AD 244857

AUTHORITY: NRL ltr 7-2/A4-82

BULLETIN No. 28

SHOCK, VIBRATION AND ASSOCIATED ENVIRONMENTS PART IV

AUGUST 1960

OFFICE OF
THE SECRETARY OF DEFENSE
Research and Engineering

Washington, D. C.

BULLETIN No. 28

SHOCK, VIBRATION AND ASSOCIATED ENVIRONMENTS PART IV

AUGUST 1960

OFFICE OF
THE SECRETARY OF DEFENSE

Research and Engineering

The 28th Symposium on Shock, Vibration and Associated Environments was held in the Departmental and Commerce Auditoriums, Washington, D. C., on February 9 - 11, 1960. The Department of the Air Force was host.

Washington, D. C.

The Theme of the Symposium was:

"The Survival of Military Equipment in a Hot War Environment"

DISTRIBUTION

Aberdeen Proving Ground, Md.
- Att: Ballistic Research Lab. 1
- Att: Development & Proof Services 1
- Att: Physical Test Lab. 1
- Att: Mr. W. J. Taylor 1
- Att: Mr. C. N. Kingery 1
- Att: Mr. J. W. Apgar 1
- Att: Mr. J. R. Tomlinson 1
- Att: Mr. W. C. Olson 1
- Att: Mr. O. T. Johnson 1
- Att: Mr. R. E. Reisler 1

Aeronautical Standards Group, D. C. 1

Air Defense Command, Ent AFB
- Att: Deputy for Civil Engineering 1

Air Force Ballistic Missile Division, L.A.
- Att: Technical Data Division 3
- Att: Director of Installations 1

Air Force Cambridge Research Ctr., Mass.
- Att: Library 1

Air Force Flight Test Ctr., Edwards AFB
- Att: FTOTL 1

Air Force Flight Test Ctr., El Centro
- Att: Mr. E. C. Myers, Tech. Dir., 6511th Test Group (Parachute) 1

Air Force Headquarters, D. C.
- Att: AFCOA, Library 2
- Att: AFCIN-3V 2
- Att: AFDRD-GW, Capt. A. R. Deptula 1
- Att: AFOCE-5, Plans Group 1
- Att: AFOCE-ES 6
- Att: Maj. Gen. A. M. Minton 1

Air Force Missile Dev. Ctr., Holloman AFB
- Att: MTHTP 2
- Att: HDOIL 1

Air Force Missile Test Ctr., Patrick AFB
- Att: Chief, Tech. Systems Lab. 2

Air Force Office of Scientific Research, D. C.
- Att: Library 1

Air Force Regional Civil Engineer
- Att: Mediterranean Region 1
- Att: Missouri River Region 1
- Att: New England Region 1
- Att: North Atlantic Region 1
- Att: North Pacific Region 1
- Att: Ohio River Region 1
- Att: South Atlantic Region 1
- Att: South Pacific Region 1
- Att: Southwest Region 1

Air Force Special Weapons Ctr., Kirtland AFB
- Att: Development Test Div. 1
- Att: Dr. E. H. Wang 1
- Att: Mr. R. Birukoff 1
- Att: Mr. H. G. Mason 1

Air Proving Ground Ctr., Eglin AFB
- Att: Weapons & Missiles Br. 1
- Att: 3208th Test Group (TF), Lab. Div., Chief, Airborne Instr. Br. 1

Air Material Command, Wright-Patterson AFB
- Att: Civil Engineer 1

Air Research & Dev. Cd., Andrews AFB
- Att: Aerodynamics Br. 1
- Att: Directorate of Equipment 1
- Att: RDTAEF 1
- Att: Dir/AI 1

Air Research & Dev. Cd., Wright-Patterson AFB
- Att: RDZSPA 2
- Att: Lt. Col. J. S. Stone 1

Air Training Command, Randolph AFB
- Att: DCS/CE 1

Alaskan Air Command, Seattle
- Att: DCS/CE 1

Armed Services Tech. Info. Ag., Arlington 10

Army Air Defense Ctr., Ft. Bliss
- Att: AKBAAC 337 1

Army Ballistic Missile Agency, Ala.
- Att: ORDAB-HST 1

Army Chemical Ctr., Md.
- Att: Mr. H. L. Solomonson 1
- Att: CMLEN-DE-S 1

Army Engineer District, N. Y.
- Att: NANGD 1

Army Engineer R&D Labs., Ft. Belvoir
- Att: Package Development Br. 1
- Att: Mr. F. J. Lindner 1
- Att: Dr. T. G. Walsh, Chief, Spec., Proj. Br. 1
- Att: Director of Research 1
- Att: Capt. R. H. Sievers, Jr. 1

Army Engineer Waterways Exp. Sta., Vicksburg
- Att: Mr. J. M. Strange 1
- Att: Mr. W. J. Flathau 1

Army Field Forces, Ft. Bragg 1

Army Field Forces, Ft. Monroe
Att: ATDEV-9 1

Army, Off. Chief of Engineers
Att: Asst. Chief for Military Operations, Engineer R&D Division 2
Att: ENGEB 1

Army, Off. Chief of Ordnance
Att: ORDFA-T 1
Att: ORDFM 1
Att: ORDTB, Mr. J. Kaufman 1

Army, Off. Chief of Res. & Dev.
Att: Mr. A. L. Tarr 1

Army, Off. Chief of Staff
Att: Surface-to-Surface Missiles Div. 1

Army, Off. Chief of Transportation
Att: Executive for R&D 1

Army Ordnance Missile Command, Ala.
Att: Mr. R. E. Cuthill, Chief Engr. 1

Army Security Agency, Md. 1

Army Signal Equipment Support Ag., N. J.
Att: SIGFM/ES-PFM-4 1

Army Signal R&D Labs., N. J.
Att: Tech. Documents Ctr. ESL 1
Att: Spec. & Drafting Br. ESL 1
Att: Thermionics Br. ESL 1
Att: Spec. & Drafting Components Dept. 1
Att: Suppl. & Gen. Engr. Components Dept. 1
Att: Components & Materials Br. SSL 1
Att: Spec. & Drafting Br. SSL 1
Att: Mr. J. J. Oliveri 1

Army Transportation Research Cd., Ft. Eustis
Att: Library 1

Arnold Engineering Dev. Ctr., Tenn.
Att: AEOIM 1

Atomic Energy Commission, Oak Ridge 3

Atomic Energy Commission, D. C.
Att: Library 1
Att: Div. of Reactor Development, Tech. Evaluation Br. (Army Reactors) 1

Boston Naval Shipyard
Att: Code 250c 1

Bureau of Medicine & Surgery, D. C.
Att: Research Div. 1

Bureau of Naval Weapons, D. C.
Att: DLI-3 15
Att: SP Tech. Library 1
Att: FWAA, C. H. Barr 1
Att: RREN-5 5
Att: RRMA 1
Att: RAAE-2 1
Att: RM-3 2
Att: RM-2 1
Att: RSSH 2
Att: FWAE 1

Bureau of Naval Weapons Rep., E. Hartford 2

Bureau of Naval Weapons Rep., Pomona
Att: Chief Engineer 1

Bureau of Naval Weapons Rep., Sunnyvale
Att: Mr. C. M. Fitch 1

Bureau of Ships, D. C.
Att: Code 423 20

Bureau of Supplies & Accounts, D. C.
Att: Code H43 1

Bureau of Yards & Docks, D. C.
Att: Code P-306 1
Att: Code C-304 1
Att: CDR W. J. Christensen 1
Att: Tech. Library (Unclassified Parts) 1

Civil Engineering Ctr., Wright-Patterson AFB
Att: AFIT 2

Coast Guard Headquarters, D. C. 1

David Taylor Model Basin, D. C.
Att: Library 3
Att: Mr. Harry Rich 1
Att: J. A. Luistro, Code 591L 1
Att: Mrs. S. C. Atchison 1
Att: Contract Research Administrator, Code 513 1

Defense Atomic Support Agency, D. C.
Att: Technical Director 1
Att: Weapons Development Div. 1
Att: Mr. John G. Lewis 1

Defense Atomic Support Agency, Livermore
Att: Administrative Officer 1

Detroit Arsenal, Michigan
Att: Technical Library 2
Att: Engineering Standards Unit 1

Dept. of Interior, Bureau of Mines, D. C.
Att: Dr. L. Obert, Applied Physics Res. Lab. 1

Diamond Ord. Fuze Labs., D. C.
Att: Mr. W. S. Hinman, Jr. 2
Att: Components Lab., 300 1
Att: Industrial Div., 700 2
Att: Mr. R. G. Barclay, Br. 220 1
Att: Tech. Ref. Ctr., .012 1

Electronics Supply Office, Great Lakes 1

Federal Aviation Agency, Atlantic City
Att: Lt. Col. J. Abellera, USAF, Emergency Readiness Officer 1

Federal Aviation Agency, D. C.
Att: Emergency Readiness Div., Off. of Plans & Requirements 2

Frankford Arsenal, Phila.
Att: Fire Control Lab. 1
Att: Physics Research Lab. 1
Att: Electronic VT Fuze Dept. 1
Att: Mr. A. L. Jamieson 1

InsMat San Francisco 1

InsMat St. Louis 1

InsMat Syracuse
Att: Code 5 3

Long Beach Naval Shipyard, Cal.
Att: Code 240 1

Los Alamos Scientific Laboratory, N. M.
Att: Report Librarian 1

Los Angeles Air Procurement District, Cal.
Att: Quality Control Division 1

Los Angeles Ordnance District, USA, Cal.
Att: ORDEV 1

Mare Island Naval Shipyard
Att: Electronics Officer 1
Att: Industrial Laboratory 1

Marine Corps Equipment Board, Quantico 2

Marine Corps Headquarters, D. C.
Att: Research & Dev. Section 1
Att: Code AO4E 1

Maxwell Air Force Base, Ala.
Att: Air Command & Staff School 1
Att: USAF Institute of Tech. 1

Military Air Transport Service, Scott AFB
Att: Chief, C.E.D. 1

NASA, Ames Research Ctr., Moffett Field
Att: Dr. S. J. DeFrance, Dir. 1

NASA, High Speed Flight Sta., Edwards AFB 1

NASA, Goddard Space Flight Ctr., D. C.
Att: Mr. John C. New, Code 9440 1
Att: Code 9401 1

NASA, Langley Research Ctr., Va.
Att: Mr. E. I. Garrick 1

NASA, Lewis Flight Propulsion Lab., Cleveland
Att: Library 1

NASA, Washington, D. C.
Att: Library 1

National Bur. of Standards, Colorado
Att: AEC Cryogenic Engr. Lab. 1

National Bur. of Standards, D. C.
Att: Dr. Walter Ramberg 2
Att: Mr. W. A. Wildhack 1
Att: Mr. S. Edelman, Mech. Div. 1

Naval Air Development Ctr., Johnsville
Att: Mr. E. R. Mullen 1
Att: Aviation Armament Lab. 1
Att: Materials & Components Br. 1
Att: Aeronautical Instruments Lab. 1

Naval Air Engrg. Facility, Phila.
Att: Library 1

Naval Air Material Ctr., Phila.
Att: Library 1

Naval Air Rocket Test Station, Dover
Att: Technical Library 1

Naval Air Station, Alameda
Att: Aeronautical Engrg. Group 1

Naval Air Station, Patuxent River
Att: Armament Test Div. (Mr. Regan) 3

Naval Air Test Center, Patuxent River
Att: Electronics Test Div. 1

Naval Ammunition Depot, Earle
Att: Mr. J. E. Kelly, Chief Engr., Materials Handling Lab. 1

Naval Attache, Navy 100
Att: Logistics Division 1

Naval Civil Engineering Lab., Pt. Hueneme
Att: Library 1
Att: Mr. R. A. Breckenridge 1
Att: Mr. C. R. White 1
Att: Mr. J. R. Allgood 1

Naval Engrg. Experiment Sta., Annapolis
Att: Code 705 1

Naval Medical Field Res. Lab., Camp Lejeune 1

Naval Medical Research Inst., Bethesda
Att: Dr. David Goldman 1

Naval Mine Engrg. Facility, Yorktown 1

Naval Missile Ctr., Pt. Mugu
Att: Library 1
Att: Launcher & Environment Div. 1
Att: Mr. S. R. Melcher 1
Att: Mr. M. R. Beckman 1

Naval Nuclear Ord. Eval. Unit, Albuquerque 1

Naval Operations, Office Chief of, D. C.
Att: Op 31 1
Att: Op 34 1
Att: Op 75 1
Att: Op 51 1
Att: Op 91 1
Att: CDR P. H. Shropshire, Jr. 1

Naval Ordnance Lab., Corona
Att: Quality Eval. Lab. 1
Att: Code 56, Sys. Eval. Div. 1

Naval Ordnance Lab., White Oak
Att: Technical Director 1
Att: Library 3
Att: Code UN 2
Att: Shock Branch 1
Att: Vibration Branch 1
Att: Environmental Branch 1
Att: Mr. J. Petes 1
Att: Mr. W. S. Filler 1
Att: Mr. L. W. Slifer, Jr. 1

Naval Ordnance Test Sta., China Lake
1 Att: Code 55514
1 Att: Technical Library

Naval Ordnance Test Sta., Pasadena
3 Att: P8087
1 Att: P8092
1 Att: P8073
1 Att: P80962
1 Att: Mr. F. L. Baldwin

Naval Postgraduate School, Monterey
1 Att: Library

Naval Propellant Plant, Indian Head
1 Att: Mr. K. M. Carr, Code R5B

Naval Radiological Def. Lab., San Fran.
3 Att: Library
1 Att: Mr. H. A. Zagorites

Naval Repair Facility, San Diego
1 Att: Tech. Library, Bldg. 38

Naval Research Laboratory, D. C.
1 Att: Code 6250
1 Att: Code 6260
1 Att: Code 6201
1 Att: Code 6261, Mr. M. W. Oleson
2 Att: Code 4021

Naval Supply R&D Facility, Bayonne
1 Att: Library

Naval Torpedo Station, Keyport
1 Att: QEL, Technical Library

Naval Training Device Ctr., N. Y.
1 Att: Library Branch

Naval Underwater Ord. Sta., Newport
1 Att: Tech. Documents Library

Naval Weapons Laboratory, Dahlgren
1 Att: Technical Library

Naval Weapons Plant, D. C.
6 Att: Aviation Ordnance Unit
4 Att: Design Dept. Code DE-740
1 Att: Engrg. Dept. Code 733.2
Att: Missile Systems Engrg. Div., Code 760

Navy Central Torpedo Office, Newport
1 Att: Quality Evaluation Lab.

Navy Electronics Lab., San Diego
1 Att: Library

Navy Mine Defense Lab., Panama City
1

Navy ROTC & Admin. Unit, MIT
1

Navy Underwater Sound Lab., New London
1 Att: Dr. J. M. Ide
1 Att: Mr. J. G. Powell

Navy Underwater Sound Ref. Lab., Orlando
1 Att: Mr. J. M. Taylor

New York Naval Shipyard
1 Att: OinC, Naval Material Lab., Code 912b 3

Norfolk Naval Shipyard, Va.
1 Att: Design Superintendent
3 Att: Underwater Explosions Res. Div., Code 281A
1 Att: Mr. G. J. Vogler
1

Norton AFB, Calif.
1 Att: 1002d IG, D/RM1, Supply Services and Transportation
1

Off. Naval Material, D. C.
1

Off. Naval Research, D. C.
6 Att: Code 439
1 Att: Code 104

Off. Naval Research Branch Off., Boston
1

Off. Naval Research Branch Off., Pasadena
1

Off. Naval Research Branch Off., San Fran.
1

Off. Secretary of Defense, Dir. of Defense R&E
1 Att: Technical Library
1 Att: Dir. of Electronics
1 Att: Dir. of Fuels, Matls. & Ord.
1 Att: Dir. of Aeronautics
1 Att: Dir. of Guided Missiles
1 Att: Mr. L. M. Ruth, Rm 3E127
1 Att: Mr. G. B. Wareham
1

Off. Secretary of Defense, Dir. of Defense R&E Advisory Group on Electron Tubes, N. Y.
1 Att: Secretary
1

Oklahoma City Air Material Area, Tinker AFB
1 Att: Engineering Div.
1

Ordnance Ammunition Ctr., USA, Joliet
1 Att: ORDLY-M-P, H. S. Stein
1 Att: NNSC/A
1

Pacific Air Force
1 Att: ACS/CE
1

Pearl Harbor Naval Shipyard
2 Att: Code 264
1

Philadelphia Naval Shipyard
1 Att: Ship Design Section
1

Picatinny Arsenal, Dover
1 Att: Library
1 Att: Packaging Sec., Tech. Div.
1

Portsmouth Naval Shipyard
1 Att: Code 251b
1 Att: Mr. E. C. Taylor
1

Puget Sound Naval Shipyard
1 Att: Design Supt., Code 251
1 Att: Material Labs.
1 Att: K. G. Johnson, Design Div., Planning Dept.
1

Quartermaster Food & Container Inst., Chicago
Att: Dir., Container Lab. 1
Att: Technical Library 1
Att: Mr. E. F. Williams 1

Quartermaster General, Off. of, D. C.
Att: Military Planning Div. 1

Quartermaster Res. & Dev. Ctr., Natick
Att: Technical Library 2

Radford Arsenal, Va.
Att: ORDCB, W. B. Helbert 1

Randolph AFB, Texas
Att: USAF School of Aviation Medicine 1

Redstone Arsenal, Ala.
Att: Technical Library 4
Att: Mission Planning & Coord. Off. 1
Att: Guided Missile Dev. Div. 1
Att: Mech. Branch, T&E Div. 1
Att: Rocket Development Div. 1
Att: James M. Taylor, RDL-Bldg. 855 1
Att: ORDDW-GMTB 1
Att: ORDDW-IDES-J 1

Rome Air Development Center, N. Y.
Att: Mr. E. A. Catenaro, RCSGE-1 3

Rossford Ordnance Depot, Ohio
Att: Ordnance Packaging Off. 1

San Francisco Naval Shipyard
Att: Code 250 1
Att: Code 254T 1

Savanna Ordnance Depot, Illinois
Att: Ammunition Instructor's School 1

Signal Corps Supply Agency, Phila. 1

Signal Officer, Off. of Chief, Arlington
Att: Engineering Control Div. 1

Signal Officer, Off. of Chief, D. C.
Att: R&D Division 1

Springfield Armory, Mass.
Att: Library 2

Strategic Air Command, Offutt AFB
Att: Operations Analysis Off. 1
Att: Director of Civil Engineering 1

Tactical Air Command, Langley AFB
Att: Director of Installations 1

U. S. Air Forces in Europe
Att: DCS/I 1

Watertown Arsenal, Mass.
Att: Dr. R. Beeuwkes, Jr., Ord. Matls. Res. Off. 2
Att: Technical Information Sec. 1

Watervliet Arsenal, N. Y.
Att: ORDBF-RR 1

White Sands Missile Range, N. M.
Att: Electro Mechanical Div. 1
Att: ORDBS-TS-TIB 3
Att: Mr. A. O. Crobaugh 1

Wright Air Development Division, Ohio
Att: Chief, WCRT 1
Att: Chief, WCLE 1
Att: Chief, WCRD 1
Att: Chief, WCLS 1
Att: Chief, WCLB 1
Att: Chief, WCLP 1
Att: Chief, WCLF 1
Att: Chief, WCRR 1
Att: Chief, WCLG 1
Att: WCRTH-5 1
Att: WCLSY, Mr. H. A. Magrath 1
Att: WCLEMD, Mr. D. C. Kennard 1
Att: WCLKM, Mr. C. Golueke 1
Att: WCLNKT, Mr. McDowell 1
Att: WCLREP, Mr. McCormick 1
Att: WCLODC, Mr. Hankey 1
Att: Dr. M. G. Scherberg 1
Att: Forest Products Lab. Library (via WCRTH-5) 1

FOREWORD

This section of the Bulletin contains unclassified papers discussing design, test methods, instrumentation and data analysis. The material discussed at the panel session on the Collection, Analysis and Presentation of Shock and Vibration Data is also included. A Table of Contents for all four Parts of the Bulletin and an attendance list for the 28th Symposium may be found in Part I.

Constructive suggestions for the improvement of the Symposia and the Bulletins are earnestly solicited. Address communications to: Code 4021, U.S. Naval Research Laboratory, Washington 25, D.C., or to a member of the Interservice Technical Group whose names are listed on the following page.

August 1960

INTERSERVICE TECHNICAL GROUP FOR SHOCK, VIBRATION, AND ASSOCIATED ENVIRONMENTS

ARMY MEMBERS

Mr. A. O. Crobaugh
Electro-Mechanical Laboratories
White Sands Missile Range
Las Cruces, New Mexico

Mr. E. F. Williams
Quartermaster Food and Container Institute
1819 W. Pershing Road
Chicago 9, Illinois

Mr. Joseph Kaufman
Office of the Chief of Ordnance
U.S. Army
Pentagon
Washington 25, D. C.

Mr. Frederick J. Lindner
Packaging Development Branch
U.S.A. Engineer Research and Development Laboratories
Fort Belvoir, Virginia

Mr. Joseph J. Oliveri
Elec. Parts and Material Division
U.S.A. Signal Research and Development Laboratories
Fort Monmouth, New Jersey

Dr. Joseph S. diRende, Director
Research Directorate
U.S.A. Transportation Research Command

NAVY MEMBERS

Mr. J. M. Crowley
Office of Naval Research
U.S. Navy Department
Washington 25, D. C.

Mr. E. R. Mullen
U.S. Naval Air Development Center
Johnsville, Pennsylvania

Mr. R. H. Oliver
Bureau of Ships
U.S. Navy Department
Washington 25, D. C.

Mr. Harry Rich
David Taylor Model Basin
Washington 7, D. C.

Dr. Harold Leibowitz*
Head, Structural Mechanics Branch
Office of Naval Research
U.S. Navy Department
Washington 25, D. C.

AIR FORCE MEMBERS

Mr. Emil A. Catenaro
Rome Air Development Center
Attn: RCSGE-E
Griffiss Air Force Base, New York

Mr. Carl Golueke
Wright Air Development Division
Attn: WCREM
Wright-Patterson Air Force Base
Akron, Ohio

Mr. D. C. Kennard
Wright Air Development Division
Attn: WCLES-3
Wright-Patterson Air Force Base
Akron, Ohio

Mr. H. A. Magrath
Wright Air Development Division
Attn: WCLSY
Wright-Patterson Air Force Base
Akron, Ohio

NATIONAL AERONAUTICS AND SPACE ADMINISTRATION MEMBER

Mr. John C. New
Head, Systems Test Branch
Payload Systems Test Division
Goddard Space Flight Center
Washington 25, D. C.

*Deputy for Mr. J. M. Crowley

CONTENTS

Instrumentation and Data Analysis

Panel Session and Discussion

Information Exchange

DESIGN PROBLEMS AND SOLUTIONS

A METHOD FOR PREDICTING ENVIRONMENTAL VIBRATION LEVELS IN JET-POWERED VEHICLES

P. T. Mahaffey and K. W. Smith
Convair
Fort Worth, Texas

A method for predicting environmental vibration levels for jet-powered vehicles is described. A quantitative relationship is determined between structural vibration and acoustic noise level on the external super of a structure by statistical analysis of measured data. Comparisons of measured and predicted levels are shown.

INTRODUCTION

One of the most difficult problems facing the vibration engineer is that of predicting environmental vibration levels on a new vehicle. Another problem almost as difficult is that of quoting vibration levels on a current vehicle in a region where no measurements have been made. Yet questions on these matters are frequently asked by equipment designers and must be answered in some manner by the vibration man.

It is the purpose of this paper to present a method which can be used to obtain good engineering answers to these questions. This particular method was developed to aid in establishing vibration test requirements for the B-58 airplane. However, it appears that it would be equally applicable to other vehicles according to the checks which have been made at Convair. The basic principle lies in relating vibration level to noise level, and curves are presented which permit a prediction of vibration level from a knowledge of noise level on the external surface of the vehicle.

BASIC CONCEPTS

In jet-powered vehicles, most of the environmental vibration comes from response of the structure to intense engine noise. Thus, the vibration level should be proportional to the noise level in some manner. If this relationship could be established, then it should be possible to predict vibration level from a knowledge of the engine noise level distribution.

There are two basic ways which can be used to relate vibration level to noise level. One way is to calculate the response of the structure to the excitation provided by the noise. The other way is to use statistical methods to predict the most probable structural response level to a given noise level.

To follow the course of direct response calculation, an investigation has to adopt the approach of looking at a specific location. He has to examine the physical make up of the structure and to calculate as best he can the natural modes of vibration of this location. He has to determine the damping

associated with each natural mode, and he has to determine whether or not the response is linear. These obstacles have been sufficiently formidable to deter most investigators, and to prevent any from achieving a universally applicable solution to the problem.

Let us now examine the statistical approach. One important advantage is immediately obvious. It is now possible to look at the problem in the broad sense rather than having to deal with each specific instance. The structural response can be categorized into that for primary structure and that for secondary structure. One can also adopt the viewpoint of average response, or of most probable response instead of dealing with a specific response value.

If we now formulate the problem in terms of predicting the most probable vibration level for primary structure exposed to a given noise level, we begin to see a chance for success. What we need is a sufficient body of measured data to analyze. These data need to be in the form of vibration level measurements and sound pressure level measurements for a large number of locations. We then need to reduce these data on an octave band basis and to correlate the results in terms of the relationship between vibration acceleration level and sound pressure level. If we do this, we can construct a plot for each octave band of the type illustrated in Fig. 1. Acceleration level in g's is plotted on a log scale against sound pressure level in decibels. Statistical analysis can be employed to determine a regression line giving the average trend of the data, and the scatter in the data can be expressed in terms of confidence levels.

With a plot of this type for each octave band and a knowledge of the octave band sound pressure level, a prediction of the envelope of probable vibration level can be made in the form illustrated in Fig. 2. Any desired degree of conservatism can be incorporated by basing the predicted envelope on the appropriate upper confidence level boundary.

These methods have been applied to measured data from the B-58 airplane with gratifying results as described in the following section.

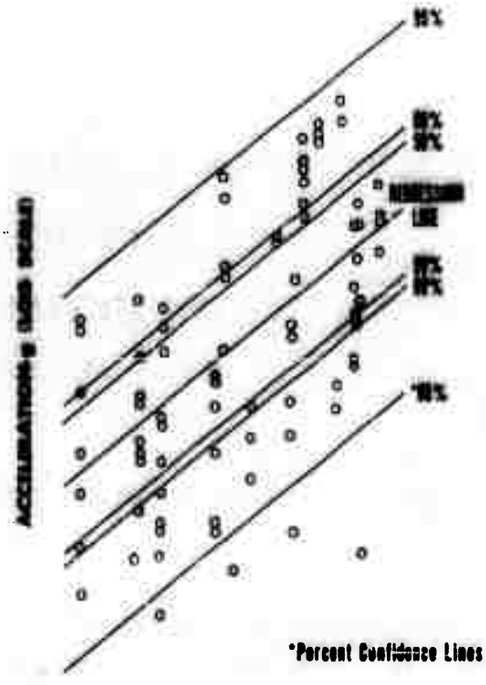

Fig. 1 - Example of plot acceleration vs sound pressure level

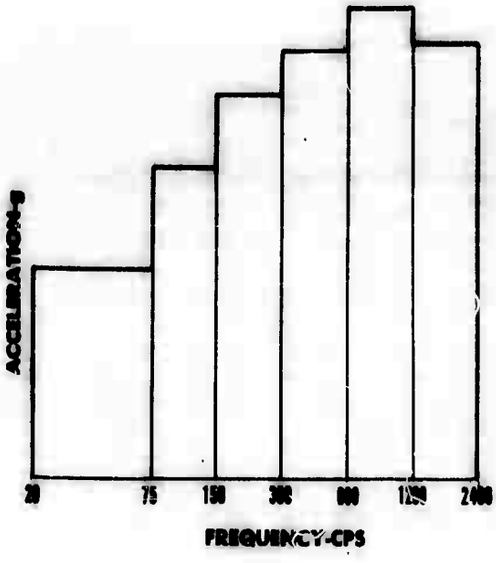

Fig. 2 - Example of predicted envelope of probable vibration levels

ANALYSIS OF B-58 VIBRATION DATA

Both an acoustic noise survey and an environmental vibration survey were made for the B-58 airplane for the condition of maximum afterburner power on all four engines during ground run-up.

The noise data were collected by using microphones spaced judiciously over the surface of the airplane so that lines of equal sound pressure level could be constructed

from the measurements. The microphone outputs were recorded on magnetic tape and reduced on an octave band basis. Isointensity line plots were then made for the overall levels and for each octave band as shown in Figs. 3 through 9.

The vibration data were collected by using velocity pickups, crystal accelerometers, and a tape recorder. These data were reduced on a one-third octave band basis through a peak detection circuit. Within the limitations of the filters, the reduced data were peak acceleration readings of the sort one would expect to obtain from a hand analysis of an oscillograph trace of the transducer signal. Sixty-five pickups were used. These were mounted on primary structure at various points in the airplane. At most points, accelerations were measured in three perpendicular directions.

The first step in correlating the data was to tabulate acceleration level in g's for each frequency octave band along with the noise level in decibels in the corresponding octave bands. This was done for each pickup for all octave bands. The noise levels were picked off the isointensity line plots made for each octave band, as shown in Figs. 4

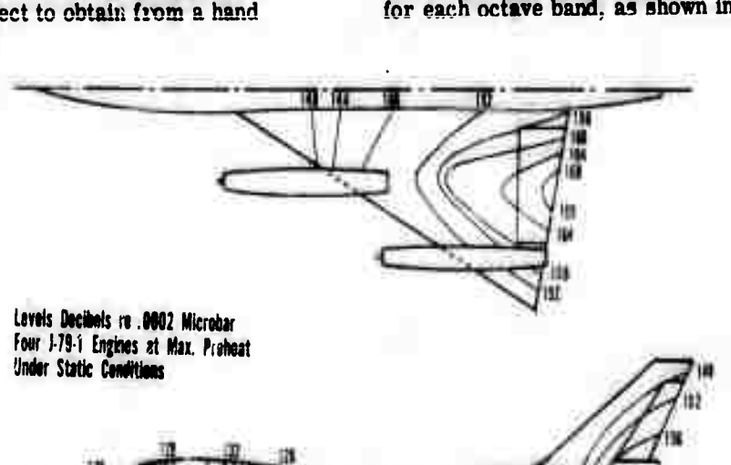

Fig. 3 - Overall sound pressure level contours

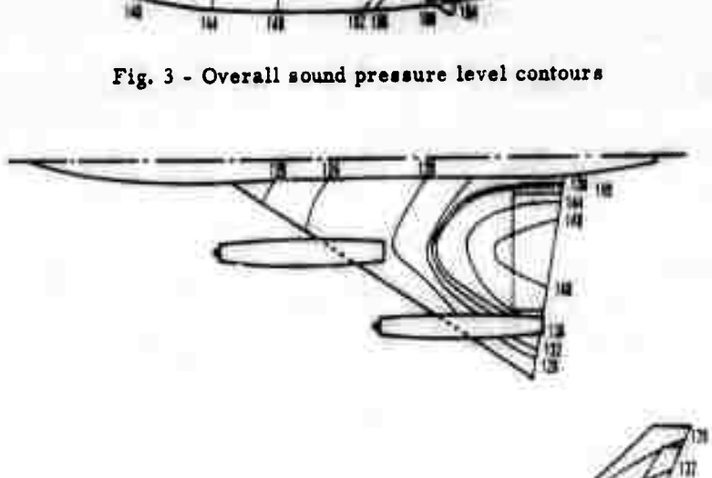

Fig. 4 - Twenty to 74-cps octave band sound pressure level contours

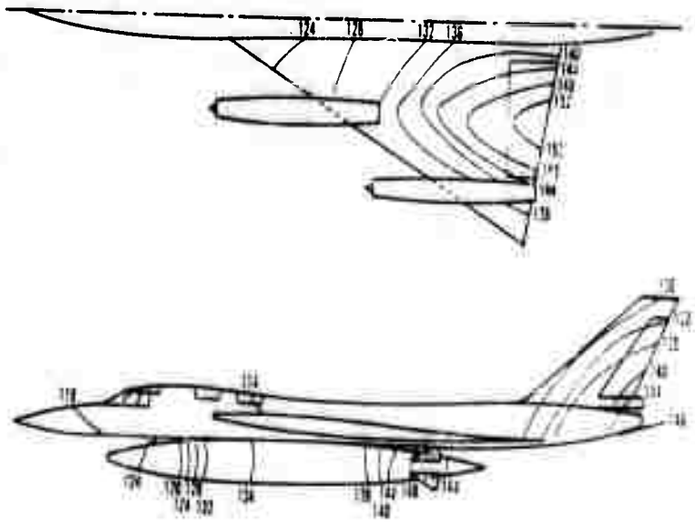

Fig. 5 - Seventy-five to 150-cps octave band sound pressure level contours

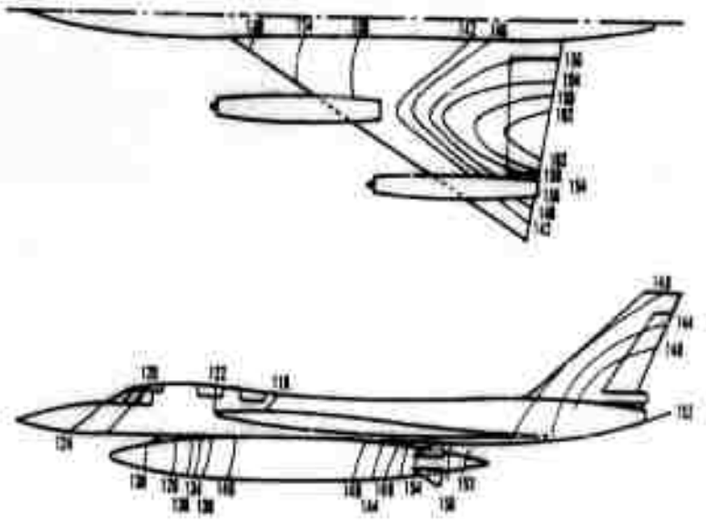

Fig. 6 - 150- to 300-cps octave band sound pressure level contours

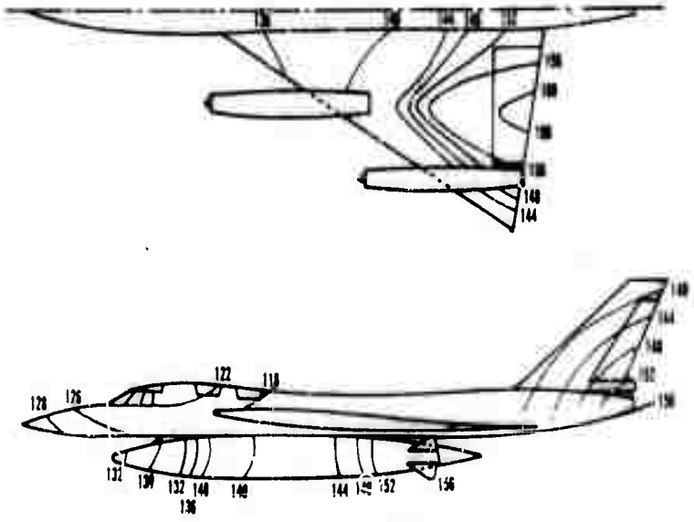

Fig. 7 - 300- to 600-cps octave band sound pressure level contours

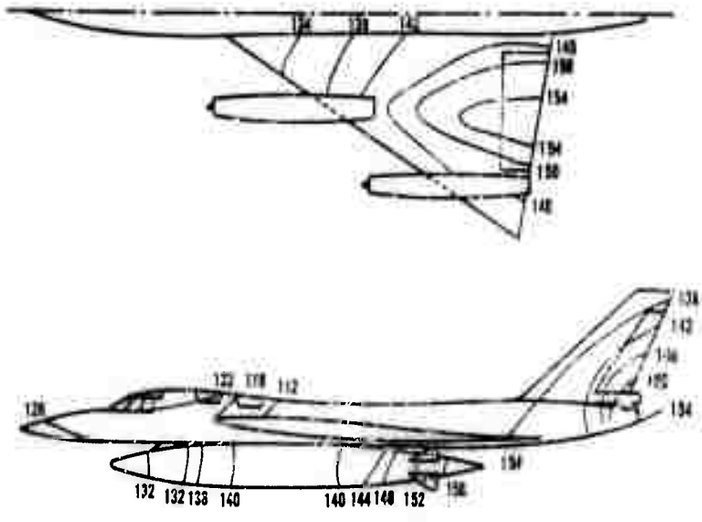

Fig. 8 - 600- to 1200-cps octave band sound pressure level contours

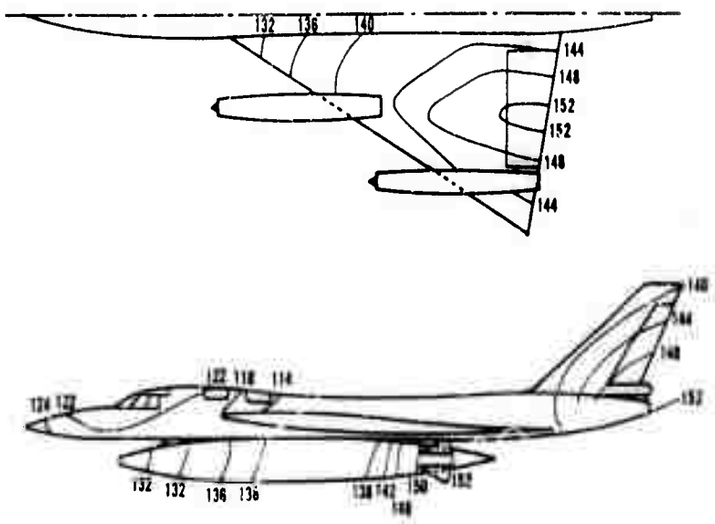

Fig. 9 - 1200- to 2400-cps octave band sound pressure level contours

through 9 according to the location of the vibration pickup. These values were first plotted on ordinary graph paper bearing uniform scales. As expected, a wide scatter was observed, so statistical correlation methods were employed to determine a mathematical equation best fitting these data.

The vibration acceleration values together with their corresponding acoustic noise levels were then processed by electronic calculating machines. Here the statistical correlation coefficients were calculated for a number of different equation forms (linear, parabolic, exponential, etc.). These statistical correlation coefficients are a mathematical representation of the following two methods of prediction:

1. Each peak acceleration level is predicted by using the empirical equation line.

2. Each peak acceleration level is predicted by using the average of the measured vibration levels. Then

$$r = \pm(1 - \sigma_1^2/\sigma_2^2)^{\frac{1}{2}}, \qquad (1)$$

where

r = Pearsonian correlation coefficient,

σ_1^2 = sum of squares of data point deviations from the empirical equation line,

σ_2^2 = sum of squares of the data point deviations from the average line.

When r approaches ± 1, then the fit of the data is good. If r approaches zero, then the data are randomly arranged. The correlation coefficients calculated for the different empirical equation forms revealed that the exponential equation provided the best fit for the data in each frequency octave band. The exponential equation has the form

$$\log_e g = (M)(SPL) + \log_e A, \qquad (2)$$

where

g = peak acceleration level divided by the acceleration due to gravity,

M = slope of the empirical equation line,

SPL = sound pressure level in decibels (re .0002 dynes/cm^2),

A = intercept of the empirical equation line on the g-axis.

The method of least squares was used to determine values of M and $\log_e A$ so that the sum of the squares of the data point deviations from the empirical equation line was at a minimum. In addition the statistical variance of the data from the empirical equation line was calculated. Figures 10 through 15 show the plots of the empirical equations and statistical confidence levels for each frequency octave band in the range from 20 to 2400 cps.

With the octave band noise plots of Figs. 4 through 9 and the plots of vibratory

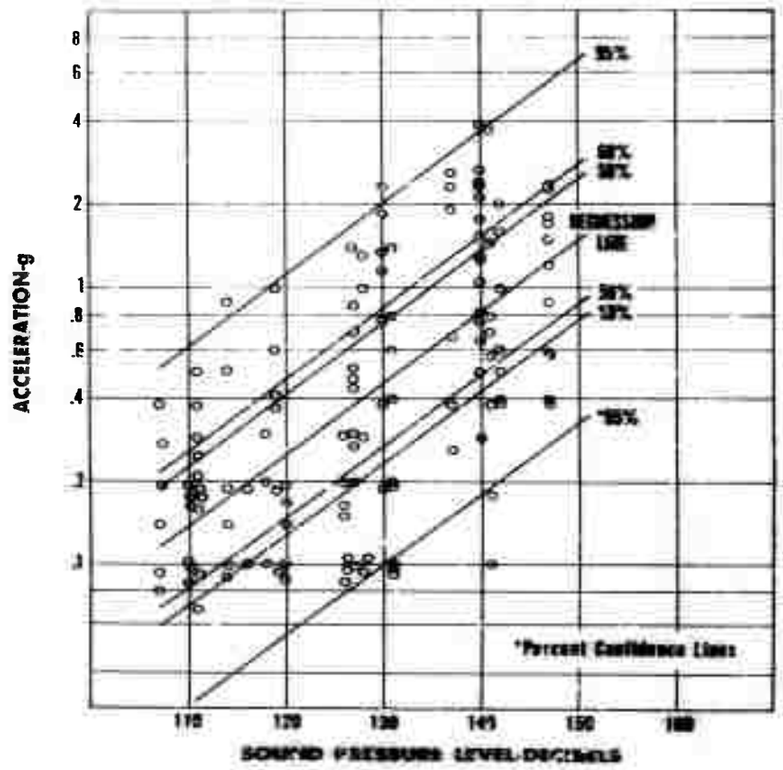

Fig. 10 - Acceleration vs sound pressure level, 20- to 75-cps octave band

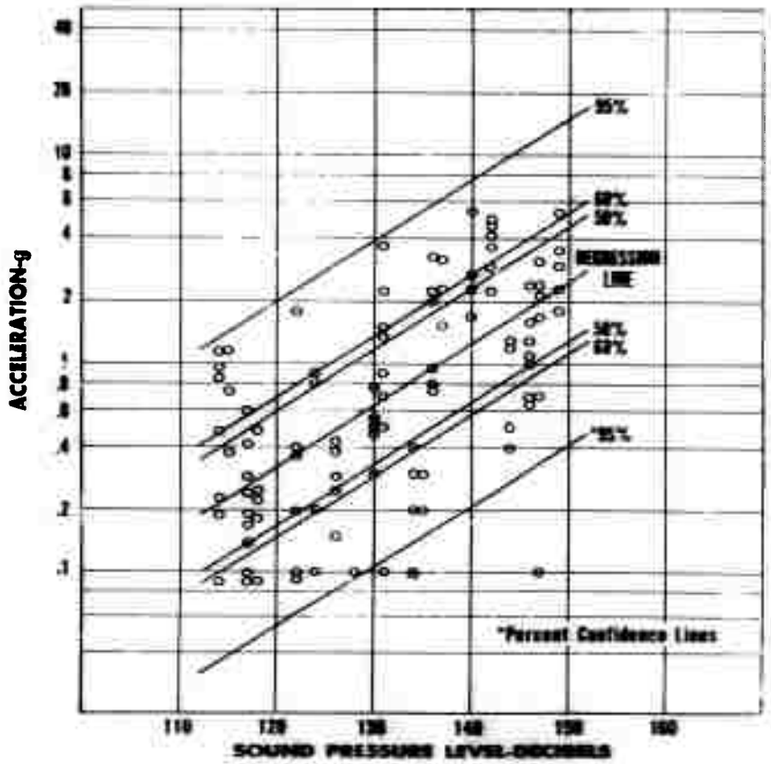

Fig. 11 - Acceleration vs sound pressure level, 75- to 100-cps octave band

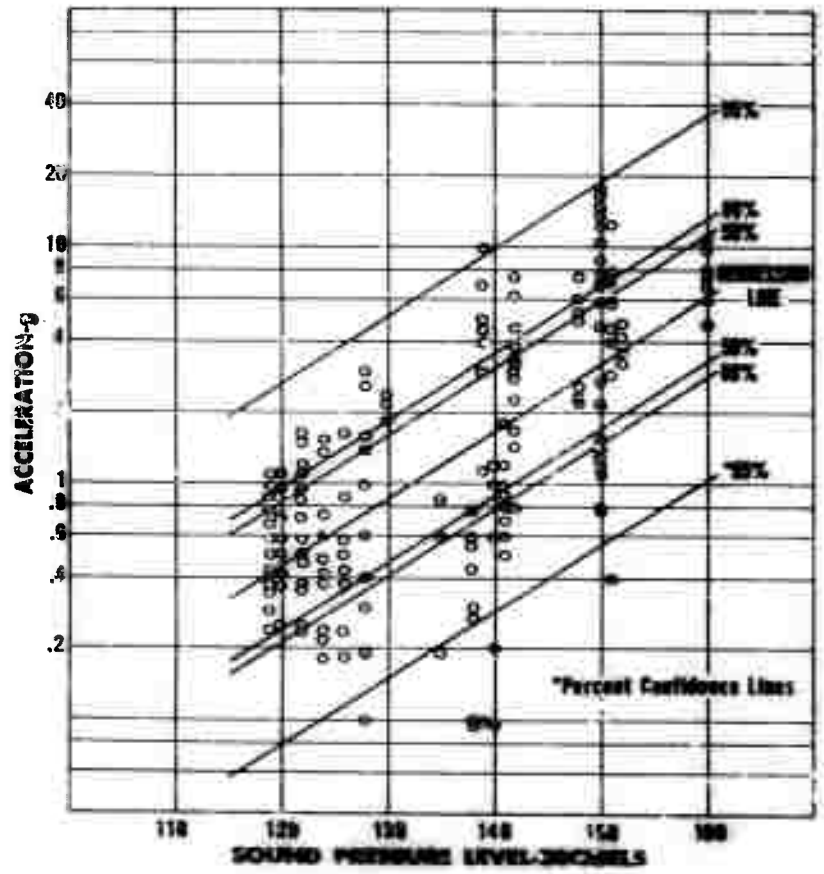

Fig. 12 - Acceleration vs sound pressure level, 150- to 300-cps octave band

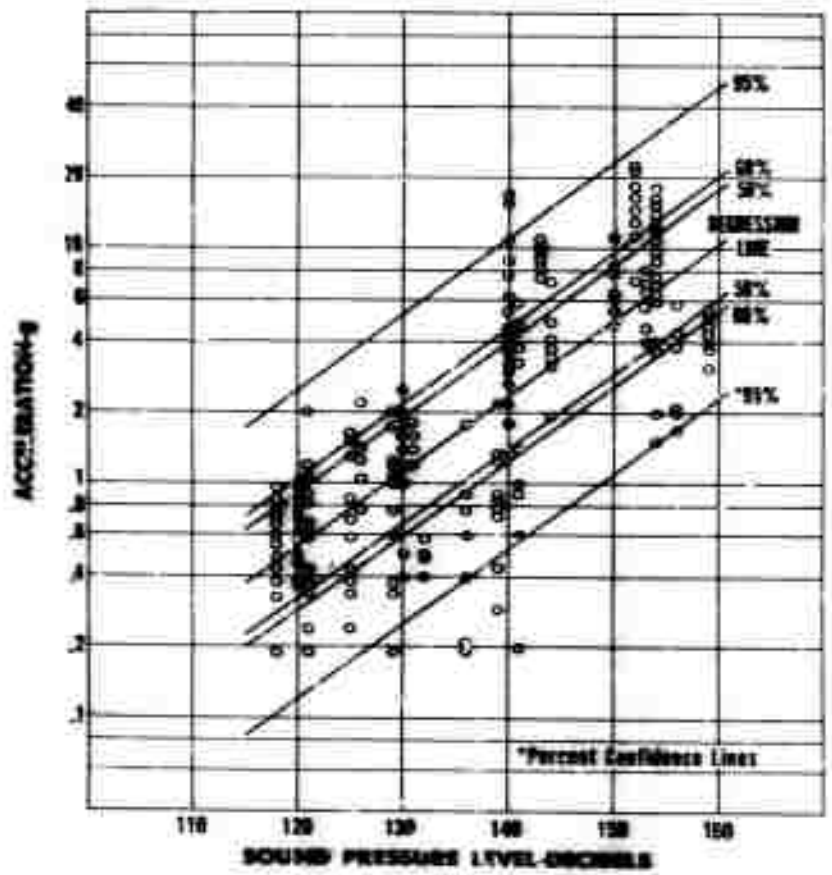

Fig. 13 - Acceleration vs sound pressure level, 300- to 600-cps octave band

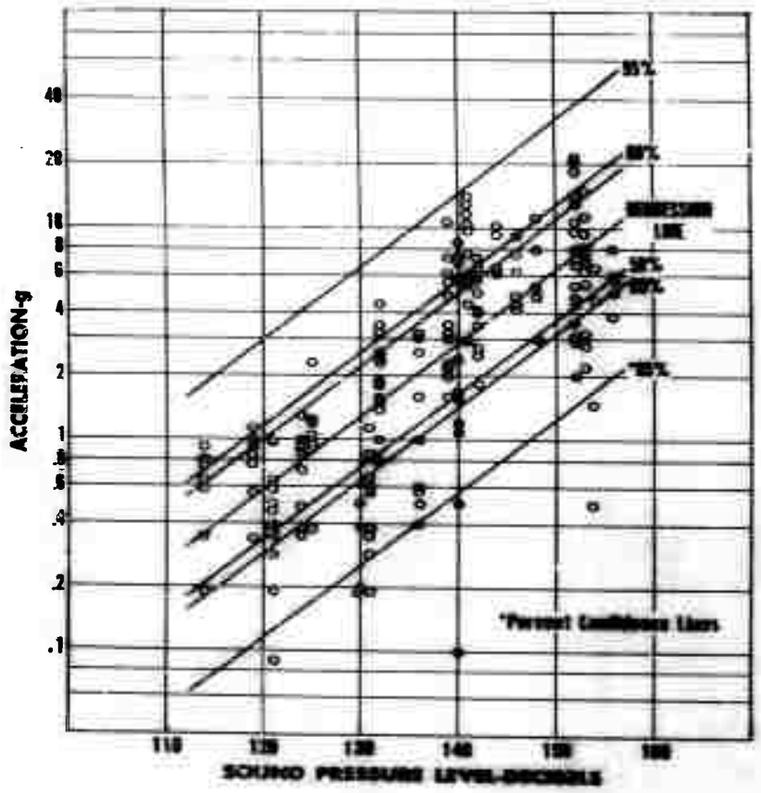

Fig. 14 - Acceleration vs sound pressure level, 600- to 1200-cps octave band

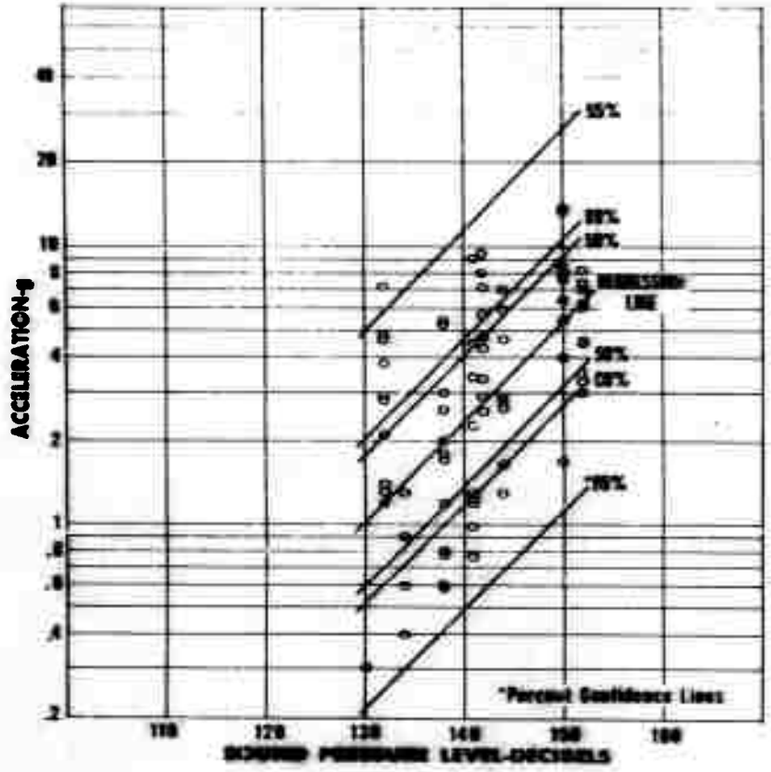

Fig. 15 - Acceleration vs sound pressure level, 1200- to 2400-cps octave band

acceleration versus noise level of Figs. 10 through 15, it is now possible to predict a vibration level envelope such as illustrated in Fig. 2 for any point on the airplane. From such envelopes, one may further proceed to derive range curves for vibration qualification testing along the lines specified in MIL-E-5272.

DERIVATION OF VIBRATION TEST ENVELOPES

The first step in deriving a series of vibration test envelopes for the B-58 was to divide the airplane into vibration zones. The preliminary selection of these zones was made on the basis of the exterior sound pressure levels on the surface of the airplane. The final boundaries were selected so that the transition from one zone to another would not represent in an unduly large step changes in the predicted environment. These zones are shown in Fig. 16. The representative sound pressure level for each vibration zone was then read from the isointensity sound level plots for each frequency octave band in the 20 to 2400 cps range.

By using these sound pressure levels from each vibration zone, the plots in Figs. 10 through 15 were entered and the predicted peak acceleration levels were read opposite one of the upper confidence lines. The choice of upper confidence line depends upon the risk one is willing to assume that the actual acceleration level will exceed the predicted level. For the B-58 it was determined that predicted vibration levels corresponding to the upper 60-percent confidence line provided a reasonable fit to data collected but not used in the correlation. The vibration level predicted with this confidence line will encompass the measured vibration levels during 80 percent of the prediction trials.

The predicted peak acceleration values read from the upper 60-percent line in each frequency octave band were tabulated and plotted for each vibration zone. A test envelope suitable for use with a sinusoidal vibration shaker system was then drawn over the predicted vibration values. Figures 17 through 19 show predicted vibration levels and derived test envelopes for three representative test zones. Included in these figures for comparison purposes are plots of the measured vibration data collected in each of the zones and used in the statistical correlation. These plots are representative of the fit between the derived envelope and the measured data. Note that although a few measured points fall outside the envelopes, the fit is generally good.

Vibration range curves were thus derived for all the zones shown in Fig. 16, and were used with the basic MIL-E-5272 procedure to produce a qualification test procedure tailored to fit the B-58 airplane.

Very little measured vibration data were obtained for some of the zones of Fig. 16, and no data at all were obtained for others. Yet, the application of this procedure made it possible to establish predicted levels and

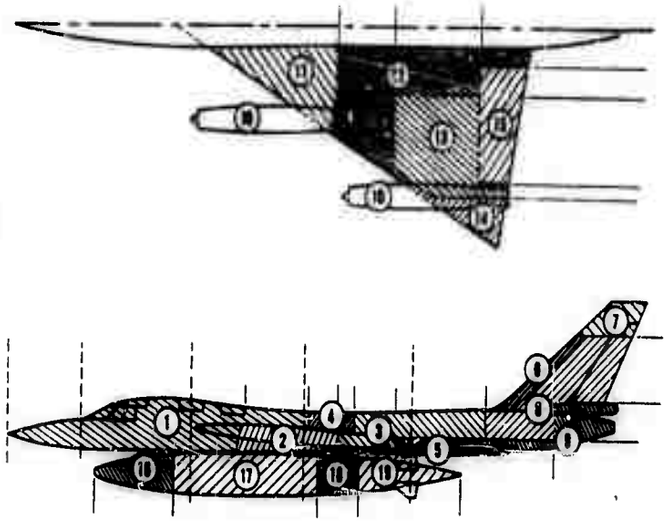

Fig. 16 - Vibration zones

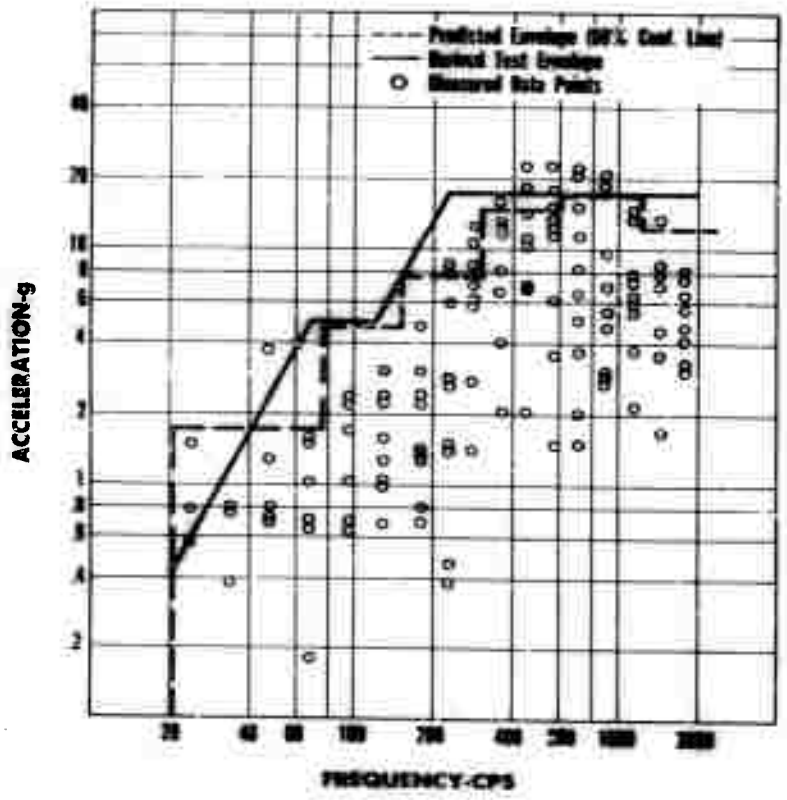

Fig. 17 - Comparison of predicted envelope and derived test envelope with measured vibration for Zone 9

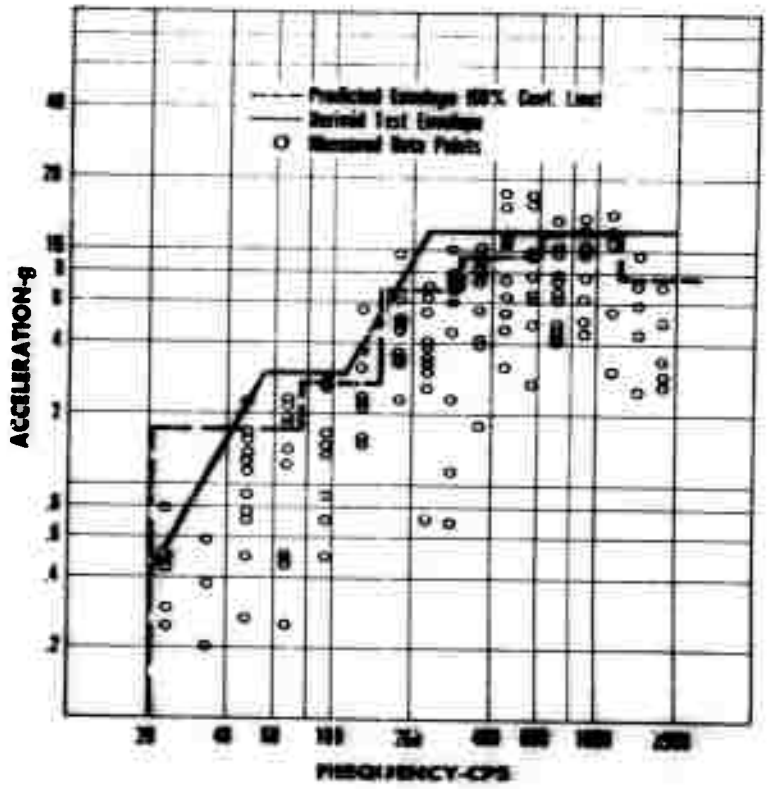

Fig. 18 - Comparison of predicted envelope and derived test envelope with measured vibration data for Zone 12

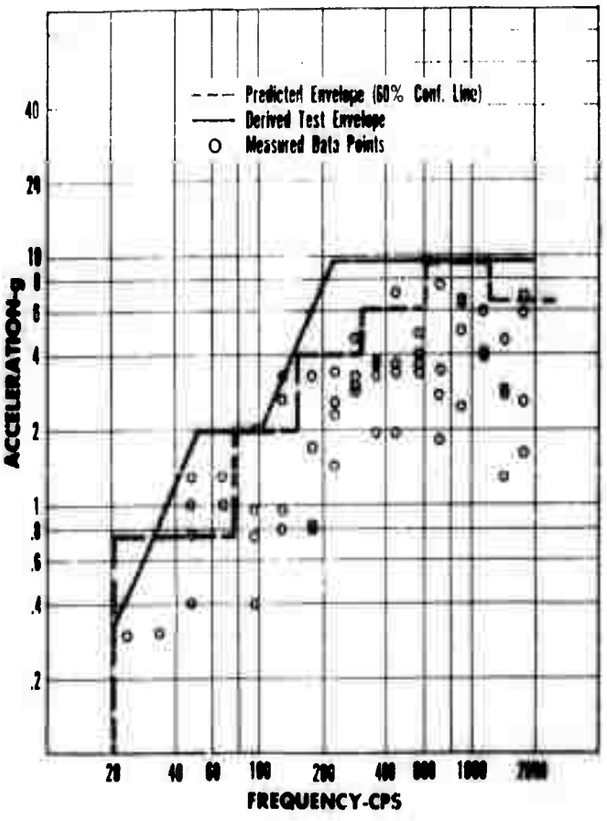

Fig. 19 - Comparison of predicted envelope and derived test envelope with measured vibration data for Zone 14

test range curves for these areas with a good degree of confidence.

EARLY DESIGN USES

While the data shown were collected from the B-58 airplane, these empirical curves have been used to predict vibration levels for other vehicles where both jet engine noise and vibration data are available. The predicted vibration levels for the different frequency octave bands fit the measured data with about the same degree of accuracy as they do the B-58 data. Therefore, by choosing a suitable risk level (upper confidence line), the curves presented in Figs. 10 through 15 may be used with reasonable success on other jet powered vehicles. Furthermore, when used with estimates of the external surface acoustic noise levels on new designs, these curves will provide a good first estimate of the vibration environment and may be used to specify vibration qualification tests in the early procurement specifications.

While the prediction curves presented are in terms of peak acceleration readings, the same correlation procedure may be used with true root-mean-square or average values read from a particular frequency band. By experimentation it was determined that the peak acceleration values read from Figs. 10 through 15 are about 3.3 times the true root-mean-square values. Thus the prediction values from these figures can be converted to rms values by dividing by 3.3 if desired.

DISCUSSION

Mr. Barber (Chance-Vought Aircraft): I have three questions, Bill. Has Convair been able to determine what proportion of the vibration environment is due to structureborne vibration and what proportion is due to airborne noise input?

Mr. Mahaffey: No, we haven't, Walt. We have not attempted to try to separate these two. By basing your data on actual measurements in the structure you get both, so that I think that the combination is represented in the data.

Mr. Barber: Has a separate correlation of sound and vibration been made for the B-58 flying supersonically? If so, has this correlation agreed with those obtained from the ground run-out and taxiing you presented here? This would give you some better idea of what proportion was coming from sound and what was coming from vibration.

Mr. Mahaffey: We have made an inflight vibration survey, and the levels are considerably lower than they are on the ground. We do not have a measurement of external noise levels in flight. We tried to measure some at about three different locations, but we were unsuccessful, as I guess a lot of other people have been in this respect. So that there is no way that we can correlate inflight noise level with inflight vibration data.

Mr. Barber: I was wondering whether you had the opportunity to attempt to estimate inflight vibration levels on the basis of estimated aerodynamic noise levels.

Mr. Mahaffey: We are working on this, and we have a method for predicting inflight noise level patterns of these sorts. Naturally you'd think that if you could do this in flight you could also predict inflight vibration levels. But we do not have any experimental data to be able to tell whether our inflight noise predictions are any good or not. That's where we stand on that.

Dr. Vigness (NRL): I am glad you gave the coefficient which related the peak value that you obtained to the rms value. That might be more useful to some of the rest of us. I would be interested in knowing how you happened to pick such a number as a peak value for a rather nonsinusoidal condition of vibration, and I certainly would expect you to get a very wide range of measurements when the peak value is measured for this type of vibration. Could you give any information as to why you picked that?

Mr. Mahaffey: We didn't exactly pick it. That's the way it came out. Actually we set up this data reduction system some several years ago before we hit upon this scheme of reducing the data, and we set up our peak detection system to detect peaks which would occur about one percent of the time.

Dr. Vigness: I think that's the answer. Thank you very much.

Mr. Brown (Douglas Aircraft): Would it be permissible to ask whether a great deal of variation, let's say in the range of about 10 to 1 that you get in your readings, is due to the measurement technique rather than the data itself because of this peak measurement technique?

Mr. Mahaffey: I'm not sure that I understood your question. Were you asking could the large amount of scatter in the data be due to the peak method of measurement?

Mr. Brown: Right. In other words, let's say if you did this by the power spectral approach would this give you less variation in the measurements?

Mr. Mahaffey: Of course one can never be entirely sure of his data system. All I can say is that we did everything in our means to check out the data system, including running out records from the tape on oscillograph and reducing it by hand to be sure that the data system was reading the right numbers. However, I don't believe that the large amount of scatter is due to the data system. I think that the large amount of scatter is inherent in the process. You remember that these were readings taken all over the airplane at a number of different locations, and each location is going to be different. So that what we are trying to get at is the most probable vibration level.

Mr. Karnesky (Aero-Jet General): Do you think perhaps your scatter is due to the fact that you are measuring vibration of different types of structures at different points? You wouldn't expect the launcher arm, for example, to have the same response to an acoustical environment as a frame. Did you try to break your data down as to the typical type of structure, either frame, launcher arm, size of frames perhaps?

Mr. Mahaffey: No, we didn't, Al. It's quite probable that there is some of that in this data. But if you start trying to break it down in terms of the particular type of structure then you will complicate the situation in trying to lay out vibration zones. Now I won't say this can't be done, and maybe it is a valuable extension to this technique, but we have not tried to do that.

Mr. Koppamaki (Lockheed, Sunnyvale): I have a comment concerning the last figures you presented on amplitude versus frequency. The presented statistics show an increasing trend in amplitudes up to the 2-kc limit of the graph. How about higher up? The usual excuse for stopping at 2-kc amplitude (when the telemeter channel used is not the limiting factor) is that information of vibration amplitudes above this level can be omitted because there is no equipment available to perform component testing at higher frequencies. Such excuse, however, cannot be readily justified. Information on amplitudes of higher frequency bands should be solicited (whenever within reach) in order to find out whether or not simulation techniques in component testing have to be extended to cover higher frequency bands than possible without modification with the gear presently in use. The shown increasing trend of vibration amplitudes in higher frequencies would definitely justify extension of the measurements beyond the 2-kc limit of the presented data.

Mr. Mahaffey: Actually the highest acceleration values in the data I presented occur in the 600- to 1200-cps range and the acceleration has begun to drop off as we approach 2 kc. There may be significant vibration above 2 kc. On the other hand, the signal from the transducer may be mainly electrical noise. It is very difficult to tell from a practical standpoint. While I cannot really disagree with you that we should try to measure and test for the entire range of vibration present, there comes a point in laboratory simulation where we are kidding ourselves on the significance of the test. Sometimes I wonder if we are not kidding ourselves when we try to test above 1 kc, particularly on the larger pieces of equipment.

* * *

THE INFLUENCE OF MASS AND DAMPING ON THE RESPONSE OF EQUIPMENT TO SHOCK AND VIBRATION

Ralph E. Blake and Torsten Ringstrom
Lockheed Missiles and Space Division
Sunnyvale, Calif.

Much present practice in designing for shock and vibration environments is highly conservative because impedance effects have largely been neglected. Theoretical results are reported on the amount of reduction to be expected from such effects and the way in which mass, natural frequency, and damping will influence design stress.

INTRODUCTION

In earlier papers, it was shown (1,2,3) that equipment can be very much overstrength when our present procedures for designing and testing for shock and vibration are used. The reason for the present conservatism is that shock and vibration measurements made in the past must be extrapolated to apply to equipments not yet in use. An envelope of available data, usually in the form of a frequency spectrum, is used to define a test or design input motion of the equipment mounting points. Contrary to the assumption that is usually made, the reaction of the equipment against its foundation can produce significant reductions in the severity of the motion of its foundation.

However, a reduction in equipment strength cannot be made safely until it can be shown how much reduction in severity can be guaranteed in each instance. It is necessary to obtain better understanding of the factors which influence the dynamic loads in equipment. As a step in this direction, some theoretical results are reported which show the manner in which a simple model of an equipment can affect the shock and vibration which it feels when mounted on a simple model of a vehicle.

Of course, our real interest is in the behavior of complex systems but it has not yet been found possible to reduce the complex mathematical expressions to a form which can be "understood." Since a simple system obeys a simplified form of the equation for a complex system, one can hope to find useful clues in the behavior of the simple model.

NORMAL MODE EQUATION

The equation expressing the acceleration $\ddot{x}$ of a mass of an equipment as it responds to an arbitrary force $F(t)$ on the vehicle is (4)

$$\ddot{x} = \sum_n T_n R_n(t) . \qquad (1)$$

There is one term of this series for each normal mode of vibration of the equipment-vehicle system. The factor $R_n(t)$ is known as the dynamic response factor or Duhamel's integral. It is a function of time t determined by the applied force and the natural frequency of the mode. It is the factor which depends upon whether the excitation is a transient pulse, a sinusoidal force, a random force, etc.; but it will not be discussed further. The other factor T_n, the "Mode Transmission Factor," is determined entirely by

the properties of the system, and is independent of $F(t)$. The question under investigation here is the effect of the distribution of mass and stiffness in the equipment and vehicle on the values of T_n. The factors T_n apply regardless of the form of $F(t)$; that is, they affect the response to any shock, sinusoidal vibration, or random vibration.

The factor T_n is expressed in terms of the normal mode amplitudes φ_n of the Nth mode by

$$T_n = \frac{\varphi_{ni}\,\varphi_{nf}}{\sum_j m_j\,\varphi_{nj}^2}, \qquad (2)$$

where φ_{ni}, φ_{nf}, and φ_{nj} are the normal mode amplitudes at the point of measurement of $\ddot{x}$, the point of application of force, and the j^{th} mass of the system, m_j, respectively.

A SIMPLE MODEL

The system that was studied is shown in Fig. 1; it is about the simplest system that could be expected to show the desired effects. The equipment is represented by a mass supported by a spring and damper; the vehicle is represented by two masses connected together by a spring and damper. To simplify the analysis the ratio of damping coefficient to spring coefficient for both spring-damper pairs is assumed to be the same. This assumption of "uniform damping" makes the mode shape and T_n independent of the amount of damping.

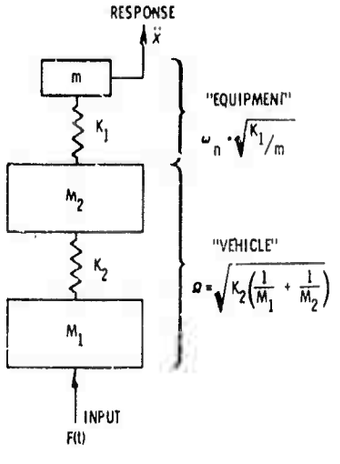

Fig. 1 - A simplified equipment-vehicle system

The parameters used to define the system are ω_n, the natural frequency which the equipment would have if it were attached to an infinite mass; Ω, the natural frequency of the vehicle by itself, and the mass ratios m/M_1 and M_2/M_1. The damping, expressed either by ζ, the percent of critical damping or $Q(= 1/2\zeta)$, the resonant amplification factor, will not be considered yet.

The combined system will have two natural frequencies associated with two modes of vibration; hence there are two Mode Transmission Factors, T_1 and T_2. Values of T_1 and T_2 have been computed as a function of ω_n/Ω, m/M_1, and M_1/M_2. A dimensionless plot of M_2T_1 and M_2T_2 vs. ω_n/Ω are shown in Fig. 2 for the case $M_1 = M_2$ and several values of m/M_2. The following features of Fig. 2 are considered to be significant:

1. The largest response in both modes occurs when ω_n is about equal to Ω.

2. The transmission is reduced as the equipment mass is increased.

3. The largest values of T_1 and T_2 are nearly equal but of opposite sign.

Since the largest loads are developed when the equipment is "tuned" to the vehicle natural frequency, all further studies were for the case $\omega_n = \Omega$ and $M_1 = M_2$.

The equation for the two natural frequencies of vibration of modes is

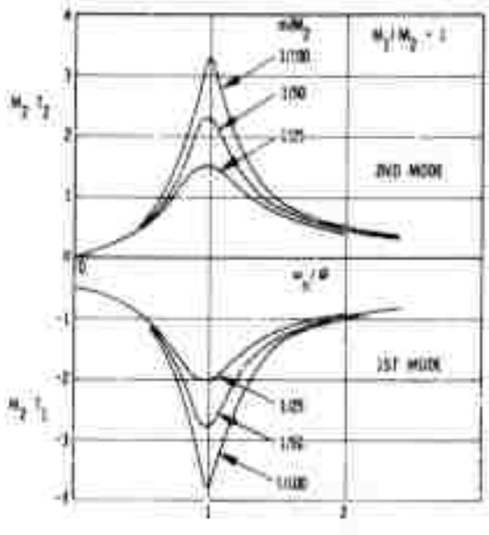

Fig. 2 - Model transmission factors for three-mass system

$$\omega_{1,2}^2 = \frac{\Omega^2 + \omega_n^2\left(1 + \frac{m}{M}\right)}{2} \pm \sqrt{\left(\frac{\Omega^2 + \omega_n^2\left(1 + \frac{m}{M}\right)}{2}\right)^2 - \Omega^2\omega_n^2\left(1 + \frac{m}{2M}\right)}. \quad (3)$$

The difference between the two natural frequencies is

$$\omega_1 - \omega_2 = \left[\frac{\left(\Omega^2 + \omega_n^2\left(1 + \frac{m}{M}\right)\right)^2 - 4\Omega^2\omega_n^2\left(1 + \frac{m}{2M}\right)}{\Omega^2 + \omega_n^2\left(1 + \frac{m}{M}\right) + 2\Omega\omega_n\sqrt{2 + \frac{m}{M}}}\right]^{1/2}. \quad (4)$$

Examination of these equations shows that the difference in frequency becomes smaller if $\omega_n \to \Omega$ and as m becomes smaller.

As a result of the small difference in the two natural frequencies and the nearly equal but opposite values of T_1 and T_2, the acceleration of m which will result from an impulsive force I is almost a perfect example of vibration beats. The acceleration is

$$\ddot{x} = \frac{I\Omega}{2\sqrt{2Mm}}\, e^{-\zeta\Omega t}(\sin\omega_1 t - \sin\omega_2 t), \quad (5)$$

if $\omega_n = \Omega$, $M_1 = M_2$ and $m \ll M_1$.

An example of equipment response to an impulse is sketched in Fig. 3. The oscillations of the two modes cancel each other out initially, then reinforce each other later. The lower curve shows the corresponding acceleration of the foundation mass M_2; this also shows beats at the same rate but the amplitude is large when the equipment amplitude is small, and vice versa. The appearance is that the impulse sets up an oscillation

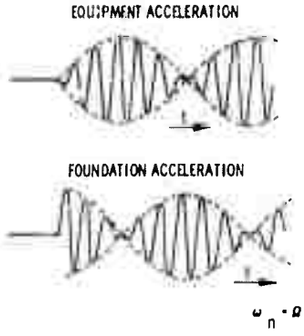

Fig. 3 - Response of tuned system to impulse

of the vehicle as if the equipment were not there. The equipment responds to this oscillation with a resonant buildup of amplitude. Since this buildup drains energy out of the vehicle, the amplitude of the equipment reaches a maximum when the vehicle oscillation is stopped.

This picture of the phenomenon led to the question of how much of the total energy gets into strain energy of the equipment spring. It was found that the total energy transferred to the system by the impulse can be expressed as the sum of the kinetic energy of rigid body translation of the system plus an oscillatory energy. If the energy in the equipment spring were equal to the energy input minus the rigid body energy, the acceleration of the equipment would be

$$\ddot{x} = \frac{I\Omega}{\sqrt{2M_1 m}} \quad (6)$$

assuming $m \ll M_1$ and no damping. Thus the effect of tuning is to allow all of the oscillatory energy to find its way into the equipment spring.

But this energy builds up to a maximum by increments on each cycle, so that one could expect damping to reduce the maximum acceleration considerably. By finding the time at which the envelope of Eq. (5) reaches a peak and by using Eq. (3) the peak acceleration was calculated to be

$$\ddot{x}_{max} = \frac{\left(\frac{I\Omega}{2M_1}\right)}{\sqrt{4\zeta^2 + \frac{m}{2M_1}}}\, e^{-2\zeta\sqrt{\frac{2M_1}{m}}\cot^{-1}2\zeta\sqrt{\frac{2M_1}{m}}}. \quad (7)$$

This is plotted on Fig. 4, showing that for small damping an increase in equipment mass produces considerable reduction in acceleration; or for small equipment mass an increase in damping is very beneficial. But if one of these factors is already fairly large, the other is not very important. With zero damping the acceleration varies inversely with $\sqrt{m}$.

If one knows the response of a system to an impulse, he can find the response to other inputs. The response to a step force F is derived easily; it is the same as Fig. 4 if F is substituted for $I\Omega$.

The response to a random white-noise force is of interest to those in the missile industry. The root-mean-square acceleration

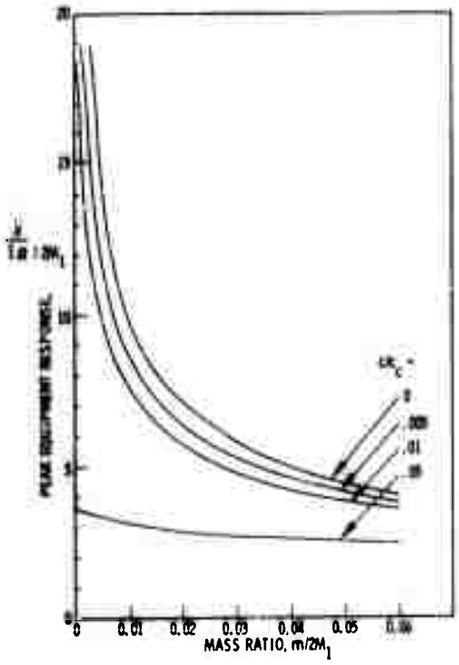

Fig. 4 - Effect of mass and damping on tuned equipment

of this system was calculated by D. A. Aspinwall at Lockheed to be

$$\ddot{x}_{rms} = \frac{\sqrt{\frac{\pi}{2}\,\frac{\Omega}{2\zeta}\,\frac{\Phi}{4M_1^2}}}{\sqrt{2\left(4\zeta^2 + \frac{m}{2M_1}\right)}}, \qquad (8)$$

where Φ is the spectral density of force. The expression in the numerator is the rms acceleration of the foundation when the equipment is not in place. Again it is seen that an increase in either mass or damping will decrease the equipment acceleration.

RECIPROCITY OF MODE TRANSMISSION FACTORS

In Eq. (2) the factor T_n contains the product of mode amplitudes at the point of acceleration measurement and at the point of force application. It is evident that the factor will remain the same if the points are interchanged. Thus we should expect large response throughout a heavy vehicle if the force is applied to a lightweight tuned mass-spring system.

APPLICATION TO PRACTICAL PROBLEMS

It has not yet been proved mathematically that the phenomena and curves for this simple model can be applied to more complex systems. It is hoped that some judicious combination of the theorems in Refs. 2 and 5 might be made to provide a sound basis for working with complex systems. In the meantime these results can be regarded as possibly useful clues to understanding the systems with which we work.

Some examples in our recent work tend to show some of the effects just described. In one case, a computer was used to compute the normal modes of a 20-mass system with and without a mass-spring "equipment" tuned to one of the vehicle modes. The peak acceleration of the equipment for a step-force input corresponded quite well with the energy of the vehicle mode flowing into the equipment spring.

In a Lockheed rocket it was observed that a certain mode of the structure responded very strongly to random forces in flight. In another missile this response was mysteriously missing. It is now suspected that the region of force input of the first missile involved a local structure tuned to the frequency of the missile mode.

As a final example, it seems significant that the largest oscillations seen on shock and vibration records are very often characterized by beats. Although a vehicle may have a large number of modes in the frequency range of a recording instrument, very few of these are prominent on a given record. Only a few satisfy the conditions for good transmission and these often show the beat effect found to accompany good transmission in the simple model.

REFERENCES

1. R. E. Blake, "The Need to Control the Output Impedance of Shock and Vibration Machines," Shock and Vibration Bulletin No. 23, Office of Secretary of Defense, June 1956, pp. 59-64.

2. R. E. Blake and R. O. Belsheim, "The Significance of Impedance in Shock and Vibration," ASME Colloquium on Mechanical Impedance Methods, ASME, 1958.

3. G. J. O'Hara, "Shock Spectra and Design Shock Spectra," U.S. Naval Research Laboratory Report 5386, Nov. 1959.

4. W. T. Thomson, "Mechanical Vibrations," Prentice-Hall, New York, 1953.

5. R. H. MacNeal, "Vibrations of Composite Systems," Cal. Inst. of Tech. Report No. 4 for ARDC, Oct. 1954. (ASTIA AD No. 63118.)

* * *

ON THE PREDICTION OF DYNAMIC ENVIRONMENTS

R. W. Mustain
Northrop Corporation, Norair Division
Hawthorne, California

Estimates of jet engine noise, rocket engine noise, and boundary-layer noise have been computed and are presented. Actual field data are compared with predictions, and predicted vibration response is also discussed. Field data of vibration levels created by acoustic inputs are presented. Predictions for a hypothetical rocket of 2×10^6-pound thrust are also presented.

INTRODUCTION

What is the basic dynamic environmental problem on aircraft and missiles? When and where did this environmental difficulty originate?

In order to answer these fundamental questions, the reader must return to the beginning of the Air Age on December 17, 1903. On that historic date the Wright brothers piloted the world's first flights in a motor-driven, heavier-than-air plane and thus ushered in the era of flight with its transports, fighters, bombers, helicopers, missiles, satellites, glide-bombers, etc. Then it was that man first successfully faced the basic dynamic problem of building an optimum strength/weight airframe with the required equipment capable of enduring the specific dynamic environment. In contradistinction to the mighty and complex weapon systems of this modern period, the Kitty Hawk biplane with its 12-horsepower motor presents but a whisper of dynamic excitation. Yet, the task accomplished by the Wright brothers in constructing a suitable frame for that small motor with its relatively minor excitations compares well with the gigantic tasks confronted by the dynamic engineers of today.

It is safe to assume that Orville and Wilbur Wright knew practically nothing of such sophisticated terms as power spectral density, spatial correlation, randomness, stochastic processes, stationary processes, power transfer functions, autocorrelation function, ensemble, etc. However, sophisticated as these terms appear to the layman, the foundation, the framework, and the building blocks for present day dynamic formulations had been established already by men like Newton, Gauss, Rayleigh, Strouhal, etc. For example, Karl Friedrich Gauss had made valuable mathematical contributions in the early part of the 19th Century that are recognized today in any concept of normality and randomness. In 1877 Lord Rayleigh provided an early foundation for modern theories on stochastic (random) methods. In The Theory of Sound, he discussed vibrations with "phase accidentally determined" and formulated the circular distribution that describes the amplitude r, or envelope of random vibrations. The Rayleigh distribution shows the probability of a resultant amplitude occurring between r and r + dr when a large number, n, of unit vibrations are compounded at random. This is how the probability was given originally by Rayleigh

$$\frac{2}{n\alpha^2} \exp \frac{-r^2}{n\alpha^2} r\, dr \ . \qquad (1)$$

For power spectra mathematics this probability can be expressed in the modern form

$$P(r)\, dr = \frac{r\, dr}{\sigma^2} \exp \frac{-r^2}{2\sigma^2} . \qquad (2)$$

(See References 1 and 2.)

It is interesting to point out that Strouhal had predicted Strouhal values, fD/V, in 1878 that may be considered reasonably accurate at this date. His calculations displayed a maximum Strouhal number of 0.2 for a Reynolds number of 2000.

This brief discussion has been inserted for the purpose of inference. Imagine that the founders of aviation, Orville and Wilbur Wright, had advanced to a technical state wherein acoustical and vibration analyses were deemed beneficial. Then, it can be inferred that the essential technical ingredients were available for development under a desired and guided impetus. This impetus has gradually evolved during the past decades and has gained stature concomitantly with each advance in propulsion, airframe, and airborne equipment. The transition from one type of propulsion system to newer and more powerful units has resulted in greater velocities, flights to higher altitudes, equipment complexities, and more severe dynamic environments. Throughout this continuous advancement of power and velocity performance with its concurrent additional dynamic penalty, the basic dynamic environmental problem has remained the same.

The trend to greater power plants has accompanied the tremendous expansion of the aviation industry through two World Wars, the Korean War, and one major depression. World War I provided the first real encouragement in this rapid development as the airplane began to revolutionize warfare. Then, in the twenties and thirties, the advent of in-line engines and powerful radial engines created noticeable vibration problems and minor acoustic enigmas. With the second World War the airplane came into its own as a mighty weapon of attack and destruction. During the accelerated developments of World War II, manned aircraft became complex systems with powerful engines capable of inducing relatively large vibrations in relation to previous environments. Furthermore, development of delicate airborne electronics for controls and guidance created components with low-fragility levels. A major transition in aircraft engines occurred near the end of World War II when the first jet-propelled aircraft appeared (the P-59 and the P-80) to present a new dynamic environment containing troublesome acoustic excitations. In due time the dynamic engineers became acquainted with the many pitfalls of the jet engines and their attendant vibrations and their random-type forces that cause equipment and structural failures.

Then, before the jet dynamic problem could be conquered, the next type of propulsion system entered the scene. The last decade has seen the space age become a reality with its multistage vehicles and its thunderous rocket engines producing thrusts in the hundreds of thousands of pounds and even threatening to enter the million-pound class. Phasing into the high-thrust rocket systems created severe shock, vibration, and acoustic environments. Although, the previous engines had provided some dynamic difficulties, these difficulties were magnified by several degrees in the missile and space programs. The dynamic environment has accounted for numerous incomplete missile missions attributed to equipment and structural failures.

The many recent equipment and structural failures on aircraft and missiles have enhanced the value of predicting dynamic environments. Solution of the basic dynamic problem requires: (1) an adequate definition of the dynamic environment, (2) the determination of fragility levels, and (3) the design of equipment and structures so that their fragility levels exceed the dynamic environmental levels. There is a fundamental requirement for a reasonable definition of the dynamic environment during early design stages in aircraft and missile programs. Experience has shown that lack of awareness of these dynamic excitations and their damaging responses has resulted in mission failures, numerous design changes, and manufacturing delays. On the other hand, a sensible consideration of the expected vibration and acoustic forces will result in improved performance and greater reliability of aircraft and missiles.

Several methods of predicting dynamic environments have been formulated by individuals and organizations within the dynamics

field. Some of these prediction techniques have been studied and investigated. Perhaps the most important acoustic predictions are those that provide estimates of acoustic levels generated by: (1) jet engines, (2) rocket engines, and (3) boundary layers. Example predictions which use some of the investigated methodologies are given in this paper. Actual calculations of acoustic levels for jet engines, rockets, and aerodynamic propagations are listed in the Appendices.

Acoustical predictions for a hypothetical rocket engine with a thrust of 2×10^6 pounds have been made. Assuming certain required data (i.e., weight flow, nozzle diameter, missile length, and trajectory), the following estimations were made and are included in this paper:

(1) Rocket exhaust noise spectrum,

(2) Sound pressure levels for the various stations,

(3) Boundary-layer noise levels.

JET ENGINE NOISE

Soon after the appearance of jet engines it became apparent that the high-intensity noise levels generated by the jet exhaust flow were not only troublesome to personnel, but were so intense that they contributed to equipment and structural failures. This sonic fatigue problem hastened the analyses and measurement of jet engine noise. So that in the intervening years there has accumulated a vast amount of valuable literature and data on jet noise. The jet phenomena have been well described and defined during the past decade. This has resulted in the formulation and verification of several prediction and estimation procedures. Fortunately, these predictions have been primarily based on and confirmed by the wealth of available empirical data (3,4,5). For this reason, this paper will practically circumvent the jet engine noise problem. However, a brief review of some salient points will be presented with a sample prediction and a few empirical data points.

The noise produced by the jets is primarily aerodynamic noise that is generated by the turbulent mixing which occurs at the boundary of the jet stream. In general, most prediction methods and analytical solutions have neglected the least understood and perhaps, negligible effects of other minor noise sources found in jet engines. It is entirely possible that, depending on the engine configuration, sources such as compressor whine, combustion noise, duct noise, combustion instabilities, engine resonances, etc., may radiate considerable acoustic energy and in some individual cases might even cause structural and equipment failures. For example, the high fluctuating pressures developed within jet engine inlet ducts have created sonic-fatigue failures. These failures are a function of several possible sources. To exemplify, they may result from forces caused by (1) compressor noise radiated forward, (2) boundary-layer noise within the duct or (3) radial, sloshing, or longitudinal modes within the duct. The absence of these and similar functions from acoustic predictions may yield unconservative answers.

Whereas the aerodynamic noise created aft of the jet exit has been the principle factor in most jet engine considerations, some aspects of this forcing function will be reviewed. Beginning at the plane of nozzle there exists a central core or cone wherein the flow is approximately sonic and wherein there is little or no turbulence. Surrounding this potential cone is an annular mixing region that runs downstream from the orifice to the end of the cone. At this point (approximately 5 diameters downstream) the cone has vanished and has been replaced by the turbulent front which now reaches the jet axis. The shear differential between the jet efflux and the ambient atmosphere generates a turbulent boundary layer commencing in the annular region and spreading downstream. These eddies travel almost with the speed of the jet flow. It has been found that the angle of spread of the jet boundaries is between 7.5 degrees to 10 degrees for subsonic jets (6). Certain investigations have indicated that the maximum noise is generated near the tip of the jet core (7). Analytical results by Powell (8) imply that most of the noise power is generated at constant rate along the jet from exit to the end of the cone. Ribner (9) found that this power is constant with X (distance from the nozzle) in the initial mixing region (X^0 law), then farther downstream (about 8 to 10 diameters) it falls off extremely fast (X^{-7} law or faster) in the fully developed jet. Studies of these turbulent flows show that as the boundary layer is thin in the annular region adjacent to the jet exit, high-frequency excitations will be generated near the nozzle. In like manner, the larger eddies produce low-frequency excitations downstream.

Quadrupole sources were considered as the principal noise generators in a fluctuating flow by Lighthill (10,11) when he derived the parameter for acoustic power. Lighthill's parameter or the $V^8 D^2$ law is

$$P \sim \frac{D^2 V^8 \rho_1^2}{\rho_2 a^5}, \qquad (3)$$

where

P is the total acoustic power,

ρ_1 is the jet density,

D is the nozzle diameter,

V is the jet velocity,

ρ_2 is the density of the atmosphere,

a is the atmospheric speed of sound.

The $V^8 D^2$ term is characteristic of jet noise power which appears to be generated by a mixture of lateral and longitudinal quadrupoles (8).

Estimations of jet acoustic power may be made when certain engine parameters are known. By using the required engine data, (1) the acoustic power, (2) the sound power level, and (3) the sound pressure levels at various locations were estimated for the T-38 airplane. The calculations are given in Addendum A which accompanies this paper. The estimated sound pressure levels for 50-foot, 100-foot, and 250-foot radii are displayed in the polar plot of Fig. 1. Measurements for the 50-foot radius on two T-38 airplanes have been included for comparative purposes. It can be observed that the field values are higher than the predictions near the nose of the aircraft. A possible explanation for this difference is that the estimation reflected only the noise generated by the turbulent exhaust jet. That is, the calculations did not consider individual aircraft variables such as engine and duct design. As a matter of fact it was later found that the duct design induced high-pressure fluctuations.

THE MISSILE ENVIRONMENT

A primary design consideration for any rocket-boosted vehicle is the effect of acoustic and vibration excitations on the vehicle structure and on delicate airborne equipment. Naturally, these dynamic forcing functions display magnitudes in agreement with spatial

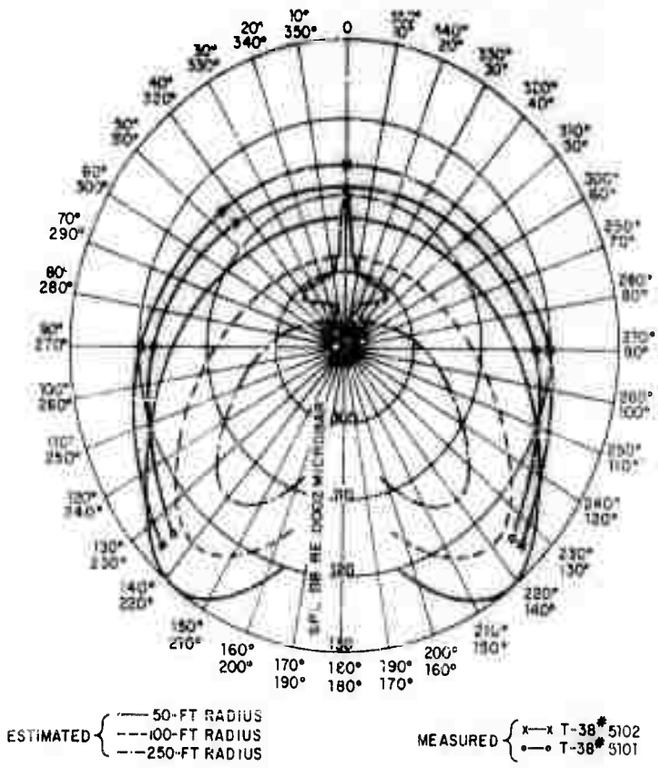

Fig. 1 - Estimated vs measured engine noise levels for a T-38. Overall sound-pressure level as a function of angular position from exhaust jets during military power operation (100 percent rpm without after burner).

patterns and are variant also with time and the mission profile. The following list of forcing functions presents some of the vibro-acoustic sources that must be considered, predicted, measured, and analyzed during the course of any missile program.

1. Acoustic Source

   a. Aerodynamic noise
   b. Rocket noise
   c. Auxiliary equipment
   d. Secondary acoustic source
   e. Interaction of shock wave and boundary layer

2. Vibration Sources

   a. Main power-plant oscillations
   b. Auxiliary equipment
   c. Aerodynamic gusts
   d. Separation of stages
   e. Coning vibrations
   f. Guidance-system reactions
   g. Spin-rocket excitations.

It can be expected that the space vehicle will experience the most severe dynamic environment during the launch phase. There can be no doubt, but that the sound field of the rocket engine is the most important source of vibration and that aerodynamic noise ranks second in source severity. An example of high-intensity noise levels from solid-propellant rocket bottles is displayed in Fig. 2. This field diagram depicts external sound pressure levels as a function of fuselage station and frequency for a typical firing at Cape Canaveral on the SM-62 Snark missile. The high peak in the background of this three-dimensional plot displays a sound-pressure level of 190 db overall. These measurements were obtained by external microphones mounted so that the microphone buttons were flush with the outer skin of the missile. Numerous instrumented launches and firings were conducted on the Snark missile that verified the field data of Fig. 2 (12). Although the Snark missile has been operational for many years, is launched in a horizontal angle, and is not supersonic, it is felt advantageous to exhibit and discuss these high levels. The astonishing fact is that the acoustic levels surrounding the dependable SM-62 missile are more severe than those upon any present day missile and missiles in the near future. The reason for the higher levels on the Snark missile is the configuration of the rocket-bottle installation which places the exhaust nozzles at fuselage station 647 and consequently, the aft missile structure receives the direct blast of the 260,000 pounds of thrust and excitation. Perhaps, it will be some time before any vertically-launched missile is exposed to intensities as great as those found within and external to the SM-62 missile. Furthermore, the environmental conditions presented by the Snark launches provided the stimulus for Norair engineers to select optimum designs and to conduct meaningful qualification tests. The results of this stimulus were the design and manufacture, on a production scale, of delicate airborne equipment capable of withstanding extreme acoustic environments that will not be exceeded for some time in the future. This is exemplified by the predictions in this paper which show the levels for a hypothetical two-million-pound thrust vehicle to be less than those on the SM-62 missile.

Whereas a vast amount of vibration and acoustic data were compiled from Snark firings and launches, it was considered desirable to establish some type of correlation between vibration levels and acoustic levels. Some typical correlations of vibrations per acoustic levels vs frequency are given in Figs. 3, 4, and 5. Even though these graphs indicate the slopes for three different axes, there appears to be a reasonable agreement. These data provide an indication of expected vibration increments for acoustical inputs. Many factors such as structural configuration, structural damping, material damping, resonant frequencies, impedance of the structure, coincidence, ground plane effects, etc., enter into any correlation study. For this reason the specific case is not applicable to generalizations. It is suggested that the data of Figs. 3, 4, and 5 be applied in specific cases where, at least, the damping and frequencies are known. Another possibility is the usage of classical transmissibility curves scaled correspondingly to yield responses per the acoustic forcing functions. These solutions would be similar to single-degree-of-freedom solutions and would be based on the normal assumptions.

The vibrational environment at any point in a space vehicle is the complex product of external and internal exciting forces accompanied by the transmission of these forces through the vehicle to the point. During the launch phase of a missile, the tremendous noise generated by the rocket motors is transmitted through the atmosphere and reflected by the ground plane in a symmetrical pattern around the vertical missile. Since the rocket noise is essentially random or "white" in nature, it creates resonant

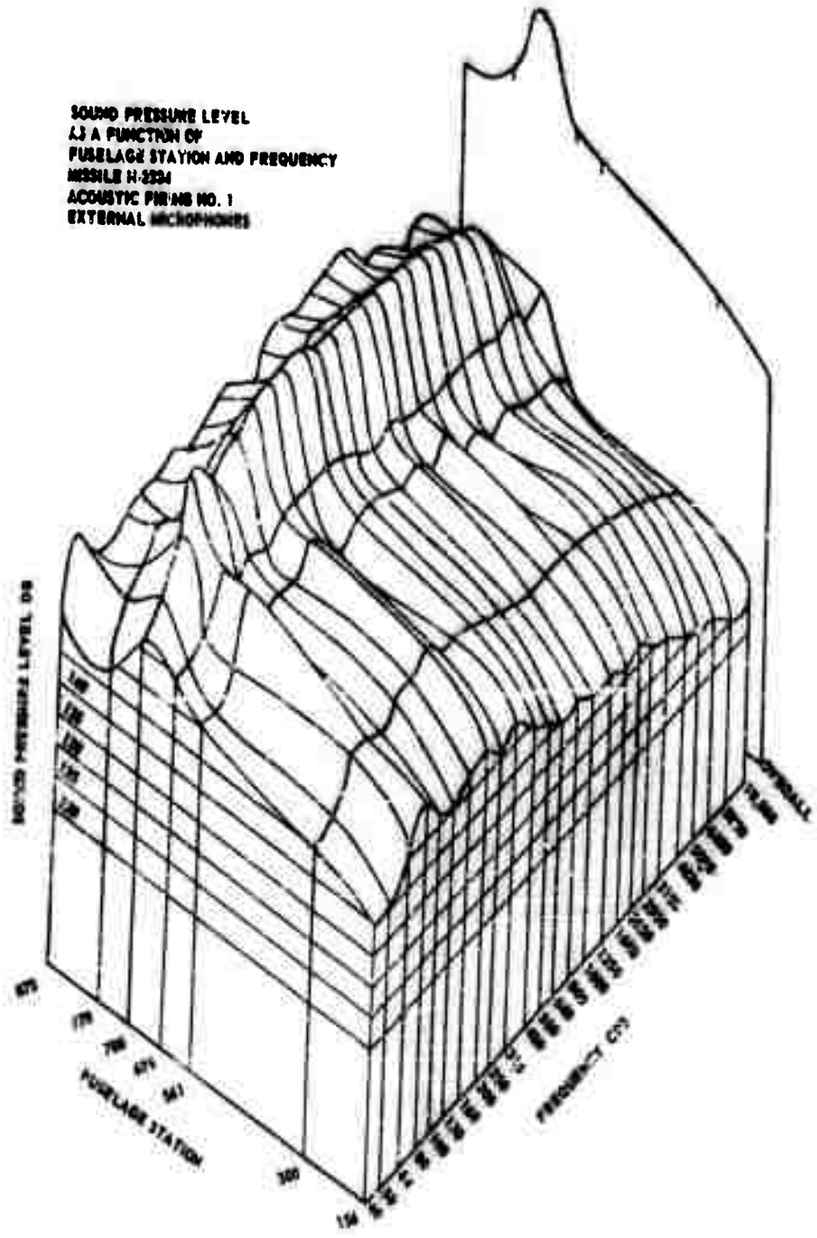

Fig. 2 - Sound-pressure level as a function of fuselage station and frequency. Missile N-3304, acoustic firing No. 1, external microphones

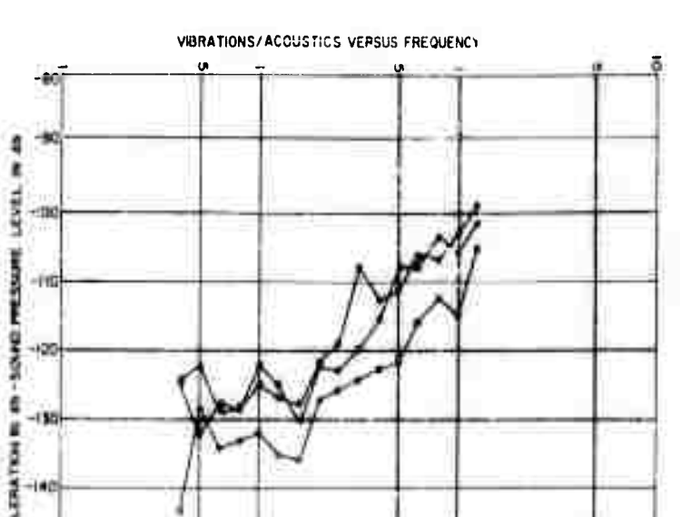

Fig. 3 - Vertical vibrational acceleration and acoustic pressure measurements on structure F.S. 561, SM-62 missile N-3304

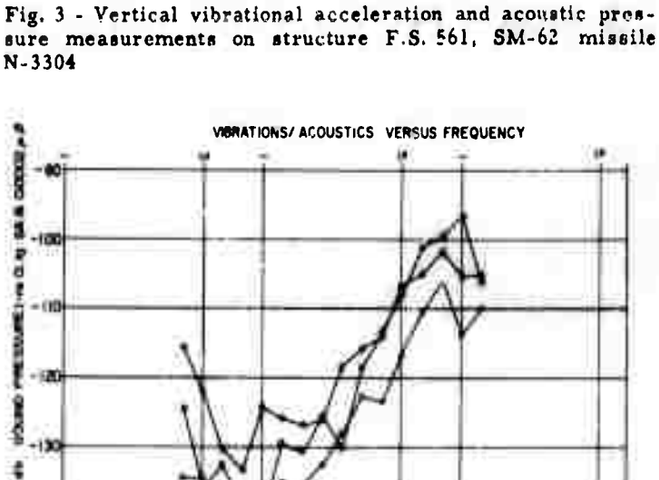

Fig. 4 - Longitudinal vibrational acceleration and acoustic pressure measurements on structure F.S. 561, SM-62 missile N-3304

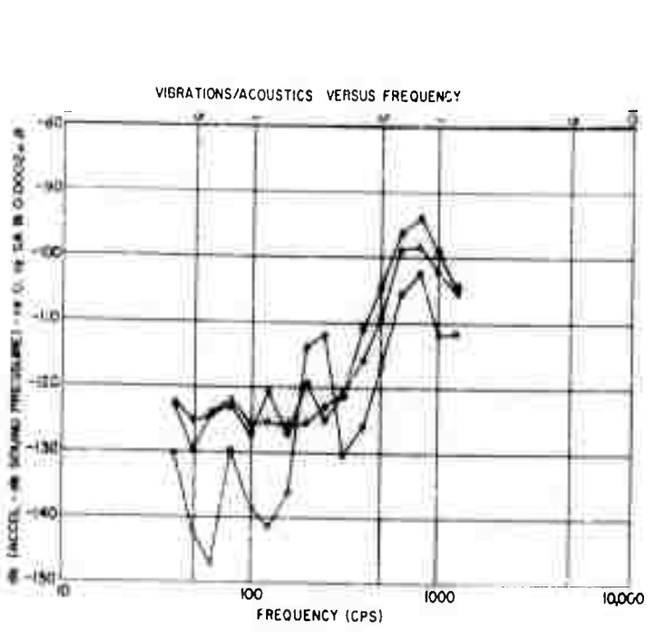

Fig. 5 - Lateral vibration acceleration and acoustic pressure measurements on structure F.S. 561, SM-62 missile N-3304

responses of skin panels and structures. The magnitude of this excitation depends upon the frequency spectrum, the amplitude, the space correlation of the noise, and the mechanical impedance of the structure. The resulting vibrational energy is transferred throughout the missile to substructure and equipment. Some of the panels act as secondary noise sources and radiate acoustic energy into the vehicle's compartments. In turn, some of these bays become semireverberant chambers to maintain fairly high acoustic levels.

The noise generated by a rocket motor results primarily from turbulence in the subsonic mixing portion of its jet stream. The amplitude and spectrum of this noise are dependent upon various jet-stream parameters, distance from the jet stream, and upon direction relative to the exhaust stream direction. The spectra can be treated mathematically in spectral density terminology. All data indicate that the rocket noise reaches a maximum during launch; its exact level depending somewhat on the launch pad configuration. Rocket noise reflected from the ground plane dominates the environment for the first 1 to 2 seconds of flight until the nozzles reach an altitude on the order of 50 nozzle diameters (7). By this time the missile is at an altitude wherein the rocket exhaust flow is unobstructed. Whereupon, at this point, the effect of forward vehicle motion reduces the noise environment surrounding the missile. As the missile velocity increases, rocket noise forward of the nozzle decreases approximately with the square of the missile's velocity until Mach 0.5 is reached, after which it decreases more rapidly, approaching zero at Mach one. This decrease in noise level with increased missile motion is shown in Fig. 6 (13). Some controversy exists over this relationship. Modifications of this effect can be found in Refs. (7) and (14). It is contended that the display in Fig. 6 provides realistic values.

The spectra and levels in the rocket's near field are dependent on additional factors which include shock-wave formation and stability, and the formation and stability of afterburning in the jet stream. The noise has, in general, a continuous random level spectrum, but may contain some discrete frequencies. Two different methods for predicting acoustic power levels are listed below for comparison. (Note – these are included in the Appendices.)

1. From Reference (15).

$$OA\ PWL = 78 + 13.5 \log_{10} W_m \quad \text{in db re } 10^{-13} \text{ watts,} \qquad (4)$$

where W_m = mechanical power of jetstream in watts,

$$W_m = 0.676\ tv = 0.676\ (t^2 g)/w,$$

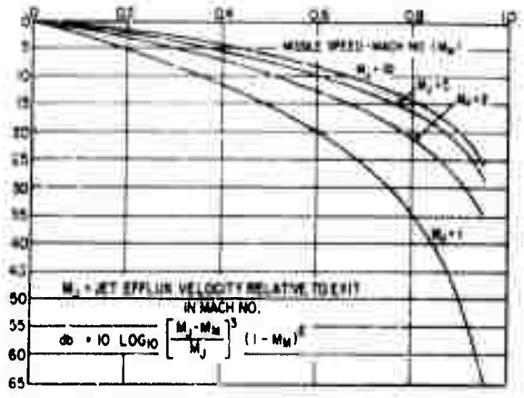

Fig. 6 - Effect of missile motion on exhaust noise. Mach number based on speed of sound in ambient atmosphere. From Journal Acoust. Soc. Am., Vol. 30, No. 11, November 1958.

with $v = (tg)/w$ = gas velocity at nozzle in feet per second,

t = thrust in pounds,

g = gravitational constant = 32.2 ft/sec^2,

w = weight flow in lb/sec,

then $PWL = 78 + 13.5 \log_{10} 0.676\ (t^2 g)/w$.

2. From Reference (16).

$$PWL = 10 \log_{10}\eta + 10 \log_{10} \frac{MV^2}{2 \times 10^{-13}} \quad (5)$$

where η = efficiency of conversion of mechanical power to acoustical power.

$$SPL = SPL_o - 20 \log R + 10 \log G^2,$$

where the reference sound pressure level SPL_o is given relative to the overall power level and is based on Strouhal numbers, fD/V.

SPL_o = PWL - Strouhal number factor.

In addition to the acoustic energy generated by the rocket-motor exhaust, vibratory forces from the rocket-motor casing are mechanically transmitted through the vehicle structure. This energy includes random forces resulting from thrust variation, combustion instability, etc., together with transient excitations during ignition. The internal vibratory energy resulting from the rocket can occur either in space or in the sensible atmosphere, whenever a rocket is used for propulsion or steering.

An important external source is the aerodynamic noise which results from turbulence in the boundary layer. Its magnitude and spectra appear to correlate with local flow parameters in a manner which allows mathematical spectral density treatment and reasonably accurate prediction, depending upon the aerodynamic prediction of flow conditions. Three different equations for predicting aerodynamic noise are presented below for comparison and for general interest:

1. Reference (17).

$$OA\ SPL = 20 \log Q/500 + 130\ db. \quad (6)$$

2. Reference (16).

$$OA\ SPL = 20 \log Q + 86\ db, \quad (7)$$

where SPL is the level of the overall pressure fluctuations at the surface and Q is the free stream dynamic pressure in lbs/sq ft.

3. Reference (7).

$$OA\ SPL = 82 + 20 \log Q. \quad (8)$$

THE HYPOTHETICAL VEHICLE

A research study was conducted to determine the acoustic environment surrounding a hypothetical missile powered by a two-million-pound-thrust engine. Acoustic predictions were made of (1) the noise generated

by the rocket-exhaust stream and (2) the noise generated by the boundary layer.

The trajectory shown in Fig. 7 plus the following basic design data were required for this investigation:

1. Thrust, 2 million pounds,
2. Weight flow, 2500 pounds per second,
3. Nozzle diameter, 25 feet,
4. Length, 301 feet.

The trajectory used in this study is assumed to be typical of a nuclear-powered rocket which uses liquid hydrogen as a propellant. The specific impulse (I_{sp}) associated with this trajectory is 900 seconds which is indicative of a high-performance rocket.

The trajectory is based on an initial tip-over at an altitude of 5000 feet with the end of tip-over occurring at an angle with the local horizontal of between 60 and 70 degrees. The burnout velocity is approximately 36,000 fps, which is about equal to the earth's escape velocity. A trajectory with an initial thrust to weight ratio of 1.5 was selected as being representative of a typical mission. The trajectory graph of Fig. 7 displays the dynamic pressure, the altitude, longitudinal acceleration, and velocity vs time for the hypothetical vehicle.

Prior to a detailed examination of the estimated acoustic levels for this mission, it appears appropriate to review briefly the major acoustical effects on a chronological pattern. As stated previously, the rocket-exhaust noise will manifest itself most severely before the vehicle rises a distance equivalent to approximately 50 exit nozzle diameters. The severity of this condition is caused by the deflection of the exhaust stream, the static condition of the vehicle, and the ground reflection. After the vehicle leaves the launch pad it begins to gain velocity and then the effect of missile motion (shown in Fig. 6) becomes apparent until, on approaching Mach one, the rocket noise disappears. On the other hand, as the vehicle moves with increased velocity through the atmosphere another sound source emerges—boundary-layer noise. Originally, the boundary-layer noise is masked during the launch phase by the intense rocket noise and is not propagated in any degree until the sonic speed range is reached. This propagation of noise in the boundary layer is a function of dynamic pressure (see Eqs. (6), (7), and (8)).

In line with the above time pattern of describing the dynamic environment of the missile, the first major consideration becomes the rocket-exhaust noise. The two-million-pound-thrust engine produces an overall sound power level somewhere in the range from 215 to 220 db overall (re 10^{-13} watts). For comparative purposes the overall sound power level was computed by both Eq. (4) and Eq. (5). The former equation provided a value of 220 db and the latter yielded a level of 215.4 db. Many of the calculations for this mission are listed in the Appendices. They have been provided for the convenience and perusal of the design engineer who desires to become familiar

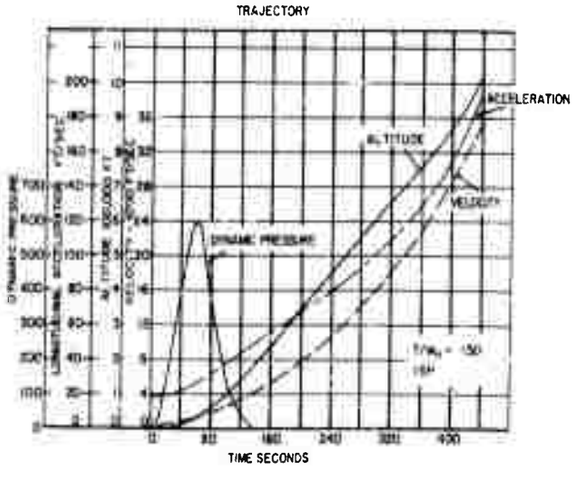

Fig. 7 - Trajectory for two-million-pound thrust missile study

with this methodology. The power level spectra for the rocket noise were computed also and are presented with the overall value from Eq. (4) in the graph of Fig. 8. These octave-band data show clearly that the greatest concentration of energy for this spectrum occurs in the low-frequency end. This peaking of energy in the low end of the spectrum is reasonable for such a large sized rocket. It must be pointed out that these low-frequency excitations can be injurious to delicate airborne equipment and structure and, in addition, are not easily dissipated.

Next, calculations were made of the sound-pressure levels surrounding seven spatial points on the huge 301-foot missile and these levels are presented graphically in Figs. 9, 10, 11, and 12. For the static firing, the assumption was made that a turning bucket was located 30 feet below the vehicle during the initial launch phase. Theoretically, this tends to increase the levels on the missile over free-field conditions. Thus, the sound-pressure levels on the structure are higher for the static firings than they are in flight. For the static firings the turning bucket geometry was included in the calculations to establish source distance for the calculations. These data are not given in this paper or its Appendices. Figure 9 portrays the static ground-firing noise spectra with the turning bucket for octave bands and 50-foot increments forward of the nozzle. The positive slope shown by the zero data points indicates that the high-frequency excitations are generated close to the exhaust nozzle while the low-frequency sources can be found further downstream of the nozzle. The three-dimensional spectrogram of Fig. 10 provides a visual view of sound-pressure levels as a

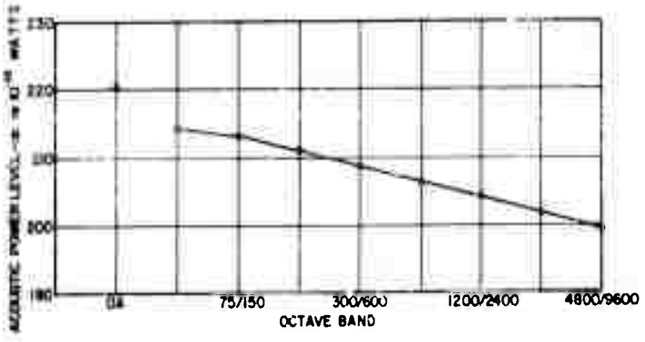

Fig. 8 - Two-million-pound thrust missile study, acoustic power level spectra of exhaust stream

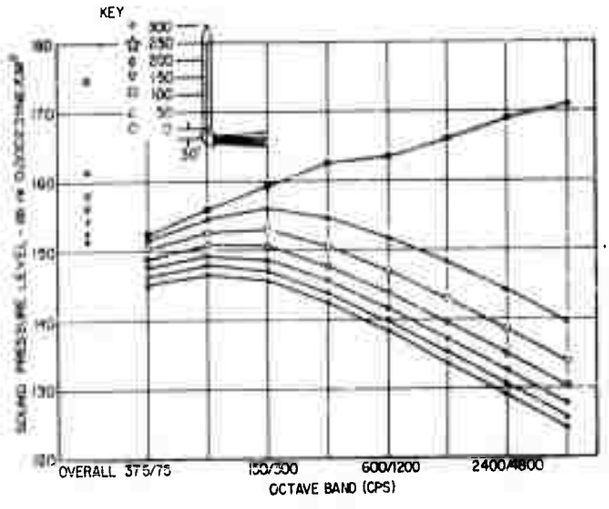

Fig. 9 - Static ground firing noise spectra for two-million-pound missile. Turning bucket 30 feet below vehicle

function of missile location and of octave bands. This three-dimensional plot provides an excellent indication of the spectrum distribution and shows the low-frequency excitations to be fairly constant in magnitude throughout the missile while the high frequencies peak up near the exhaust nozzle.

Slightly lower levels are found in the pictorial plots of the low-altitude launch phase. These data occur when the missile has attained sufficient altitude to escape the ground plane effect and thus allow the exhaust stream to flow unobstructed. This condition can be found somewhere in the altitude region from 20 to 60 nozzle diameters above the ground. In order to be more specific, the value of 50 nozzle diameters has been selected for this discussion. The levels for this low-altitude launch phase have been increased over the free-field condition so as to compensate for the missile configuration (structure, skin panel effects, etc.). A portion of the free-field calculations has been included in Appendix C for interested parties. The launch phase spectra curves exhibited in Fig. 11 are similar to the data displayed in the static firing plot of Fig. 9. The positive slope for the sound-pressure levels near the nozzle (zero distance) shows the high-frequency peak again. Also, the constancy of the low-frequency acoustic levels can be seen for excitations below 1200 cps. These effects are more vividly depicted in the three-dimensional spectrogram of Fig. 12. A study of this pictorial display indicates that the spectra become uniformly "white" somewhere between the nozzle and 50 feet forward of the nozzle. The usual atmospheric attenuation shapes the spectra so that peaks occur in the low-frequency region with increased distance forward of the nozzle.

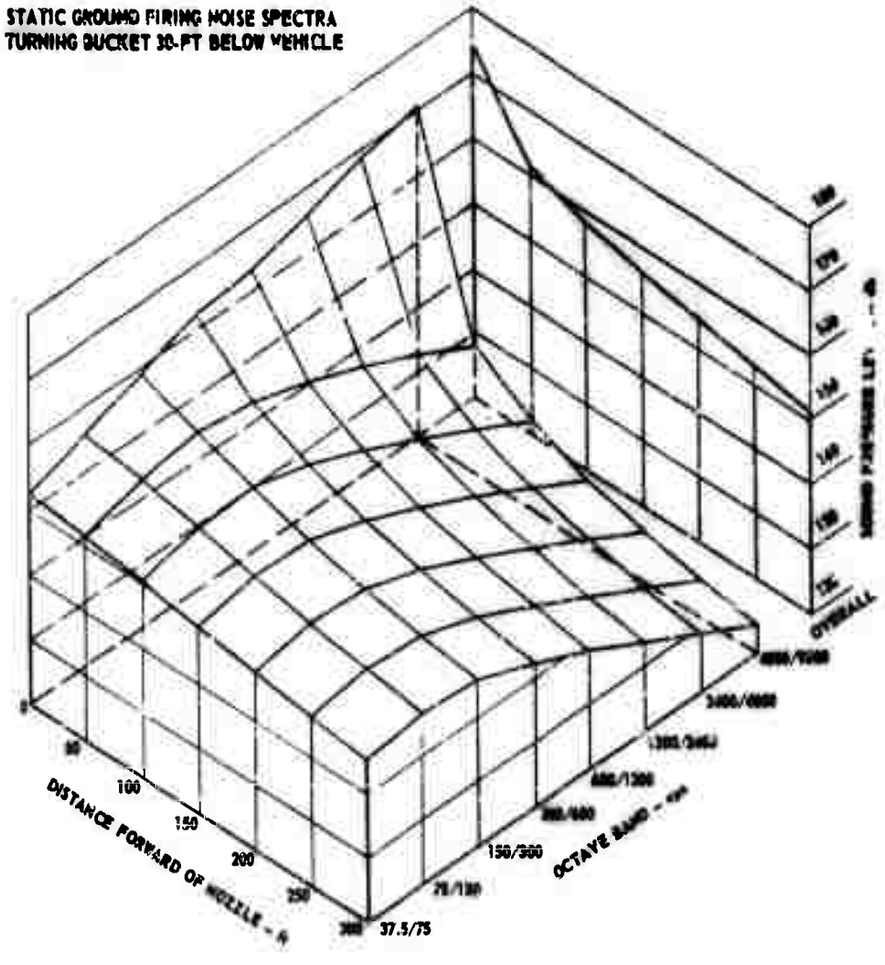

Fig. 10 - Three-dimensional plot of static firing noise spectra shown in Fig. 9

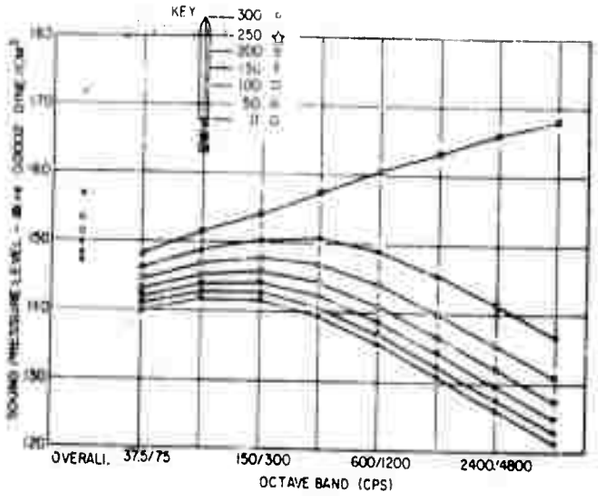

Fig. 11 - Launch phase noise spectra for two-million pound missile. Low-altitude, low-velocity flight.

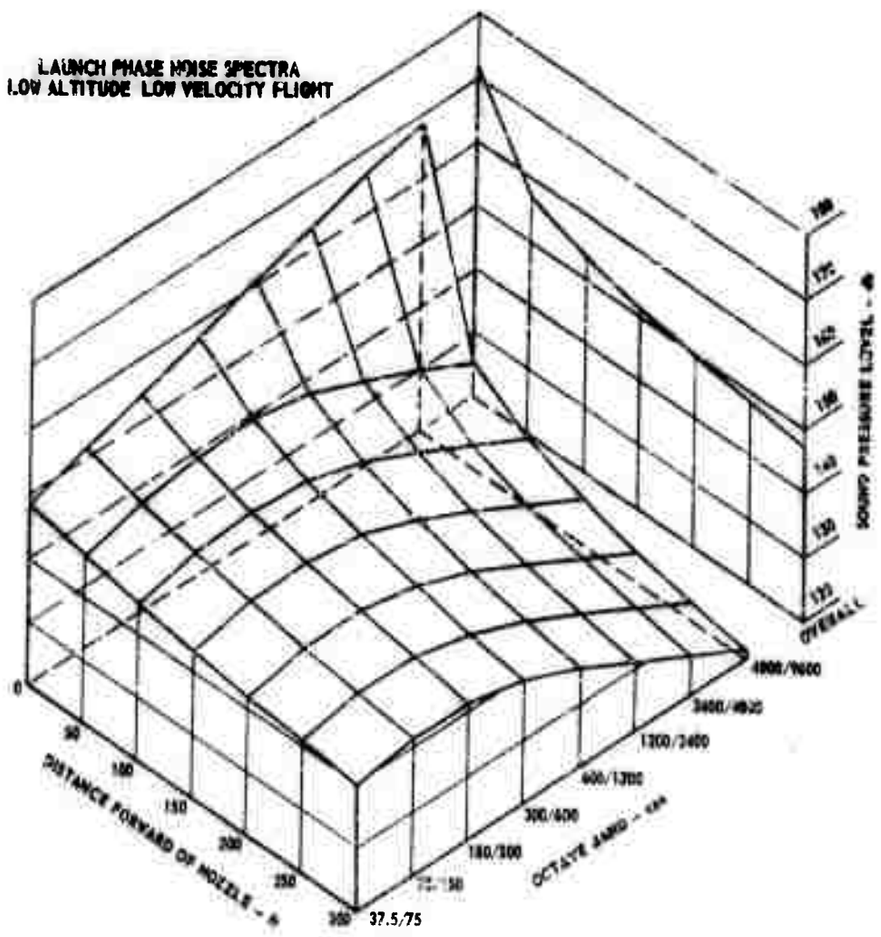

Fig. 12 - Three-dimensional plot of launch phase noise spectra shown in Fig. 11

In regard to transmission loss through the missile skin and structure it can be expected that the overall levels within the missile will be diminished by 5 to 15 db. A suitable average or "ball-park" figure for this diminution in level is a value of 10 db. Certainly, the transmission loss will vary for each individual missile configuration and will vary with many factors such as skin thickness, material damping, resonant frequencies, coincidence effects, cavity resonances, reverberation effects, the amount of fuel or equipment in the bays, etc. Field data from Snark booster firings (12) provide actual results of transmission effects under high-intensity excitations. External microphone measurements on the Snark missile disclose a uniformity of frequency that indicates the boosters are essentially a white noise source. This can be observed in the spectrum of Fig. 2 which shows a relatively uniform distribution at fuselage station 825. This location is very close to the booster nozzles and is representative of the booster excitations. Reference (12) discloses that peaked and skewed curves are found on Snark acoustic measurements where the booster blast is attenuated by obstructions or resistances. The internal microphones on the Snark missile exhibit launch spectra with the highest acoustic energy in the low frequencies. Most of the internal microphone spectra follow a negative slope after low-frequency maxima and decline to minima at 10,000 cps. These data show that the major portion of the acoustic energy is somewhere below 300 cps. Maxima are observed at 80, 100, 125, 160, 200, 250, and 315 cps for Snark internal electroacoustic measurements. The Snark data indicate that an average transmission loss of 10 db is reasonable.

The noise level surrounding the hypothetical vehicle decreases immediately after the launch phase until a sufficient velocity is attained to develop boundary-layer noise. These "pseudo-sound" fluctuations are proportional to the freestream pressure (see Eqs. 6, 7, and 8). Therefore, an examination of the trajectory in Fig. 7 indicates that the maximum value of boundary-layer noise will occur after launch when the dynamic pressure reaches its maximum value of 590 psf. These randomly fluctuating hydrodynamic pressures can be decomposed by Fourier methods into a pattern of sinusoidal waves (6) spreading downstream with various angles of yaw. It is further assumed that this wave pattern is idealized and moving uniformly by convection (the pressure fluctuation at any point is thus caused by the motion). A running ripple in the skin follows underneath each wave, and the noise is actually the result of these ripples.

The boundary layer or "panting" noise exhibits a broad spectra which can be estimated from calculations of the Strouhal number, $f\delta/V$. Where f is the frequency, δ is the boundary-layer thickness and V is the free stream velocity. The maximum octave-band frequency of the boundary layer noise is

$$f_m = 0.4 \frac{V}{\delta} \text{ cps.}$$

A typical boundary layer noise spectrum based on these relationships is plotted in Fig. 13. It can be discerned from this plot that the overall sound-pressure level (Eqs. (6), (7), or (8)) is approximately 5 db above the maximum noise frequency. The boundary layer noise spectra at the maximum Q were calculated and are presented in Fig. 14. The

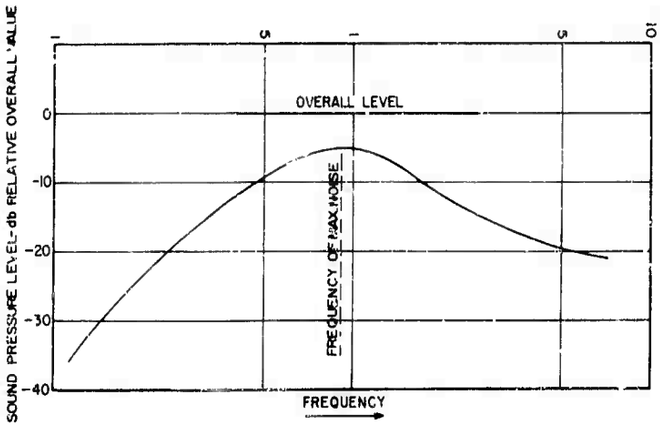

Fig. 13 - Typical boundary-layer noise spectrum

necessary calculations can be found in Appendix C. Sound-pressure levels are displayed in Fig. 14 as a function of frequency and distance forward of the nozzle. It can be seen in this three-dimensional illustration that the high frequencies are propagated near the leading edge. This is a result of the frequency relationship given above where it is shown that frequency is a function of boundary-layer thickness. Supporting the frequency distribution of Fig. 14 is aerodynamic theory which shows an extremely thin boundary layer near the leading edge. The equation for estimating boundary-layer thickness is

$$\delta = d\ 0.129\ (R_e)^{\frac{1}{7}},$$

where d is the distance from the leading edge, and R_e (Reynolds number) is $(Vd)/\nu$, where ν is kinematic viscosity.

Figure 15 summarizes the previously described acoustic environment of the hypothetical vehicle with the two-million-pound-thrust rocket engine. This chronological history of the major acoustic sources depicts the sound-pressure levels for 50-foot intervals forward from the exhaust nozzle. Thus, the static firing levels, the launch phase, the diminution immediately after launch, the increase in level to the maximum Q value, and the final decline to negligible noise levels are included in this summation. This family of curves shows that the most severe environment exists during the first few seconds of the mission.

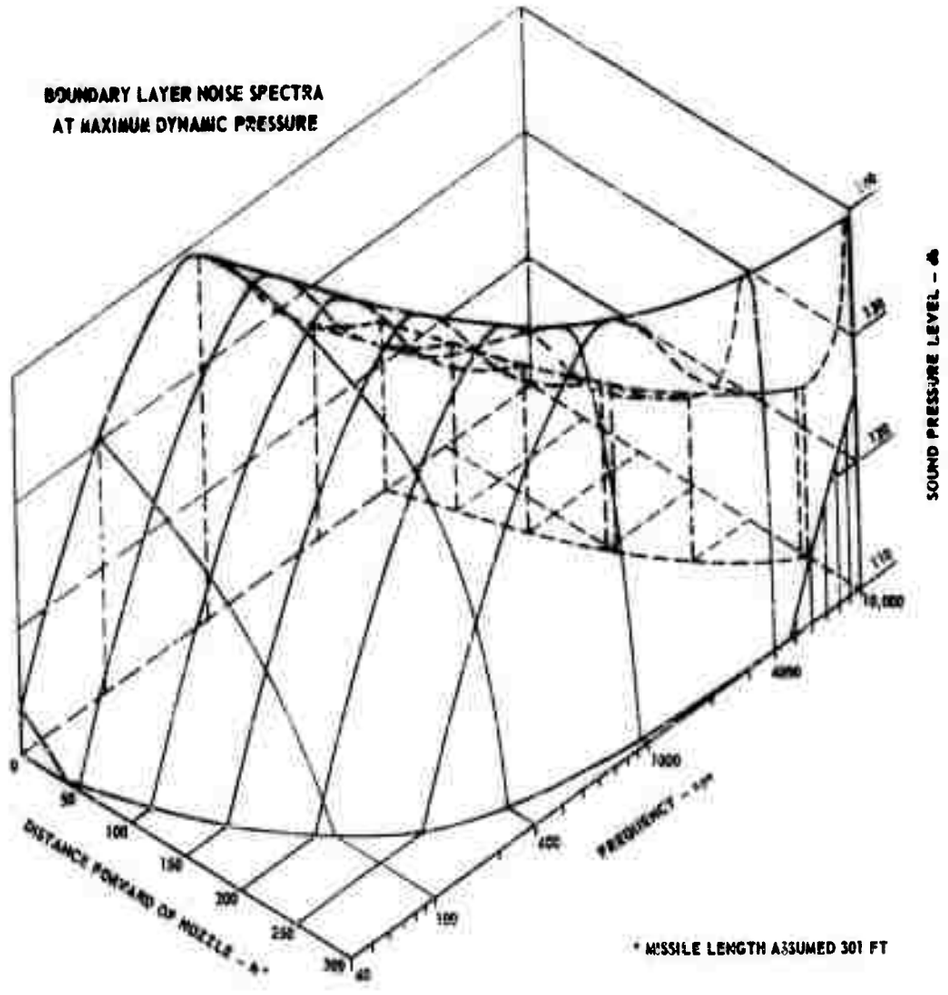

Fig. 14 - Boundary-layer noise spectra at maximum dynamic pressure calculated for the hypothetical vehicle

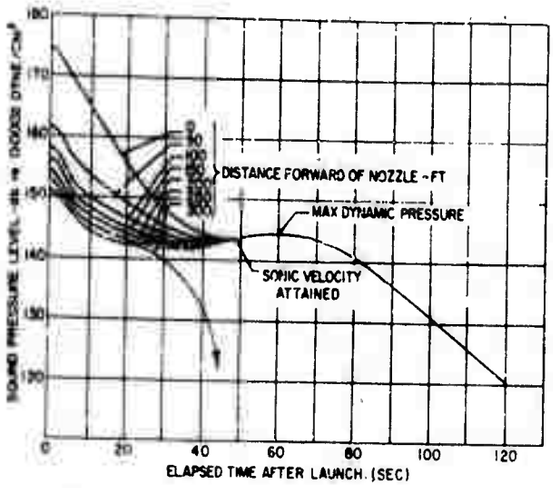

Fig. 15 - Summary of predicted time histories of overall noise levels for the hypothetical vehicle with two-million-pound thrust rocket engine

SUMMATION AND RECOMMENDATION

This paper has discussed three of the principal dynamic environments:

1. Jet engine noise.
2. Rocket-exhaust noise.
3. Boundary-layer noise.

In addition, a hypothetical mission of a vehicle with two-million pounds of thrust has been described and analyzed. Estimated acoustic levels for the launch phase and for the maximum boundary-layer noise were presented. As expected, the most severe environment was displayed during the launch phase before the missile cleared the ground plane. However, the levels obtained on the missile structure were not as great as anticipated. If these estimations are considered reasonable, then it is felt that structure and equipment can be designed, with presently available techniques, to withstand this hypothetical acoustic environment. It is noted that the launch acoustic environment of the SM-62 Snark missile is more severe than that shown for the powerful hypothetical vehicle. The booster installation configuration accounts for the greater environment measured on the Snark missile.

In a search for dynamic data during the past year, it was found that only a limited amount of acoustic measurements have been obtained during recent missile firings and flights. Therefore, it is recommended that more missile programs take an interest in acoustic environments and that adequate measurements be made so as to define these field environments.

Many momentous aeronautical and space developments have occurred since that historic day in 1903 when the Wright brothers ushered in the Air-Space Age. Yet, today the basic dynamic problem is the same – designing and building the structure and the equipment to withstand the dynamic environment with a minimum weight penalty.

ACKNOWLEDGMENT

The writer is greatly indebted to C. L. Gray, J. A. Mallick, and D. L. Van Ert of the Norair Dynamics Branch for preparing the estimations and the supporting pictorial data that made this paper possible.

REFERENCES

1. R. W. Mustain, "Power Spectral Density Nomogram," Environmental Quarterly, July 1959.

2. R. W. Mustain, "Extended Environmental Tests of SM-62 Missile Components," Shock and Vibration Bulletin No. 27-Part II, Office of The Secretary of Defense.

3. WADC Technical Report 54-401, "A Compilation of Turbojet Noise Data," July 1956.

4. WADC Technical Note 56-280, "Noise Characteristics of Air Force Turbojet Aircraft," December 1956.

5. WADC Technical Note 56-60, "Noise Prodeced by Aircraft During Ground Run-up Operations," June 1957.

6. L. R. Fowell and G. K. Korbacher, "A Review of Aerodynamic Noise," Inst. of Aerophysics, Univ. of Toronto, July 1955, UTIA Review #8.

7. Northrop Report, NOR-60-26, "Structural Vibration in Space Vehicles," Phase I Report, Investigation of Structural Vibration Sources and Characteristics.

8. A. Powell, "On the Generation of Noise by Turbulent Jets," ASME Publication 59-AV-53, March 9, 1959.

9. H. S. Ribner, "On the Strength Distribution of Noise Sources Along a Jet." Univ. of Toronto, Inst. of Aerophysics, UTIA Report 51, 1958.

10. M. J. Lighthill, "On Sound Generated Aerodynamically, Part I—General Theory," Proc. Roy. Soc., Vol. A211, pp 564-587, 1952.

11. M. J. Lighthill, "On Sound Generated Aerodynamically, Part II—Turbulence as a Source of Sound," Proc. Roy. Soc., Vol. A222, pp 1-32, 1954.

12. R. W. Mustain, "Summary of Acoustic and Vibration Data: Acoustic (Noise) Test Program," Northrop Report No. NA I-57-588, Oct. 1958.

13. A. Powell, "Effect of Missile Motion on Exhaust Noise," Journal of the Acoustical Society of America, Vol. 30, No. 11, Nov. 1958.

14. I. Dyer, "Estimation of Sound-Induced Missile Vibration," Random Vibration, The Technology Press of MIT.

15. WADC Technical Report, 57-354, "Noise Radiation from Fourteen Types of Rockets in the 1000 to 180,000 Pounds Thrust Range," December 1957.

16. WADC technical Report 58-343, "Methods of Flight Vehicle Noise Prediction," November 1958.

17. Personal communication K. Eldred, Western Electro-Acoustic Labs. to B. R. Vernier, Northrop Corp.

18. H. S. Ribner and B. Etkin, "Canadian Research in Aerodynamic Noise," Inst. of Aerophysics, Univ. of Toronto, UTIA Review No. 13.

19. NACA TN 1428.

20. D. M. A. Mercer and I. Dyer, "The Influence of Turbojet Engine Design Parameters on Noise Output," IAS Preprint No. 544.

APPENDIX A

ACOUSTIC POWER, J85-GE-5 ENGINE, T-38 AIRPLANE

1. Operating Conditions

Military power (100 percent RPM w/o A/B); Static, sea level operation; one engine

2. Performance Characteristics

Engine speed	16,500 RPM
Net static thrust	1934 lb
Weight flow	37.7 lb/sec.
Nozzle exit area	114.2 in.^{2}; 0.793 ft^2
Total temperature at exit	1660° R
Total pressure at exit	26.4 psia

Compression ratio	7.0
Compressor efficiency	83 percent
Turbine efficiency	87 percent

3. **Calculated Jet Conditions**

Velocity

$$V = \frac{F}{\dot{m}}$$

$$= \frac{1934 \times 32.2}{37.7} = 1650 \text{ fps.}$$

Density

$$\rho = \frac{\dot{m}}{A\,V}$$

$$= \frac{37.7}{32.2 \times .793 \times 1650} = .000895 \text{ slugs/ft}^3.$$

Mach Number

$$\rho = \frac{P}{gRT}$$

$$P = P_T \left[1 + \frac{\gamma - 1}{2} M^2\right]^{\frac{-\gamma}{\gamma - 1}}$$

$$T = T_T \left[1 + \frac{\gamma - 1}{2} M^2\right]^{-1}$$

$$\rho = \frac{P_T}{gR\,T_T} \left[1 + \frac{\gamma - 1}{2} M^2\right]^{\frac{1}{\gamma - 1}}$$

$$\left[\frac{\rho g R T_T}{P_T}\right]^{-(\gamma - 1)} = 1 + \frac{\gamma - 1}{2} M^2$$

$$M^2 = \frac{2}{\gamma - 1} \left\{\left[\frac{gR\,T_T}{P_T}\right]^{1-\gamma} - 1\right\}$$

$$= \frac{2}{1.4 - 1} \left\{\left[\frac{.000895 \times 32.2 \times 53.3 \times 1660}{26.4 \times 144}\right]^{(1-1.4)} - 1\right\}$$

$$= .875$$

$$M = .935.$$

Static Temperature

$$T = k_1\, T_T \qquad (k_1 \text{ from Ref. 19})$$

$$= .85 \times 1660 = 1410^\circ R.$$

Static Pressure

$$P = k_2 P_T \qquad (k_2 \text{ from Ref. 19})$$

$$= .57 \times 26.4 = 15.0 \text{ psia.}$$

4. Calculated Acoustic Power

$$P_A = 4.2 \times 10^{-3} WK^2. \qquad \text{(Ref. 20)}$$

Stream Power

$$W = \frac{1}{2} \rho A V^3$$

$$= \frac{1}{2} \times .000895 \times .793(1650)^3 \times \frac{746}{550}$$

$$= 2.16 \times 10^6 \text{ watts.}$$

Parameter K

$$K = \frac{W}{(T)^{1.8} d}$$

$$= \frac{2.16 \times 10^6}{(1410)^{1.8} \times 12.0}$$

$$= .386.$$

Acoustic Power Generated

$$P_A = 4.2 \times 10^{-3} \times 2.16 \times 10^6 (.386)^2$$

$$= 1.35 \times 10^3 \text{ watts}$$

$$PWL = 10 \log_{10} \frac{P_A}{P_{REF}}$$

$$= 10 \log_{10} \frac{1.35 \times 10^3}{10^{-13}}$$

$$= 161.3 \text{ db.}$$

5. Operating Conditions

Military power (100 percent RPM w/o A/B); static, sea level operation; one engine

6. Sound Pressure Levels

$$SPL = PWL - 10 \log_{10} A - B$$

PWL = Acoustic power level re. 10^{-15} watts

= 161.3 db

A = Area of advancing sound pressure wave (hemisphere)

$= 2\pi r^2$

B = Constant determined by ambient conditions

= -0.5 db for std. s.l. atm.

At r = 50 feet

$$SPL = 161.3 - 10 \log_{10} 2\pi(50)^2 + 0.5$$

$$= 120 \text{ db}.$$

At r = 100 feet

$$SPL = 161.3 - 10 \log_{10} 2\pi(100)^2 + 0.5$$

$$= 114 \text{ db}.$$

At r = 250 feet

$$SPL = 161.3 - 10 \log_{10} 2\pi(250)^2 + 0.5$$

$$= 106 \text{ db}.$$

At r = 500 feet

$$SPL = 161.3 - 10 \log_{10} 2\pi(500)^2 + 0.5$$

$$= 100 \text{ db}.$$

7. Dual Engine Operation

Operation of both engines would produce a maximum of twice the acoustic power, or 3 db. However, because of the proximity of the exhaust streams, no acoustic energy can be assumed to be generated between the jets, and an increase of 2 db is estimated. The full RPM operation can then be expected to produce overall SPL's of

122 db at 50 feet
116 db at 100 feet
106 db at 250 feet
102 db at 500 feet

8. Directivity

Typical directivity factors in db above and below the space average SPL are as follows:

Angle from Aircraft Nose (Degrees)	Relative SPL (db)
0	-15
30	-14
60	-12
90	- 7
120	+ 2
140	+ 8
150	+ 7
160	+ 1
170	- 8

APPENDIX B

SOLID PROPELLANT CALCULATIONS

Thrust	= 101,700 pounds
Exit Velocity	= 6310 fps
Mass Flow	= 16.12 slugs/sec
Nozzle Diameter	= 1.794 feet

Method used - WADC 58-343

1. $10 \log \eta = -20$ db for large rockets.

2. $$PWL = 10 \log \eta + 10 \log \frac{\frac{1}{2} mv^2}{10^{-13}}$$

$$PWL = -20 + 10 \log \frac{\frac{1}{2}(16.12)\ 14.6 \times (6310)(.3048)^2}{10^{-13}}$$

$$PWL = -20 + 10 \log 4.35286 \times 10^{21}$$

$$PWL = -20 + 216.4$$

$$PWL = 196.4 \text{ db}.$$

3. Computing Strouhal No. for Octave Bands, we find source distance (fD/V):

Octave (cps)	Mean Frequency (cps)	$\frac{fD}{V}$	$\frac{X_o}{D}$	X_o (ft)	M 1 Position R_o (ft)
37.5/75	53	.0151	9.9	17.76	19.69
75/150	106	.0301	8.5	15.25	17.10
150/300	212	.0603	7.2	12.92	14.78
300/600	424	.1205	5.5	9.87	11.76
600/1200	849	.2414	3.5	6.28	8.236
1200/2400	1698	.4828	1.48	2.66	4.775
2400/4800	3390	.9638	0.59	1.06	3.353
4800/9600	6930	1.9703	0.24	0.43	2.846

4.

Octave (cps)	20 log R	$K = \frac{2\pi f}{c_a}$	KR	10 log G^2	SPL_o (db)
37.5/75	25.6	.3063	6.00	1	165.7
75/150	24.7	.6127	10.48	0	169.4
150/300	23.4	1.2254	18.11	0	171.9
300/600	21.4	2.4507	29.92	0	172.4
600/1200	18.3	4.9072	40.42	0	170.9
1200/2400	13.6	9.8144	46.86	0	167.0
2400/4800	11.5	19.5942	65.70	0	162.1
4800/9600	9.1	40.0554	114.00	0	157.1

5.

Octave (cps)	SPL (db)	Octave (cps)	SPL (db)
37.5/75	140.9	600/1200	152.6
75/150	144.7	1200/2400	153.4
150/300	148.5	2400/4800	150.6
300/600	151.0	4800/9600	156.0

OA - 159.3 db

APPENDIX C

HYPOTHETICAL VEHICLE

PWL CALCULATIONS

Given:

Weight flow = 2500 lb/sec

Thrust = 2×10^6 lb = 8.93×10^6 newtons

1 pound = .453 K grams; weight flow = $2500 \times .453 = 1134$ Kg/sec

Diameter = 25 feet or 7.62 meters

1 foot = .3048 meters

(1) $\frac{V}{C_a}$ using C_a = 1116 fps

$$V = \frac{tg}{w} = \frac{2 \times 10^6 \times 32.2}{2500} = 25,760 \text{ fps}$$

$$\frac{V}{C_a} = \frac{25760}{1116} = 23.1$$

$10 \log \eta = -20$. (Taken from Ref. 16)

(2) Mechanical Stream Power = $\frac{1}{2} mV^2$ in watts.

$$= \frac{1}{2}(1134)\, V^2 \qquad V = 25,760 \times .3048 = 8851.6 \text{ m/sec}$$

$$= \frac{1}{2}(1134)(7851.6)^2 = 3.51 \times 10^{10} \text{ watts}.$$

(3) $PWL = 10 \log_{10}\eta + 10 \log_{10} \frac{\frac{1}{2} mV^2}{10^{-13}}$ (re Ref. 16)

$$PWL = -20 + 10 \log \frac{3.51 \times 10^{10}}{10^{-13}} = -20 + 10 \log 3.51 \times 10^{23}$$

$PWL = -20 + 10 \times 23.544 = -20 + 235.44 = 215.44$ db.

Check on PWL using equations from Ref. (15).

OA $PWL = 78 + 13.5 \log_{10} W_m$ in db re 10^{-13} watts,

where

W_m = mechanical power of jetstream in watts

$W_m = 0.676\, tV = 0.676\, (t^2 g)/w$,

with $V = (tg)/w$ = gas velocity at nozzle exit in fps,

t = thrust in pounds,

g = acceleration due to gravity = 32.2 ft/sec^2,

w = weight flow in lb/sec.

Then

$$PWL = 78 + 13.5 \log W_m = 78 + 13.5 \log 0.676 \frac{t^2 g}{w}$$

$$PWL = 78 + 13.5 \log 0.676 \frac{(4 \times 10^{12})(32.2)}{2500}$$

$$PWL = 78 + 13.5 \log 3.48 \times 10^{10} = 78 + 13.5 \ (10.542)$$

PWL = 78 + 142 = 220 db.

SPECTRUM CALCULATIONS

Given:

D = 25 feet,

$$V = \frac{tg}{w} = \frac{2 \times 10^6 \ (32.2)}{2500} = 25{,}760 \text{ fps.}$$

(1) Compute df/V values; f = geometric mean of octave band $\sqrt{f_1 \times f_2}$.

(2) Determine power spectrum level re. zero reference at each df/V value on Fig. 45A of Ref. 15.

(3) Determine power spectrum level re. 10^{-13} watt by computing zero reference level which equals OA PWL - 10 $\log_{10}$ V/d and algebraically adding this reference level to each power spectrum level determined in previous step.

(4) Convert these power spectrum levels at the geometric mean frequencies to Octave Band PWL's by adding the appropriate 10 $\log_{10} \Delta f$ correction factors on Fig. 45A of Ref. (15) to each power spectrum level.

Given:

D = 25 feet,

V = 25,760 fps.

Octave Band (cps)	Geom. Mean Frequency (cps)	Strouhal No. Df/V	Power Spectrum Level (db) (from Fig. 45A Ref. 15)	Octave Band OB PWL (cps)
37.5-75	53	.0514	8.2	214.4
75-150	106	.1029	4.0	213.2
150-300	212	.2057	-1.1	211.1
300-600	424	.4115	-6.3	208.9
600-1200	849	.8240	-11.7	206.5
1200-2400	1698	1.648	-16.6	204.4
2400-4800	3390	3.290	-22.2	202.0
4800-9600	6930	6.726	-27.7	199.5

Power spectrum level at a specified frequency is the PWL in db within a band one cps wide centered at that frequency.

$$\text{Octave Band PWL} = \text{Power Spectrum Level} + 10 \log_{10} \Delta f ,$$

where Δf = bandwidth in cps.

$$\text{Zero reference} = \text{OA PWL} - 10 \log \frac{V}{D}$$

$$= 220.3 - 10 \log \frac{25,760}{25} = 220.3 - 10(3.013) = 190.2 \text{ db.}$$

Then

$$\text{OB PWL} = \text{zero reference} + \text{power spectrum level} + 10 \log \Delta f .$$

Example: 37.5 to 75 cps band

$$\text{OB}_{37.5\text{-}75}\,\text{PWL} = 190.2 + 8.2 + 16 = 214.4 \text{ db} .$$

SOURCE DISTANCE FROM EXIT

Strouhal No.	$\frac{X_o}{D}$	X_o (ft)	Octave Band (cps)
.0514	7.5	187.5	37-75
.1029	5.8	145.0	75-150
.2057	3.75	93.75	150-300
.4115	1.73	43.25	300-600
.8240	.71	17.75	600-1200
1.648	.30	7.5	1200-2400
3.290	.125	3.125	2400-4800
6.726	.055	1.375	4800-9600

$$X_o = \frac{X_o}{D} 25 ,$$

where

D = 25 feet = nozzle diameter

X_o/D taken from Fig. 22 of Ref. (16).

SPL for 37.5 to 75 cps

$$K = \frac{2\pi f}{C_a} = \frac{2\pi 53}{1116} = .294 .$$

Distance = S Up on Missile from Nozzle (ft)	R $(X_o + X)$ (ft)	KR	10 log G^2
0	187.5	55	0
50	237.5	69.8	0
100	287.5	84.5	0
150	337.5	99.2	0
200	387.5	113.9	0
250	437.5	128.6	0
300	487.5	143.3	0

$$\text{SPL} = \text{SPL}_o - 20 \log R + 10 \log G^2 ,$$

where the reference sound pressure level SPL_o is given relative to the overall power level in Fig. 24 of Ref. (16).

Then

$$SPL_o = PWL - 25 = 215.5 - 25 = 190.5 \text{ db}.$$

S	R	20 log R	SPL (db)
0	187.5	45.5	145
50	237.5	47.5	143
100	287.5	49.2	141.3
150	337.5	50.6	139.9
200	387.5	51.8	138.7
250	437.5	52.8	137.7
300	487.5	53.8	136.7

Add 3 db to above SPL's for missile configuration.

SPL for 75 to 150 cps

$$K = \frac{2f}{1116} = .591,$$

$$SPL = SPL_o - 20 \log R + 10 \log G^2.$$

From Fig. 24 of Ref. (16)

$$SPL_o = PWL - 24 = 215.5 - 24 = 191.5 \text{ db}.$$

S (ft)	$R = (X_o + X)$ (ft)	KR	$10 \log G^2$	$20 \log R$	SPL (db)
0	145	> 10	0	43.24	148.3
50	195	> 10	0	45.80	145.7
100	245	> 10	0	47.8	143.7
150	295	> 10	0	49.40	142.1
200	345	> 10	0	50.8	140.7
250	395	> 10	0	51.9	139.6
300	445	> 10	0	53.	138.5

To conserve space, the remaining octave band SPL calculations have been deleted. The above are considered typical. Add 3 db for missile configuration.

DECREASE IN PWL DUE TO MOTION

From Journal of ASA-Powell, Vol. 30, No. 11, November 1958. Use

$$M_J = \infty.$$

M_M	t (sec)	V_e (fps)	Distance	Δ PWL (db)
.23	1	257.6	128.8	-2.2
.46	2	515.2	515.2	-5.5
.695	3	772.8	1159.2	-10
.93	4	1030.4	2060.8	-23

From WADC 58-343, Fig. 32

Correction for T_a, P_a, in ΔB,

t = 1 sec.	ΔB = .1 db	ΔSPL = -2.3 db
t = 2 sec.	ΔB = .1 db	ΔSPL = -5.6 db
t = 3 sec.	ΔB = .3 db	ΔSPL = -10.3 db
t = 4 sec.	ΔB = .4 db	ΔSPL = -23.4 db

NOISE ESTIMATION

Boundary Layer Noise for Q_{max} at t + 60 sec.

$$SPL = 20 \log Q + 86 \text{ db}$$

$$SPL = 20 \log 590 + 86 \text{ db}$$

$$SPL = 20 (2.77085) + 86$$

$$SPL = 141.4 \text{ db} + 3 = 144.4 \text{ db}$$

$$R_e = \frac{Vd}{\nu} = \frac{1300\ d}{368 \times 10^{-6}} = 3.53 \times 10^6\ d \qquad \nu = \frac{\mu}{e} \text{ Alt. } 32{,}000 \text{ feet}$$

$$\nu = \frac{3.041 \times 10^{-7}}{.826 \times 10^{-3}} = 3.68 \times 10^{-9}$$

$$\frac{\delta}{d} = .129\ (R_{e_d})^{-\frac{1}{7}}$$

$$\delta = \frac{.129\ d^{\frac{6}{7}}}{(3.53 \times 10^6\ d)^{\frac{1}{7}}}$$

$$\delta = \frac{.129\ d^{\frac{6}{7}}}{10\ (.353)^{\frac{1}{7}}}$$

$$\delta = \frac{.0129\ d^{\frac{6}{7}}}{.8618}$$

$$\delta = .015\ d^{\frac{6}{7}}$$

$$f_{max} = .4\ \frac{V}{\delta}$$

$$f_{max} = \frac{.4\ (1300)}{.015\ d^{\frac{6}{7}}} = \frac{320}{150 \times 10^{-4}\ d^{\frac{6}{7}}}$$

$$f_{max} = \frac{3.47 \times 10^4}{d^{\frac{6}{7}}}$$

Distance from Leading Edge (ft)	Distance from Aft Nozzle (ft)	f_{max} (cps)	98
1	300	34,700	
51	250	1,190	6-2400
101	200	665	6-1200
151	150	470	3-600
201	100	368	3-300
251	50	304	150-600
301	0	259	150-300

To conserve space, the remaining boundary layer calculations have been deleted. The above sample is considered typical.

DISCUSSION

Mr. Harvey (Lockheed Aircraft Corporation): I take it that your equations would predict an increase in vibration somewhere around the max of dynamic pressure. I would like to just note that in our experience in launching the Agena satellite on the end of the Thor, we expected to get an increase in vibration at max Q, but we didn't get it there. We got it in a very strange region which we can't explain, and that is it started to pick up at a Mach number of about seven tenths, increased to a Mach number of about nine tenths, and then dropped off to zero just before Mach one. We thought it should happen at Mach one, but it didn't, and the best thing we can figure out is that our calculations of the Mach number vs time were incorrect. So I wonder if you have anything to say about this, if you have any information that might explain why this happened.

Mr. Mustain: First of all, boundary-layer noise is what you are talking about? We didn't make vibration predictions on a boundary-layer noise.

Mr. Harvey: Well, let me say what we did and you can shoot me down. We had a measurement made with a vibration pick up inside the missile, and we assumed that if you had an increase in boundary-layer noise you should see some rise in the vibration measurement in the missile. Maybe this is what went wrong, but certainly the results are unusual. Maybe you would like to explain that if you can.

Mr. Mustain: Just guessing, without knowing, I would say that, with forward motion in the missile as you approach Mach 1, your excitation should go down externally acoustically, and if that is causing your vibrations they should go down also. If you have some other internal vibrations like machinery in there, equipment that mechanically induces vibrations from the power plant, it naturally wouldn't go down. I have no actual measurements to cover your problem, but I certainly can guess as well as the next person, or I can try. Maybe I am wrong. But this is what I do.

Mr. Kuoppamaki (Lockheed, Sunnyvale): I would also like to add a comment. Data from two other types of Lockheed test vehicles have also shown interesting differences. The type-one vehicle behaved normally in respect to increase in vibration level with increasing Q, the aerodynamic pressure. Accordingly, high-vibration levels were expected at maximum Q also in the flights of the type-two test vehicle, but no appreciable increase in vibration amplitudes showed up. Some increase in the structural response to the aerodynamics at Mach one has been experienced also in the type-two vehicle but nothing appreciable in proportion to the increase in aerodynamic pressure. Ralph Blake explained in the previous presentation the basics of structural response concerning this peculiar characteristic. It would be of interest, from the standpoint of missile design in general, to actually determine the internal relationships of the masses and damping ratios involved in two different test vehicle types, which have a significant difference in the flight characteristics in respect to the smooth riding through the region of maximum aerodynamic pressure.

Mr. Hall (Douglas Aircraft Corp.): Roy, I have just a quickie. I would say that you might as well forget all this talk about aerodynamic-induced vibration because I

don't think it is at all important to the vibration problem. On payloads, I agree, we are designing to specifications that might be too low. In this case the aerodynamic noise may be the most considerable vibration encountered. But generally, I submit to the audience that aerodynamic noise is negligible in most design cases.

Mr. Mustain: I would like to see more measurements on acoustics during launch on these missiles and during flight. I have tried to get vibration and acoustic measurements, and so far I have gotten only one set of measurements from the contractors. Most of them are not interested in acoustic measurements. I got that from people who were at the top of several projects. They told me they weren't interested in acoustic measurements and weren't taking any.

* * *

EXTERNAL NOISE FIELDS OF A BOOST-GLIDE HYPERSONIC VEHICLE

Werner Fricke and William Squire
Bell Aircraft Corporation
Space Flight and Missiles Division

The paper presents a time history of the external noise fields of a high-speed, high-altitude manned glide vehicle during a global flight. After a discussion of the flight parameters to which the noise fields are related, an analysis of the two noise phases, originated from the rocket booster and from the boundary layer, is presented. At subsonic speed, the effect of motion of the noise source and the decreasing characteristic impedance of air change the noise field around the cockpit. Its time history was calculated as function of the Mach No.

At supersonic speed, boundary layer noise is the only noise source. After a discussion of the most important parameters of the flow behind the shock wave around a blunt body moving supersonically, a method for a prediction of the overall sound pressure is derived, based on the conception of Newtonian flow. The following quantities were required: location of the transition point between laminar and turbulent boundary layer and distribution of the local dynamic pressure along the cockpit.

The spectrum was estimated from a published spectrum of turbulent flow measured in a boundary layer, plotted as a dimensionless spectral density-frequency diagram. Application of this graph to the cockpit configuration required a calculation of the boundary layer displacement thickness to be calculated from quantities measured on a flat plate. The sequence of the analysis will be discussed and demonstrated.

INTRODUCTION

This paper presents a description of the noise environments of a high-speed, high-altitude manned glide vehicle during a global flight. The analysis was performed about one year ago at Bell Aircraft Corporation. Knowledge of the complete time history of the external and internal noise fields is required to establish design requirements for the structure and adequate noise control for the cockpit and the equipment compartment. Moreover, it allows preliminary specifications of test equipment prior to production release of the first test vehicle.

The noise environments are closely related to certain flight parameters (Fig. 1), such as altitude h, free stream Mach No. M_∞, ambient density ρ_∞, and dynamic pressure q. All units are expressed as ratios with the maximum value as reference. The highest Mach No. occurs during the intermediate phase which is not of interest here. The dynamic pressure peaks during the first part of supersonic flight. The density during boost decreases rapidly from its sea level value to 1 percent within 2 minutes. During landing, about 5 minutes are required for the same range.

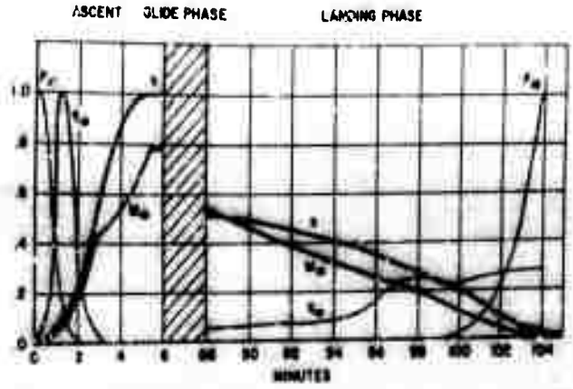

Fig. 1 - Altitude (h), free-stream Mach No. (M_∞), ambient density (ρ_∞), and free-stream dynamic pressure (q_∞) during boost and landing

During a complete global flight of a boost-glide vehicle, two external noise phases have to be considered and are shown in the noise-time history (Fig. 2). The first and most severe noise period occurs during ascent. The analysis shows a sequence of two noise maxima, the first originating from the booster rocket, the second from the fluctuating pressure in the turbulent boundary layer.

The second booster stage operates at an altitude, where neither sound transmission from the rocket engine to the vehicle through the ambient air nor noise from the turbulent boundary layer will be observed. During this period and during the following glide, the noise inside the vehicle will be entirely produced by the airborne equipment, and can be limited by suitable noise control.

The other external noise phase will occur during the last part of the mission, as the dynamic pressure rises during descent into the denser atmosphere. The methods used for the prediction of these two noise phases are demonstrated in the next section.

CALCULATION OF OVERALL ENGINE NOISE DURING BOOST

The overall external noise along the airplane, caused by the first stage booster, was calculated from octave band levels, recorded with a spectral analyser during ground tests of a single rocket engine of the type to be used in the booster rocket under consideration (in the launching position).

During ascent, the noise field will be changed because of the noise source and decreasing characteristic impedance of the ambient air. If it is assumed that the acoustic power W of a rocket engine is proportional to the square of the jet velocity relative to the ambient air (1), the proportionalities shown below may also be assumed:

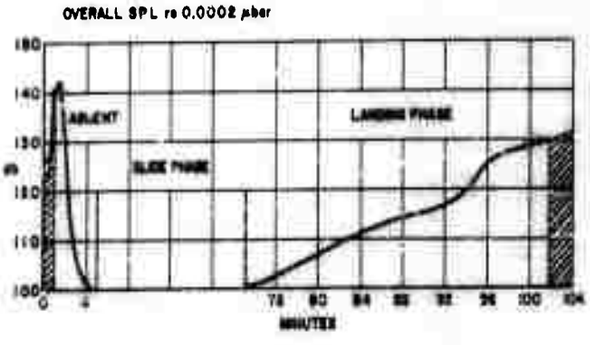

Fig. 2 - External overall noise levels during global flight. (Shaded area indicates subsonic flight.)

$$p \sim W^{\frac{1}{2}} \sim \frac{v_j - v_v}{v_j} \sim \left(1 - M_\infty\right) \cdot \frac{c}{v_j} , \qquad (1)$$

$$p^2 \sim \rho c , \qquad (2)$$

where

v_j = jet velocity,

v_v = vehicle velocity,

M_∞ = free stream Mach No.,

c = speed of sound,

ρ = ambient density of air,

p = rms sound pressure,

W = acoustic power.

Theoretical studies about the effect of motion on the noise source resulted in the prediction of a forward radiation increasing with the Mach No. at subsonic speed (2 and 3). Different multiplicators for the sound pressure level were derived, depending on the type of elementary noise sources (quadrupoles or dipoles) and on the orientation of their axes relative to the direction of motion. In our analysis, the rms pressure was assumed to be proportional to the factor $1/(1-M_\infty)$ for points upstream of the nozzle exit. This is obtained by putting $\theta = 180°$ in Eq. (26) of Ref. (3).

$$p \sim \frac{1}{1 - M_\infty} . \qquad (3)$$

It has to be pointed out that this proportionality holds only for dipoles and for subsonic speed below a Mach No. of 0.9. It results in an increase of the noise field in front of the moving noise source. Application of this correction to noise field predictions of this or similar types of manned vehicles might require a revision as soon as airborne noise field measurements of rocket powered vehicles have been evaluated.

Finally, for a cluster of n booster rocket engines, the total rms sound pressure p_t will be

$$p_t \sim \sqrt{n} \cdot p , \qquad (4)$$

and combination of Eqs. (1 - 4) results in

$$p_t^2 = n \cdot p_o^2 \left[\left(\frac{1 - M_\infty \frac{c}{v_j}}{1 - M_\infty} \right)^2 \times \left(\frac{\rho c}{\rho_o c_o} \right) \right] . \qquad (5)$$

The subscript o refers to the quantities of a single rocket at sea level. Application of this equation to the boost phase of the rocket powered vehicle with a jet velocity $v_j = 8000$ fps shows that the effect of motion predominates over the influence of the other quantities. Hence, an increase of the overall SPL to 142 db at Mach 0.9 can be expected and is indicated as the first peak in the noise time history. The contribution of the turbulent boundary layer to the noise level is included in this curve.

NOISE SOURCES IN SUPERSONIC FLIGHT

The principal sources of noise in the supersonic phase of the flight are the irregular fluctuations in the turbulent boundary layer. In order to understand this mechanism we must discuss the nature of the flow field around the body when it is moving supersonically.

Figure 3 is a shadowgram of the supersonic flow about a blunt body showing the detached shock wave and the boundary layer. The transition area between laminar and turbulent flow in the boundary layer is indicated. Figure 4 is a schematic representation of the flow. Outside the shock wave the flow is undisturbed. The air passing through the almost normal portion of the shock is heated, compressed, and slowed down. In the region of subsonic flow, which is bounded by the sonic lines, the flow field is very similar to the conventional incompressible flow around a similar body. Further back where the incoming air crosses the shock wave at a small angle, the change in temperature, density, and velocity across the shock is small and the flow resembles that over a flat plate. After crossing the shock wave, the flow along each streamline is isentropic, but the entropy is different on each streamline, being determined by the inclination of the shock wave.

Except in the boundary layer, the flow can be computed on the basis of inviscid theory and this calculation will give the shape of the detached shock and the pressure distribution on the body. The inviscid calculation uses the boundary condition on the body that there is no normal velocity, but cannot satisfy the physical condition that there is no tangential velocity. The boundary layer is a thin region close to the wall where the tangential velocity falls rapidly from the inviscid value to zero. Two typical flow profiles in the boundary layer for laminar

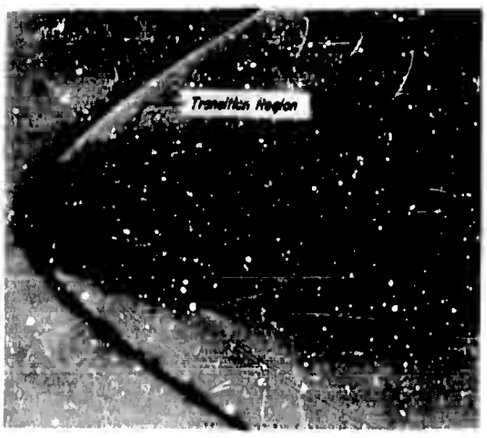

Fig. 3 - Shadowgraph of a supersonic flow field around a blunt body. (Courtesy U. S. Naval Ordnance Laboratory.)

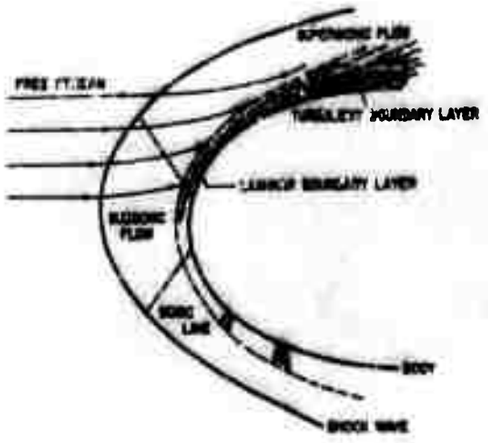

Fig. 4 - A schematic representation of the flow field around a blunt body

and turbulent flow are indicated in Fig. 4. This region is important in determining the friction and heat transfer, and has been studied extensively from that viewpoint. The turbulent boundary layer is also important as a source of aerodynamic noise but relatively little work has been done on this aspect. The noise is dependent on the random fluctuations in the turbulent flow and these are more difficult to study than the mean properties which determine heat transfer and skin friction.

Figure 5 shows a hot wire record of the fluctuations in an incompressible boundary layer at various positions. The change from the periodic oscillations (attributed to amplification of tunnel noise) in the laminar portion to the typical random turbulent pattern is illustrated.

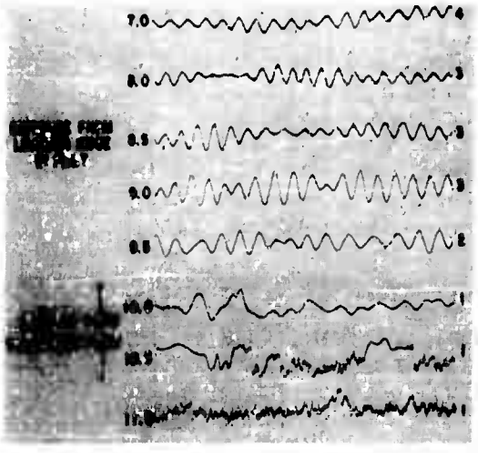

Fig. 5 - Hot-wire records of turbulent fluctuations in incompressible flow. (Courtesy of National Bureau of Standards.)

Unfortunately, at the present time the theory of turbulent shear flow is not developed sufficiently to predict accurately when the boundary layer will be turbulent. At the relatively low altitudes where we have intense noise, the boundary layer will be turbulent over most of the vehicle, but as the altitude increases the transition point moves back. When the dynamic pressure has its maximum, the transition point will be about 3 feet from the stagnation point and the cockpit will be completely surrounded by a turbulent boundary layer.

The random boundary layer fluctuations have been described in the literature as "pseudosound" (4 and 5). While they register on a receiver as sound, their propagation and attenuation differs from sound waves. These fluctuations excite a forced oscillation of the wall which generates sound in the interior. Analyses of this mechanism have been published by Corcos & Liepmann (6), and by Ribner (5). However, because of lack of knowledge of the structure of the turbulence, it is not possible to compute the interior sound level in terms of the external flow and panel parameters if double wall panels are used.

CALCULATION OF BOUNDARY LAYER NOISE

For practical calculations we have used empirical results, based on subsonic flow experiments that the ratio K of the fluctuating surface pressure p, produced by a turbulent

boundary layer, to the local dynamic pressure q_ℓ is independent of Mach No., Reynolds No., and boundary layer thickness. Measurements indicate values between 4.5×10^{-3} to 6×10^{-3} (7, 8). The higher value has been reported by NASA in recent experiments, conducted in a duct, where no appreciable difference between local and free stream dynamic pressure exists. This value was applied to our analysis. An approach to calculate and locate the maximum of the local dynamic pressure is given in the next paragraphs.

Certain general statements can be made concerning the local dynamic pressure, q_ℓ, behind the shock and on the surface of a blunt body. The local dynamic pressure,

$$q_\ell = \frac{1}{2} \rho_\ell V_\ell^2 = \frac{\gamma}{2} p_\ell M_\ell^2 ,$$

is zero at the stagnation point where the local velocity, V_ℓ, is zero, but increases as the flow expands along the body surface reaching a maximum value at some point on the curved surface. Continued expansion beyond this point results in a progressively decreasing local dynamic pressure.

In order to analyze the flow over a blunt body, it is possible to use the theory of Newtonian flow. This theory relates the local static pressure, p_ℓ, on the body surface, to the stagnation pressure aft of the shock (Eq. 1 in Appendix) as a function of the local body contour angle θ_ℓ, shown in Fig. 6. Using the Newtonian flow theory in conjunction with the isentropic flow equations for the expanding flow (Eq. 5) permits a calculation of the ratio of the local dynamic pressure at some point on the blunt nose surface to the pressure at the stagnation point.

$\frac{p_\ell}{p_s} = \sin^2 \theta_\ell$

p_ℓ = LOCAL STATIC PRESSURE
p_s = STAGNATION PRESSURE
θ_ℓ = LOCAL CONTOUR ANGLE

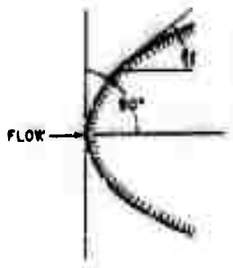

Fig. 6 - Modified Newtonian Equation

This expression together with the normal shock relationship (Eq. 6), relating the stagnation pressure aft of the shock to the free stream ambient pressure, combines to give the ratio of the local dynamic pressure to the free-stream ambient pressure (Eq. 8). Since the free-stream dynamic pressure, q_∞, can also be expressed in terms of the ambient pressure and free-stream Mach No., the ratio of the local dynamic pressure to the free-stream dynamic pressure (Eq. 9), may be derived for any given flight Mach No. and ambient pressure. It should be pointed out that this application of the Newtonian theory is restricted to the forward portion of the body, that is, in the region of large local contour angles. Consequently, for aft portions of the body where this angle is less than 10°, the local static pressure must be estimated from other data.

It has already been stated that the maximum free-stream dynamic pressure corresponds to a flight Mach No. of 2.00. Figure 7A,

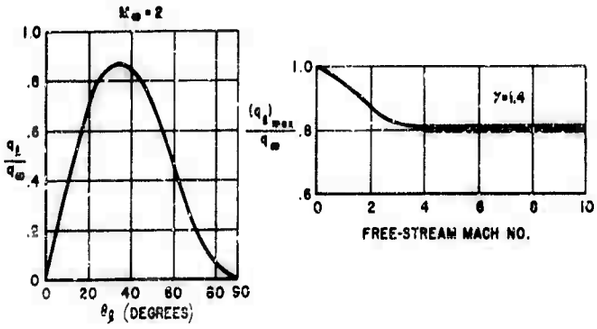

Fig. 7 - Ratio of local dynamic pressure to free-stream dynamic pressure as a function of contour angle for a blunt nose body and free-stream Mach Number. (q_ℓ = local dynamic pressure, q_∞ = free-stream dynamic pressure, and θ_ℓ = local contour angle.)

a plot of (q_ℓ/q_∞) versus θ_ℓ at this given Mach No., indicates a maximum value of (q_ℓ/q_∞) at $\theta_\ell = 35°$. An investigation of the quantity $(q_\ell/q_\infty)_{max}$ discloses that it decreases with increasing Mach No. as shown in Fig. 7B. In view of this, it appears, that for our configuration, the maximum local dynamic pressure occurs on the forward part of the cockpit at a flight Mach No. of 2.00. The estimates presented in this paper are based on this maximum value of the local dynamic pressure.

The spectral distribution was estimated by using a typical power spectrum measured in a subsonic turbulent boundary layer (7). The dimensionless spectral density is plotted versus the dimensionless frequency (Fig. 8). Application of this graph requires the boundary layer displacement thickness δx. This quantity is a function of Mach and Reynold's No. The incompressible boundary layer thickness is given by

$$\delta_1 = 0.38 \times R_c^{-\frac{1}{5}},$$

where x = distance from stagnation point, and must be corrected for compressibility (9) by the top curve in Fig. 9. The lower curve shows the ratio of displacement thickness to boundary layer thickness versus Mach No. For our cockpit configuration, the displacement thickness is 0.13 inch where maximum boundary layer noise is encountered.

From this quantity, the high-frequency part of the boundary layer noise spectrum

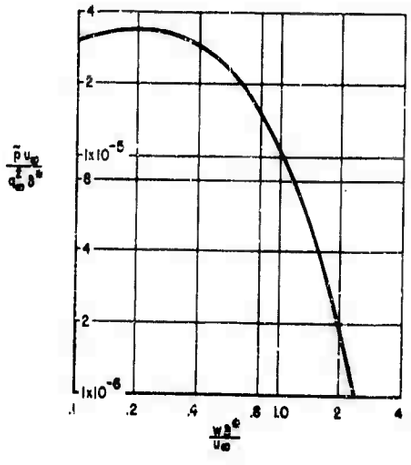

Fig. 8 - Power spectrum of fluctuating wall pressure in a turbulent boundary layer at u_∞ = 761 fps; q_∞ = 507 lb/ft^2; δ^* = .0073 ft. (Courtesy of NASA.)

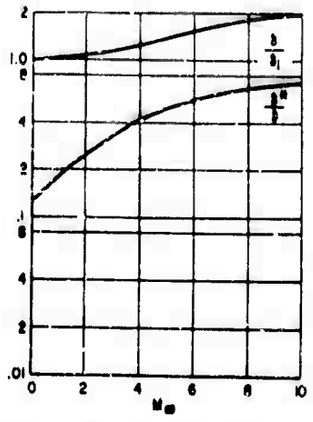

Fig. 9 - Effect of free-stream Mach Number on thickness associated with boundary layer. (δ = thickness of compressible boundary layer; δ_1 = thickness of incompressible boundary layer at same Reynolds Number; δ^* = displacement thickness.

was calculated (Fig. 10). Since it does not include low frequencies, the low octave bands were estimated from unpublished measurements performed by WADC. The complete spectrum is very flat, extends far into the ultrasonic range and peaks between 3000 and 6000 cps. It is compared with the booster engine noise spectrum at a distance of 100 feet upstream, the approximate location of the cockpit.

EXTERNAL OVERALL NOISE LEVELS

The external overall noise levels during ascent and descent are demonstrated in Fig. 11. During the first seconds, the booster engine noise level will decrease by several db's, the difference between the values obtained under static firing and free-field condition. With increasing vehicle speed, the rocket engine noise increases because the effect of motion of the noise source predominates. It results in a first peak that drops sharply at Mach 1 to the boundary layer noise. The exact level between M = 0.9 and M = 1 is uncertain. A second flat peak coincides with the maximum of the local dynamic pressure at M_∞ = 2.0. The overall levels will never exceed 145 db, and the duration of intense noise (above 125 db) is limited to 2 minutes.

During descent, a continuously increasing boundary layer noise will be observed. The

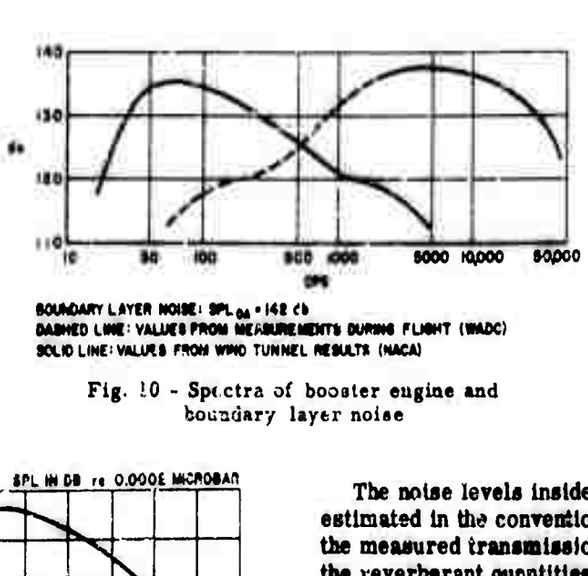

Fig. 10 - Spectra of booster engine and boundary layer noise

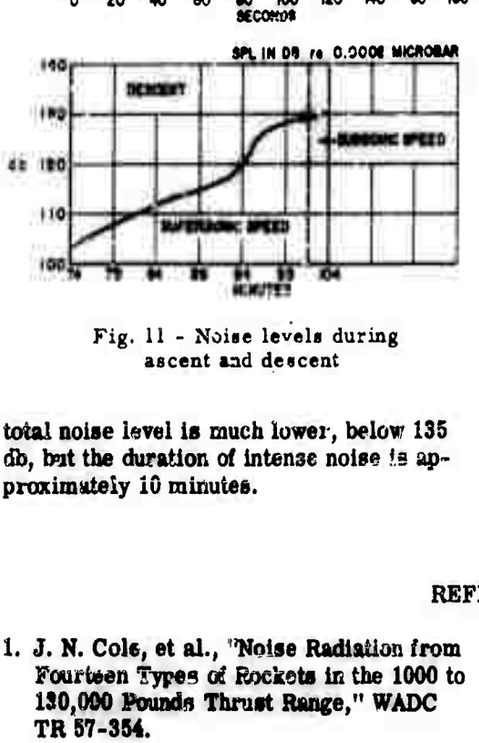

Fig. 11 - Noise levels during ascent and descent

total noise level is much lower, below 135 db, but the duration of intense noise is approximately 10 minutes.

The noise levels inside the cockpit were estimated in the conventional manner from the measured transmission loss of the panel, the reverberant quantities of the inner walls, and the characteristic impedance of the cockpit atmosphere. The last quantity decreases during ascent from sea level pressure to 5 psi. This pressure will be kept constant during the global flight.

On the basis of our analysis of the internal noise levels, no temporary hearing loss is anticipated for this type of boost-glide vehicle. Also, satisfactory communication can be maintained if a pressure suit and a high attenuation helmet are provided. However, electronic equipment may be affected if it is sound-sensitive. In the case of a double wall structure, fatigue damage of the outer wall is not anticipated because of the short duration of the peak noise. Acoustical fatigue tests performed on this type of heat sustaining panels at 150 db did not result in any failures and we will not exceed 145 db.

REFERENCES

1. J. N. Cole, et al., "Noise Radiation from Fourteen Types of Rockets in the 1000 to 130,000 Pounds Thrust Range," WADC TR 57-354.

2. J. J. Lighthill, "On Sound Generated Aerodynamically," Proc. Royal Soc. of London, 211, A, 1952, p. 504.

3. H. L. Oestreicher, "The Field of a Spatially Extended Moving Sound Source," J. Acous. Soc. of Am. 29:1223, 1957.

4. D. I. Blokhintsev, "Acoustics of Nonhomogeneous Moving Medium," NACA TM 1399, Feb. 1956.

5. H. S. Ribner, "Boundary Layer Induced Noise in the Interior of Aircraft," UTIA Report No. 37, April 1956.

6. G. M. Corcos and H. W. Liepmann, "On the Transmission Through a Fuselage of Boundary Layer Noise," Douglas Aircraft Report SM 19570, December 1955.

7. W. W. Willmarth, "Space-Time Correlations and Spectra of Wall Pressure in a Turbulent Boundary Layer," NASA Memo 3-17-59W, March 1959.

8. E. E. Callaghan, "An Estimate of the Fluctuating Surface Pressures Encountered in the Re-entry of a Ballistic Missile," NACA TN 4315, July 1958.

9. H. U. Eckert, "Characteristics of the Turbulent Boundary Layer on a Flat Plate in Compressible Flow from Measurements of Friction in Pipes," J.I.A.S. 17:573, September 1950.

APPENDIX

DERIVATION OF THE RATIO OF THE SURFACE LOCAL DYNAMIC PRESSURE TO FREE STREAM DYNAMIC PRESSURE

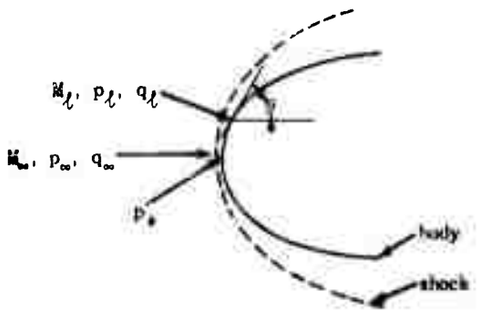

M = Mach No.

p = static pressure

q = dynamic pressure

Subscripts:

∞ = free stream values

ℓ = local values

s = stagnation value

Considering the application of a modified form of the Newtonian relationship between the local pressure and the stagnation pressure aft of the shock results in the following expression:

$$\frac{p_\ell}{p_s} = \sin^2\theta_\ell \,. \qquad (1)$$

From isentropic flow relationships

$$\frac{p_\ell}{p_s} = \left(1 + \frac{\gamma-1}{2} M_\ell^2\right)^{-\frac{\gamma}{\gamma-1}} , \qquad (2)$$

where $\gamma = 1.4$ is the ideal gas value of the ratio of specific heats. By definition, the local dynamic pressure is

$$q_\ell = \frac{\gamma}{2} p_\ell M_\ell^2 \,. \qquad (3)$$

Combining Eqs. (1) and (2) results in

$$\frac{p_\ell}{p_s} = \sin^2\theta_\ell = \left(1 + \frac{\gamma-1}{2} M_\ell^2\right)^{-\frac{\gamma}{\gamma-1}}$$

$$(\sin^2\theta_\ell)^{-\frac{\gamma-1}{\gamma}} = 1 + \frac{\gamma-1}{2} M_\ell^2$$

$$M_\ell^2 = \left[(\sin^2\theta_\ell)^{\frac{1-\gamma}{\gamma}} - 1\right] \frac{2}{\gamma-1} \,. \qquad (4)$$

Substituting Eqs. (4) and (1) into (3) gives the expression (q_ℓ/p_s)

$$q_\ell = \frac{\gamma}{2} p_\ell \left[(\sin^2\theta_\ell)^{\frac{1-\gamma}{\gamma}} - 1\right] \frac{2}{\gamma-1}$$

$$q_\ell = \frac{\gamma}{2} (p_s \sin^2\theta_\ell) \left[(\sin^2\theta_\ell)^{\frac{1-\gamma}{\gamma}} - 1\right] \frac{2}{\gamma-1}$$

$$\frac{q_\ell}{p_s} = \frac{\gamma}{\gamma-1} (\sin^2\theta_\ell) \left[(\sin^2\theta_\ell)^{\frac{1-\gamma}{\gamma}} - 1\right] . \qquad (5)$$

From normal shock equations

$$\frac{p_s}{p_\infty} = \left[(\gamma + 1)\,\frac{M_\infty^2}{2}\right]^{\frac{\gamma}{\gamma-1}} \left[\frac{\gamma + 1}{2\gamma M_\infty^2 - (\gamma - 1)}\right]^{\frac{1}{\gamma-1}} \quad (6)$$

Also by definition

$$q_\infty = \frac{\gamma}{2}\, p_\infty M_\infty^2 \,. \quad (7)$$

Substituting Eq. (6) into Eq. (5)

$$\frac{q_\ell}{p_\infty} = \frac{\gamma}{\gamma - 1}\,(\sin^2\theta_\ell)\left[(\sin^2\theta_\ell)^{\frac{1-\gamma}{\gamma}} - 1\right] \left[\frac{(\gamma+1)\,M_\infty^2}{2}\right]^{\frac{\gamma}{\gamma-1}} \left[\frac{\gamma + 1}{2\gamma M_\infty^2 - (\gamma - 1)}\right] \quad (8)$$

Eliminating p_∞ between Eqs. (7) and (8) gives the desired expression (q_ℓ/q_∞).

$$\frac{q_\ell}{q_\infty} = \frac{2\,\sin^2\theta_\ell}{M_\infty^2(\gamma - 1)}\left[(\sin^2\theta_\ell)^{\frac{1-\gamma}{\gamma}} - 1\right] \left[\frac{(\gamma + 1)\,M_\infty^2}{2}\right]^{\frac{\gamma}{\gamma-1}} \left[\frac{\gamma + 1}{2\gamma M_\infty^2 - (\gamma - 1)}\right]^{\frac{1}{\gamma-1}} \quad (9)$$

* * *

APPLICATION OF THE VIBRATION ABSORBER PRINCIPLE FOR THE PROTECTION OF AIRBORNE ELECTRONIC EQUIPMENT

Harry R. Spence and James H. Winters
Space Technology Laboratories, Inc.
Los Angeles, California

A novel application of the vibration absorber principle for the vibration protection of airborne electronic component parts and subassemblies with particular reference to circuit boards is presented. The mathematics for the solution of this problem covers any base excited, damped two-mass system. The application of this solution is extended, through the use of an equivalent mass concept, to include multiresonant systems where the fundamental resonance is of primary concern.

The principle is illustrated through the application of a vibration absorber on a circuit board, and readily applied design information has been generated for this type of application. A dramatic decrease in vibration transmission is obtained for this case with vibration absorbers comparable in size and weight to subminiature component parts. Typical numbers for this would be a 400 percent reduction in transmissibility for 3 percent increase in weight.

The vibration absorber is expected to have its most fruitful application as a "fix" on existing designs; however, planned use is also anticipated for some applications.

INTRODUCTION

In contrast to the time-honored approach to vibration protection of electronic equipment through controlling the transmission path, the vibration absorber concept consists of adding an appendage to the end of the path. Figure 1a and b illustrate the contrast.

The vibration absorber does not provide the same degree of vibration control which may be obtained at the transmission path; however, sufficient control may be derived to make it practical for many applications. Specifically, its application is preferred for areas where altering the transmission path is undesirable or impractical and, secondly, for cases where vibration control has to be supplied to existing hardware. An example for both cases is a circuit board. The vibration transmission through the circuit board from its support to a certain component part (say at the antinode of the board) may be altered by changing the board material, the board thickness, or the supports. Generally, all three changes have the effect of shifting the frequency at which the maximum Q occurs without materially affecting the Q. The vibration absorber, on the other hand, reduces the maximum Q without altering significantly the frequency at which it occurs. Keeping the resonance frequency the same is often of no particular consequence; however, there are occasions when this is desirable. If for instance, the fundamental resonance frequency of the circuit board is

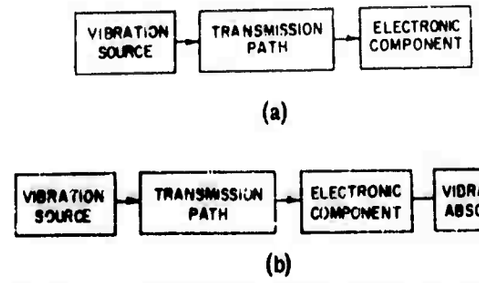

Fig. 1 - Vibration control through adjustment of (a) transmission path and (b) vibration absorber

optimum from the standpoint of component part fragilities, it may be necessary to reduce Q while holding the resonance frequency the same. The reduction of Q through the application of a vibration absorber on a circuit board is illustrated in the body of this presentation.

NOTATION

m_e = main mass, $FL^{-1}T^2$

m_a = absorber mass, $FL^{-1}T^2$

k_e = main mass stiffness coefficient, FL^{-1}

k_a = absorber mass stiffness coefficient, FL^{-1}

c_e = main mass damping coefficient, $FL^{-1}T$

c_a = absorber mass damping coefficient, $FL^{-1}T$

x_o = base displacement, L

x_e = main mass displacement, L

x_a = absorber mass displacement, L

A_o = base displacement amplitude, L

A_e = main mass displacement, L

A_a = absorber mass displacement, L

ω = forcing frequency, T^{-1}

ω_e = main mass undamped natural frequency, T^{-1}

ω_a = absorber mass undamped natural frequency, T^{-1}

DAMPED VIBRATION ABSORBER AND MAIN MASS WITH BASE EXCITATION

The dynamic system which is treated in this presentation is shown schematically in Fig. 2. The equations of motion for this system may be written

$$\ddot{x}_e m_e + c_e(\dot{x}_e - \dot{x}_o) + k_e(x_e - x_o) + c_a(\dot{x}_e - \dot{x}_a) + k_a(x_e - x_a) = 0, \quad (1)$$

$$\ddot{x}_a m_a + c_a(\dot{x}_a - \dot{x}_e) + k_a(x_a - x_e) = 0. \quad (2)$$

For a sinusoidal base excitation

$$x_o = A_o \sin \omega t. \quad (3)$$

Substituting Eq. (3) into Eq. (1) and utilizing the following identities,

$$\beta_e \equiv \frac{c_e}{2m_e\omega_e}, \quad \beta_a \equiv \frac{c_a}{2m_a\omega_a}, \quad \mu \equiv \frac{m_a}{m_e},$$

$$k_e = \omega_e^2 m_e, \quad k_a = \omega_a^2 m_a,$$

Eqs. (4) and (5) are obtained

$$\ddot{x}_e + 2\dot{x}_e(\beta_e\omega_e + \mu\beta_a\omega_a) + x_e(\omega_e^2 + \mu\omega_a^2) - \mu\omega_a(2\beta_a\dot{x}_a + \omega_a x_a) = \omega_e A_o(2\beta_e\omega \cos \omega t + \omega_e \sin \omega t), \quad (4)$$

$$\ddot{x}_a + 2\beta_a\omega_a\dot{x}_a + \omega_a^2 x_a - 2\beta_a\omega_a\dot{x}_e - \omega_a^2 x_e = 0. \quad (5)$$

Applying the Laplace Transform to Eqs. (4) and (5) and letting initial displacements and velocities be zero, leads to Eqs. (6) and (7).

$$\bar{x}_e[s^2 + 2S(\beta_e\omega_e + \mu\beta_a\omega_a) + (\omega_e^2 + \mu\omega_a^2)] - \mu\omega_a\bar{x}_a(2\beta_a S + \omega_a) = \omega_e A_o \mathcal{L}(2\beta_e\omega \cos \omega t + \omega_e \sin \omega t), \quad (6)$$

$$\bar{x}_o[2\beta_a\omega_a S + \omega_a^2] - \bar{x}_a[S^2 + 2\beta_a\omega_a S + \omega_a^2] = 0. \quad (7)$$

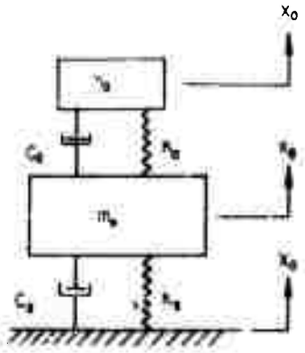

Fig. 2 - The dynamic system

For a steady-state solution $S = j\omega$, and Eqs. (6) and (7) become

$$x_e[(\omega_e^2 + \mu\omega_a^2 - \omega^2) + 2j\omega(\beta_e\omega_e + \mu\beta_a\omega_a)] - x_a\mu\omega_a[\omega_a + 2j\beta_a\omega] = \omega_e A_o[2\beta_e\omega\cos\omega t + \omega_e \sin\omega t], \quad (8)$$

$$x_e\omega_a[\omega_a + 2j\beta_a\omega] - x_a[(\omega_a^2 - \omega^2) + 2j\beta_a\omega_a\omega] = 0. \quad (9)$$

Solving Eqs. (8) and (9) for x_e/A_o and taking its peak value (A_e/A_o) results in the following expression:

$$\frac{A_e}{A_o} = \frac{\frac{\omega_e}{\omega}\sqrt{\left(\frac{\omega_e}{\omega}+4\beta_e^2\right)\left\{\left[\left(\frac{\omega_a}{\omega}\right)^2-1\right]^2+4\beta_a^2\left(\frac{\omega_a}{\omega}\right)^2\right\}}}{\sqrt{\left\{\left(\frac{\omega_e}{\omega}\right)^2\left[\left(\frac{\omega_a}{\omega}\right)^2-1\right]-\left(\frac{\omega_a}{\omega}\right)^2(\mu+1)-4\frac{\omega_e}{\omega}\frac{\omega_a}{\omega}\beta_e\beta_a+1\right\}^2 + 4\left\{\left(\frac{\omega_e}{\omega}\right)\left(\beta_e\left[\left(\frac{\omega_a}{\omega}\right)^2-1\right]+\frac{\omega_e}{\omega}\frac{\omega_a}{\omega}\beta_a\right)-\frac{\omega_a}{\omega}\beta_a(\mu+1)\right\}^2}}. \quad (10)$$

By letting $g = \omega/\omega_e$ and $f = \omega_a/\omega_e$, Eq. (10) can be brought into a form similar to Den Hartog's (1) for a main mass excited system.

$$\frac{A_e}{A_o} = \frac{\sqrt{\left[1+(2g\beta_e)^2\right]\left[(f^2-g^2)^2+(2\beta_a gf)^2\right]}}{\sqrt{\left[f^2-g^2-(fg)^2(\mu+1)-4fg^2\beta_e\beta_a+g^4\right]^2 + 4g^2\left[\beta_e(f^2-g^2)+f\beta_a-fg^2\beta_a(\mu+1)\right]^2}}, \quad (11)$$

where

A_e/A_o = transmissibility

β_e = percent critical damping, main mass

β_a = percent critical damping, absorber

f = natural frequency, absorber/natural frequency, main mass

g = forcing frequency/natural frequency, main mass

$\mu = m_a/m_e$.

To obtain $(A_e/A_o)_{max}$ Eq. (11) must now be maximized with respect to g. This operation was found to be very laborious and was therefore set up on an analog computer. The computer solution provided the g corresponding to the $(A_e/A_o)_{max}$ for optimum f and β_a values. These computer solutions are shown graphically in Figs. 3a, b, c, and d. It can be seen in these figures that for the range of μ and β_e considered, $f = 0.95$ for optimum conditions. With the values of f, g, and β_a established from the computer solution, it is possible to solve Eq. (11) for $(A_e/A_o)_{max}$ in terms of μ and β_e. Figure 4 depicts $(A_e/A_o)_{max}$ for typical values of μ and β_e. For design purposes of the absorber system it is necessary to know the maximum relative motion between the absorber and the main mass, i.e., $(A_a - A_e)_{max}$ or in normalized form $[(A_a - A_e)/A_o]_{max}$. Similar to the derivation for $(A_e/A_o)_{max}$ the equation for maximum relative motion is derived from Eqs. (8) and (9). The steps in arriving at the final equation below are omitted for the sake of brevity.

$$\frac{A_a - A_e}{A_o} = \frac{g^3\sqrt{1+(2\beta_e g)^2}}{\sqrt{\left[f^2-g^2-g^2f^2(1+\mu)+g^4+4\beta_e\beta_a g^2 f\right]^2 + 4g^2\left[\beta_e(f^2-g^2)+f\beta_a-fg^2\beta_a(\mu+1)\right]^2}}. \quad (12)$$

As for the computation for $(A_e/A_o)_{max}$ the same computer solutions for g, f, and β_a are applied in Eq. (12). Values for $[(A_a - A_e)/A_o]_{max}$ have been determined for the same typical values of μ and β_e as for $(A_e/A_o)_{max}$ and are given in Fig. 5. The optimum absorber mass damping β_a associated with $(A_e/A_o)_{max}$ and $[(A_a - A_e)/A_o]_{max}$, is given in Fig. 6 as a function of the mass ratio μ.

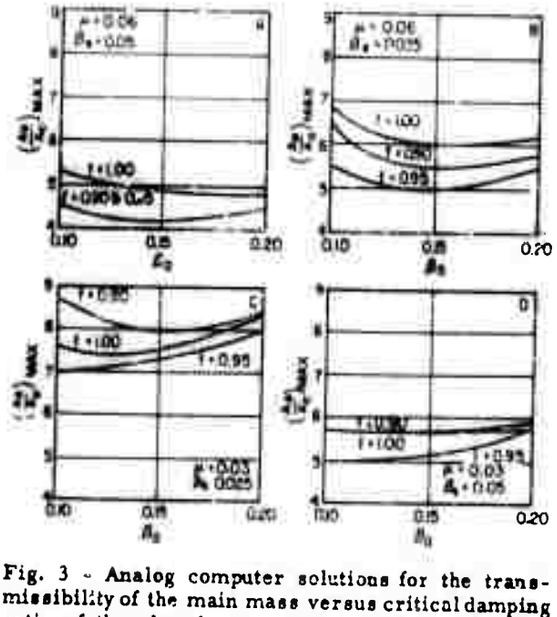

Fig. 3 - Analog computer solutions for the transmissibility of the main mass versus critical damping ratio of the absorber system for various constant mass ratios and main system critical damping ratios

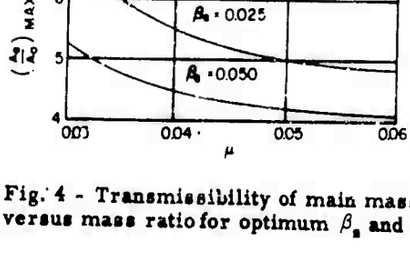

Fig. 4 - Transmissibility of main mass versus mass ratio for optimum β_a and f

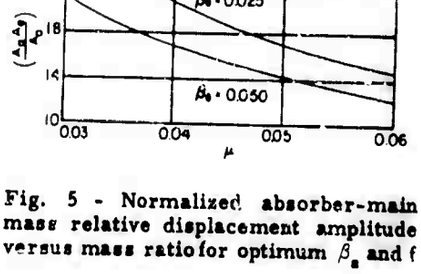

Fig. 5 - Normalized absorber-main mass relative displacement amplitude versus mass ratio for optimum β_a and f

DESIGN ILLUSTRATION FOR A VIBRATION ABSORBER SYSTEM

In approaching an absorber system design, the designer must know three things about the structural member whose vibration is to be controlled by a vibration absorber. These are:

1. The frequency of its resonance,
2. The effective mass of the resonant member,
3. The damping of the resonant member.

For simple structural members, items 1 and 2 can be calculated, and 3 can be found in material handbooks. For complicated structural members or if the structural member is at hand, a simple vibration test will provide

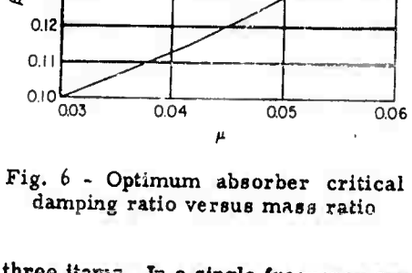

Fig. 6 - Optimum absorber critical damping ratio versus mass ratio

all three items. In a single frequency sweep test, the transmissibility of the resonant member $(A_e'/A_o)_{max}$ and the corresponding resonant frequency (ω_e) are easily determined. For a lightly damped resonator $(\beta_e < 0.1)$,

$$\beta_e \cong \frac{1}{2\left(\frac{A_e'}{A_o}\right)_{max}}, \qquad (13)$$

where $(A_e'/A_o)_{max}$ is the transmissibility of the resonant member without the vibration absorber.

For a distributed mass resonator the effective mass is equal to the mass of a one-degree-of-freedom system with identical kinetic energy at resonance. The expression for this is

$$m_e = \frac{1}{a_e^2} \sum_{i=1}^{k} \Delta m_i a_i^2 , \qquad (14)$$

where

m_e = effective mass

Δm_i = mass of the i^{th} portion of the distributed mass

a_i = displacement amplitude of Δm_i at resonance, i.e., at ω_e

a_e = displacement amplitude at antinode of structural member which should also be the absorber system location

In Eq. (14), a_i and a_e is determined experimentally and Δm_i may be measured or calculated. The application of Eq. (14) is best illustrated by an example. Consider a circuit board supported along two opposite edges as shown in Fig. 7a. Imagine this circuit board divided into sections as indicated by the dotted lines in Fig. 7a with the mass of each section lumped at the cg as shown in Fig. 7b. With a vibration probe the peak deflection may then be measured at each cg location. It must be remembered that these deflection measurements are made with the circuit board at the resonance to which the absorber system is to be tuned. This approach is perfectly general and holds for any mode shape. For a large number of Δm, it may be profitable to tabulate the data on a form such as that illustrated in Fig. 8. The number of Δm_i must be chosen with discretion. Too large a number may be unnecessarily cumbersome while too small a number may introduce too large an error in m_e.

Once m_e, ω_e, and β_e have been determined, it is possible to obtain all necessary design information for the absorber system from Figs. 4, 5, and 6 (within the range of the curves presented). The following four steps should provide all the information necessary for the design of the absorber system.

1. Corresponding to a desired transmissibility of the main mass system $(A_e/A_o)_{max}$ read a μ in Fig. 4.

2. Solve for m_a and k_a by using the expressions below.

$$m_a = \mu m_e ,$$
$$k_a \geq (0.95\ \omega_e)^2 m_a . \qquad (15)$$

(For the range of μ and β_e considered in this presentation $f = 0.95$ without serious loss of engineering accuracy.)

3. Obtain $[(A_a - A_e)/A_o]_{max}$ from Fig. 5 and solve for the minimum allowable excursion of m_a by using the following expression:

$$D = 2A_o \left(\frac{A_a - A_e}{A_o} \right)_{max} , \qquad (16)$$

where

D = minimum allowable excursion of absorber system,

$2A_o$ = double displacement amplitude of sinusoidal base vibration.

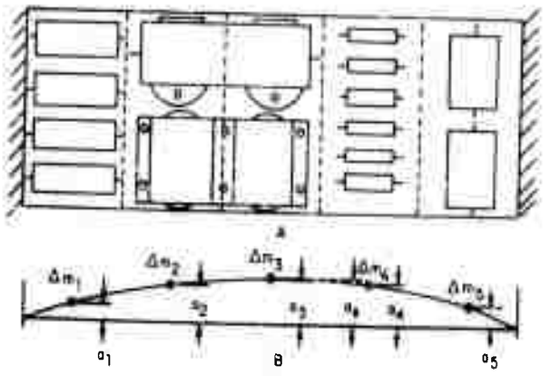

Fig. 7 - Example of deflection measurements

:	Δm_i	a_i	a_i^2	$\Delta m_i a_i^2$
1				
2				
3				
h				

$\sum_{i=1}^{h} \Delta m_i a_i^2 =$ _____

Fig. 8 - Form for tabulating a large number of Δm

4. Obtain absorber critical damping ratio β_a from Fig. 6.

During the physical design of the absorber system some experimentation may be necessary to check the parameters ω_a and β_a. This check is in principle the same as the determination of ω_e and β_e for the main mass.

Based on the design data presented herein an absorber system was constructed and tested. Figure 9 depicts the design of this absorber system. It consists of a thin acrylic tube closed at both ends which houses two compressed coil springs separated by a steel ball. In addition to the ball and the springs, the tube is partially filled with a silicone oil. Clearance between the ball and the tube allows the oil to pass to either side of the ball when the ball is in motion. The correct clearance and ratio oil volume to total volume had to be determined to avoid excessive spring and mass effects of the oil. To demonstrate the effectiveness of this vibration absorber design, vibration transmissibility measurements were made on a

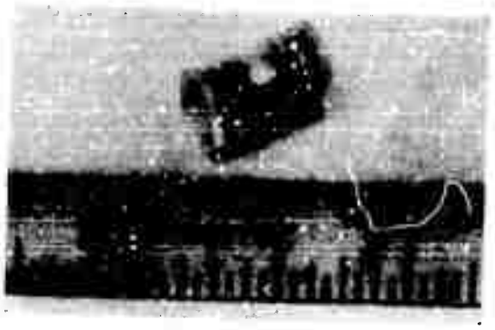

Fig. 9 - Vibration absorber system

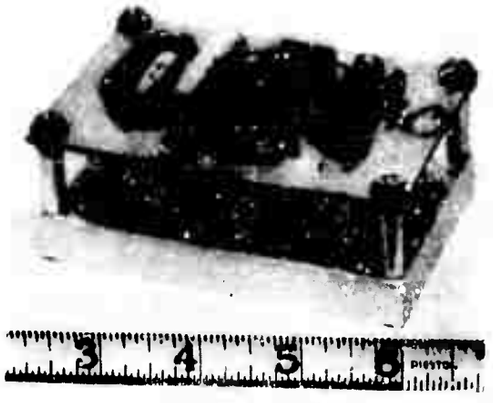

Fig. 10 - Circuit board with vibration absorber attached

circuit board with and without the absorber in place. The circuit board with the absorber in place is shown in Fig. 10 and transmissibility plots corresponding to these two configurations in Fig. 11. This illustrates that an absorber system having a mass comparable

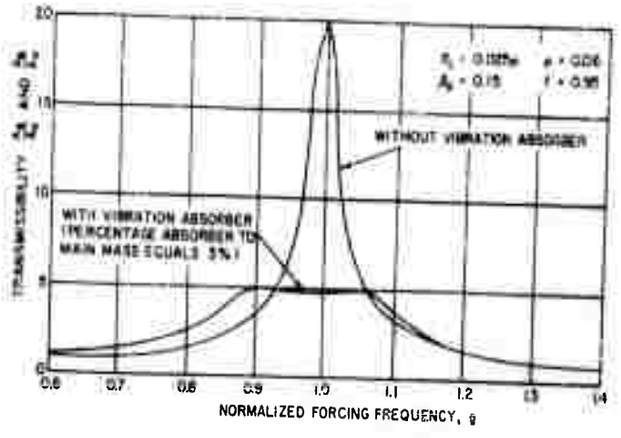

Fig. 11 - Transmissibility vs normalized forcing frequency plot for circuit board with and without absorber system

to that of a subminiature component part can very appreciably reduce the Q of a circuit board and thus provide an improved vibration environment for the board and mounted components. Figure 11 illustrates a 400 percent reduction in transmissibility at the expense of a 3 percent increase in weight. Greater convenience in the application of the absorber system may be envisaged in the form of ready-made absorber systems (such as the type illustrated) covering a certain range of absorber mass, natural frequency, and damping ratio. Much like the selection of a resistor or capacitor, an absorber system, suitably marked for identification, may be readily selected for each application.

CONCLUSION

Although the virtues of the vibration absorber application to circuit boards and other electronic assemblies appear very promising, the designer is cautioned not to rely on the vibration absorber as a crutch for poor design.

In the case of circuit boards, for instance, the principle design criteria is the board deflection at the fundamental resonance. For typical board designs this occurs in the frequency range between 100 and 300 cps. If the fundamental resonance can be controlled, the higher modes are of no particular consequence, since the corresponding deflections become very small. For the sake of illustration a poorly designed board may have its fundamental resonance at 50 cps which can be "taken out" by a vibration absorber; however, the third mode resonance may still cause damage. Transmissibility measurements at the higher modes indicate some improvement due to the absorber; however, more work will have to be done for any conclusive data.

REFERENCE

1. J. P. Den Hartog, "Mechanical Vibration," McGraw-Hill, 1947, pp. 112-131.

DISCUSSION

Mr. Foster (Collins Radio Company): Your device I believe you said was for use in a fix situation. Suppose that you were going into production on something and you could be about 10 percent off in natural frequencies by having tolerances in your manufacturing process, and suppose that you were ten percent off in the manufacture of your little absorber. Have you done any work to indicate any type of reduction that you would get in that situation?

Mr. Winters: Yes. The question was what happens when we have approximately a ten-percent variation in our absorber parameters. The equations presented there and in the paper will allow you to calculate your resulting maximum transmissibility for any parameters that you so desire. You would use 5, 10, 20 percent limits, just depends on what you felt you could work with as manufacturing tolerances.

Mr. Thomas (Lord Manufacturing Company): In your experimental work did you work with any shapes other than the rather simple rectangular board supported on the corner as you showed in your slide, or did you work with any cantilevered boards or anything of that nature?

Mr. Winters: No, we didn't. However, you could use different boards, different shapes, different edge conditions, because the treatment in the paper, for instance when we are computing the effect of mass, is a very general type of approach and can be extended to other edge conditions.

Mr. Thomas: If you didn't do that with your experimental work did you try working out anything to find a more critical type of board where you might have to use two absorbers or what would occur in the case where you had a very long board?

Mr. Winters: I think the question you are asking is, if you have a long board you are actually worried then not only about the first mode, but higher modes, what the effect would be. For all the odd number of modes, first, third, fifth, and so forth, you will derive some degree of protection from the absorber by using the end conditions shown.

For your even numbered modes such as the second, then your absorber would be sitting at the nodal point and would offer no protection. Generally in circuit boards where you figure displacement is your primary enemy, your fundamental mode is the most severe. This is the application we had in mind when we designed the system.

Mr. Yoshimoto (Hughes Aircraft): In your absorber design did you have anything in the way of an artificial method of controlling your damping?

Mr. Winters: The damping was controlled by substituting different viscosities of silicone fluid.

Mr. Yoshimoto: You had fluid in that capsule?

Mr. Winters: Yes. In fact, the one we used here was approximately 125 70 silicone.

Mr. Yoshimoto: What happens versus temperature?

Mr. Winters: That's the reason we used the silicone fluid, because of the small change in viscosity due to temperature. Actually when the temperatures become higher and the viscosity goes down, you will have a corresponding decrease in damping, and you can determine the net result on your circuit board with this decrease in damping from the equations given.

Mr. Yoshimoto: Does the viscosity change too much at minus 65? Is it a fairly reasonable figure there also?

Mr. Winters: Actually we tried it at room temperature. We haven't gone to extended temperatures yet.

Mr. Golueke (Wright Air Development Division): The size of the absorber as related to the dimensions of the circuit board in a perpendicular direction; what are the approximate dimensional penalties involved?

Mr. Winters: Well, this would depend upon the particular design that you had undertaken. One of the problems or parameters that must be examined is this relative motion, and you must permit enough space for your absorber mass to move so that it doesn't bottom. Otherwise you then have a nonlinear phenomena that would throw off your calculations. So for each specific application you have to design the absorber in such a way that you have an optimized mass and damping and clearance ratio for your particular application.

Mr. Preis (Hazeltine Corporation): I read your original paper and I recall you mentioned something about making experiments in order to find the damping ratio. You mentioned also you used silicone fluids. Have you got any method for synthesizing prior to testing to get that damping without doing any test work?

Mr. Winters: Actually we haven't as yet. We used the rule of thumb and we came out with a pretty good looking thumb this time, but I couldn't guarantee anything beyond what we have done already. I am sure that some relationships could be brought about from the amount of clearance you have, the ratio of the clearance between your cylinder and the wall and the viscosity of the fluid that you are using.

* * *

A PRACTICAL APPROACH TO SHOCK MOUNTING

W. G. Soper
Los Alamos Scientific Laboratory
and
R. C. Dove
University of New Mexico

In the design of shock-mounting systems it is desirable, if not mandatory, to have analytical means for evaluating different materials before a full-scale device is built and tested. Unfortunately, mathematical analysis is often difficult. This paper describes an approximate method for solving shock-mounting problems. Application is illustrated by examples, and experimental proof of its validity is given.

INTRODUCTION

The practice of shock-mounting fragile components is becoming increasingly common in today's technology. In the design of shock-mounting systems it is desirable, if not mandatory, to have analytical means for evaluating different materials before a full-scale device is built and tested.

Unfortunately, mathematical analysis of the problem is hampered by several factors. First, there is a scarcity of data on the dynamic behavior of available materials, particularly those which are rate-sensitive. Second, even if data are obtained, it is very difficult to express it in analytical form. Also, the relationships between such variables as stress, strain, and rate of strain are usually nonlinear and create serious mathematical difficulties in the solution of problems.

This paper describes an approximate method for solving shock-mounting problems. A procedure is given for experimentally determining the dynamic stress law of a material. The law is expressed in graphical form with no attempt being made to write it as an equation. A plausible estimate is made of the state of strain in the material of the shock-mounting system. This strain state, together with the stress law, is used to calculate the response of the system to any applied forcing function. The differential equations are solved by numerical procedures.

Application of the method is illustrated by examples, and experimental proof of its validity is given.

By using this method, a sufficient number of examples have been solved to determine how the cushioning effectiveness of a given material will be altered by such variables as cushion thickness, mass supported, duration of loading pulse, etc. This information is present in graphical form.

DEFINITION OF PROBLEM

Figure 1 illustrates the problem under consideration. A rigid case experiences an acceleration pulse $\bar{a}(t)$, where t denotes time. Within the case is a rigid mass m mounted in a flexible material. It is desired to calculate the acceleration response $a(t)$ of the mass. The purpose of the calculations

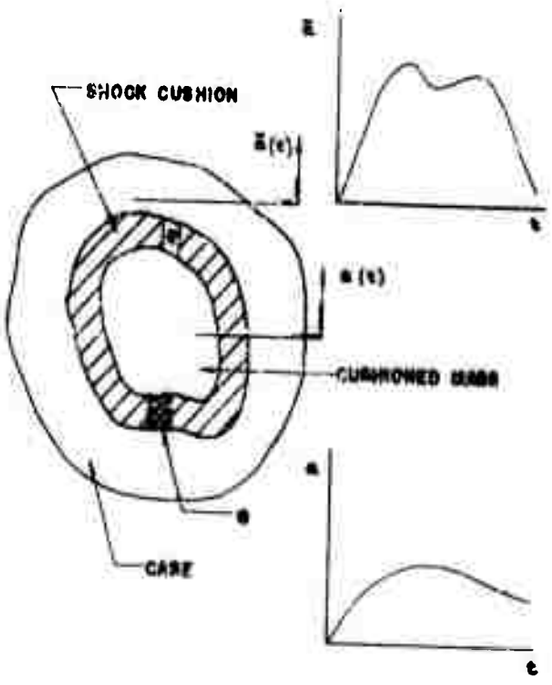

Fig. 1 - Shock-mounting system

is, in most applications, to select a material which will give the smallest peak value of $a(t)$.

In general, the problem involves large deformations of a material of complicated shape and unknown stress law. Certain simplifications concerning the state of strain in the material are necessary before the analysis can proceed. Conditions will be placed on the problem to insure that each material element e is in a state of approximately uniform compression and shear. If variation in strain state occurs from one element to another, it must take place slowly, that is, only over distances comparable to the over-all system dimensions.

It will be assumed that the material thickness everywhere is small compared with the dimensions of the system. This requires the strain to be approximately constant through the thickness of the material, at least under static loading. This will also be true under dynamic loading if the magnitude of the strain waves is small compared with the maximum strain attained. If there are free surfaces of the material, such as around the cavity c in Fig. 1, the strains in the neighborhood of these surfaces may violate the above conditions. The dimensions of this boundary region will be comparable to the material thickness, however, and the effect on the problem as a whole will be insignificant.

The material thickness can vary from point to point, but variations must occur only in distances comparable to over-all system dimensions.

In the special case of compressive or tensile loading of a material exhibiting negligible Poisson effect, the condition on the material dimensions can be relaxed somewhat. Since no strains tend to occur in directions perpendicular to the direction of applied strain, each material element acts independently of the elements adjacent to it. No strain deviation near free surfaces occurs, and the requirement of large lateral dimensions of the material can be dropped. The system dimensions perpendicular to the material must still be large compared with the material thickness, however.

The writers have found that many materials useful in shock mounting exhibit little Poisson effect. The fact that such materials behave the same whether confined or unconfined makes their performance more predictable and simplifies the task of obtaining experimental data on their dynamic behavior. This point will be discussed later.

Figure 2 depicts the assumed state of strain of the material for points sufficiently

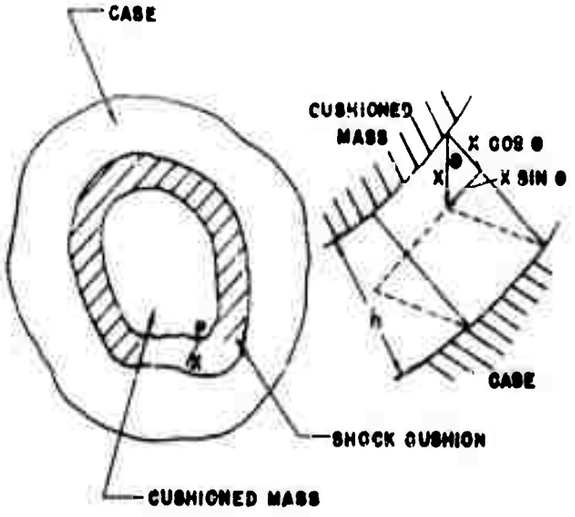

Fig. 2 - Assumed state of strain

far from free surfaces. For an arbitrary displacement, consisting of translation and rotation of the mass m within the case, the displacement of any boundary point p with respect to the case can be calculated. This displacement is denoted by x. The normal to the material surface at the point p makes an angle θ with the direction of x. As a consequence of the displacement x, the material element at point p receives a compressive strain of $\epsilon = (x \cos \theta)/h$ and a shear strain of $\gamma = (x \sin \theta)/h$, since the material is assumed fastened to both the case and the mass. The rates of change of the strains with respect to time are $\dot{\epsilon} = (\dot{x} \cos \theta)/h$ and $\dot{\gamma} = (\dot{x} \sin \theta)/h$, where the dot denotes differentiation with respect to time. Note that the definition of the strains rests on the previous assumption of uniform strain through the thickness.

For a given displacement, the above formulas define the strain at every point in the material. If the stress law is known, the stress at each point can be calculated. The stresses can then be summed to give the total force and moment on the mass.

Simple stress laws and geometries can be treated analytically. For example, consider a material of constant thickness h surrounding a sphere of radius R. Let the sphere-material interface be frictionless, so that no shear occurs. Assume the stress law $\sigma = E\epsilon + c\dot{\epsilon}$, where σ denotes compressive stress and the quantities E and c are constants. The total force for a uniform translation x is

$$f(x) = \int_0^{\frac{\pi}{2}} \sigma(\theta)\, 2\pi R^2 \sin\theta \cos\theta \, d\theta$$

$$= \int_0^{\frac{\pi}{2}} 2\pi R^2 \sin\theta \cos\theta \left(E \frac{x}{h} \cos\theta + \frac{c\dot{x}}{h} \cos\theta \right) d\theta.$$

$$= \frac{2\pi R^2}{3} \left(E \frac{x}{h} + c \frac{\dot{x}}{h} \right).$$

Because of the symmetry of the problem and the absence of rotational displacement there are no moments, and the force f(x) is parallel to the displacement x. It is seen that the force is given by the product of the stress at the point $\theta = 0$ and two-thirds of the projected area of the sphere. Note that the integration occurred over only one-half of the sphere, since the material was assumed not fastened to the sphere.

When the stress law and/or the geometry are complicated, direct integration is impossible and further approximation must be made. For example, when the problem is axially symmetric, the surfaces of revolution can be replaced by series of conical segments, each segment having associated with it an average material thickness. Strain and strain rate are then constant over the surface of each segment. The contributions of all segments can be added to obtain the total force on the mass. This is illustrated in the sample problem in the Appendix.

DETERMINATION OF THE STRESS LAW

A stress law is defined here as a relationship between the two functions stress and strain and their time derivatives. Familiar cases are (1):

$\sigma = E\epsilon + c\dot{\epsilon}$ .... Voigt model

$\sigma + K\dot{\sigma} = c\dot{\epsilon}$ .... Maxwell model

$\sigma + K\dot{\sigma} = E\epsilon + c\dot{\epsilon}$ .... standard linear model.

To date, the writers have investigated the dynamic behavior of materials under compressive stress only. It has been found that, for every promising material tested, the stress can be satisfactorily represented for purposes of response calculations as a function only of strain and strain rate. This is demonstrated as follows: Samples of material are placed on a rigid foundation and compressed by a falling mass. Acceleration of the mass during the impact is obtained by a crystal accelerometer. Under the assumption of negligible Poisson effect, the stress is taken to be uniform over the sample area and is calculated as a function of time from the acceleration curve. Strain rate and strain are obtained from the first and second integrals of acceleration, respectively.*

Regarding strain rate as a function of strain, each drop is represented by a trajectory on a strain rate vs strain chart, Fig. 3, solid line. The initial impact occurs at zero strain and at a strain rate given by impact velocity divided by material thickness. Compression then proceeds with decreasing strain rate and increasing strain. Termination of compression occurs at zero strain rate and maximum strain. Associated with each point on the trajectory is a known value of stress. This is illustrated in Fig. 3 by a few discrete stress values.

It is quite easy to perform a second drop on the same material such that the trajectory, dotted line in Fig. 3, will cross the first trajectory. This is accomplished by using a heavier mass and a lower impact velocity. At the point common to both trajectories, both material samples have the same strain and strain rate, but different strain histories. Also, the point is reached at different times for the two samples. If the stress is a function

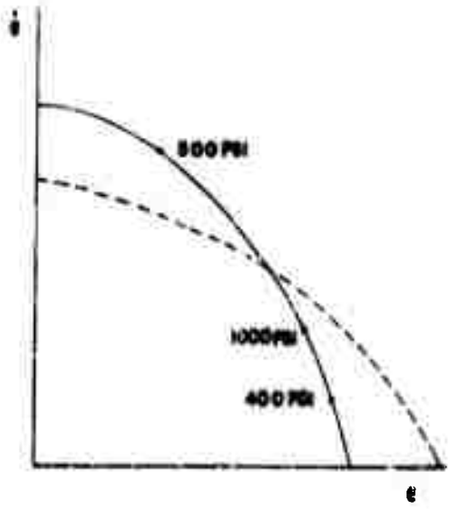

Fig. 3 - Strain vs strain rate for simple drop test

only of strain and strain rate, the stresses in the samples should be equal at the common point.

The writers have found that this is approximately true for a large number of materials over all values of ϵ and $\dot{\epsilon}$ that are of importance in the impact problems being considered. It must be emphasized, however, that each new material must be checked.

When a material has been proven to have a stress law involving only strain and strain rate, the law is represented on an "isostress plot," Fig. 4. Here, the data obtained in the tests described previously are used to plot lines of constant stress in strain, strain rate coordinates. This is accomplished by drawing in a large number of $\epsilon - \dot{\epsilon}$ trajectories and connecting with a smooth curve all trajectory points having the same value of stress. Sufficient curves are drawn to insure that the stress value for any point $(\epsilon, \dot{\epsilon})$ can be accurately obtained by interpolation. At low values of strain rate, where the drop test data becomes inaccurate, a cam-driven device described in the literature (3) is used.

If a material exhibits significant Poisson effect, the data for the isostress plot should be obtained from laterally-confined samples. In this manner, the conditions experienced by the material in actual use will be most accurately duplicated. Lateral confinement can be easily introduced by placing the material specimen in a snugly fitting metal ring. The inner surface of the ring should

*An alternate method for obtaining stress, strain, and strain rate from such drops is discussed in a previous paper (2).

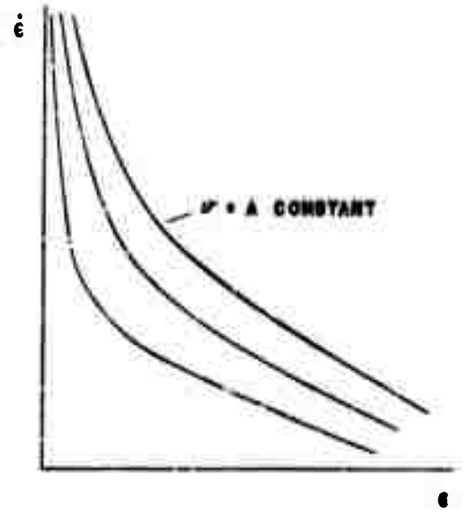

Fig. 4 - Isostress plot

be smooth and well-lubricated to minimize friction. Confinement can also be obtained by compressing the sample between rough surfaces, the sample thickness being small compared with its other dimensions. Under these circumstances, only a negligible amount of material is free to expand laterally.

The category of materials representable by an isostress plot includes the Voigt model as a special case. The plot for a Voigt material is a family of parallel straight lines with negative slope. The Maxwell and standard linear models involve rate of stress and are not included in this category.

CALCULATION OF RESPONSE

While the foregoing principles are applicable to problems with multiple degrees of freedom, the writers have to date dealt only with single-degree systems.

The numerical procedure chosen for solution of the problems was selected for its rapidity and ease of comprehension. To begin, the time scale of the applied pulse is divided into a number of finite intervals Δt. Let

$\bar{a}(t)$ = case acceleration

$x(t)$ = displacement of inner component relative to case, positive in direction of negative $\bar{a}(t)$

$\dot{x}(t)$ = velocity of inner component relative to case

$\ddot{x}(t)$ = acceleration of inner component relative to case

f = force on inner component, positive in direction of negative x

m = mass of inner component

$a(t)$ = absolute acceleration of inner component, positive in direction of positive $\bar{a}(t)$.

The subscript n will denote a value at the end of the nth time interval. $\Delta_n(\bar{a}, x, \ldots)$ = change of corresponding quantity during nth time interval. The initial conditions are $x(0) = x_0$, $\dot{x}(0) = \dot{x}_0$.

The formulas used are:

$$\Delta_n\dot{x} = \frac{\ddot{x}_{n-1} + \ddot{x}_n}{2}\Delta t \qquad \Delta_n x = \frac{\dot{x}_{n-1} + \dot{x}_n}{2}\Delta t$$

$$\epsilon_n = \frac{x_n \cos\theta}{h} \qquad \dot{\epsilon}_n = \frac{\dot{x}_n \cos\theta}{h}$$

$$\gamma_n = \frac{x_n \sin\theta}{h} \qquad \dot{\gamma}_n = \frac{\dot{x}_n \sin\theta}{h}$$

$$f_n = m(\bar{a}_n - \ddot{x}_n) \qquad a_n = \frac{f_n}{m} = \bar{a}_n - \ddot{x}_n$$

$$x_n + \Delta_{n+1}x = x_{n+1} \qquad \dot{x}_n + \Delta_{n+1}\dot{x} = \dot{x}_{n+1}$$

The expressions involving $\Delta_n\dot{x}$ and $\Delta_n x$ are approximate for finite Δt but become exact as Δt approaches zero.

The procedure for using these equations in a step-by-step solution of the problem is illustrated by the operations necessary to pass from the nth time interval to the $n+1$ time interval: Given the values x_n, $\dot{x}_n$, $\ddot{x}_n$, and $\bar{a}_{n+1}$, estimate a value of $\ddot{x}_{n+1}$. Calculate $\Delta_{n+1}\dot{x}$ and $\Delta_{n+1}x$, and from these get x_{n+1} and $\dot{x}_{n+1}$. When x_{n+1} and $\dot{x}_{n+1}$ are known, ϵ_{n+1} and γ_{n+1} can be calculated at every point of the material. The isostress chart then gives the stress over the body. These stresses are summed in the direction of $-x$ to give f_{n+1}. Using this f_{n+1}, calculate

$$\ddot{x}_{n+1} = \bar{a}_{n+1} - \frac{f_{n+1}}{m}$$

and compare with the estimated value. If it is not close, use the $\ddot{x}_{n+1}$ which was calculated for an improved guess and repeat. This method of successive approximations converges very rapidly. In fact, an experienced computer will often make so

accurate a first estimate that further approximations are not necessary.

To avoid erroneous answers resulting from time intervals being too large, the calculation must be repeated with a smaller interval. The response $a(t)$ should agree well with the first calculation. If it does not, the time interval must again be reduced, and so on.

In practice, it is found that even very coarse time meshes give satisfactory results. This is due in part to the fact that good shock-mitigating materials give highly damped responses without rapid fluctuations and steep slopes. It follows that only a few mesh points will accurately represent such functions. It has been the writers' experience that for smooth forcing functions such as half-sine pulses, a dozen mesh points will give good accuracy.

The numerical procedure described above is well suited for use by semiskilled personnel. The operations can be indicated in tabular form and performed quickly. It was found that an individual can plot as many as 10 to 15 responses per day for a problem involving a flat geometry and half-sine forcing pulse. More complicated geometries require more time.

A sample calculation of the response of a spherical mass mounted in cushioning material of varying thickness is given in the Appendix. This calculation illustrates all of the operations required to solve a problem with nonplanar geometry and one degree of freedom.

COMPARISON OF THEORY AND EXPERIMENT

To ascertain the value of the method described in this paper, a number of experiments were performed and the results compared with computations. The drop vehicle used in the tests consisted of two masses, one within the other. The inner mass was separated from the outer by a thin, uniform layer of cushioning material. Two geometries of the inner mass were used, a right circular cylinder with material on the plane lower end and a sphere with material covering the lower half.

Since dynamic shear and tension have not yet been investigated, these deformations were excluded from the test by not gluing or otherwise fastening the material to the inner mass. Of course, in the case of the sphere, a small amount of shear must have resulted from sliding friction between the mass and the material.

The vehicle was dropped on an elastic block and the acceleration-time functions were recorded from both masses. The acceleration of the outer mass and the isostress plot for the mounting material were used to calculate the response of the inner mass.

Figure 5 shows the comparison of experiment and calculations. The curves labeled $\bar{a}$ are the case accelerations. The solid curves labeled a are the measured responses of the inner mass. The dotted curves are the calculated responses. The diagram on each plot indicates the geometry used. It is seen that for both geometries the correlation between theory and experiment is satisfactory.

THE INFLUENCE OF PERTINENT VARIABLES

In the usual design problem, the cushioning material is not specified and the cushion dimensions are not given. These must be selected so the resulting acceleration-time pulse on the cushioned mass and cushion compression will be acceptable.

Problems of this type may be solved by using the method just developed only through trial and error. That is (1) assume a material and cushion dimensions; (2) solve the problem; (3) if results are not satisfactory, make new assumptions and resolve the problem until the results are satisfactory. Since this method is time-consuming, a better understanding of the effect of the pertinent variables on the response is needed.

Since time can be saved if the number of variables is reduced by grouping them into nondimensional terms, the following analysis has been made. The variables considered are as follows:

(a) Cushion thickness, h,

(b) Magnitude of cushioned mass per unit area of cushion, m/A,

(c) The nature of the acceleration pulse applied to the case, $a(t)$.

The acceleration of the cushioned mass at any time can be written as: $a = f(\bar{a}, h, m/A, \sigma, t)$, in which

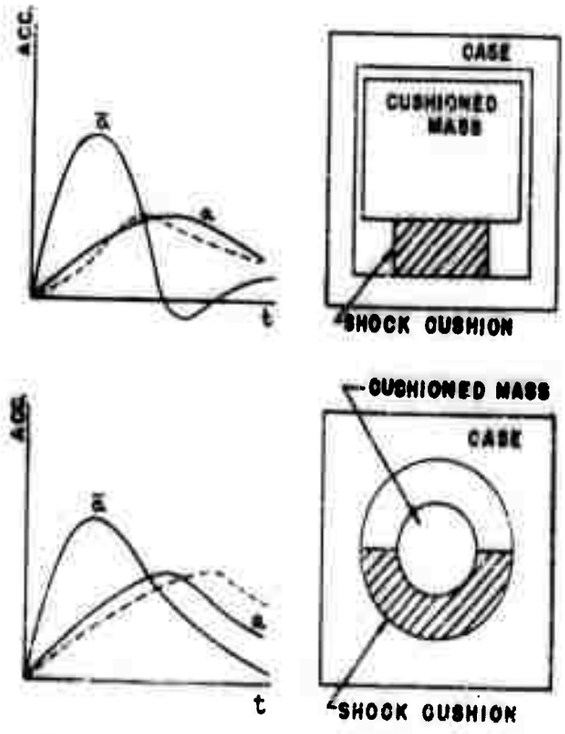

Fig. 5 - Comparison of theory and experiment

a = the acceleration of the cushioned mass,

$\bar{a}$ = the acceleration of the case,

h = the thickness of the cushion,

m/A = the mass per unit area of cushion,

σ = stress,

t = time.

Grouping these quantities as dimensionless terms we have

$$\frac{\bar{a}}{a} = \varphi\left(\frac{\bar{a}t^2}{h}, \frac{m\bar{a}}{A\sigma}\right).$$

Likewise:

$$x = f'(\bar{a}, h, m/A, \sigma, t),$$

where x = the displacement of the mass relative to the case. Again, by grouping into dimensionless terms:

$$\frac{x}{h} = \phi'\left(\frac{\bar{a}t^2}{h}, \frac{m\bar{a}}{A\sigma}\right).$$

If a' and $\bar{a}'$ are now used to denote the maximum values of the mass and case acceleration, it is seen that with the time scale and shape of applied pulse fixed, and for a given material, we may investigate the effect of the other variables on a' by plotting $\bar{a}'/a'$ vs $m\bar{a}'/A$ for a range of values of $\bar{a}'/h$. Likewise the effect of the variables on x' may be investigated by plotting x'/h vs $m\bar{a}'/A$ for a range of values of $\bar{a}'/h$, where x' now denotes the maximum relative displacement.

The curves presented as Figs. 6, 7, and 8 have been calculated for an applied pulse defined as a half-sine. The isostress diagram for a mixture of polyrubber and stafoam which was used in these calculations is presented in the Appendix. This material was selected since its isostress graph is typical of those for foamed plastics. These curves are the result of the solution of numerous problems by using the method previously described.

On these figures the term "isolation factor" (R) is used as the ratio of the maximum (or peak) case acceleration to the maximum acceleration of the cushioned mass. The displacement of the mass relative to the case, x', appearing on these figures is the maximum value. Values of R greater than unity indicate that some attenuation of acceleration has been achieved. The greater the value of R, the greater this attenuation.

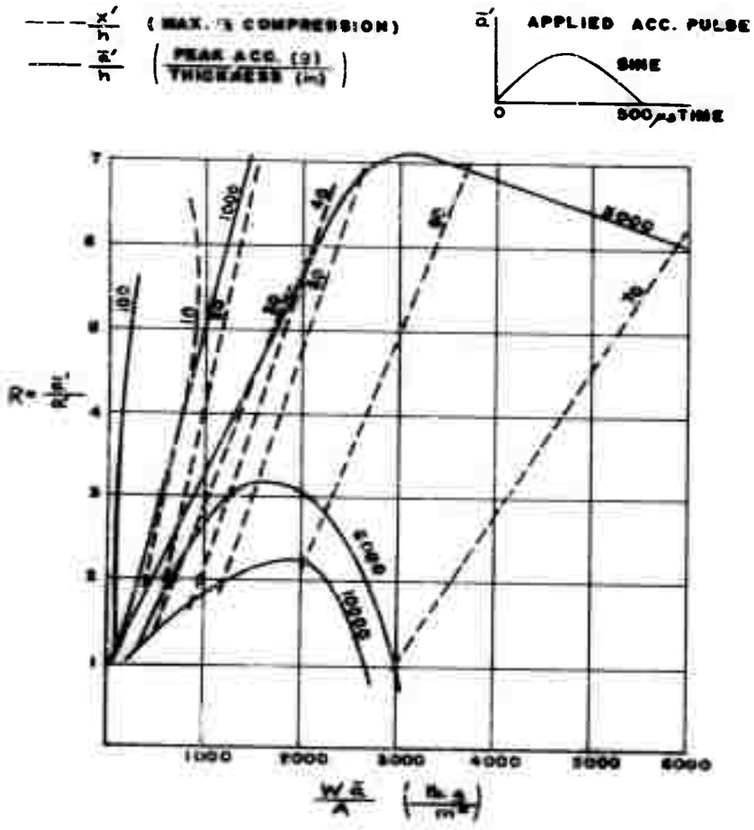

Fig. 6 - Isolation factor (R) vs unit loading

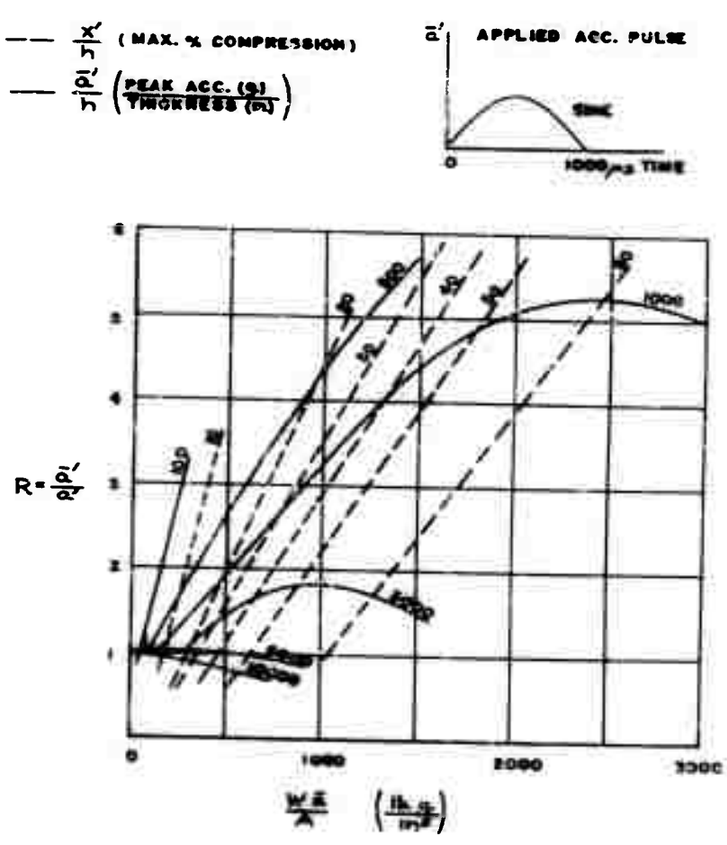

Fig. 7 - Isolation factor (R) vs unit loading

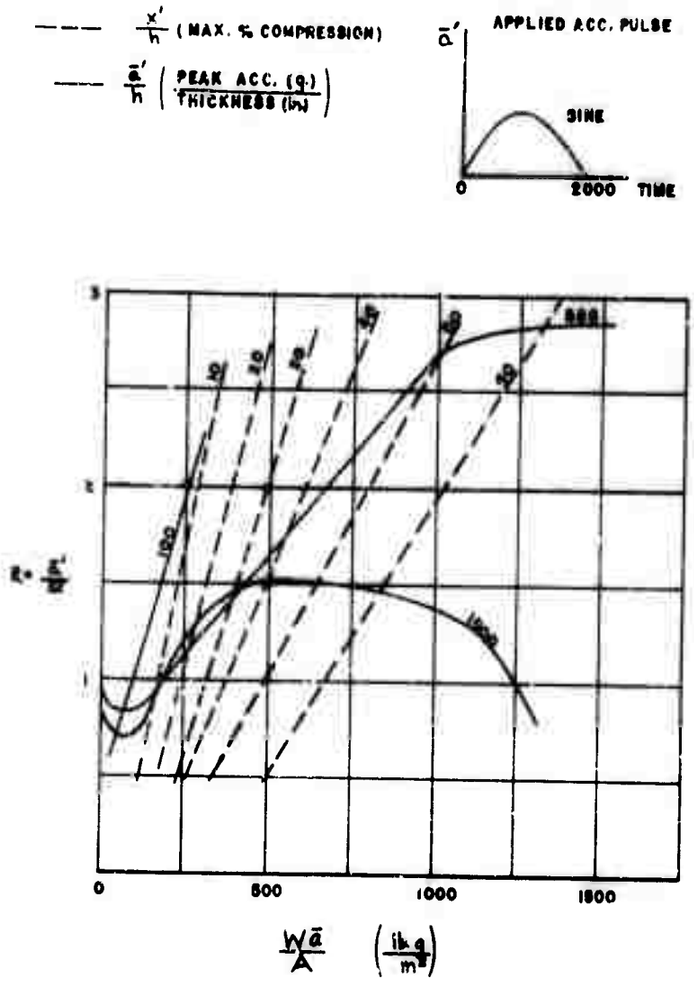

Fig. 8 - Isolation factor ($\bar{R}$) vs unit loading

Inspection of these curves reveals that if the supported mass per unit area of cushion, m/A, is either too small or too large, the value of R may be less than 1, i.e., the cushion produces an amplification of the applied pulse.

It is important to recognize that the grouping of variables used here is not restricted to materials expressible by an isostress plot. This scaling includes any material whose stress law is a function only of strain, time, time derivatives of stress and strain, and time integrals of stress and strain. For purposes of calculations, however, we must restrict ourselves to materials represented on an isostress plot, i.e., those whose stress law is a function only of strain and its first time derivative.

Another point of interest is that these calculations can be made for nonplanar geometries and plotted in exactly the same manner. It is only necessary to define A as some area, e.g., projected area of the body. The plotted curves will, of course, apply only to geometrically similar systems.

CONCLUSIONS

A method has been presented for solving shock-mounting problems for which the material stress law depends only on strain and strain rate. The usefulness of this method has been demonstrated by experiment for the case of compressive loading of the material. The application of the method to problems involving shear and tension should be the subject of future research.

REFERENCES

1. Schmidt and Marlies, "Principles of High-Polymer Theory and Practice," McGraw-Hill Book Company, Inc., New York, N. Y., 1948.

2. Engineering Experiment Station, University of New Mexico, Albuquerque, New Mexico. "The Effect of Loading Rate on Mechanical Properties," Quarterly Report Number 3 on Project 57-1ME, January 1, 1958.

3. Engineering Experiment Station, University of New Mexico, Albuquerque, New Mexico. "The Effect of Loading Rate on Mechanical Properties," Annual Report on Project 57-1ME, June 30, 1958.

APPENDIX

SAMPLE CALCULATION OF RESPONSE OF A SPHERICAL MASS MOUNTED IN CUSHIONING MATERIAL OF VARYING THICKNESS

Problem

Determine the acceleration of the sphere, Fig. A1, as a function of time. The material thickness varies linearly with angle from 0.25 inch to 0.080 inch, or $h = 0.25 - 0.34\theta/\pi$. The isostress plot is provided, Fig. A2. The case acceleration is a half-sine pulse, Fig. A3. The initial conditions are $x_0 = 0$, $\dot{x}_0 = 0$.

First divide the sphere into conical segments, for which strain and strain rate are constant. Three segments will be used, Fig. A4. The edges of the segments are circles on the surface of the original sphere. The material thickness for each segment is the value associated with the center of the angular range of the segment. If h_1, h_2, h_3, are the three thicknesses,

$$h_1 = 0.25 - \frac{0.34}{\pi}\,\frac{15}{180}\pi = 0.222 \text{ inch},$$

$$h_2 = 0.25 - \frac{0.34}{\pi}\,\frac{45}{180}\pi = 0.165 \text{ inch},$$

$$h_3 = 0.25 - \frac{0.34}{\pi}\,\frac{75}{180}\pi = 0.108 \text{ inch}.$$

The notation of the paper will be used. Let superscripts refer to the segments. Thus, $\epsilon_n^{(2)}$ is the compressive strain in the second segment at the end of the nth time interval.

$$\epsilon_n^{(1)} = x_n \frac{\cos 15^\circ}{0.222} = 4.35\, x_n,$$

$$\epsilon_n^{(2)} = x_n \frac{\cos 45^\circ}{0.165} = 4.29\, x_n,$$

$$\epsilon_n^{(3)} = x_n \frac{\cos 75^\circ}{0.108} = 2.40\, x_n,$$

$$\dot{\epsilon}_n^{(1)} = \dot{x}_n \frac{\cos 15^\circ}{0.222} = 4.35\, \dot{x}_n,$$

$$\dot{\epsilon}_n^{(2)} = 4.29\, \dot{x}_n,$$

$$\dot{\epsilon}_n^{(3)} = 2.40\, \dot{x}_n$$

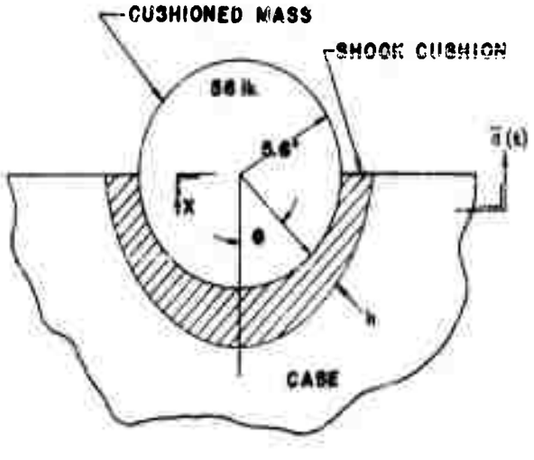

Fig. A1 - Illustrative problem

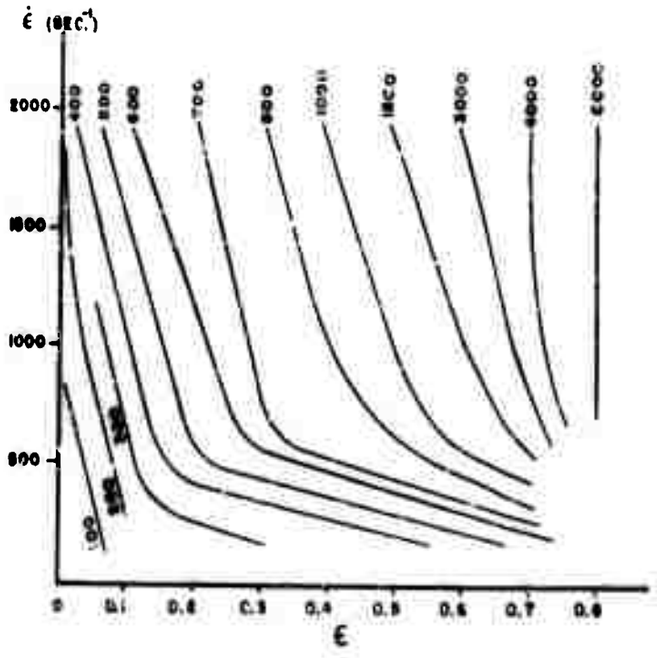

Fig. A2 - Isostress plot

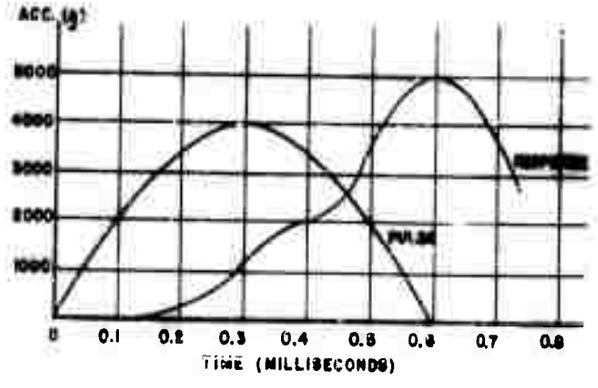

Fig. A3 - Applied pulse and response of sphere

The surface areas of the segments are 26.4, 72.0, and 98.5 square inches for segments 1, 2, and 3, respectively.

If $\sigma_n^{(1)}$, $\sigma_n^{(2)}$, and $\sigma_n^{(3)}$ are the stresses corresponding to the strains, the total forces on the segments are:

Segment 1: $26.4\ \sigma_n^{(1)}$,

Segment 2: $72.0\ \sigma_n^{(2)}$,

Segment 3: $98.5\ \sigma_n^{(3)}$.

However, only the components of these forces parallel to x affect the motion of m. The components in the direction opposite to x are:

$$25.4\ \sigma_n^{(1)} \cos 15^\circ = 25.5\ \sigma_n^{(1)} ,$$

$$72.0\ \sigma_n^{(2)} \cos 45^\circ = 50.9\ \sigma_n^{(2)} ,$$

$$98.5\ \sigma_n^{(3)} \cos 75^\circ = 25.5\ \sigma_n^{(3)} .$$

Finally, the total vertical force on the mass is $25.5\ \sigma_n^{(1)} + 50.9\ \sigma_n^{(2)} + 25.5\ \sigma_n^{(3)} = f_n$.

For the first calculation, let the time interval, Δt, equal 50×10^{-6} sec. The initial conditions are $x_0 = 0$, $\dot{x}_0 = 0$. All strains and strain rates are therefore zero at $t = 0$. The total force f_0 on the mass is zero and the case acceleration $\bar{a}_0$ is zero. The quantity $\ddot{x}_0 = \bar{a}_0 - (f_0/m)$ is therefore also zero.

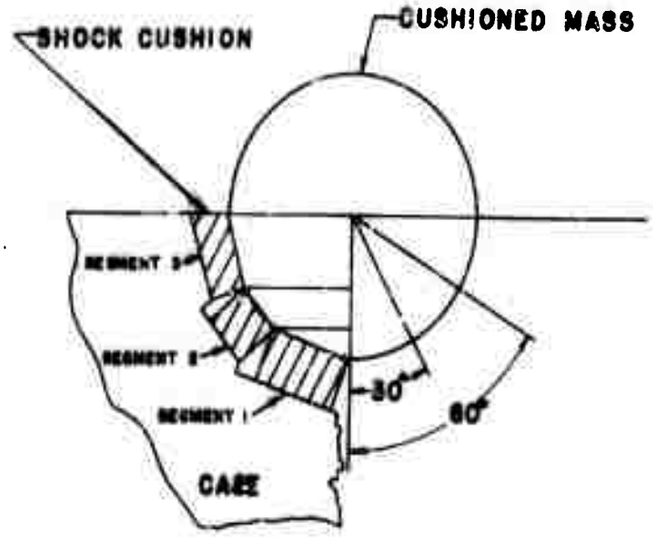

Fig. A4 - Replacement of sphere by conical segments

Guess

$$\ddot{x}_1 = 15g = 5790 \frac{\text{in.}}{\text{sec}^2}$$

$$\dot{x}_1 = 0.145 \frac{\text{in.}}{\text{sec}}$$

$$\Delta_1 x = \frac{0 + 5790}{2} (50)10^{-6}$$

$$\Delta_1 x = \frac{0 + 0.145}{2} (50)10^{-6} = 3.62 \times 10^{-6} \text{ in.}$$

$$\Delta_1 \dot{x} = 0.145 \frac{\text{in.}}{\text{sec}}$$

$$x_1 = 3.62 \times 10^{-6} \text{ in.}$$

$$\epsilon_1^{(1)} = 4.35(3.62)10^{-6} = 15.7 \times 10^{-6}$$

$$\epsilon_1^{(2)} = 4.29(3.62)10^{-6} = 15.5 \times 10^{-6}$$

$$\epsilon_1^{(3)} = 2.40(3.62)10^{-6} = 8.68 \times 10^{-6}$$

$$\dot{\epsilon}_1^{(1)} = 4.35(0.145) = 0.631 \text{ sec}^{-1}$$

$$\dot{\epsilon}_1^{(2)} = 4.29(0.145) = 0.622 \text{ sec}^{-1}$$

$$\dot{\epsilon}_1^{(3)} = 2.40(0.145) = 0.348 \text{ sec}^{-1}$$

Reference to Fig. A2 shows that the stresses $\sigma_1^{(1)}$, $\sigma_1^{(2)}$, and $\sigma_1^{(3)}$ are essentially zero. Therefore $f_1 = 0$ and $\ddot{x}_1$ is calculated to be $\ddot{x}_1 = \bar{a}_1 - (f_1/m) = 0.259(4000\ g) = 1040$ g, quite different from 15 g.

As a second guess, choose

$$\ddot{x}_1 = 1040 \text{ g} = 401{,}000 \frac{\text{in.}}{\text{sec}^2}$$

$$\Delta_1 \dot{x} = \frac{0 + 401.000}{2} (50)10^{-6} = 10.0 \frac{\text{in.}}{\text{sec}}$$

$$\Delta_1 x = \frac{0 + 10.0}{2} (50)10^{-6} = (25)10^{-5} \text{ in.}$$

$$\epsilon_1^{(1)} = 4.35(25)10^{-5} = (1.09)10^{-3}$$

$$\epsilon_1^{(2)} = 4.29(25)10^{-5} = (1.07)10^{-3}$$

$$\epsilon_1^{(3)} = 2.40(25)10^{-5} = (0.600)10^{-3}$$

$$\dot{x}_1 = 0 + 10.0 = 10.0 \frac{\text{in.}}{\text{sec}}$$

$$x_1 = (25)10^{-5} \text{ in.}$$

$$\dot{\epsilon}_1^{(1)} = 4.35(10.0) = 43.5 \text{ sec}^{-1}$$

$$\dot{\epsilon}_1^{(2)} = 4.29(10.0) = 42.9 \text{ sec}^{-1}$$

$$\dot{\epsilon}_1^{(3)} = 2.40(10.0) = 24.0 \text{ sec}^{-1}$$

Figure A1 again gives stresses equal to zero. Therefore $f_1 = 0$ and $\ddot{x}_1 = 1040$ g, $\dot{x}_1 = 10.0$ in./sec, and $x_1 = (25)\ 10^{-5}$ in. satisfy all equations. The absolute acceleration of the mounted mass is f_n/m. For the end of the first interval, $f_1/m = 0$.

For the second interval, guess

$$\ddot{x}_2 = 2000 \text{ g} = 773{,}600 \frac{\text{in.}}{\text{sec}^2}$$

$$\Delta_2\dot{x} = \frac{401{,}000 + 773{,}000}{2}(50)10^{-6} = 29.4 \frac{\text{in.}}{\text{sec}}$$

$$\Delta_2 x = \frac{10.0 + 39.4}{2}(50)10^{-6} = (1.24)10^{-3} \text{ in.}$$

$$\epsilon_2^{(1)} = 4.35(1.49)10^{-3} = (6.48)10^{-3}$$

$$\epsilon_2^{(2)} = 4.29(1.49)10^{-3} = (6.40)10^{-3}$$

$$\epsilon_2^{(3)} = 2.40(1.49)10^{-3} = (3.58)10^{-3}$$

$$\dot{x}_2 = 10.0 + 29.4 = 39.4 \frac{\text{in.}}{\text{sec}}$$

$$x_2 = (25)10^{-5} + (1.24)10^{-3} = (1.49)10^{-3} \text{ in.}$$

$$\dot{\epsilon}_2^{(1)} = 4.35(39.4) = 171 \text{ sec}^{-1}$$

$$\dot{\epsilon}_2^{(2)} = 4.29(39.4) = 169 \text{ sec}^{-1}$$

$$\dot{\epsilon}_2^{(3)} = 2.40(39.4) = 94.6 \text{ sec}^{-1}$$

Figure A2 gives approximately

$$\sigma_2^{(1)} = 10 \text{ psi} \qquad \sigma_2^{(2)} = 10 \text{ psi} \qquad \sigma_2^{(3)} = 0$$

$$f_2 = 25.5(10) + 50.9(10 + 25.5(0)$$

$$= 255 + 509 = 764 \text{ lb}$$

$$\ddot{x}_2(\text{calculated}) = \bar{a}_2 - \frac{f_2}{m} = 2000 - \frac{764}{56}$$

$$= 2000 - 14 = 1986 \text{ g} = 767{,}000 \frac{\text{in.}}{\text{sec}^2}$$

This is sufficiently close to the 2000 g estimate. The absolute acceleration, a_z, of the mass at the end of the second interval is 14 g.

For the third interval, estimate

$$\ddot{x}_3 = 2700 \text{ g} = 1{,}040{,}000 \frac{\text{in.}}{\text{sec}^2}$$

$$\Delta_3\dot{x} = \frac{.767 + 1.04}{2}(50) = 45.3 \frac{\text{in.}}{\text{sec}}$$

$$\Delta_3 x = \frac{39.4 + 84.7}{2}(50)10^{-6} = 0.00310 \text{ in.}$$

$$\epsilon_3^{(1)} = 4.35(0.00459) = 0.0200$$

$$\epsilon_3^{(2)} = 4.29(0.00459) = 0.0197$$

$$\epsilon_3^{(3)} = 2.40(0.00459) = 0.0110$$

$$\dot{x}_3 = 39.4 + 45.3 = 84.7 \frac{\text{in.}}{\text{sec}}$$

$$x_3 = 0.00149 + 0.00310 = .00459 \text{ in.}$$

$$\dot{\epsilon}_3^{(1)} = 4.35(84.7) = 368 \text{ sec}^{-1}$$

$$\dot{\epsilon}_3^{(2)} = 4.29(84.7) = 363 \text{ sec}^{-1}$$

$$\dot{\epsilon}_3^{(3)} = 2.40(84.7) = 203 \text{ sec}^{-1}$$

From Fig. A2,

$$\sigma_3^{(1)} = 50 \text{ psi} \quad \sigma_3^{(2)} = 50 \text{ psi} \quad \sigma_3^{(3)} = 25 \text{ psi}$$

$$f_3 = 25.5(50) + 50.9(50) + 25.5(25)$$

$$= 1200 + 2550 + 637 = 4467 \text{ lb}$$

$$\ddot{x}_3(\text{calculated}) = 2830 - \frac{4467}{56} = 2830 - 80$$

$$= 2750 \text{ g} = 1{,}060{,}000 \frac{\text{in.}}{\text{sec}^2}$$

This is sufficiently close to the estimate of 2700 g.

For the fourth interval, estimate

$$\ddot{x}_4 = 3300 \text{ g} = 1{,}270{,}000 \frac{\text{in.}}{\text{sec}^2}$$

$$\Delta_4\dot{x} = \frac{1.06 + 1.27}{2}(50) = 58.3 \frac{\text{in.}}{\text{sec}}$$

$$\Delta_4 x = \frac{84.7 + 143.0}{2}(50)10^{-6} = 0.00569 \text{ in.}$$

$$\epsilon_4^{(1)} = 4.35(0.0103) = 0.0448$$

$$\epsilon_4^{(2)} = 4.29(0.0103) = 0.0442$$

$$\epsilon_4^{(3)} = 2.40(0.0103) = 0.0247$$

$$\dot{x}_4 = 84.7 + 58.3 = 143.0 \frac{\text{in.}}{\text{sec}}$$

$$x_4 = 0.00459 + 0.00569 = 0.0103 \text{ in.}$$

$$\dot{\epsilon}_4^{(1)} = 4.35(143) = 622 \text{ sec}^{-1}$$

$$\dot{\epsilon}_4^{(2)} = 4.29(143) = 615 \text{ sec}^{-1}$$

$$\dot{\epsilon}_4^{(3)} = 2.40(143) = 343 \text{ sec}^{-1}$$

From Fig. A2,

$$\sigma_4^{(1)} = 160 \text{ psi} \quad \sigma_4^{(2)} = 155 \text{ psi} \quad \sigma_4^{(3)} = 50 \text{ psi}$$

$$f_4 = 25.5(160) + 50.9(155) + 25.5(50)$$

$$= 4080 + 7900 + 1275 = 13{,}255 \text{ lb}$$

$$\ddot{x}_4 \text{ (calculated)} = 3460 - \frac{13,255}{56}$$

$$= 3460 - 237 = 3220 \text{ g}$$

Although this is quite close to the assumed value of 3900 g, a second approximation will be calculated for illustrative purposes:

Estimate

$$\ddot{x}_4 = 3220 \text{ g} = 1,240,000 \frac{\text{in.}}{\text{sec}^2}$$

$$\Delta_4\dot{x} = \frac{1.06 + 1.24}{2} (50) = 57.5 \frac{\text{in.}}{\text{sec}}$$

$$\Delta_4 x = \frac{84.7 + 142}{2} (50)10^{-6} = 0.00567 \text{ in.}$$

$$\dot{x}_4 = 84.7 + 57.5 = 142 \frac{\text{in.}}{\text{sec}}$$

$$x_4 = 0.00459 + 0.00567 = 0.0103 \text{ in.}$$

Clearly, the accuracy of the isostress plot is not sufficient to indicate any difference between f_4 for this case and the previous f_4. The calculated value of $\ddot{x}_4$ is therefore 3220 g, the estimated value.

The calculation for the remainder of the time intervals proceeds in exactly the same manner. When the calculation has been completed, the time interval must be reduced and the calculation repeated to assure that the answer is accurate.

The response for this problem is also shown in Fig. A3. The quantity plotted is $a(t)$, the absolute acceleration of the cushioned mass. It is seen that, in this example, the cushioning material amplifies the applied pulse.

* * *

SIMPLIFIED APPROACH TO DESIGNING SHOCK ISOLATION FOR THE ROTATIONAL DROP TEST*

Gordon S. Mustin†
Douglas Aircraft Company
Santa Monica, California

Previously published papers (1, 2, 3, 4) on the rotational drop test appear to be analyses of existing designs or require certain unwarranted assumptions concerning distributions of accelerations. No satisfactory designer's approach to the use of nonlinear cushioning materials for rotational drop test cushioning has been found in the literature. This paper summarizes an approach found to be useful in designing with shock mounts and covers an extension of the method to tangent elasticity.

THE ROTATIONAL DROP TEST

Consider the situation shown in schematic form in Fig. 1. The pivot end is on a block h_2 inches above the floor, and the opposite end is raised some specified height h_1 inches above the floor. The designer's objective is to control the acceleration, G_m, some distance x_3 inches away from the c.g. or x_2 inches from the pivot point. Usually the point at which G_m is to be controlled is the impact end of the contents. Natural frequencies of the final design must also be considered.

It is reasonable to assume that the container designer is given maximum values of acceleration and firm values on geometry, weight, and moments of inertia (or preferably radii of gyration) concerning the contents.

Height of drop of the center of gravity is given by

$$h = y_1\left(\frac{h_1}{L}\cdot\frac{x_1}{y_1} + \sqrt{1-\left(\frac{h_1-h_2}{L}\right)^2} - \sqrt{1-\frac{h_1^2}{L^2}}\right). \quad (1)$$

In the special case where $h_2 = 0$ (as for example in a tip over test)

$$h = y_1\left(\frac{h_1}{L}\cdot\frac{x_1}{y_1} + \sqrt{1-\frac{h_1^2}{L^2}} - 1\right). \quad (2)$$

Most conveniently, the approximate formula

$$h \cong \frac{x_1}{L} h_1 \quad (3)$$

is sound for preliminary design. Both Eqs. (1) and (2) require assumptions concerning a specific value of y_1. x_1 can be most conveniently determined quite accurately by designing for the end impact condition first. (This latter is almost mandatory for cushion packs.)

THE RATIO M

Use of the energy method leads to an expression for the ratio of total deflection at the end to translational deflection normal to the base at the center of gravity which, for convenience, is dubbed M:

*This paper was not presented at the Symposium.
†Current Address: Reed Research, Inc., 1048 Potomac Street, N. W., Washington 7, D. C.

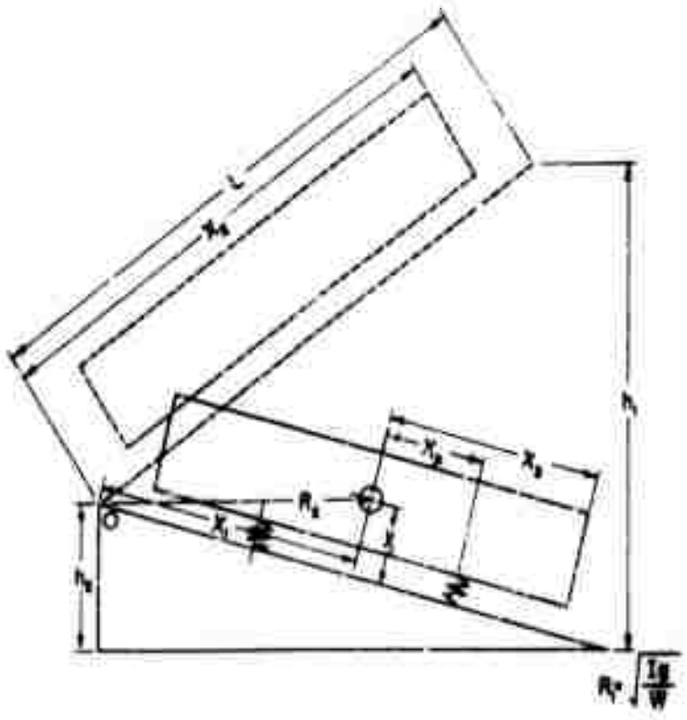

Fig. 1 - The rotational drop test

$$M = \frac{d_T}{d_1} = 1 + \frac{d_R}{d_1} = 1 + x_3 \sec \theta_1 \sqrt{\frac{E_2}{E_1}\frac{K_T}{K_\theta}}$$

$$= 1 + x_3 \sec \theta_1 \sqrt{\frac{R_1^2 K_T}{R_2^2 K_\theta}} = 1 + \frac{x_3 R_1}{x_1}\sqrt{\frac{K_T}{K_\theta}}, \quad (4)$$

where

K_T = translational spring rate,

K_θ = rotational spring rate.

In the special case where three-fold symmetry can be obtained (and note that the designer is almost invariably forced to at least two-fold symmetry to achieve the pleasing appearance of the contents riding level), the ratio $K_\theta/K_T = x_s^2$ and Eq. (4) becomes

$$M = 1 + \frac{x_3 R_1}{x_1 x_s}. \quad (5)$$

This special case teaches certain practical limits tc the value of M. Thus x_s will rarely exceed x_3 because excessive cube would be lost. Similarly, limited experience indicates that rotational natural frequency becomes very low when x_s is less than $(1/3) R_1$. Hence, we can write practical designer's limits on the value of M for a specific object as

$$1 + \frac{R_1}{x_1} \leq M \leq 1 + 3\frac{x_3}{x_1}. \quad (6)$$

which limits may be expected to remain reasonably valid regardless of types of symmetry involved in the final design. An even rougher approximation of the range of M is to state that its most probable value lies between 1.0+ and 4.0. Note particularly that the limits of M derived above are independent of drop height, spring rate, or allowable acceleration.

USE OF M WITH SHOCK MOUNTS

Total required deflection at the end can be estimated by

$$d_T = \frac{2h}{G_m} \cdot \frac{x_2^2}{R_3^2}, \quad (7)$$

where

$$R_3^2 = R_1^2 + R_2^2 = R_1^2 + x_1^2 + y_1^2.$$

Note that an estimate of the value of y_1 is required. This value is made up of components

from the container, the contents, and an allowance for movement of the item. Since both x_2^2 and k_3^2 are fairly large numbers (often of the magnitude 10^3 or 10^4, accurate estimation is not essential. A useful preliminary approximation can be achieved by considering the drop as a flat drop with an arbitrary additional allowance. If found wrong after the next step, a better approximation does not introduce appreciable delay.

Translational spring rate, the controlling element in the design, is given by

$$K_T = \gamma \alpha M^2 , \qquad (8)$$

where

$$\gamma = \frac{2}{d_T^2} \quad \text{for linear elasticity,}$$

$$\alpha = \frac{x_1^2}{k_3^2} Wh .$$

α and γ are constants for the problem. A range of K_T is available through variation in M. Select stock mounts fitting the range, solve Eq. (8) for M and, if three-fold symmetry is possible, solve Eq. (5) for x_s. If not possible, solve Eq. (4) for K_θ/K_T and proceed by trial and error on the basis of known or feasible offsets.

Ratio of translational acceleration normal to base to total acceleration at the end is given by

$$\frac{G_1}{G_n} = \beta M , \qquad (9)$$

where

$$\beta = \sec \theta_1 \frac{x_1^2}{x_2^2} .$$

Natural frequencies are given by

Vertical: $$f_v = 3.13\sqrt{\frac{K_T}{W}} \qquad (10)$$

Rotational: $$f_R = \frac{f_v}{R_1}\sqrt{\frac{K_\theta}{K_T}} . \qquad (11)$$

For three-fold symmetry Eq. (11) simplifies to

$$f_R = \frac{x_s}{R_1} f_v . \qquad (12)$$

and, all things appearing satisfactory, the design is complete.

The technique outlined above was applied to the problem enumerated by Goodill (3) in the Guided Missile Handbook. It was found that K_T could vary between 4350 lb/in. and 21,000 lb/in. To make the problem the same, it was then assumed that the only stock mounts available gave K_T = 9070 lb/in. The results are summarized in Table 1.

Note that there are differences between the two approaches but most are attributable to inherent slide-rule error. The appeal of the method outlined here is its speed and flexibility.

TABLE 1
Comparison of Preliminary Values in a Specific Design Problem

	Goodill	This Paper	Difference
Maximum Deflection, in.	5.21	5.21	0
Deflection at Mount, in.	3.46	3.62	0.11
Deflection at c.g., in.	2.31	2.26	0.05
Mount Spacing, in.	21.5	23.0	1.5
Acceleration at c.g., g.	10.0	11.2	1.2
Vertical Natural Frequency, cps	6.67	6.67	0
Rotational Natural Frequency, cps	3.96	4.27	0.29

MINDLIN VS JANSSEN

If the same simple technique found for linear elasticity could be applied to certain classes of nonlinear elasticity, design would be greatly simplified. Before entering into an analysis of the rotational drop, however, it is expedient to compare the two main streams of cushioning theory to demonstrate their close relationship. For simplicity, the comparison will be made by using the flat drop test first. The comparison established, we will proceed to the rotational drop.

It will be recalled that Mindlin's classic paper (5) deals with specific initial spring rates of materials. From this he derives an expression of the optimum initial stiffness. Janssen, in effect, deals with another characteristic (called Jopt) of the stress-strain curve of a material, at which the

energy stress ratio is minimized. It has been clear for some time that the two workers were talking about two different properties of the same load-deflection (stress-strain) curve. What has been lacking, heretofore, is a clear bridge between the two techniques.

To illustrate, Mindlin states that minimum bottoming deflection, d_b, in tangent elasticity is given by

$$d_b = \frac{3.9\,h}{G_m}. \tag{13}$$

Janssen's theory, in its latest developments (6), states that minimum thickness is given by

$$T = \frac{Ch}{G_m}, \tag{14}$$

where C is the cushion factor.* Now, if we set s_b as the bottoming stress in a given material, it is obvious that

$$T = \frac{3.9\,h}{G_m\,s_b} = \frac{Ch}{G_m}. \tag{15}$$

Of course, the bridge is not clear yet since there are no readily available data concerning the bottoming stresses of cushioning materials. Equation (15) only indicates that there is a bridge, not its dimensions.

Mindlin's equation for tangent elasticity can be written in the form

$$y' = \frac{K_o'}{A} = \frac{\pi f_o}{2T\,s_b \tan\frac{\pi}{2}\cdot\frac{s_o}{s_b}} = \frac{3.1\,Wh}{AT^2\,s_b^2} \tag{16}$$

where

y' = initial stiffness, lb/in.^{3}

K_o' = optimum initial spring rate, lb/in.

A = area of cushion, in.^{2}

f_o = optimum stress, psi (Janssen's Jopt)

T = thickness, in.

s_o = optimum strain, in./in.

s_b = bottoming strain, in./in.

W = weight, lb

h = height of drop, in.

In an extensive analysis, Yurenka and Giacobbe (7) have shown that f_o always occurs at .707 s_b of tangential materials.*

From this, we obtain

$$\left.\begin{aligned} T &= \frac{Ch}{G_m} = \frac{2.75\,h}{G_m\,s_o} \cong \frac{5\,h}{G_m}, \\ y' &= \frac{.55}{T}\cdot\frac{f_o}{s_o} = \frac{1.55\,Wh}{AT^2\,s_o^2} \cong \frac{5.13\,Wh}{AT^2}, \\ f_c &= \frac{2.82\,Wh}{AT\,s_o} \cong \frac{5.13\,Wh}{AT}. \end{aligned}\right\} \tag{17}$$

In tangent elasticity, it has been shown that

$$\left.\begin{aligned} d_m &= \frac{2}{\pi}\,d_b \cos^{-1}\exp\left(-\frac{\pi^2 z^2}{8}\right), \\ G_m &= \frac{2\,G_o}{\pi z}\sqrt{\exp\left(\frac{\pi}{2}\cdot z\right)^2 - 1}, \end{aligned}\right\} \tag{18}$$

where

d_m = actual deflection,

d_b = bottoming deflection,

z = ratio d_o/d_b, i.e., the deflection which would occur if initial spring rate remained constant to the bottoming deflection of that material with the same spring rate.

Since

$$\left.\begin{aligned} d_b &= \sqrt{\frac{3.1\,Wh}{K_o'}}, \\ d_o &= \sqrt{\frac{2\,Wh}{K_o'}}. \end{aligned}\right\} \tag{19}$$

The value of d_o/d_b for optimum initial spring rate, initial stiffness parameter or best f_o value is given by

$$z = \sqrt{\frac{2}{3.1}} = 0.803, \tag{20}$$

and the value of z for any stiffness parameter differing from the optimum value will be given by

*Cushion factor as defined by Janssen is the ratio of stress to energy per unit volume.

*For the equally common algebraic elasticity, they have shown s_o/s_b = 68.4%.

$$z = .803\sqrt{\frac{K_o'}{K}} = .803\sqrt{\frac{y'}{y}} = .803\sqrt{\frac{f_o}{f}}, \quad (21)$$

where K, y, and f are the significant stiffness parameters of the material actually used.

Now, Mindlin's K_o' is defined as optimum in a restricted sense, i.e., as the initial spring rate using as much of the available space as feasible without encountering excessive multiplication of acceleration from the effects of bottoming. It is obvious that, once thickness is fixed by some means, it is not essential that only K_o' material be used. For example, a material with considerably greater stiffness parameter could be used with the logical limit being the initial stiffness which would cause the material to behave as though it were linear throughout the range of deflection required. Simple rearrangement produces

$$K'_{max},\ y_{max},\ f_{max} = 2.45\ (K_o',\ y',\ f_o). \quad (22)$$

When $z = 1.0$, G_m is twice what it would be for linear elasticity of the same initial spring rate. Above $z = 1.0$ the multiplication factor rises so rapidly as to be definitely unwise to use considering material variation. Again, simple rearrangement produces

$$K'_{min},\ y_{min},\ f_{min} = 0.64\ (K_o',\ y',\ f_o). \quad (23)$$

Thus, for a given problem, an envelope of materials is defined by solution of Eqs. (17), (22), and (23). The designer is free to use any particular computing procedure he finds convenient and can shift from one basis to another at will. Table 2 summarizes the design formulas involved.

ROTATIONAL DROP WITH TANGENT ELASTICITY

Having shown the relationship between Mindlin's methods and the methods based on Janssen's technique, we are now in a position to proceed to the rotational drop test. The analogy with the rotational drop with linear elasticity is clear. Hence, using Mindlin's notation, we may write

$$\left.\begin{aligned} d_b &= \frac{3.9\,h}{G_m}\cdot\frac{x_2^2}{R_3^2} \\ K_o' &= \gamma\,\alpha M^2 \\ \gamma &= \frac{3.1}{d_b^2} \end{aligned}\right\}. \quad (24)$$

Limits of initial stiffness are given by Eqs. (22) and (23). Basis shifting to the Janssen method is given by Table 3. The value of z can then be taken from Eq. (21). Ratio of end deflection to c.g. deflection normal to the base can then be estimated by rearranging the first of Eqs. (18) to give

$$M^1 = \frac{\cos^{-1}\exp\left(-\frac{\pi^2 z^2}{8}\right)}{\cos^{-1}\exp\left(-\frac{\pi^2 z^2}{8 M^2}\right)}. \quad (25)$$

TABLE 2
Design Formulas for Flat Drop with Tangent Elasticity

Quantity	Mounts	Cushions	
		Basic Method	Short Cut Approximation
Bottoming deflection, d_b	$\frac{3.9\,h}{G_m}$	--	--
Minimum thickness, T	$\frac{.707\,d_b}{s_b}$	$\frac{2.75\,h}{G_m\,s_o}$	$\frac{5h}{G_m}$
Optimum initial stiffness	$K_o' = \frac{3.1\,Wh}{d_b^2}$	$y' = \frac{1.55\,Wh}{AT^2\,s_o^2}$	$y' = \frac{5.13\,Wh}{A\,T^2}$
Best optimum stress, f_o	--	$\frac{2.82\,Wh}{AT\,s_o}$	$\frac{5.13\,Wh}{A\,T}$

TABLE 3
Design Formulas for Rotational Drop Test with Tangent Elasticity

Quantity	Mounts	Cushions	
		Basic Method	First Approximation
Bottoming deflection, d_b	$\frac{3.9\,h}{G_m} \cdot \frac{x_2^2}{R_3^2}$	--	--
Minimum thickness, T	$\frac{.707\,d_b}{s_o}$	$\frac{2.75\,h}{G_m s_o} \cdot \frac{x_2^2}{R_3^2}$	$\frac{5\,h}{G_m} \cdot \frac{x_2^2}{R_3^2}$
Optimum initial stiffness	$K_o' = \gamma \alpha M^2$	$y' = \gamma \alpha M^2$	$y' = \gamma \alpha M^2$
γ	$\frac{3.1}{d_b^2}$	$\frac{1.55}{AT^2 s_o^2}$	$\frac{5.13}{AT^2}$
Best optimum stress, f_o	--	$\gamma \alpha M^2$	$\gamma \alpha M^2$
γ	--	$\frac{2.82}{ATs_o}$	$\frac{5.13}{AT}$

While the answers to Eq. (75) can be obtained with a log-log slide rule, Fig. 2 plots this function for several values of z. Similarly, the second of Eqs. (18) can be modified to express acceleration ratios as

$$\frac{G_1}{\beta G_m} = s = M^2 \sqrt{\frac{\exp\left(\frac{\pi z}{2M}\right)^2 - 1}{\exp\left(\frac{\pi z}{2}\right)^2 - 1}}. \qquad (26)$$

s versus M for several values of z is plotted in Fig. 3.

An estimate of natural frequencies for small excursions is then obtained by using Eqs. (10) and (11). Equation (10) can be rewritten as

$$f_v = 3.13\sqrt{\frac{y'}{f_s}} = 2.32\sqrt{\frac{f_o}{f_s} \cdot \frac{1}{Ts_o}} \cong 3.13\sqrt{\frac{f_o}{f_s} \cdot \frac{1}{T}}, \qquad (27)$$

where f_s = static stress on the cushion.

DISCUSSION

The preceding section gives a design method applicable to tangent elasticity. As noted, it is approximately accurate for algebraic elasticity.

The method shows that a rather wide range of cushioning materials is usable to solve a specific design problem. Since drift, permanent set and static deflection are usually proportional to stiffness, it is usually better to work towards the stiffer allowables insofar as economically feasible.

In actual practice with cushioned packs, an uncoupled system seems extremely unlikely. Further, in large containers, thickness and area on ends and tops are often entirely different from bottom thicknesses and areas because of differing test conditions and the lesser energy involved in rebound. Top and end cushions must, of course, be used in determining rotational spring rates and, therefore, estimation of accelerations, etc., requires one or two successive approximations. Nevertheless, the method still offers a practical plan of attack on an otherwise very difficult problem.

REFERENCES

1. D. M. Chase and I. Vigness, NavResLab Rept. 4719, Mar. 30, 1956.
2. R. S. Ayre and J. I. Abrams, Chapter 11, RD219/3.

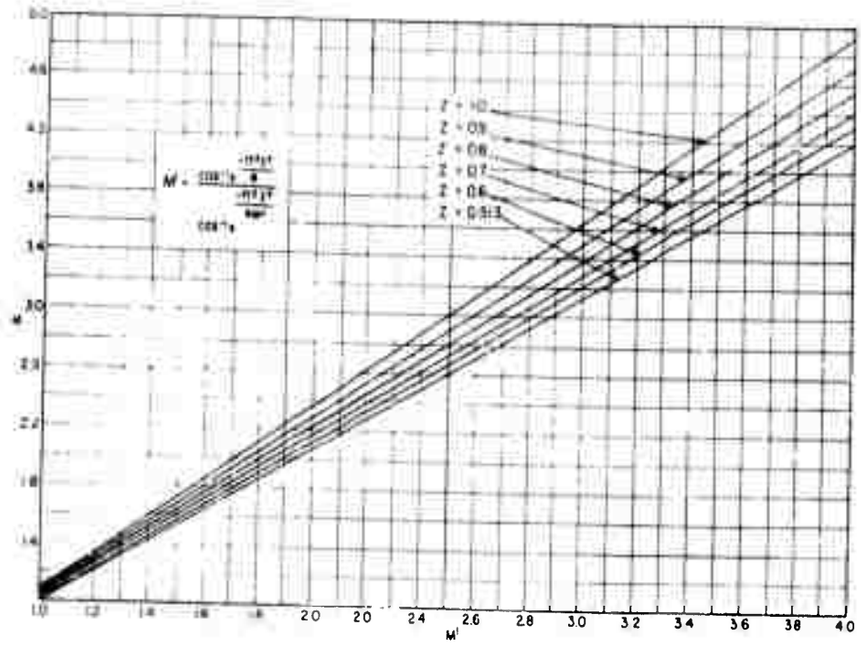

Fig. 2 - M^1 vs M for various values of z

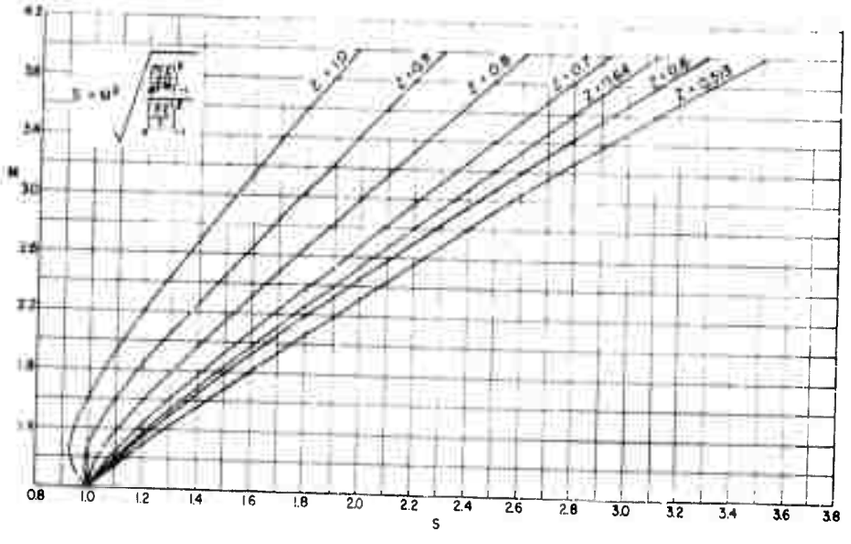

Fig. 3 - s vs M for various values of z

3. J. J. Goodill, Appendix 8, p. 15, RD219/3.

4. M. J. Peterman, Chapter 8, Section II-L, RD219/3.

5. R. D. Mindlin, Bell System Technical Publications Monograph B-1369.

6. R. E. Jones and W. L. James, Chapter 9, RD219/3.

7. S. Yurenka and C. R. Giaccbine, Douglas Aircraft Co. Testing Division Report No. Dev.-2128, 20 July 1956.

* * *

TEST METHODS AND TECHNIQUES

THE REVERSE-ACTION SHOCK-TESTING METHOD

J. W. Apgar and G. R. Thomson
Development and Proof Services
Aberdeen Proving Ground, Maryland

A versatile shock-testing method has been developed in which a deflected structural member, such as a cantilever, is suddenly released. At the bottom of the second quarter cycle, the object being tested is disconnected. Selection of pulse duration is flexible, and the device can be designed for testing large items.

DEVELOPMENT

In the spring of 1959, Development and Proof Services, of Aberdeen Proving Ground, conducted high-g low-frequency tests on crystal accelerometers. Greater than 2000 g were achieved at frequencies below 500 cps by means of a 2 × 3-inch cantilever beam of 4140 steel heat-treated to a C-45 Rockwell hardness. A universal testing machine with an upper range of 600,000 pounds was used to provide both a massive base and a large clamping force for the fixed cantilever end. Originally, the clamping force was distributed through two, large, rectangular, steel blocks over a foot of the cantilever bar. By use of this bar the length of the cantilever could be varied between 8 and 16 inches. Tests conducted at the 10-inch length indicated a fundamental frequency 26 percent below that calculated from the formula

$$f = \frac{3.515}{2\pi}\sqrt{\frac{GEI}{wl^4}},$$

where f = frequency,
E = Young's modulus of elasticity,
I = moment of inertia,
w = weight per unit length,
l = length of cantilever.

At first this rather startling difference was attributed to the fixed-end conditions of the bar. A fixture was built to distribute the clamping force over four sides of the beam. The design, as shown in Fig. 1, provided an internal space around the beam into which could be inserted a filler to distribute the force. A 2 × 4 × 36-inch beam, also of 4140 steel heat-treated to a Rockwell hardness of C-45, was fabricated for the new fixture. Tests on the new cantilever, conducted under the same conditions as those on the old, revealed a fundamental frequency 15 percent below that calculated. These differences for the two beams are shown in Table 1 for a 10-inch cantilever length.

TABLE 1
Calculated vs Experimental Fundamental Frequencies

Beam (in.)	Fundamental Experimentally Determined (cps)	Fundamental Calculated (cps)	Difference (%)
2 × 3	475	645	26
2 × 4	550	645	15

Other tests followed in which lead and then rubber were used as fillers. Clamping forces from 1000 to 10,000 psi were applied. In no case was the fundamental frequency of

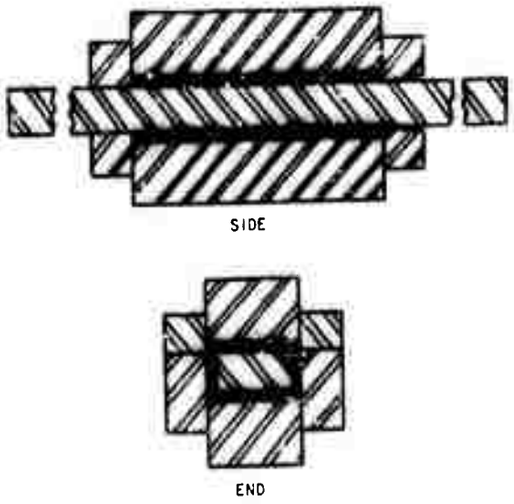

Fig. 1 - End constricting fixture variable length cantilever beam

the beam appreciably altered. As might be expected, the damping of the beam was somewhat affected by the end conditions. In spite of being completely constrained, rubber and lead each exerted an influence on the damping factor, with rubber exerting the most. The damping factor also decreased slightly with increase in clamping load in the range from 1000 to 6000 psi. Beyond this point, change in load seemed to have little effect. Figure 2 and Table 2 show the influence of these end conditions.

SHOCK TESTING

Although we didn't account for the differences between fundamental frequencies determined theoretically and those determined experimentally, we did build fixtures, develop techniques, and establish conditions which could be used in shock tests. The need for a specific type of shock-testing machine arose when we were asked last August to shock test a number of tank periscopes in accordance with methods described in

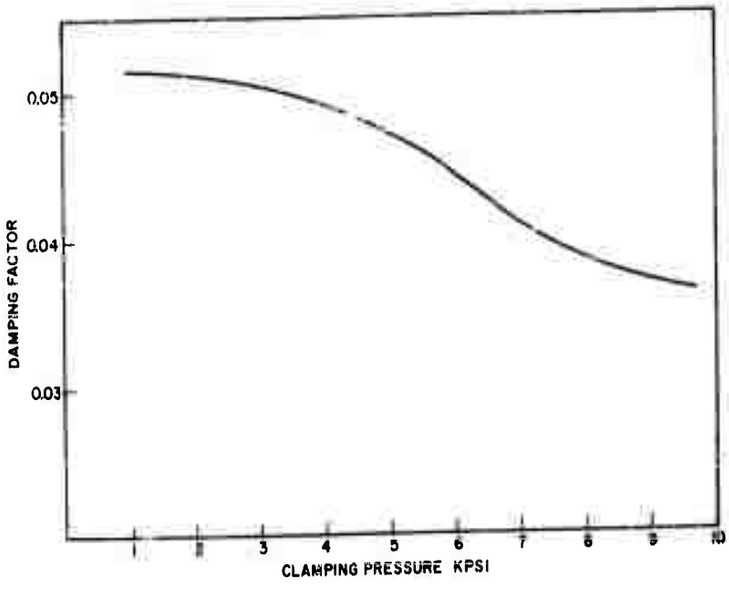

Fig. 2 - Damping factor vs clamping pressure

TABLE 2
Damping Factors for Various Clamping Materials

Clamping Material	Damping Factor
Steel	0.033
Lead	0.048
Rubber	0.078

specification JAN-S-44. Although we lacked the equipment described, we were able to use our cantilever setup to produce the desired shocks. The requesting group asked for a peak shock of 150 g during a pulse of approximately 7 ms. If the pulse is converted to frequency, the approximate length of the cantilever can be determined from the formula

$$f = \frac{1}{2\pi}\sqrt{\frac{3EIG}{\left(W + \frac{33}{140}wl\right)l^3}},$$

where W = weight of test item plus holding fixture. This length then can be experimentally adjusted to provide the desired frequency. A 7-ms pulse corresponds to a 70-cps frequency, and 150 g corresponds to a 0.3-inch amplitude at this frequency. Thus, if the cantilever is properly adjusted for length, deflected 0.3 inch, and suddenly released, an object represented by w should undergo a 150-g peak acceleration. Our previous work has produced a sudden-release method, which is indicated in Fig. 3. This involved attaching a bolt to the free end of the cantilever and linking the bolt to a strain-gaged drawbar. The drawbar in turn extended through a hollow jack and terminated in a nut which served as a jacking surface. The hollow jack was supported by two 12-inch I-beams which were fixed to the universal testing machine. With this arrangement, the drawbar could be jacked until the bolt broke. If measurements of drawbar strain vs cantilever deflection had been made, then an oscillograph-recording strain would have revealed the deflection of the cantilever at the time that the bolt broke. The cantilever thus set in motion would have produced an acceleration trace of the form shown in Fig. 4a.

To prevent the object under test from being subjected to all the pulses shown, a

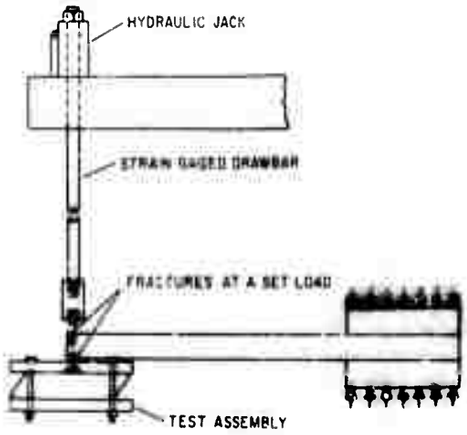

Fig. 3 - Setup for cantilever beam shock test

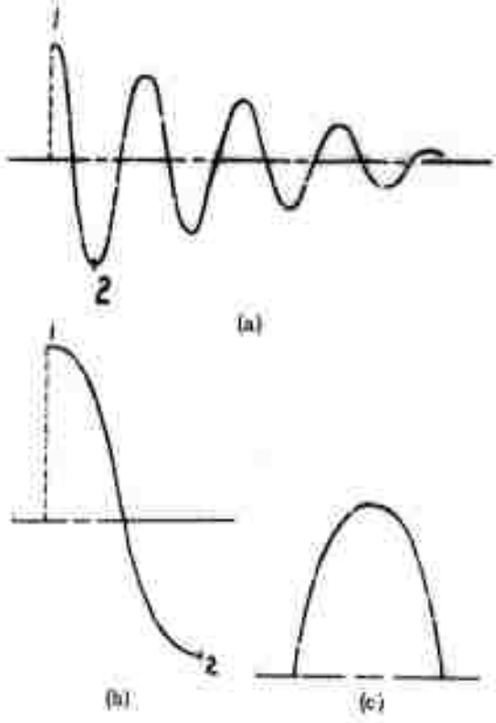

Fig. 4 - Acceleration vs time curves (a) Transient cantilever vibration decay, (b) Typical pulse of cantilever shock device, (c) Typical pulse of JAN-S-44 shock device

second quick release was required. This second release was accomplished by a method similar to that of the first. A test object undergoing the acceleration (indicated by the trace between points 1 and 2 in Figs. 4a and 4b) will exert a steadily decreasing upward force during the first quarter cycle

and a steadily increasing downward force during the second quarter cycle. The maximum downward force will never equal the initial upward force because of the hysteresis in the system. If the bolt holding the test object is sufficiently weaker than the drawbar bolt, it will be ruptured by the downward force, and the test object will drop under conditions approaching free fall. There are certain inherent advantages to this method. If the acceleration pulse thus obtained (Fig. 4(b)) is compared with that obtained by the JAN-S-44 method (Fig. 4(c)), it is evident that they both represent the same amount of energy. Under the JAN-S-44 conditions, however, the shock is unidirectional and, depending on the mounting of the test item, can produce either compression or tension failures but not in the same test. Under the conditions of the cantilever tests, the test item is exposed to shock successively in opposing directions and therefore can produce compression and tension failures in the same test. If desired, the reversal shock can be greatly reduced by making the holding arrangement of comparatively elastic material. Another advantage of this system is that the tester has a wide range for pulse selection by the change, individually or collectively, of cantilever length and test mass.

In this system, it was necessary to know the breaking strength of the bolts used to control the applied shock. Breaking strength of ordinary bolts could be estimated to an accuracy of ±5 percent by hardness checks. These accuracies could be much improved through the use of bolts made of 4130 or 4140 steel. Later tests have indicated that the values estimated were within ±1 percent of the tensile values. In all cases, the bolts were heat treated to produce brittle fracture. As a rule of thumb, the bolts releasing the test specimen were selected to have a strength equal to one half the value calculated from the formula

$$F = WAg ,$$

where F is the downward force, W is the weight of the test assembly, and Ag is the maximum acceleration in g's. Consequently, the test items were released with a small downward thrust. By determining the cantilever damping factor, bolts strong enough to practically eliminate this thrust could be selected. As pointed out previously, this damping factor could be minimized by applying damping pressures of 6000 psi at the fixed beam end.

OTHER CAPABILITIES

In addition to the properties previously listed, this testing device has the following other capabilities. It can be used to apply shock in three planes if the mounting position of the test item is changed with respect to the cantilever. It is also possible to mount the cantilever so that its plane of action is horizontal. In the latter way gravitational effects can be neutralized. With this device items weighing up to 100 pounds can be accelerated up to 100 g, and items weighing less than 1 pound can be accelerated up to 2000 g. The bolt-fracture release method suggests itself as a tool for the study of the behavior of materials under impulsive loads. A small tensile specimen could be substituted for the release bolt. By selection of cantilever conditions, the duration of the fracturing pulse could be selected. In this way, the breaking strengths of materials could be determined under dynamic conditions.

In conclusion, it should be stated that both larger and different structural members can be used to achieve shock in this manner. The elastic system could be a simple or fixed beam or a spring to which the deflection release-bolt combination could be applied. Figure 5 shows an arrangement in which there is a beam fixed at both ends and a platform in the middle. This setup will be investigated in the near future. An advantage that the fixed-end beam should have over the cantilever is that the test item should travel in a straight line instead of in a slight arc. By proper proportioning of the structional members, it should be possible to build a device to test more massive items.

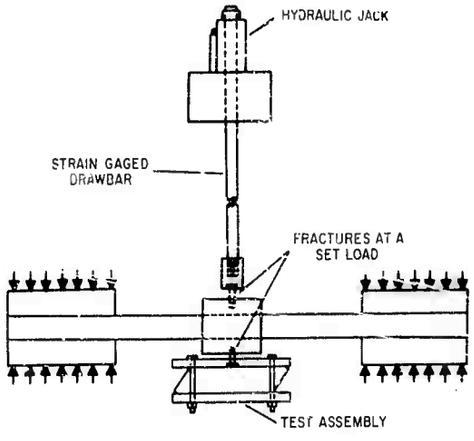

Fig. 5 - Setup for fixed end beam shock test

We are now investigating the feasibility of utilizing this method for the shock testing of items weighing up to 2000 pounds.

SUMMARY

1. Fundamental frequencies of a 2 × 3 × 10-inch and a 2 × 4 × 10-inch cantilever determined experimentally were 26 percent and 15 percent lower, respectively, than those determined theoretically.

2. Distributing the clamping pressure over four sides of a 2 × 4 × 10-inch cantilever beam had no appreciable affect upon its fundamental frequency.

3. Lead and rubber under conditions of total constraint at the base of the cantilever appreciably increase the cantilever damping factor.

4. Increasing the clamping force decreased the damping factor asymptotically. Above a force of 6000 psi the affect was not appreciable.

5. A shock-testing method was developed from this work in which a deflected structural member, such as a cantilever, was suddenly released. At the bottom of the second quarter cycle, the object being tested disconnected. Accelerations opposite to the initial provided the disconnecting action.

6. This method provides great flexibility for selection of pulse duration.

7. Breaking strengths of ordinary bolts used to obtain quick releases can be estimated to within ±5 percent by hardness checks. This accuracy can be much improved through use of bolts made of 4130 or 4140 steel.

8. Shock so applied can be used to produce compression and tension failures in a single test. If desired, the reversal shock can be minimized.

9. This method can be used to apply shock in three mutually perpendicular planes.

10. Other structural members, such as simple or fixed-end beams and springs, can be used to achieve this type of shock.

11. This device can be designed for the shock testing of large items.

12. The bolt-fracture release method could be used for the determination of strengths of materials under controlled dynamic conditions.

13. Unidirectional shock can be approached by making the holding arrangement for the test object of comparatively elastic material.

BIBLIOGRAPHY

1. W. T. Thomson, Mechanical Vibrations, Prentice Hall, Inc., 1953.
2. T. H. H. Pian, Random Vibration (S. H. Crandall, Ed.), Technology Press of M.I.T. Ch. 5.
3. R. Middleton, Vibration Notebook, M. B. Co. Publications, April 1959.

DISCUSSION

Dr. Mains (General Electric): I would like to inquire what particular reason you had for wanting to stop at the end of the first downward cycle?

Mr. Apgar: Well, there was no basic reason, except that we were trying to produce a pulse similar to what the requesting group asked for; and we had this equipment already at hand, it enabled us to produce a shock pulse which satisfied our requesting agency.

Dr. Mains: You see, I had an ulterior motive for asking this question. The JAN spec, with the half sine pulse, is tailored to suit a particular kind of testing machine, not necessarily to suit the kind of excitation that you would like to simulate.

Mr. Apgar: Right

Dr. Mains: Now, you have here a device which can come a lot closer to simulating the shock pulse that is wanted than a sand-drop tester can. This is the time to go to bat and ask for a waiver on the JAN spec in favor of a much better test that you can produce with your damped sinusoid shock.

Mr. Apgar: Well, this was my feeling toward the device, but, as I say, I am a tester, not one who works up the specs.

Mr. Stern (General Electric): At the beginning of the talk you mentioned the calculation of a natural frequency of the cantilevered beam, and you indicated that the observed as against the calculated values disagreed appreciably. Then you had two formulas--you discussed only the first one, for the simple cantilever beam. Then you had a second formula which took into account the weight, is that right?

Mr. Apgar: Yes, that's true. Now, as I said in the initial part of the talk, there was no weight attached to the cantilever, merely the accelerometer. Actually, we had no holding device. We also made calculations to show what amount of weight would be taken into account by the accelerometer. We were really straining.

Mr. Stern: It seemed that nowhere in your discussion did you take into account shear and rotary inertia—and you had a rather stubby cantilevered beam there.

Mr. Apgar: Right.

Mr. Stern: There is a book out by Jacobson and Ayre which has two plots in it, one for cantilevered beams and one for simply supported beams, and they show you what is the correction for shear and rotary inertia in stubby beams. If you use this, it might show you why you had this discrepancy. Perhaps the second formula, even though you took into account the weight, did not cover everything.

For the other point you mentioned, breaking the bolt, you might want to try a device (I think it's J. C. Fisher's, from NOL). He used this in an air gun to release a piston where you have a bolt with a V-groove in it. The device is hit with a hammer when the desired load is reached, then the breaking load can be controlled much more accurately.

Mr. Apgar: Well, I thought that, actually, with the bolt heat-treated for brittle fracture, ±1 percent wasn't too bad for this type of operation.

Mr. Stern: No, it isn't, but sometimes it doesn't always break, even with 1 percent. Sometimes it won't always break exactly where you'd want it; but when you have a V-groove it will.

Mr. Apgar: I might say that we did notch our bolts to give us exactly what we wanted, and we checked many bolts beforehand to be sure that this would be so. We also have a final judgment because we can look at our oscillograph and see exactly what the deflection of the cantilever was at the time that the bolt broke. I might say that in almost all our tests we didn't find too much to worry about.

Mr. Jones (Army Ballistic Missile Agency): In Fig. 5 you showed a clamped-clamped beam. Because one of your problems was clamping force you used the big machine, and you probably still had a terrific clamping force necessary. I wondered why you didn't use a hinged-hinged beam.

Mr. Apgar: Well, we have had just enough time to play around with the cantilever. I might say that one could play around with this thing exhaustively. We are primarily a testing agency, but I would certainly love to have the time to explore all the different possibilities —

Mr. Jones: Oh, I wasn't trying to make any accusations. I was merely asking if there is anything wrong with a hinged-hinged beam.

Mr. Apgar: Well, I can't see anything at all wrong with it. I merely showed Fig. 5 to indicate that this method could be applied to almost any spring-mass system. It depends upon the ingenuity of the designer and the person who is playing around with it. The device which I showed happened to be another beam which we had already made up for another test, and it came in very handy.

Mr. Hancock (Radiation Incorporated): Do you feel that this method of testing would be directly replacing the half-sine wave shock pulse, and in so doing would it eliminate one of the objectionable features of, say, the sand-drop testing method, the effects of mechanical coupling between specimen and table?

Mr. Apgar: Let me state that in the first place we don't have that type of a test device. Probably if we had had the one specified in JAN-S-44, we wouldn't have used this, so I am not in a position to tell whether it should be used to replace it, or not. I feel that people who are in a specifying department, those who work up shock pulses, what should be used, are the ones who should state what should be used or what shouldn't. I merely wanted to suggest it, as what I thought would be a very useful device for somebody who had another Universal testing machine like I have.

* * *

THE AIR SHOCK TUBE AS A SHOCK TESTING FACILITY

Stanley R. Melcher
U.S. Naval Missile Center
Pt. Mugu, California

At the Naval Missile Center a shock tube has been used to generate square wave shock pulses for shock testing of components. This paper describes the facility, typical test configurations, and results.

INTRODUCTION

Shock tests are normally employed to determine if a test article can withstand the mechanical shocks likely to be encountered in the field. The test package is bolted to the shock-testing facility and subjected to impact shocks at various amplitudes and pulse durations. The ability of a shock pulse to excite natural frequencies is dependent on the pulse shape and duration. Since present shock facilities are limited in their ability to produce the desired pulse spectrum, it is difficult to obtain quantitative shock-test data.

These difficulties may be partially overcome by using a step function or rectangular shock pulse and defining the response characteristics of the test configuration in terms of this pulse. The air shock tube has the ability to produce a high-pressure region for a usable time duration. This high-pressure region may be used to shock a test configuration with essentially a step function.

SHOCK TUBE THEORY

The shock tube is a long tube that is divided by a thin diaphragm material into a high-pressure and a low-pressure chamber (Fig. 1a). The bursting of this diaphragm causes a shock wave, a contact surface, and a rarefaction wave to be developed in the tube (Fig. 1b). If air is used in both chambers and is initially at a uniform temperature, the pressure of the shock wave P_s may be related to the initial pressure ratio P_c/P_o in the following manner:

$$\frac{P_c}{P_o} = \frac{\frac{P_s}{P_o}}{\left[1 - \left(\frac{P_s}{P_o} - 1\right)\left(7 + 42\,\frac{P_s}{P_o}\right)^{\frac{1}{2}}\right]^7} \qquad (1)$$

Ref. (1)

where P_c and P_o represent absolute pressures in the high-pressure and low-pressure chambers. This relationship may be shown by plotting P_s/P_o vs P_c/P_o (Fig. 2).

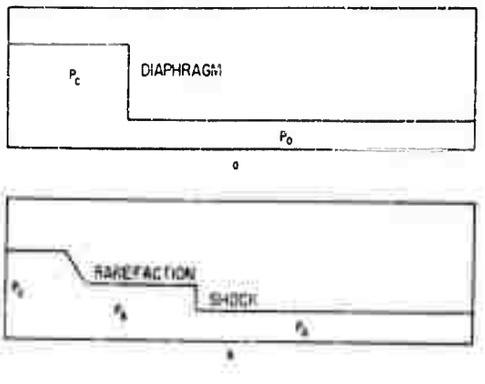

Fig. 1 - Schematic of shock tube operation: (a) Before diaphragm burst, (b) After diaphragm burst

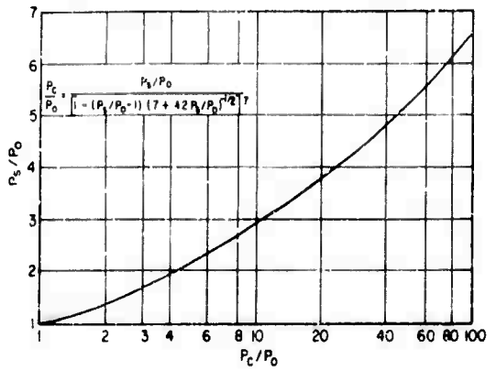

Fig. 2 - Shock strength

The shock wave will travel down the low-pressure chamber at a theoretical velocity of

$$V_s = c\left[\frac{1 + 6\frac{P_s}{P_o}}{7}\right]^{\frac{1}{2}}, \quad \text{(2) Ref. (2)}$$

where c is defined as the local velocity of sound. The shock MACH number V_s/c or M_s may be plotted as a function of P_s/P_o (Fig. 3). The region behind the shock and across the contact surface has a constant pressure P_s and travels at a velocity of

$$U = \frac{\left(\frac{P_s}{P_o} - 1\right)}{\left(7 + 42\frac{P_s}{P_o}\right)^{\frac{1}{2}}}\cdot \quad \text{(3) Ref. (1)}$$

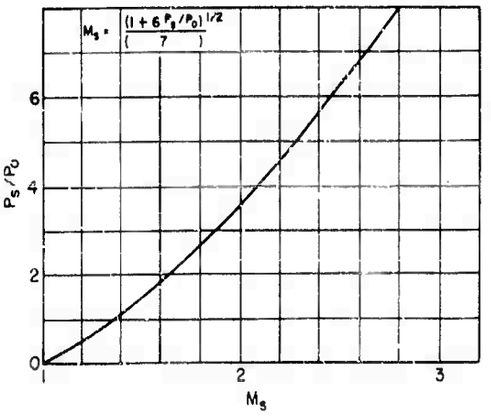

Fig. 3 - Shock velocity

A rarefaction fan develops at the diaphragm and is reflected back from the closed end of the high-pressure chamber. The velocity of this rarefaction wave is equal to the sum of local sound and gas velocities and may be determined by an iteration procedure (3). This means the rarefaction wave may overtake the shock wave if the shock tube is of sufficient length (Fig. 4a).

The shock wave is reflected from the end of the tube and leaves behind it a gas at a pressure (Fig. 4b

$$P_r = 2P_s\frac{(7P_o + 4P_s)}{7P_o + P_s}\cdot \quad \text{(4) Ref. (1)}$$

The pressure ratio P_r/P_o may be plotted vs the MACH number, Fig. 5). The pressure difference $P_r - P_o$ is greater than twice the pressure difference across the shock and may be represented by the equation

$$\frac{P_r - P_o}{P_s - P_o} = \frac{6 + 8\frac{P_s}{P_o}}{6 + \frac{P_s}{P_o}}\cdot \quad \text{(5) Ref. (2)}$$

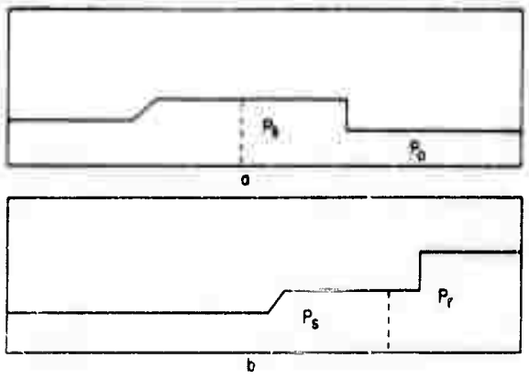

Fig. 4 - Reflaction of rarefaction and shock waves in shock tube: (a) After reflection of rarefaction, (b) Reflection of shock wave

The velocity of the reflected shock may be determined by the equation

$$V_r = \frac{c\left(2\frac{P_s}{P_o} + 5\right)}{\left(7\left(6\frac{P_s}{P_o} + 1\right)\right)^{\frac{1}{2}}}\cdot \quad \text{(6) Ref. (1)}$$

The contact surface between the gas initially in the low- and high-pressure chambers has a temperature and density discontinuity across it. The reflected shock wave is therefore reflected from this surface back toward the end of the shock tube (4). The

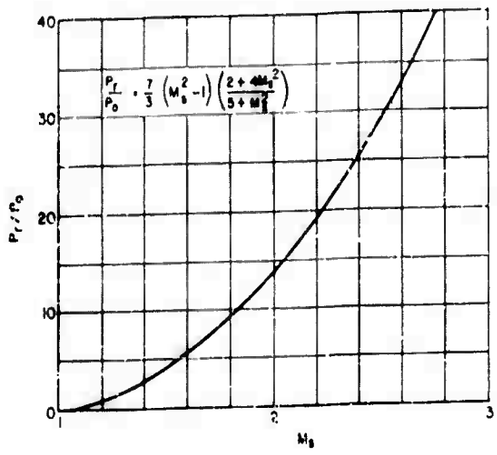

Fig. 5 - Reflected shock amplitude

time difference between the two shock reflection and rarefaction wave reflection represents the testing time at the high pressure P_r (Fig. 6).

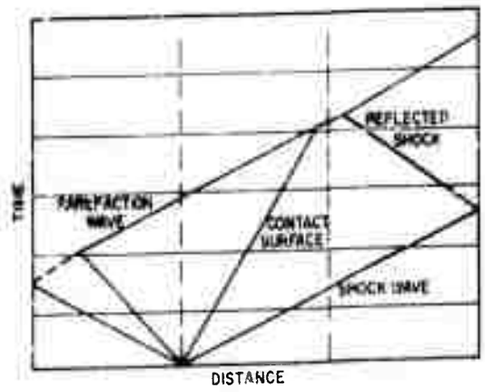

Fig. 6 - Time-distance plot of shock tube waves

CONFIGURATION

The U. S. Naval Missile Center shock tube is six inches in diameter and has an overall length of 28 feet (Fig. 7). The high-pressure chamber is five feet long with a plunger extending along its entire length. The plunger is used to burst the diaphragm which is placed between the high-pressure chamber and the low-pressure or expansion chamber. Photographic film is used as a diaphragm material and the thickness is varied to obtain catastrophic rupturing for various pressure ratios. The diaphragm material is sealed on the high-pressure chamber side with a rubber "O" ring and supported on the low-pressure side with a grid network (Fig. 8).

The end of the low-pressure chamber is fitted with a plug. The test component is attached to this plug and the entire configuration suspended as a pendulum. The test specimen and plug are allowed to move out and away from the shock tube as a result of the shock (Fig. 9). This allows the test configuration to be designed to simulate approximately the field assembly.

SHOCK THEORY

An analysis of the response of simple spring mass system to various pulses may be obtained by the use of Duhamel's integral (5). A calculation for a rectangular pulse indicates an amplification factor of two, provided the pulse duration is equal to or greater than 1/2 f_n where f_n represents the lowest natural frequency of the test configurations. An analysis of various other pulse shapes indicates amplification factors dependent upon the pulse duration, pulse shape, and leading-edge rise time. The rectangular pulse therefore represents the ideal shock pulse to obtain amplifications and frequency-response characteristics. A system with several degrees of freedom will have amplification factors dependent on the driving point as well as the forcing function. A step function will represent the most severe shock, and data may be obtained accordingly.

USE OF THE SHOCK TUBE

The theoretical rise time of a shock tube pulse is approximately 10^{-8} seconds. The rise time observed in practice is generally greater than the instrumentation capabilities and is dependent on the diaphragm burst characteristics and shock wave interference in the tube. This interference is primarily due to wall roughness and diaphragm particles that are carried along with the shock wave. The higher shock amplitudes are found to be somewhat less than that predicted by theory and these experimental results may be attributed to the same interference.

The pulse durations that may be obtained are dependent on the shock-tube length, the relative pressures, temperatures, and densities of the gases and may be calculated for the various conditions. These basic shock-tube characteristics may be improved

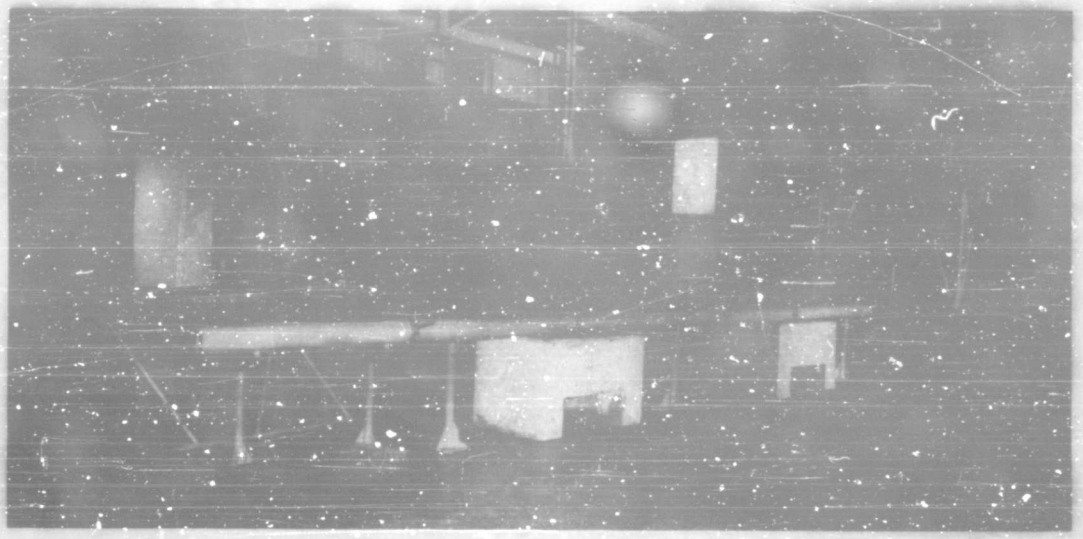

Fig. 7 - Air shock tube at the Naval Missile Center

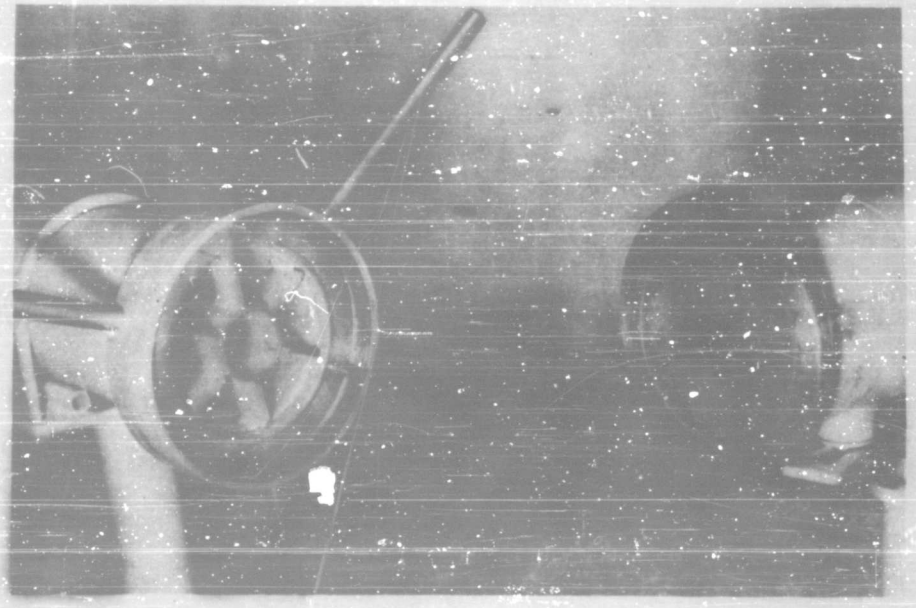

Fig. 8 - Diaphragm assembly

by resorting to various modifications which are covered in the literature on the subject.

The shock tube equations presented are for a basic shock tube with a closed end. When the shock tube is used as a shock testing facility, the end is allowed to move out as a result of the forcing function. Theoretically, this should result in a decrease in the forcing function or high-pressure gas P_r. In practice, the effect of this decrease in pressure is usually negligible. This high-pressure region is relatively long compared with the movement of the test configuration, resulting in very little change of the PV equations. A noticeable effect may be observable for light test configurations which are accelerated to high velocities. The effects of secondary shock reflections are also observed for some test situations. This

Fig. 9 - Klystron test assembly showing end plug

phenomena may be observed in the oscillograph recordings of Fig. 10. Figure 10b is the response of the accelerometer on the plug and indicates a rapid drop in pressure. This pressure decrease is attributed to an interaction between the rarefaction wave and the reflected shock wave and is dependent on the shock-tube length and initial pressure ratio.

The klystron test configuration of Fig. 9 was shock tested to determine the frequency variation of the klystron tube (Fig. 10a) as a result of shock. The frequency variation was found to be a function of shock amplitude and varied at definite discrete frequencies corresponding to natural resonance. The klystron mounting accelerometer was used to obtain the natural frequency of the mounting (Fig. 10c). This information may be used to evaluate the performance of the assembly in its natural environment.

Figure 11 is a missile configuration test setup. The missile is suspended from an "A" frame and is attached to the plug. Figure 12 represents the frequency response and transmissibility characteristics observed at various stations along the missile.

CONCLUSION

The shock tube has the ability to produce a single, rectangular pulse with a sharp leading edge. The proper design of the shock tube will result in pulse durations in excess of 10 ms. Longer pulse durations may be obtained with low-pressure ratios.

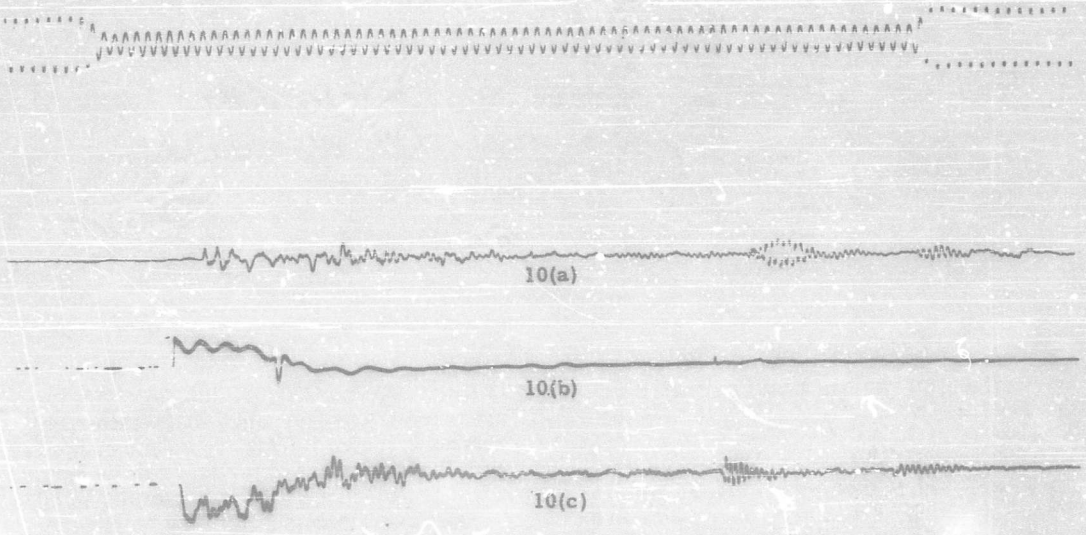

Fig. 10 - Oscillograph recordings of klystron test: (a) Klystron frequency variation under shock, (b) Forcing function from accelerometer on plug, (c) Klystron mount response from accelerometer on the mounting

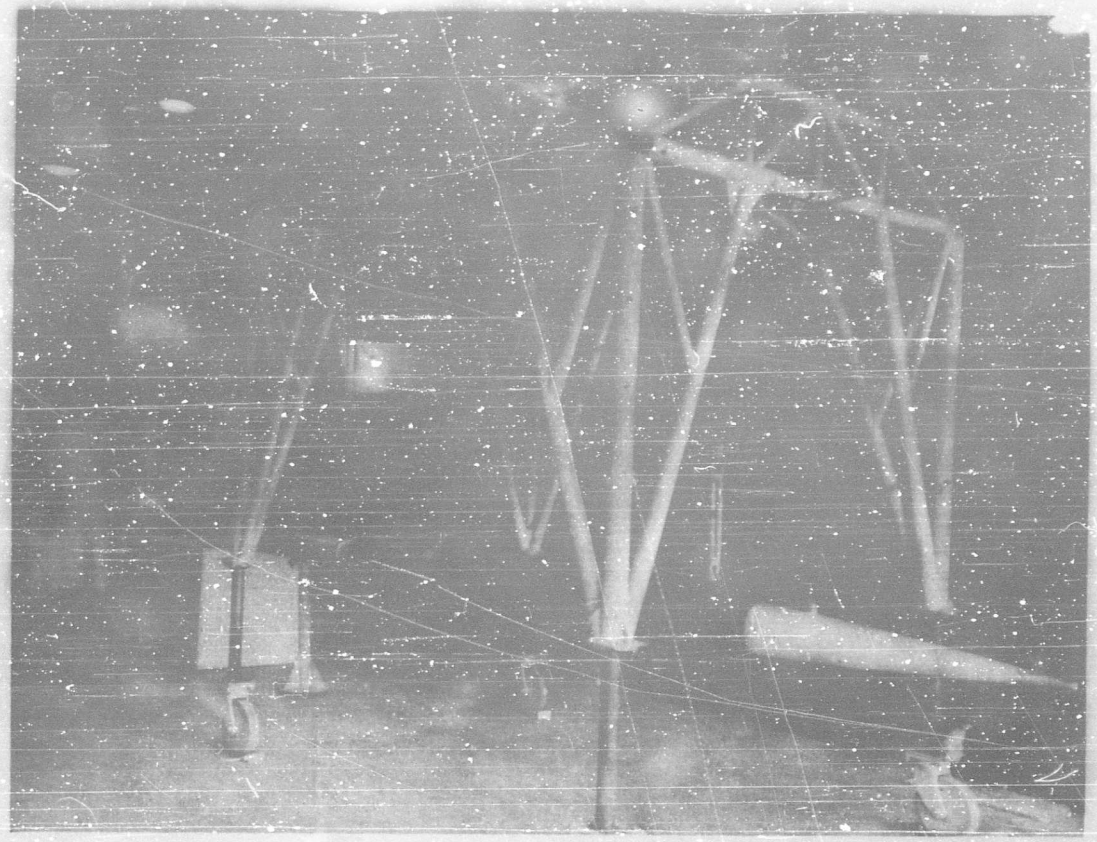

Fig. 11 - Missile test configuration

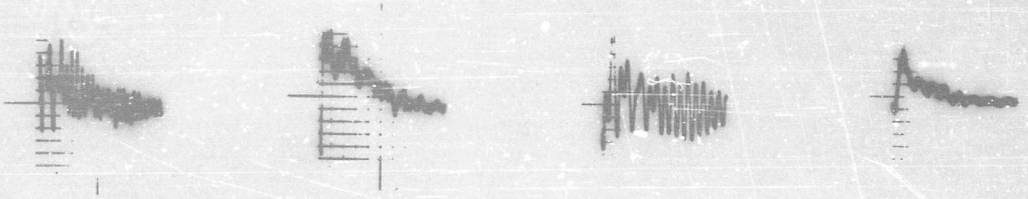

Fig. 12 - Missile response characteristics

This allows the determination of resonance and frequency response characteristics for most mechanical systems. The extremely sharp leading edge of the pulse allows structures to be excited at any high natural frequencies inherent in the structure.

Relatively high shock amplitudes may be obtained with a simple air-to-air shock tube and normally available air supplies. The adaptability and versatility of the shock tube allows test configurations to be designed to simulate field assemblies closely and to reduce the effect of mechanical impedance inherent in most test facilities. These features of the shock-tube facility simplify the design of quantitative tests for a wide range of test situations and analytical studies.

REFERENCES

1. P. O. Smith and P. S. Lederer, "The Shock Tube as a Facility for Dynamic Testing of Pressure Pickups," NBS Report 4910, (March 1957).
2. Allen E. Wolfe, "Shock Tube for Gage-performance Studies," JPL Report 20-87 (May 1955).
3. George Rudinger, "Wave Diagrams for Nonsteady Flow in Ducts," D. Van Nostrand Company, Inc., 1955.
4. Herman Mark, "The Interaction of a Reflected Shock Wave with the Boundary Layer in a Shock Tube," Cornell University AFOSR-TN-57-345, AD132 418 (June 1957).
5. M. Kornhauser, "Prediction and Evaluation of Sensitivity to Transient Accelerations," J. Applied Mechanics, Vol. 21, No. 4.

DISCUSSION

Mr. Baranoff (Aeronutronics): Would you state specific g levels and pulse durations?

Mr. Melcher: The g levels obtained will depend upon the mass of the test configuration. With missiles we have obtained shocks of 50 g, as for example, with the missile configuration you saw in Fig. 11. For small test configurations we went to 60 g, say, but we could have gone higher on those things.

As for the pulse duration, this may be determined theoretically from the basic shock-tube equations, and for very-low-pressure ratios we have obtained pulse durations in excess of 20 ms. For some of the higher pressure levels with this particular shock tube, we have been down to perhaps 4 or 6 ms—in that area—but this has depended upon the design of the shock tube, the length, the pressure ratio, and so on.

* * *

SHOCK TESTING POLARIS MISSILE RE-ENTRY BODIES WITH AN ELECTRODYNAMIC SHAKER

H. O. Lewis
Lockheed Missiles and Space Division
Sunnyvale, California

This paper describes a method devised for shock testing Polaris re-entry bodies wherein any available electrodynamic shaker of 25,000 pounds force output can be used. The versatility of the system is emphasized in that the shock pulse can be modified within wide limits and may be superimposed on vibration.

INTRODUCTION

Early in 1959, a difficult shock test requirement was presented to the Polaris Missile System Test Services laboratory. A Polaris re-entry body, weighing nearly 1000 pounds with its test fixture, had to be excited with shocks of 50 g for 2 ms, and 25 g for 7 ms. Various types of shock test equipment were considered in terms of ability to duplicate the required pulses with a reasonable degree of fidelity, availability, amount of required setup time, number of preliminary shocks required to achieve fidelity, cost, and adaptability to our security requirements.

A 13-inch Hyge impact tester was being installed in the laboratory at the time, so it received initial consideration. Unfortunately, the manufacturer, when contacted concerning our problem, was unsure of the ability of the Hyge to handle the large mass of the test specimen. In addition, the metering pins necessary to generate a 2-ms shock were not available. If the correct pins had been available, the Hyge still would have required disassembly between shock pulses. This is necessary since metering pins of different sizes are required for each different pulse duration.

Drop testers, ballistic hammers, and other similar testing schemes were eliminated because of poor repeatability characteristics and the large number of trial shocks required before a desired amplitude is attained. Electro-dynamic shakers were considered next as an excitation source for the shock pulses. It was felt that the shaker should duplicate the required shock pulses unless an extreme amount of damping was present in the armature suspension system. The idea seemed to warrant further investigation.

INITIAL EXPERIMENTS

The shaker employed in the endeavor was a Calidyne, Model A182, 25,000 force-pound system with a 170 KVA Westinghouse amplifier. This shaker system was to be used to vibrate the re-entry bodies, regardless of the outcome of the shock experiments. To approximate the test specimen, a crude mass was quickly fabricated from available steel scrap. It was intended to duplicate the weight and length of the re-entry body and its fixture. Figure 1 shows this test-mass spring-suspended in front of the shaker.

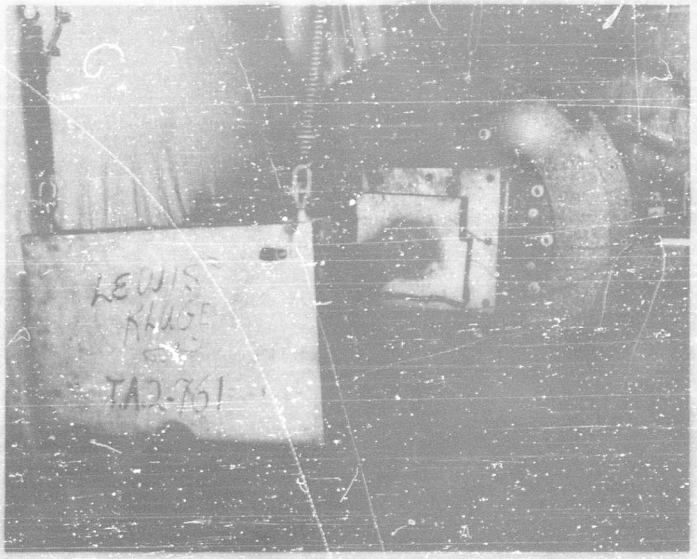

Fig. 1 - Dummy test mass used to simulate weight and length of re-entry body. The dummy is shown spring suspended and attached to the shaker in the manner employed for shock test experiments.

Our first problem was the introduction of a pulse to the shaker system. This was solved very nicely by an accidental discovery. When operating in the direct, or analog, reproduce condition with CEC 14-channel tape systems, the starting and stopping operation produces a full sine transient switching pulse, an example of which is shown in Fig. 2. This pulse appears in the output of the tape system reproduce amplifier. The duration of the full sine pulse is approximately 6 ms when operating at a tape speed of 30 inches per second. The pulse was recorded on another tape system and used in initial experiments. The pulse was played from the tape system output into the shaker control console. An Endevco, 2213 series, crystal accelerometer was mounted on the shaker head to monitor its reaction to the shock pulse. The accelerometer was connected to an Endevco, 2614 series, cathode follower-amplifier whose output was presented on an oscilloscope. Results were recorded on a Polaroid oscilloscope camera.

To introduce the pulse, the taped signal was played into a 60-watt power amplifier in the shaker control console. The power amplifier was used as a preamplifier and impedance matcher ahead of the system gain control. The tape system operator warned the shaker operator 5 seconds before the pulse was introduced. Upon receiving the warning, the shaker operator turned the system gain control up until the pulse occurred, then turned the gain down immediately. This prevented spurious signals or other switching transients from exciting the shaker.

Early testing with the taped switching transient produced completely discouraging results. Figure 2 shows the switching transient as recorded at the output of the tape system; Fig. 3 shows it as recorded on the shaker head. The shaker seemed to react to the pulse as if a dc signal had been applied then bled off slowly. A week of work with the test setup could not solve the problem.

At this point in the program an effective method was employed for obtaining a single, full sine pulse of any time duration. An electronic counter having a control binary (start-stop) circuit and a control binary output jack, such as the Berkeley, 735OR Eput meter, was used to obtain a single pulse. An audio oscillator fed a sine wave to the counter at a frequency corresponding to the pulse duration. The start-stop circuit allowed the passage of a single pulse only in the form of a square wave. Next, a variable bandpass filter was employed to extract the fundamental from the square wave. Fig. 4 shows this full sine wave, and Fig. 5 the reaction of the shaker with a 1200-pound

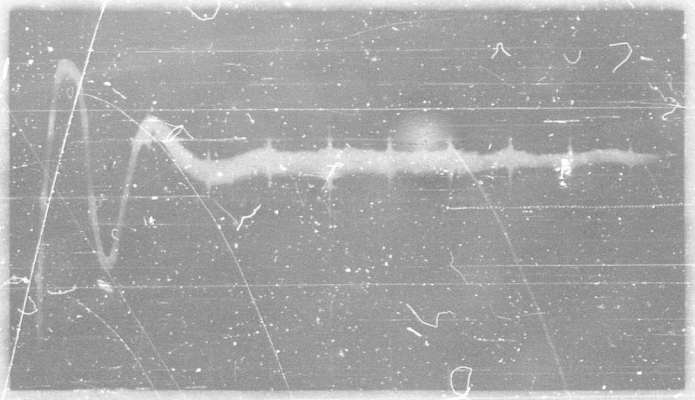

Fig. 2 - Switching transient pulse from CEC recorder. Oscilloscope horizontal sensitivity: 10 ms per division.

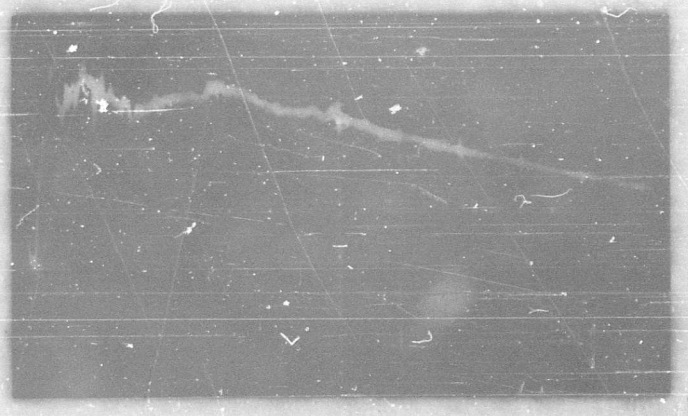

Fig. 3 - Output of accelerometer on shaker head. This shows the reaction of the shaker and dummy to the switching transient of Fig. 2 in early experimentation. Oscilloscope sensitivities per division: Vertical--30-g vector; Horizontal--10ms.

mass attached. A half-sine pulse was desired, but further experimenting was halted because the first test specimen was ready for excitation.

The apparent inability of the shaker to follow the pulse mentioned earlier was found to be the result of a simple instrumentation problem. The accelerometer was putting out such a large signal that the Endevco amplifiers were saturating. This was discovered when work was started with the new pulse, which was of a much lower amplitude than the switching transient.

TEST EXPERIENCE

The test specified two shocks. One was to be a 50-g, 2-ms shock; the other was to be a 25-g, 7-ms shock. A representative of the structural dynamics group felt that a more revealing test might result if the re-entry body could be subjected to a duplication of an actual flight shock. A duplicate tape was obtained which was a transcription of the reaction of an accelerometer to first-stage motor ignition. This was used to excite the dummy to ensure reasonable reproduction. When it was found that reproduction was quite close, (Figs. 6 and 7) an actual re-entry body was inserted in the test stand.

Crystal accelerometers were mounted at crucial points, both externally and internally, and their outputs were recorded on tape. Figure 8 shows a sketch of a typical re-entry body shock test setup. In addition, the external accelerometer locations for all tests are

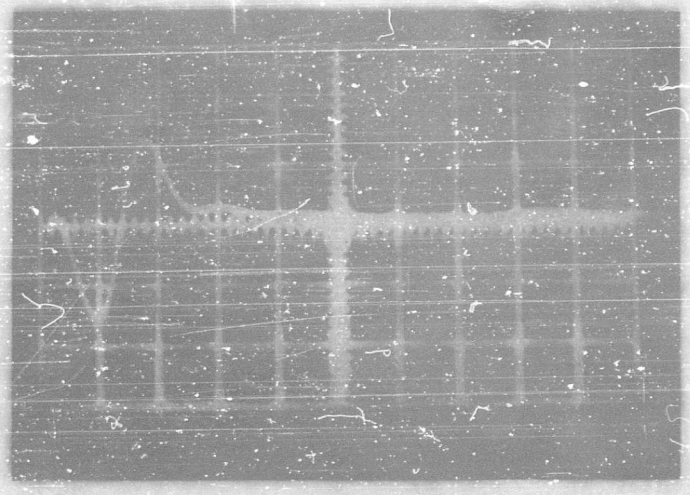

Fig. 4 - Test pulse produced by oscillator-counter-filter method. This pulse was used in two different re-entry body tests. Oscilloscope horizontal sensitivity: 2 ms per division.

Fig. 5 - Output of accelerometer on shaker head. This shows the reaction of the shaker and dummy to the pulse shown in Fig. 4. Oscilloscope sensitivities per division: Vertical--12-g vector; Horizontal--10 ms.

Fig. 6 - First-stage motor ignition pulse. This was recorded on an accelerometer mounted in the re-entry body during a missile flight and played through a filter adjusted to pass the 20- to 1300-cps frequency band. Oscilloscope horizontal sensitivity: 10 ms per division.

Fig. 7 - Output of accelerometer mounted on test mass when shaker was subjected to the pulse of Fig. 6. Oscilloscope sensitivities: Vertical—14-g vector per division; Horizontal—10 ms per division.

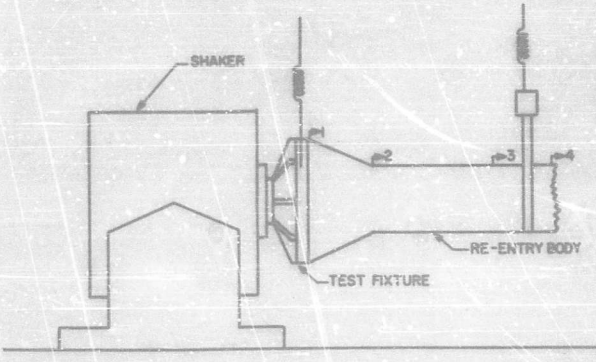

Fig. 8 - Sketch of re-entry body as attached to shaker for shock testing

shown. The two traces shown in each of Figs. 9 through 13 are the reaction of the re-entry body to a 2-ms pulse and the first stage ignition pulse. Accelerometer 3, which was mounted on the heat shield, shows a pronounced 250-cycle response. This was confirmed later in the analysis of random vibration test data. This condition was due to the heat-shield attachment and was corrected in later missiles. In this test the bottom lobe of the pulse was reduced considerably in amplitude. This was accomplished by varying the frequency settings of the bandpass filter to allow harmonics of the desired frequency to distort the wave shape.

Recently a more satisfactory method of obtaining a half-sine pulse was discovered. This procedure employs a pulse generator, such as the Dumont type 404, for a signal source. Its output was fed to an SKL model 302 bandpass filter. The signal was directed from the bandpass filter to an oscilloscope for viewing. In addition, a diode across the output of the filter clipped the bottom lobe. Figure 14 shows the square wave which appears at the output of the pulse generator. Figure 15 shows the pulse as it appears at the output of the bandpass filter. In this instance both sections of the bandpass filter were set in the low-pass position. One side was set at 2100 cps, low pass, and the other at 330 cps, low pass. Figure 16 shows the final pulse as it appears after being clipped by the diode, in this instance an IN1313.

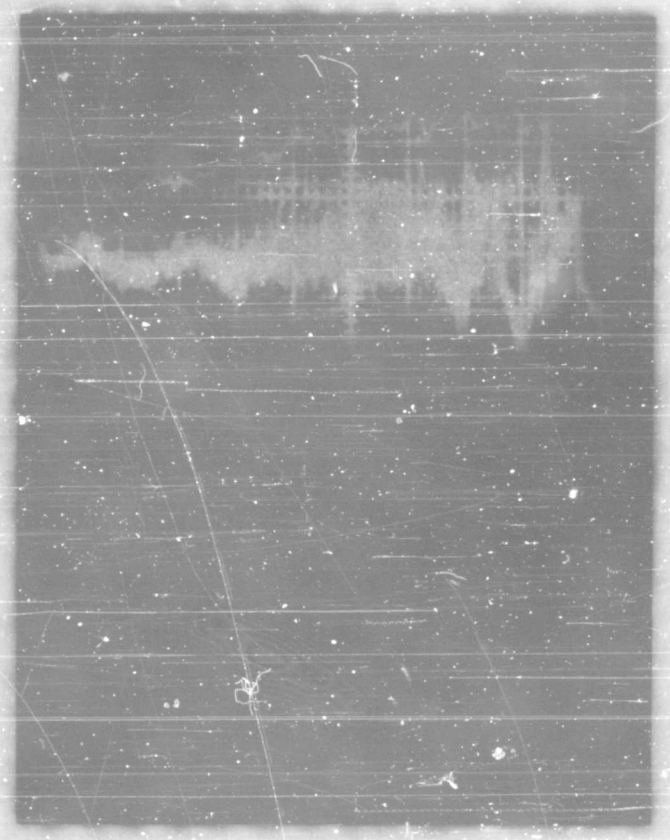

Fig. 9 - Pulses introduced to the shaker for re-entry body shock testing. The top picture shows a second-stage motor ignition pulse as recorded in a re-entry body. The bottom picture shows a 2-ms pulse. Oscilloscope horizontal sensitivity for both pictures is 2 ms.

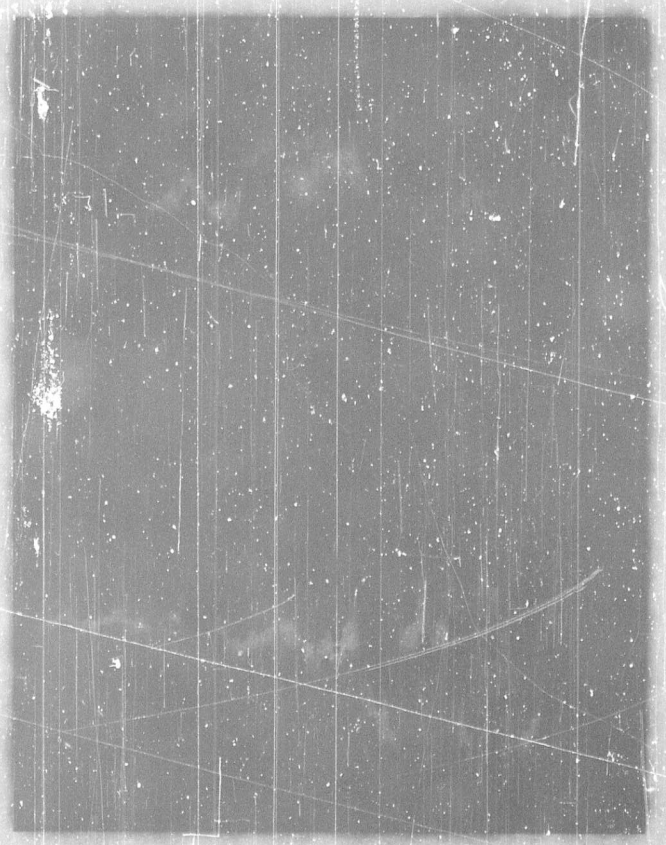

Fig. 10 - Reaction of an accelerometer mounted at location 1 to the pulses of Fig. 9. The reaction to motor ignition is shown in the top picture. The reaction to the 2-ms shock is shown in the bottom picture. Oscilloscope sensitivities per division:

	Vertical	Horizontal
top	25-g vector	2 ms
bottom	50-g vector	2 ms

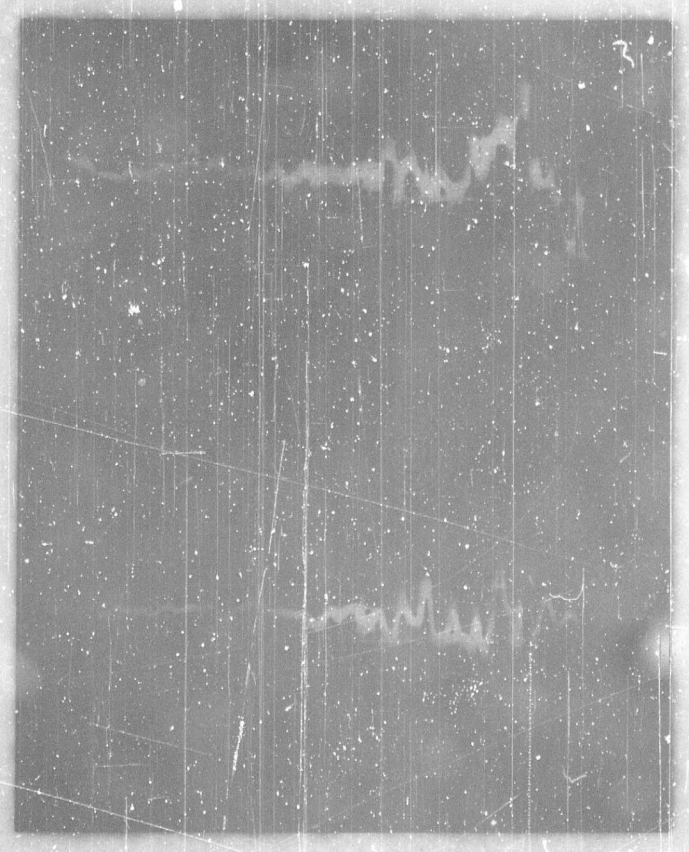

Fig. 11 - Reaction of an accelerometer mounted at location 2 to the pulses of Fig. 9. The reaction to motor ignition is shown in the top picture. The reaction to the 2-ms shock is shown in the bottom picture. Oscilloscope sensitivities per division:

	Vertical	Horizontal
top	25-g vector	5 ms
bottom	125-g vector	2 ms

Fig. 12 - Reaction of an accelerometer mounted at location 3 to the pulses of Fig. 9. The reaction to motor ignition is shown in the top picture. The reaction to the 2-ms shock is shown in the bottom picture. Oscilloscope sensitivities per division:

	Vertical	Horizontal
top	25-g vector	2 ms
bottom	50-g vector	1 ms

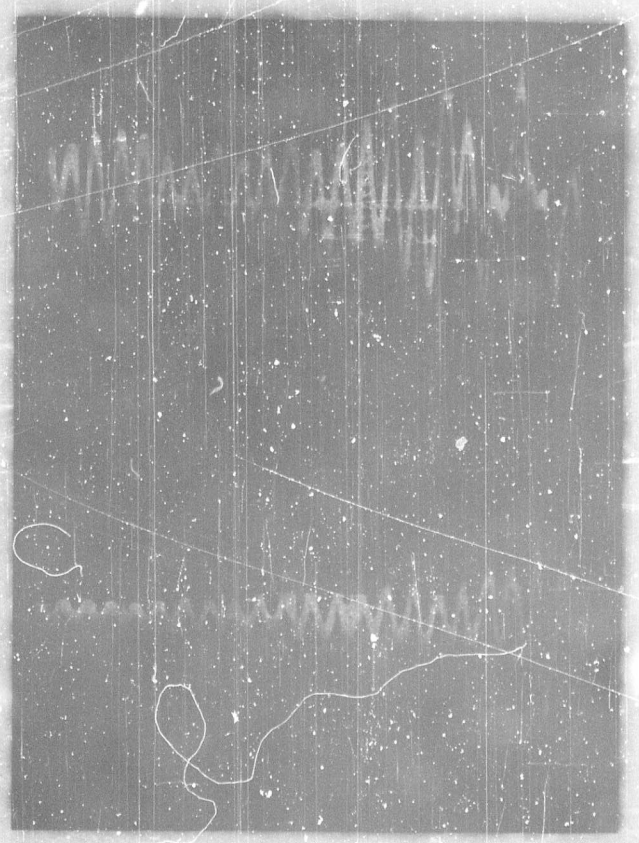

Fig. 13 - Reaction of an accelerometer mounted at location 4 to the pulses of Fig. 9. The reaction to motor ignition is shown in the top picture. The reaction to the 2-ms shock is shown in the bottom picture. Oscilloscope sensitivities per division:

	Vertical	Horizontal
top	25-g vector	10 ms
bottom	50-g vector	10 ms

Fig. 14 - Oscilloscope photograph of square wave at output of pulse generator. Oscilloscope horizontal sensitivity: 100 microseconds per division.

Fig. 15 - Oscilloscope photograph of pulse after bandpass filter. Both filter sections were in the low-pass position, one at 2100 cps, the other at 330 cps. Oscilloscope horizontal sensitivity: 1 ms per division.

Unfortunately, we have not been able to establish a predictable method for producing a desired pulse with either the oscillator-counter filter system or the pulse generator-filter-diode system. Shaping the pulse is performed by trial and error, by varying the admission of harmonics with the bandpass filter.

All accelerometer outputs from re-entry body shock tests were recorded on tape. This requires two separate tape systems: one to introduce the pulse, and one to record the accelerometer outputs. An accelerometer mounted at the rear of the re-entry body was used as a monitor to determine the amplitude of the shock. All other channels were reduced at the conclusion of the test.

In the data reduction process the accelerometer outputs were played back on the tape system and recorded with an oscilloscope camera, one channel at a time. Experience showed that the triggering level on the oscilloscope required adjustment for each channel to prevent the loss of data. This has always been a major data reduction problem. The triggering level of the oscilloscope must be set so that low amplitude excitation preceding the main pulse will be recorded. The output of the accelerometers could be recorded on an oscillograph provided

Fig. 16 - Oscilloscope photograph of pulse after an IN1313 diode was added at the output of the bandpass filter. Oscilloscope horizontal sensitivity: 1 ms per division.

the galvanometers have a sufficiently flat frequency response.

ADVANTAGES OF SHAKER SHOCKING

A considerable saving in setup time can be affected if vibration as well as shock is included in the environmental requirements. The same fixtures and test setup used for vibration may be utilized when shocking with the shaker. An estimated 2-1/2 days of test time, or about 120 manhours, are saved on each re-entry body test by shocking with the shaker instead of an impact tester.

This must be considered the most versatile type of shock test available. Practically any type of half or full sine pulse in the frequency range from 30 cps up to the resonance of the shaker armature can be programmed. This can be best accomplished by making a master programming tape of all the pulses desired. Amplitude control can be made fairly precise by maintaining a predetermined setting on the tape system reproduce amplifier and all shaker system gain controls. With this knowledge, gained empirically, the shaker operator can determine the exact gain settings required for a given amplitude.

Exciter amplitude restrictions limit the range of the pulse duration to a maximum of about 15 ms half-sine. Greator durations require other forms of excitation. If desired, the shock pulse can be introduced during a random vibration test to simulate powered vehicle separation. With this arrangement the shaker compensation arrived at for vibration may be employed.

Utilization of shaker shocking can reduce the amount of money required for investment in test equipment. In many instances the shaker will fulfill shock as well as vibration requirements, and thus eliminate the need for separate shock test equipment. If a testing agency is short of funds, the pulse can be programmed into the shaker directly by using the pulse generator-filter method. If a minimum of data is required, the resulting pulse from the table can be displayed on an oscilloscope and photographed. This eliminates the need for two costly tape systems when simple tests are being performed.

The major disadvantage associated with shaker shock testing is the inability of the exciter to handle long pulse durations. This is partly offset by the theory which maintains that shocks with durations of over 10 ms can be duplicated on a centrifuge. This was advanced recently by the Polaris Missile System Structures Department.

SUMMARY

This report can be considered only as a preliminary description of shock testing with electro-dynamic shakers. Because of severe time limitations, the technique has been developed only to the point where testing is merely possible.

In the Polaris Missile System Test Services laboratory shakers are employed exclusively for shock testing articles from 200 to 1000 pounds within the pulse duration limitations noted earlier. Plans are under way to extend the use of the technique to all items requiring pulse durations up to 14 ms.

There are several areas that require development before the technique can be considered of age. First, an effective and repeatable method of producing the desired pulses must be developed. Secondly, the shaker manufacturers should market their exciters with longer stroke capabilities, if this technique enjoys sufficient acceptance. This would allow this type of shock testing to be extended over a wider range of pulse duration. Finally, effective control of all shaker system gain settings is mandatory if repeatable data is to be obtained. It is hoped that other testing agencies will participate in the development of this technique so that it can become an accepted part of environmental testing.

DISCUSSION

Mr. Gertel (Allied Research): I think the use of a shaker offers some very interesting possibilities in shock testing; however, I would like to inject a word of caution in regard to the attempt to make shock on a shaker look like shock on some other area. Very often you can get into difficulty merely by making two shocks look alike. I think experience in past symposia, recorded in the proceedings, points out that shock spectra, even for two shocks of reasonably identical damaging characteristics, can vary considerably.

Mr. Lewis: Well, let me say that I am a test type, and essentially if we are presented with a requirement we will do the best we can as far as fulfilling the requirement is concerned, and we leave it to the more theoretical types to determine whether or not we are absolutely correct, nearly correct, or somewhere in the same county.

Mr. Brown (Douglas Aircraft): I would like to second in effect the previous remark and add to it just a little bit in that the technique of using a transient pulse and then shaping it through a bandpass filter holds very great possibilities of matching shock spectra rather than shock pulses and it would seem that this sort of technique should be developed much further. There is somewhat of a danger here in using the shape and the shock pulse without looking at the frequency spectra. For example a 10-ms pulse has no energy at a hundred cycles and 200 cycles and maximum energy at 50 cycles and 150 cycles. This could be very easily overlooked in this sort of approach.

Mr. Lewis: Well, as I said, we have developed this method practically under a shotgun, and we would be grateful if we could get other experiences with this sort of thing, because frankly we haven't had time to develop it to its fullest extent. We have developed it only to the point where we can run a test.

Mr. Blake (Lockheed): I would like to point out that we did use shock spectra in this program. The fact was that in the time scale allowed for this particular development we had to use our judgment as to what the shock spectra would look like based on past experience in looking at these time histories. But we certainly do use shock spectra to judge the comparison between shocks on the missile and shocks in a test.

Mr. Lewis: Thanks a lot, Ralph. Mr. Blake is in the Polaris Structures Unit and he is our ready reference whenever we run into trouble.

Mr. Barnes (Boeing Airplane Co.): I was looking at your last picture (Fig. 16), of this shock pulse showing a half-sine input and I am just curious as to what you do with the velocity that would be built up under a pulse with only a positive or negative magnitude? What is the response of the shaker part to this particular input?

Mr. Lewis: We haven't paid an awful lot of attention to this, other than to note that when you include the bottom lobe, the shaker will generally follow like this. When you clip the bottom lobe, the shaker will still give you some excitation in the other direction, but the amplitude of this other load is decreased. I think if you consider any form of shock testing, given a test article, if you excite it with a shock in one direction, it will compress and then it will lose its compression so that you would still get energy in the bottom lobe from the test specimen itself.

Mr. Hunt (Abma): Of the data that I have seen, very little of it is what you could call a pure shock anyway, and in our case we normally specify shock conditions, mainly because we don't have equipment large enough. I think with your 25,000-lb shaker this is an excellent idea.

Mr. Lewis: Let me say this. The method should not be considered as a test that should be restricted to large shakers. You can probably figure the force output obtainable for shock testing at three to three and a half times the peak vector force rating of any particular shaker, because, as you know, the limiting factor in obtaining a particular force rating is the cooling ability of the shaker, so inasmuch as the pulse is played out of a tape recorder, a warning is given to the shaker operator so many seconds before the pulse will occur, he turns his shaker up at that time, bang, he turns the shaker off. The shaker armature is seeing current only for just a few seconds, so you can go ahead and overload a shaker in an instance like this and get away with it.

Incidentally, let me add one other thing. Ray Yaeger of Chrysler questioned this sort of testing because he felt that we would seriously damage armatures. Well, we had the armature out of that 25,000-lb calidyne once because the leads had pulled loose. If you are familiar with this thing, the leads that feed current t the armature come up through the bottom, and then they fan out over webs on opposite sides of the armature. But we haven't yet physically damaged the armature, and we found that during initial experimentation, as I showed you there in some of the early slides, we were—God forgive us—getting about 200 g on the shaker head.

Mr. Adams (A C Sparkplug): About a year ago we received a requirement to maintain a 1-g orientation on a package, and we felt that the only way to do it was by shaker shock testing. It required an 11-ms, 15-g shock pulse and we went into this same program. I was very interested to hear your comments. We tried to approach it from the theoretical aspect, however, and tried to put on tape a signal which we felt would give us the necessary shock pulse.

This particular approach did not work out too well. We then went back into the shaker a little bit, determined its gain and phase shift characteristics, resonant frequency, expanded our mathematical model, placed it on the computer and determined the voltage which we felt we had to put into our shaker in order to give this shock. Unfortunately, the test was pulled out from under us, so we have never completely tested a live package. We have been trying to get a half sine wave with a leading and trailing secondary pulse and have run into some difficulty getting that. We feel that one of our problems is possibly that the gain and phase angle versus frequency characteristics of these amplifiers may shift with time or other things like that. There is something written up, and I would be very glad to swap information with you, sir.

Mr. Lewis: Fine. Let me say I certainly wish we had had the time you did to develop this technique. Let me also say that you should be very careful of the level of the input pulse, consider all of the system gain that you have in your shaker control consol and in your shaker amplifier. If you go in on Day-1 and run a test at a certain gain setting on the shaker control consol and then somebody from your maintenance department goes inside the amplifier at night, you come in the next morning and you try to run the same gain setting and, well, look out!

Mr. Yeager (Chrysler Corp.): Unfortunately this is a very nice approach, a very sophisticated approach. In the matter of the equipment involved, we are using a rather expensive piece of equipment in the first place, and I worry about things like shaker armatures. Frankly another thing I would like to add is that you can get away with a lot simpler approach. A number of years ago on the meteor program we simply discharged capacitors into the shaker armature. You can work this out if you do a little figuring. You get a beautiful half sine wave pulse out of such a system. Now the reason I worry about armatures is that we succeeded in damaging one quite seriously that time. But it's quite feasible to do it this way, and it's a very easily reproducible system, since you only have to excite the field in your power supply and do it with just a bank of capacitors.

Mr. Galef (Radioplane): I want to refer back to what the speaker said when he took a pulse to the structural dynamics people and asked if it was o.k. They told him to make a half sine wave or a full sine wave. Well, these have quite different shock spectra, but the structural dynamics people said o.k. I think this is fairly common. I think that they probably would have said o.k. if he had performed a test by dropping it on some sand, or maybe by kicking it as he walked by.

In general, the structural dynamics people, of which I am one myself, don't know the shock spectra well enough to be fussy, so I would like to comment that when any of you test-type people get something from structural dynamics, if it looks like it's going to

be hard to do, please don't knock yourselves out. Come back and ask them "is that what you really want." It will save a lot of worry.

Mr. Cohen (Naval Material Lab.): Could you and Mr. Adams tell me if your systems were equalized?

Mr. Lewis: No. We have a set of home-made peak notch filters, and we are somewhat afraid that we might have R C time constant problems in the filters, but we do intend to try this when we get a commercial compensation system.

Mr. Adams: No, our system was not equalized.

* * *

A QUASI-SINUSOIDAL VIBRATION TEST AS A SUBSTITUTE FOR RANDOM VIBRATION TESTING

A. E. Galef
Radioplane, a Division of Northrop Corporation
Van Nuys, California

A vibration test, using a modulated sinusoid, is shown to be a reasonable compromise between the random vibration often measured in the field and the sinusoidal vibration of many test specs. It may be performed with existing electrodynamic shakers with only minor modifications, the input required is relatively insensitive to damping in the test specimen, and a good approximation to a Rayleigh distribution of stress amplitudes can be attained.

INTRODUCTION

It has been shown, in past symposia of this series and elsewhere, that flight vibration data are generally random, with approximately Gaussian distribution. Data of that type are best analyzed and presented in the form of power spectral density.

A typical spectral-density plot for a particular point on an airframe is presented in Fig. 1. It is typical in the sense that when we measure vibration at a mounting point of a "black box," we often find only one rather narrow band of high spectral density with negligible density at other frequency regions. Less often, we find two or occasionally three "spikes" in the power density. If our vibration pickup had been located at some other point close by (perhaps at another mounting point of the same piece of equipment), we would probably find that the frequency band of possibly destructive spectral density is different from the frequency shown in Fig. 1. At another point on the same aircraft, still another frequency band would be most prominent.

The explanation of the peaked power-density spectra, with peaks occurring at different frequencies at different points, lies in the selective filtering action of the airframe-equipment system. The excitation energy (usually emanating from the power plant, or from boundary-layer turbulence) typically has a broad, fairly smooth spectrum (Fig. 2). However, when that energy is converted to vibration energy and measured at a particular point, the complicated acoustic and mechanical path between the source

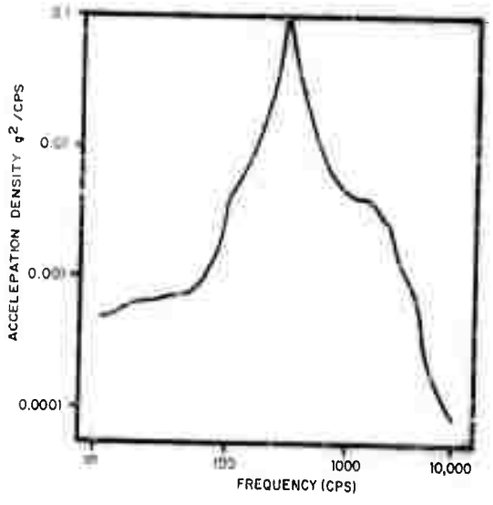

Fig. 1 - Typical acceleration density plot

and the measuring point will have done some tuning of the frequencies which were originally present, and typically only narrow frequency bands will appear prominently. At another point, the acoustic-mechanical path will have been sufficiently different that a different frequency will appear. If spectral-density plots from a large number of points within the vehicle were superimposed, an envelope could be drawn (Fig. 3) which would have approximately the same shape as the excitation function.

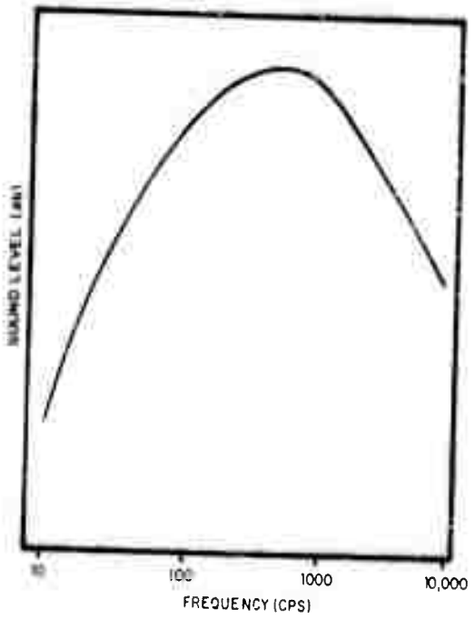

Fig. 2 - Typical acoustic noise spectrum

When we attempt to transform data of the above form into a suitable laboratory qualification test, marked differences of opinion are encountered. One school of thought suggests that the envelope of Fig. 3 is the most useful result of any measurement program. An envelope of that type is further smoothed, and, after multiplication by a safety factor, is considered to be the laboratory test. (Fig. 4.) Objections to such treatment of data, as presented in some previous symposia, have been based largely upon the practical difficulties in performing the test. As an example of the practical difficulties, consider a representative test requirement, which calls for power spectral density of at least $0.2g^2/cps$ over the frequency band of 10 to 2000 cps. This requires rms acceleration of 20 g, with peak accelerations (clipped at 3σ) of 60 g. If the test specimen is moderately large and heavy, the difficulties of equalization become very great, and an extremely rigid shaker armature and vibration test fixture are required to cope with the equalization problem. For a test specimen weight of 50 pounds, a total moving mass (specimen, fixture, and armature) of at least 500 pounds is typical, and a total shaker force of 30,000 pounds is required.

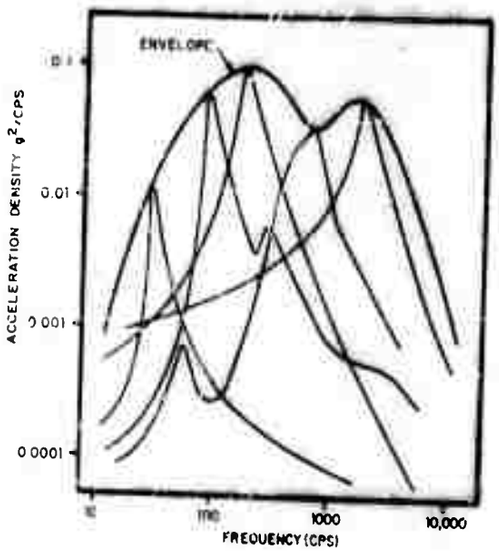

Fig. 3 - Superposition of acceleration density measured at several points

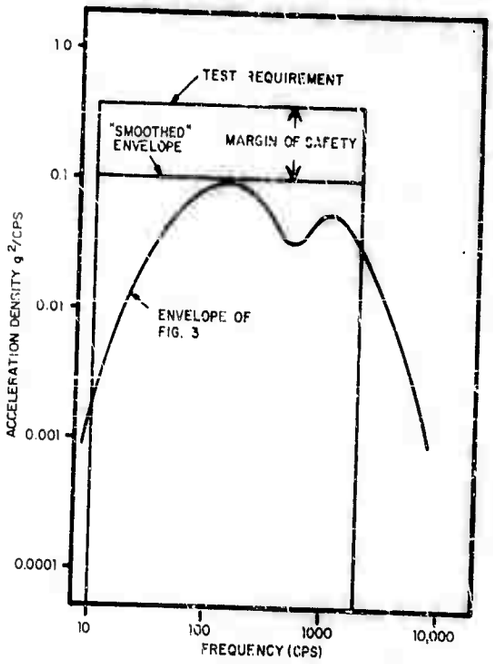

Fig. 4 - Evolution of test requirement

Although the above example shows that performance of a wide band random test is indeed difficult, it would appear that a more forceful objection to specifying tests of that sort would be that it is simply not a valid test. The writers of such requirements, by looking at the envelope of spectral densities are observing the forest and not noting that the forest is made of individual trees. That type of test is excessively conservative for test specimens with several degrees of freedom, and results in the rejection of equipment which would work adequately in the field.

Another common response to the data previously presented is perhaps more logical. This school of thought properly observes the output of an individual vibration pick-up, and sees a signal which can be adequately described as a sine wave modulated by a random function with, typically, a Rayleigh probability distribution of amplitudes (Fig. 5). Our observer, after carefully noting that the forest is indeed made up of individual trees, then often says, "A tree is a tree, and a modulated sinusoid is a sinusoid. We will test with sinusoids." However, there are important differences between a modulated sinusoid and a uniform sinusoid. The most important of these differences has been shown to be in the resonant responses of the test item; a damped mass-spring system, excited by random vibration, will respond proportionately to the square root of the "Q" and will respond proportionately to the first power of the "Q" if excited by sinusoidal vibration. Therefore, in order to get equal response to a sinusoidal excitation as would have occurred under random excitation at an appropriate level, it is necessary to first measure the "Q" of the test specimen, and adjust the level of the excitation accordingly. That complication is often avoided by ignoring it, resulting in excessively severe tests for specimens which have high "Q" resonances (Fig. 6).

Fig. 5 - Typical random acceleration time history

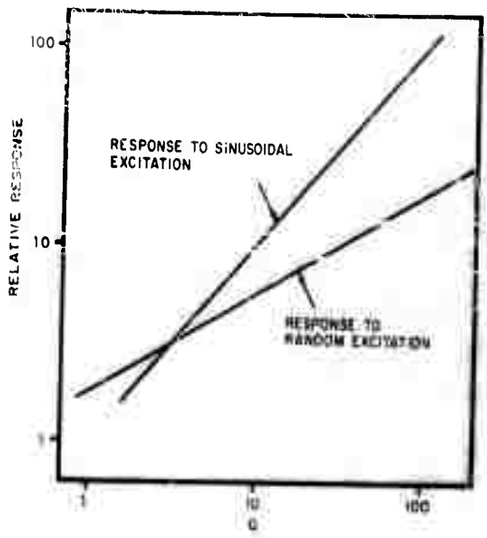

Fig. 6 - Response of damped spring mass system

Even when appropriate adjustments for "Q" are made in the test procedure, it is possible to object to the sinusoidal test because of the important differences between the probability distribution of peak amplitudes resulting from response to sinusoidal excitation and the Rayleigh distribution which describes the peak amplitude distribution of response to Gaussian random excitation. This difficulty could be surmounted if an adequate theory of cumulative damage in fatigue were at hand; however, no such theory exists.

The above discussion, summarizing the objections to both broadband random vibration tests and sinusoidal tests when the field environment is described by narrow-band random vibration, has perhaps suggested that we test with narrow-band random vibration. This has been suggested previously (1, 2), but apparently aroused little interest. The purpose of this paper will be to redirect attention to that suggestion, and, also, to suggest another test procedure which will have many of the desired characteristics of a narrow-band random test but which will generally be easier to perform.

A QUASI-SINUSOIDAL VIBRATION TEST

Consider an excitation function which can be written as,

$$\ddot{y} = A \sin \frac{\omega}{\eta} t \sin \omega t . \qquad (1)$$

That function represents a sine-modulated sinusoid. In appearance, (Fig. 7), it has some resemblance to a random-modulated sinusoid, but we may not expect its effects to be identical to the effects of the random excitation. The effects of the sine-modulated sinusoid may be evaluated in a direct manner by applying it to a damped spring-mass system with natural frequency ω, and with variable "Q." The amplification factor, T (ratio of rms acceleration of mass, to rms acceleration of base), may be shown to be

$$T = Q\eta^2 \sqrt{\frac{Q^2(2+8\eta^2)+2\eta^4+2\eta^2}{Q^4(1-4\eta^2)^2+Q^2(8\eta^6-6\eta^4+2\eta^2)+(\eta^4-\eta^2)^2}}. \qquad (2)$$

The amplification factor versus Q, for several values of η, is shown in Fig. 8. Also shown in Fig. 8 is transmissibility which is proportional to the square root of Q, as would result from random excitation. It is seen that the square root curve may be made to intersect a curve of Eq. (2) at two values of Q, with higher than desired transmissibility between those values of Q and lower than desired transmissibility for Q's outside that range. Depending upon a statement of an acceptable deviation from the "correct" transmissibility, a rather wide range of Q may be covered. Thus, if ±10 percent deviation from the desired transmissibility is allowed, it may be achieved over the Q range from 4.5 to 38 using the $\eta = 25$ curve, or over the Q range from 8 to 65, using the $\eta = 40$ curve. It is often true that the data upon which a vibration test is based is not accurate within ±10 percent, in which case a wider tolerance on transmissibility is warranted, and a wider range of Q for acceptable transmissibility may be found.

It is now necessary to consider the probability distribution of peak values of response

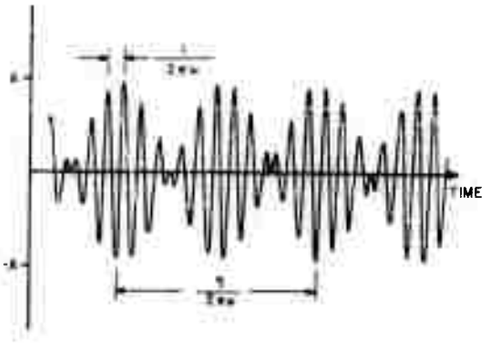

Fig. 7 - Modulated sinusoid
(A sin (ω/η)t sin ωt)

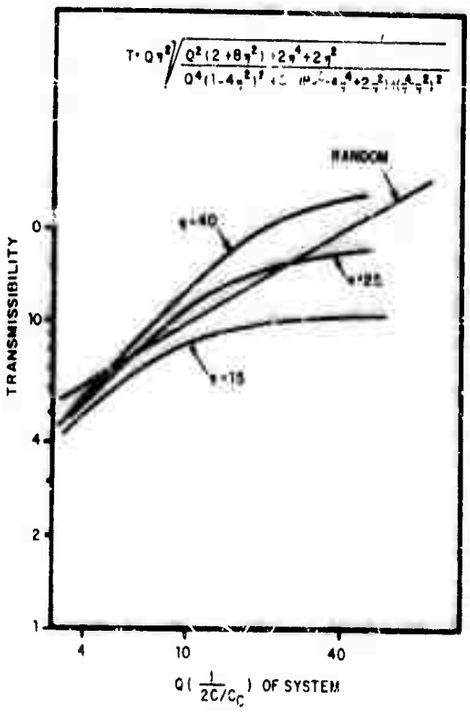

Fig. 8 - Response of damped spring-mass system to modulated sinusoid excitation

because of the importance attached to that distribution in fatigue. The probability distribution of the modulated sinusoid is shown in Fig. 9, together with a Rayleigh probability distribution. It is seen that the two distributions are not sufficiently similar so that equal rms values could be expected to cause identical fatigue effects independent of whether the vibration was random- or sine-modulated sinusoid. However, if a small portion of the test period is spent in vibration at an rms level slightly higher than the random vibration rms level, then a much better comparison of probability distributions is attained. Figure 10 compares the probability distribution of a two-level modulated sinusoid test (12 percent of time at a value of 1.1σ; 88 percent of time at a value of 0.70σ) with the Rayleigh distribution. Lacking an adequate theory of cumulative damage in fatigue, we cannot rigorously establish the equivalence of the two distributions, but it is intuitively clear that the effects should be similar.

The above technique is obviously not appropriate when the operational vibration is truly sinusoidal. However, it will be satisfactory in many cases where the operational vibration is nearly white noise. Broad-band, relatively smooth power density, similar to the envelope of Fig. 3, is most often observed

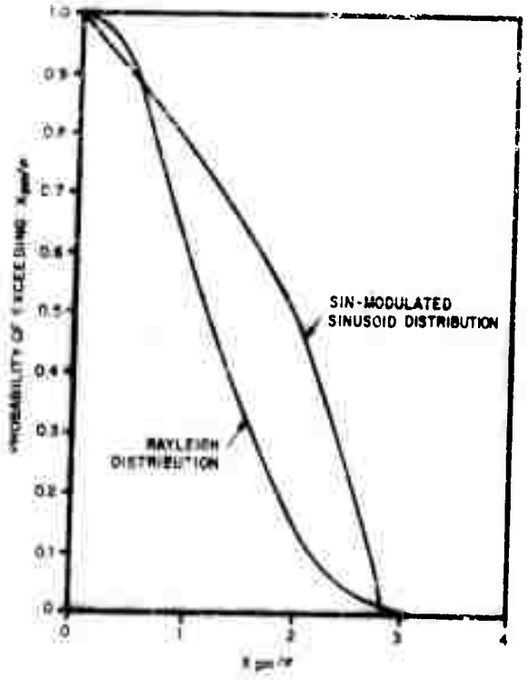

Fig. 9 - Rayleigh probability distribution and sine-modulated sinusoid probability distribution

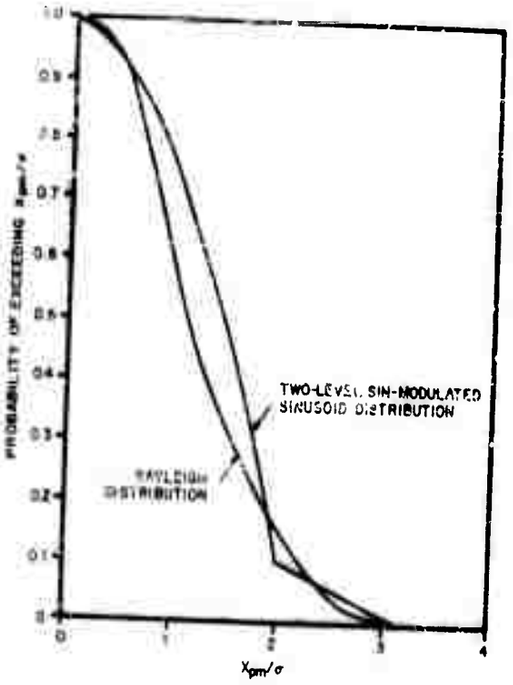

Fig. 10 - Rayleigh probability distribution and a two-level sine-modulated sinusoid distribution

when the vibration transducer is at the mounting point of a small, lightweight item of equipment. If that equipment is sufficiently simple that there is only one resonant frequency, it would be approximately correct to perform a modulated sinusoid test only at that frequency using an rms excitation acceleration of the same level as would have been used if the measured power density had been negligible except within approximately ±1/6 octave of the critical frequency.

It is now appropriate to consider the modifications required on an existing sine-wave shaker system in order to perform the test described above. Since shaker force is proportional to the product of the field strength and the armature current, the modulated sinusoid may be achieved by varying either the armature excitation or the field strength. In all shakers which employ electromagnetic fields (which includes the great majority of all shakers), it would only be necessary to replace the dc field power supply by a variable frequency ac generator. This would be especially convenient in shaker systems employing rotating machinery power supplies, since a generator could be readily geared to the existing shaft. If the shaker system has an electronic power supply, then modulation of the armature current may be simpler and can be accomplished in several ways: perhaps the most convenient technique makes use of the fact

$$A \sin \frac{\omega}{\eta} t \sin \omega t$$

$$= \frac{A}{2}\left[-\cos \omega\left(1 + \frac{1}{\eta}\right)t + \cos \omega\left(1 - \frac{1}{\eta}\right)t\right].$$

Therefore, by adding the outputs of two signal generators, we achieve the desired function. This technique is especially convenient if sharp resonances in the shaker-fixture system exist, since such resonances may be readily compensated by adjusting the relative outputs of the two signal generators.

In conclusion, an alternate test technique has been proposed which has the advantages of (a) being more nearly correct than either of the vibration test techniques commonly used and (b) simplicity of performance.

REFERENCES

1. M. Gertel, "Establishing Vibration and Shock Tests for Missile Electronic Equipment," Barry Report 230-C, February 1955.

2. R. E. Blake and M. W. Oleson, "Substitutes for Random-Vibration Testing," 24th Shock and Vibration Bulletin, February 1957.

DISCUSSION

Mr. Lewis (Lockheed Sunnyvale): I would like to take issue with you and cite an example. When I was at Boeing I remember an airborne telemetry system which sailed right through a sinusoidal test with flying colors, but when the system was subjected to random vibration we found that there was a panel on the side and right next to the panel there was a cantilevered terminal board. We subjected both of these to random vibration at the same time, and shorts occurred. Well, with this modulated sinusoid system, how can you be sure that you will excite two resonances of this sort at the same time?

Mr. Galef: The question might be avoided instead of answered by asking why we think we should have to excite two resonances at one time? Now if it is true that the field environment consists often of a single peak, then not only do we not have to excite two resonances at one time; we absolutely shouldn't or we shall be too conservative. On the other hand, if the field environment is a smooth environment, what you say is correct, we do have to excite them both at the same time. It is quite true that we often find troubles in random shaking which we do not find in sinusoidal shaking.

Another question might be, though, do we find troubles in the field which would not have occurred in sinusoidal shaking, or perhaps in this kind of shaking. If we cause troubles in a random white noise shake which do not occur in the field, we are simply doing something we shouldn't do. I hope that answers your question.

Mr. Daniels (Bell Aircraft Corp.): Mr. Lewis' problem of co-resonance has been tackled by Professor Rona of MIT. He says you should shake a little harder. That is—up your sinusoidal levels and you will then get the same kind of failure. However I think the point is a good one. (Here Mr. Adams described a somewhat complex example, with the aid of a blackboard, which could not be recorded.)

Mr. Lewis: Well let me describe my example of the panel next to a cantilevered terminal board. The panel had the lower resonant frequency. Now as the frequency was increased the panel passed through resonance and then isolated, then the board resonated and isolated. But at any one time only one or the other was resonating. Now if you excite both into resonance simultaneously they may touch. In a random vibration test you just turn up the gain on the shaker. But I feel that if you were to excite sinusoidally to the level where only one or the other will come into contact at their respective resonances, then you may wind up blowing your part right off the shaker.

Mr. Galef: This seems to be the old argument whether we should use random vibration or sinusoidal vibration with the same old problem involved of translating random to mean white noise. Random does not necessarily mean white noise, and I don't believe this confusion should exist.

Mr. Finocchi (ITT Laboratories): You mentioned that you are dealing with systems that have essentially a sharp peak of resonance. In some of the systems I am familiar with this does not occur. If you could delineate a separation between the types of systems, between those that have isolated peaks and those which do not, this may be resolved.

Mr. Galef: I believe any system which has a bandwidth of resonance which is less wide than the peak which might occur in the field can be and should be treated in the manner that we are talking about. If the Q of the resonance of the system is sufficiently low that the bandwidth of the field excitation is much narrower than the bandwidth of the piece of equipment, then I don't think any of the equations we have been showing are applicable.

* * *

RECOVERABLE DATA CAPSULE DESIGN AND ITS APPLICATION TO THE PROTECTION OF MILITARY EQUIPMENT

E. M. Mazur
General Electric Company
Missile and Space Vehicle Department
Philadelphia, Pennsylvania

This paper presents a brief history of the design and development program for the GE Recoverable Data Capsule used on Thor and Atlas re-entry vehicles as part of the instrumentation required to record in-flight environment and to recover the data intact. Since the capsule free-falls into the sea, high g loadings are involved.

INTRODUCTION

The concept of a Recoverable Data Capsule was initiated early in the research and development phases of the Atlas and Thor Ballistic Missile Programs. Since meager re-entry information was available at that time and since it was presumed that some of the initial vehicles would not survive re-entry, a method for assuring collection of data through this critical portion of the flight regime was needed. Ordinary telemetry methods for data gathering were not satisfactory during re-entry because of the formation of a sheath of ionized gases over the vehicle which completely blanked out radio transmission. The solution to the problem pointed toward utilization of a magnetic-tape recorder which would store the vital re-entry data and transmit it to the ground station after completing re-entry. Since this system relied on survival of the vehicle until the data was transmitted, it was also decided to use a recoverable recorder mounted in a capsule capable of survival of independent re-entry. The capsule was to be ejected from the re-entry vehicle prior to, during, or after re-entry through the earth's atmosphere, free fall from many thousands of feet above the earth, impact at terminal velocity upon the ocean, protect the precious tape record of the flight from the tremendous deceleration forces upon impact, and finally automatically activate recovery aid devices within itself so that search crews could successfully be directed to it. All of this was to be done with an 18-inch-diameter sphere which could weigh no more than 100 pounds.

Since the primary reason for the Data Capsule was the recovery of the tape transport within it, the packaging of the capsule's components was based primarily upon the size and location of the tape transport itself. The choice of recovery aids within the capsule required a comprehensive study of search and recovery procedures, facilities, and equipment. Dispersion studies were also conducted since the problem of finding an 18-inch ball bobbing upon the vast ocean obviously requires tremendous effort. The studies indicated that the best recovery aids were a radio beacon, a SOFAR bomb, high-intensity flashing lights, and dye markers of various kinds. In addition, the capsule had to carry its own battery packs to power the recovery aids. The final configuration of the recoverable part of the capsule is shown in Fig. 1. This assembly is housed within a plastic shell that protects the inner capsule

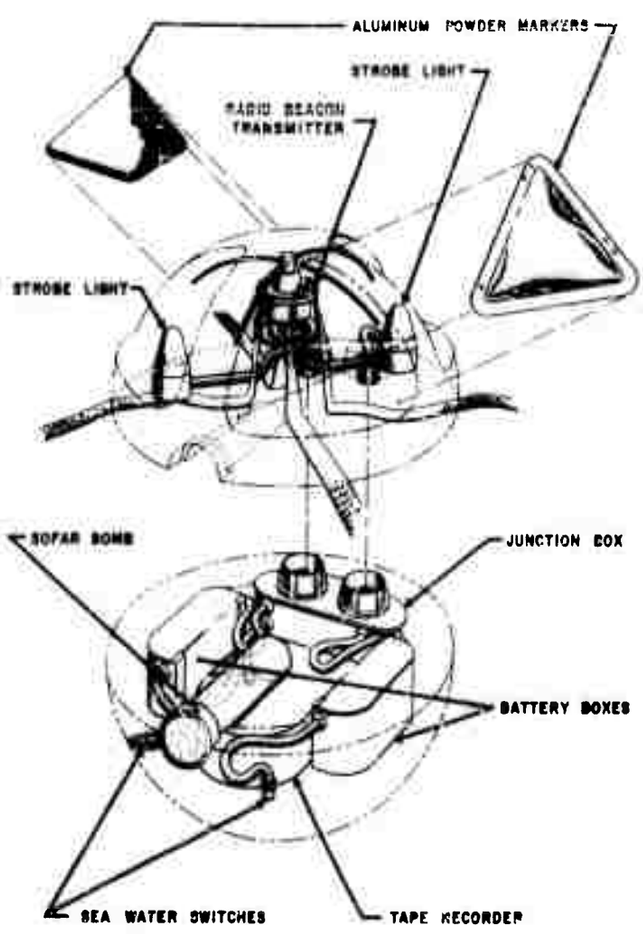

Fig. 1 - Phantom view of MARK 2 MOD 6 data recovery capsule

if independent re-entry is required. The location of the various components within the sphere was based upon predicted impact locations, susceptibility of components to impact damage and final positions of the electronic components when the capsule floats upon the water. As an example, the recovery beacon is located at the top of the capsule (with respect to the impact location) so that its chances of survival are greater.

A small drogue chute of 6-inch diameter is employed to enhance the aerodynamic stabilization forces which orient the impact of the capsule so that its maximum survival capabilities are utilized. Also, the center of gravity of the capsule is such that the beacon and antenna float above the water line, thereby reducing the possibility of continuous attenuation of the beacon signal.

SYSTEM OPERATION

In general, the sequence of system operation of the Data Capsule and its associated ejection mechanism assembly is as follows. After successful re-entry through the earth's atmosphere, the capsule and its associated ejection mechanism is propelled from the re-entry vehicle by means of a JATO unit. The capsule and ejection cylinder (Fig. 2) are separated by aerodynamic forces thereby allowing the Data Capsule itself to fall freely away from and at a higher velocity than the cylinder. The capsule impacts the ocean with a terminal velocity of approximately 450 fps. During free fall, the capsule stabilizes in the desired impact attitude (beacon up) because of the effect of the small drogue chute attached to the capsule's outer shell. The capsule impacts the water in this attitude

Fig. 2 - Data recovery capsule system

at which time the outer shells fragment and separate from the inner sphere assembly. Almost simultaneously, aluminum powder packets burst open and the finely-divided powder is spread over the surface of the ocean, leaving a large reflective slick. The capsule submerges, then returns to the surface because of its natural buoyancy. A seawater switch then completes the inner circuitry of the capsule thus applying battery power to the beacon transmitter and the flashing lights. Current is also supplied to an explosive charge which ejects the SOFAR bomb. The bomb sinks and is detonated at approximately 4200 feet below the surface of the water. This explosion can be detected at great ranges and provides a rough fix on the capsule's location.

The problem then becomes one of pinpointing the position of the floating sphere. The primary device used for locating the capsule is the radio beacon. The beacon signal is received by the search aircraft which carry direction-finding equipment.

The visual aids in the capsule provide a back-up in case of failure of the radio beacon. The aluminum powder marker, the reflective paint on the capsule itself, and the flashing strobe lights, are all visible at ranges of several miles under conditions of either daylight or night time. For maximum reliability, the location aids are designed so that failure of one aid will not result in failure of the others.

IMPACT LOADING

When the data capsule impacts the ocean, it is traveling at approximately 450 fps. Three hundred thousand pounds of kinetic energy has to be dissipated, and impact point loadings have been measured between 40,000 and 60,000 g's. This tremendous energy presents formidable problems in protecting the recovery components in the capsule.

Obviously, one means for insuring survival of the data capsule is to reduce the impact

velocity. However, this approach was discontinued early in the program because of the design complexities involved and the state of the art in terms of parachute shock loads and deployment velocities.

The solution to the problem rested in the proper choice of capsule structure material associated with proper configuration of recovery components in the weight/volume realm. Proper separation of components within the vehicle was also mandatory since the effects of component interaction after impact was known to have increased the local "g" levels.

Many materials were studied and evaluated for use in the inner sphere of the capsule. Little data existed on the performance of any material at the high shock levels that would be encountered upon impact, so an extensive program of testing was conducted. Results obtained from these tests provided a range of desirable characteristics which included flexibility, strength, low water absorption, low density, and slow return after initial shock. The material finally selected for use in the Data Capsule was a plasticized polyurethane foam which produced a structure that was well suited for high-velocity impact shock with a rapid deadening effect. This material also has the ability to adhere to the components molded within the package which contributes greatly to the capsule's structural integrity.

The capsule's outer shell serves basically as a re-entry protection for the inner sphere and as such does not appreciably change the effect of impact upon the inner sphere or its components since it fragments in the initial phase of water entry prior to the time that the inner sphere and its components respond to the deceleration forces. This phenomenon has been verified both analytically and by test.

ANALYTICAL APPROACH

It has been established by researchers such as Shiffman and Spencer, Birkhoff, Carr, et al., that the phenomenon of water entry by a blunt object such as a sphere consists basically of three phases. The first phase occurs during the first several microseconds of initial contact with the water and is called the compressible-flow phase. This phase is characterized by the propagation of a trapped pressure wave confined to the point of impact, subjecting it to very high pressures. The second or flow-forming phase, begins immediately after the moment where the horizontal component of velocity falls below that of wave-propagation velocity in water. At this point, the trapped pressure wave will tend to move away from the intruding shape and relieve all of its energy by raising a mass of water in the form of a splash to a specific height. The third and last phase is less complex to analyze; it begins when the flow around the body has stabilized itself and all that remains is a pure hydrodynamic force acting on the body.

The compressible-flow phase is the most difficult of the three phases to predict analytically, as verified by the extremely empirical approach that most experts use.

One approach, proposed by the Admiralty Research Laboratory, Teddington, England (1), is to solve for the peak pressures experienced at the surface of the body that is in immediate contact with the trapped pressure wave and to then calculate the area of this contact surface. The expression for pressure is $p = \rho c V_o \sin \alpha$,

where

p = pressure,

ρ = density of water,

c = velocity of sound in water,

V_o = impact velocity,

α = entry angle.

The time (t_1) during which this pressure (p) acts is estimated by the following equation:

$$t_1 = \frac{V_o R}{c^2 \sin \alpha},$$

where R = radius of sphere.

The penetration depth (s) of the sphere during the time (t_1), assuming $s\Delta V \geq 0$, is $s = vt_1$. For the Data Capsule, using the above equations, $p = 30{,}000$ psi, $t_1 = 16$ microseconds, and $s = .085$ inch. The wetted area of the Data Capsule for .085 inch is approximately equal to 5.6 square inches. Therefore, the force acting on the capsule is equal to 168,000 pounds. The amount of kinetic energy (K.E.) transferred during the compressible-flow phase can then be approximated by the amount of work expended in the water. Assuming an average force of

100,000 pounds moving a distance of .007 feet we have an energy loss of 700 foot pounds.

In order to solve for the velocity change that occurs during this energy transfer, it is assumed that only the outer shells respond to the 16 microsecond pulse duration since the inner isofoam sphere and its components have extremely low natural frequencies. The energy loss can then be stated as follows:

$$\frac{MV_o^2}{2} - \frac{MV_1^2}{2} = 700 \text{ ft lbs},$$

where V_o = 450 fps and M = shell mass ≅ 1. Therefore $V_o^2 - V_1^2$ = 1400 and V_1 = 447 fps. (Velocity at time t_1.)

This gives a velocity loss (ΔV) for the shell mass of 3 fps and an acceleration (assuming a constant acceleration) equal to

$$a = \frac{3}{.000016} \times \frac{1}{32} = 6000 \text{ g's}.$$

This figure is conservatively low since it is based upon the assumption that all of the shell mass absorbs the change in kinetic energy. Experience gained from impact tests performed on the capsule shows that a large portion of the shell disintegrates at impact; therefore it would seem safe to assume that the impact shock would be absorbed by only a fraction of the shell mass.

A method of analysis for determining the critical velocity shock, suggested by M. Kornhauser, refers to work done at the David Taylor Model Basin (2). The solution for the effects of the damage caused by a shock pulse on a structure is based on the assumption that when the duration of loading is less than 1/4 of the natural period of the structure, the response is independent of peak acceleration or duration, but depends only on the velocity change, ΔV.

The critical velocity change required to produce damage of the structure is given by

$$V = 0.3\ \epsilon_o\ c_o,$$

where ϵ_o = strain and c_o = velocity of sound in the structure.

When the above expression is applied to the Data Capsule shell structure,

$$V = (0.3)\ (.002)\ (7000) = 4.2 \text{ fps}.$$

Therefore, a 4.2-fps change in velocity at impact is enough to induce damage to the shell structure. This figure roughly corroborates the calculated results obtained by means of the first method of analysis and test experience in which shell fragmentation has always occurred.

The effect of this first phase shock pulse on the recoverable inner sphere is minor as shown by the results of impact tests, since the critical velocity for the isofoam material is approximately 60 fps, as shown in the following analysis.

The application of the above critical velocity (ΔV) equation to nonrigid structures such as the isofoam core of the capsule is of questionable value. However, by using .10 for ϵ_o as determined by laboratory tests and 2000 fps as the velocity of sound in the isofoam core, a ΔV of 60 fps is obtained.

As shown in the following paragraph, the foam inner sphere is subjected to velocity changes in the order of 70 fps. This would bear out the fact that in certain impact tests minor foam damage has been incurred. The characteristic of the second or flow-forming stage in water impact is that of a transient drag pulse that changes in magnitude with data capsule wetted area rate of change and therefore with entry velocity. Kornhauser provides a method for determining this transient drag (3).

First, the ballistic density (σ) of the sphere is calculated, since the impact coefficient is dependent on the "virtual mass" of the projectile.

$$\sigma = \frac{M}{\frac{4}{3}\pi\rho R^3},$$

where

M = mass of sphere,

R = radius of sphere.

By using the ballistic density (σ), an impact drag coefficient (C_p) is determined. A plot of C_p versus penetration and subsequently a plot of deceleration vs penetration can be obtained by using the expression

$$G = \frac{3}{8} C_p \frac{V_o^2}{R\sigma}.$$

This value of acceleration represents overall capsule deceleration and is based upon the assumption that the capsule is fairly rigid (which it is not) and helps only to arrive at an approximation of the acceleration-time history of the second phase of the water entry.

By using the above methods for the Data Capsule, it was predicted that the maximum forces and velocity changes occurred during the first water penetration of one radius and that the velocity shock (ΔV) amounted to approximately 70 fps. This velocity shock was used to predict the "g" loading experienced by each component within the capsule as will be discussed subsequently.

The third and final phase of water impact by blunt bodies begins when the body is completely submerged and is characterized by a lessening of the deceleration forces. This phase has no effect upon the life of the capsule or its components.

The methods used for the shock analysis of the Data Capsule components consisted of the following. Each component was considered as a single-degree-of-freedom nonlinear system where the spring is the polyurethane foam between the component and the mass on which it impacts. Thus for zero impact direction, the foam between the recorder and the shell was used to determine the deceleration response of the recorder and the foam between the SOFAR bomb and the recorder determined the deceleration response of the SOFAR bomb. This procedure assumes no coupling effects or interaction between the masses. Computer studies were run to determine the validity of this approach and indicated that the single-degree-of-freedom analysis was quite valid except for one component, which was the beacon. Interaction between the beacon and the SOFAR bomb accounted for higher "g" levels on the beacon.

The nonlinear spring was assumed to be the tangent type whose restoring force is given by

$$F = \frac{2Kh}{\pi} \tan \frac{\pi\delta}{2} ,$$

where

h = thickness of foam (in.),

K = linear spring constant (lb/in.),

δ = compression of spring (in.).

This type of spring was chosen since it is essentially linear for small δ and infinite if $\delta = h$. The linear spring constant K is

$$K = k \times \frac{\text{area}}{h} ,$$

where k = linear spring constant for a one inch cube in compression. The value of k was obtained from dynamic tests.

The response of a single-degree-of-freedom tangent-type nonlinear system to a velocity shock is adequately discussed in many texts. The maximum force in the spring due to the absorption of the kinetic energy is

$$F_{(max)} = \frac{2Kh}{\pi} \sqrt{e^{\left(\frac{\pi\delta_o}{2h}\right)^2} - 1} ,$$

where δ_o, the maximum deflection of a linear spring of stiffness K, is the ratio of the velocity shock divided by the natural frequency of the linear system $\Delta V/\Omega_n$.

Since the force in the spring is due to the mass times the deceleration, the maximum deceleration is given by

$$A\ (g's) = \frac{F_{(max)}}{W} ,$$

where W is the weight of the component.

TEST PROGRAM

Many aircraft drop tests were conducted throughout the development program and valuable design information was obtained in this manner. However, the precise point of impact of the capsule and the velocity of impact were actually somewhat in doubt. Therefore, as a final qualification test program, a series of controlled water-impact tests were conducted at the U. S. Naval Weapons Laboratory, Dahlgren, Virginia. The primary objective of the water-impact tests of the data capsule was to determine the boundaries of a spherical sector on the surface of the capsule within which the capsule would reliably survive water impact at specified striking velocities.

The test facility (Fig. 3) consisted of a 110-foot rocket launcher, depressed 10° from the horizontal, a stripper device used to separate the capsule from its rocket-propelled carriage, and a water recovery tank for impacting and recovering the

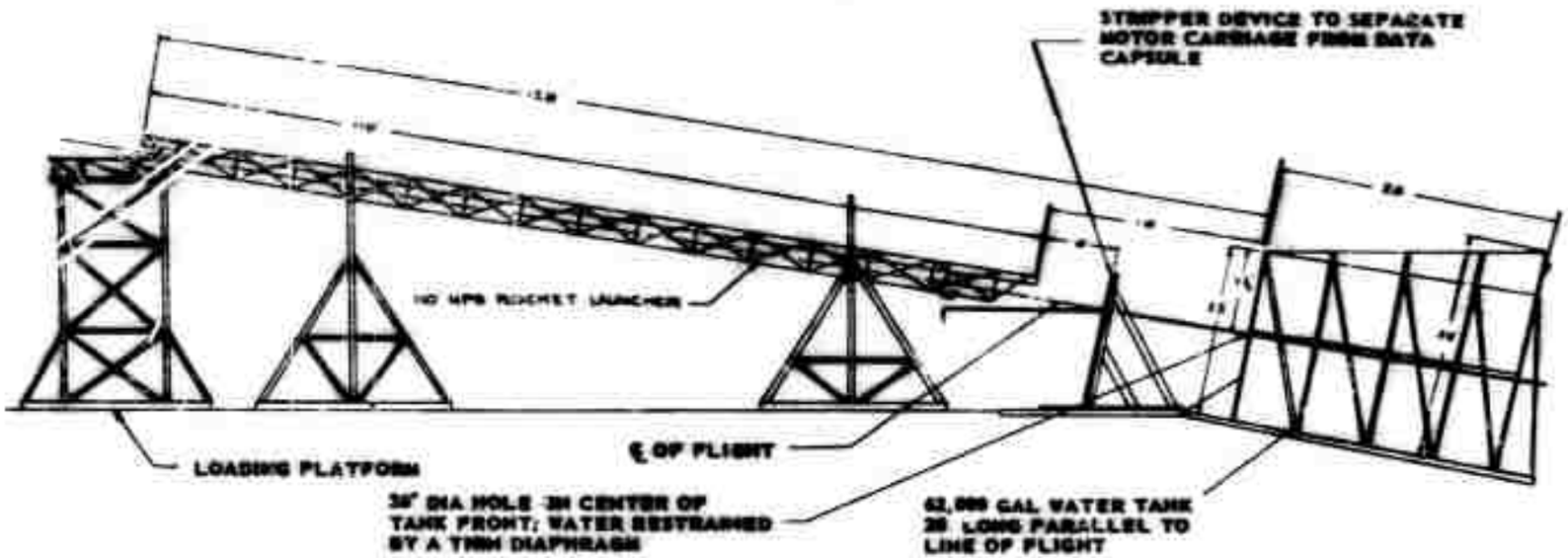

Fig. 3 - Elevation view of Dahlgren Naval Proving Ground Test Facility

capsules. The capsule entered the tank through a 36-inch-diameter opening over which was clamped a .010-inch cellulose triacetate diaphragm. A sluice gate was utilized to close the opening in the tank to protect the diaphragm from turbulence while the tank was pumped full of water. Just before actual firing of the capsule the sluice gate was opened and immediately after entry of the capsule into the tank, the gate was closed. The dimensions of the water tank were approximately 28 feet long, 16 feet wide and averaged 17.5 feet high.

The carriage holding the data capsule was propelled by means of four 3.25-inch Mk. 7 Mod 0 rocket motors, temperature conditioned to 140° F. Total weight fired was approximately 400 pounds. The stripper plate was located 8 feet from the end of the 110-foot launcher. The stripper separated the motor carriage from the capsule allowing the capsule to fly freely approximately 10 feet before impacting the water tank diaphragm.

High-speed photographic instrumentation was used to verify the capsule's velocity and point of impact (Fig. 4). Four data capsules were constructed by using spent components upon which were secured copper ball, peak reading type accelerometers mounted in the planes of impact. The test results indicated that the analytical approach using the single-degree-of-freedom nonlinear system is quite valid for obtaining design "g" levels for components packaged and protected as was done within the Data Capsule.

Table 1
Results of Typical Test

Component	Peak g (test)	Peak g (calculated)
Battery box	1750	1780
Junction box	1500	1700
Recorder	2300	2250
Beacon	4500	1880
Sofar bomb	5800	4100

It should be noted, as stated before, that the test results corroborated the computer study which indicated that interaction would occur between the beacon and SOFAR bomb thereby increasing the actual peak g's experienced by these components.

The Dahlgren tests proved conclusively that the Data Capsule could reliably survive water impact at velocities of about 450 fps if the impact were restricted to the bottom hemisphere within a spherical sector whose diameter lies 70° from the bottom of the capsule and is parallel to the horizontal diameter.

In addition to the tests performed on the capsule which contained a SOFAR bomb (Mod 6), tests were conducted by using a Mod 7 capsule in which the SOFAR bomb was replaced with a 16-mm camera. Nine Mod 6 capsules and three Mod 7 capsules were successfully tested. It should be noted that three of the Mod 6 Data Capsules were impacted twice (using new outer shells for the second shot) at different locations without failure due to impact, indicating the rugged nature of the foam material.

The final proof of design however, rests in its successful use in actual flight. The Data Capsules have been flown in both the Thor and Atlas re-entry vehicles. The record of successful recoveries of both types of capsules has been very impressive considering the complexities of a missile system, the rigorous environmental conditions that the capsule must survive and finally, the "needle in a haystack" aspects of the recovery system.

Much valuable data has been collected by using this technique. Complete storable records of missile flights have been recovered, both on tape and on film. Extraordinary photographs of the earth (Fig. 5) have been obtained from altitudes up to 900 miles which have revealed interesting weather patterns and which have paved the way for more research into meteorological and reconnaisance satellites.

APPLICATION TO PROTECTION OF MILITARY EQUIPMENT

The use of foamed plastics for the protection of delicate equipment during the handling and transportation phase is not new. Many manufacturers have utilized this technique and have effected considerable savings as a result.

The ability of foamed plastics to absorb energy is put to good use in packaging.

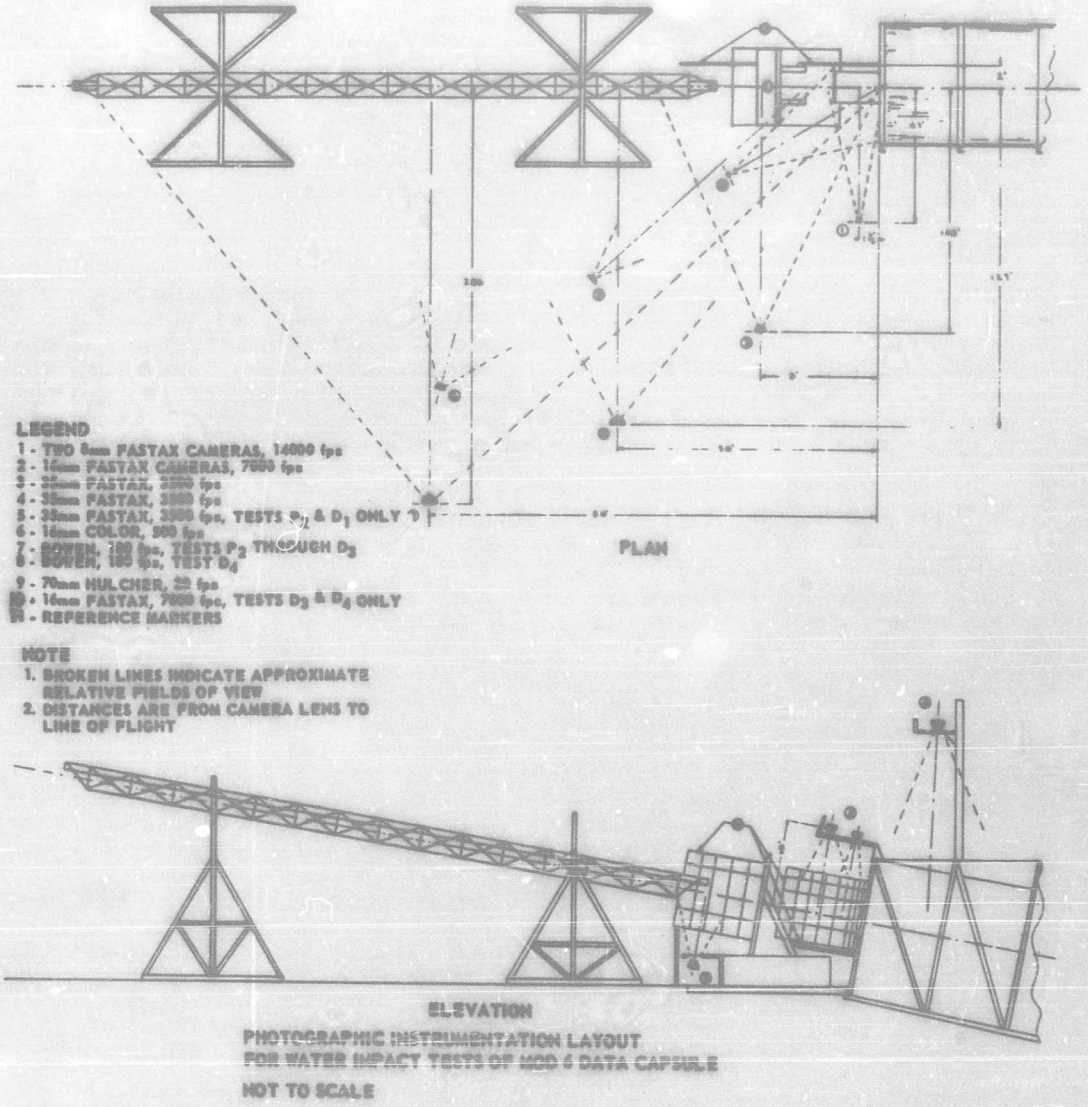

Fig. 4 - Plan and elevation views of the test facility showing camera instrumentation

Fig. 5 - Photograph of earth from altitude of 350 miles recovered from data recovery capsule

Here, contoured foamed-in-place packages as well as slitted slab stock can be used. It is conceivable that parachute delivery of supplies and equipment could be made faster and more accurate if the allowable impact velocity of the packages could be increased. With proper foaming techniques, descent velocities of parachutes could be increased, thereby lessening the vulnerability of large packages to enemy action.

Electronic equipment used for homing or guidance purposes, such as a radio beacon or flashing lights as utilized in the Data Capsule could be dropped accurately on an enemy beach without parachute retardation of the impact velocity. For example, a Data Capsule of special design was dropped from an aircraft from 8000 feet upon a sandy beach. The capsule impacted the wet sand at a velocity of 420 fps. The radio beacon within the capsule functioned just as well as it did before the test even though it had experienced a shock of 10,000 g's.

There has been speculation recently about the feasibility of a "logistics missile;" that is, a missile which could accurately deliver hypercritical supplies or possibly personnel to an embattled outpost where all other conventional methods of delivery had been deemed impossible. The missile would have a separable nose cone which would "home in" on electronic equipment set up on the ground station. It is proposed that a parachute be used to retard the descent of the cone with its payload protected by foamed-in-place plastics, both rigid and semi-rigid. The principle of energy absorbing by shock collapsing of semi-rigid foam to protect delicate instruments has been found to work well. The advantage of using plastics for this application rather than honeycomb aluminum structures, for instance, lies in the ease of handling of the foam and its ability to fill all voids in a structure thereby affording uniform support to the payload. The high "g" tolerance of the payload would therefore be increased since the tendency for differential deflections in the payload would be minimized. In addition, removal of the payload from the foam protection is quickly and easily accomplished simply by cutting the plastic away from the package. In the case of a human cargo, a contoured foam seat oriented properly upon impact would serve as adequate protection. Studies involving space capsules for human occupancy have indicated the feasibility of this approach.

Interesting military applications of the use of controlled-density urethane foams have been under experiment at the Dayton Rubber Co. A series of tests were conducted

in which rubber tire tubes were filled with foam. To test the tire, holes were drilled through the sidewall and pie shaped wedges were cut across the tire to simulate battle damage. The tire remained intact during subsequent driving. The foam-filled tire showed greater stability and better shock absorption without the reciprocal "bouncing" effect shown by air-filled tires.

Another technique involving use of urethane in creating protective foxholes for wartime use has possibilities. By using a portable mixing machine, the shoulder-depth foxholes can be sprayed with urethane foam which sets in a matter of minutes. When hardened, the foam forms a rigid coating that provides excellent insulation and prevents water seepage. A dome-shaped cover complete with vision slit can then be formed by using strips of preformed flexible urethane and wrapping paper as a base coated with several successive layers of rigid foam. The resulting foxhole cover is strong enough to support several hundred pounds of weight and to afford protection from stray shrapnel and debris. The use of a similar technique to construct fully-insulated and water-proofed storage depots and bomb shelters has been under consideration.

CONCLUSION

The successful application of the use of foamed plastics for the protection of sensitive electronic equipment from high-shock environments has been adequately demonstrated by the recovery of many Data Capsules. A reliable, yet simple method for analytically determining the design "g" levels for components packaged in this manner has also been formulated and verified by a series of unique, controlled water-impact tests.

A few interesting and perhaps thought-stimulating suggestions of military applications of this technique have been presented. Undoubtedly, these, or similar concepts will be utilized in the near future as our "know-how" and technology in the field of foamed plastics increases.

REFERENCES

1. "Impulsive Forces at Work," Admiralty Research Laboratory, Teddington, England, No. A.R.L./R1/G/2/3, dated 1952.
2. M. Kornhauser, "Impulse and Structural Failure at High Speed Water Entry," Applied Mechanics Memo No. 52, General Electric Co.
3. M. Kornhauser, "Water Entry of Buoyant Bodies," Applied Mechanics Memo No. 62, General Electric Co.
4. "Summary of the Development Program for the Data Recovery Capsule," TIS R59SD357, General Electric Co.
5. "Test Plans and Facilities for the Water Impact Tests of the Mod 6 Data Capsule," Tech. Memo No. T-1/50, Warhead and Terminal Ballistics Laboratory, U. S. Naval Proving Ground, Dahlgren, Va.

DISCUSSION

Mr. Cordes (Lockheed Aircraft Corp.): Do you have any data on the frequency response of your instrumentation, and how long were these shock impulses?

Mr. Mazur: Actually, we know that the copper ball type accelerometers probably gave us a rebound effect and, the g levels that we read were possibly too high. The pulse time actually was about two to three milliseconds in this second phase of impact. However, the g levels experienced were so high that if actually we did read 3000 g's instead of 2500 g's we felt that in design of the components the difference was insignificant.

* * *

DEVELOPMENT OF A COMBINED CLIMATIC, STATIC, AND DYNAMIC ENVIRONMENTAL TEST FACILITY

J. J. Hendrix, E. H. Moore, and K. M. Murphy
Missile Division
North American Aviation, Inc.

The Missile Division Testing Laboratory's capability for combined environmental testing has long permitted the combination of climatic environments such as temperature, altitude, humidity, etc. The Laboratory has employed this capability effectively in numerous ways without ever seriously considering the addition of both vibration and linear acceleration to extend the capacity for testing under multiple environments. Some eighteen months ago, however, several inquiries were received including one from USAF BMD as to capabilities for testing under combined sustained inertial and vibratory loading. Pursuit of these inquiries revealed a strong indication that such combinations of environments are to be significant in future missile and aircraft development testing. An adequate capability for such combined testing therefore appeared to be desirable, and means for acquiring this capability were considered. It is the purpose of this paper to outline factors which entered into this consideration, to describe design and development of the facility, and to indicate the degree of capability achieved.

CONSIDERATION OF FACILITY DESIGN

The combination of vibration and sustained acceleration can be obtained in two ways. First, by placing an accelerator on a vibrator, and second, by reversing the process and providing some method of vibration excitation on the accelerator. Consideration of the methods stated above was governed by the following design precepts:

1. Existing equipment was to be used
2. Development cost was to be held to a minimum
3. Facility was to be available for use in six months
4. Facility capability to be 25 g's in the frequency range, 25 to 2000 cps, with 15 g's of sustained acceleration, additive
5. Equipment used was to retain its capability for general use

A survey of existing test equipment based on the above design precepts dictated that the means of vibration excitation should be mounted on the accelerator. No decision was required relative to providing linear acceleration since only one piece of equipment suitable for this application (a Genisco Model C-159 accelerator) was available.

Conversely, several possible means of providing vibration excitation were considered. Mechanical methods of excitation

were available but their use was rejected because of their limited range of frequency. Resonant beams were attractive from the standpoint of weight but the number required to cover fully the frequency range was considered excessive and they were also rejected. It was decided that the most practicable means of providing vibratory excitation would be the conventional electrodynamic shaker, and design consideration proceeded upon this basis.

Since the source of sustained acceleration was to be a Genisco Model C-159, its capability was evaluated in terms of the design precepts. A preliminary static and dynamic analysis of the accelerator beam led to the following observations:

1. The manufacturer was conservative in rating the capacity of the accelerator.
2. Additional beam torsional stiffness was required for compatibility with anticipated requirements.
3. The beam would not withstand the expected dynamic test loads.
4. The moment acting through the c.g. of the exciters accounted for greater than 90 percent of the total moment.

As a result of the above analysis, it was concluded that the accelerator beam would need to be stiffened or, alternatively, that the dynamic load would have to be restrained. This latter alternative was selected in the expectation that it would entail the expenditure of less time and money. During test, the accelerator required both static and dynamic balancing, so the decision was made to mount two identical, dynamically-opposed shakers on the accelerator beam. The MB Model C-6-C shaker was found to satisfy basic problem conditions of size, weight, force output, and frequency range. Additional considerations which influenced the selection of this type shaker include an advantageous "force output to mass" ratio, a wide frequency range (5 to 5000 cps), and electrical requirements which were compatible with the rated capacities of the silver alloy slip rings provided on the accelerator.

The selection of the C-6-C shaker limited test-specimen gross weight, exclusive of the armature table, to approximately 5 pounds. Heavier specimens reduced vibration levels below the required 25-g maximum. A sketch of the accelerator-vibrator combination is shown in Fig. 1.

With decisions regarding equipment selection accomplished, attention turned to ways of putting the equipment to optimum use. Orientation of the vibration exciters on the accelerator beam and incorporation of provisions for climatic environments were primary considerations in this new decision phase.

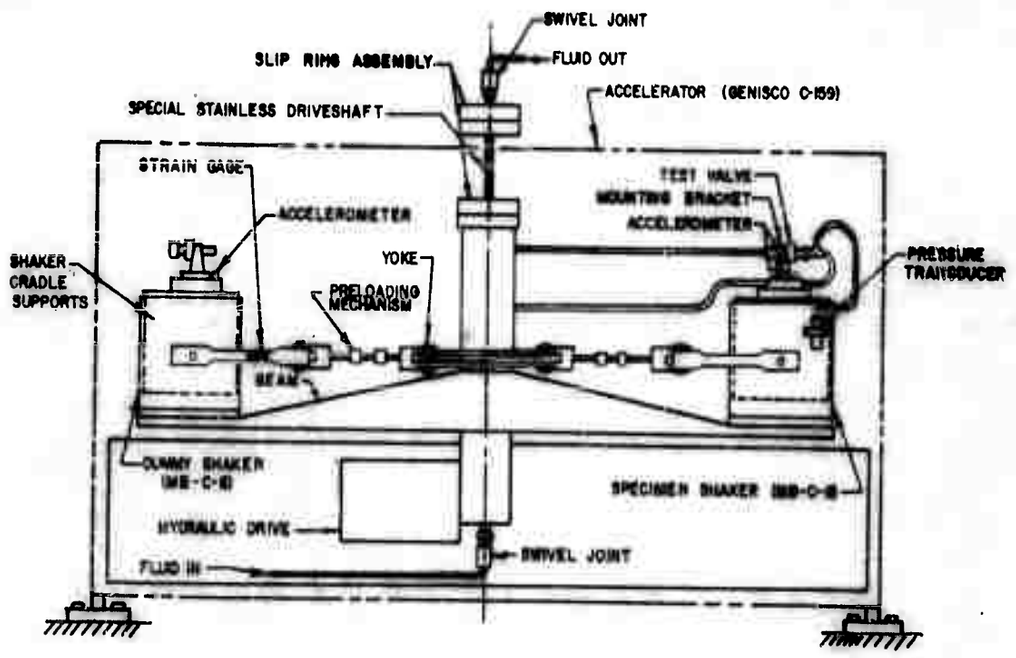

Fig. 1 - Configuration of combined environment test

Standard procedure for the combination of vibration and sustained acceleration in orthogonal axes usually includes exposure in all orientations. As previously mentioned, however, analysis showed the accelerator beam to be weak in torsion, and for this reason it was not considered advisable to vibrate in the axis tangential to accelerator rotation. Therefore, two axes of vibration with respect to the axis of sustained acceleration were chosen, namely, the axes normal to and coaxial with that of linear acceleration. Any disadvantage arising from the elimination of tangential vibration was expected to be offset by careful consideration of component symmetry in fixture design.

Because of space and weight limitations, it was found necessary to restrict means of imposing climatic environments to the simplest form possible. The means evolved consisted simply of wrapping conventional insulation material around the test specimen and permeating this material with heating or cooling fluid, as the case demanded. Space limitation further dictated that hot and cold fluid be stored outside the accelerator and be piped through swivels to the desired area of heating or refrigeration. Some additional modifications of the accelerator were found to be required to perform this function but initial planning proved the feasibility of the general scheme.

EQUIPMENT MODIFICATION AND DESIGN

Removal of the accelerator optical system and replacement with 3000-psi stainless steel lines and swivels for conveying climatic control fluid was one of the first accelerator modifications. Some difficulty was experienced with performance of swivels in this service and the problem demanded specific design effort for solution. An outgrowth of this effort has been a superior swivel, which cannot be discussed in this paper because patent protection has not yet been obtained. It will suffice to say that the resultant system has proven to be highly satisfactory.

Other modifications made to the accelerator included raising of the protective enclosure sides (Fig. 2), reinforcement of the beam to increase torsional stiffness, and the replacement of manual operation with servo

Fig. 2 - Vibration normal to centrifugal acceleration axis

control. Additional slip rings were installed to permit more extensive instrumentation, and the wiring was changed to allow operation at higher temperatures. The change to remote control was made necessary by the Laboratory Safety classification of the facility as "dangerous."

As far as structural integrity of the vibration exciters was concerned, no major problems with the 15-g sustained acceleration requirement of the design precepts were envisioned. A yoke device (Fig. 3) was designed and fabricated to strap the shakers together at c.g. locations, both to avoid imposing moment loads upon the beam incidental to the imposition of sustained acceleration and also to assure simplicity of the dynamic system. A means of prestressing the accelerator beam in bending was also incorporated in the design of this strap for better control of load paths. A final modification consisted of the redesign of vibration exciter cradles to provide a means of more positive locking in a given orientation and also to lower the c.g. as much as possible, again for minimization of centrifugal load in the beam.

A problem of major concern caused by the imposition of vibration and steady-state acceleration in the same axis was the provision of a means for keeping the shaker armature centered in its magnetic field. Conventional flexures are designed for performing this function under normal gravitational loading only. The flexures for the intended application were required to have a range of stiffness some fifteen times greater than that required for normal operation and to be adjustable over the entire range of vibration and acceleration as well. It was decided that pneumatic springs offered the best means of providing the desired range of adjustability. Actuators suitable for this application were adapted in accordance with the design procedure of Appendix A. A modification arising from the choice of actuators was the removal of the vibrator degaussing coils to provide space for mounting of the pneumatic cylinders. Figure 3 shows the exciters mounted for coaxial vibration and the actuators in use.

Fig. 3 - Vibration coaxial to centrifugal acceleration axis

FACILITY SHAKEDOWN

After all major design and modification problems were resolved, a series of tests was planned to prove design. Figure 2 shows the assembled facility ready for the first shakedown test. With the vibration exciters oriented as shown, with the combined system instrumented with strain gages as described in Appendix C, and without operating the shakers, the accelerator was rotated and readings of load data were taken in single g increments. As will be seen in Fig. C1, the prestress beam load is neutralized by centrifugal action in accordance with the requirement set forth in the preliminary analysis. The stress recorded in the straps was well below design limits.

The procedure described above was repeated with the shakers oriented for coaxial vibration as shown in Fig. 3. Loads were considerably greater for this case since the radius of gyration as measured to the shaker armature decreased while the distance to the c.g. of the exciter remained constant. However, total loads were still within the safe operating limits of the tie rods.

The facility was now considered ready for dynamic study under conditions of the simultaneous application of vibration and linear acceleration. For this purpose, the beam, tie rods, and specimen jigs were instrumented with accelerometers to permit detection of resonant response, and the system was set in operation. Initial data were extremely noisy because of ground loop and line bundling problems.

One source of noise was identified as a voltage induced by the magnetic field of the shaker as it passed the instrumentation terminal strip. Figure 4 is a schematic presentation of the configuration which produced this problem. It also shows how the difficulty was corrected by rerouting the coil hot wire to induce opposing voltages in two legs of the looped instrumentation line. Instrumentation signals were further improved by providing maximum separation between power leads and instrument leads.

Vibration data taken in the course of facility shakedown showed dynamic response throughout the range of operational frequency. Violent response was noted at several frequencies below 25 cps, but in general the response above this frequency was easily controlled by the test operator. A check of system simplicity against the analysis (Appendix B) showed good agreement.

Checkout of the pneumatic spring flexures on the vibration exciters was successful with minor modifications. Some misalignment between the armature and spring axes caused binding of piston rods initially, but the installation of self-aligning rod-end bearings corrected this difficulty. The only other problem was due to excessive friction of piston O-rings. This situation was easily corrected by removing two of three O-rings on the piston. Success in the use of these pneumatic

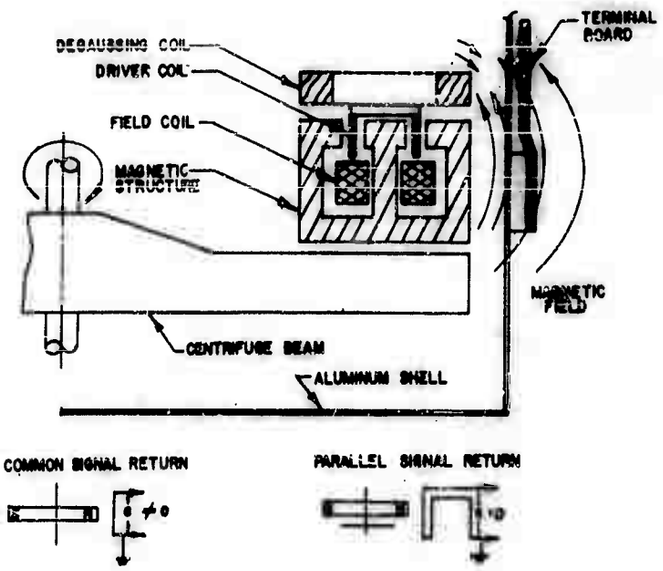

Fig. 4 - Induced voltage caused by shaker magnetic field

springs for centering the armature in its magnetic field at all sustained accelerative loads to 15 g's confirmed the design procedure of Appendix A.

Provisions for remote control (Figs. 5 and 8) proved to be highly satisfactory. Control of accelerator load to within a tenth of one gravity permitted good load regulation, and vibration sensed at the shaker armature could be controlled with the same accuracy either with or without the influence of sustained acceleration. That is to say, insofar as vibration control was concerned, that operation of the accelerator had no deleterious effect.

COMMENTS AND CONCLUSIONS

The equipment just described has demonstrated its importance to qualification testing throughout the past year. Its operational versatility in the combination of environments has been shown to be a material contribution to the continuing effort toward more faithful reproduction of tactical environments in the Laboratory. Its size lends itself well to the testing of many components and small assemblies and, although it has not to date been used as a portable unit, its convertibility, in accordance with the design precepts, makes possible this highly desirable use. The convertibility feature also permits other than combined testing use of all elements of equipment integrated into this test unit. Facility rentals required to be absorbed by test costs are therefore less. Combined testing is very expensive at best, but it is apparent that the use of convertible equipment results in minimum combined test equipment rental and lower test cost.

Size limitations are found to contribute both favorably and unfavorably to use of the facility. A costwise advantage is realized, of course, from the minimization of specimen size range, since the use of a small facility for testing small specimens is economical. This becomes a serious disadvantage in any case where specimen size exceeds facility capability. Needs in this regard, pertinent to a given application, are worthy of careful study.

The facility which resulted from the effort described, has been found to be close to

Fig. 5 - Control and instrumentation panel

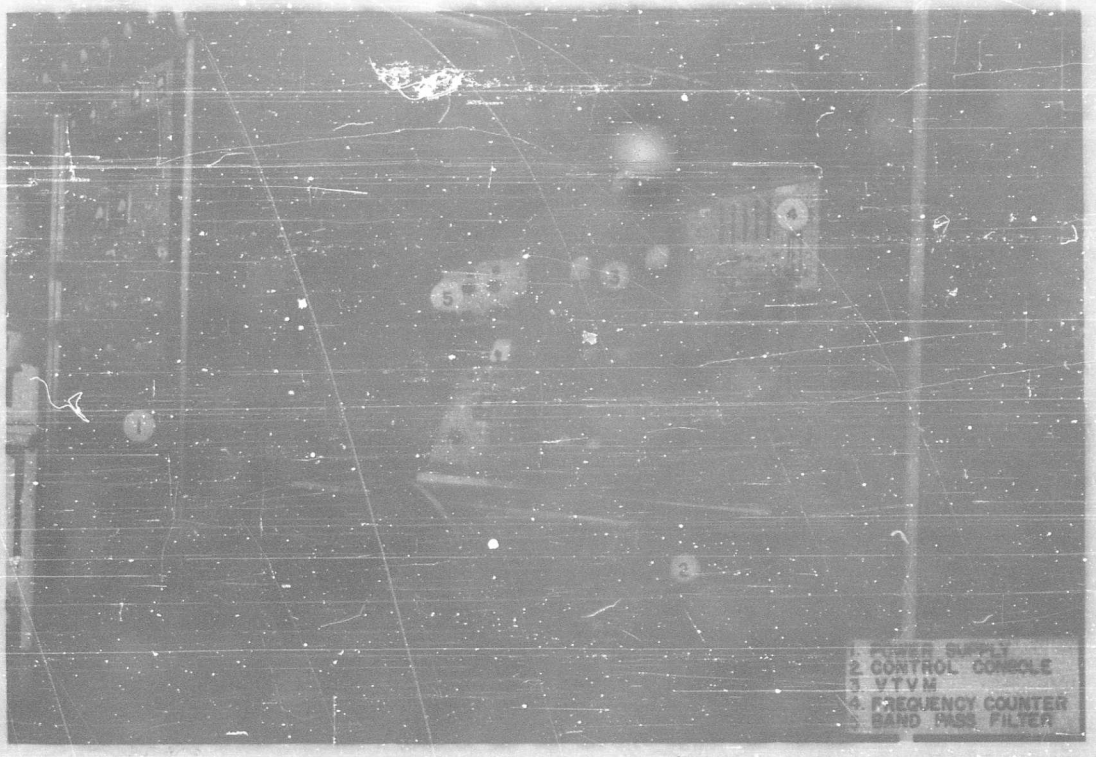

Fig. 6 - Vibration power supply and control console

optimum design, in terms of the above considerations. Although several tests have been rejected upon the basis of facility size limitation, the equipment has been almost completely occupied since its completion and is scheduled heavily for future work.

APPENDIX A

DESIGN OF A PNEUMATIC SPRING

The geometry of a pneumatic spring is shown in Fig. A1, where,

R = radius to centrifuge center,

M = mass of shaker armature, jig, specimen, etc.,

ℓ = piston clearance

ℓ_o = static (mean dynamic) piston clearance,

P_o = static (mean dynamic) cylinder pressure,

A = piston area,

F = centrifugal force $MR\omega^2$,

ω = rotational velocity $2\pi(\text{rpm})/60$.

If a polytropic dynamic process is assumed, then

PV^n = constant,

P = instantaneous pressure,

V = instantaneous volume,

n = polytropic process coefficient.

By differentiating,

$$P n V^{n-1}\, dV + V^n\, dP = 0,$$

$$P n dV + V\, dP = 0,$$

$$\frac{dP}{dV} = -\frac{Pn}{V}.$$

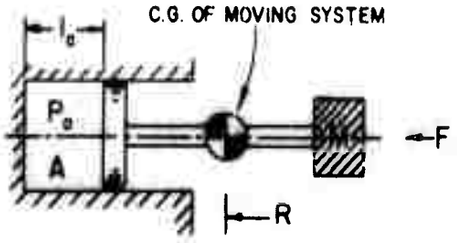

Fig. A1 - Schematic of pneumatic spring

The spring constant of the pneumatic spring is

$$k = \frac{\Delta F}{\Delta \ell} = \frac{A\,\Delta P}{\frac{\Delta V}{A}} = \frac{\Delta P}{\Delta V} A^2 = -\frac{Pn}{V} A^2$$

$$= -\frac{Pn}{\ell A} A^2 = -\frac{Pn\,A}{\ell}$$

and referencing to mean pressure and clearance,

$$k = \frac{P_o\, n A}{\ell_o}.$$

For the range of audio frequencies, an adiabatic process may be assumed. This assumption also applies, without serious error, in the range of frequencies to 5 cps. Employing a value of $n = 1.4$, an expression useful for design purposes, from the above derivation, is as follows:

$$\frac{k}{m} = 1.4\,\frac{P_o\, A}{M\,\ell_o} = \frac{1.4}{\ell_o} \cdot \frac{4\pi^2}{3600} \cdot R\,(\text{rpm})^2 .$$

The spring may be designed in terms of limiting dimensions, available actuators which may be employed as cylinders, etc. The procedure is to select values of non-critical parameters which are compatible, in terms of the above expression, with those which are fixed or sharply restricted in range. Simple system natural frequency, proportional to the square root of this quantity, should be kept below 10 cps for this application if possible.

APPENDIX B

ACCELERATOR/SHAKER SYSTEM RESPONSE FREQUENCIES

Figure B1a shows the principal features of the accelerator/shaker system for shaker orientation in the axis normal to that of the accelerator arm. A similar schematic applies for shaker orientation in the axis parallel to that of the accelerator arm. Figure B1b shows a simplification considered to be valid in consideration of the system and anticipated forcing-function symmetry. Note that this simplification combines strap stiffness and that of the beam into one spring constant. This is done since it is not expected that its value will need be obtained; the analysis being in terms of significant frequencies. Figure B1c shows the equivalent two-degree-of-freedom system employed as an analytical model. This analysis produced a determinant as follows:

$$\begin{vmatrix} \omega_1^2 - \omega_n^2 & \omega_{12}^2 \\ \omega_{12}^2 & \omega_2^2 - \omega_n^2 \end{vmatrix} = 0 ,$$

where

$$k_{12} = \frac{k_1\, k_2}{k_1 + k_2}, \qquad \omega_1^2 = \frac{k_1}{m_1},$$

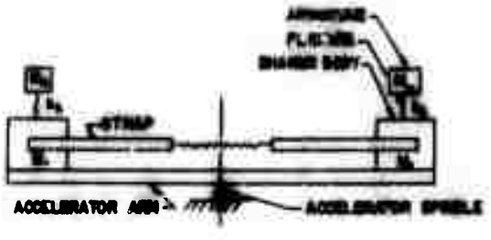

(a) Schematic of accelerator/shaker system

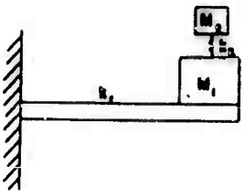

(b) Simplified schematic of above system

(c) Analytical model of above system

Fig. B1 - Geometry and analytical model of the accelerator/shaker system

$$\omega_2^2 = \frac{k_{12}}{m_2} , \quad \omega_{12}^4 = \frac{k_2^2}{m_1 m_2} .$$

This determinant may be expanded to the form of a quadratic as follows:

$$\omega_n^2 = \frac{1}{2} (\omega_2^2 + \omega_1^2) \pm \sqrt{\frac{1}{4} (\omega_2^2 - \omega_1^2) + \omega_{12}^4} .$$

In this form, it is convenient to insert observed frequencies for identification and verification of design assumptions embracing system simplicity, constituent stiffness, etc.

APPENDIX C

DETERMINATION OF MINIMUM PRELOAD FOR CENTRIFUGE BEAM

As noted in the body of this paper, a yoke device was designed to counteract the severe loading of the centrifuge beam which would result if the forces acting on the vibration exciters under sustained acceleration were reacted by the beam only. In order to determine the minimum preload in the yoke system which allowed safe operation of the system at 15-g sustained acceleration, strain gages and load transducers were installed on the centrifuge beam and load straps of the yoke device so that preload and bending stress in the beam was read as the centrifuge rotated.

The strain-gage-type load transducers installed on the load straps of the yoke were calibrated by loading in a universal testing machine and recording strain readings vs load throughout the usable range of the straps. The beam stress was measured by installing eight A-7 type strain gages at critical locations on the beam structure as shown in Fig. C1

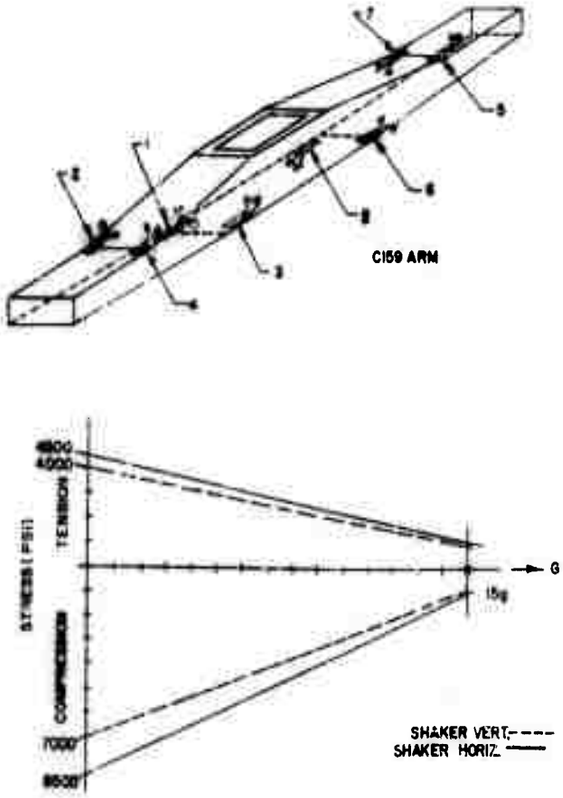

Fig. C1 - Strain gage location and stress curves

During the tests to determine the minimum preload requirements, all strain gage and load instrumentation was set to zero readings with the yoke device unloaded and the centrifuge not rotating. Prior to starting the centrifuge, the yoke was tightened to approximately 2000 pounds load, and all instrumentation readings were recorded. The centrifuge was then rotated at various speeds between zero and that which produced 15 g, and all instrumentation readings were recorded at each speed. At the conclusion of the test, the beam stress vs acceleration curves were plotted and examined to verify the loading characteristics. A typical stress-acceleration curve is shown in Fig. C1.

It can be seen from the curve in Fig. C1, that the beam is deflected upwards by the preload and, as the centrifugal load is increased, the stress in the beam approaches a balanced condition at approximately 15 g. With this preload, the beam is therefore subjected to a minimum bending stress at the actual operating speed. This condition of operation agrees with requirements of the design precepts.

DISCUSSION

Mr. Johnston (Western Electric Co.): I have three questions. One, what did you find in your test results that would have been different from the testing in the individual environments? Two, did you have to provide any special protection to the shaker because of the additional side thrust stress you placed on it? And three, how did you choose the planes of vibration and sustained acceleration? We normally test in the three different planes for vibration and in two directions in each of those three planes for a sustained acceleration. How do you mix these up and what results did you get?

Mr. Hendrix: If I may work backward and answer number three first, the choice of axes. This was of our own choice, because the beam showed itself to be very weak in torsion. If the shaker was oriented for tangential vibration in regard to the beam, then this would give us our maximum torsional loads. This we decided to do without. As it turned out, all our components so far have been symmetric and we can get the third axis by changing a fixture rather than reorienting the shaker. Question number two, I believe, was the side loads. One thing that did arise was that the velocity coils of the shaker did get this side load, and we removed them. And question number one, here I don't know if we can reach definite conclusions. We did one job for an outside concern that had claimed to go up to 40 g in cold environments with no sign of failure, with 25 g's of vibration and 15 g's of acceleration combined. We failed four out of four units. The exact reasons for failure, we don't know. This is up to the customer.

Mr. Griffith (Bendix Aviation): Did you consider using hydraulic shakers at all?

Mr. Hendrix: Yes, we did. One of our ground rules was that we tried to use our own equipment. We do not have a hydraulic shaker. We did approach Wiley Test Laboratories on the West Coast, but their asking price for their small hydraulic shaker was way beyond our means.

Mr. Griffith: What was the maximum specimen size that you tested?

Mr. Hendrix: The maximum in our case has been up to this date one and a half pounds actual specimen. We have been up to four pounds including the jig.

Mr. Heller (U. S. Naval Avionics Facility): Do you have any data or information on cross talk?

Mr. Hendrix: Yes, we do. It is not presented in this paper, but in some of the preliminary runs we instrumented the jigs for cross talk and we don't feel that you get any more than you would normally get: this depends on fixture design.

Mr. Shipley (Jet Propulsion Laboratory): I have a comment concerning the value of this combined environment testing. It seems to me this would be extremely valuable for testing inertial components. We found some very significant differences in the performance of an accelerometer just due to a skewed amplitude distribution in shaking. The rectification characteristics were entirely different. I imagine the same thing would come out in a combined test like this.

Mr. Hendrix: The wave forms through the complete range of frequency looked pretty well, although I believe temperatures probably bother it more than the acceleration, or anything like that

* * *

HYDRODYNAMIC IMPACT TESTING OF A RADIOMETRIC SEXTANT RADOME

S. Leonard Spitz
Allied Research Associates, Inc.
Boston, Massachusetts

A new method has been established for water-impact testing of those devices subject to hydrodynamic loading. The appropriate test structure is described as it specifically relates to the hydrodynamic loading of a radiometric sextant radome. Instrumentation capability of the test structure especially with reference to the radome is discussed. Data recorded during the radome test program are presented and analyzed. Both the structural integrity of the radome under simulated hydrodynamic impact loads and that of the test structure are verified.

INTRODUCTION

The radar antenna for a radiometric sextant navigational aid for new submarines is to be encapsulated in a radome which is supported by a retractable mast and extends to position the radome above the surface of the sea when navigational data are required.

The radome employed for the antenna enclosure must be capable of withstanding the hydrodynamic wave-impact loads associated with heavy seas without structural failure and without excessive deflections which would cause spurious signals and concomitant navigational errors. In addition, of course, the radome must be capable of fabrication within the close tolerance boresight limits prescribed for satisfactory antenna operation.

Allied Research Associates, Inc. has been engaged in a program to develop the test equipment and to conduct such tests as are necessary to determine the stresses and deflections produced in radomes by the hydrodynamic loadings associated with various water-impact conditions. The wave-impact loadings associated with particular sea conditions were simulated by attaching the radome to a pendulum which was raised to predetermined heights and allowed to fall, thereby impacting the radome on the surface of a body of water. Different wave-impact conditions were simulated by releasing the pendulum from various heights. Sufficient inertia is incorporated in the pendulum through a mass attached to the free end to preserve the impact velocity within 5 percent during radome water penetration. The radome was instrumented so as to measure radome deflection, radome stress, imposed water pressure, the total moment and lift and drag forces on the radome, the speed of impact, and the radome internal pressure.

Because of the large system inertia and the concomitant high system energy required to preserve the entrance velocity within 5 percent of its initial value, it would have been extremely difficult and costly to stop the radome-carrying pendulum by mechanical means after water entry. However, calculations showed that hydrodynamic braking could be efficiently accomplished by the use of a triangular shaped member (entering the water apex first) at the end of the pendulum. Accordingly, the inertia providing ballast is wedge-shaped and it, together with the buoyancy of the pendulum, was designed to

arrest the structure within 20 feet of water penetration.

To obtain the desired impact velocities associated with a State 5 Sea (42.7 fps) a drop height of at least 34 feet was needed. The size of the necessary test pendulum obviously required an outdoor test installation. A study of possible test sites showed abandoned flooded quarries to be almost ideal. Such quarries provide a natural foundation for the installation of the test rig, and the depth of water is sufficient to preclude reflection effects and to bring the pendulum to rest after radome penetration but before contact with the bottom. Nelson's Quarry, which Allied Research selected for the program, is located in Gloucester, Massachusetts. It has good accessibility, an ideal rock ledge 34 feet high, and a water depth varying from 40 to 100 feet. A photograph of the quarry is shown in Fig. 1.

DESCRIPTION OF PROTOTYPE RADOME

The radome chosen as the prototype of that which is to be installed on the new submarines is made of layers of Number 181 Volan fiberglas cloth (per Mil P-8013C) and Number 828 Resin (per Mil-R-9300A). It is essentially a cylinder 30 inches long capped on one end with a hemisphere and mounted on the other end to a conic base. The final thickness of the laminate is approximately 0.380 inch. Although inherently rigid, the radome was internally pressurized to 75 psig to further insure its stability.

To determine whether the mechanical properties of the fiberglas fell within the range specified in Ref. (1), standard tensile specimens were prepared and subjected to axial loading in tension until fracture. A typical stress strain diagram is shown in Fig. 2 and the modulus of elasticity from $E = S/\delta$ was found to be 3.259×10^6 psi. This elastic modulus is in good agreement with the referenced values.

DESCRIPTION OF TEST EQUIPMENT

Test Structure

Naval specifications require a radome to function satisfactorily when exposed to the

Fig. 1 - Nelson's Quarry, Gloucester, Massachusetts

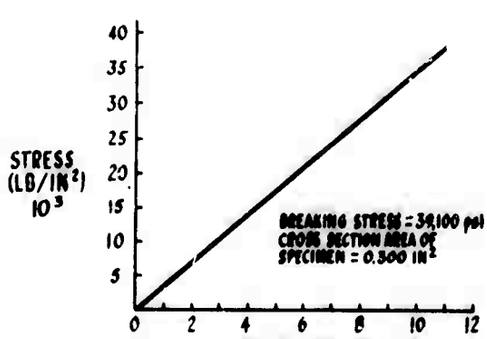

Fig. 2 - Stress vs strain for fiberglas radome material

hydrodynamic loadings associated with a moving submarine operating in a State 5 Sea. The wave velocity characterized by the State 5 Sea together with the operating velocity of the submarine define the relative velocity between the radome and the wave as 42.7 fps. The test equipment therefore is required to simulate this velocity both at impact and during penetration of the radome into the water.

The final design concept of the drop-test structure is illustrated in Fig. 3. The radome was to be mounted to a pendulum which would be raised to various heights and allowed to drop, thereby impacting the radome on the surface of a body of water. The structure consisted of four primary members, viz: the main pipe acting as the pendulum and contributing buoyancy to the structure; the hinge by means of which the pendulum was attached to the quarry wall while providing the axis of pendulum rotation; the wedge to contribute both the inertia mass for maintaining impact velocity during water penetration and also to absorb together with the pendulum buoyancy the high system energy and so arrest the structure after water entry; the support beam providing a rigid cantilever support for the radome. The two secondary members were the sting balance, an instrumented pipe for measuring total forces and the instrument support structure within the radome. However, the actual choice of material, size of primary and secondary members, method of joining members, wedge inertia mass were all in whole or in part dependent upon the loadings imposed upon the radome and wedge as they impacted the water.

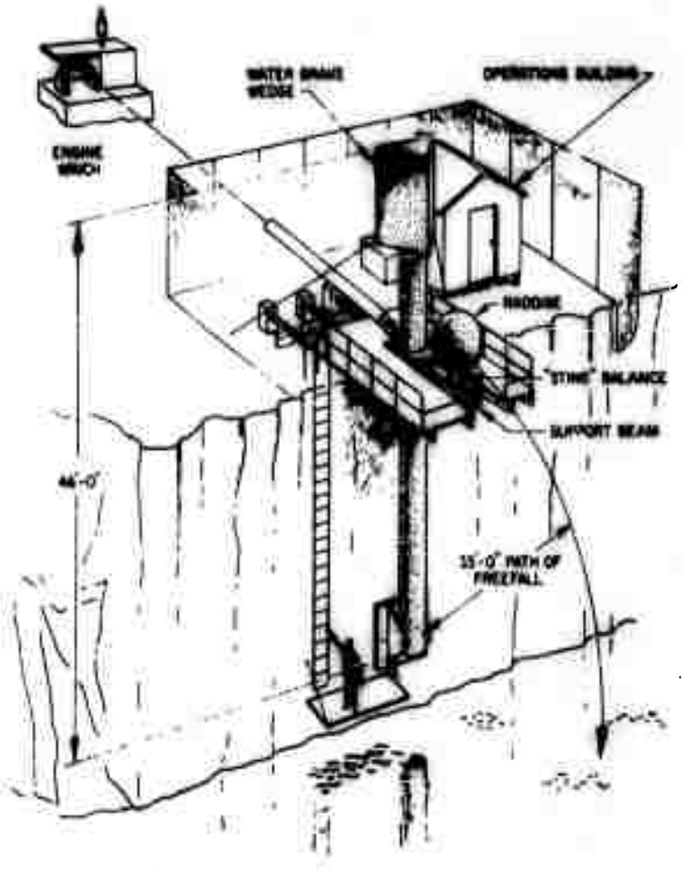

Fig. 3 - Field test area

The hydrodynamic forces on the radome and the wedge were predicted by calculations based on the work described in Ref. 2. The expression for the impact force of a body penetrating the surface of a liquid at constant velocity in terms of the virtual mass, assumed to be variable is

$$F_i = A(C_1)_e \frac{\rho}{2} V_o^2 , \qquad (1)$$

where

F_i = the hydrodynamic force,

A = the cross-sectional area normal to the applied force,

$(C_1)_e$ = a semiempirical force coefficient and is a function of the dead-rise angle β and the shape of the penetrating mass,

ρ = the fluid density,

V_o = the impact velocity.

A curve of hydrodynamic loading on the radome as a function of penetration time after impact is shown in Fig. 4. It may be seen that the predicted maximum force with the radome impact velocity of 42.7 fps is 81,000 pounds occurring 0.01 seconds after impact. Solution of wedge loadings is similarly obtained by Eq. (1). An iterative procedure is utilized for the final wedge design whereby having chosen the shape, dimensions are assumed and attendant loads calculated until the final geometry-load configuration is compatible with the strength capability of the main pipe and the inertia mass required for maintenance of impact velocity during penetration. The maximum predicted force on the wedge was 230,000 pounds.

To absorb these large predicted hydrodynamic loads without failure, the pendulum was fabricated from United States Steel T-1 (tensile strength of 118,000 psi) into a pipe, 16 feet long and 3 feet in diameter. The wedge cross section is an isosceles triangle with an altitude of 5 feet, a base of 7.5 feet and having an over-all length of 8.5 feet. The total weight of the entire structure is 16,710 pounds and is carried by the hinge, 5.5 feet high and 6 feet long, which in turn is bolted to the quarry's granite wall with 64, 1-1/8-inch diameter bolts. A photograph of the structure as it is installed is shown in Fig. 5.

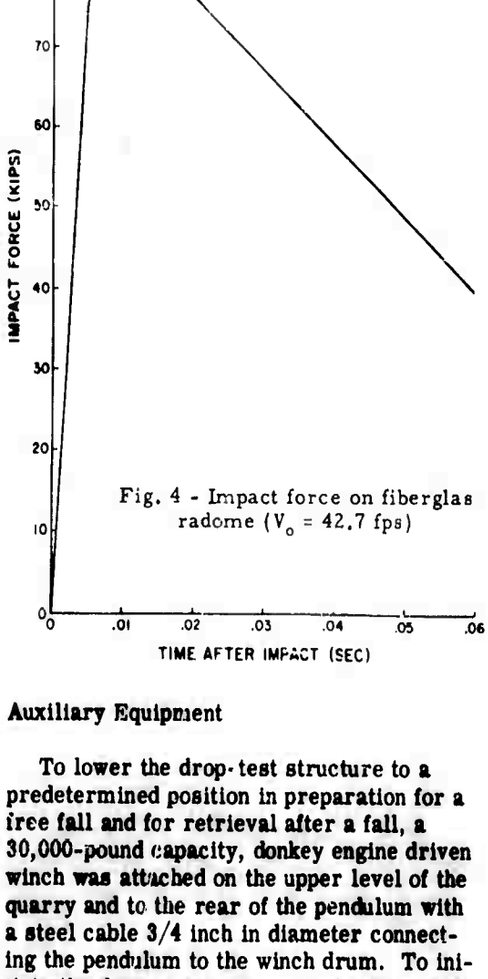

Fig. 4 - Impact force on fiberglas radome (V_o = 42.7 fps)

Auxiliary Equipment

To lower the drop-test structure to a predetermined position in preparation for a free fall and for retrieval after a fall, a 30,000-pound capacity, donkey engine driven winch was attached on the upper level of the quarry and to the rear of the pendulum with a steel cable 3/4 inch in diameter connecting the pendulum to the winch drum. To initiate the drop, a remote-control cable cutter was hung from the pendulum and in cutting position was attached to the winch cable. The cutter derived its energy from an exploding cartridge, electrically fired and remotely energized. A work platform was cantilevered over the top edge of the cliff for easy access to the radome and a second was attached to the wall near the hinge.

Instrumentation

The radome was instrumented so as to measure radome deflection, radome stress, imposed water pressure, the total moment and lift and drag forces on the radome, the speed of impact and the radome internal pressure. Stress, deflection, and pressure measurements were made at such stations on the radome as are required for reasonable determination of the maximum values of these quantities and their distribution in

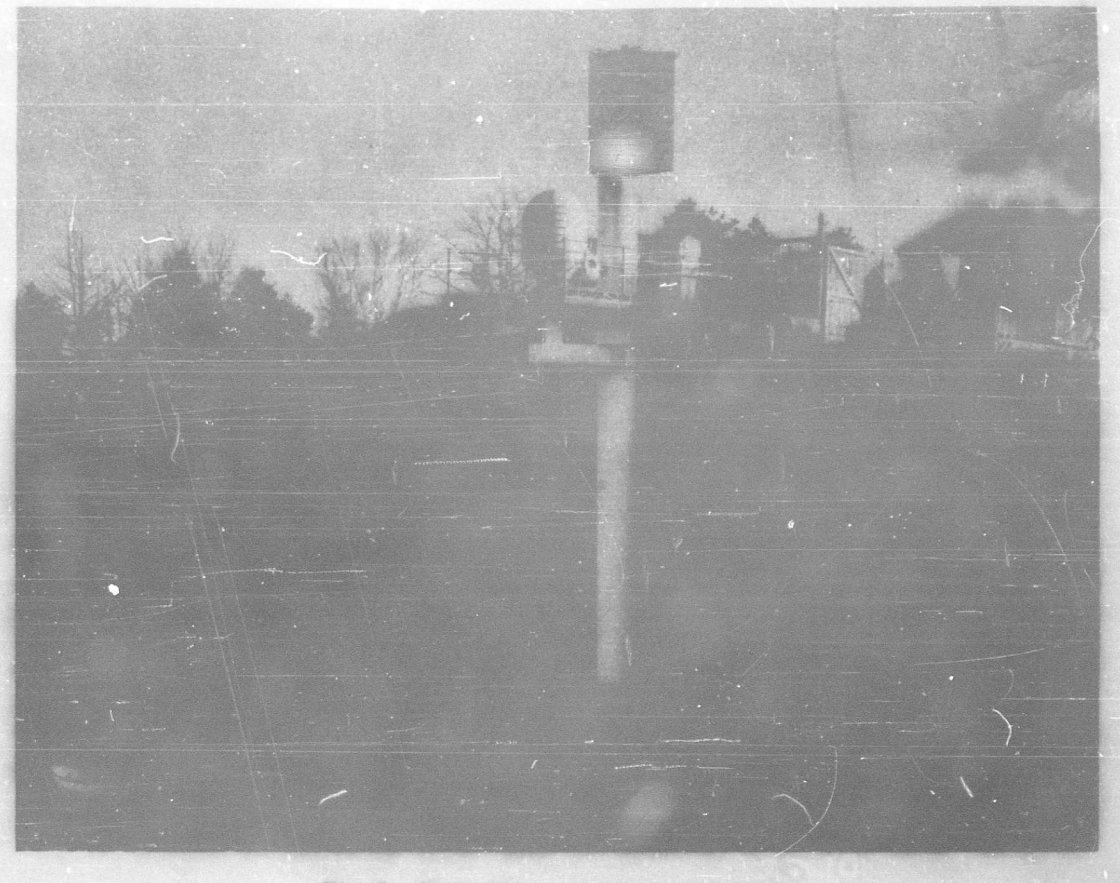

Fig. 5 - Drop-test structure installations

the vicinity of the maximum. The majority of the pressure, deflection, and stress measurements were made on the impact side of the radome. Some measurements were also made at the side and rear of the radome. It should be noted that since the radome is geometrically symmetrical about the plane D-D (Fig. 6) a symmetry of pressure, stress, and deflection measurements about this plane was expected. This symmetry has been utilized to minimize the number of transducers that were used. A complete pressure, stress, and deflection survey was made on one side of the plane D-D centerline and only pilot, correlative measurements on the other side. Radome deflections were measured by self-aligning translatory potentiometers whose shafts were attached to the radome skin and whose bodies were connected to a central instrument carrier within the radome as shown in Fig. 7. A placement pattern of the potentiometers is shown in Fig. 6. The potentiometers employed were a modification of a standard translatory potentiometer manufactured by Technology Instrument Corporation that Allied Research has redesigned to withstand the anticipated acceleration forces imposed at impact.

The water pressure imposed on the radome was measured by using small, lightweight (0.062 pound) pressure transducers installed so as to have their pressure-sensitive face flush with the external surface of the radome. The locations of the pressure transducer stations are shown in Fig. 6. The pressure pickups that were used for impact-pressure measurements and for monitoring the radome internal air pressure are Consolidated Electrodynamic Corporation's Model 4-312A.

Stresses were measured on the rigid radome with conventional Baldwin-Lima-Hamilton strain gages. Two-gage rosettes with the gages placed at right angles to each other were used at the locations shown in Fig. 8 and the gages were cemented directly

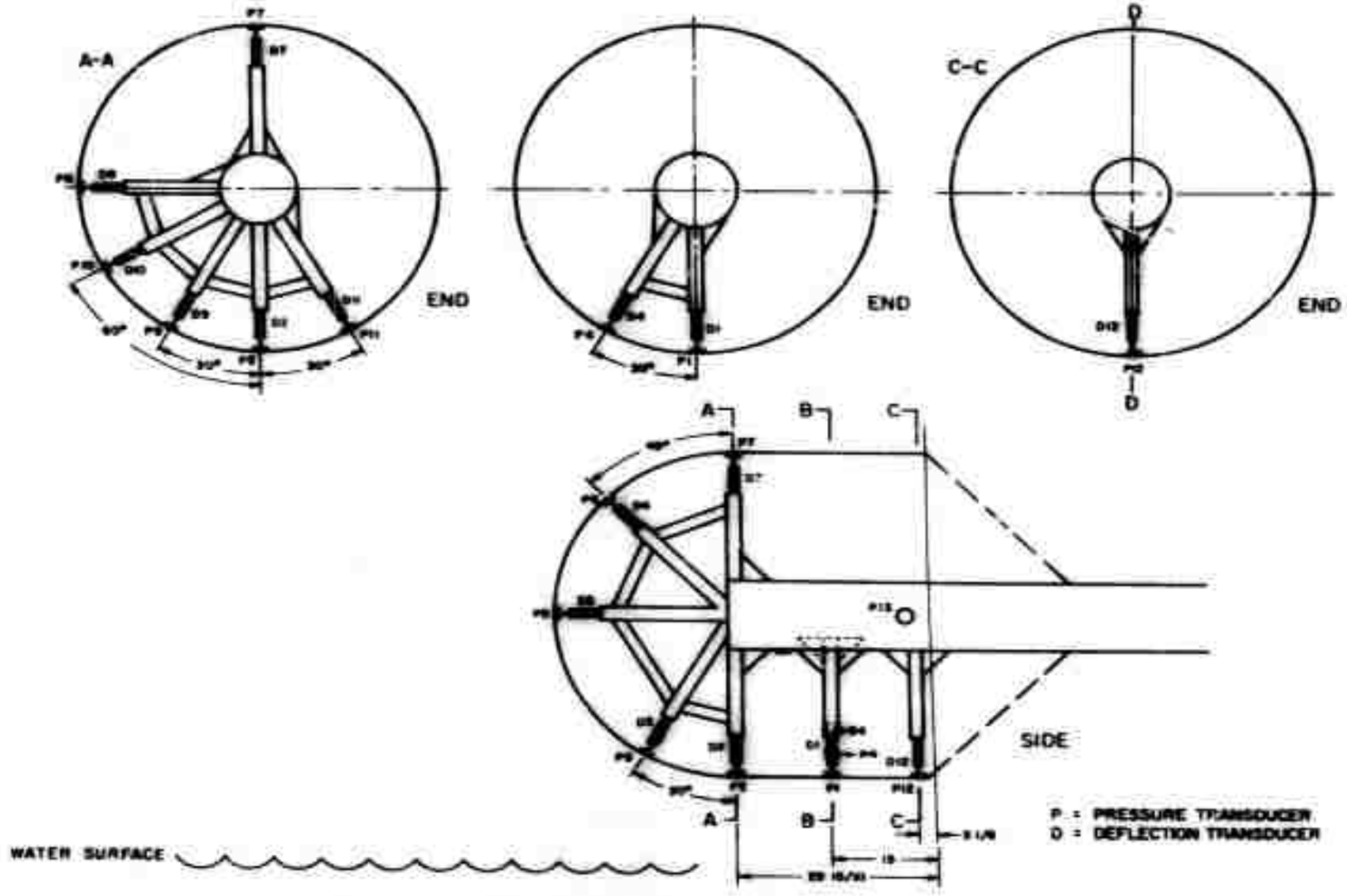

Fig. 6 - Deflection and pressure transducer instrumentation

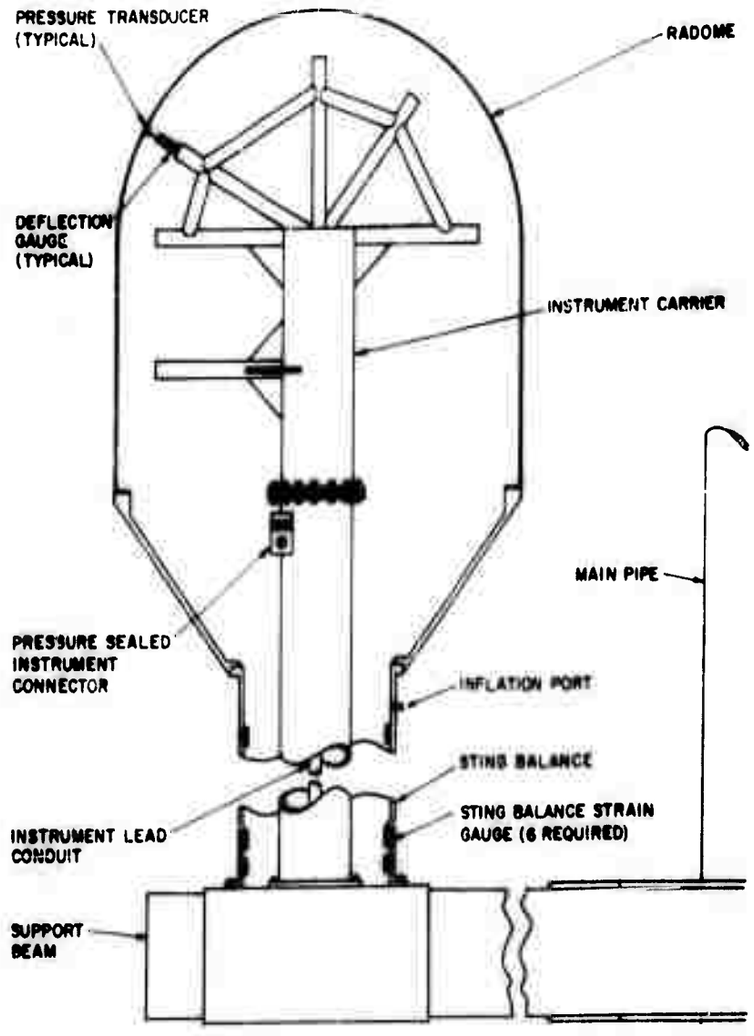

Fig. 7 - Radome "string" balance

to the interior skin surface of the fiberglas. The angular displacement and velocity of the pendulum were measured by an Ohmite Type R-500-watt rotary potentiometer which is connected to the pendulum hinge shaft.

Fifty data-recording channels were required for the instrumentation described above. Of these, twenty-two were used for strain-gage data; twelve for external-pressure measurements; one for recording internal-pressure data; eleven for deflection measurements; three for net lift, moment, and force as applied to the sting balance and support beam; and one to record pendulum velocity. One sixteen-channel and two twenty-four channel recording oscillographs were used to simultaneously record all data. The amplifiers and galvometers which were used for data recording have flat frequency responses to 3300 cps. This insured an accurate, undistorted record of all impact data. The recording equipment was controlled so as to operate the instant the pendulum was released and continued to do so until the pendulum had come to rest. A block diagram of instrumentation and recording circuitry is given in Fig. 9.

TEST PROCEDURE

The events describing a typical drop test include lowering the pendulum by means of the winch to a predetermined height from which free fall would be initiated, balancing and calibrating all instrumentation, remotely firing the cable cutter, and simultaneously starting the recording equipment which was manually shut off when the structure assumed

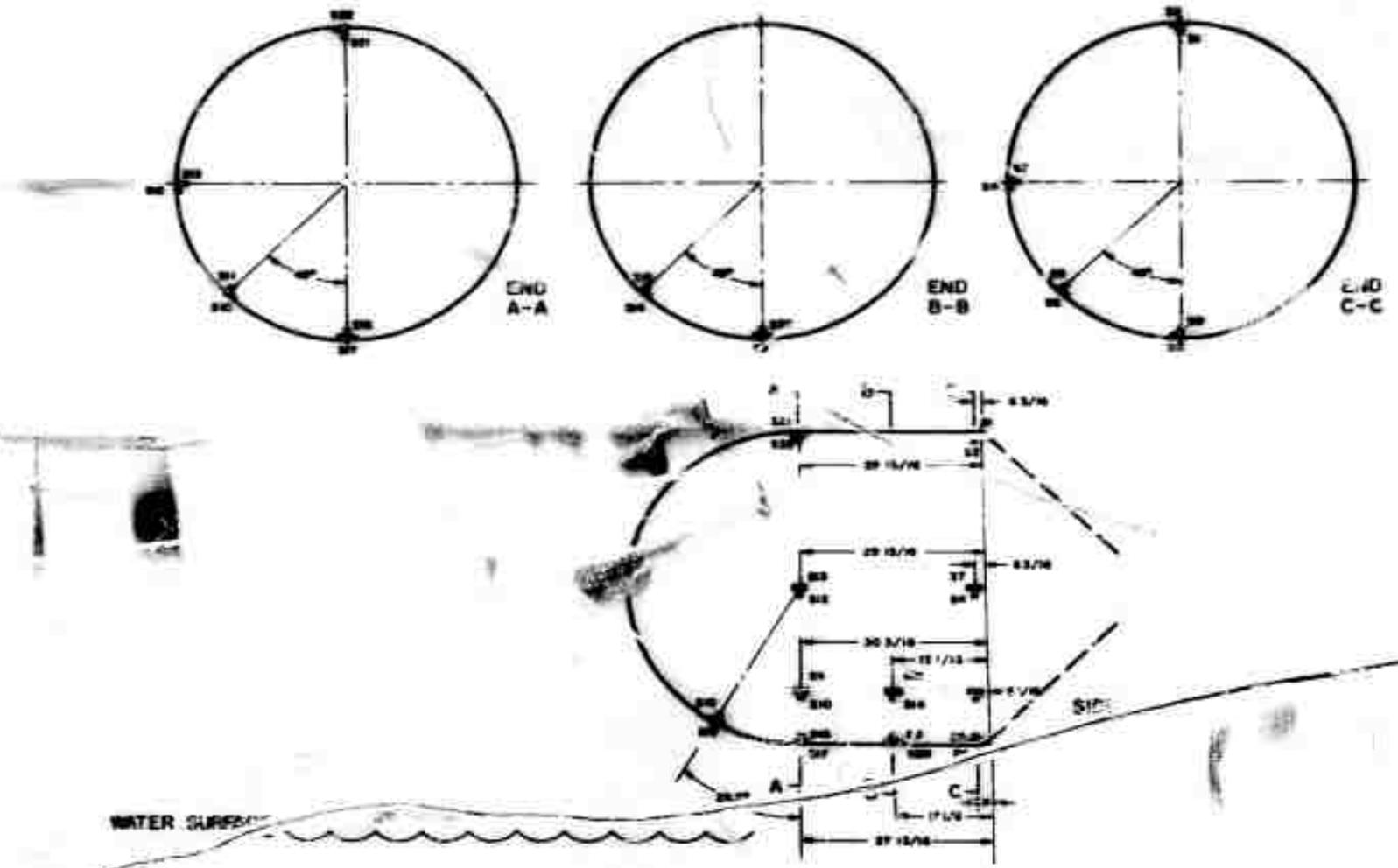

Fig. 8 - Strain-gage instrumentation

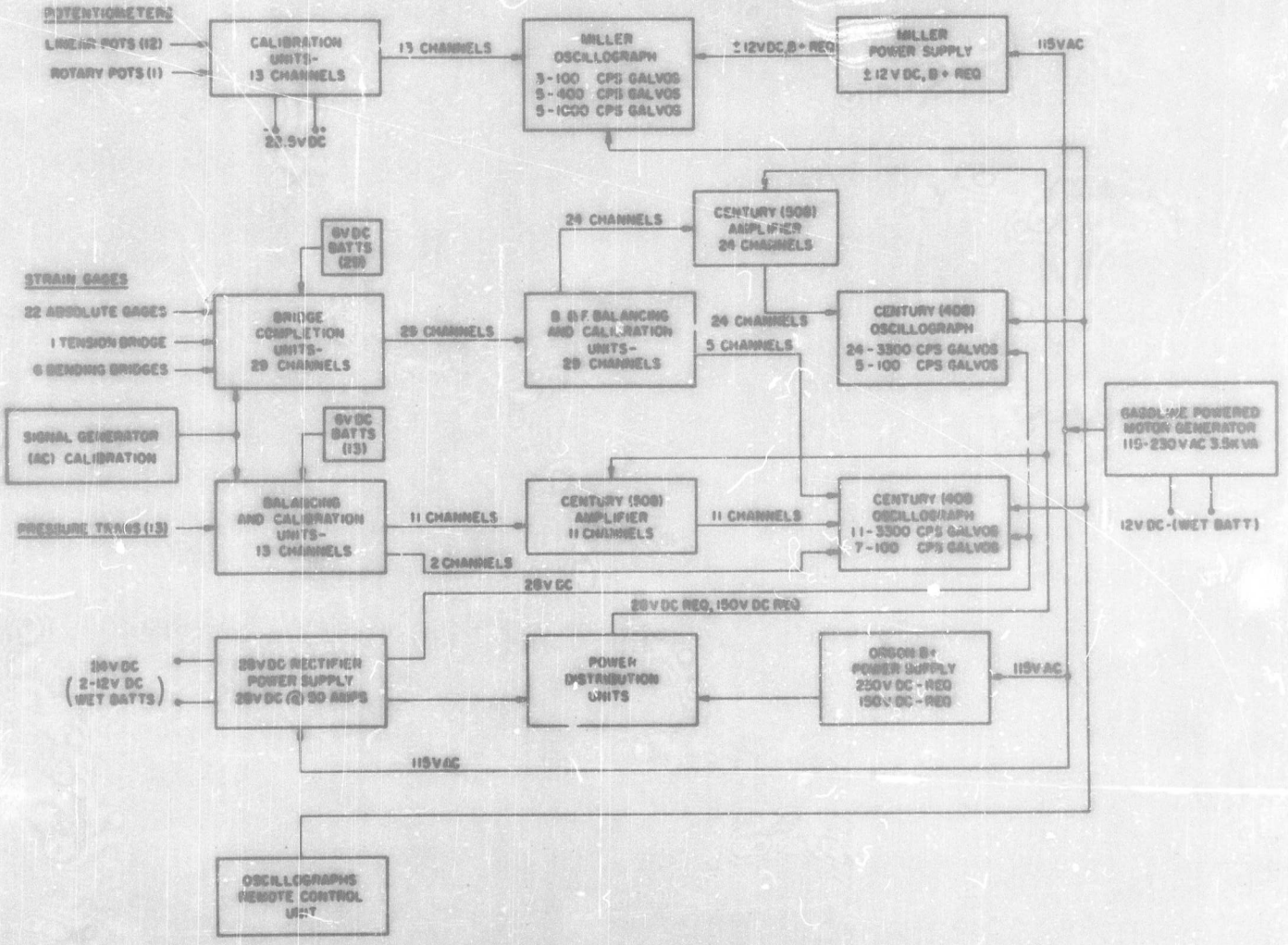

Fig. 9 - Instrumentation and recording circuitry

a floating position. Figure 10 illustrates a typical drop sequency from drop initiation to final flotation.

To predetermine the drop height an upper and lower bound of impact velocity as a function of height was predicted. The upper-bound velocity is calculated from $V = \sqrt{2gh}$, the expression for a freely falling body in our gravitational environment. The lower-bound velocity is an inertial type calculation based on the conservation of energies for a pendulum system and is given by $P.E. = 1/2\ I\omega^2$. The actual velocity of impact was measured by a rotary potentiometer attached to the hinge shaft as described above.

TEST RESULTS AND DATA ANALYSIS

A total of nine drop tests was made during the field program wherein all active transducers were monitored. The drop height varied from about 3 feet to 41 feet providing an impact-velocity increment to maximum averaging 3 fps. The fundamental objectives of the experimental program, viz: measurement of radome deflection, strain and pressure under the hydrodynamic loadings associated with a State 5 Sea, were effectively realized.

Reproductions of the oscillograph traces recording the transducer data for that drop test simulating State 5 Sea conditions are shown in Figs. 11, 12, and 13. The numbers that may be seen adjacent to the traces key the particular trace with the position of the associated sensing transducer on the radome. Velocity at impact and at full radome penetration, hydrodynamic loading, radome deflection and strain have been determined by reducing the above recorded data and reducing similar records taken during other test drops.

The relationships between measured impact velocity and drop height and a comparison of these results with the upper- and lower-bound calculations described above are shown in Fig. 14. It may be seen that at relatively low drop heights having low impact velocities, the measured velocity closely conforms with the upper-bound values; however, as the drop height increases with its concomitant increase in impact velocity, the measured velocity becomes even less than that predicted by the lower bound. This may be explained by the fact that the lower-bound calculations neglect the hinge friction which becomes more significant as the drop height increases and is most important when the pendulum is close to the vertical.

The hydrodynamic loadings were calculated by means of a dynamic analysis based on energy conservation wherein the work done by the externally-applied load is related to the internal strain energy in the structure. Such an analysis is described in Ref. (3). The load-time history for the actual maximum impact velocity of 41.7 fps yielded by the dynamic analysis is shown as a curve in Fig. 15 contrasted with the predicted load pulse at the same velocity. It is apparent that the predicted values for both the load magnitude and time pulse are conservative by a factor of about two. Maximum load on the radome as a function of impact velocity is shown in Fig. 16. The curve shows the load increasing exponentially with velocity.

Translatory potentiometers measured the deflection of the radome due to imparted motion from the deforming radome skin. The position of principal interest is the impact face of the radome. Figure 17 shows the relationship between the deflection at this point and the velocity of impact. It can be seen that impact face deflection increases almost linearly with impact velocity. A survey of maximum radome deflection with respect to the position of this deflection on the radome was attempted for each velocity; however, because of potentiometer failures insufficient data were recorded on the simulated State 5 Sea drop. A deflection distribution curve associated with a radome impact velocity of 21.5 fps is shown in Fig. 18. The section illustrated refers to section A-A from Fig. 6 with the positions noted corresponding to those on the section. It can be seen that the radome deforms locally at the impact face while bulging at a point about 90° away from the impact face. It also appears as if the deflection pattern is symmetrical from the similarity of deflection at positions 9 and 11. It would be reasonable to expect this deflection pattern to be reproduced similarly with an increase in magnitudes at greater impact velocities.

As a first approximation for the determination of radome stresses and assuming that the direction of the principal stresses are coincident with the orientation of the radome two-gage rosettes, the equations associated with membrane theory are utilized. These equations which neglect bending are given in Ref. (4) as

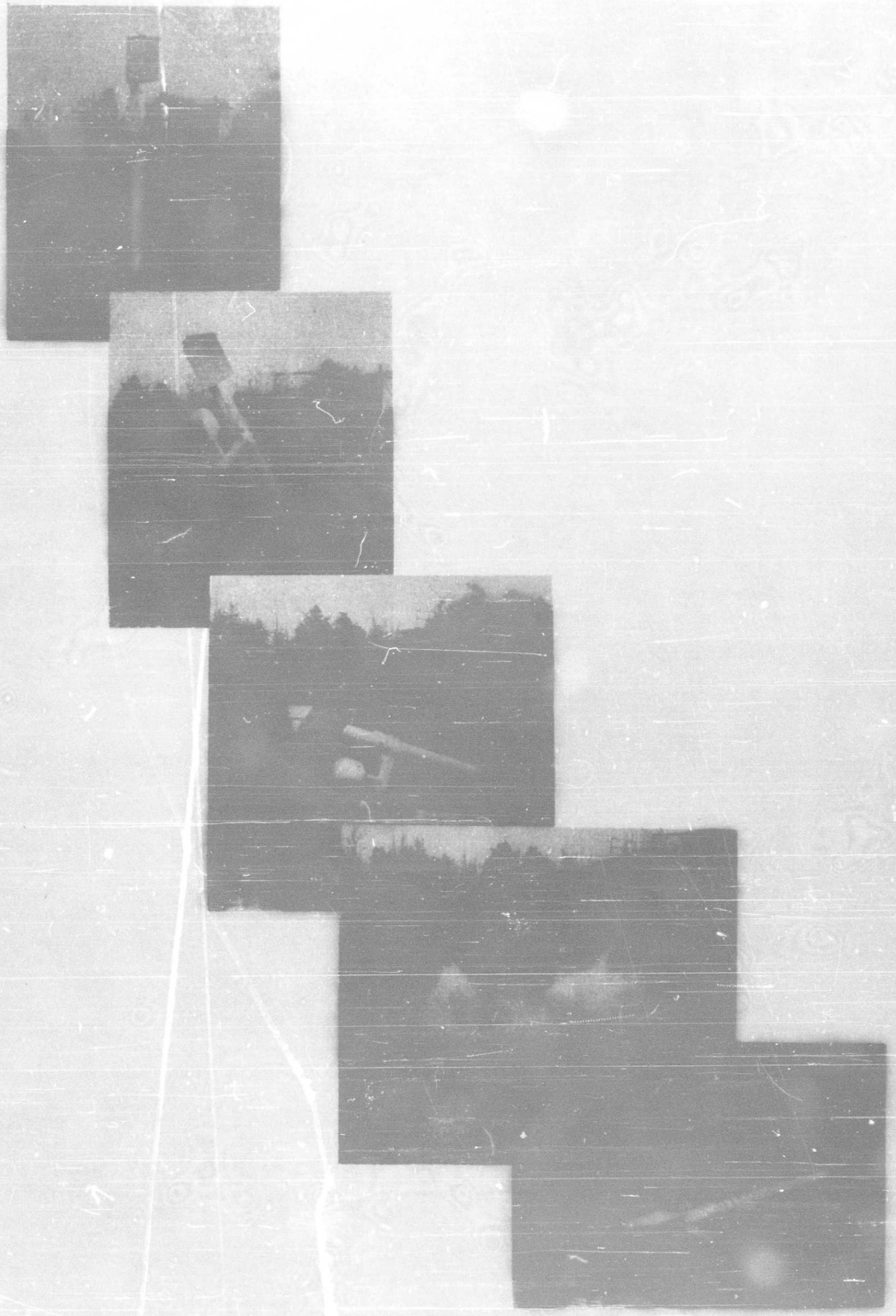

Fig. 10 - Typical drop-test sequence

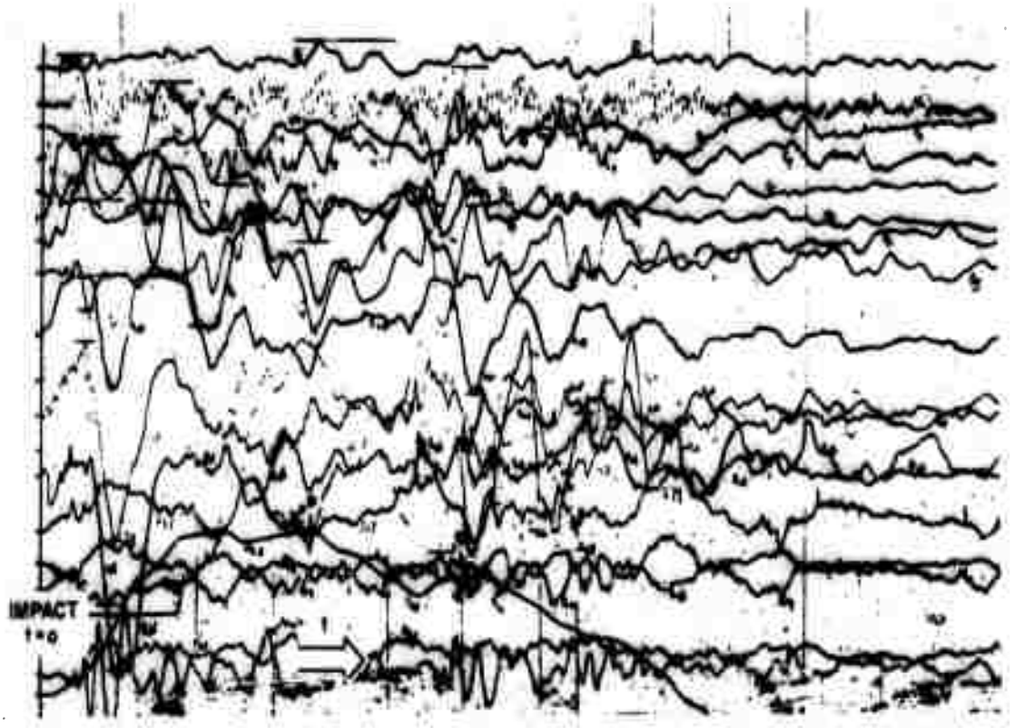

Fig. 11 - Strain data

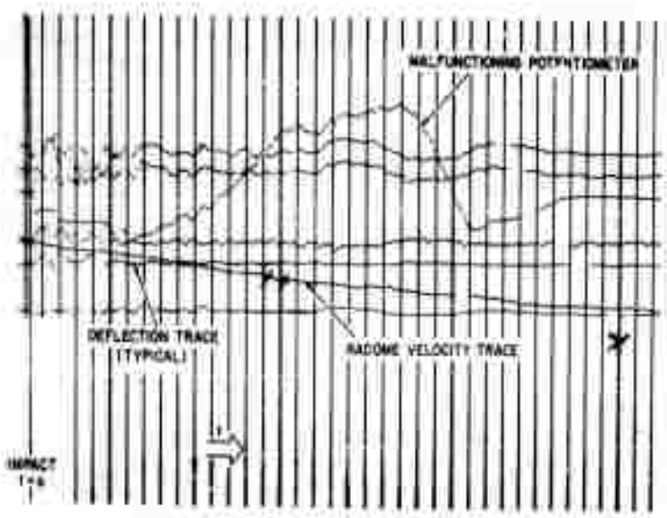

Fig. 12 - Potentiometer (translatory and rotary) data

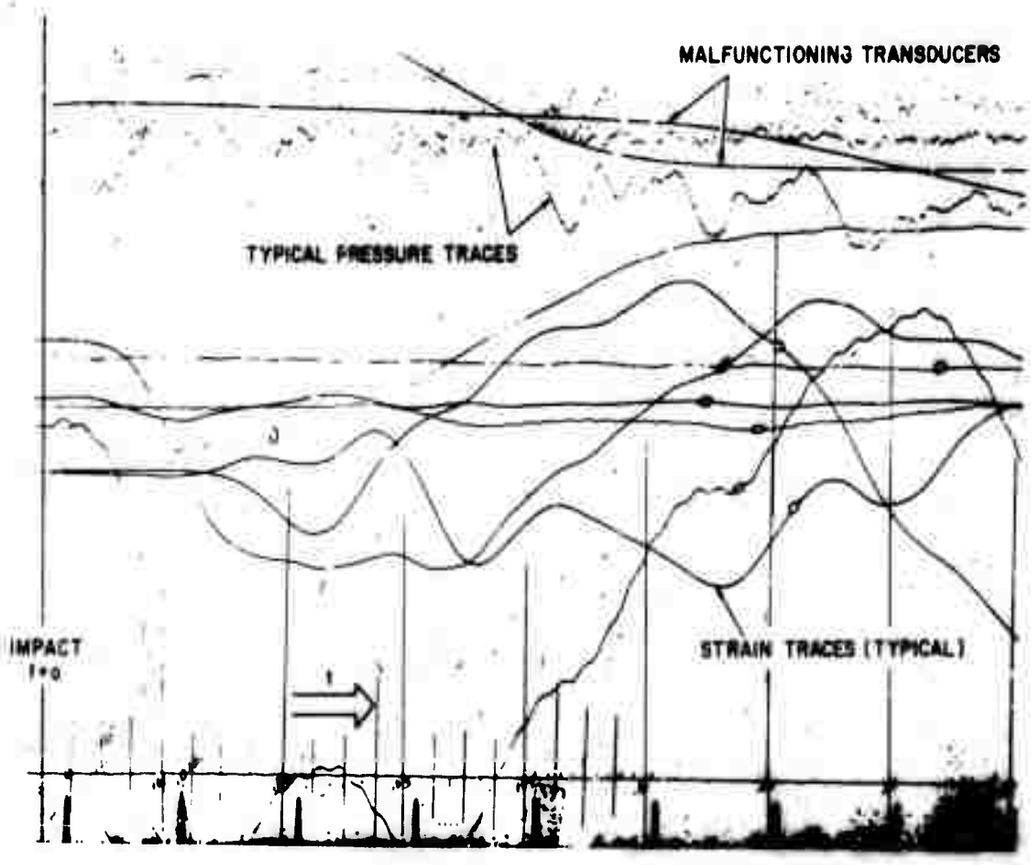

Fig. 13 - Pressure and strain data

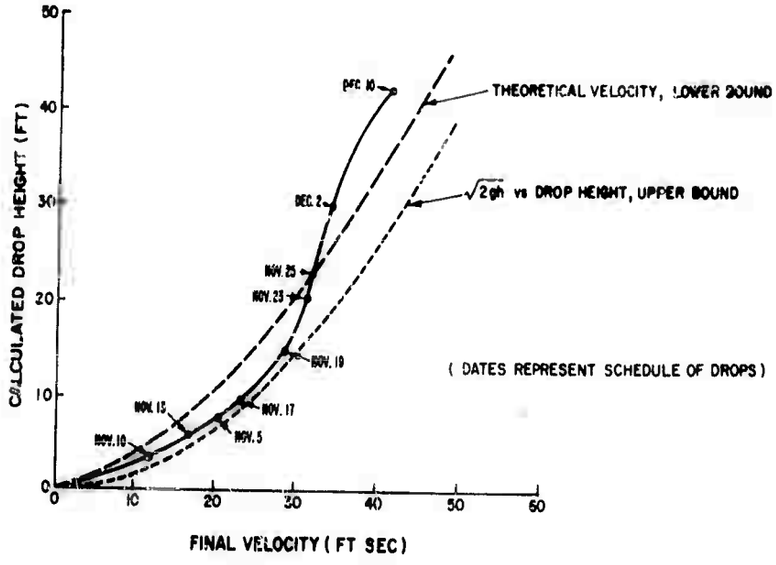

Fig. 14 - Final impact velocity of radome vs calculated drop height

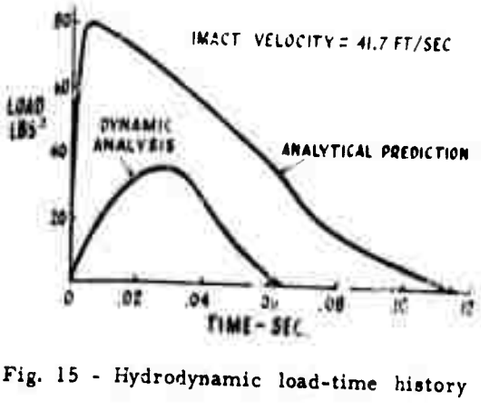

Fig. 15 - Hydrodynamic load-time history

$$\sigma_x = \frac{E}{1 - \mu^2} (\epsilon_x + \mu \epsilon_y), \qquad (2)$$

$$\sigma_y = \frac{E}{1 - \mu^2} (\epsilon_y + \mu \epsilon_x), \qquad (3)$$

where

σ_x and σ_y = the principal stresses in psi,

E = the modulus of elasticity in psi,

μ = Poisson's ratio (0.17 from Ref. 1),

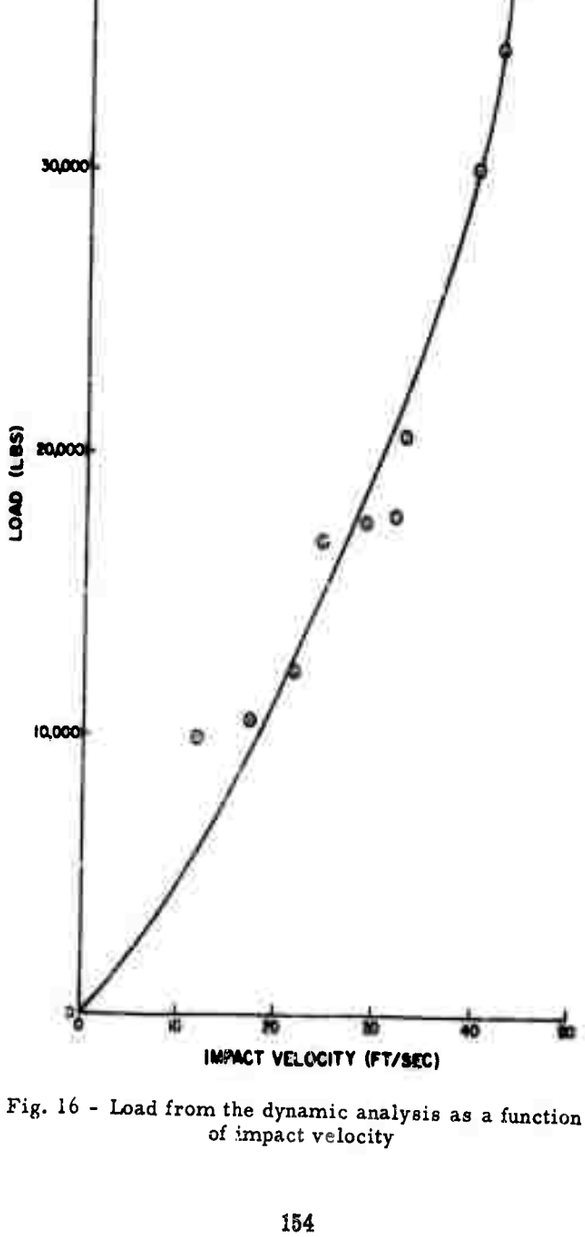

Fig. 16 - Load from the dynamic analysis as a function of impact velocity

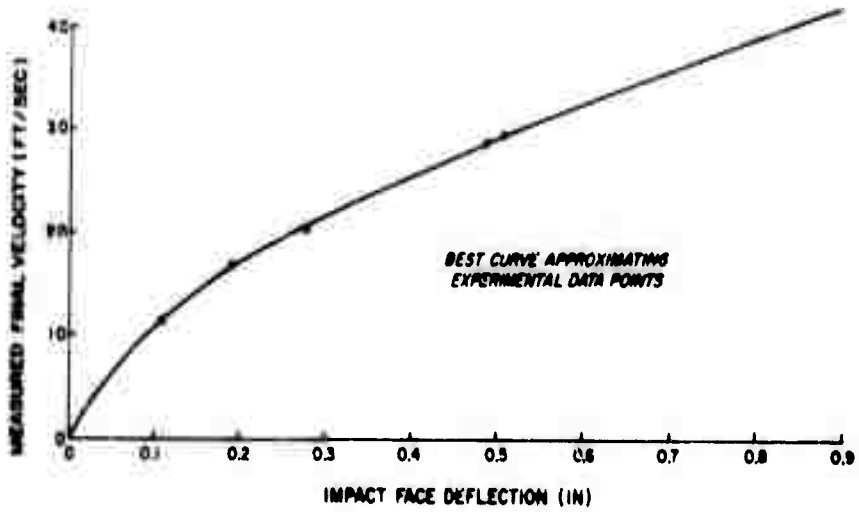

Fig. 17 - Maximum deflection of radome impact face

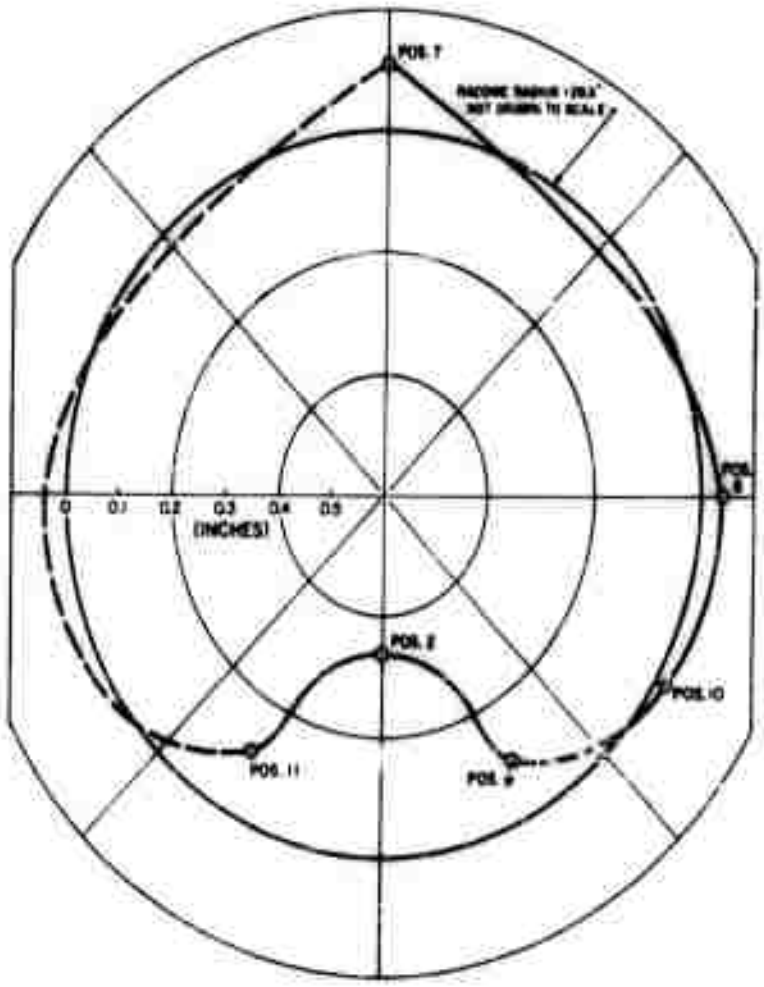

Fig. 18 - Maximum deflection

ϵ_x and ϵ_y = the principal strains in in./in. (The subscripts x and y refer respectively to planes perpendicular and parallel to the longitudinal axis of the radome.)

Principal stress-time histories associated with the simulated State 5 Sea impact velocity are shown in Figs. 19 and 20. The strain measurements were taken at positions 5 and 6 as noted in Fig. 8. From Fig. 20 it can be seen that the maximum stress is 5000 psi in compression perpendicular to the longitudinal axis of the radome.

CONCLUDING REMARKS

This new method of simulating water-impact loadings on bodies by means of a free-falling inertia-driven pendulum has provided significant data for the parametric study of a radiometric sextant radome. Accordingly, it is expected that the facility can be employed in other water-impact test applications. Submarine radomes of all types including flexible air-supported radomes are prime candidates for this facility. Shipboard bubbles located close to the water and thus exposed to heavy seas lend themselves to such testing. Capsules, recovery systems, and launching systems may also be tested. It is possible that such testing can provide design criteria for ejection seats, sonar transducers and housings, torpedoes and hull elements. Although the maximum attainable free-fall impact velocity is about 42 fps, an initial velocity can be imparted to the pendulum by an auxiliary device such as a jet booster to provide an impact velocity of close to 100 fps. Accordingly the structure may be applicable to prototype or model nose-cone testing. Heavier and larger devices than radomes may be tested by minor modifications to the mounting pad.

ACKNOWLEDGMENT

The author wishes to express appreciation to Mr. Leonard E. Smollen for his contribution to the project with reference to the conception of the test structure and its design.

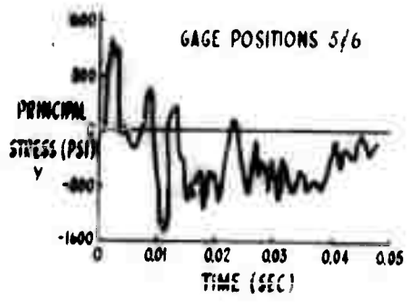

Fig. 19 - Time history of principal stress, y

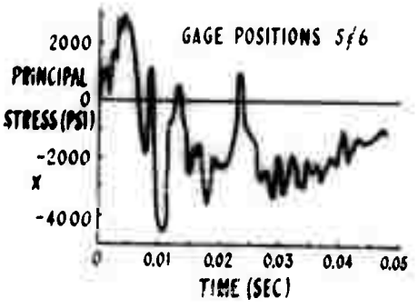

Fig. 20 - Time history of principal stress, x

REFERENCES

1. Forest Products Laboratory, Forest Service, United States Department of Agriculture, "Plastics for Aircraft, Part I, Reinforced Plastics," Department of the Air Force, Air Research and Development Command, June 1955.

2. L. W. Ward, "Methods for Estimating Impact Forces on Ship Appendages," Experimental Towing Tank, Stevens Institute of Technology, Report No. 616, December 1956.

3. C. H. Norris et al., "Structural Design for Dynamic Loads," McGraw-Hill Book Company, Inc., New York, 1959.

4. C. C. Perry and H. R. Lissner, "The Strain Gage Primer," McGraw-Hill Book Company, Inc., New York, 1955.

* * *

INSTRUMENTATION AND DATA ANALYSIS

A CRITIQUE OF THE TECHNIQUES USED IN THE MEASUREMENT, ANALYSIS, AND SIMULATION OF MISSILE VIBRATION ENVIRONMENT

Merl R. Beckman
Laboratory Department, U. S. Naval Missile Center
Point Mugu, California

The vibration qualification tests performed on missile equipment in the laboratory typically are very different from actual flight environments. Some causes may be found in the confusion that exists within the fields of vibration measurement, data analysis, and laboratory simulation. Even more important is the lack of coordination that exists between these specialties.

INTRODUCTION

This paper deals primarily with the shock and vibration problem in missiles, but it would not be out of context to apply many of its conclusions to other electromechanical devices.

WHY VIBRATION MEASUREMENTS ARE MADE

In polite philosophical circles, it would generally be agreed that the ultimate reason for measuring missile vibration is either to prove or improve the product by using added knowledge the measurements would bring to light.

In actual practice, the measurements occasionally are made because "the contract says we have to." Or sometimes "we have serious trouble and can't seem to find it. Let's measure the flight shocks and vibration. While the experts are arguing about the true significance of the data, we'll have six months to come up with a fix." In short, the motives for measuring missile vibration are often not very scientific.

However, the poor initial attitude is only the beginning of a long series of misconceptions and technical errors that typify a vibration environment program. The telemetry system to measure vibration is typically designed and adjusted with little regard for system information capacity, system noises, and system distortion characteristics.

The data analysis is performed and the data presented in a format that will satisfy the data requestor. Frequently, the format is determined by equipment availability and by the personal prejudices of the analyst. Rarely is the format determined with shock or vibration simulation in mind.

Following the analysis, someone from somewhere converts the data into test procedures to be used by the shock and vibration laboratory. Those charged with performing the laboratory tests typically are preoccupied with obtaining or fabricating the right jigs, fixtures, adaptors, and mounts that mate the test specimen with the testing equipment. There is also concern about scheduling equipment time, assignment of personnel, and the funding of the test. There is usually little interest in what the original data looked like, the limitations of the equipment that measured the vibration or analyzed it, the manipulation of the data by the

analysts, or the conversion of the data into a test procedure.

To state it briefly, nobody seems to care what anybody else is doing, or why. As a result, the laboratory vibration tests commonly bear no recognizable relationship to the flight vibration environment. One could ask in such instances, "why bother?"

Unfortunately, there is no easy road to achieving a good laboratory simulation of flight shocks and vibration; however, with a consistent attention to fundamentals, meaningful simulations can be achieved.

HOW FLIGHT VIBRATION MEASUREMENTS ARE MADE

When it is decided to measure missile flight vibrations by radio telemetry, there often seems to be some initial confusion. If IRIG telemetry standards are adhered to literally, the maximum information frequency that can be accommodated is about 2 kc. A question then arises as to whether the 2-kc response is adequate (it is not) or whether it might be possible to increase the response a little, still using IRIG standard equipment. Another possibility is to use systems completely at variance with IRIG standards. Because of limitations of time and space, only systems "expanding" the nominal IRIG frequency limitations will be discussed at any length. Various systems of this type and others are described in Ref. (1).

The nominal frequency response capabilities of standard IRIG fm-fm telemetry can be expanded considerably for the purpose of accommodating high-frequency vibration data. However, the process is not without its pitfalls and dangers.

A block diagram of a typical vibration data channel with commercial hardware is shown in Fig. 1. The amplitude and distortion characteristics of a channel with a 70-kc subcarrier is shown in Fig. 2. The various curves indicate some of the highly important characteristics of band-limited fm systems in general and fm-fm telemetry in particular. For example, the distortion is highly frequency sensitive. Another interesting characteristic can be noted from the curves if the fundamental information

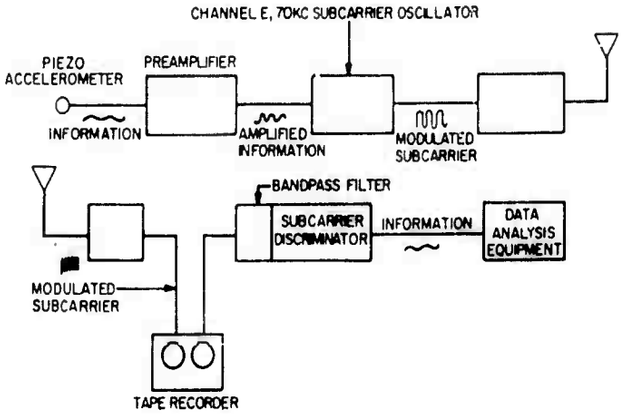

Fig. 1 - Standard subcarrier system

frequency component is added to its harmonics. Under these conditions (which would normally prevail) the rms output of

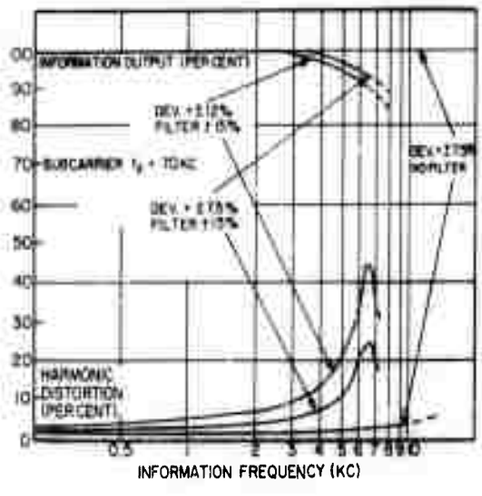

Fig. 2 - Amplitude and distortion characteristics of a channel with a 70-kc subcarrier

the subcarrier discriminator does not drop as the signal frequency is raised to the point of maximum distortion. This means that a flat information frequency response is not an indicator of good system performance.

An important point to note is that these distortion products do not arise from the use of nonlinear circuit elements, but are fundamental to the fm modulation process followed by predetection filtering. The effect is not similar to filtering the original information, and the distortion effects are not similar to simple amplitude distortion of the original information. Stated differently, the final data cannot be corrected by any simple scheme of frequency response correction or amplitude correction.

Opposing this idea, there is a persistent notion among mathematical sophisticates that if the detailed operating characteristics of a system are known, all the data errors can be corrected. They are to be reminded that after (and if) the ingenious data correction schemes have been reduced to practice, they can do no more than would be achieved by using a different band-limiting filter in the first place.

Except as a rather pointless exercise in time consumption, it is not recommended that any corrections be applied to data modified by fm band limiting; instead, band-limiting effects should be avoided or minimized by careful attention to, and coordination of, the relationship between the deviation of the subcarrier and the band limiting employed in the analysis station.

And now to discuss some of the proposed schemes for reducing the required information handling capacity of vibration telemeter systems. To set a proper framework of perspective for considering these systems, some fundamental principles should be borne in mind. First, whenever vibration data is operated on, i.e., "reduced" or analyzed, information is lost in the process. That is to say, when the data has been broken down to some form that is easy to study, invariably some salient features of the original data are missing and it is impossible to reconstruct, in detail, the original vibration information function. In short, when the original data is simplified for easier human comprehension, an irreversible loss of information has occurred.

The second point is simply an extension of the first: The information loss may or may not be important. Whenever the vibration information is to be analyzed, or reduced, or encoded (all meaning the same thing) before transmission from the flight vehicle, extreme caution should be exercised in determining the suitability of the system for use in the particular missile. The reason for this emphasis on the limitations of in-flight data analysis system is that in-flight analysis is basic to most bandwidth reduction schemes.

Spectrum Analyzer

One system gaining in popularity analyzes vibration by essentially tuning a filter slowly across the vibration spectrum and telemetering the magnitude of the filter voltage. To achieve adequate frequency resolution, the filter must sweep quite slowly, typically taking several seconds for one sweep of the spectrum. It is obvious that the system is not usable if significant spectral changes occur within the period of one frequency sweep. This renders the device useless for transient or impulsive type shocks or a rapidly changing random type function. This means it is not suitable for short burning motors (the motor should burn for several frequency sweeps). Also, it is not suitable for use in missiles where ordnance explosions or other intermittent mechanical shocks may occur.

Amplitude Analyzer

This device determines what portion of the total time a number of different amplitudes are exceeded. When the vibration is similar to random noise, the data is useful. However, as was true with the sweeping spectrum analyzer, impulsive shocks of truly catastrophic magnitude may show up in the data as only minor or unnoticeable perturbations.

Analog Frequency Meter and Voltimeter

There is a certain attractive simplicity in the idea of feeding the vibration signal into two simple data converters. One puts out a voltage proportional to the vibration frequency; the other puts out a voltage proportional to the amplitude of the vibration signal. The significant point to remember is that analog frequency meters can read one frequency, usually by the process of summing up the number of polarity reversals

per unit time which occur in the input function. Thus, the system yields no spectrum data and cannot handle random type signals; it yields nothing usable with impulsive type inputs; it does not even work with discrete frequency inputs, if more than one significant frequency component is present. In short, the system works only in the highly improbable circumstance that the vibration consists of a single discrete frequency.

Before any of the airborne data analysis schemes can be used, as an absolute minimum precaution, the nature of the missile vibration first should be determined by some wideband system; one that transmits the vibration in its "raw" form to the ground. Even after this precaution is observed, a strange situation exists. As long as the band reduction systems yield similar data flight after flight, they can reasonably be trusted. However, when the data suddenly departs from the expected pattern, a dilemma arises. What does the new vibration environment really look like? The environment obviously has changed, but has it changed its basic nature to the point where the particular type of in-flight analysis is no longer valid? In short, unusual or unexpected data cannot be trusted. This characteristic may be of no importance or it may prove to be a fatal deficiency, depending on test objectives.

An extremely important point to remember is that only if the nature of the vibration function is already known is it possible to use or trust any of the band-reduction schemes. Assumptions, guesses, and assurances are not a permissible method of determining the nature of the vibration function. This can be accomplished only by measurement with suitable, wide-band (high information capacity) systems. There are no short cuts!

DATA ANALYSIS OF FLIGHT VIBRATION

The data analyst has the job of transforming a measured vibration function into a form suitable for easy human comprehension and suitable for creating a laboratory test procedure to simulate the flight environment.

The responsibilities of the analyst obviously are very great. Perhaps they are too great. He must be schooled in the basic data gathering systems so he can determine the validity of the data. He must have the courage and ingenuity to operate on the particular data the best way; not just the easy way or the habitual way. He must have a thorough knowledge of the characteristics of the simulation equipment. He must also have a good "feel" for the general nature of vibration or shock susceptibilities in missile equipment. If he is forced to design his tests to use unsuitable simulation equipment, he must have the competence and courage to label the simulation tests as inadequate or unsuitable, or even as having no validity whatsoever. Such protestations are almost always justified but are very rarely heard and even more rarely heeded. Meanwhile, back in the laboratory, the simulation tests continue in the same old way, with the same old equipment, using the same old procedures, with the same old lack of meaning.

CHARACTERISTICS OF VIBRATION DATA

The type of vibration most commonly produced by rocket motors is essentially random in nature. The most common data format for this type of information is the familiar power spectral density presentation. The averaging time for each presentation may range anywhere from milliseconds to minutes. The spectral data for an entire flight may sometimes be found presented on an inch or two of 35-mm film, or other times, on a stack of large sized sheets of graph paper, with still other presentations falling between these two extremes. But the variety of ways in which this data appears is not the important point. The important point is "Are power spectra useful or valuable?" The answer is not yes or no, it is "usually." Now we are reduced to talking about probabilities and likelihoods. To put the problem in perspective, consider the two following examples. If this city were wiped off the map by the simultaneous explosion of ten of the largest fusion bombs, the atmospheric pressure during the day was "usually" 14.7 pounds per square inch here at sea level; or, one could safely say that the man who was beheaded one minute ago "usually" has his head firmly on his shoulders.

These remarks are intended to emphasize that although missile vibrations are usually random, this provides no excuse whatsoever for assuming that all significant missile vibrations are random in nature. They are not! Discrete frequencies, damped waves, and impulses can occur at destructive amplitudes even if it is not the usual case, but to jump back a moment, beheading is not

the usual way to die, but it certainly influences the personality of the person on whom it is practiced, ever if it happens only rarely.

There has, so far, been some discussion of the use and misuse of telemetering information capacity and some comments about the possible nature of missile vibration data. Because these things have been essentially technical in nature, it would now be profitable to look at some problems arising from human idiosyncrasies.

ANALYTICAL SCHOOLS

All too often, the data analyst clings to analysis methods and data formats which are really a matter of habit rather than technical appropriateness. Many analysts are distinctly classifiable as belonging to a certain "school" of analysis, to the exclusion of all others. Here is a list of some of them:

Power Spectral Density

The adherents of this school apparently have had most of their experience with long-burning motors having essentially a random vibration output. Typically, they have yet to stumble at some of the pitfalls already mentioned.

Amplitude Probability Distribution

Those who are preoccupied with amplitude probability distribution (to the exclusion of other methods of analysis) are dangerous in the extreme. Typically, they are interested in statistics but not in simulation. For example, it has happened in the past that an analyst has gone out to perhaps three sigma on the amplitude distribution curve and used this g level for the slow sweep (single frequency) vibration level specification. By this means, data indicating a mild flight environment can be converted into a ground simulation which is guaranteed to turn high-priced missile electronic equipment into high-priced junk.

The "g-Frequency" School

The members of this school are believers in simplicity and, typically, they convert all data (whether transient, random, or discrete frequencies) into a pair of numbers; namely, g and frequency. An analyst of this school would do well to ask what kind of mind reading a stranger would have to do, to reconstruct the original information from the two numbers. The answer is consistently embrassing.

The "g" School

To pervert the words of the late Gertrude Stein, many people seem to believe that "a g is a g is a g." It is sad almost beyond measure that many of the people of this school are senior administrators or executives who have at last found a small area of the engineering disciplines where they can quote concrete numbers as well as anyone else. The situation is worse when the guilty party is a competent engineer. It is totally inexcusable when the guilty one is an environment engineer. Yet it continues to happen, almost as a rule instead of an exception. In summary, missile shocks and vibrations can take many different forms. Any stereotyped approach to data analysis is going to run into trouble sooner or later.

LABORATORY SIMULATION

Vibration Testing

One basic tool in most simulation laboratories is a vibration shaker. Typically, it is used to impress sinusoidal vibrations of various or varying frequencies on the missile or missile components. This test is ordinarily used to simulate the flight vibration which most often is random (not sinusoidal) in nature. For those who disdain abstract or analytical arguments about the deficiencies of a single frequency simulation of random vibration, the following example is presented.

Let us assume we have a structural element with a resonant frequency of 1 kc and a Q of 100. This means that if we excite the element properly at 1 kc, with say 5 g, the points of maximum deflection can build up to a maximum acceleration of 500 g. But even more important, to a first order approximation, the system responds only to frequencies between 995 cps and 1005 cps, a bandwidth of 10 cps.

So with 1-kc drive, we are putting in 5 g and finding a maximum response of 500 g. Now, let us distribute the same input energy over the relatively narrow range of 900 cps to 1100 cps. This modest spectral dispersion of the energy reduces the maximum response from the original 500 g to slightly over 100 g. Spreading the driving energy over the range

of 500 cps to 1500 cps reduces the maximum response to 50 g. (Moving all these figures down a couple of octaves, one encounters the very practical case of quartz crystals used for frequency control. Moving up through nearly five octaves, many vacuum tube microphonic problems are described.) The significant point is that anything, but anything, that will spread out the vibration spectrum, will provide a better simulation of random vibration than does a single frequency. Stated differently, a single frequency is just about the poorest simulation of a random function that could possibly be created. Why, then, is the single frequency (or slowly sweeping frequency) used as such a popular substitute for reality. Historically speaking, only a few years ago missile components were qualified by shaking at a single frequency of 55 cps, a standard evolved for equipment in propeller driven aircraft. When it became obvious that such a standard was inadequate, the frequency range was simply increased, but the feature of essentially single frequency shaking was retained. It remains invalid wherever high mechanical Q is encountered.

What, then, can be done to simulate random vibration by using present shakers or vibrators? A direct approach would be to generate a random electrical function and drive the shaker with it. This technique is in use, and it works. The random function may be derived from noise generators or from tape recordings of actual flight vibrations.

It should be noted that a good simulation of the effects of random vibration can be achieved by using a distributed but not necessarily continuous spectrum. This type of function can be generated by frequency modulating the oscillator which drives the shaker. As a point of economic interest a substantial increase in the rms g level can be achieved by using a frequency modulated signal instead of a true random function, assuming that a fixed maximum force can be generated by the shaker. Reasonable simulations of flight vibration can be made without buying whole new laboratories full of equipment.

Shock Testing

The lead ball, the drop table, the sand pit, and probably many other devices and installations have been used to induce impulsive accelerations. Again, however, one encounters a serious disparity between flight test results and the usual shock test procedures.

In flight, the shocks produced by metal-to-metal banging, and by ordnance explosions of various sorts, can contain powerful frequency components up to many kilocycles, indeed to tens of kilocycles. The "average" shock specification allows such long rise times for the shock that the test could be tailored to produce virtually no frequency components above 1 kc.

For those who wish to argue the advisability of shock testing equipment by applying really sharp impulses, an example may be in order. One of the first subminiature ceramic tubes was afflicted with a very serious microphonic susceptibility at 22 kc. Standard shake tests and soft shock tests would never show up this susceptibility. A description of one device for producing broad spectrum impulses may be found in the paper "The Air Shock Tube as a Shock Testing Facility," by Stanley R. Melcher.*

GENERAL REMARKS

To avoid becoming too embittered by the present inadequacies in many vibration environment programs, it is well to remember that in the not too distant past, missiles have gone through design, production, and obsolescence without once having the flight vibration adequately measured. Unfortunately, we have not progressed as far as we should have since then. The employment of blind empirical fixes for environmental deficiencies in missiles would seem old fashioned in this day of lunar probes, ICBM's, megaton bombs, and earth satellites. But, the blind empirical fixes will continue until the various specialties in the field of environment are merged into a meaningful whole.

*See P. 94.

REFERENCES

1. Merl R. Beckman, "The Determination of Missile Vibration Environment," U. S. Naval Missile Test Center, Conference proceedings of Second National Convention on Military Electronics, p. 354.

Mr. Salberta (Gulton Industries): You mentioned that prior to using an airborne spectrum or amplitude distribution analyzer the properties of the signal must be very well understood and in order to understand these properties you need a wide-band channel. My question is what method of analysis do you use to determine the properties of this signal?

Mr. Beckman: Often one of the things which will keep you out of trouble is an elementary eyeball look at the data. That is certainly one method. This is not a quantitative test, but it is certainly indicative of whether you have something which, for example, has discrete impulses in it. That is the thing that can kill you which you won't see with the more sophisticated inflight analysis schemes. You have to be sure that none of these exist and indeed when they don't exist you can often economize on your bandwidth by a very, very large factor by using the inflight data reduction scheme.

Mr. Kuoppamaki (Lockheed): When you speak about your missile environmental data, you speak, of course, of flight data. Now in flight data we are limited in frequencies and bandwidths and our techniques don't go very much above 2 kc. You speak about 20 kc. What techniques do you suggest for us to get the information from the higher regions?

Mr. Beckman: They are very, very painful. The telemetry people and the procurement people almost turn blue because about the only technique you can use is to go completely nonstandard in your high-frequency subcarriers. You can get substantially more than 2 kc out of a 70-kc subcarrier, for example. You can get quite easily 15 or 20 kc provided, in the first place, you have no adjacent subcarriers and your data analysis equipment has bandpass filters that are wide enough to accommodate it. These are not standard at the stations.

Mr. Kuoppamaki: Don't you use the standard channel?

Mr. Beckman: Well, the only limitation on the bandwidth of these channels is in the receiving station. Ordinarily the equipment, the airborne equipment, is not particularly limited. You can use any deviation you want. Typically the voltage control oscillator, for example, can cover, if you desire; a full octave range, with a reasonable linearity, but ordinarily you would only use much smaller deviation than that and modulate with the higher frequencies and then use a wider bandwidth filter in the play back and it stretches out to the order of 15 or 20 kc this way.

Mr. Kuoppamaki: I first wanted to point out that the techniques which are available for analysis of data during flight and for transmitting the data down in a different form. This, of course, effectively expands the bandwidth. By using these techniques, you can exceed the bandwidth within any practical limit at frequencies above 2 kc.

Mr. Beckman: Oh, indeed, there are certainly non-standard techniques of both digital and indeed analog which have appeared in the literature which are capable of going far beyond the normal IRIG limits. As a matter of fact, you can go to an almost infinite capacity if you want to pay the penalty and the penalty ordinarily is bandwidth. My personal impression is that it is worth paying almost any penalty to get the information we are after. Unfortunately, this attitude is not completely supported by people who have to provide the room, provide the money for the new equipment, and sacrifice the channels of data that are necessary to accommodate the new data. There is not universal agreement that this should be done.

Dr. Morrow (Space Technology Laboratories): I would just like to make one or two comments. First of all, I think this points out that it is very easy to find difficulties in the techniques we are using and I have pointed them out occasionally. I think this should be done from time to time.

Mr. Beckman: Annually, if I might interrupt.

Dr. Morrow: It is also very much more difficult to point out something constructive to do about the situation. I would like to extend one bit of comfort, however, and that is that missiles 50 percent or more reliable are not uncommon. While we would like these to be better they can be effective weapons even if they are not the most economical weapons. Furthermore, if you translate these overall system reliabilities into subsystem and equipment reliabilities a little bit crudely, you can get some quite high numbers and the bulk of the subsystem and components, therefore, are surprisingly

good. So even though we would like to do very much better I think we can draw the conclusion that we are building better as things are than we know how to build.

Mr. Beckman: If I may interject, no one can argue that we are not building better automobiles than we did in 1910, although I don't think the people building them are too terribly much smarter than they were then. It was a little bit gradual, a little bit too gradual.

Dr. Morrow: One other point which has been touched upon already in the question period – the question of the high-frequency limit on data. I don't want to take much time, but there is a question about what you are going to do with data, to 20 kc or so, if you get it. Now in addition to the fact that there are many pitfalls in getting it, even if you are presented with the data you can't be sure you can trust it this high for a number of reasons even if the accelerometer calibrates flat to 20 kc, but once you have got it there is a good deal of question what you can do with it, and the simulation equipment that we have available now certainly is not capable of doing much more than 1500 cps or so on large items and maybe 3,000 cps or so on small ones. There is a certain amount of waste effort involved in gathering large amounts of such data.

Mr. Beckman: May I interject again, I concur.

Dr. Morrow: And it is not possible either in connection with equipment design problems to use the data in any straightforward design approach. So one suggestion I have here is that we should take an occasional look at the high-frequency data, be alert for problems that may arise there, but trying to get data in a routine manner to frequencies much higher than we do now could very well increase the dollar expenditure without very much return.

Mr. Beckman: I wish we could disagree but I largely agree with what you said. I don't think we do disagree particularly.

Mr. Shipley (Jet Propulsion Laboratory): I second most of the things that Dr. Morrow just said, and I would like to point out that on the Explorers there were no failures due to any vibration or shock problems. With the Sergeant missile we have never had a problem attributed to shock or vibration. And with regard to the telemetering problem if you do want to look at this wide-band data, occasionally, you can always go to carrier modulation by using channels A + B, and get this data without increasing the net information bandwidth of the system. This can be done by using essentially no increased power requirements for a long-range communication system.

Then with regard to amplitude distribution, having used an amplitude distribution analyzer for some time I find it very uncommon to find anything that looks much different from a gaussian amplitude distribution even when we have low-level sliding tones.

Mr. Beckman: Then you have a perfectly legitimate reason for using it and I think you should.

* * *

APPLICATION OF A SPECIAL TEST FIXTURE TO VIBRATION MEASUREMENT DURING STATIC FIRING OF ROCKET MOTORS

M. W. Oleson
U. S. Naval Research Laboratory

Measurement of vibration induced during rocket motor static firings is one technique for obtaining environmental data applicable to rocket vehicle components. However, the usefulness of such data may be compromised by conditions peculiar to the static test itself. The accuracy of data obtained may be improved by the use of special test fixtures during the static firings, as shown by measurements on two different types of rocket motor.

INTRODUCTION

In attempting to provide pertinent vibration data early in rocket development programs it has become common practice to instrument developmental static firings with vibration pickups. The usefulness of data so obtained depends upon an assumed correlation with flight vibration. At present it is difficult either to challenge or verify this assumption in general. Previously reported data have shown good correlation in some instances, and none in others.

It seems obvious that a major deterrent to correlation is the difference which exists between most static test configurations and the subsequent flight configuration. During static testing, the rocket structure is seldom completed, rigid mechanical restraints are employed, and acoustic excitation is exaggerated by nearby reflecting surfaces.

In the last year and a half a series of vibration instrumented static firings have been completed, with the motor and an assembled structure mounted in a special test fixture. The fixture, which has been dubbed "coffin," was designed to (1) accommodate payload structures attached to the motor, (2) provide flexible mounting restraints which would not inhibit vibration at frequencies above 15 to 20 cps, and (3) provide acoustic isolation of the motor casing and attached structure. The "coffin" static tests, it was anticipated, would provide conditions approximating those of flight in-so-far as motor-induced vibration was concerned. This report will discuss experience in the application of the coffin fixtures.

FIXTURE DESIGN

Two different rocket motors have been fired in coffins. The Arcon motor (Atlantic Research Company) had a cylindrical steel case which was approximately 6 in. in diameter and 8 ft long. The X-248 motor (Allegany Ballistics Laboratory) had a fiberglass case which was approximately 18 in. in diameter and 3 ft long. Fixtures employed for the two motors were similar in principal, but differed in detailed design because of the necessity of accommodating the different motor and payload configurations.

Both fixtures were of welded aluminum panel construction (Fig. 1 and Fig. 2). Ribs

Fig. 1 - X-248 motor and attached payload in coffin fixture

Fig. 2 - Arcon motor and attached payload in coffin fixture

and longitudinal beams were employed for strength, and also for panel rigidity. In cross section, the fixtures were rectangular on three sides, with a "V" shaped bottom which conform d to roller V-blocks in use at the rocket test sites. The top panels, removable for motor installation and working access, were secured by a large number of bolts during firings. Interiors of the coffins were lined with fiberglass for acoustic absorption.

For the Arcon motor thrust was transmitted to the coffin through commercial type vibration isolators, and a collar secured by payload mounting bolts at the head end of the motor (Fig. 2). To prevent excessive forward motion upon development of thrust, and at the same time allow a low natural frequency of the suspension, the vibration isolators were preloaded in the thrust direction with a force somewhat less than that of the motor thrust. Laterally, the motor was supported by the forward thrust collar and by a loose-fitting vibration-isolating clamp somewhat forward of the tail fin assembly.

Restraint of the X-248 motor was complicated by the necessity of taking thrust on a forward fitting having a smaller diameter than that of the motor case (Fig. 1). Thrust from this fitting was coupled into a larger diameter collar by a number of extra-flexible steel cable strands (aircraft control cable), and thence through four thrust springs to the coffin. Similar to the Arcon arrangement, these thrust springs were preloaded to prevent excessive forward motion.

During the coffin tests, it was also necessary to prevent the gravity torque load of the X-248 simulated payload from being applied to the motor. For this purpose the payload was neutrally suspended by four counter weights which hung down outside the coffin.

FIXTURE APPLICATION

The coffins were designed for incorporation into standard static firing procedures with minimal interference. Measurements of operating pressure and thrust were taken during all of the firings. Thrust measurements, taken at the forward end of the coffin, were not effected by the coffin itself (except in frequency response) since the entire assembly was free to move on roller V-blocks. Handling of the coffins at the test sites required no more than regular motor handling equipment. The X-248 coffin, heaviest of the two, weighed about 600 lbs.

Motor handling time, important in the case of temperature conditioned motors, depended considerably upon familiarity with the assembly techniques. After some practice, the motor insertion, mechanical assembly, final instrumentation check, and securing of the lid could be accomplished in about 30 minutes.

EFFECT ON DATA

In the case of these two motors, it appears that the introduction of acoustic isolation by the coffin was of major importance. Sound pressure levels measured in the Arcon and X-248 test bays were in the order of 145 to 150 db. The coffins introduced about 25-db attenuation, resulting in acoustic fields near the payload structures of 120 to 125 db. In addition the spectral profiles of acoustic energy were modified from approximately uniform spectra outside the coffins to spectra which maximized at frequencies below 400 cps inside the coffins (Fig. 3).

The effect of acoustic isolation on the vibration level was most clearly demonstrated by a set of measurements taken during the Arcon tests. The Arcon rocket employs an end-burning grain which is inserted into a cylindrical steel case. Accelerometers were attached directly to the case wall. During the course of normal burning, the grain backing the case wall at the pickup station was burned away resulting in a marked increase in vibration level. In the standard static test configuration the rms level of vibration increased from 1.5 g to 15 g. Most of the energy was distributed in the frequency range from 500 cps to 3000 cps. For the coffin firings, the corresponding rms levels were .75 g to 3 g, and the energy was concentrated at several case modal frequencies (Fig. 4). Comparative maxima in spectral density values were 1 g^2/cps and .01 g^2/cps respectively. (It should be noted that these measurements were made on the motor case and are not necessarily an accurate representation of the change in payload vibration level. However, in the normal static test a payload is not included).

In addition, the character of the vibration induced in the two test configurations was quite different. In the coffin shots, the vibration appeared as a series of damped transients, probably caused by particle impacts in the nozzle area. These transients had been obscured in other measurements by the large acoustically-induced vibration.

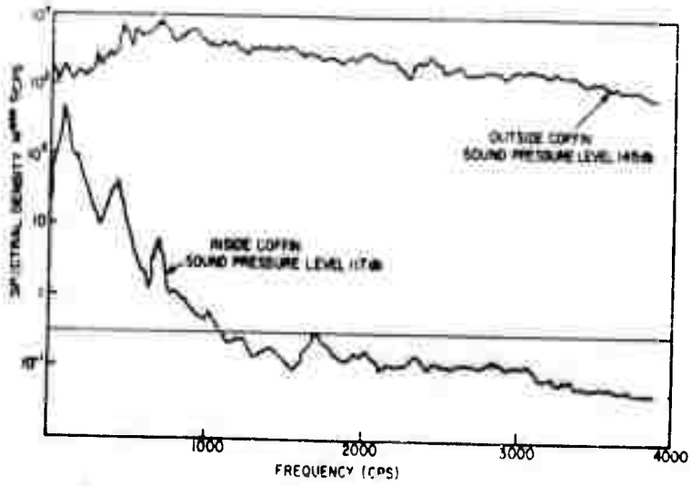

Fig. 3 - Spectral analysis of sound pressure levels measured during Arcon firing (SR 158)

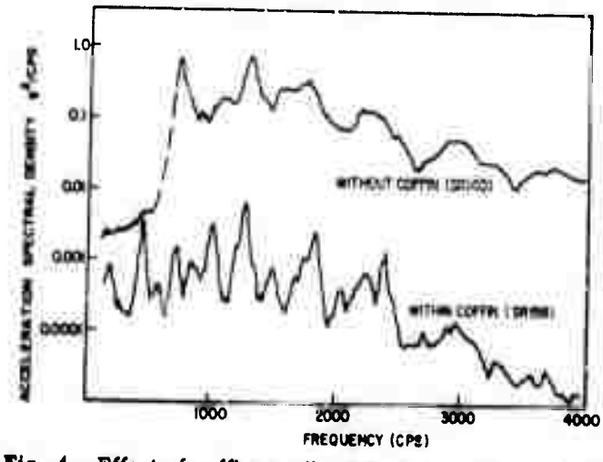

Fig. 4 - Effect of coffin on vibration of Arcon motor wall during static firing

CORRELATION WITH FLIGHT DATA

The correlation between vibration measurements taken during the coffin tests and vibration measurements taken during flights appears quite good*. Available data includes that from three Arcon coffin firings, one Arcon flight, four X-248 coffin firings, and two Javelin rocket flights in which the X-248 motor was the final stage of a four-stage vehicle.

Spectral analyses of vibration at the base of the Arcon payload show the same general profiles and levels both during the coffin tests, and during flight (Fig. 5 and Fig. 6). In addition, the impulsive transients observed from the coffin data were also evident from the flight measurements.

The coffin firings had indicated that the X-248 motor induced quasi-periodic vibrations of significant amplitude, but no random vibration of consequence. Quasi-periodic vibrations are characterized as "almost periodic," but of varying frequency or amplitude. As pertaining to the X-248 motor, they are associated with oscillatory burning modes in the gas cavity. These modes, in turn, are functions of the cavity dimensions. During the coffin tests, measured vibration levels at the payload attachment plane ranged as high as 50 g rms at frequencies above 2000 cps, and averaged 4 g to 10 g rms. Comparable measurements during the flight produced quasi-periodic vibration levels in

*It should be noted that the flight vibration environment includes aerodynamic turbulence as a possible source. In some situations, aerodynamically induced vibration has obscured lower levels of motor induced vibration, in which case the correlation of results as cited here cannot be expected.

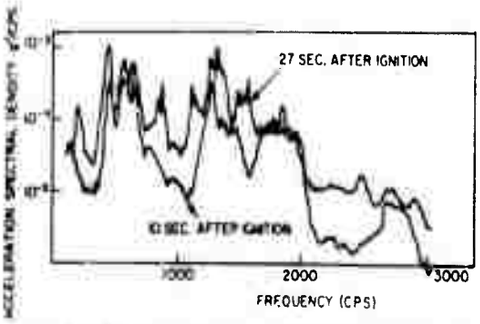

Fig. 5 - Motor induced vibration at base of Arcon payload during coffin firing (SR 159)

the same frequency range to 60 g rms. Flight data also substantiated the absence of random vibration excitation which was noted from the coffin data (1).

CONCLUSION

The difficulties of obtaining reliable environmental vibration data are familiar to many whose concern is rocket reliability, and measurements obtained during static firings provide one way of circumventing at least some of these difficulties. The cost of statically fired motors is comparatively modest, their scheduling precedes and is more flexible than that of actual flights, and there is no immediate limit to the instrumentation which can be employed. From the evidence cited above, it appears that the use of special test fixtures such as those described, can contribute materially to the reliability and accuracy of such measurements.

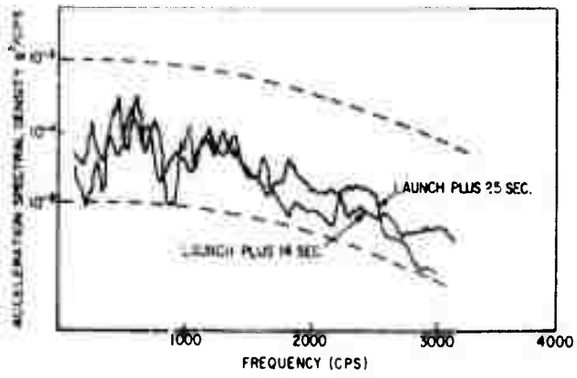

Fig. 6 - Vibration at base of Arcon payload during flight (SEL 47)

REFERENCES

1. M. W. Oleson, "Preliminary Report on Acceleration and Vibration Data from Javelin (8.01) Vehicle," NRL Memorandum Report No. 1024, February 1960.

DISCUSSION

Mr. Charles Skillas (Bendix Aviation): Have you found any degree of correlation between the vibration data you have taken on the static firings with that taken from actual flights of the same motors?

Mr. Oleson: Yes. We found a substantial correlation. Of course, flight data are sometimes difficult to come by so that in the statistical sense our flight data are inadequate. However, what flight data we have does agree very well with the measurements we have taken during the coffin tests.

Mr. Stern (General Electric): In the design of the fixture from an acoustic standpoint, did you consider the fact that the coffin might have acted as a Helmholtz resonator? It seems that when you got your correlation between the free flight and the box that you might have introduced an error. I wonder if this was considered?

Mr. Oleson: The answer to that question is no, we didn't consider it. To the best of my knowledge this wasn't a condition inasmuch as the measurements inside the coffin,

while they did indicate certain maximum frequencies of acoustic energy, might well be attributed to the reflection inside the coffin even though we did have acoustic absorbent material in there.

Dr. Fricke (Bell Aircraft Corporation): I think this question can be answered. I think the motor casing resembles more or less an anechoic chamber having a very high absorption. For this reason no standing waves can be expected.

Mr. Shipley (Jet Propulsion Laboratory): I noticed on the Vanguard motor that the nozzle was running separated. I wonder if you ran the same test in a vacuum chamber or with a lower expansion ratio nozzle and if you saw any difference?

Mr. Oleson: We did. The X-248. Of the four coffin firings we made, two of them had altitude nozzles such as the one I pictured, and two had sea level nozzles in which the nozzle was cut off to prevent overexpansion. It was interesting to note that there was a difference. I mentioned in the talk that we saw little random vibration of consequence. The only time we did see what appeared to be random vibration, this is in the payload area, was on the two firings in which we used altitude nozzles. This maximized at somewhere between two and four hundred cycles and had levels on the order of, we will say, less than .01 g^2/cps. Generally, we didn't see it in the sea level nozzles. With flight data one has an additional problem, the signal-to-noise ratio becomes difficult at times, but to the best of our knowledge, or to the best of our instrumentation I should say, there was no random vibration induced during flight above the level of 1 g rms which means again that it would be of little consequence and in essence this substantiates the coffin measurements.

* * *

THE SIGNIFICANCE OF POWER SPECTRA AND PROBABILITY DISTRIBUTIONS IN CONNECTION WITH VIBRATION

Charles T. Morrow
Space Technology Laboratories, Inc.
Los Angeles 45, California

The two most fundamental descriptions of random vibration are in terms of power spectra and probability distributions. Usually, the two are not of equal importance. Which is more significant depends on the application at hand. In respect to describing the environment of equipment mounted in a missile, ordinarily the power spectrum, not the distribution, is significant. In respect to laboratory testing to determine material properties under random stress, the rms stress and the probability distribution of the stresses have particular significance. Likewise, in respect to failure of the airframe, the rms stress and the probability distribution of stresses at the point of failure are likely to be more important than the details of the power spectrum.

INTRODUCTION

It may be taken as a fundamental principle that the details of the probability distribution of a vibration (i. e., the deviations from a Gaussian distribution) are of primary importance only when the measurements are made at the point where the failure or malfunction under consideration would take place. The details of the power spectrum, on the other hand, are of importance when the vibration cannot be associated with one or two major resonances of the structure where it is measured, for purposes of the failure or malfunction under consideration. Three different cases are considered in this paper. As the considerations and conclusions pertinent to each are somewhat different, they will be treated separately, in succession.

EQUIPMENT ENVIRONMENTS

Equipment fails under vibration primarily because of excitation of mechanical resonators. As typical equipment resonates at many frequencies, the shape of the power spectrum at various frequencies is important.

On the other hand, the probability distribution of the motions or stresses at any point of failure or malfunction within the equipment tends to be independent of the distribution of the excitation at the mounting points of the equipment; thus detailed measurements of the distribution of the exciting environment are of minor significance. Linear filtering, which is one of the influences involved in the transmission of vibration from any one point in the airframe structure or equipment to any other, tends to change the distribution if it is not already Gaussian. Usually, the sharper the filtering accomplished by a resonator, the more nearly Gaussian the response becomes. Simple nonlinearities tend to produce deviations from the Gaussian distribution. Imagine a vibration transmission path through a lightly-damped resonator and through a nonlinear element to a region of stress concentration, as shown in Fig. 1.

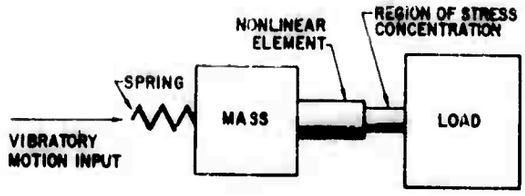

Fig. 1 - Mechanical system with filtering and nonlinearity

Whether the original distribution was Gaussian or not, the resonator tends to have a Gaussian response. The nonlinear element in turn produces a non-Gaussian distribution at the point where failure, if any, occurs. Thus, the final distribution may be non-Gaussian, but it tends to be independent of the distribution at the input of the system. In short, testing with Gaussian random vibration may ordinarily be expected to have the same effects as testing with the actual distributions of flight. Even in exceptional cases, the differences in the effects are still likely to be much less than the differences inherent in the policies for deriving test requirements from flight data. It is doubtful, as a practical matter that any data on flight vibration distributions are of use even in evaluating the realism of vibration test requirements. Thus, for application to environmental testing, it is sufficient to assume that the excitation of equipment in flight is Gaussian even when perceptible discrepancies can be observed.

The development of equipment to withstand shock and vibration is accomplished primarily by testing and redesign. The engineer who would like to use more sophisticated techniques and actually calculate responses, taking changes in probability distributions into account in theoretical detail, faces formidable problems. To be sure, exceptional cases can be devised where filtering does not make vibration more Gaussian. There are mathematical techniques that can be applied to the alteration of distributions by filters or nonlinear elements, but they are cumbersome. In general they assume special properties such as statistical independence in different frequency bands, which are least likely when the vibration is distinctly non-Gaussian. Some investigation of distributions for the sake of fundamental understanding is to be encouraged, but there is little practical utility to routine detailed measurements of distributions at points, such as the mounting points of equipment to the airframe, where few of the equipment failures or malfunctions are expected.

MATERIAL PROPERTIES

There has been some discussion recently of the possibility of measuring the fatigue properties of materials with random excitation as opposed to periodic. This would avoid either the somewhat difficult problem of deriving random fatigue characteristics from periodic fatigue characteristics on theoretical grounds or provide a better understanding of the relationship so as to put theory on a firmer basis.

Fatigue, especially in equipment, frequently occurs as the result of one dominant resonance. It is seldom that more than two or three contribute significantly. It would appear that a somewhat pessimistic basis for estimating fatigue is readily obtainable by considering the overall rms vibration to be concentrated at the highest frequency of resonance that contributes significantly. Thus, a logical first step, at least, in investigating random fatigue is to excite materials with a narrow-band random vibration of an approximately Gaussian distribution and a prescribed rms stress. So long as the band is narrow, one-third octave or preferably less, the fatigue data will be affected little by the detailed shape of the power spectrum. The details of the probability distribution, on the other hand, may be more significant.

Consider such a question as, "Will steel under random excitation have a fatigue limit?" If the tails of the probability distribution at the point of failure are sharply limited, the answer is a clear-cut yes.* If

*However, electronic limiting of the current to a shaker does not result in similar sharp limiting at the failure point if there is a mechanical resonator in the transmission path.

there is no deviation from the Gaussian distribution, it is difficult, without actual data, to say whether there would be a random fatigue limit—some fatigue might occur for all rms levels of excitation.*

Careful examination of the conditions where fatigue is expected in the airframe or within equipment during flight may very well disclose some deviations from the Gaussian distribution, well out on the tails. The nonlinearities inherent in fatigue and the nonlinearities of the test apparatus also tend to produce these during test if their influence is not controlled. Isolated half cycles of high strain or stress seldom occur under random excitation. Usually, large stresses or strains are attained in the course of a long series of cycles of progressively increasing magnitude. The duration of the wave train, until the largest cycle is reached, is of the order of the response times of the resonators through which the vibration was transmitted. Fatigue is an energy absorptive mechanism, with little tendency to scatter energy about the spectrum in comparison with chattering. Its absorption is particularly effective in a resonator that otherwise has little damping. When the wave train builds up above a fatigue limit, for example, energy is absorbed from successive cycles so that the maximum stress finally attained is much less, as suggested by the sketch in Fig. 2. Thus, when the tails of a Gaussian distribution representing stress in a lightly damped resonator extend beyond a fatigue limit, they will tend to be rolled off.

It can be seen that fatigue data will be quite dependent on the character of the tails of distribution, especially with materials that tend to be brittle or exhibit definite fatigue limits. Some standardization is necessary before measurement of random fatigue becomes a routine materials test. Two approaches appear promising. One is to test with a distribution as close to Gaussian as practical. Just what actual compromise is possible without affecting the data can be determined by preliminary experiments with typical materials. Small amounts of tail clipping may result in large discrepancies for fatigue by low-level excitations. It may be necessary to decide on the range of levels of greatest interest and place tolerances on

*Some steels, in particular, exhibit no fatigue for sinusoidal stresses below a certain level; this level is known as the fatigue limit.

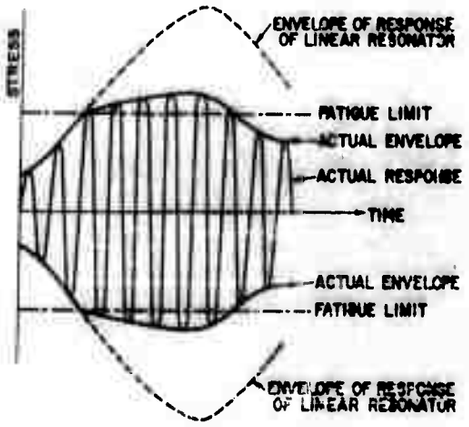

Fig. 2 - Effect of fatigue on the occurrence of a large stress

the probability distribution accordingly. The other approach is to shape the tails of the test distribution as closely as possible after the distributions that occur where the materials are in use, with the intent of making the simple comparison of rms levels as indicative as possible of the fatigue properties of materials as they are used.

AIRFRAME FAILURE

In respect to fatigue of an airframe structure, measurements of vibration at some distance from the point of failure have limited significance. It may be possible to estimate the power spectrum at the point of failure. On the other hand, it will seldom be practical to compute deviations from the Gaussian distribution at the failure point from deviations at other points in the structure or from deviations in the exciting acoustic noise or turbulence outside the skin.

When measurements are made at the point of failure, it is likely that the vibration will be found to be concentrated in a small number of resonances.* If so, the details of the

*It does not follow that the excitation of equipment mounted to the airframe can be considered to be concentrated in a small number of resonances. Equipment is not ordinarily mounted where the noise level is high enough to induce vibration fatigue of the airframe. Even if the equipment were mounted exactly where this fatigue takes place, the equipment would have resonators of its own. These could easily accentuate portions of the spectrum that do not happen to be important to the particular airframe fatigue problem under consideration.

power spectrum at other frequencies are of little importance. The most significant factors appear to be the frequencies of resonance, the corresponding rms responses, and the overall probability distribution.

Some nonlinearities tend to broaden the tails of a distribution. However, the nonlinearities associated with fatigue tend primarily to absorb energy from the cycles of larger amplitude, especially for materials exhibiting a definite fatigue limit. Thus, for low and moderate-level excitation they tend to narrow the distribution and decrease the damage.

A brief survey of the distributions at possible airframe failure points would be helpful either in determining the best distributions to use in fatigue testing of materials or in determining the best corrections to apply to fatigue data measured with an essentially pure Gaussian distribution.

CONCLUSION

It thus appears that for the excitation of equipment, the power spectrum in detail, but not the over-all probability distribution nor the distribution within any restricted frequency band, is of significance. As fatigue measurement can be accomplished by resonant excitation, details of the power spectrum are unnecessary, but some aspects of the distribution are important. In relation to airframe failures, some details of the power spectrum and some details of the probability distribution will undoubtedly be found to be important.

DISCUSSION

Mr. Mustain (Norair Division, Northrop Corp.): I was interested in Fig. 2, Dr. Morrow, where you showed the decay of the response. This is a type of picture I would get when I put excitation into an airplane panel and then take the excitation off. Obviously you kept the excitation going but your response was going down. I don't understand what caused the decay. I wondered if partially this is material damping, nonlinearities? Would you clear me up on that?

Dr. Morrow: Well, this would not necessarily happen in practice, but it could happen. There is a sizeable interval in the figure when excitation goes above the fatigue limit and during that interval energy is absorbed. Now it is quite possible then that once the excitation comes down below the fatigue limit, the response one gets would be less than it would be if this energy had not been absorbed. Furthermore it is quite possible for the response to go on decreasing much as it would have if the absorption had not taken place. I won't guarantee that this will occur in all cases because just what happens will depend on a lot of details. You can have beating effects between the transients remaining when the thing comes below the fatigue limit and the excitation still persisting. This is one possible thing that can happen.

Mr. Moore (North American Aviation): In listening to your paper, Dr. Morrow, I was reminded of two things. First of all was my recollection of the student's prayer, "Oh, Lord, please make nature linear and Gaussian." This, of course, you emphasized in your paper. The other was that I was wondering if you had extended your thinking to the nonlinearity that exists in the higher acoustic levels—an explanation of this nonlinearity perhaps along the same lines.

Dr. Morrow: We can expect nonlinearity at high acoustic levels for the reason that the pressure can never drop lower than a vacuum, and so if we arrive at levels that are high enough to suggest peaks greater than 15 pounds per square inch we can expect positive peaks to exceed the negative peaks. However, there is no reason to expect the same situation to persist by the time you look at the excitation in the airframe. There is enough filtering that takes place in between, perhaps nonlinearity too, to make the situation look quite different.

Mr. Stern (General Electric): The theme of the paper was quite interesting. This brought up a question asked me about a month ago and I think a lot of designers are concerned with this. In many designs people have, let's say, satisfactorily designed a chassis that would take 10 g's (10 to 2,000 cycles per second) and they have done this successfully. Suddenly someone comes along with a random spec and we would like to know what is the equivalent in damage between the sinusoidal spec and the random spec we have now been asked to perform.

I wonder if you can give a number, say 10 g, 10 to 2,000 cycles per second equals xg^2/cps. What is x?

Dr. Morrow: I can say on good authority that I don't know. [Laughter] However, I would like to say that if one looks at the Gaussian distribution very literally and makes a criteria on the basis of a chance of collision in a particular length of time such as a missile flight, one can often arrive at an extremely conservative design criteria which is not very realistic and I think part of the point is that when you do get fatigue there will be some reduction in the tail. A little investigation of this might be helpful.

Mr. Galef (Radioplane): I was wondering just how nonlinear some of the equipment that we are talking about might actually be. It would appear that if the stresses are well above the elastic limit they will cause excessive deformation and almost immediate damage. If the stresses are down sufficiently low that fatigue is a consideration and I believe this is usually the case, our equipment will be very close to linear and the probability distribution at the base will then be important. Now how nonlinear are these?

Dr. Morrow: I disagree that the distribution at the base is important if the equipment is linear. The distribution gets reshuffled anyway. It just gets shuffled in a different manner and the filtering by itself will be shuffling.

Mr. Galef: Perhaps it would be appropriate to arbitrarily use a Rayleigh distribution. I think the probability distribution is definitely important both from the point of view of extreme limits at the edge of your tail and also from the point of view of fatigue. The Rayleigh distribution might be as close as we can possibly find; in some cases you may be able to find something a little better.

Dr. Morrow: Well, one thing that I have indicated is that even though the distribution at the excitation point in flight may be non-Gaussian, the fatigue or malfunction produced by a Gaussian excitation may be quite common.

Another point I think we should be clear on is that if we have a complex wave shaker system and use it to apply a random test and we limit the distribution to, say, 3 Sigma, it does not follow that the distributions at the point where the failure or malfunction occurs are limited at 3 Sigma and there is pretty good chance they will never know that limiting took place.

Mr. Curtis (Hughes Aircraft): Before we get away from using the probability distribution entirely, I think for data analysis we need it, or correlation analysis, or some method that enables us to determine what kind of a time history we have so that the data analyst doesn't express sine waves in terms of power spectral density and random functions in terms of sinewave. It seems to me that probability distribution is one of the most useful techniques of doing this.

Dr. Morrow: I quite agree that we should not try to use periodic techniques in the analysis of random vibration or vice versa. However, there are more powerful techniques for telling the difference than looking at the probability distribution.

If you want to take the time to examine these things closely the correlation function is a better indication than the distribution.

Mr. Curtis: I agree with your comments although I do believe that the expense of data reduction using correlation techniques at this time is much greater than for the probability distribution.

Dr. Morrow: Let me point out there is a great deal of difference between (1) just telling whether vibration is random or periodic when you are presented with a curve and no other information about it, and (2) saying whether vibration is random or periodic when there is a flight about to take place and you are trying to guess what is going to happen. If you know a little bit about what the sources of the vibration are, you know a good deal more about what to expect than you can decipher just from looking at a record. I think in working with a particular rocket engine, especially if there have been some captive firings, one can get some idea in advance of where to expect quasi-periodic functions due to combustion instability and look for them. In between one can expect primarily a random excitation.

Mr. Curtis: Right, but I always feel that when we are talking about how should we analyze the data, let's assume the worst condition, that the analyst has absolutely no idea what is on that tape and what are its characteristics; because often I think he really doesn't. Maybe he should; perhaps he should talk to a few other people around the company, but usually I think he is flying

blind and so he should have the capability of doing this.

I am not saying that the way to do it is probability distribution. I am merely saying, let's find out these things, let's not just keep on assuming them the way we often do.

Dr. Morrow: I think the data reduction engineer should be informed about what he is trying to analyse thereby saving him from making mistakes. I think that one should take a real good qualitative look at the vibration before one attempts to produce spectra, but I think of the probability distribution as a relatively weak tool for discovering quasi sinusoids and there are a number of other things that are quite informative for a small amount of effort. For example, you can play the thing into a loud speaker and listen. While this will not disclose the feeble periodic content it will certainly disclose the more violent things. You can look at what happens when you put the thing through bandpass filters which you can do very quickly before you begin an elaborate routine data reduction and the sinusoids will tend to stand out.

There was a device that was invented several years ago at JPL* which could be used to track a quasi sinusoid produced by a solid propellant and it locked on that thing and tracked it. If one has a device of this nature one can give it an initial tuning roughly where one expects difficulty and see whether it tracks, and with a little skill with a device of this nature one can get a rather sensitive indication of whether there is periodic content or not.

Mr. Brown (Douglas Aircraft): I would just like to comment on the correlation method of finding periodicities. It is not necessary to go through the effort of computing a whole correlation function but just to look at the correlation function for very large time differences which is not a great deal of effort and can be accomplished very rapidly.

Dr. Morrow: Yes. Just to elaborate a little further, if you have purely random vibration then the correlation function is something that tends to decay very rapidly over a time interval that corresponds roughly to the response time of the resonators involved, whereas if you have some periodic content then the thing persists much longer.

Now there is a little bit of a problem here if the frequency is changing at the same time, as it would be in a solid propellant rocket, but I think there are a number of techniques here that can be used and used fairly quickly that are more powerful, than just investigating the probability distribution.

*Shock and Vibration Bulletin No. 24, p. 99.

* * *

MEASUREMENTS FOR THE RESPONSE OF SUBSTRUCTURES TO THE EXHAUST NOISE OF A TURBOJET ENGINE

H. J. Parry
Lockheed Aircraft Corporation
California Division, Burbank, California

This paper describes some recent measurements of the near noise field of a turbojet engine and the response characteristics of complex panel specimens. The work reported is part of a program concerned with developing methods for predicting response and fatigue life of aircraft type structures.

INTRODUCTION

The problem of acoustic fatigue of airframe structures and components is well known. Recently work has been completed (1) on the initial phases of a study program to develop methods of predicting the response and fatigue life of complex structures excited by turbojet engine noise. This program may be considered to consist of three phases: theoretical, laboratory test, and field test. The purpose of this paper is to describe the field test portion of the program, associated data processing techniques, and a few of the results obtained.

RATIONALE OF THE EXPERIMENTS

The main objective of the field tests to be described was to provide data for determining the validity of theoretical response prediction methods. A secondary objective was to obtain information on the near sound field of the engine both inside and outside the jet wake. These two objectives were the basis for establishing the types of measurements that were made.

REQUIREMENT FOR CORRELATION MEASUREMENTS

Consider a test panel having an area A and excited by a force $F(t)$. In essence, simple theory says that the mean-square deflection, (ξ^2), in mode will be proportional to the mean-square force, $\overline{F^2(t)}$, acting on the panel. Thus

$$\overline{\xi^2} \sim \overline{F^2(t)}. \tag{1}$$

Also the total force may be considered as the sum of the forces acting on a set of elementary areas which comprise the total panel area,

$$F(t) = F_1(t) + F_2(t) + F_3(t) + \cdots + F_n(t) \tag{2}$$

and

$$F_k(t) = (P_k)\left(\frac{A}{n}\right), \tag{3}$$

where n = the number of elementary areas,
$F_k(t)$ = force on an elementary area,
P_k = pressure on an elementary area.

For example if $n = 2$ the total force is the sum of two pressure-area products

$$F(t) = F_1(t) + F_2(t) = \frac{A}{2} P_1(t) + \frac{A}{2} P_2(t) = \frac{A}{2} (P_1(t) + P_2(t)) . \quad (4)$$

In this case the mean-square force is given by

$$\overline{F^2(t)} = \left(\frac{A}{2}\right)^2 (\overline{P_1^2} + \overline{P_2^2} + \overline{2P_1 P_2}) . \quad (5)$$

A general expression for the mean-square force considering (n) equal areas is

$$\overline{F^2(t)} = \left(\frac{A}{n}\right)^2 \left[\overline{P_1^2} + \overline{P_2^2} + \overline{P_3^2} + \cdots + \overline{P_n^2} + \overline{2P_1 P_2} + \overline{2P_1 P_3} + \cdots + \overline{2P_1 P_4} + \overline{2P_2 P_3} + \overline{2P_2 P_4} + \cdots + \overline{2P_2 P_4} + \cdots + \overline{2P_{n-1} P_n}\right] . \quad (6)$$

This involves the product of an area factor and a quantity including the sum of (n) mean-square pressures plus a series of $n(n-1)/2$ pressure cross-products.

For stationary random processes the mean-square and cross-product terms may be evaluated (2) thus

$$\overline{P_1(t)\, P_2(t)} \doteq \frac{1}{T} \int_0^T P_1(t)\, P_2(t)\, dt , \quad (7)$$

and

$$\overline{P^2(t)} \doteq \frac{1}{T} \int_0^T P^2(t)\, dt . \quad (8)$$

The normalized correlation function, a correlation coefficient, r, is given by

$$r = \frac{\overline{P_1(t)\, P_2(t)}}{(P_1 \text{ rms})\, (P_2 \text{ rms})} . \quad (9)$$

Corresponding relations for the steady state sinusoidal case are

$$P_1(t)\, P_2(t) = (P_1 \text{ rms})\, (P_2 \text{ rms}) \cos \alpha , \quad (10)$$

and

$$r = \cos \alpha . \quad (11)$$

These equations and the notion of elementary areas define data processing and field test requirements for evaluating the panel forcing function.

The relation between mean-square force and panel deflection implies the requirement for measurement of panel motion. The fatigue aspect of the problem dictates the necessity of measuring panel strain.

FIELD TEST METHODS AND PROCEDURES

A close-up view of the YJ-79 engine with the free field survey microphones is shown in Fig. 1. The engine is an axial flow turbojet with afterburner and a variable converging-diverging exhaust nozzle. Engine RPM and exhaust gas temperature were selected as operating criteria since thrust instrumentation was not available. Jet velocities computed from the operating criteria and manufacturers data on thrust and airflow, were 1740 fps and 2290 fps for Military and afterburner engine conditions respectively.

Measurements to determine the panel forcing function were performed at two locations in the noise field; 40.1 feet and 14.2 feet aft of the nozzle-exit and 15 feet and 10 feet respectively from the jet centerline. Test panels were placed parallel to and at the same height as the centerline of the jet. The panel holding and backing frame with microphones and test panel are shown in Fig. 2. This photo illustrates a typical arrangement of six Altec-Lansing 21BR microphone systems used to obtain simultaneous sound pressure recordings. Similar test setups were made at both field locations for several boundary conditions: free field, rigid panel and various panel specimens. The panel shown in Fig. 2 (Flat Panel A) is a skin-stringer substructure 20 by 40 inches with individual skin panels 6 by 9 inches.

Panel deflections were measured indirectly with Glennite miniature barium titanate accelerometers. SR-4, F25 type strain gages were used for measurement of panel strain. Maintenance of electrical attachments on these transducers presented one of the most serious problems encountered during the tests.

Figure 3 shows the jet wake probe containing three flush-mounted water-cooled microphones, manufactured by Photocon Research Products. This assembly was used for measurements of sound pressures inside the engine wake.

Fig. 1 - YJ-79 jet engine and free-field survey microphones

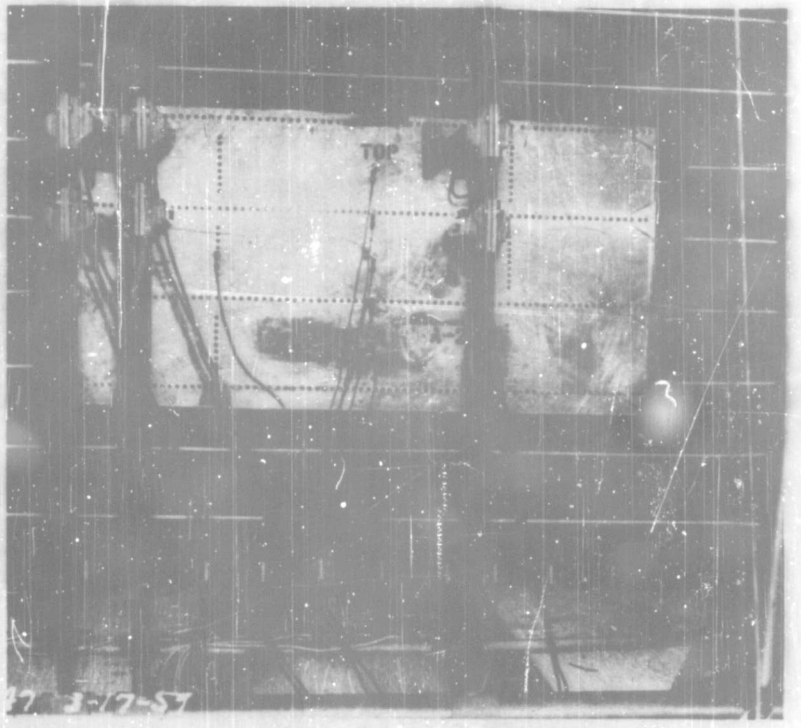

Fig. 2 - Field test setup for cross-correlation measurements on Flat Panel A

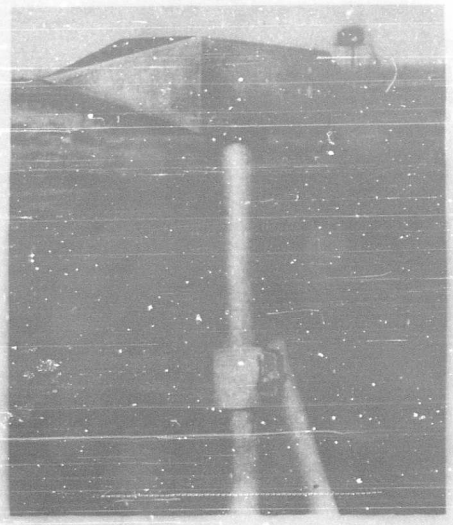

Fig. 3 - Jet wake probe assembly

Signals from all transducers were recorded on a 14-channel Ampex Type FR-114 tape recorder. Individual attenuator and amplifier systems were employed with each data channel to allow a 15-db peak overload factor.

DATA PROCESSING

Two data processing systems were used to analyze the tape recorded signals. In order to determine correlation coefficients and wide-band mean-square quantities a special purpose analog correlation computer was constructed, Figs. 4 and 5. This computer is a major part of the correlation data processing system of Fig. 6. Narrow-band results in both logarithmic and mean-square forms were produced with the system shown in Figs. 7 and 8.

The special purpose analog computer utilizes commercially available components with the exception of the Tape Transport Control unit and special switching circuitry for tape channel, computation function, filter band selection, and card punch programming. The operational integrator is time controlled allowing a 30-second averaging interval.

The punched card output of the analog computer together with transducer calibration data and information regarding field-test conditions complete the input to an IBM 709 digital computer. This computer is programmed to solve the data system performance equations in terms of the desired results; i.e., mean-square, root-mean-square, pressure level or correlation coefficient.

RESULTS AND DISCUSSION

During the investigation cross-correlation measurements were made for three sound-field boundary conditions: free field, rigid panel, and representative substructure test panels. Measurements were performed at two field locations, as mentioned previously, for most of these boundary conditions. The field test recordings were analyzed with the correlation computer described above by using a pair of 1/3-octave band filters. These results have been plotted as correlograms of correlation coefficient against microphone longitudinal separation. A representative set of these correlograms are presented in Fig. 9. The Row C and Row D notations refer to the two examples of area-pair sequences of Fig. 10. That is, these correlograms are all referred to the sound pressure

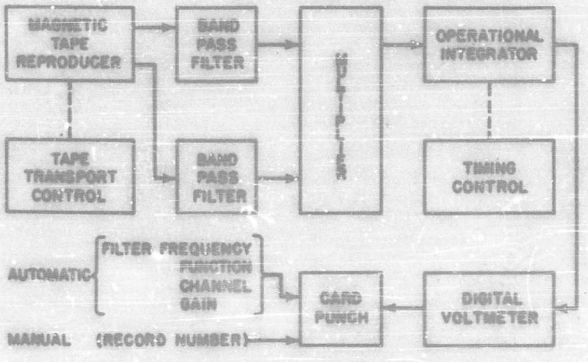

Fig. 4 - Simplified block diagram of correlation computer

Fig. 5 - Special purpose analog correlation computer

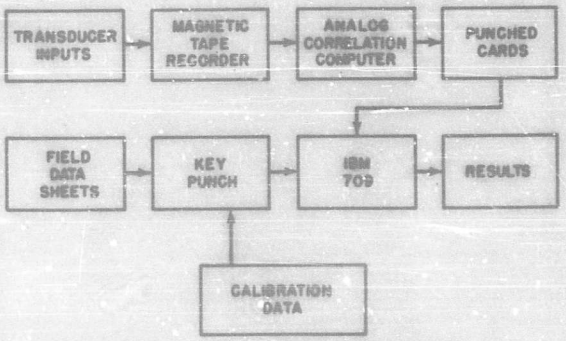

Fig. 6 - Block diagram of correlation data processing system

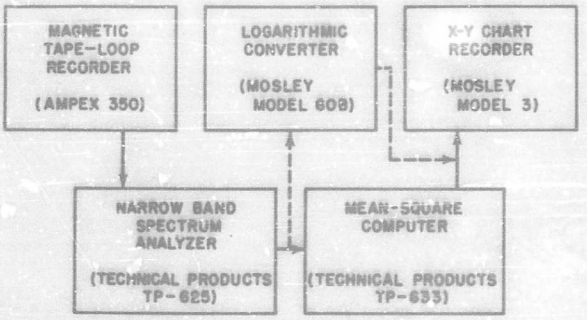

Fig. 7 - Block diagram of narrow-band analysis system

Fig. 8 - Narrow-band analyzing equipment

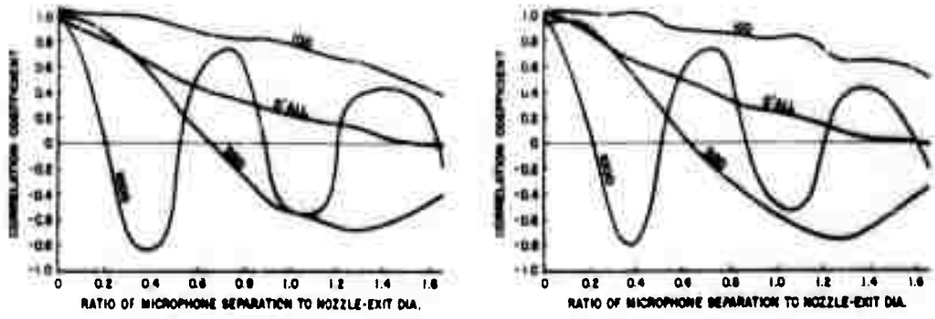

(a) Rigid panel, Row C; engine condition—military operation; Location: Aft—40.1 ft, Radial—15 ft

(b) Rigid panel, Row D; engine condition—military operation; Location: Aft—40.1 ft, Radial—15 ft

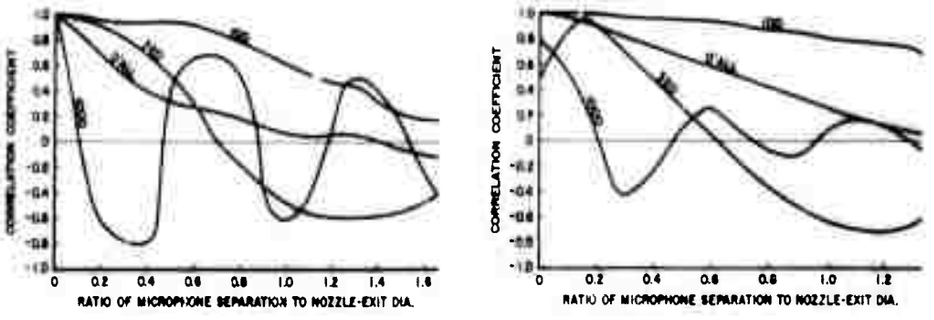

(c) Free field, Row C; engine condition—military operation; Location: Aft—40.1 ft, Radial—15 ft

(d) Rigid panel, Row D; engine condition—afterburner operation; Location: Aft—40.1 ft, Radial—15 ft

Fig. 9 - Longitudinal sound pressure correlation

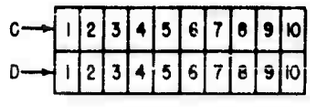

ELEMENTARY AREAS

TOTAL NUMBER OF AREA PAIRS = $\frac{n(n-1)}{2} = \frac{20(20-1)}{2} = 180$

EXAMPLES:

(1) ROW C; $\overline{P_{c1}P_{c1}}$, $\overline{P_{c1}P_{c2}}$, $\overline{P_{c1}P_{c3}}$, $\overline{P_{c1}P_{c4}}$,... $\overline{P_{c1}P_{c10}}$

(2) ROW C-D; $\overline{P_{c1}P_{d1}}$, $\overline{P_{c1}P_{d2}}$, $\overline{P_{c1}P_{d3}}$, $\overline{P_{c1}P_{d4}}$,... $\overline{P_{c1}P_{d10}}$

Fig. 10 - Correlation over the panel area

of area C1. Consequently, the initial coefficient for Row C would be expected to be unity, whereas the initial coefficient for Row D is the vertical correlation between areas C1 and D1.

These correlograms all have the form of damped cosine functions. If the exciting pressures had been steady state, the correlograms would be simple cosine functions. For the Military condition the correlograms for both Row C and Row D approach cosine functions at the 40.1-feet aft location. At the same location, for the afterburner condition, the correlograms decay to an uncorrelated state quite rapidly. This of course implies a significant sound source change between the two engine conditions. Also, at this same location, the decay of vertical correlation is more apparent for the afterburner.

Longitudinal sound pressure correlations 14.2 feet aft of the nozzle-exit and 10 feet from the jet centerline are presented in Fig. 11. These are for Military, Rigid Panel conditions, Row C and D. Compared with the data for 40.1 feet aft these correlograms approach the uncorrelated state much more rapidly in all cases. Since these effects are related to boundary location, they are indicative of "apparent" changes in source characteristics with position. In other words, close to the nozzle-exit the source tends to appear to be a spatially distributed random-phase phenomenon while farther downstream the source tends to resemble a simple generator.

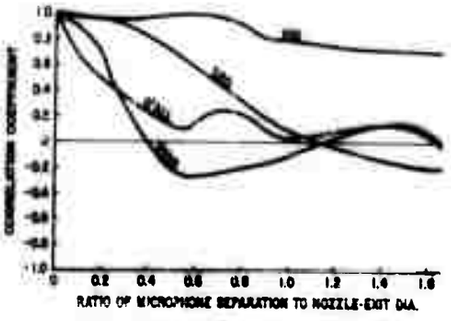

(a) Rigid panel, Row C; engine condition—military operation; Location: Aft—14.2 ft, Radial—10 ft

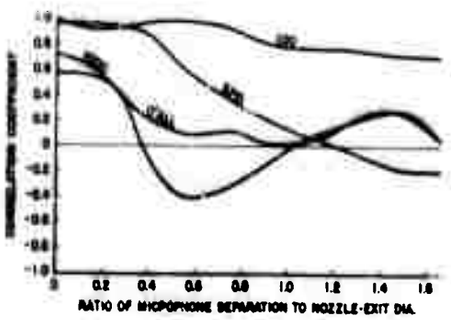

(b) Rigid panel, Row D; engine condition—military operation; Location: Aft—14.2 ft, Radial—10 ft

Fig. 11 - Longitudinal sound pressure correlation

Narrow-band sound pressure spectra for three boundary conditions at two locations are presented in Fig. 12 for the afterburner only. The ordinate for these curves has been reduced to spectrum level (re: 0.0002 dynes/cm^2) and have been redrawn from the originals which exhibit normal plotting scatter. The general shape of these curves is characteristic for the locations selected, greater low-frequency content downstream and increased high-frequency content upstream. Average overall sound pressure levels shown do not account for correlation but are ensemble averages for a large number of engine runs.

Typical sound pressure excitation and response spectra for Flat Panel A, described previously, are shown in Fig. 13. Ordinates for these curves are in mean-square units per cycle (power spectral density). The strain gage and accelerometer were attached to the center-left-half and center respectively of an individual skin panel 6 by 9 inches. The difference in mode response is obvious. In particular, the resonant frequencies for the fundamental and 1 by 3 mode (first two peaks) are observed to occur more nearly at the same frequency for the strain gage location compared with the accelerometer location.

Jet wake spectra and constant sound pressure level free-field contours for a limited set of conditions are presented in Figs. 14 and 15. The frequency bands referred to are the center frequencies of the octave band filters used for these analyses. Sound pressure levels have been reduced to spectrum level values (re: 0.0002 dynes/cm^2).

Spectra for microphone locations along the jet centerline show a slight decrease in high-frequency content with increased distance from the nozzle exit (1). Nearly all of the sound energy appears to be concentrated in the frequency range below 200 cps. In this

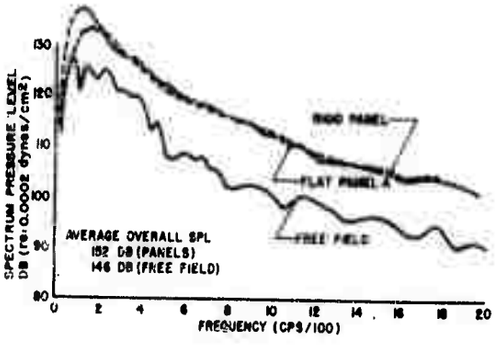

(a) Afterburner operation; Location: Aft—40 ft, Radial—15 ft

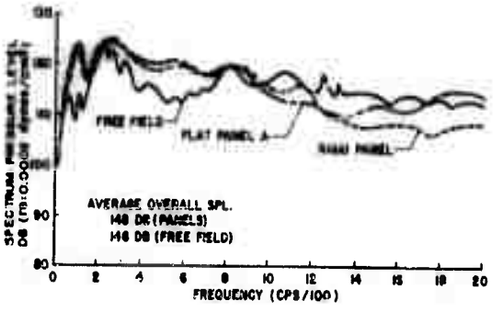

(b) Afterburner operation; Location: Aft—14.2 ft, Radial—10 ft

Fig. 12 - Comparison of sound pressure spectra (10-cps bandwidth)

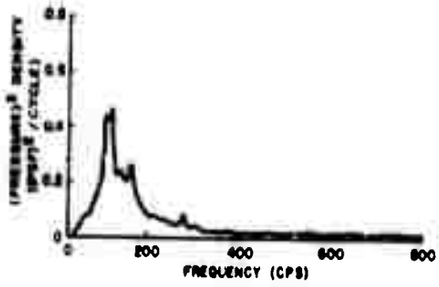

(a) Panel excitation

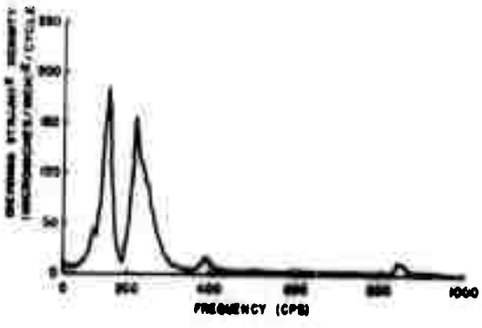

(b) Panel response (bending strain)

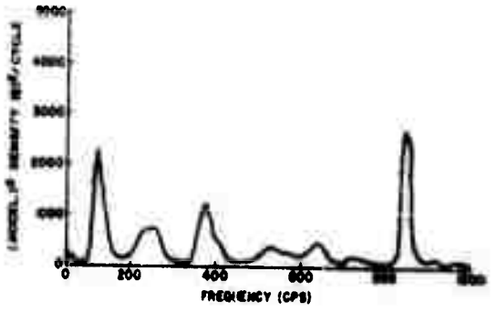

(c) Panel response (acceleration)

Fig. 13 - Flat Panel A, excitation and response for military operation at location: Aft--40.1 ft, Radial--15 ft (10-cps bandwidth)

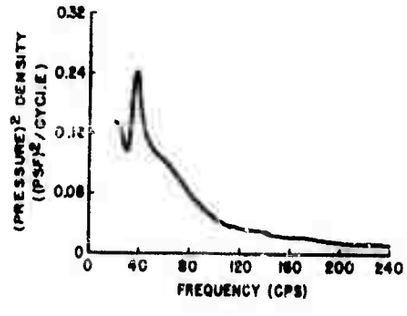

(a) For military operation and location: Aft—40 ft, Radial—0

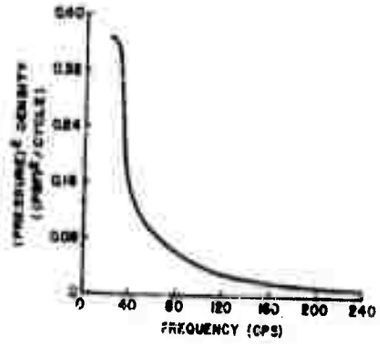

(b) Afterburner operation at location: Aft—40 ft, Radial—0

Fig. 14 - Jet wake sound spectrum analysis (2-cps bandwidth)

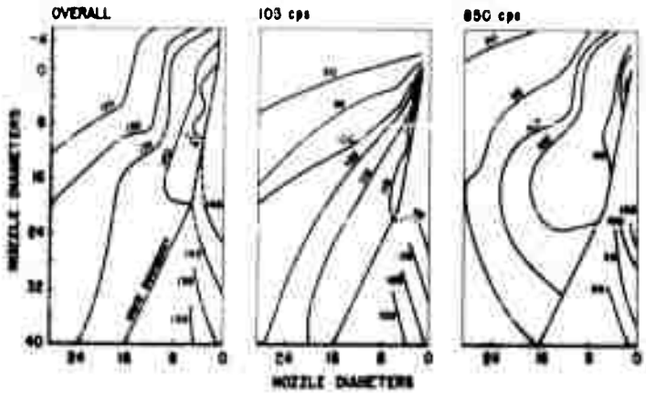

(a) For military operation

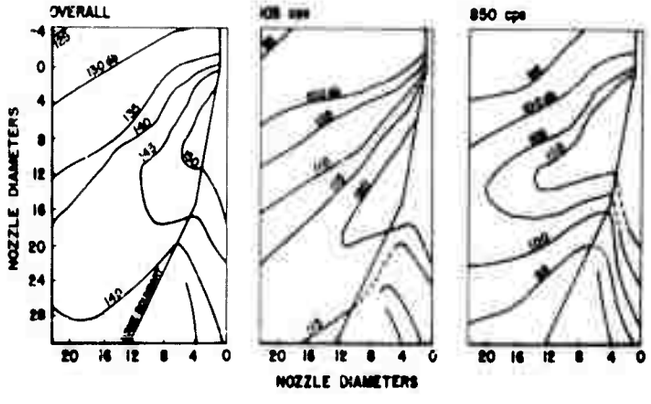

(b) For afterburner operation

Fig. 15 - Sound pressure iso-level contours, free field

respect the spectra are similar to the spectral density of turbulence data of Ref. (3), for distances greater than 16 nozzle-exit diameters.

The constant sound pressure level contours in the region outside the exhaust exhibit the now well-known form of the near noise field of a turbojet engine (5). The present results, however, include contours for the interior of the exhaust wake. Since the primary objectives of this program were concerned with structural response, no serious attempt has been made to explain these portions of the contours. However, even casual observation reveals a certain degree of continuity along the nominal wake boundary. Also, the general form of the wake contours appears to be in agreement with the idea of inward radiated sound suggested in Ref. (4).

CONCLUSION

Measurements of excitation and response of substructures in the near-noise field of a turbojet engine have been completed. These have served a useful purpose in providing a basis for determining the validity of theoretical prediction methods. Also, some measurements of sound pressures within the engine wake were obtained. Further investigations in this research area are being both planned and proposed including additional correlation and response studies, effects of multiple jet sources, and development of improved measurement techniques.

The work described in this paper was supported under Air Force Contract Number AF 33 (616)-5546.

REFERENCES

1. "Study of the Characteristics of Modern Engine Noise and the Response Characteristics of Manned Vehicle Structures," Lockheed Report 13,700 (Final Report Contract No. AF-33(616)-5546).

2. Davenport and Root, Random Signals and Noise, McGraw-Hill Book Co., 1958.

3. James C. Lawrence, "Intensity, Scale, and Spectra of Turbulence in Mixing Region of Free Subsonic Jet," NACA Report 1292, 1956.

4. Erik Mollo-Christensen, "Jet Noise Generation and Suppression," M.I.T. Fluid Dynamics Research Group Report #59-5, May 1959.

5. Walton L. Howes, et al., "Near Noise Field of a Jet-Engine Exhaust," NACA Report 1338, 1957.

DISCUSSION

Mr. Trotter (Boeing Airplane Co.): I would like to ask if you have made any narrow-band cross correlation measurements where your bandwidth was of the order of a panel resonance perhaps?

Mr. Parry: No.

Mr. Stern (General Electric): At the opening of your paper I got the impression you were going to give some correlation between random and sinusoidal damage, and I tried to follow your talk very closely and perhaps you indicated it someplace but I didn't get it. So I would like to ask a specific question again. If, as a result of this work (a man) came to you and said he had a 10 to 2000-inch bandwidth, 10 g excitation and he wanted an x g^2/cps equivalent for when the thing would be likely to fail these panels, what would x be?

Mr. Parry: This is a good question. I don't feel ashamed to say I can't answer it. I really don't think there is anybody here who can. In fact, I think from the way things are going it will be some time before it can be answered, but I would like to say this, that the problem of sonic fatigue is not a simple one, at least I don't think it can be nailed down to one number.

What I am trying to do here this morning is to show you the measurements that we made, why we made them, what we are trying to get at, what the actual numbers are. There are some people back at Lockheed, unfortunately they are not here with me, but there are people who have been working on theory. They have got some pretty good theories. They feel they can predict, for instance, the resonant frequency of a complex structure, such as we showed, to about 10 or 20 percent. They are always a bit on the low side, and right now they don't know why. I don't know why either, but there are essentially two problems. One is, do you have a fatigue theory which says essentially why, in the first place, does the material fail? How many cycles of loading do you put into it and which way do you put them in and so forth, to make it fail consistently so you can predict that failure? Secondly, you have to know in complex panels like these, how does the darn thing move. In other words, how much stress are you getting at what frequencies so you can compute how much and how many cycles you are putting into it for how long? Then in a complex structure like this you have a third problem, can you locate the stress concentrator? Because really you can't say just because you know how it is moving that you know exactly where the thing is going to fail. So it is pretty complicated. That is the best I can do for you.

Mr. Mustain (Norair Division, Northrop Corporation): I have a question. I am used to seeing values of 0.1 maybe up to around 1 g^2/cps. You showed values up to 2000 g^2/cps which to me is of earthquake proportions. Would you clear me up on that one?

Mr. Parry: Well, I don't really know what data you are used to looking at. All I can say is if, for instance, you have on one of these curves here, a mean-square density of a thousand, then you have about 50 g's in that particular mode. I really don't know what your data is so I really can't compare it.

Mr. Mustain: Actually I am concerned with your data, not my data. I just don't see values like yours. That is what I don't understand. You have g^2/cps in values of 2000, and we are usually talking in values

around 1 g^2/cps which are considered fairly high.

Mr. Parry: Let me say this. On your visual observation if you look at the panel, for instance, the panel from which this data was taken, if you observe it, look at it, see how it is moving, if you look at the accelerometer that is mounted on it you see that it is moving on the order of two-tenths to a quarter of an inch double amplitude under this sort of excitation. So really it depends upon how much excitation is that you have on it. If you don't drive it very hard it won't move very much, you know.

Mr. Mustain: [Shakes head negatively.]

Dr. Morrow: I think we can add one or two comments to the question of levels of power spectral density. What we have been talking about here is not typical of the excitation of equipment for two reasons. In the first place, you don't normally mount equipment on the portions of the airframe that are real close to the jet exhaust. You try to avoid it if you can, and yet these areas are of interest in connection with acoustical fatigue of the airframe. In the second place, if you did mount equipment there it would load the airframe and the vibration observed would be very much less than it is now. So for these reasons I don't think there is a conflict. It's just that the vibration we are concerned about at the moment – is not typical of equipment excitation.

* * *

SUPERSONIC AIR-TO-SURFACE MISSILE VIBRATION PROGRAM

J. L. Frarey and P. W. Kinnear, Jr.
North American Aviation, Downey, Calif.

This paper gives some results of the rather critical vibration test program of the "Hound Dog" missile carried by the B-52. The data showed strong discrete signals at the electrically coincident frequencies of 400, 800, 1200, and 2400 cps. Some aspects of the effort to establish confidence in this data and to separate electrical noise from vibration will be treated.

INTRODUCTION

The Hound Dog is an air-to-surface cruise missile, about two thirds the size of a small fighter aircraft, powered by a single conventional turbojet engine and carried in pairs by a B-52. The missile is mounted between the B-52 inboard engine pod and the fuselage with the aft portion of the missile aft of the inboard engine nozzle and about 10 feet from the engine. Figure 1 shows the missile location when mated to the bomber. This location produces a very severe acoustical and vibrational environment during ground run-up and take-off. The runway and B-52 wing serve as reflectors, actually forming a chamber for the acoustic energy. As the Hound Dog becomes standard armament on later model B-52 aircraft, operational missiles must withstand the stresses of a very large number of take-offs and many hours of captive in-flight cruise environment. This in-flight environment is also severe; therefore, these factors made the obtaining of vibration and acoustic data of prime importance.

Fig. 1 - Acoustical energy chamber. A one-sided outline of the B-52 Aircraft with a Hound Dog missile attached. The aircraft body and engine nacelle form the walls of a chamber for acoustical energy while the wing and runway complete the box effect.

One of the most important questions asked during a flight test program is "How good are the data obtained?" In ordinary measurements, such as the many temperatures and pressures secured during a flight test program, this question can be resolved by a detailed error analysis. Then, a figure may be quoted for the accuracy of the data. While this type of analysis may be made on vibration data as well, an even more important first step is to have a general feeling of confidence or trust in the recorded data. The ability to separate the vibration data from the system noise is of prime importance. The question is not the accuracy of the data obtained but whether the signal is useful data or system noise. The GAM-77 (Hound Dog) missile vibration program is the subject of this paper, with emphasis placed on the effort made to establish confidence in the data.

In obtaining early vibration data, full-scale dummy missiles were used. The prime objective of these dummy missiles was to obtain initial captive flight load data and the use of these same tests for vibration and acoustic data was a bonus, both in time money. Full-scale dummies allowed direct mass—center of gravity simulation of components, hopefully assuring realistic vibration response. Spatial simulation of components afforded, again hopefully, acceptable acoustic response. Although there were no operating missile systems or engine, it was known that the missile engine should add less than three decibels to the overall sound pressure level, while the major contribution from the operation of missile systems should be the generation of discrete frequencies. Using information obtained from these dummy flights, and data from later powered missile flights, a reliable basis for evaluation of the vibration and acoustic environment was expected.

In making vibration measurements on powered missiles, enough measurements had to be taken to establish discrete system inputs as well as to verify the dummy missile data obtained previously. The major effort on powered missiles was to have been on early missiles so that, after a few flights, enough data would be available to either validate or change the environmental criteria. Because of instrumentation malfunctions and enough surprises in the data to reduce the confidence in early dummy missile data, totally acceptable data has only recently been available to either validate or change the environmental criteria. As detailed later, the dummy data differs from the powered missile data in a predictable manner.

INSTRUMENTATION SYSTEM

The vibration measuring system employed was a conventional arrangement. It consisted of piezoelectric accelerometers, cathode followers, and amplifiers. The B-52 contained an instrumentation capsule located in the bomb bay and a one-inch tape recorder in the crew compartment to allow tape changes in flight. The missile data amplifiers, for measurements recorded in the bomber, were located in the B-52 bomb bay capsule. This arrangement facilitated calibration of the system and provided a temperature controlled area.

The accelerometers used were medium output, high-capacity units, with a natural frequency of approximately 10 kc. These units had a minor resonance at approximately 4 kc and were listed by the manufacturer as being good to 3500 cps. No filtering was used in the system. The cathode follower was powered by +36 volts on the plate with the cathode returned to -36 volts in the transistorized amplifier. The amplifier had a variable gain up to 100 and was flat ±1 percent from 5 cps to 4000 cps and ±1 db to 12 kc.

The instrumented powered missiles contained a telemeter sometimes used for vibration measurements. The top three standard IRIG (narrow) telemeter channels have a normal frequency response of 1050, 790, and 600 cps respectively. To widen the response, the filters in the ground station demodulators were changed. Several methods of improving frequency response of a telemeter were discussed by Beckman (1) in a previous Symposium. The telemetry was used to check discrete responses and low-frequency random signals during free flight.

The B-52 contained a receiver for the reception of the telemeter signal. The composite audio signal output of the receiver was recorded on the B-52 recorder for a backup or check on the ground recorded telemeter data. In obtaining the necessary frequency response to record the telemeter signal, the recorder was run at 30-inch per second. As this tape speed in turn sets the frequency response of standard fm electronics used, the frequency response of the vibration measurements recorded in the B-52 was 5 to 5000 cps. This wide response exceeded the accelerometer manufacturers specified frequency range by 1500 cps.

GENERAL INSTRUMENTATION PROBLEMS

Before detailing some of the more subtle points in the data that caused concern, a few of the more obvious problems will be examined. While results from the early tests were plainly not data and necessary system modifications were straightforward, although not always easy, these problems delayed the schedule. Probably more important, they caused the data to be analyzed more critically, particularly for any electrical interference.

The most common problem in any aircraft instrumentation system is the necessity to minimize 400-cps electrical noise. The problem was compounded in this case, because

both the powered missiles and the bomber have their own electrical generating systems and the instrumentation is one of the few common points of both systems. The dummy's instrumentation was, of course, powered from the B-52.

Time code generator pulses in the B-52 occur at rates of 10 pulses per second, 1 pulse per second, and 1 pulse per 10 seconds. These are heavy current pulses and are used to advance counters and cameras in the B-52. Transients at all these rates were observed in the instrumentation system until electrical contact noise suppressors eliminated this problem.

Loose connectors in the system can of course produce transients that are easily mistaken for actual mechanical transients. Coax connectors were the most common offenders in this respect. A positive method of locking these connectors was necessary. Also, any momentary interruption in the power supply voltages to the amplifier would produce large transients.

DATA ANOMALIES

After eliminating or reducing the above problems, the data still showed several anomalies. At times, an analysis of these anomalies was made difficult because of the data reduction equipment available. The equipment available for frequency analysis had a 160-cps bandwidth filter and a one-second sweep time. Since considerable trouble had already been experienced with the measurement system, unexpected results always made the measurement system suspect.

Data were expected to be below 2000 cps. Some measurements indicated considerable vibration energy in the range of 2000 to 5000 cps. At the time it was not known that the accelerometer had a minor resonance at 4000 cps, but a subsequent report from the accelerometer manufacturer indicated the possible presence of this resonance. Thus, at the time the data appeared to go all the way out to 5 kc and peak at the higher end. Filters which cut off at 2 to 3 kc could have been used since the accelerometers were being used beyond the manufacturers recommendation. However, the use of filters at this point was rejected until the nature of these high-frequency signals could be determined.

High-frequency system noise is most likely to be obtained from either of two sources: acoustic pickup in the accelerometer and cathode follower, or from the reproduction of discriminator hiss in an fm recording and playback system. Acoustic response was checked in two ways. The transducer and cathode follower were tested in an acoustic chamber. The results of this test showed that the sound pressure level at a single frequency would have to exceed 163 db in order to produce signals of the magnitude measured in the 4000-cps region. As a further test, the accelerometer was shock mounted in the dummy missile and another flight was made. Thus, any signals above the cutoff point of the shock mounts would be either electrical noise or acoustic response of the accelerometer or cathode follower. Only small signals at the electrical power frequency and the odd harmonics of this frequency were observed.

Many locations in both the powered and dummy missiles produced complex signals larger than predicted. These large voltage signals, when injected into an fm voltage controlled oscillator, would over deviate it. In the ground playback of these signals, the frequency modulated signal is passed through a bandpass filter. If the frequency modulated signal exceeds the response of the bandpass filter, the discriminator sees the equivalent of an open circuit and the familiar discriminator hiss occurs. To insure against over driving the fm oscillators, the measurement ranges were increased to better contain the complex signal. Later, when the high-frequency random vibration had been properly identified, it was proved that there was no fm distortion.

Dummy missile data also showed a strong discrete signal at 800 cps for some locations. This 800-cps signal varied in magnitude with applied B-52 engine power just as would be expected of a vibration signal. However, regardless of the fact that the 400-cps power showed only odd harmonic content, the reasonable doubt that this signal was the result of some spurious electrical interference could not be erased. To further complicate the problem, powered missile data, when it became available, showed strong signals at 1200 cps and 2400 cps at many locations. One location also indicated a very strong 400-cps signal.

SPECIAL DUMMY MISSILE FIELD TEST PROGRAM

The confidence level in the data obtained by this time was low or at least controversial.

Tests had been run on the measurement system in the field and in the laboratory and all these tests seemed to indicate that the disputed discrete signals were not electrical noise. However, the coincidence of obtaining these frequencies seemed too great to believe. Also, the presence of high frequency, high-amplitude broadband data was still questioned. In order to establish confidence in the data or correct any measurement system problems, a special program was instigated. The prime objective of these special tests was to investigate the vibration data gathering system. An instrumented dummy missile and a B-52G aircraft were assigned to this program for one month. It was agreed that ground run-up tests would be the most advantageous to this program.

To investigate electrical interference in the B-52 on-board recording system, a completely independent ground recording system was established to be used during ground engine run-ups. While the selection of a dummy missile for this test was a schedule necessity, it proved an advantage because all 400-cps power could be removed from the missile during these ground tests and instrumentation could be powered from 60-cps sources.

Test Descriptions and Results

The ground run-up tests were conducted in two parts: data were recorded on the ground recorder for one part, and on the B-52 recorder for the second part. Data from these tests were then analyzed and the next tests were determined.

The existence of three main sources of error was investigated. These were the production of beat frequencies or harmonic frequencies of legitimate signals; the existence of electrical interference which could be amplified only under certain conditions, and the general content and source of random noise. The production of beat frequencies was checked by mixing two signals and feeding them into both the ground and airborne system. One signal was held constant while the other signal was swept over the frequency range. The amplitude of these signals was also varied. The data were then analyzed to detect the presence of any signals at the sum or difference frequencies. No beat frequencies were detected. To investigate harmonic generation, missile accelerometers were excited at given frequencies and the reduced data was examined for the presence of harmonics. The excitation of the accelerometers was first tried by striking a tuning fork and placing the base on the top of the accelerometer. Unfortunately however, to produce a significant signal, the forks had to be struck quite hard producing a tone that was itself rich in harmonics. The test is recommended however, if anyone cares to elicit the kind of interest that is aroused when one is observed descending on the missile with an armload of tuning forks. The pure signal was finally produced by installing a small, 2-pound peak force, Goodman shaker in the missile and mounting an accelerometer on the shaker. No harmonics could be detected in any of these missile shaker tests.

The search for electrical interference was centered mainly on the 800-cps signal found most strongly at the aft attach point between the missile and the pylon. Various tests were conducted at this and other locations. Accelerometers of different natural frequencies, manufactured by different concerns, and a velocity pickup were mounted side by side at the aft attach fitting. The accelerometer systems were powered both from the ground and from the B-52. Outputs of these instruments were recorded both on the ground and in the B-52.

A black box, containing a battery powered cathode follower and amplifier, was installed in the missile. The accelerometer connected to this system was mounted side by side with an accelerometer that was routed to a system powered in a conventional manner. The signals produced by these two instruments were recorded both on the ground and in the bomber.

Ground loops were simulated in the system by placing a resistor to ground from the ground side of the signal and also by shorting the signal shield to the missile frame at several points. This was done to simulate the condition of the missile at the beginning of the test after it had been flown in captive flights for six months with little instrumentation maintenance. Data was scanned after each test by use of photographs taken of each signal, both on a Panoramic Sonic Analyzer and on an oscilloscope.

Figure 2 shows the comparison of the ground recording and the B-52 recording of the station showing the 800-cps discrete frequency. The ground recorded signal was produced when all 400-cps power had been removed from the missile. This comparison

along with supporting data from the velocity pickup and battery powered system confirmed the fact that the signal was an actual mechanical vibration and not electrical pick-up. When equipment became available which utilized a two-cycle wide filter, it was found that this apparent discrete frequency was actually composed of two signals, 650 cps and 740 cps. Had this reduction equipment been available early in the program, much more confidence in the data could have been obtained without these special confidence tests. In particular, this 800-cps problem would not have occurred.

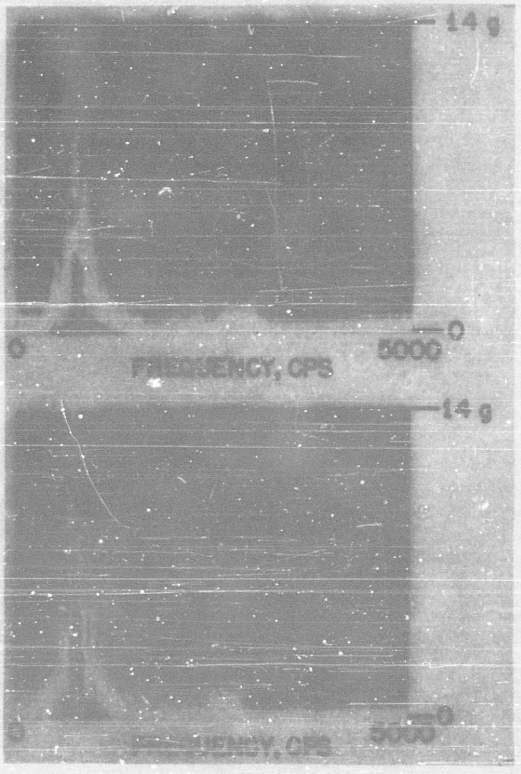

Fig. 2 - 800 cycle data comparison. Discrete response measured at the aft attach fitting between the missile and the pylon. The top photo is a B-52 recording while the bottom photo was recorded on the separate ground recording system.

Signals showing high-frequency broadband data were checked to insure that they were not spurious in nature. Figure 3 is presented to show that high-frequency signals were present when the fm system was not being overdriven. Early representations of the high-frequency data had tended to overemphasize it because of the display technique chosen plus the error introduced by the high-frequency response of the accelerometer. This response is plotted in Fig. 4. This high-frequency data is now considered to be of no greater amplitude than would be expected when the missile is in a high-level acoustic field.

No definite conclusions could be determined from the attempt to simulate a poorly maintained instrumentation system. However, the data produced at some locations were of different character than earlier data and the only explanation could be the poor condition of the instrumentation. After the ground run-up tests had been concluded and the data from the above tests analyzed, the first truly "acceptable" data was finally recorded during taxi runs and actual take-offs.

POWERED MISSILE DATA

The suspicion that 400-cps harmonics still existed in the vibration signals did not end with the dummy missile data. Powered missile data showing a strong 400-cps output had been all but discarded as being invalid. The location of this 400-cps signal was a rack used to support instrumentation components. Upon further investigation in the laboratory, it was found that this rack had an inopportune resonance at 400 cps with magnifications between 5 and 10. This rack has since been redesigned. Further, large 1200-cps, and occasionally smaller 2400-cps signals, appeared in the powered missile data and were traced to the constant speed hydraulic motor used to drive the alternator. This motor is a nine-piston wobble plate unit turning at 8000 rpm, or 133 cps. Thus, if an impulse is created when the pistons are either driving or exhausting, an impact rate of 1200 per second is created. If a hydraulic disturbance is created by both the inlet and exhaust stroke, 2400 impacts per second are created.

At this point a description of the hydraulic system will aid in appreciating the scope of this problem area. The system is conventional; it uses a pump driven by the jet engine through a gear box and a combination single port accumulator-reservoir. The system drives the constant speed hydraulic motor, the flight surfaces including the forward elevator, and the jet engine air inlet spike positioner. Since the hydraulic motor is located in the aft compartment, hydraulic lines must be routed to, or through, all

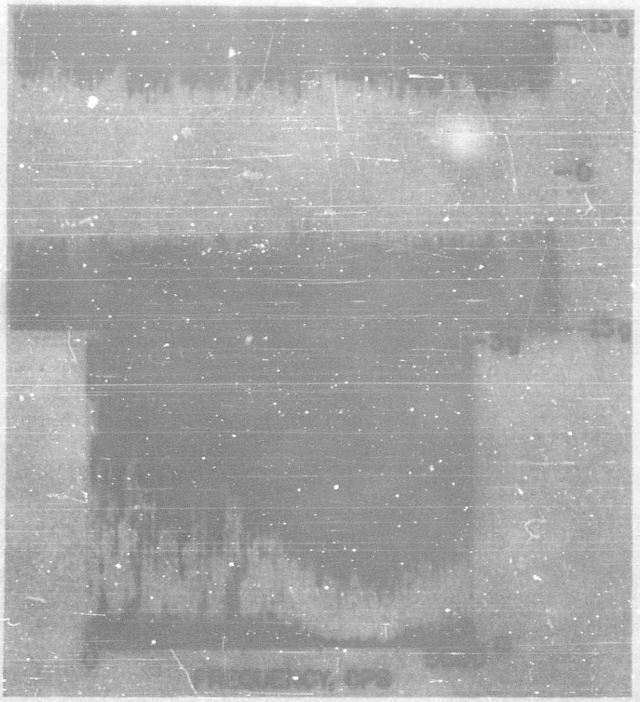

Fig. 3 - High-frequency data. Oscilloscope and Panoramic Sonic Analyzer representation of a signal showing high-frequency data.

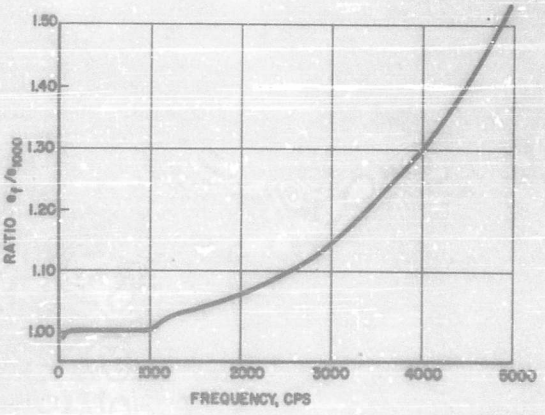

Fig. 4 - Accelerometer response. This figure indicates the response of the accelerometers used in the majority of the vibration program. The curve was made by using a high natural frequency accelerometer as a standard. Therefore, it is only an indication of the actual response experienced.

compartments. Thus, all line tie-downs, or bulkhead feed-throughs, may become point sources of vibration.

The magnitude of this 1200-cps vibration varied from ±10 g or more in the aft compartment to ±0.5 g or less in some forward sections of the missile. Figure 5 shows the wave form and magnitude of this vibration in the aft compartment. Magnitude varied with the distance from the hydraulic motor and the local line tie-down conditions. The 2400-cps vibration, when it appeared, was small by comparison.

An unfortunate facet of this problem is the inverse relation of vibration magnitude to electrical load; i.e., the lighter the electrical load, the greater the vibration magnitude. This is important because the alternator is running light during most of the ground checkout periods. Of course, during captive and free flight the electrical loads are higher, thus minimizing this problem. Figure 6 shows the 1200 cps still predominate but of much lower magnitude in flight at a midbody station.

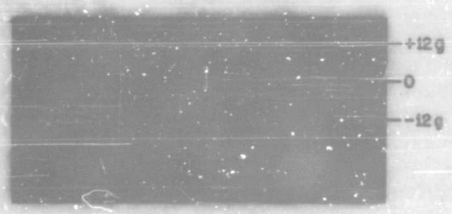

Fig. 5 - 1200-cycle vibration. Top: Almost pure 1200-cps vibration obtained at station 472 in the aft body. Bottom: 1200-cps signal for comparison.

With the determination of the source of the 1200-cps and 2400-cps signals, the problem of confidence in data showing frequencies coincident with the electrical power frequency and its harmonics was resolved. One other strong discrete signal that poses a serious problem should be noted as a matter of interest. This vibration currently appears to be generated by the missile hydraulic pump. Knowing the measured rpm and the pump gear box ratio, and again working with a nine piston unit, the pump impact frequency can be calculated. This discrete vibration signal was found to have magnitudes which vary from ±5 g to ±15 g and frequencies, depending on engine rpm, which vary from 385 cps to 530 cps. An unfortunate, but not unexpected condition, is that the pump vibration is a maximum at a low engine rpm, i.e., at engine idle the pump must increase its stroke to maintain system pressure. When it is recalled that the Hound Dog will operate at engine idle during most of the captive phase of its mission in order to keep all systems powered and ready, the importance of this problem is obvious. This high-amplitude vibration generated by the pump is also evident during missile dive-in when the engine is windmilling. An example of this vibration is given in Fig. 7.

CONCLUSION

Instrumentation of a dummy missile was vital to the vibration program because of its early availability. The use of the dummy missile to trouble shoot the measurement system and to obtain confidence in the data produced a system that was virtually fault-free early in the powered missile program.

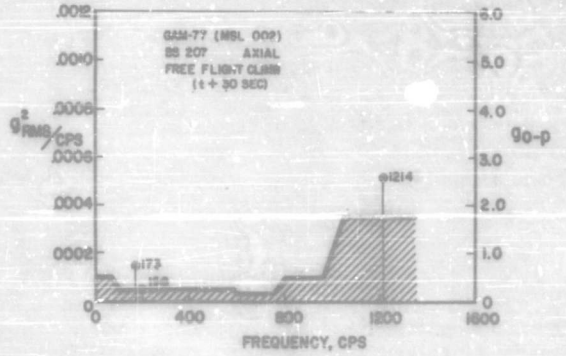

Fig. 6 - Free-flight data. The average random levels are related to the g^2_{rms}/cycle scale while the discrete g levels are related to the g zero-to-peak scale.

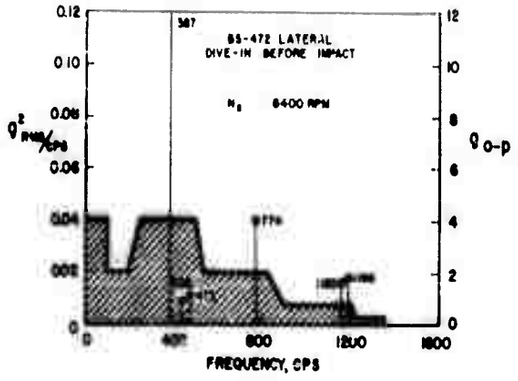

Fig. 7 - Dive-in data. Data obtained during the dive-in phase of a free flight showing the strong discrete vibration obtained from the hydraulic pump. The random levels are related to the g^2_{rms}/cp scale while the discrete frequencies are related to the g zero-to-peak scale.

Satisfactory answers to the problems might never have been worked out in powered missiles alone because of much tighter schedule demands. While the vibratory response of the dummy missile was substantially comparable with the powered missiles, as predicted, the random vibration level was found to be somewhat higher than that of the powered missiles. This difference was probably due to improper spatial simulation of components. Figure 8 shows a comparison of the data obtained during take-off of the B-52 with a dummy and a powered missile.

The program was plagued with two unpredictable and very misleading problems. These problems were coincidence of vibration frequencies and 400-cps electrical harmonics, and the high-frequency response of the test accelerometers, which indicated a large magnitude of high-frequency broadband and random vibration. Hydraulically generated vibration had totally unexpected high-level magnitudes and provided frequencies and levels beyond the regime of the predicted environmental specification.

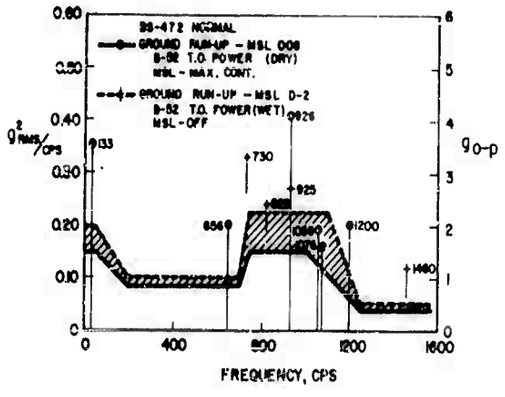

Fig. 8 - Dummy vs powered missile comparison. This data is for an aft body location. The B-52 was using water injection and take-off power for the dummy missile data. The B-52 engines were running dry, at take-off power, and the missile engine was at maximum continuous power for the powered missile.

REFERENCE

1. M. R. Beckman, "Special Consideration in Telemetering Missile Vibration," Shock and Vibration Bulletin No. 26, Part II, Dec. 1958, pp. 96-101.

* * *

SHOCK DATA HANDLING SYSTEMS AT DAVID TAYLOR MODEL BASIN

Mrs. S. C. Atchison
David Taylor Model Basin
Washington, D. C.

The David Taylor Model Basin has recently revamped its methods of handling large quantities of shock data. New methods incorporate high-speed digital computer techniques and types of components which may be useful to others involved in correcting, reducing, and interpreting large quantities of transient data. Computer programs for computing the response of mechanical systems to transient inputs, e.g., shock spectra, are also available.

INTRODUCTION

Since World War II the David Taylor Model Basin has been conducting full-scale shock tests to measure the response of ships' structure and equipment to underwater explosions. Test data consist of transient motions lasting from 50 to several hundred milliseconds. The seismic velocity meter has generally proved to be the most useful sensing device for obtaining a history of the shock motion. This meter, which is not too bulky for most shipboard applications, is a simple device consisting of a bar magnet seismically mounted inside a rigidly mounted coil. Meter output is recorded on magnetic-tape recorders and on electromagnetic oscillographs, the latter without amplifiers.

Usually two objectives sought from test data are:

1. Accurate documentation and correlation of the shock motions of the entire target with the explosion parameters and observed damage;

2. Derivation of input motions to equipment for use in the design of equipment and specification of design criteria.

Selection of a data-handling system was based on the preceding objectives in conjunction with the known characteristics of the recording and measuring instruments.

Desirable computations include (1) statistical combinations of large groups of motions as functions of the explosion parameters to reduce the data to a comprehensible unit, and (2) computations of the response of both linear and nonlinear mechanical systems simulating equipment to the input motions.

The fortuitous circumstance that the Bureau of Ships computing facility is located at the Model Basin meant that digital handling of the data could be effected without costly outlay for equipment. A variety of equipment as well as the advice of trained personnel were readily available. Therefore, it was decided to utilize the open-shop program of the Applied Mathematics Laboratory in developing needed computer programs. With this arrangement programming for the computers is done by the engineer or physicist initiating the problems by using one of the scientific compilers. In the examples discussed herein the computer was the IBM-704 and the compiler was Fortran.

COLLECTION OF DATA

Generally shock data is collected at sea during full-scale underwater explosion tests against a combatant-type ship and occasionally from model tests conducted at the Model Basin and elsewhere. Some 20 to 100 velocity meters may have been installed throughout the ship to measure the response of ships' structures and equipments to one or more shots. The number of instruments and shots would depend upon the purpose and extent of the tests. The output of the velocity meter will always differ from the actual motion of the structure to which it is attached by the motion of its seismic element. If large displacements are encountered, an additional error is introduced by the bottoming of the meter against its stops. Thus two corrections may need to be applied to measured data before further computations can be made with it.

The two recording systems commonly employed for velocity-meter output introduce negligible error; they are (1) electromagnetic oscillographs and (2) magnetic-tape recorders.

DATA-HANDLING SYSTEM

The first step in processing the data is preparation of a single computer input from one or both of two quite different media. Because it was anticipated that part of the data would be processed more than one time on the computer, binary digitized magnetic tape of a specified format was selected as the standard input for all shock-data-reduction programs. Binary magnetic tape is handled more efficiently by the computer and can be stored more compactly than punched cards.

In Fig. 1 is seen typical test records which were recorded on an electromagnetic oscillograph. The handling system for such optical records is diagrammed in Fig. 2. The typewriter is simply a monitoring device. The essential components are the Data Reducer on which amplitudes of the records are read at even increments in time and the Telecordex which takes output from the reader and converts it into input for the IBM Summary Punch. A record of 200 to 300 points is digitized in approximately 30 minutes with this system. The next step in the reduction of oscillograph data involves

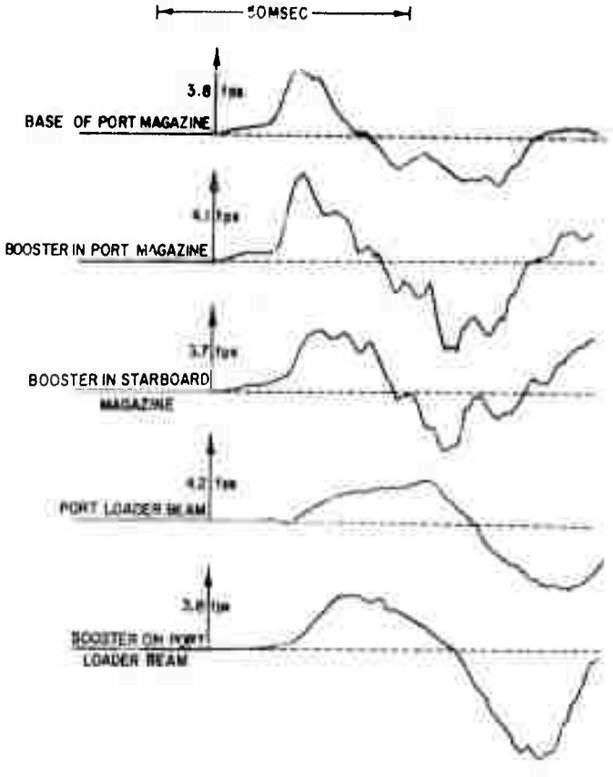

Fig. 1 - Typical shock motions on missile ship

processing of the decks of cards through a short computer program to make the binary input tape.

An alternate method of data reduction is available for data which is recorded directly on analog magnetic tape. These records will be processed through the Computer Language Translator (1) which is roughly diagrammed in Fig. 3. This facility of the Math Laboratory is just becoming operational; however, trial runs with this equipment are promising. For the test runs, sampling rate and playback speed were adjusted to yield 9600 points per second of real time, and the digitized output agreed quite satisfactorily with playback of the original analog record on a string oscillograph. Once the input tape was properly positioned the 9600 points were obtained in 32 seconds. It is hoped that the processing time per record allowing for such things as mounting and alignment of input tape will be no more than 3 minutes per record.

The second step in data handling is processing of the binary input data through selected IBM-704 programs. Each of the programs contains one subprogram to correct for motion of the seismic element and another to correct for possible meter bottomings. The output of such programs is normally obtained in the form of tables of corrected and uncorrected velocity, corrected and uncorrected displacement, and an average

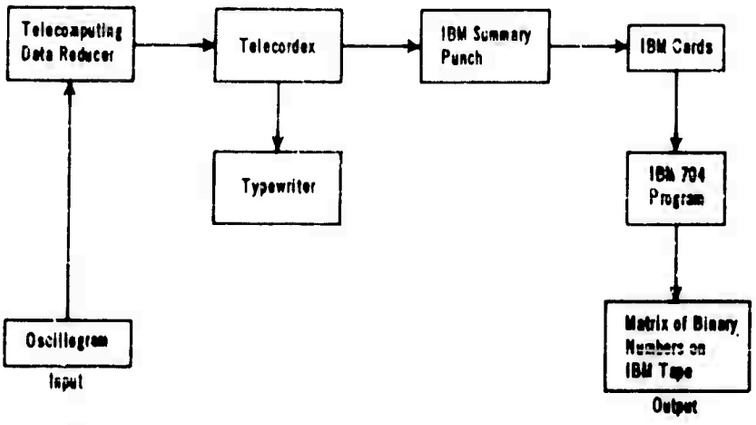

Fig. 2 - Initial data-reduction procedure for optical records

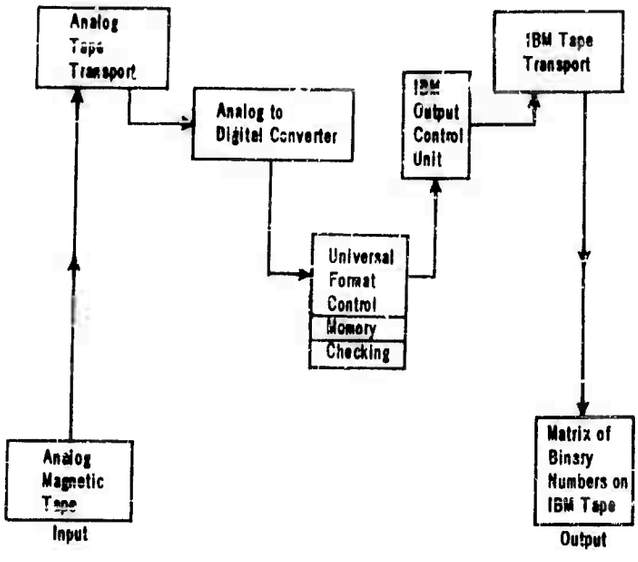

Fig. 3 - Initial data-reduction procedure for analog magnetic-tape records

acceleration, each corresponding to a listed time. In addition, time histories of shock spectra may be obtained.

In addition to the usual tables of output from the computer, graphs of amplitude vs time can be obtained with the Charactron Plotter (2) which operates as an on-line component of the IBM-704. The essential components of the Charactron Plotter are the charactron shaped-beam tube similar to the familiar television picture tube, a Traid high-speed camera, and a Kelvin Hughes fast-developing camera. The maximum plotting rate is 15,000 points per second with an accuracy of 0.5 percent. Because time histories of motions are preferred, most computer output from shock analysis programs will eventually be in graphical rather than tabular form.

ANALYSIS PROGRAMS

Several shock analysis programs for the 704 have been in use for the past year. A block diagram of the latest version of the most commonly used program is shown in Fig. 4. Beyond the point at which plots and tables of corrected velocity, displacement, and acceleration are obtained the output becomes both optional and variable with the user. The response of a single-degree-of-freedom system can be computed for a maximum of 20 values of frequency and 10 values of damping. Output consists of relative displacement across the spring and acceleration and velocity of the mass. Relative displacement and acceleration are used in design criteria while velocity of the mass is used mainly in correlating observed motion of an equipment with observed motion of its foundation. Output from this portion of the program consists of graphs of the time histories and tables of peak absolute values only.

A program for finding the bodily velocity of a ship from the digitized measured motions has been used. By proper choice of constants the same program will compute relative displacement and has been used to find relative displacement across shock mountings from the observed motion of the equipment and its foundation.

FUTURE EXTENSIONS OF THE SYSTEM

The data-handling system was set up so that it could be easily extended in the direction of more sophisticated analysis programs. The standard input and subprograms readily lend themselves to response calculations for nonlinear systems or for multidegree-of-freedom linear systems. It is planned to extend the system in the area of simulation of nonlinear equipment mountings particularly.

Future plans include greater use of magnetic-tape recording of test data to permit more statistical analysis in the determination of sets of typical shock motions for a given type of ship. The displacement program mentioned above has been extended in that direction, and currently an extensive set

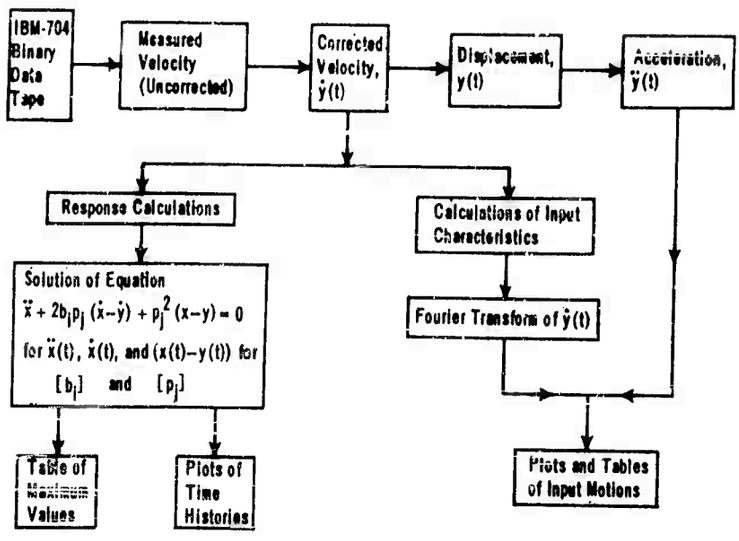

Fig. 4 - General purpose shock analysis program

of magnetic-tape records from a cruiser model test are being processed to obtain typical shock motions for use in weapon effects predictions and shock design criteria.

In conclusion it should be noted that this data-handling system has resulted from cooperative pooling of ideas from personnel involved in the design of sensing devices, collection of data in the field, and analysis and use of data in the laboratory. There has been a constant feedback of information in the three areas as the procedures and capabilities in each area either limit or extend the capabilities in the other areas. Thus the handling system itself will be continually changing to make use of improvements in other areas.

REFERENCES

1. Robert Goldsteen, "Introduction to the Computer Data Format Translator," David Taylor Model Basin AML Report 87 (July 1959).

2. E. Cuthill and R. Mejia, "Preliminary Programming Manual for SC4020 Microfilm Recorder," David Taylor Model Basin AML Report 87 (August 1959).

DISCUSSION

Mr. Abstein (Hughes Aircraft): Would you describe the nature of the correction that is applied to take into account the bottoming of velocity pickups?

Mrs. Atchison: It's really a very simple correction. We indicate where we want the correction applied in the data, and the computer as it processes the data applies the correction. When the meter hits the stops, there is a reversal of velocity. The output is completely reversed and the correction that needs to be applied is simply shifting the record at some point up to its previous level.

Mr. Curtis (Hughes Aircraft): Is this a conventional MB pick-up or one especially designed by DTMB?

Mrs. Atchison: One especially designed by DTMB. The frequencies of our meters are six cycles and under ordinarily and well, one meter has a travel of four inches, another has one inch, so we can find when we need to correct it actually by looking at the displacement.

* * *

A THERMAL POWER DETECTOR*

B. L. Mattes
Lockheed Aircraft Corporation
Missiles and Space Division
Palo Alto, California

A thermal power detector has been developed to measure intense, transient heat levels. This detector was designed to operate at close range in the heat environment generated by the Polaris missile at launch, but its use is readily adaptable to other, similar requirements. Its main features as a thermal power detector are: (1) broad spectral sensitivity (0.3μ to 20μ), (2) fast transient response (10 μsec or better), (3) ability to withstand intense heat levels for short periods (1000 watts/in.^{2} for 0.5 secs), (4) continued use for succeeding tests without calibration, and (5) ease of installation, requiring a minimum in circuitry to record the heat levels. The thermal power detector consists of a pyroelectric ceramic disk placed in a shock-absorbent mount. The ceramic disks used were either barium titanate or lead zirconate-titanate, depending upon the thermal power level.†

THE TRANSDUCER

The transducer detects thermal power-convective and radiative heat by instantaneously responding to the average temperature rise of the detector element. The detector element is a pyroelectric ceramic. The ceramic generates a current output directly proportional to the net thermal power absorbed.

The response of the ceramic to the thermal power absorbed can be explained thermodynamically as follows (1): The rate at which the heat energy is absorbed into the ceramic determines the rate of increase in temperature. Thermal agitation results in the individual polarized domains of the ceramic (the ceramic is composed of many sintered crystalline grains polarized in one direction, each grain consisting of several domains). The rise in temperature within each of these domains decreases the net polarization. As a result of the decrease in polarization (P), a charge (Q) is induced to the electrodes (electrodes are on two sides of the ceramic, forming a capacitor). The rate of change in charge (dQ/dt), or current (i), is directly related to the rate at which energy is absorbed into the ceramic:

$$i = \frac{dQ}{dt} = A\frac{dP}{dt}, \qquad (1)$$

where A = area of the electrode.

The current is related to the rate in change of temperature (T):

$$i = A\frac{dP}{dT}\left(\frac{dT}{dt}\right)_{ave}$$

or

$$i = A\gamma\left(\frac{dT}{dt}\right)_{ave}, \qquad (2)$$

where γ is the pyroelectric coefficient.

*This paper was not presented at the Symposium.
†Work carried out under U. S. Navy Contract NOrd 17017.

The average rate of increase in temperature follows from the transfer of heat into the ceramic:

$$\left(\frac{dT}{dt}\right)_{ave} = \frac{W}{c\rho Ad}, \qquad (3)$$

where

W = thermal power absorbed,

c = specific heat of ceramic,

ρ = density of ceramic,

d = thickness of ceramic,

A = area of electrode.

Hence, the current output is directly proportional to the thermal power absorbed:

$$i = \frac{\gamma W}{\rho cd}. \qquad (4)$$

Several different pyroelectric ceramics have been used as the detector element. Table 1 lists these ceramics and their sensitivities.

TABLE 1
Some Pyroelectric Ceramics Used as Detector Elements

Element	Thickness (in.)	Sensitivity (μa/watt)	Upper Average Temperature Limit (C)†
$BaTiO_3$	0.125	0.023	90°
$BaTiO_3$	0.0625	0.046	90°
PZT-5*	0.125	0.030	300°

Typical values of the constants in Eq. (4) for $BaTiO_3$ are:

$\gamma = 2.0 \times 10^{-8}$ coulombs/cm^2 °C

c = 0.12 Cal/gm °C

$\rho = 5.7$ gm/cm^3

*Clevite Corporation trade name for lead zirconate-titanate.

†The upper average temperature limit (limited to below the Curie temperature) is the temperature at which either all or partial polarization is lost within the ceramic element.

The ceramic elements are circular disks, varying in thickness depending on the sensitivity required. Typical elements were four inches in diameter and 0.125 inch thick. Each element has silver electrodes bonded to the ceramic. Leads were attached to the electrodes by means of a phosphor-bronze clip.

A high emissivity surface with broad spectral sensitivity is required to absorb the incident heat energy into the detector element. Black Glyptal enamel* met this requirement as well as being resistant to high heat levels, corrosion, and abrasion. Figure 1 gives the spectral sensitivity for the enamel's emissivity. The enamel's total emissivity is independent of temperature from 0°C to 100°C and increases slightly above this range. This enamel bonded excellently to the silver electrodes or to the ceramic and could be applied in thin layers. The thickness of the enamel layer limits the time response of the detector because of its low thermal conductivity.

The detector element is housed in a rigid container, as shown in Fig. 2. To reduce the response of the ceramic to shock and vibration, the ceramic element was placed between two layers of glass wool. The glass wool served also as an electrical and thermal insulator for the element.

The ceramic element acts as a current generator when shunted with a resistance low compared with its output impedance (on the order of 10^{11} ohms). Thus the output signal can be fed directly into regular coaxial or twin lead shielded cable to a high-sensitivity recording galvanometer. A C.E.C. 7-339 galvanometer (4.6 μa/in.) with a coil resistance of 30 ohms, shunted with 350 ohms, was used in the recorder.

The time response of this galvanometer was considerably larger than the inherent time response of the detector. The time response of the detector is determined by its capacitance plus the cable capacitance and the shunt resistance across the cable. The capacitance for a four-inch diameter and 0.125-inch-thick $BaTiO_3$ disk is about 0.02 μf. With a shunt resistance of 1000 ohms, the response time of the detector is about 20 μsec. The lower limit in time response has not been determined.

*Manufactured by General Electric Company, Schenectady, New York.

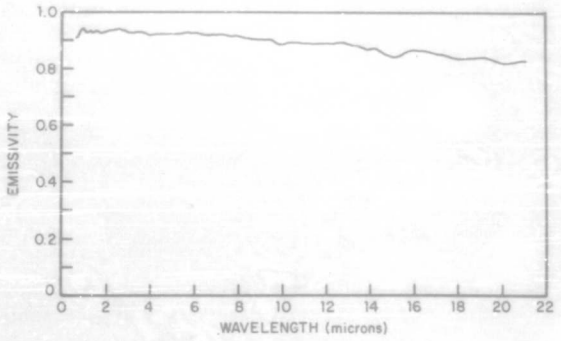

Fig. 1 - Emissivity of Black Glyptai enamel for perpendicular incidence

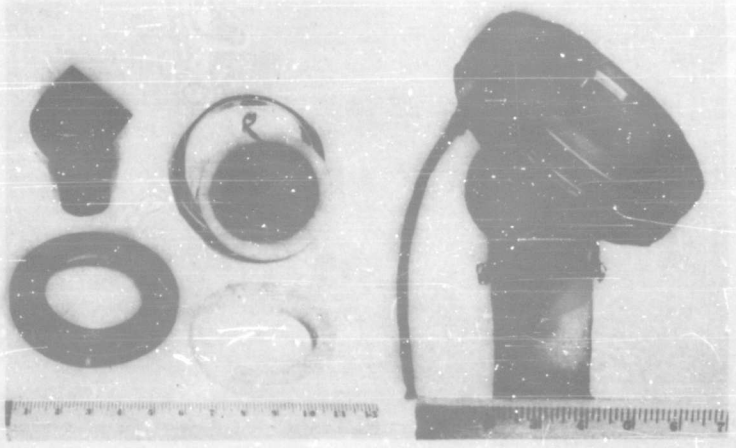

Fig. 2 - The detector element and its assemblage

The detectors do not require calibration in the field. Once calibrated in the laboratory, their calibration has remained within 5 percent of their original value after a year in the field. Some elements were used twelve times without any maintenance. Should the average temperature of the element exceed the upper average temperature limit (Table 1), then the disk has to be replaced (this is very uncommon for transient heat measurements of short duration). All elements of the same composition, diameter, and thickness are interchangeable within a few percent difference in calibration. The laboratory calibration was accomplished by calibrating a 200-watt heat lamp at a given point over a known area with a calorimeter consisting of a copper disk and a thermocouple. The ceramic element was then placed at this point, and the current output was recorded.

APPLICATION

The thermal power detector can be readily applied to measure either convective or radiative heat. A quartz window can be placed in front of the detector to measure radiant heat if convective heat is also present. With an open detector (directly exposed element within the container), the sum of convective and radiative heat can be measured. The field of measurement to be covered by a detector can be varied by the angle subtended through the aperture of the container. In addition, a 4π detector could be constructed if a hollow, spherical ceramic element were used.

The thermal power detectors in the field have been subjected to average heat rates as high as 1000 watts/in.^{2} for a period of 0.5 sec; yet there was no observable change in

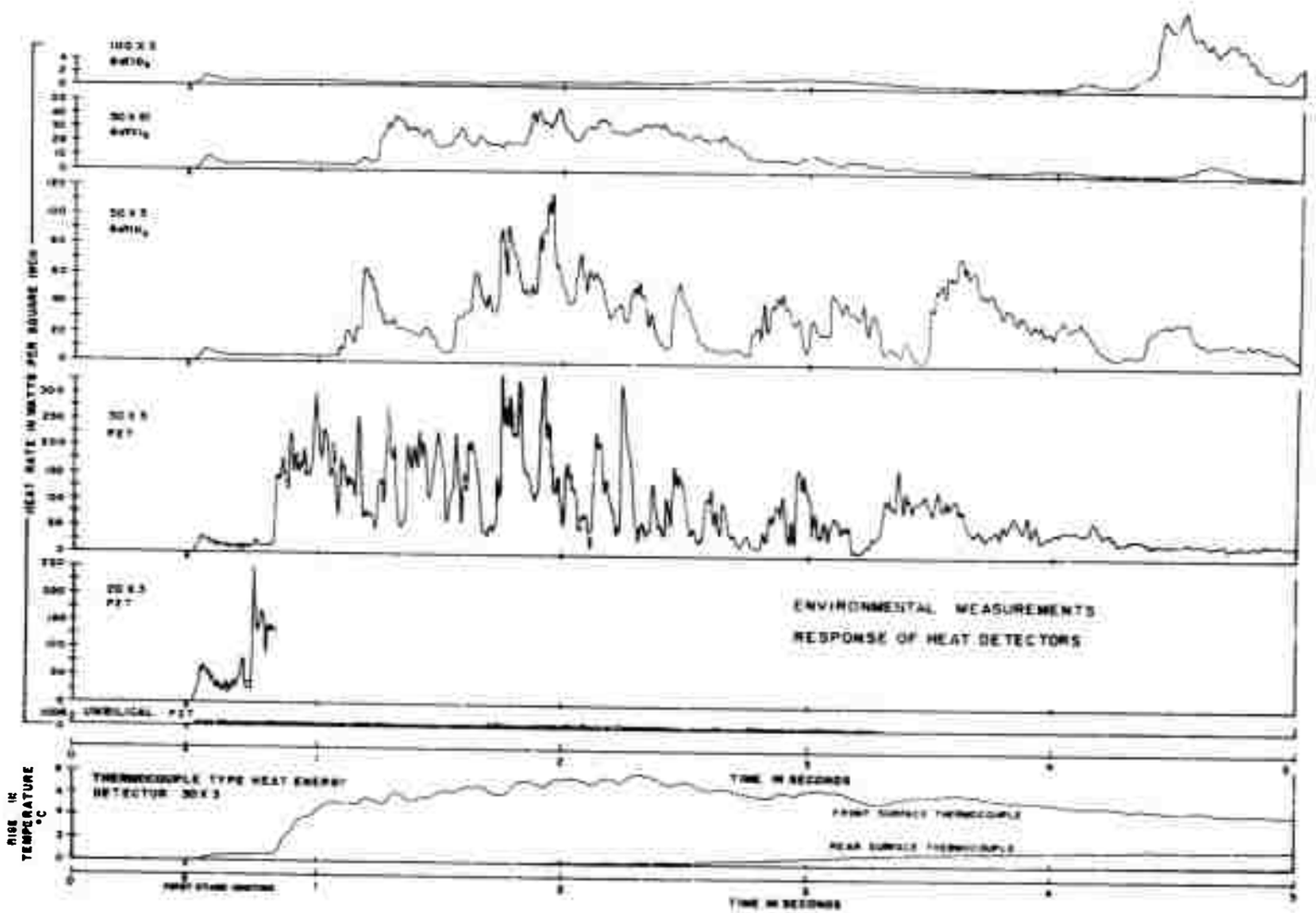

Fig. 3 - Typical recorded thermal power levels

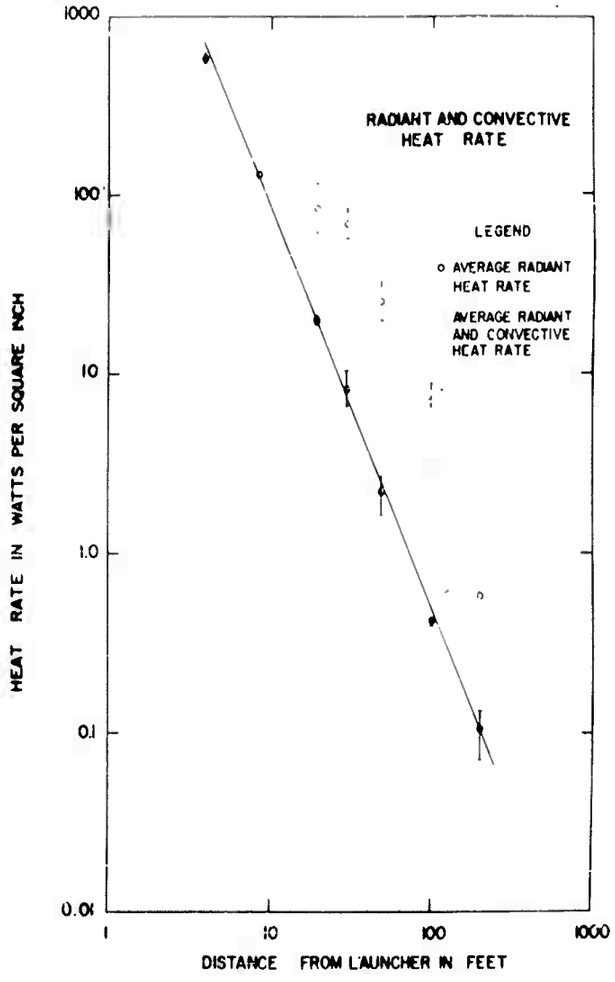

Fig. 4 - Radiant and convective thermal power distance

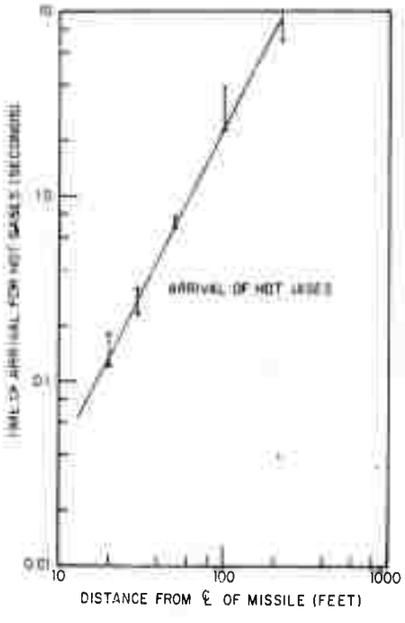

Fig. 5 - Time of arrival of convective gases indicating their inverse square relationship of translational kinetic energy per unit area with distance

their calibration and time response. However, the Black Glyptal enameled surface had burned off.

Figure 3 is a typical set of recorded data as obtained from these detectors. The radiative component of energy can be noted preceding the convective heat from turbulent gases. The large peaks are associated with large swirls of gases. The lower record is from a thermocouple-type heat energy detector used to evaluate and to verify the thermal power levels indicated by the pyroelectric-type detector. The front and rear surface thermocouple outputs are analyzed by the "Schmidt diagram" method (2). The thermocouple-type heat energy data gives an integrated thermal power level. The results were in agreement between the two detectors. The advantage of the thermal power detector over the thermocouple-type is that the heat rate levels can be read directly from the recording.

Figure 4 shows data combined over a series of different tests. The radiant heat level drops off approximately with the inverse square of distance. The convective heat levels drop off much more rapidly because of the mixing with cooler gases. The gases also lose their translational kinetic energy per unit area as the inverse square with distance, as shown in Fig. 5.

The thermal power detector should, in addition, provide accurate data for purposes of correlation with skin flash burns. The ceramic acts as a thermal insulator as does skin. The combined fast time response and broad spectral sensitivity should give almost instantaneously the surface absorption rates of heat energy.

ACKNOWLEDGMENTS

The author is indebted to T. A. Perls, J. J. Bartog, and E. C. Barkofsky for their help and suggestions in the development of this transducer. Pyroelectric $BaTiO_3$ ceramic was suggested as a detector for measuring heat radiation by T. A. Perls, T. J. Diesel, and W. I. Dobrov (3). The emissivity data on Black Glyptal was obtained from Clyde Shaw. The work was carried out under U. S. Air Force Contract AF 04(647)-347.

REFERENCES

1. T. A. Perls, T. J. Diesel, and W. I. Dobrov, "Primary Pyroelectricity in Barium Titanate Ceramics," J. Applied Physics 28:1297-1302, Sept. 1958.
2. W. H. Giedt, "Principles of Engineering Heat Transfer," Van Nostrand, 1957, pp. 315-319.
3. Perls, op. cit.

* * *

A DATA SYSTEM FOR THE DESCRIPTION OF MISSILE ENVIRONMENTS

D. Brown
Douglas Aircraft Company
Santa Monica, Calif.

A comprehensive set of digital computer programs is being developed for use on IBM 709-7090 computers to produce environmental descriptions for quasi-stationary random data and transient data. The programs are expected to be applicable to shock, vibration, flutter, and acoustic environmental description.

GENERAL

The collection of data on the environment of a system is most often for one of two applications – the design of laboratory tests that aim in some sense to simulate the environment, or the presentation of data that will give an engineer information for redesign. Most environmental description is the direct presentation of measured data – temperature, humidity, pressure, radiation levels, etc. The problems occur primarily in the description of transient effects or a continuous process having a wide bandwidth. The direct presentation of the measured data from these sources results in long time-history plots or tables of figures that are extremely difficult to interpret and apply. This is the situation in the area of shock, vibration, and acoustics. The data system must operate on the data in a manner that will produce concise, meaningful descriptions of these phenomena. A simplification is the notion of a standard source or driving function.

The simplest satisfactory description for these processes is shown in Fig. 1. Note that for some purposes, the real system may be nonlinear. However, the linear model may be sufficient to reconstruct a typical waveform for laboratory testing. The specification of the environment thus reduces to the specification of a linear "black box," and a standard source, which is very good for reconstruction or simulation of the environment in the laboratory.

The most common description for these "black boxes" is in the frequency domain – the frequency response or Fourier spectra.

$$Y(f) = \int_{-\infty}^{\infty} x(t)\, e^{-2\pi i f t}\, dt . \qquad (1)$$

There are additional advantages gained by frequency presentations: the transducers employed for shock and vibration instrumentation are linear filters. Also, all data-transmission schemes have a limited channel capacity. If the frequency handling capacity of these systems is exceeded, some form of distortion results – frequency folding in time sampled systems or nonlinear effects (for example, crosstalk, or amplitude distortion) in continuous systems. To avoid these effects, data-transmission systems contain filters which modify the data. Compensation for these filters and for the resonant effects of environmental simulation devices is most straightforward in the frequency domain.

An alternate description that has some definite advantages in the simulation problem is the expansion of the shock waveform in

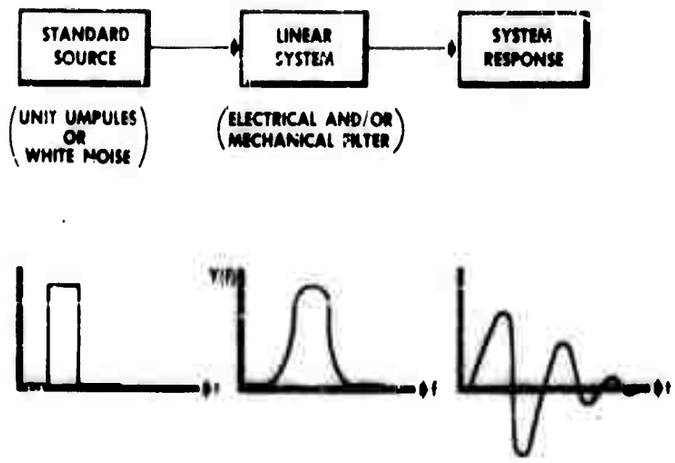

Fig. 1 - Environmental model

Laguerre polynomials. Here we describe the source, shock, and shaping network by an orthogonal expansion of the form:

$$g(t) = e^{-kt} \sum_n a_n L_n(kt) . \qquad (2)$$

However, frequency representations have advantages in familiarity and in availability of design techniques; therefore they will be treated here.

Stationary random data can be treated in a similar manner, except that direct Fourier transformation involves too much computer effort, and statistically is not as meaningful as a (smoothed) power spectral density estimate.

Some amplitude descriptions are also desirable, especially if there is a good possibility that the amplitude distribution is not gaussian. For this purpose the frequency of occurrence of amplitude of a selected portion of data may be counted and a standard statistical hypothesis test accomplished. Another useful description for fatigue analyses is the number of peak accelerations as a function of amplitude in a transient waveform.

THE DATA SYSTEM

Once the meaningful descriptions are decided upon, it is then possible to design the data collection and reduction machinery. Manual computation is out of the question – a spectral computation often requires on the order of 10^5 multiplications – some form of automata is required. The three most common approaches are diagrammed in Fig. 2.

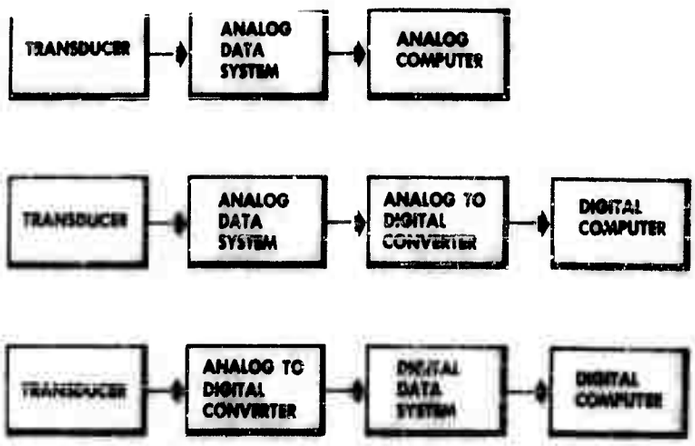

Fig. 2 - Data systems

The analog computer has a number of disadvantages compared with the digital machine:

1. Programming is more difficult – the various descriptions outlined each require an entirely new computer set-up.

2. The machine is less versatile in accomplishing frequency resolution and accuracy trades and in handling data at very low frequencies.

3. The computation is considerably slower than that possible on the newer high-speed digital computers.

4. The use of previously computed calibration information is difficult.

The ideal data system would accomplish the analog-to-digital conversion directly at the transducer, as a digital transmission system is less subject to noise effects in transmission and storage.

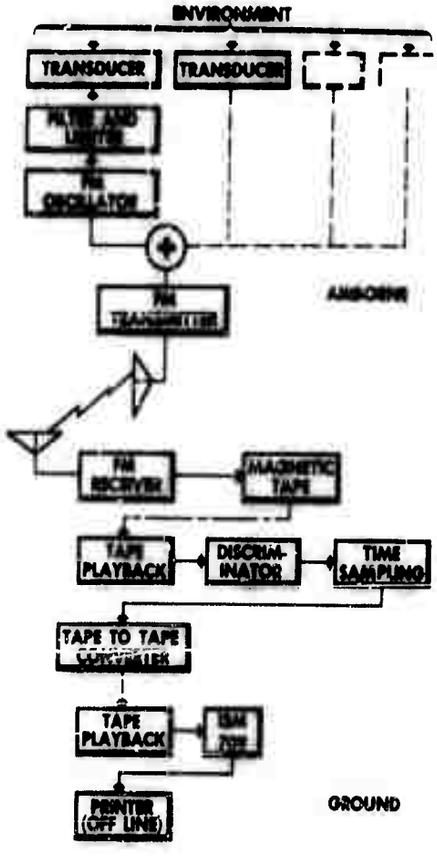

Fig. 3 - The present data system

A block diagram of the present system at Douglas Aircraft is shown in Fig. 3. The weak link is the fm/fm modulation and transmission system. This system has a very narrow dynamic range for gaussian data – only a 22-db range in σ for the best tapes analyzed to date; and an inflexible and insufficient frequency capacity. If time sampling and analog-to-digital conversion is accomplished directly at the transducer filter outputs, the system flexibility, dynamic range, and frequency capacity can be greatly improved. The information is transmitted as a sequence of frequency of phase shifts of a rf carrier representing a train of binary numbers. The binary numbers are coded in floating point (fraction and exponent) to increase dynamic range, and bits for error correction added. This is a PCM/FM or PCM/PM data system. A 200,000-bit/second PCM/FM system may be transmitted in the 220-mc telemetry band.

If each sample of data is coded into a 7-bit fraction and 4-bit exponent, a system may be constructed with a 104-db dynamic range for gaussian data and with 5400 cps of usable frequency response, divided among any reasonable number of channels.

THE ENVIRONMENTAL COMPUTER PROGRAMS

The computer programs are diagrammed in Fig. 4. The following paragraphs treat some of the details generated by the digital approach to an environmental data system.

Digital Sampling Requirements

If the data is to be analyzed in a digital computer, it is necessary to time sample the data at some point in the data system. If the data is sampled at a constant rate, f_s, any frequencies higher than the Nyquist folding frequency $f_{s/2}$, will be folded into the interval $(0, f_{s/2})$, thereby eliminating the possibility of computing a unique spectrum. It is therefore necessary to filter before sampling with a low-pass filter. The required sampling rate may be chosen as shown in Fig. 5.

Calibration

As long as nonlinear effects are small, the entire data system may be considered as a "black box" with a particular frequency

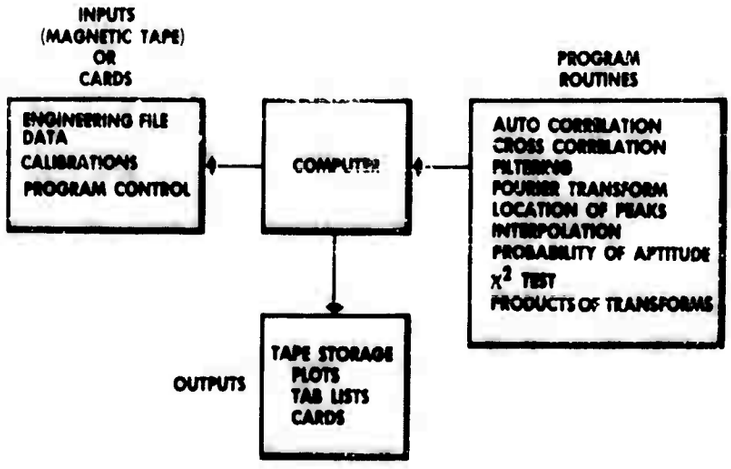

Fig. 4 - The computer programs

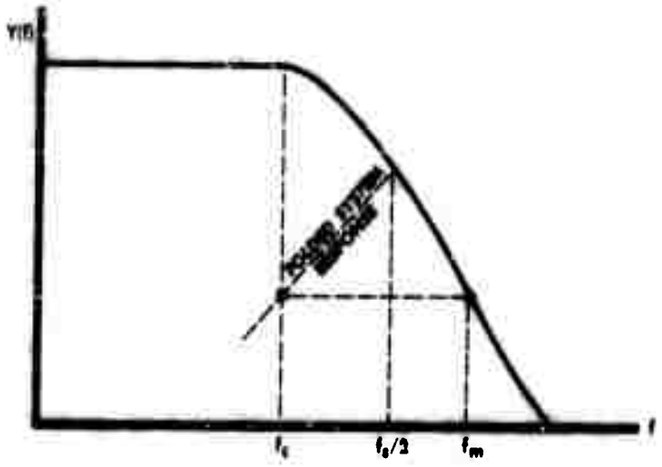

$$f_s \geq f_m + f_c$$

Fig. 5 - Determination of sampling rate where f_m = maximum frequency of analysis and f_t = the point above which the filter attenuation remains acceptable

transfer function on each channel. The availability of Fourier transform programs allows for a simple automatic system calibration: a known time function, $x(t)$, (for example, a unit step function) is simultaneously applied to all data channels and the output, $y(t)$ recorded. The system transfer function, $Y(f)$, is then just the ratios of the transforms, i.e.,

$$Y(f) = \frac{\bar{F}_y(f)}{F_x(f)}, \qquad (3)$$

providing $F_x(f) \neq 0$ in the desired range.

It is usually difficult to apply a known input to a transducer installed in a missile, so the transducer response, $Y_t(f)$ may be determined in a test laboratory. Then $x(t)$ is a voltage pulse applied by a simulated transducer, and

$$Y(f) = \frac{F_y(f)}{F_x(f)} Y_t(f). \qquad (4)$$

The spectral computations are very simply corrected for the data system's response, i.e., if $z(t)$ is the time data function in the computer, and $F_z(f)$, $\omega_z(f)$ a shock spectra and power spectral density computed from $z(t)$, then the corrected spectra are:

$$F(f) = \frac{F_x(f)}{Y(f)} , \qquad (5)$$

$$\omega(f) = \frac{\omega_x(f)}{[Y(f)]^2} . \qquad (6)$$

Amplitude presentations may be corrected by filtering the data with a time weighting function

$$K(t) = \int_{-\infty}^{\infty} \frac{e^{2\pi i f t}}{Y(f)} \, df , \qquad (7)$$

which again may be computed and applied automatically.

Statistical Considerations and Computing Effort

In any sampling procedure, we obtain the most information per data point if the sample points are statistically independent, i.e., the autocorrelation, $R(i\Delta\tau)$ is zero for $i \neq 0$, $\Delta\tau = 1/f_s$. Then each point corresponds to one degree of freedom. The number of degrees of freedom (or independent samples), n, is then

$$n = f_s T \qquad (8)$$

in a data sample of length T. If such is not the case, the information is redundant, i.e., the data has fewer degrees of freedom in any given time interval. If we wish to compute the spectrum at M equally spaced frequency points in the interval $(0, f_{s/2})$, then the spectral estimate at each point has at most N_0 degree of freedom where

$$N_0 = \frac{n}{M} = \frac{f_s T}{M} . \qquad (9)$$

Now, if the spectrum is computed by direct transform methods, the process is to compute the Fourier transformation (requiring approximately n^2 multiplications) and then square and average $F(f)$ over a finite bandwidth (approximately n multiplications). By computing an autocorrelation function first (averaging before Fourier transformation) and then the power spectral density by Fourier transformation, considerable time may be saved (approximately $n + (M+1)^2$ multiplications). The trick is to compute $R(\tau)$ with the minimum number of statistics. The following formulation is one possible method:

$$R(\tau_i) = \frac{1}{N_0} \sum_{s=0}^{N_0 - 1} x(sM\Delta t) \cdot x[(sM + i)\Delta t] . \qquad (10)$$

Typically, the computer time saved by the autocorrelation approach is on the order of a factor of 100 over direct Fourier methods.

Smoothness and Fitting Considerations

Suppose the data contains a periodic (or almost periodic) function, i.e., $x(t) = y(t) + g(t)$, where $g(t)$ is periodic and $y(t)$ is white noise. The autocorrelations and power spectra for these parts are additive. Suppose y has a variance, σ^2, and

$$g(t) = A \sin 2\pi f_0 t . \qquad (11)$$

The true (aliased) power spectra from digitized data are:

$$\omega(f) = \frac{2\sigma^2}{f_s} \; \frac{A^2 f(f - f_0)}{2} . \qquad (12)$$

However, cutting off the correlation computation at τ_m results in the following smoothed spectrum (Fig. 6):

$$\hat{\omega}(f) = \frac{2\sigma^2}{f_s} + A^2 \, \frac{\sin \frac{\pi}{\tau_m}(f - f_0)}{2\pi (f - f_0)} . \qquad (13)$$

Although the frequency resolution of this estimate is $1/\tau_m$, it is easily seen from Fig. 7 that the spectrum is distorted for a considerable distance beyond that.

The truncation of the autocorrelation function may be viewed as forming the product

$$\phi(\tau) = R(\tau) \, D(\tau) . \qquad (14)$$

The smoothed spectra is then as shown in Fig. 7, where $Q(f)$ is the Fourier transform of $D(\tau)$. $D(\tau)$ is often referred to as a "lag window." By the proper choice of a window, the spectra computation will be accurate for a 20-db power range. These windows are discussed in detail in the literature. Cross spectra and transfer ratios will be attacked by similar methods.

Numerical Filtering

If the computed spectra encompass a wide power range and the lower levels contain

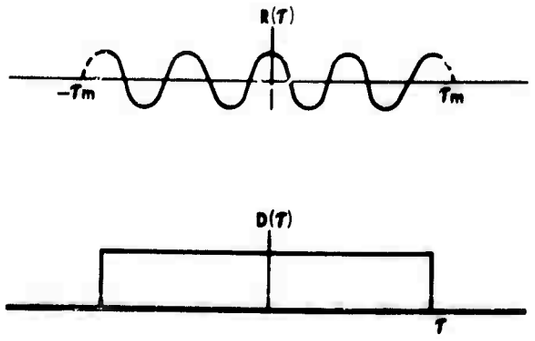

Fig. 6 - Result of truncation of the autocorrelation

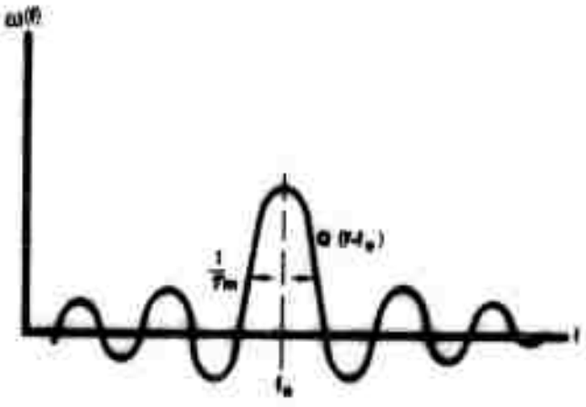

Fig. 7 - Smoothed spectrum of a sine wave

useful information, it is necessary to filter ("prewhiten") the data and recompute the power spectra. Numerical filtering is accomplished by weighting the digital values, i.e.,

$$\hat{x}(n\Delta t) = \sum_{s} k(s\Delta t)\, x([s+n]\,\Delta t)\,. \qquad (15)$$

The following is a basic low-pass filter:

$$\begin{aligned} H(f) &= 1\,, \quad f < f_c \\ &= \frac{f_T - f}{f_T - f_c}\,, \quad f_c < f < f_T \qquad (16) \\ &= 0, \quad f > f_T\,. \end{aligned}$$

The weighting function for this filter is

$$k(n\Delta t) = \frac{\cos 2\pi f_c n\Delta t - \cos 2\pi f_T n\Delta t}{2\pi^2 n^2 \Delta t\,(f_T - f_c)}\,, \qquad (17)$$

$$k(0) = (f_c + f_T)\,\Delta t\,.$$

This filter may be converted to other functions as follows:

1. Band pass around ω_0:

$$k_{\omega_0}(n\Delta t) = k(n\Delta t)\cos(\omega_0 n\Delta t)\,. \qquad (18)$$

2. High pass:

$$\begin{aligned} k'(n\Delta t) &= S_n - k(n\Delta t) \\ S_n &= 1, \quad n = 0 \qquad (19) \\ &= 0, \quad n \neq 0\,. \end{aligned}$$

3. Band reject around:

$$k'_{\omega_0}(n\Delta t) = S_n - k(n\Delta t)\cos(\omega_0 n\Delta t). \qquad (20)$$

For a finite summation, it may be desirable to normalize the filters so that the frequency transfer function at some frequency, ω_1, is unity. For this, the weights may be divided by C, where

$$C = k(0) + 2 \sum_{1}^{N} k(n\Delta t) \cos (n\omega_0 \Delta t). \quad (21)$$

Note that these filters are symmetrical in time, therefore unlike physically realizable filters, they do not phase shift data.

Fourier Transforms

The computation of frequency spectra by Fourier transformation is straight-forward for band-limited sampled data

$$F(f) = \Delta t \sum_{n} x(n\Delta t)\, e^{-2\pi i f n \Delta t}. \quad (22)$$

In many cases, it is more convenient to compute an integrated spectra:

$$H(f) = \int_{-\infty}^{\infty} F(\xi)\, d\xi = -\frac{1}{2\pi i} \sum_{n} \frac{x(n\Delta t)}{n} (e^{-2\pi i f n \Delta t} - 1). \quad (23)$$

This function has somewhat better convergence properties. If some smoothness assumptions can be made, it is then also practical to reduce computing effort by computing fewer frequency points.

Transient phenomena in a missile system are almost always accompanied by quasi-stationary random processes. The effect on the Fourier transform is diagrammed in Fig. 8. Here $F_N(f)$ has a Rayleigh probability density in amplitude and a uniform density in phase. The expected amplitude is just the rms (σ) value of the noise at that frequency and is

$$\frac{\sigma}{\sqrt{2\Delta f}} \quad (24)$$

for white noise. If the shock spectra is sufficiently smooth, the effect of added noise may be reduced by averaging adjacent spectral values. The effect of noise decreases as $\sqrt{\Delta f}$. This averaging may be accomplished by taking finite differences from the integrated spectra. If periodic or narrow-band noise is present, it may be desirable to "cut off" the transient by a time window.

Amplitude Description

From data sampled at a minimum rate, it is necessary to interpolate between points to find the peak values. The interpolation function for band-limited data is

$$x(t) = \sum_{n} x(n\Delta t) \frac{\sin \frac{\pi}{\Delta t}(t - n\Delta t)}{\frac{\pi}{\Delta t}(t - n\Delta t)}. \quad (25)$$

Interpolation between all points to locate peaks is possible but wasteful of computer time. Peaks may be located by noting that there can be at most one peak between adjacent points and that if a peak occurs in the closed interval $(j\Delta t, [j+1]\Delta t)$, then

$$\frac{dx}{dt}(j\Delta t) \cdot \frac{dx}{dt}([j+1]\Delta t \le 0; \quad (26)$$

from Eq. 23

$$\frac{dx}{dt}(j\Delta t) = \sum_{k} \frac{(-1)^k\, x([j+k]\Delta t)}{k\Delta t}. \quad (27)$$

Once it has been determined that a peak lies between two points, the approximate

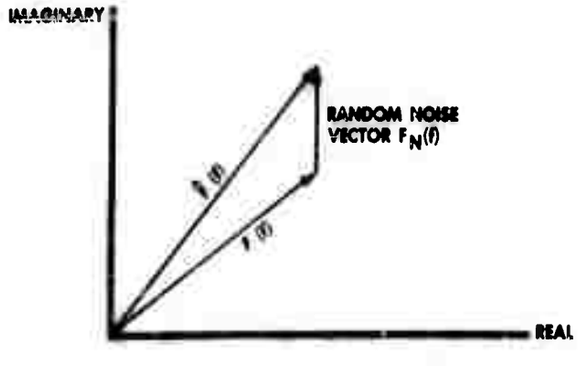

Fig. 8 - Effective random noise on the shock spectrum

time of the peak t_m may be determined from the intersection of the reciprocal of the slopes (Fig. 9). $x(t_m)$ is then determined by applications of Eq. 23. The error in the peak value as a function of frequency due to this approximation is plotted in Fig. 10. The number of peaks in a given amplitude region is then counted and displayed.

Probability Densities

If the data is a sample from a gaussian process, the power spectra is sufficient to describe it. However, it is often desirable to verify the gaussian assumption – especially near-narrow spectral peaks, where the driving function may be periodic. For this purpose, the (filtered) data is further quantized and the digital values lying between these levels are counted. A standard chi-squared test may be used to decide if the data is gaussian.

Note that in order to apply the chi-square test, the time interval, Δt, between sample points must be sufficient to insure independence if the data is narrow-band gaussian. If B is the bandwidth of the (filtered) data, then

$$\Delta t > \frac{1}{2B} . \qquad (26)$$

SUMMARY

The programs described above have all been run on an experimental basis on the IBM 704 or Bendix G-15 computer. They are at present being programmed into an integrated package for the IBM 709 computer and are expected to start producing environmental data in April 1960. It is hoped that as side effects to better environmental descriptions, we will be able to learn more about the design and utilization of simulators and test fixtures by the use of these methods. In the future we expect to add programs for the computation of ensemble averages, i.e., a presentation of the expected or average environment (with confidence limits) that is automatically updated as a series of test progress.

The author wishes to express appreciation to W. A. Kunkel for the considerable effort he has put into this program, and to V. S. Norton, H. Purvis, and J. Korhonen for their assistance in preparation of this paper.

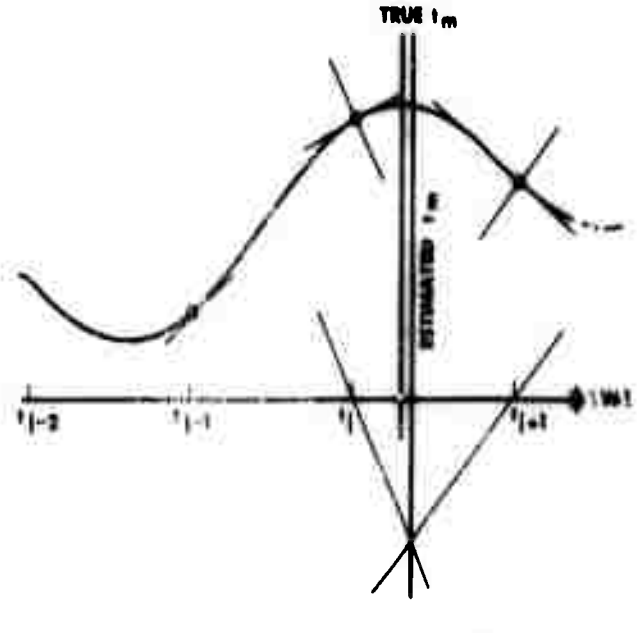

Fig. 9 - Determination of peaks

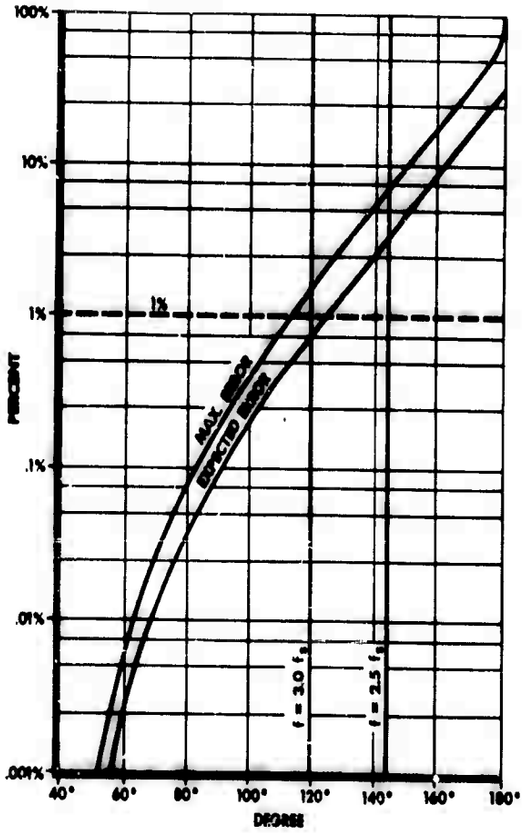

Fig. 10 - Error in peak estimates vs frequency

BIBLIOGRAPHY

R. B. Blackman and J. W. Tukey, The Measurement of Power Spectra (Dover).

M. Wiener, The Fourier Integral and Certain of Its Applications (Dover).

W. R. Davenport and W. L. Root, Random Signals and Noise (McGraw-Hill).

A. M. Mood, Introduction to the Theory of Statistics (McGraw-Hill).

C. Shannon, "Communication in the Presence of Noise" (Proc. IRE, January 1949).

J. F. A. Ormsby, "The Design of Numerical Filters" (STL Report SL 7.43-113).

D. Brown, "On the Use of PCM to Telemeter High Frequency Random Data," Douglas Aircraft Report SM-36167.

DISCUSSION

Mr. Trotter (Boeing Airplane Co.): I am curious to know what a data system like this would cost.

Mr. Brown: The problem here is that we have looked at the cost per plot of data rather than the overall cost of the system. We found that the cost of producing a power spectral density is very roughly equal to the cost we have at present by using our Technical Products Analyzers. The savings in time by automatic computation, the fact we can automatically calibrate the data, reduces considerably, the man hours involved, although the equipment cost itself is initially considerably higher. I think in our laboratory, the analog-digital conversion equipment has cost us roughly $125,000. Of course

this is spread over a large number of firings and represents probably a lot more capability along with versatility than with a lot of other installations.

Mr. Treadwell (University of California Radiation Laboratory): I would like to know some specific sampling rates that you do plan to use and what type of equipment do you plan in the analog-digital conversion to accomplish the large number of digital input points per unit of time required for digital computation of power spectral density.

Mr. Brown: The analog-digital conversion equipment we have on hand now has been operating for quite some time. We have been using it for various data reductions. Most of our data reduction now is handled in the digital computer. For example, our PDM data is digitized by a similar system. The equipment we have is EPSCO front end with variable sampling rates up to 40,000 per second and used in a multiplex mode with up to 15 channels simultaneously – it will handle a total rate of 32,000 per second. This goes into a tape-to-tape converter which was built for us by EECO to produce the tape format for the IBM 700 series computer.

Mr. Kuoppamaki (Lockheed): What sampling rate do you use when you convert the output of your Technical Products Analyzer to digital terms?

Mr. Brown: We don't actually convert the power spectral density plots to digital. We do this in the computer by sampling the raw data. The sampling rates we use are roughly about four. In an fm/fm system with standard 48 db per octave cutoff filters we are using roughly 2.7 times the cutoff frequency for a sampling rate. This is on the basis of these folding characteristics. For Gaussian filters we need roughly 3.3 times the sampling frequency.

Mr. Kuoppamaki: You did this before feeding it to the analog analyzer itself?

Mr. Brown: Right. All the computing is done in the digital computer by autocorrelation and Fourier transformation.

* * *

SOME INSTRUMENTATION REQUIREMENTS OF A NONPERIODIC 6-ms SAWTOOTH PULSE*†

R. C. Woodbury
Jet Propulsion Laboratory
California Institute of Technology
Pasadena, California

Six-ms sawtooth acceleration pulses have been demonstrated to be particularly suitable for shock testing in the laboratory. The accuracy to which shock machines can be calibrated is related to the spectral characteristics of the sawtooth acceleration pulse generated by them. Failure to observe these characteristics may introduce large calibration errors which may result in serious over testing of a given specimen.

INTRODUCTION

Considerable attention has been directed towards shock testing utilizing 6-ms sawtooth acceleration pulses. As a result of an investigation by Charles T. Morrow and H. I. Sargeant (1) this waveform was demonstrated to be particularly suitable for shock testing in the laboratory. Its use as a standard pulse shape for shock testing was proposed, based upon "the smoothness of the spectrum which results from the extreme asymmetry of the pulse shape" (2) and the ease and simplicity by which it may be produced. To this end, shock machines have been developed and are commercially available. The accuracy to which these machines can be calibrated is related to the spectral characteristics of the sawtooth acceleration pulse generated by them. Failure to observe these characteristics may introduce large calibration errors which may result in serious overtesting of a given specimen.

Shock work necessarily involves the measurement of transient accelerations, i.e., pulses of finite duration not subject to the laws of periodic phenomena. In particular, the sawtooth pulse will always yield a continuous frequency distribution in time with a greatest value at zero frequency, with contributions from higher frequencies decreasing toward zero as the frequency rises. The spectrum will always have the fundamental property of a broad frequency distribution for a pulse of short duration and a narrow one for a pulse of long duration.

The fidelity of reproducing a sawtooth pulse is directly related to the distortionless transmission of all significant frequency components. Deviation from this requirement introduces waveform distortion. The peak amplitude will be suppressed. This suppression is analogous to the failure of a series to sum to the correct value if certain terms are eliminated. In shock work, it is the peak acceleration that is of major interest. The peak acceleration determines the maximum inertial stress applied to a specimen and, hence, is a measure of design integrity.

*This paper was not presented at the Symposium.
†This paper presents the results of one phase of research carried out at the Jet Propulsion Laboratory, California Institute of Technology, under Contract No. NASw-6, sponsored by the National Aeronautics and Space Administration.

For a sawtooth pulse, the degree of amplitude attenuation depends greatly upon which end of the spectrum is attenuated. As the pulse width increases, more and more energy is concentrated in the low-frequency domain. Consequently, the low-frequency components contribute more to the overall pulse geometry than do the higher frequencies. Conversely, a sawtooth pulse of narrow width with a wide frequency distribution will (within limits) be less dependent on the lower frequencies for accurate reproduction.

The desirability of estimating the amplitude reduction or error which will occur when significant low- and high-frequency components of a sawtooth pulse are attenuated is evident when one considers that the accelerometer used to measure this particular forcing function will either have high- or low-frequency limitations, depending on whether or not it is of the strain gage or piezoelectric type.

AMPLITUDE FUNCTION OF A SAWTOOTH PULSE

A sawtooth pulse can be transformed from the amplitude-time to the amplitude-frequency domain by means of Fourier transform analysis. The result is a complex function of the form $G(w) = A(w) + jB(w)$ and is completely specified by Eq. (1).

$$G(w) = \frac{A}{Tw^2}\left[(\cos wT + wT \sin wT - 1) + j(wT \cos wT - \sin wT)\right], \quad (1)$$

where w is the angular frequency variable and T is the pulse width. This form is not completely useful since instrumentation will respond only to its absolute value. This value may be derived by extracting the square root of the sum of the squares of the real and imaginary parts of Eq. (1), from which it may be shown that the absolute value of the spectrum of a sawtooth pulse is given by

$$|G(w)| = \frac{A}{Tw^2}\left[(wT)^2 + 2 - 2\sqrt{(wT)^2+1}\,\sin\left(wT + \tan^{-1}\frac{1}{wT}\right)\right]^{\frac{1}{2}}. \quad (2)$$

This equation is plotted in Figs. 1 and 2 (curves a) for pulse widths of 6 and 12 ms, respectively. It can be seen that a 6-ms sawtooth pulse contains significant frequency components from zero frequency to about

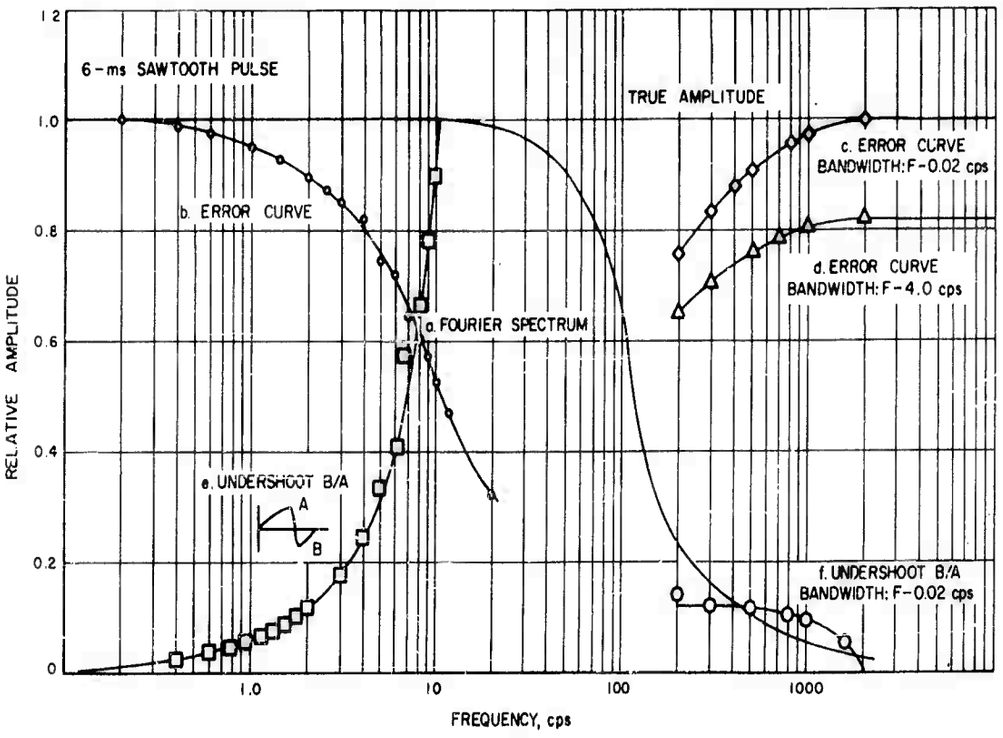

Fig. 1 - Amplitude error vs bandwidth of a 6-ms pulse

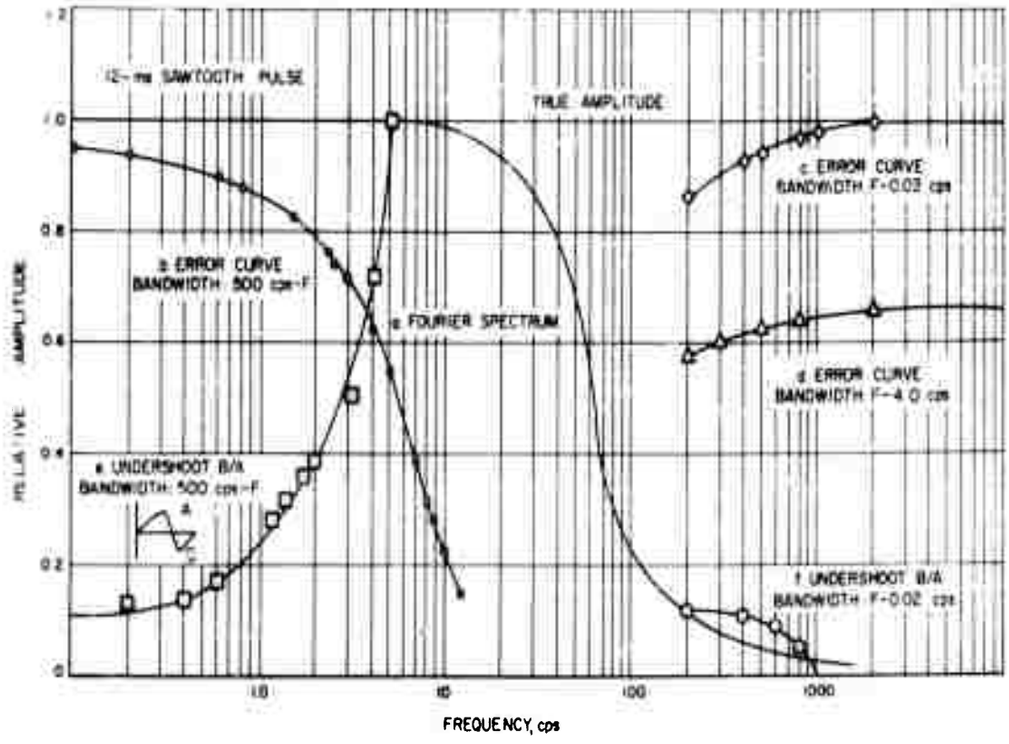

Fig. 2 - Amplitude error vs bandwidth of a 12-ms pulse

2000 cps. This in contrast to a 12-ms pulse, which requires a bandwidth to only 1000 cps.

PEAK AMPLITUDE ERROR OF A SAWTOOTH PULSE VS BANDWIDTH

The difficult mathematical problem of determining the peak amplitude of a sawtooth pulse as a function of bandwidth may be obviated through the use of a simple computer in the form of a gated linear sawtooth generator driving a bandpass filter terminated by a dc-response oscilloscope. By establishing the pulse width with the gate generator and inserting known bandlimits, it is possible to measure the peak positive and negative (undershoot) amplitudes. The block diagram of Fig. 3 represents the system used in this investigation, together with typical waveforms. The first picture (1) typifies the input pulse to the bandpass filter and is the standard of reference. Extending the high-frequency cutoff beyond 2 kc and the low-frequency response to dc will produce no measurable change in the reference pulse, providing evidence that these frequencies are not significant. The extreme left-hand column portrays the effects of low-frequency cutoff, while the top row shows the effects of high-frequency cutoff. The remaining pictures are intermediate effects. Comparison to Fig. 4 shows that as the pulse width increases, the pulse distortion becomes greater for a given bandwidth, and that the low-frequency cutoff is indeed very critical.

Curve b, Fig. 1, is a plot of the ratio of the measured peak amplitude to the true peak amplitude in terms of low-frequency cutoff. If all significant frequencies are passed, there will be no pulse distortion and hence, no amplitude attenuation. If all frequency components below 4 cps are suppressed, the peak positive amplitude will be only 80 percent of the true value. Doubling the cutoff frequency to 8 cps reduces the peak amplitude to 60 percent of the true value. Curve c is a plot similar to curve b, except that the parameter is the high-frequency cutoff. A system cutting off at 500 cps will introduce a 9-percent error in the data, while a system responding to only 200 cps will produce a 25-percent error. Curve d emphasizes the fact that a constant error will exist for a given low-frequency cutoff. This error is compounded as the high-frequency response is reduced. In general, accelerometers and associated

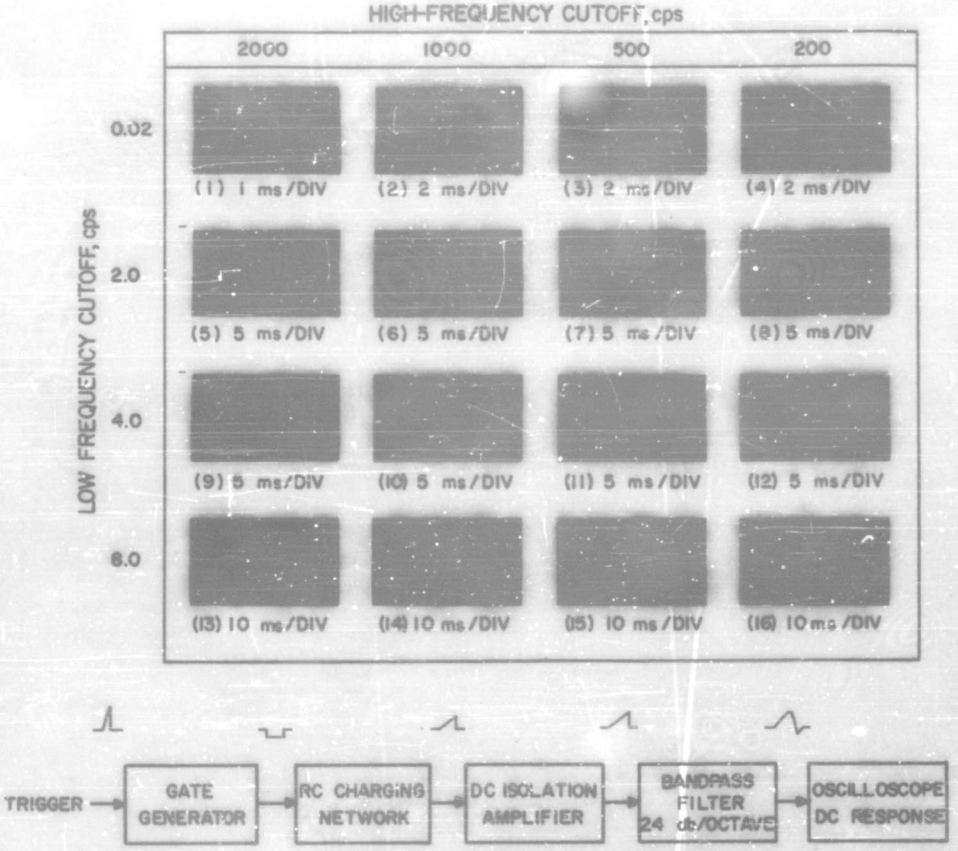

Fig. 3 - Geometry of a 6-ms nonperiodic sawtooth waveform as a function of bandwidth

instrumentation will have bandwidths falling within the limits defined by curves c and d. The low-frequency roll-off may be inherent in the instrumentation. The high-frequency response may be intentionally restricted. Consequently, errors as great as 35 percent could easily be encountered.

Curves e and f predict undershoot. They are plotted as the ratio of peak negative to peak positive amplitudes. The high frequencies contribute less to undershoot than do the low-frequency components. Obviously, attempts to measure "negative" acceleration may lead to large errors if the low-frequency response is insufficient.

The curves of Fig. 2 are similar to those of Fig. 1. They are included in an attempt to show that the high-frequency requirements of the accelerometer instrumentation tend to become less severe as the sawtooth pulse width is increased. This is in contrast to the low-frequency requirements.

ACCELEROMETERS

Acceleration is generally measured by one of two types of accelerometers: piezoelectric or strain-gage. Either accelerometer has advantages not found in the other. For shock work, the choice of accelerometer may greatly influence the accuracy of the data. Such a choice must be guided by the nature of the acceleration pulse. It cannot be overemphasized that the broadness of the Fourier spectrum of a given pulse bears an inverse relationship to its pulse width. Thus, narrow acceleration pulses (less than 1 ms), possessing broad spectra, might be adequately monitored by piezoelectric accelerometers, whereas a pulse of large width (in the 10-ms region) might be

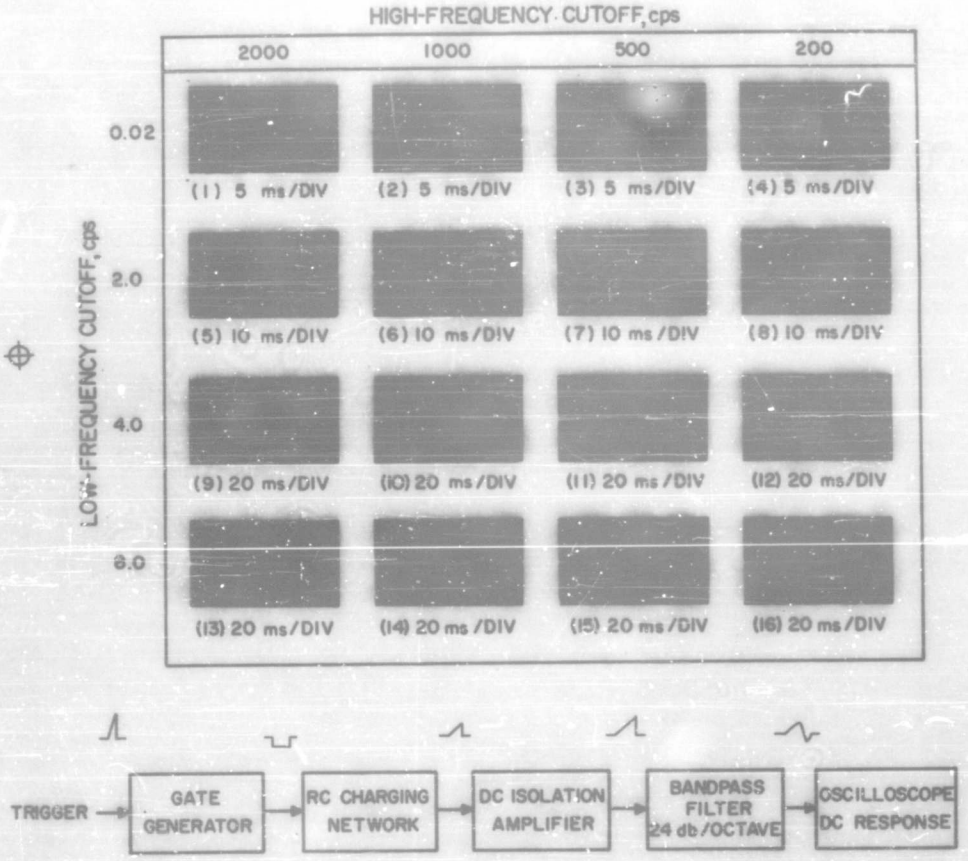

Fig. 4 - Geometry of a 12-ms nonperiodic sawtooth waveform as a function of bandwidth

completely distorted because essential low-frequency components are attenuated. In such an event, a strain-gage accelerometer may prove adequate.

A large and easily available literature exists on accelerometers. Therefore, a detailed discussion of these transducers would be redundant. However, there are certain salient points which bear reiteration and must be considered in the selection of an accelerometer system for pulse work.

Piezoelectric Accelerometers

The large dynamic range (to 10,000 g) and extremely high-frequency response (to 50 kc) are unique characteristics of piezoelectric accelerometers. A serious disadvantage for pulse work involving large pulse widths is their low-frequency limitations. A piezoelectric accelerometer generates a charge by virtue of the deformation of its piezoelectric crystal. Thus, it is an inertial device. A continuous acceleration must produce a continuous deformation, and hence, a voltage. In practice, however, the zero frequency response is only approached because the reactance of the crystal becomes very high when compared with its low resistance and the input impedance of the network which terminates the transducer. In other words, the low-frequency response is determined by the input impedance of the required matching amplifier. The best available accelerometer has a low-frequency response within ±5 percent to 0.6 cps, subject to the condition that it sees an impedance of 100 meg. If the input signal characteristics cause grid current to flow, the effective input impedance will decrease, causing an increase in the low-frequency cutoff. The corresponding attenuation of low frequencies may introduce pulse distortion. This may be greater than that experienced under the same

conditions if the generator exhibited a low internal impedance. Another factor (often neglected) which will reduce the effective input impedance to plate-loaded triode matching amplifiers is the effect of grid-to-plate capacitance. If the plate load is partially reactive, the input impedance is equivalent to a capacitance and a resistance in parallel from grid to cathode. The effective input capacitance is directly proportional to the grid-to-cathode capacitance, the grid-to-plate capacitance, the gain, and the cosine of the phase angle by which the voltage across the load impedance leads the equivalent voltage acting in the plate circuit. The effective input resistance is inversely related to the product of frequency, grid-to-plate capacitance, and the sine of the phase angle described above. The loading effect of this dynamic input impedance is usually not important when the signal source has a low impedance but may be serious when the generator is a piezoelectric accelerometer which has a very high internal impedance.

The evaluation of piezoelectric transducer systems for use in shock work by periodic waveforms (sinusoids, square waves, etc.) may not be sufficient to describe performance in terms of nonperiodic phenomena. One reason for this is that nonperiodic functions are composed of a continuum of frequencies in contrast to the discrete spectra of periodic functions. Thus, for example, a system cutting off at 10 cps will transmit accurately a 6-ms periodic sawtooth wave which contains all of its energy above 166 cps but will introduce considerable distortion to its nonperiodic counterpart, which contains most of its total energy below 100 cps. Indeed, testing the same system with a nonperiodic pulse may not be sufficient. Thus, the above system would fail to pass a 500-ms sawtooth pulse which has a narrow spectrum but would pass a 12-ms sawtooth pulse which has a broad spectrum. In addition, an amplifier that will pass a pulse generated by a low-impedance generator provides no assurance that it will transmit the same pulse if it is delivered by a high-impedance source such as a piezoelectric transducer.

In general, instrumenting shock machines with piezoelectric accelerometers may result in data subject to large errors because the true forcing function may undergo degradation through dynamic shifts in the response characteristics of the matching amplifier and accelerometer.

Strain-Gage Accelerometers

Strain-gage accelerometers have a frequency response from dc to an upper value determined by the seismograph system comprising the accelerometer. Invariably, commercial accelerometers are damped at 0.707 of critical damping. This is an optimum value which gives a flat frequency-response curve out to about 0.35 times the natural frequency of the seismic mass. The response will be down 3 db at the natural frequency. In addition, this value of damping provides a more linear phase-shift curve than is possible with other values. One commercially available accelerometer has a natural frequency of 1560 cps. Its useful frequency range extends from zero frequency to about 1092 cps. This bandwidth will introduce an 8-percent error if the forcing function is a 6-ms sawtooth pulse. Since the accelerometer is damped at 0.707 of critical, it will not ring, and all frequencies beyond the natural frequency will be attenuated. This may eliminate the need for external filtering.

The sensitivity and output impedance of strain-gage accelerometers are low. These characteristics simplify instrumentation problems. The output voltages are in the millivolt region. Consequently, electrical overload problems do not exist (in contrast to piezoelectric accelerometers, which may generate volts). The low output impedance permits the use of direct instrumentation, eliminating the necessity for complicated matching amplifiers. One possible limitation for pulse work is the high-frequency response. Strain-gage accelerometers may not be suitable for pulses which contain appreciable high-frequency components (narrow pulses, for example). The nature of the pulse must be established before these accelerometers can be used with confidence.

CONCLUSION

It was shown that the low-frequency requirements of a 6-ms sawtooth acceleration pulse demand careful selection, calibration, and operation of the transducer system used to measure it. The use of a piezoelectric accelerometer may introduce large errors because of the difficulties of maintaining the necessary high input impedance to the matching amplifier under transient conditions. A 10-percent error in the peak

amplitude of a 6-ms sawtooth pulse requires a bandwidth from 2 cps to 2000 cps. Experience has shown that a system having a 2-cps response, as measured under steady-state conditions, may actually have a response to only 8 cps under transient conditions. This is sufficient to introduce a 36-percent error in the peak amplitude of a 6-ms sawtooth pulse. By contrast, strain-gage accelerometers respond to dc but have high-frequency limitations. However, commercial accelerometers are available with sufficient high-frequency response to insure errors no greater than 8 percent. In general, strain-gage accelerometers are to be preferred in the instrumentation of 6-ms sawtooth acceleration pulses because of their stable frequency characteristics under steady-state or transient conditions.

It must be emphasized that, regardless of the type of accelerometer instrumentation used to monitor a sawtooth acceleration pulse, any evidence of undershoot which is not demonstrable "negative" acceleration must ultimately lead to the conclusion that the bandwidth is not commensurate with the frequency requirements of the pulse. Indeed, the existence of undershoot implies amplitude attenuation; the greater the undershoot, the greater the error.

BIBLIOGRAPHY

1. Charles T. Morrow and Homer I. Sargeant, "Sawtooth Shock as a Component Test," J. Acoust. Soc. Am., 28:5, 1956.

2. Ibid.

3. T. F. Hueter and R. H. Bolt, Sonics, John Wiley and Sons, New York, 1955, Ch. 4, pp. 126-130, 152-157; Ch. 8, pp. 377-382.

4. C. L. Cuccia, Harmonics, Sidebands, and Transients in Communication Engineering, McGraw-Hill Book Co., Inc., New York, 1952, Ch. 3, pp. 44-54.

5. Endevco Corp., "Instructions for Applications and Use of Piezoelectric Transducers," Bulletin 2, 31-2000, Pasadena, Calif.

6. Gifford White, "Response Characteristics of a Simple Instrument," Statham Instrument Notes Number 2, April-May 1948.

7. E. Weber, Linear Transient Analysis, John Wiley and Sons, 1956, Ch. 1, pp. 7-16.

8. Reference Data for Radio Engineers, 4th ed., American Book-Stratford Press, Inc., New York (for Int. Tel. and Tel. Corp.), 1956, pp. 1012-1015.

9. F. J. M. Farley, Elements of Pulse Circuits, John Wiley and Sons, New York, 1955, Ch. 1, pp. 3, 14-16; Ch. 2, pp. 27-36; Ch. 4, pp. 84-88, pp. 97-100

10. F. Langford-Smith, Radiotron Designer's Handbook, 4th ed., Harrison, New Jersey, RCA Division Radio Corp. of America, Ch. 12, pp. 493.

* * *

INTRODUCTION TO SHOCK AND VIBRATION SIMULATION

R. M. Mains
Knolls Atomic Power Laboratory
Schenectady, New York

Shock and vibration testing or simulation are essential for demonstrating what improvements can be or have been made in the design, for determining the adequacy and acceptability of the design, and for controlling the quality of the product. These various functions of testing or simulation are discussed in this paper.

INTRODUCTION

The service life of many kinds of equipment today involves exposure to dynamic loads. These dynamic loads are referred to as "shock loads" when they are of short duration and produce transient responses of the equipment, and as "vibration loads" when they persist long enough to produce essentially steady-state oscillatory responses of the equipment. With equipment that is structurally complex (many possible modes of response), the structural responses to dynamic loads are difficult to predict by calculation with any surety. Even more difficult to predict is the damage produced by the structural responses, so that some substitute for calculation is desirable. The natural substitute for calculation is testing, of the actual equipment if possible, or of portions or scale models of the equipment if the actual equipment is too big to test or not available.

THE PROBLEM OF DYNAMIC DESIGN

Before we pursue the subjects of shock and vibration further, let us look briefly at the overall problem of dynamic design, so that we may see how much of the picture involves testing and where it fits. For this purpose consider Fig. 1, which is an attempt to portray the dynamic design problem as a flow chart from concept to finished product. The problem begins with the conception of a need for an item which can perform a desired function with some minimum reliability and within some limiting cost. The next step, area 1 in the chart, consists of defining the loads to which the item will be subjected in service. From these loads, a design basis and a set of failure or damage criteria are then distilled, as in area 2 of the chart. Then a preliminary design is developed and its responses to the design loads are calculated. Parallel with this, a test is devised so that responses to various loads can be measured as a check against the calculations. Discrepancies between calculation and measurement are resolved, and the design is refined and carried through the production sequence to the finished article.

Now let us consider portions of this overall picture that are properly included in what we call testing or simulation. Of first concern is the measurement of the service environment, with its attendant problems of instrumentation and data processing, since special tests may need to be devised in order to measure different aspects of the environment. The interpretation of environmental measurements and their translation into design requirements are properly associated with testing or simulation since the significance of data is so intimately dependent

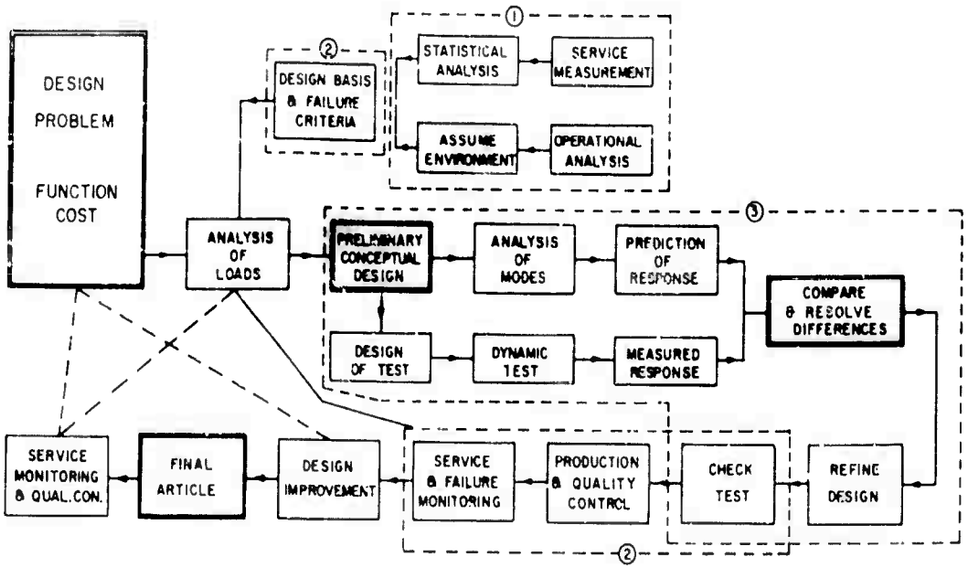

Fig. 1 - Flow chart for dynamic design

upon the end instruments used, their location, their calibration, and the whole data gathering and processing operation.

The establishment of a design basis in terms of loads, design procedures, test procedures, and failure criteria again involves testing and simulation. It may well be necessary, for example, to devise some tests that simulate the environmental loads, and then to subject various items that will be involved in the design to these tests in order to determine modes of failure and significant parameters. In other words, the failure or damage processes for items in the design must be understood (to some extent at least) before intelligent failure criteria can be established. Ideally, what is desired is a test such that the same damage processes are developed (perhaps at an accelerated rate) in the test as would be developed in service. This is true simulation or environmental testing.

The next step in the design chart involving testing or simulation is the set of tests devised to provide measured responses of a prototype or model for the purpose of checking the design calculations. This is design development testing for which a high degree of simulation of environmental loads may not be required: load intensities may be reduced, durations may be shortened, and the environmental loads may be separated or simplified so that better checking of the design calculations can be done.

Then after the design is refined and made final, we come to the box in the chart labelled "Check Test." This is the operation of "type testing" or "prototype acceptance testing," for which the ultimate in realism of simulation is desired. The more environmental loads that can be combined in this test the better, for in this way the interaction of various damage processes is developed.

The production and quality control box in the chart involves testing, but not necessarily a simulation of environmental loads. The best quality control test is the cheapest, quickest one which insures adequate quality. It does not need to bear any direct resemblance to an environmental load.

So it should be clear that simulation of, or testing within, a shock and vibration environment is interwoven through the whole dynamic design problem, from measurement of loads to quality control of the final product. In all of this, the key words are "damage process," since the objective of design is to produce a required level of reliability of function (or lack of damage). This objective can only be fulfilled if we can establish what factors in the service environment are potentially damaging to the item being designed, in what way such damage develops, and how it can be reduced or eliminated. At present we have but a small understanding of damage processes and consequently rely heavily on experience, intuition, and testing. With proper observation and accumulation of

quantitative data our understanding can be significantly increased in a relatively short time.

THE FUNCTIONS OF TESTING

In every dynamic design problem there are but three factors operating: (1) the excitation or load, (2) the response of the intervening structure to the excitation, and (3) the resistance of the particular item to damage. To minimize damage we have the choice of alleviating the excitation, reducing the response of the intervening structure, or increasing the damage resistance of the item. Shock and vibration testing or simulation are essential for demonstrating what improvements can be or have been made in the design, for determining the adequacy and acceptability of the design, and for controlling the quality of the product. These various functions of testing or simulation will now be discussed in more detail.

Design Development Testing

Testing during design development has two usual functions: the determination of the fragility levels and the damage processes for various items to be used in the design, and the determination of the response characteristics of the design. The determination of fragility levels and damage processes may be illustrated by the following example:

Consider a relay to be used in the electronic control system of a missile. Assume that a study of service vibration and shock in missiles of similar speed and propulsion method, but different in size, has revealed that:

1. Transportation, stowage, and storage of the missile (1) will probably involve long continued periods of relatively low-frequency and low-amplitude vibrations. These vibrations will be essentially at discrete frequencies, but of varying amplitude over long periods of time. The frequency will range from 2 to 500 cps at amplitudes from 0.5 g for trucks and ships to 10 or 12 g for railroads and aircraft.

2. Transportation shocks are likely to be as great as 200 g over the spectrum from a few cycles to 1000 cps, according to the particular carrier involved.

3. Missile flight vibration (2) is likely to consist of a broadbanded noise-type excitation with an acceleration spectral density of 0.1 to 0.2 g^2/cps over the range from 10 to 3000 cps.

Of course the relay will see as its excitation the responses of the intervening missile structure to these excitations, so we are concerned over the types of excitation rather than the specific amplitudes. Our problem is now defined as: how does the relay react to discrete frequency vibration, noise-type vibration, and shock? In so reacting, at what level of excitation does the relay begin to malfunction, by drop-out, chatter or fracture? The answers to these questions are determined by mounting the relay on a rigid (first mode resonance above 3000 cps, if possible) fixture and applying the different excitations to it at increasing severity until malfunction occurs. Specifically, if chatter is called damage level 1 and drop-out is called damage level 2, a sinusoidal vibration test could produce curves like Fig. 2. A vibration test with 3 sinusoids in fixed frequency and amplitude ratios could produce curves like Fig. 3. Noise-type vibration testing with flat spectra could produce a curve like Fig. 4. Shock testing with a half-sine pulse could produce results like Fig. 5. Data such as these are needed for each of the items involved in the design and can be obtained only by testing with a proper simulation of the character of the excitation, carried to levels which produce specific damage.

It is particularly worthwhile to note that, for this kind of testing in which the damage characteristics of a component are sought, the test fixture must be rigid enough (first-mode resonance sufficiently high) that its behavior does not affect the results. If a

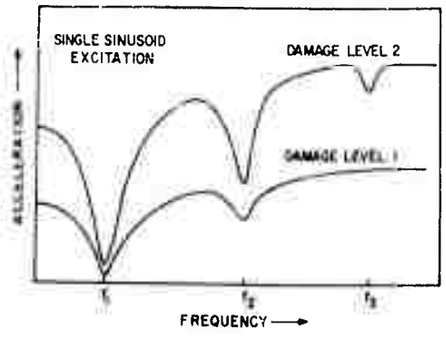

Fig. 2 - Frequency vs acceleration for various damage levels

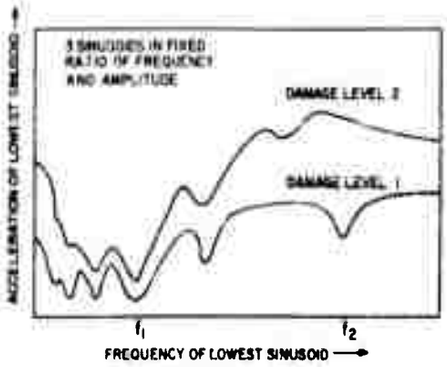

Fig. 3 - Frequency and acceleration of lowest sinusoid for various damage levels

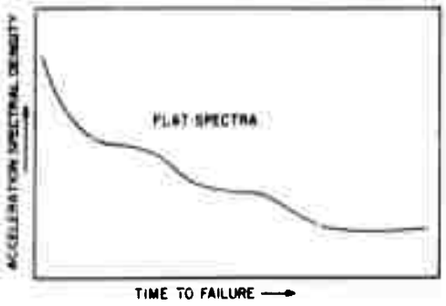

Fig. 4 - Acceleration spectral density vs time for specific damage level

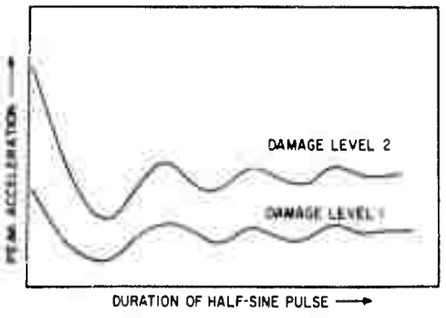

Fig. 5 - Duration and peak acceleration of half-sine pulse for various damage levels

sufficiently rigid fixture cannot be devised, then the instrumentation must be so arranged that the excitation of the component is measured, not the input to the fixture. Otherwise the data are specific for the fixture and testing machine used, and cannot be carried over into other situations.

For the second part of the design-development testing problem, we are concerned with the responses of the structure intervening between the components and the excitation source. The purpose is to determine by measurement the response characteristics, either for verification of predicted behavior or because the structure is too complex to permit a reliable prediction. The items of particular interest are: resonant frequencies, mode shapes at resonances, magnification factors or transmissibilities, effect of nonlinearities on these properties, and shock-response characteristics. In addition, it may be desirable to compare the relative merits of alternate designs, so as to be able to select the most favorable design. All of these things can be done with sinusoidal testing, provided that one is willing to do some computing. This is so because, at least for linear responses, the normal modes and frequencies and the transmissibility spectra are enough to predict the response to any excitation. Noise-type vibration testing and shock testing are needed, however, to determine the effects of nonlinear responses and of excitations which are in between vibration and shock.

Consider, for example, the same missile control system into which the relay of our previous example is to fit. The intervening structure between the relay and the excitation source might consist of a portion of the missile airframe, a control package frame, a chassis plate or deck, and a relay mounting bracket. The problem is to determine the responses at the mounting bracket, with the relay in place, of this series of structures to various excitations of the airframe. Where does one start? With what specimen and test fixture?

The procedure here is dependent upon the available testing equipment. With sufficiently large capacity equipment, the entire missile could be shaken while the transmissibility from the service source of excitation to the relay bracket were measured. This is rarely possible, either for lack of machine capacity or because of the nonexistence of a complete missile at the design-development stage. Fortunately, alternative procedures are available. The portion of the missile airframe to which the control package frame attaches plus a length from 1/2 to 1 airframe diameters on either side of the package mounting points can usually be used to get good transmissibility data. Also the various links in the structural chain can be measured for

mechanical impedance vs frequency separately, or in convenient combinations. To measure mechanical impedance between two points in a structure, it is necessary to measure the ratio of force to velocity for various frequencies at point 1 while point 2 is held fixed. The ratio of force to velocity at point 2 is then measured for various frequencies while point 1 is held fixed. These measurements then establish the four-pole parameters (3) for the structure from which the transmissibility can be calculated. This is a good procedure since it requires smaller equipment than the previously discussed methods, and it has the virtue of making it easier to determine which link in the structure needs modification and in what way. Whatever the method used, the transmissibility (or amplification factor vs frequency) from the service source of excitation to the point of interest is the desired function, since this is sufficient to establish resonant frequencies, amplification factors, and responses to the various shock and vibration inputs.

Prototype Acceptance Testing

The sole purpose of prototype acceptance testing is exactly implied by the name: to determine the capacity of a design to withstand its intended service environment so that its acceptability may be evaluated. Ideally, such testing would reproduce exactly the various damaging effects of the service environment, both in kind and in magnitude. Practically, it is rarely possible to do this because:

1. The service environment is not known exactly for a new design.

2. The service environment is too costly to reproduce in the laboratory in all of its details and complexity.

3. The service environment may cover years of time, while laboratory tests must be completed in a much shorter time to be of use.

As a consequence, if prototype acceptance testing is to fulfill its purpose, it must produce the same damage processes in the equipment as the service environment would produce, and usually at an accelerated rate of damage.

As an example, consider the same relay in a guided missile control package as before. In discussing design development testing above, the transportation vibration, transportation shock, and missile flight vibration were defined in kind and magnitude. The design development tests of the relay would have served to establish that the relay would malfunction or be damaged by one of the following procedures:

Drop-out or chatter resulting from excessive acceleration in shock, or from too high a spectral density in noise-type vibration. The same failure could occur under sinusoidal vibration at too high an amplitude or at a resonance frequency.

Fatigue and fracture of some part of the relay, structural or electrical, as a result of sustained vibration of either type.

Fracture of some structural or electrical part of the relay as a result of excessive shock.

Specific levels of excitation at the relay at which these phenomena develop are not the problem in acceptance testing. Rather it is the excitation level at the environmental source when the failure occurs that is of interest. Consequently, the test must be designed to produce this answer, and to determine the margin of safety between the environmental excitation level and the failure level. To do this properly requires either the complete control package, or some portion of it for which the electrical functioning can be monitored during testing. This complete package, or portion of the package, is then mounted on a correct structural mock-up (test fixture) of the support of the package such that:

The test article and its support show the same mechanical impedance to the testing machine as the actual missile components would show at the comparable support points.

The testing machine shows the same mechanical impedance to the test article and its support as they would see in the missile.

The point of attachment of the test article and its support to the testing machine is such that the motion of this point in service is either known by measurement or predictable by reliable calculation.

Once these conditions have been satisfied, it remains to apply through the testing machine the various kinds of service loads. These loads should be commenced at about

half the service magnitude, and increased in steps until a failure occurs for each kind of load. (It may be desirable to repair the first failure and continue until more failures are developed.) It should be observed that it is not enough simply to conduct a go-no-go test at service magnitude, because failures have a statistical distribution. The fact that one prototype passed such a test does not assure that any other article will pass the same test – in fact the probability of such success is only 50 percent. The stepwise testing to failure recommended above does make possible a determination of the margin by which the prototype passed the test and a better determination of the probability of success of subsequent articles.

For the determination of the margin of safety, account must be taken of the fact that a series of tests of increasing severity have been administered. One rule for establishing the margin of safety under such conditions that has been proposed (4) but is as yet unchecked by tests is:

$$MS = \sum_i \left(\frac{S_i}{S_s}\right)^k - 1 ,$$

in which MS = margin of safety,

S_i = severity of the i^{th} test step,

S_s = severity of the standard or specification test,

k = 5 if stress fatigue is the mode of failure, or 2 if plastic strain fatigue is the mode of failure,

$\sum_i$ is performed for all the test steps to failure.

This relationship assumes that all test steps have the same duration or involve the same number of stress or strain cycles. Additional factors could be included to account for different time durations, such as:

$$\left(\frac{t_i\ S_i}{t_s\ S_s}\right)^k \quad \text{instead of} \quad \left(\frac{S_i}{S_s}\right)^k$$

in which t_i is the duration of the i^{th} test step and t_s is the duration of the standard test. For example, if the series of test severities, S_i/S_s, each at 1/2 the standard duration were: 0.5, 0.75, 0.90, 1.00, 1.20, 1.30, 1.40, failure at 1.50, then the MS would be 1.24 for $k = 2$ and -0.53 for $k = 5$. This serves to illustrate the importance of establishing what the mode of failure is, or perhaps more properly, what the value of k is.

For the determination of the probability of success of subsequent articles, it is necessary to use the theory of finite sampling and reliability. These are available in standard texts (3) and need not be discussed in detail here.

Quality Control Testing

Probably the best quality control testing would consist of the application of the prototype acceptance test to a properly sampled sequence of production articles. Much has been done in this field (6), so much so that it would be presumptuous to attempt a brief summary here. A discussion of other feasible quality control tests would seem to be in order, however. For this purpose, the aim of quality control testing will be stated as the surveillance of production in such a manner as to insure a high probability of success in the event that any production article is subjected to a prototype acceptance test. It is not generally economical to strive for nearly 100 percent probability of success – rather some acceptable failure or rejection rate should be established as a compromise between the cost of producing reliability and the cost of probable failure. Each problem is different in this compromise, and so should each solution be.

For illustration, let us return once more to the control package for a guided missile. For this kind of equipment, it usually works out that some form of vibration test is best for quality control. In order of effectiveness, this quality-control vibration test would consist of:

1. A short-duration noise-type vibration test – perhaps with the excitation spectrum shaped to emphasize particularly troublesome frequency bands.

2. An automatic sweep of a sinusoidal excitation from high to low frequency – with amplitude and sweep rate controlled automatically to emphasize those frequency bands most likely to produce signs of failure.

3. A manually controlled sweep of a sinusoidal excitation – used in place of the automatic sweep as an interim measure.

Comments made above with regard to the test fixture in the section on prototype acceptance testing also apply to quality control testing. In addition, it is especially desirable to establish the severity and duration of the quality control test so that only some small portion of the probable life of the package is consumed in the test, say 10 to 20 percent. This may be determined only after prototype acceptance tests to failure have been conducted to establish what the probable life of the package is. A relationship such as

$$\left(\frac{S_t \times t_t}{S_s \times t_s}\right)^k = 0.1 ,$$

in which S_t = severity level of test,

S_s = severity level of standard acceptance test,

t_t = time of quality control test,

t_s = time to failure at standard acceptance test level of severity,

k = the same material constant discussed in the section on prototype acceptance testing,

would serve to establish the quality-control test level at the outset, until experience accumulated to dictate a change.

Some precautionary comments on sweep testing are offered here for their applicability to quality control testing (and acceptance and development testing as well). For a single-degree-of-freedom system, a number of cycles equal to the magnification factor is required for the amplitude response to rise from zero to 95 percent of its maximum. If this time is called τ, then a sinusoidal excitation sweep which stayed within the bandwidth, Δf_n, of the resonance of the system for a time τ should allow nearly full response of the system to develop.

$\tau \times f_n$ = number of cycles at resonance, f_n, in time τ. Then if $\tau \times f_n = Q$, or magnification factor and since

$$Q = \frac{f_n}{\Delta f_n} ,$$

$$\tau = \frac{1}{\Delta f_n} .$$

If the sweep rate is r cps/sec, then

$$r = \frac{\Delta f_n}{\tau} = (\Delta f_n)^2 = \frac{(\Delta f_n)^2}{f_n^2} \cdot f_n^2 .$$

$$r = \frac{f_n^2}{Q^2} .$$

This result suggests that the proper way to program a sinusoidal excitation sweep is to determine the largest value of Q that needs to be allowed to develop to near-maximum response, and then program the sweep rate to be maintained at f^2/Q^2_{max}. This would insure that high-frequency systems did not receive an unduly long excitation and so seem to be poorer in quality than they actually were.

This principle of sweep-rate control, together with the previously discussed one of limited life consumption control should be sufficient to point the way toward quality control testing which controls quality, rather than wears out the test article before it can see service. These same principles are important also in design development testing and in prototype acceptance testing. How much weight to place on these factors, and others discussed above, is a matter for individual judgment, to be carefully checked against experience with any particular article and modified as necessary all the way through the dynamic design problem. Dynamic design requires a dynamic approach to the testing that goes with it.

REFERENCES

1. Elias Klein (editor), "Fundamentals of Guided Missile Packaging," Dept. of Defense No. RD 219/3, July 1955, Chapter 6.
2. Ibid. Chapter 5.
3. C. T. Molloy, "Use of Four-Pole Parameters in Vibration Calculations," Jour. Acoust. Soc. Am., 29:842 (1957).
4. R. M. Mains, "A Generalization of Cumulative Damage," ASME Paper 59-MET-1.
5. H. A. Freeman, M. Friedman, F. Mosteller, and W. A. Wallis, Sampling Inspection, McGraw-Hill, 1948.
6. J. M. Juran, Quality Control Handbook, McGraw-Hill, 1951.

* * *

PARAMETRIC STUDY OF RESPONSE OF BASE-EXCITED TWO DEGREE-OF-FREEDOM SYSTEMS TO WHITE NOISE EXCITATION*

Allen J. Curtis and Thomas R. Boykin, Jr.
Hughes Aircraft Company

The response of a two degree-of-freedom system to white noise excitation is obtained analytically for a wide variation of the dimensionless parameters of the system. The interrelations of these parameters on the response are illustrated and shown to be very significant when the uncoupled natural frequencies of the system are of the same order. The limitations of approximation methods based on a single degree-of-freedom system model are indicated. The applicability of the study to dynamic vibration absorber principles is evident. The responses are compared with previously published experimental results.

INTRODUCTION

In the study of the response of mechanical systems subjected to arbitrary inputs, ideally it is desirable to know the precise motions of all the masses in the systems. When the systems themselves are generally unknown, and when the inputs are random, then the assumptions made in estimating the effects of the excitations sometimes become excessive.

To achieve some understanding of the effects of random vibration in general, one of the first obvious steps is to determine the response of a single degree-of-freedom system. This is easily found by a simple closed expression. However, although the expression for this mean-square response is easily obtained, there is no indication of the effect of other masses when added to the first, and of course no indication of the response of these added masses. It is to extend this understanding that the two degree-of-freedom system has been studied.

Figure 1 illustrates a two-degree-of-freedom system excited by motion of the base. A number of practical vibration problems may be analyzed in terms of such a system. For example, the lower mass may be visualized as basic structure excited by the random motion of the base while the upper mass represents an equipment mounted on that structure. Alternatively, the base motion may be considered as the structural excitation of the equipment represented by the lower mass while the upper mass represents a chassis or component mounted within the equipment.

The dynamic characteristics of a two-degree-of-freedom system are determined by the following dimensionless parameters: (1) the mass ratio $M = m_2/m_1$, (2) the frequency ratio $W = \omega_2/\omega_1$ between the uncoupled natural frequencies of each spring-mass system, and (3) the damping factors, S_1 and S_2, associated with each spring-mass-dashpot system. The variation of the response of the system to white-noise excitation is examined for a

*This paper was not presented at the Symposium.

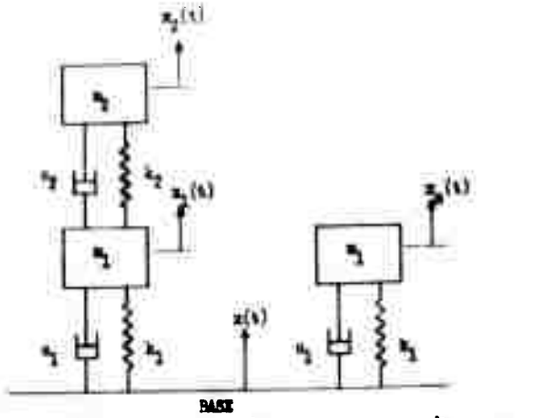

$$\omega_1^2 = \frac{k_1}{m_1} \qquad \omega_2^2 = \frac{k_2}{m_2} \qquad \omega_s^2 = \frac{k_1}{m_1} = \omega_1^2$$

$$S_1 = \frac{c_1}{2m_1\omega_1} \qquad S_2 = \frac{c_2}{2m_2\omega_2} \qquad S_s = \frac{c_1}{2m_1\omega_1} = S_1$$

$$M = m_2/m_1 \qquad W = \omega_2/\omega_1$$

$$\beta_1 = \overline{\left[x_1(t)\right]^2} \qquad \beta_2 = \overline{\left[x_2(t)\right]^2} \qquad \beta_s = \overline{\left[x_s(t)\right]^2}$$

Motion of base, x(t) is random with constant spectral density, i.e. "white noise".

Fig. 1 - Base-excited two-degree-of-freedom system

wide variation of these dimensionless parameters.

DERIVATION OF RESPONSE

The two-degree-of-freedom system analyzed in this study is shown in Fig. 1, together with the single degree-of-freedom system used for normalization and comparison purposes. The usual assumptions regarding linearity, rigid masses, massless springs, and viscous dampers are made.

The equations of motion of the two-degree-of-freedom system are

$$m_1\ddot{x}_1 + c_1(\dot{x}_1 - \dot{x}) + c_2(\dot{x}_1 - \dot{x}_2) + k_1(x_1 - x) + k_2(x_1 - x_2) = 0 , \quad (1)$$

$$m_2\ddot{x}_2 + c_2(\dot{x}_2 - \dot{x}_1) + k_2(x_2 - x_1) = 0 ,$$

while the equation of motion of the one-degree-of-freedom system is

$$m_1\ddot{x}_1 + c_1(\dot{x}_1 - \dot{x}) + k_1(x_1 - x) = 0 . \quad (2)$$

It is convenient to express these equations in terms of the following dimensionless parameters:

$\omega_1 = \sqrt{k_1/m_1}$ = undamped natural frequency of lower mass with upper mass removed (rads/sec).

$S_1 = c_1/2m_1$ = viscous damping factor of lower mass with upper mass removed.

$\omega_2 = \sqrt{k_2/m_2}$ = undamped natural frequency of upper mass if lower mass is blocked or fixed (rads/sec).

$S_2 = c_2/2m_2\omega_2$ = viscous damping factor of upper mass if lower mass is blocked or fixed.

$\omega_s = \sqrt{k_1/m_1} = \omega_1$ = undamped natural frequency of one-degree-of-freedom system.

$S_s = c_1/2m_1\omega_1 = S_1$ = viscous damping factor of one-degree-of-freedom system.

$M = m_2/m_1$ = mass ratio of two-degree-of-freedom.

$W = \omega_2/\omega_1$ = frequency ratio of two-degree-of-freedom system.

Equations (1) and (2) may then be written in the form:

$$\ddot{x}_1 + (2S_1\omega_1 + 2S_2\omega_2 M)\dot{x}_1 + (\omega_1^2 + \omega_2^2 M)x_1 - 2S_2\omega_2 M\dot{x}_2 - \omega_2^2 M x_2 = 2S_1\omega_1\dot{x} + \omega_1^2 x \qquad (3)$$

$$-2S_2\omega_2\dot{x}_1 - \omega_2^2 x_1 + \ddot{x}_2 + 2S_2\omega_2\dot{x}_2 + \omega_2^2 x_2 = 0,$$

for the two-degree-of-freedom system and

$$\ddot{x}_1 + 2S_1\omega_1\dot{x}_1 + \omega_1^2 x_1 = 2S_1\omega_1\dot{x} + \omega_1^2 x, \qquad (4)$$

for the one-degree-of-freedom system.

Response to Harmonic Basic Base Excitation

If the motion of the base is harmonic, $x(t) = Xe^{i\omega t}$, the response of the upper and lower masses are well-known to be

$$x_1(t) = \bar{X}_1 e^{i\omega t} = X_1 e^{i(\omega t - \theta_1)},$$

$$x_2(t) = \bar{X}_2 e^{i\omega t} = X_2 e^{i(\omega t - \theta_2)}, \qquad (5)$$

where

$$\bar{X}_1 = \frac{(-r^2 + ir2S_2W + W^2)(ir2S_1 + 1)X}{|D|},$$

$$\bar{X}_2 = \frac{(2irS_2W + W^2)(ir2S_1 + 1)X}{|D|},$$

$$|D| = \left(-r^2 + (1 + W^2M) + ir(2S_1 + 2S_2WM)\right)(-r^2 + ir2S_2W + W^2) - M(2irS_2W + W^2)^2,$$

where

$i = \sqrt{-1}$

$r = \omega/\omega_1$ = the ratio of the excitation frequency to the undamped natural frequency of the lower mass.

$|D| = 0$ is the frequency equation of the system.

X_1 and X_2 are the response amplitudes,

θ_1 and θ_2 are the response phase angles.

For the single degree-of-freedom system, the response to harmonic excitation is:

$$x_s(t) = \bar{X}_s e^{i\omega t} = X_s e^{i(\omega t - \theta_s)}, \qquad (6)$$

where

$$\bar{X}_s = \frac{(2iS_1 r + 1)X}{(1 - r^2 + 2iS_1 r)}.$$

The ratio of response amplitude to input amplitude for harmonic excitation as a function of the dimensionless excitation frequency, r, is defined as the transmissibility curve, i.e., X_1/X and X_2/X for the lower and upper masses respectively and X_s/X for the one-degree-of-freedom system.

Response to Random Base Excitation (1, 2, 3, 4)

If the motion of the base is a random excitation whose instantaneous values in an arbitrarily narrow frequency band have a Gaussian or normal probability density function, the excitation may be expressed by the displacement (or power) spectral density $A(f)$, (with units $(in.^2)/cps$, for example). Constant spectral density, $A(f) = A$ is termed "white noise."

For linear systems, the displacement spectral density of the response is obtained from the product of the input spectral density and the square of the transmissibility curve. Therefore, in the case of white-noise excitation, the response spectral density is directly proportional to the square of the transmissibility curve. The mean-square response is equal to the area under the response spectral density plot (1).

Thus, for the two-degree-of-freedom and one-degree-of-freedom systems of Fig. 1, the mean-square displacement responses of the two masses to white noise may be expressed as

$$\phi_1 = \overline{(x_1)^2} = A\int_0^\infty (X_1/X)^2\, df. \qquad (7a)$$

$$\phi_2 = \overline{(x_2)^2} = A\int_0^\infty (X_2/X)^2\, df. \qquad (7b)$$

$$\phi_s = \overline{(x_2)^2} = A\int_0^\infty (X_s/X)^2\, df.$$

$$= \frac{\pi}{2} f_1 \frac{1}{2S_1}(1 + 4S_1^2)A = \frac{\pi}{2} f_1 Q_1 \left(1 + \frac{1}{Q_1^2}\right)A \qquad (7c)$$

$$\approx \frac{\pi}{2} f_1 \frac{1}{2S_1} A = \frac{\pi}{2} f_1 Q_1 A,$$

where f_1 is the undamped natural frequency of the one-degree-of-freedom system and $Q_1 = 1/2S_1$ is approximately equal to the maximum value of the transmissibility curve at resonance for light damping.

From Eq. (7), the values of ϕ_1/A and ϕ_2/A are equal to the areas under the transmissibility curves plotted in Fig. 2(a), (b) and (c). The integrals of Eq. (7) are most readily evaluated by use of the Cauchy Residue Theorem (5), although graphical techniques may also be employed.

The asymptotic values of ϕ_1 and ϕ_2 for a mass ratio $M = 0$ are obtained for $M \to 0$ in the following sense. If m_2 is zero, the system of Fig. 2 becomes a single degree-of-freedom system, and thus the mean-square response ϕ_1^* of m_1 is ϕ_s, and the spectral density of this response is proportional to the square of the transmissibility curve. If it is now assumed that the upper spring-mass-dashpot system responds to this spectral density as a single degree-of-freedom system, then the mean-square response ϕ_2^* of m_2 will be proportional to the area under the product of the transmissibility curves of the two single degree-of-freedom systems with damping factors S_1 and S_2. In other words, m_2 has been assumed to be zero in the sense that its motion does not effect the motion of m_1, i.e., the systems are decoupled. Mathematically, the mean-square response of m_2 becomes

$$\phi_2^* = A \int_0^\infty \left(\frac{X_s}{X}\right)^2_{S_1} \left(\frac{X_s}{X}\right)^2_{S_2} df . \qquad (8)$$

This equation may be evaluated by the use of the Cauchy Residue Theorem. If ϕ_2^* from Eq. (8) is divided by ϕ_1^*, i.e., ϕ_s evaluated for the parameters of the lower mass, the ratio of responses is

$$\frac{\phi_2^*}{\phi_1^*} = \frac{(1 + 4S_1^2)}{\left(1 + \frac{S_2}{S_1}\right)} \left\{ 1 + \frac{1}{4S_1S_2} + \frac{S_1^2 + S_2^2 + 4S_1^2S_2^2}{S_1S_2} \right\} \qquad (9)$$

$$= \frac{1 + \frac{1}{Q_1^2}}{1 + \frac{Q_1}{Q_2}} \left\{ 1 + Q_1Q_2 + \frac{Q_2}{Q_1} + \frac{Q_1}{Q_2} + \frac{1}{Q_1Q_2} \right\} .$$

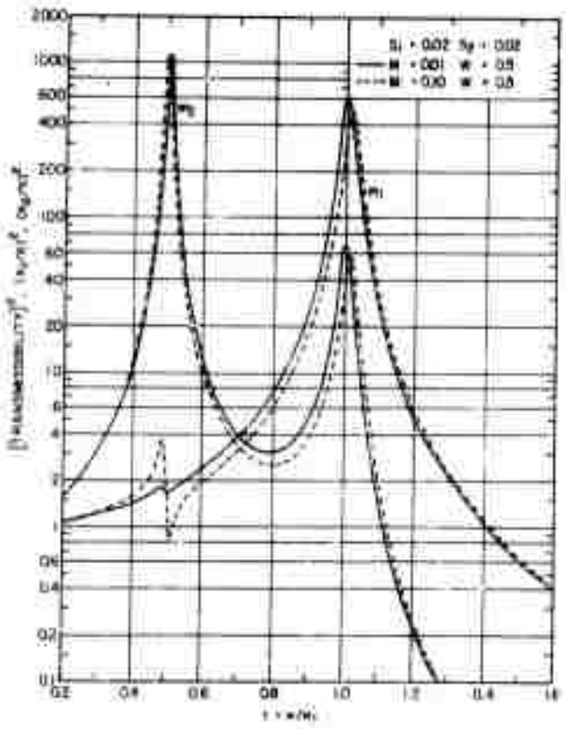

Fig. 2(a) - Transmissibility of base-excited, two-degree-of-freedom system with mass ratios and damping factors varied

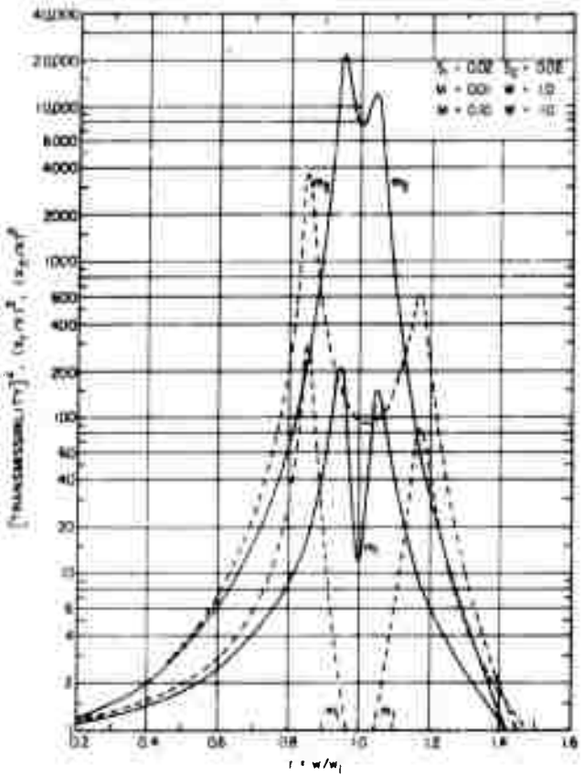

Fig. 2 (Continued)(b) - Transmissibility of base-excited, two-degree-of-freedom system with mass ratios and damping factors varied

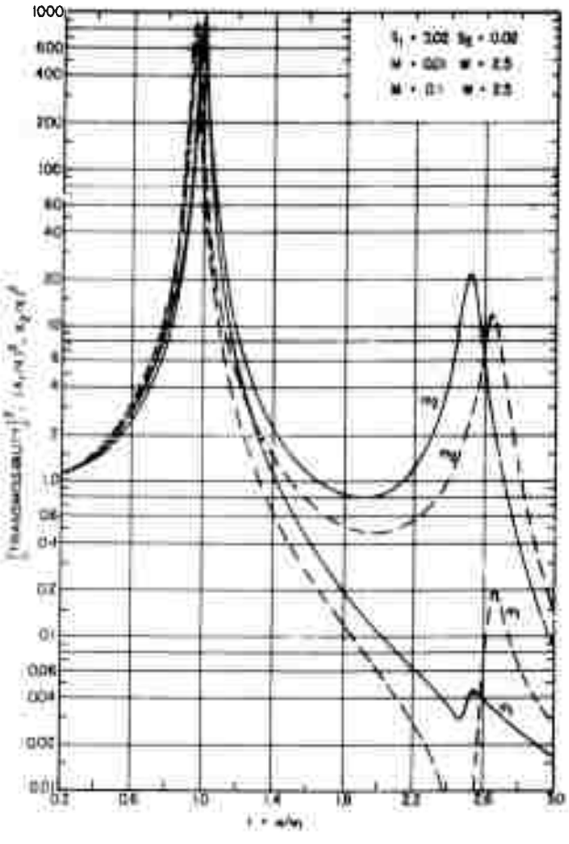

Fig. 2 (Continued)(c) - Transmissibility of base-excited, two-degree-of-freedom system with mass ratios and damping factors varied

. Results

In order to study the effects of variation of the dimensionless parameters of the two-degree-of-freedom system, i.e., mass ratio, frequency ratio, and damping factors, evaluation of the integrals of Eq. (7) was programmed for an IBM 709 computer. Figures 3 and 4 show some of these results and will be explained later. The values of the dimensionless parameters chosen are the 84 combinations of

M = 0.01, 0.02, 0.05, 0.10, 0.20, 0.50, 1.00,

S_1 = 0.01, 0.02, 0.05, 0.10,

S_2 = 0.01, 0.02, 0.05,

calculated at a sufficient number of points in the frequency ratio range $0.20 \leq W \leq 10.0$ to permit the plotting of ϕ_1/ϕ_s and ϕ_2/ϕ_s versus W. Some additional values, shown later in Table 2 were calculated for $W = 1.0$ for comparison with previously published experimental results.

It is convenient to normalize the values of ϕ_1 and ϕ_2 with respect to ϕ_s, where ϕ_s is the mean-square response of the one-degree-of-freedom system with the same dynamic characteristics as the lower mass of the two-degree-of-freedom system, i.e., to calculate ϕ_1/ϕ_s and ϕ_2/ϕ_s. Not only are the resulting plots more tractable, but the differences between one- and two-degree-of-freedom systems are more readily determined.

Figure 2(a), (b) and (c) shows plots of the square of transmissibility curves, $(X_1/X)^2$ and $(X_2/X)^2$ versus r, when the damping factors are 0.02 in each spring-mass system. The mass ratios are 0.01 and 0.10, for the three frequency ratios of 0.5, 1.0 and 2.5. The curves may also be regarded as the

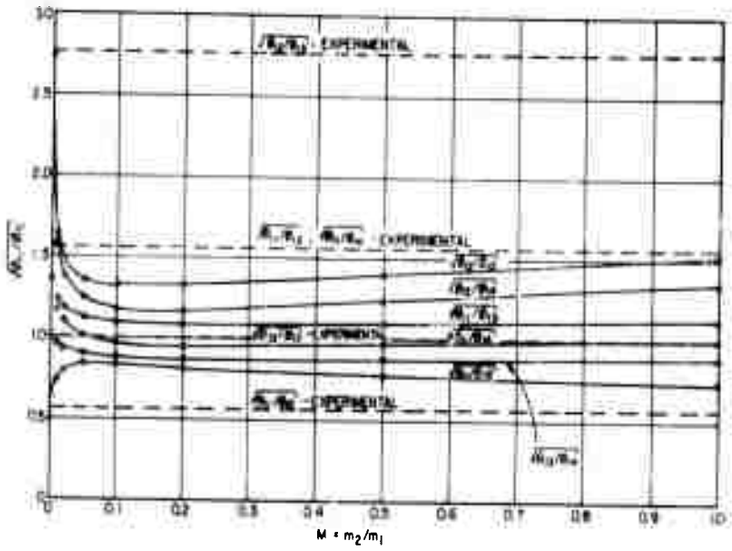

Fig. 3 - Lower mass rms response ratios, $\sqrt{\phi_{11}/\phi_{1j}}$, for combinations of damping factors, S_1, S_2 (Table 2), as a function of mass ratio M, at $W = 1.0$

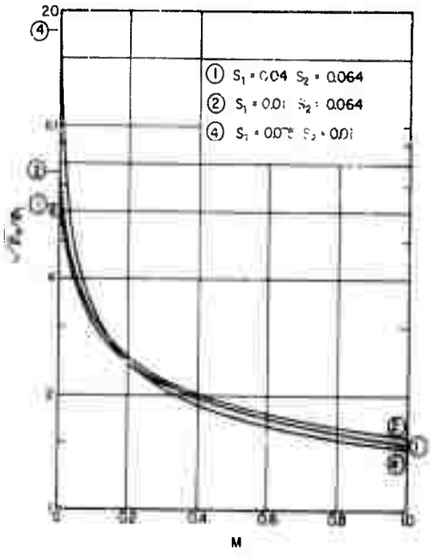

Fig. 4 - Ratio of rms response of upper mass to rms response of lower mass $\sqrt{\phi_2/\phi_1}$ for frequency ratio $W = 1.0$ as a function of mass ratio, M

response spectral density plots of the respective masses for white-noise excitation of the base.

Figures 5 thru 28 are plots of the normalized mean-square responses of each mass for the 84 combinations of damping factors and mass ratios as a function of frequency ratio. Successive pairs of odd and even numbered figures show ϕ_1/ϕ_s and ϕ_2/ϕ_s, respectively, for the seven mass ratios considered and for a particular combination of damping factors. The actual values of ϕ_1 and ϕ_2 may be obtained for a particular set of parameters by use of these curves and evaluation of ϕ_s from Eq. (7).

DISCUSSION OF RESULTS

The results in Figs. 2 thru 28 are presented in terms of the displacement response of the masses to a displacement motion of the base. It is evident that they may also be considered as the velocity response to velocity base motion or as acceleration response to acceleration base motion. However, it should be emphasized that relations between, for example, displacement response and acceleration motion of the base will differ considerably from the results presented, because of the different transmissibility curves (or transfer functions) involved. Further, the mean-square relative motion between the two masses, i.e.,

$$\phi_r = \overline{[x_2(t) - x_1(t)]^2},$$

is not obtained by the simple subtraction $\phi_2 - \phi_1$, although under certain circumstances, this may be an adequate approximation.

Because of the interrelationships between mass, stiffness, and damping coefficient in dynamic systems, some care is necessary in interpreting the effects of parameter changes. Thus in considering Figs. 5 thru 28, a change in m_2 only (Fig. 1) will affect the three dimensionless parameters, M, W, and S_2. Conversely, if the effect of mass ratio for a given W, S_1, S_2 combination is examined, it is tacitly assumed that m_2, c_2, and k_2 (or m_1, c_1, and k_1) have all been changed appropriately to preserve the values of W, S_1, and S_2.

General conclusions which may be made from examination of Figs. 5 thru 28 are as follows:

1. As the frequency ratio W becomes large compared with 1.0, i.e., the upper mass has a high natural frequency compared with the lower mass, the responses of masses asymptotically become equal to each other, i.e., $\phi_1 = \phi_2$, and approach a value:

$$\frac{\phi_1}{\phi_s} = \frac{\phi_2}{\phi_s} = 1 - \frac{1}{Q_1^2}\left[\frac{M}{1+M}\right],$$

which is very close to unity for values of Q_1 and M likely to be of interest.

2. For values of W below approximately 2.0, the response of the lower mass is considerably different than the one-degree-of-freedom system, even for mass ratios as small as 0.01, i.e., $\phi_1/\phi_s \neq 1.0$.

3. The mean-square response of the lower mass ϕ_1 is always less than ϕ_s, i.e., the upper mass "loads down" the lower mass, or acts like a dynamic vibration absorber.

4. The frequency ratio for maximum "loading" of the lower mass decreases as the mass ratio increases. For small M, maximum loading occurs at $W \approx 1.0$.

5. Significant loading of the lower mass occurs over a wider range of values of frequency ratio W as the mass ratio M increases.

6. For small W, and independent of M, the response of the upper mass is small compared with the lower mass, i.e., it is vibration isolated.

7. The maximum value of ϕ_2/ϕ_s occurs at approximately $W = 1.0$ and decreases as M increases. For small damping, the maximum value of ϕ_2/ϕ_s is, to a crude approximation, inversely proportional to M.

8. For constant S_2, the value of ϕ_1/ϕ_s is closer to 1.0 for all W as S_1 increases, i.e., as the damping in the lower mass increases, the upper mass, for given M and S_2, is less efficient as a dynamic vibration absorber.

9. For constant S_1, the value of ϕ_1/ϕ_s is closer to 1.0 for all W as S_2 decreases, i.e., as the damping in the upper mass increases, it is more efficient as a dynamic vibration absorber for given M and S_1.

10. The families of curves for varying M and a given ratio of S_1/S_2 are very similar for both ϕ_1/ϕ_s and ϕ_2/ϕ_s, except at $W \approx 1.0$. For example, compare Figs. 5, 15, and 25 and Figs. 6, 16, and 26.

The above general conclusions were drawn on the basis of the mean-square responses of the two masses. However, it is also important to consider the spectral density associated with the mean-square response. Figure 2(a), (b), and (c) illustrates the manner in which the spectral density of the response is affected by both mass ratio and frequency ratio.

It is evident from the preceding paragraphs that the calculation of the response of a two-degree-of-freedom system, although straightforward, is time consuming. The literature contains examples of calculations based on the simplifying assumption that the upper mass is small enough that its "loading" of the lower mass may be neglected. Under this assumption, it is logical to compute the response spectral densities for the two masses by use of the transmissibility curves for the two uncoupled single degree-of-freedom systems. Thus, compute the spectral density $A_1(f,m_1)$ of the lower mass from

$$A_1(f,m_1) = A(f)\left(\frac{X_a}{X}\right)^2_{S_1,r_1}, \qquad (10)$$

and the spectral density $A_2(f,m_2)$ of the upper mass from

$$A_2(f,m_2) = A(f)\left(\frac{X_a}{X}\right)^2_{S_1,r_1}\left(\frac{X_a}{X}\right)^2_{S_2,r_2}, \qquad (11)$$

where r_1 and r_2 indicate the ratio between the frequency at which the spectral density is desired and the natural frequencies of the uncoupled systems ω_1 and ω_2, and $A(f)$ is the spectral density of the base motion.

In the case of white noise base excitation, the mean-square response of the lower mass would be ϕ_a and the mean-square response of the upper mass would be approximated by the response of a single degree-of-freedom system, with characteristics f_2 and S_2, to white noise whose spectral density is equal to the response spectral density of the lower mass at f_2, given by Eq. (5), i.e.,

$$\phi_2 \approx A\phi_a(f_2,S_2)\left(\frac{X_a}{X}\right)^2_{S_1,r=1} \qquad (12)$$

Table 1 shows the comparison between approximate values of spectral density at the natural frequencies obtained by Eqs. (8) and (9) and the correct values taken from Fig. 2(a), (b), and (c). The approximate mean-square responses from Eq. (12) are compared with the correct values from Figs. 17 and 18.

The values in the first three columns indicate that for a frequency ratio $r = 0.5$, the approximation formulae yield quite accurate results for a mass ratio as high as 0.10. For larger values of M, the errors in ϕ_1/ϕ_a

TABLE 1
Comparison of Exact and Approximation Results

M	0.5			1.0			2.5		
	0*	0.01†	0.10†	0*	0.01†	0.10†	0*	0.01†	0.10†
$A_1(f_1)$ / A	626	610	480	626	12. (max = 205 at r = 0.95)	0.16 (max = 280 at r = 0.85)	626	610 at r = 0.99	660 at r = 0.95
$A_2(f_1)$ / A	99.95	97	95	391,876	7,400 (max = 21,000 at r = 0.95)	97 (max = 3,600 at r = 0.85)	687.1	890 at r = 0.99	910 at r = 0.95
$A_2(f_2)$ / A	1,113	1,110	1,110	391,876	7,400 (max = 21,000 at r = 0.95)	97 (max = 3,600 at r = 0.85)	22.6	21.3 at r = 2.51	11.7 at r = 2.63
ϕ_1/ϕ_a	1.0	0.99	0.58	1.0	0.56	0.52	1.0	0.995	0.974
ϕ_2/ϕ_a	0.889	1.00	0.[illegible]6	626.	43.	58.	0.09	1.5	1.38

*Approximation values - loading of lower mass by upper mass neglected, Eqs. (8), (9), (10).
†Exact values - see Figs. 2, 15, and 16.
$S_1 = S_2 = 0.02$ assumed for all cases.
Spectral density of base motion = A (white noise).

incurred will increase as shown by Fig. 15, although from Figs. 2 and 16, it appears that the error in ϕ_2/ϕ_s will remain small. For smaller values of W, the accuracy of the approximation formulae will improve.

The values in the last three columns indicate that for a frequency ratio W = 2.5, the approximation formulae (Eqs. (8), (9), (10)) yield quite accurate results for the spectral densities of each mass for values of M as large as 0.10. Also, the mean-square response of the lower mass is quite accurate. However, the mean-square response of the upper mass is quite inaccurate, since, referring to Fig. 2(c), it is seen that the greater part of the area under the squared transmissibility curve is in the region of f_1 rather than in the region of f_2, the natural frequency of the upper mass. Again, for larger values of M, the error in ϕ_1/ϕ_s from the approximation formulae increases. In this case, the error in ϕ_2/ϕ_s will increase as W increases since the response at f_2 will become a less and less significant part of the total response of the upper mass (Fig. 2c). The approximate values of ϕ_1/ϕ_s and the spectral densities will improve in accuracy as W increases.

The values in the middle three columns for W = 1.0 demonstrate the large errors in the approximation formulae when the frequency of the upper mass is tuned to that of the lower mass. The mean-square response of the lower mass is reduced by a factor of approximately two and the maximum spectral density is reduced by factors of three for M = 0.01 and a little over two for M = 0.10. Also important is the changed shape of the response spectral density compared with that for a single degree-of-freedom system as shown in Fig. 2(b). The implications of these changes with respect to the problem of specifying an adequate vibration test of a component or an item of equipment which might be represented by m_2 are self-evident.

COMPARISON WITH PUBLISHED EXPERIMENTAL RESULTS

The response to white noise of the two-degree-of-freedom system shown in Fig. 1 has been obtained experimentally by Crede and Lunney by using an analog computer (6, 7). The mass ratio employed was not specified although it was stated as being quite small. The experimental method precluded the measurement of the input spectral density. It was held constant for each experiment to enable comparison between experiments, rather than to make absolute measurements. A frequency ratio of W = 1.0 was used throughout. Table 2 lists the values of the system parameters together with the measured responses of the two masses. The column titled $\sqrt{\phi_{1i}/\phi_{1j}}$ tabulates the lower mass response ratios, i.e., the ratio of the rms responses of the lower mass ϕ_1 for the different damping factors associated with the experiments i and j. The next column, titled $\sqrt{S_{1j}/S_{1i}}$ is the square root of the inverse ratio of the damping factors S_1 for the lower mass, corresponding to the experiments i and j. If the mass ratio M is zero in the sense that the lower mass is not loaded by the upper mass, then the lower mass responds as a single degree-of-freedom system, and $\sqrt{\phi_{1i}/\phi_{1j}} = \sqrt{S_{1j}/S_{1i}}$, by Eq. (7c). From Table 2 it is evident that the experimental values agree quite closely with the theoretical response of such a system. Figure 3 shows plots of the lower mass rms response ratio $\sqrt{\phi_{1i}/\phi_{1j}}$ calculated from Eqs. (7a) and (7b), as a function of mass ratio M, when W = 1.0 and the (S_{1i}, S_{2i}) and (S_{1j}, S_{2j}) combinations as tabulated in Table 2 are used. In the limit as m_2 becomes zero, i.e., M → 0, the values of $\sqrt{\phi_{1i}/\phi_{1j}}$ are equal to the values of $\sqrt{S_{1j}/S_{1i}}$ tabulated in Table 2. However, for nonzero mass ratio, this relationship no longer holds and changes very rapidly in the region $0 \leq M \leq 0.01$. The actual value depends on the damping factors S_1 and S_2 for

TABLE 2
Comparison of Experimental* and Analytical Results

Experiment No.	M	W	S_1	S_2	Experiment Numbers i	Experiment Numbers j	$\sqrt{\phi_{1i}/\phi_{1j}}$ (Experimental)	$\sqrt{S_{1j}/S_{1i}}$	Q_2	$\sqrt{Q_2}$	$\sqrt{\phi_2/\phi_1}$ (M = 0)	$\sqrt{\phi_2/\phi_1}$ (Experimental)
1	Unknown	1.0	0.04	0.064	1	2	0.57	0.50	7.8	2.8	6.25	8.8
2		1.0	0.01	0.064	1	3,4	1.57	1.37	7.8	2.8	7.33	8.7
3		1.0	0.075	0.04	2	3,4	2.77	2.74	12.5	3.5	7.64	16.2
4		1.0	0.075	0.01	3	4	1.00	1.00	50.0	7.1	17.65	25.0

*After Crede and Lunney, Ref. (6).

each mass. The dotted horizontal lines represent the experimental values from Table 2.

For each experiment of the referenced report, the ratio of the rms responses of the upper and lower masses was measured and is tabulated in Table 2 as $\sqrt{\phi_2/\phi_1}$.

It is of interest to compare the mean-square response of the upper mass with that of the lower, when the frequency ratio $W = 1.0$. Figure 4 is a plot of the ratio of the rms responses of the masses, $\sqrt{\phi_2/\phi_1}$ as a function of the mass ratio M, for three combinations of damping factors from Table 2. The curve for experiment 3 was almost identical to that for the damping factors of experiment 2. The values plotted for $M = 0$ were obtained from Eq. (9), i.e., for a "decoupled" system, and are also tabulated in Table 2, along with the experimental results of Crede and Lunney. Also tabulated are the values of Q_2 and $\sqrt{Q_2}$ for the four experimental values of S_2. From Fig. 4, it is evident that $\sqrt{\phi_2/\phi_1}$ for $W = 1.0$ is little affected by the values of S_1 and S_2 until the mass ratio M becomes less than about 0.02. Values of $\sqrt{\phi_2/\phi_1}$ calculated from the curves of Figs. 5 to 28 for a number of damping factors confirmed this small variation. From the shapes of the curves in Figs. 5 to 28, it is apparent that $\sqrt{\phi_2/\phi_1}$ is close to its maximum value when $W = 1.0$ so that Fig. 4 may be used as an approximate upper bound for the value of $\sqrt{\phi_2/\phi_1}$ which will occur, independent of S_1, S_2, and W.

When the mass ratio M is very small (less than about 0.02), the ratio $\sqrt{\phi_2/\phi_1}$ is more strongly affected by the damping factors. From Eq. (9), it is seen that the ratio is not proportional to either Q or $\sqrt{Q}$ for the upper mass, even when $M = 0$, and, for the cases considered, lies somewhere between Q_2 and $\sqrt{Q_2}$. However, the important point is that the variation of ϕ_2 with S_2 cannot be approximated by the simple expression for a single degree-of-freedom system (Eq. (7c)) except for small frequency ratio, $W \lesssim 0.5$ and small mass ratio $M \lesssim 0.10$ (see Table 1).

The experimental values of $\sqrt{\phi_2/\phi_1}$ tabulated in Table 2 are consistently higher than the analytical values for $M = 0$, and thus for any other value of M (Fig. 4). From this result and the comparison of the experimental and analytical values of the lower mass rms response ratios in Fig. 3, it would appear that mass ratio used in the experiments of Crede and Lunney was effectively zero.

CONCLUSION

The response of a two-degree-of-freedom system to white-noise excitation of the base is shown to be strongly affected by the interrelations of the dimensionless parameters, i.e., mass ratio, frequency ratio, and damping factors. Approximate methods to compute the response must be used with caution and do not give satisfactory results when the frequency ratio is in the neighborhood of unity. The effectiveness of the upper mass as a "dynamic vibration absorber" for random excitation of the lower mass over a broad frequency range is demonstrated. The response magnitude is found to be very sensitive to small variations in mass ratio M for $M \leq 0.02$, for a frequency ratio $W = 1.0$.

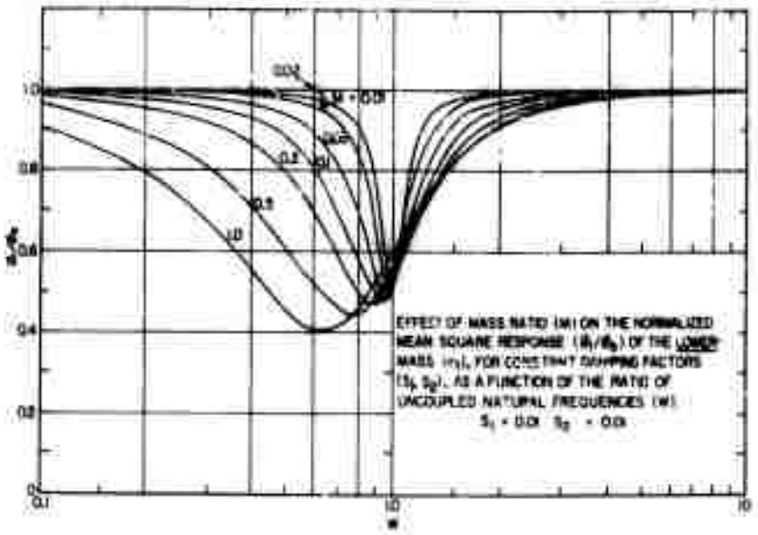

Fig. 5 - The response of a base-excited two-degree-of-freedom system to white-noise excitation

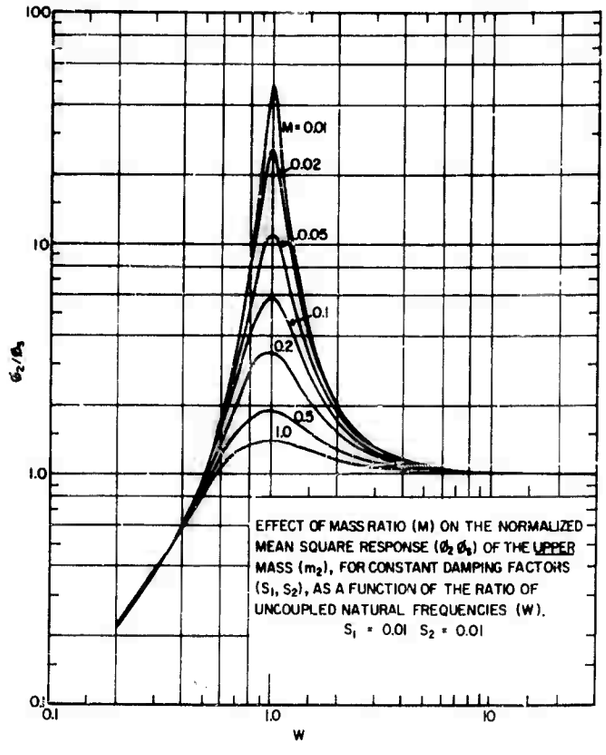

Fig. 6 - The response of a base-excited two-degree-of-freedom system to white-noise excitation

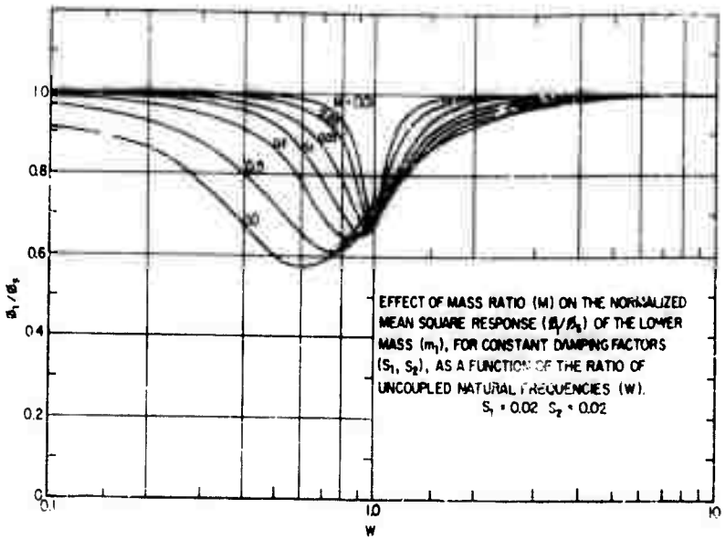

Fig. 7 - The response of a base-excited two-degree-of-freedom system to white-noise excitation

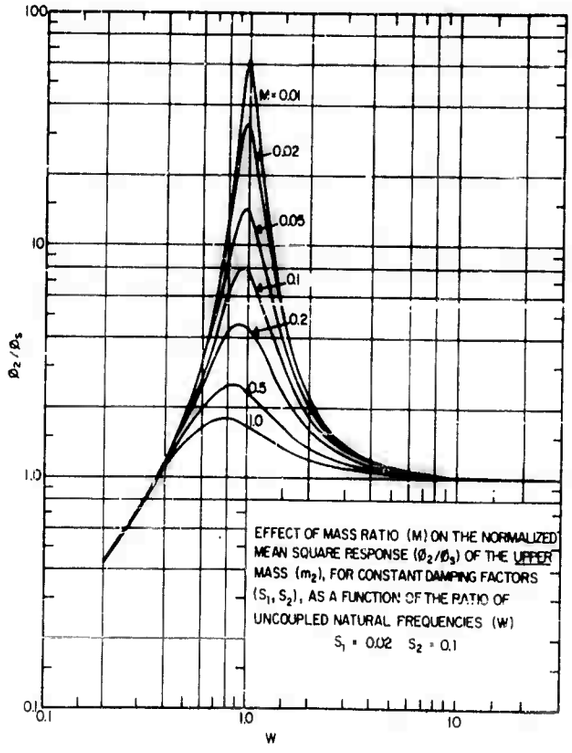

Fig. 8 - The response of a base-excited two-degree-of-freedom system to white-noise excitation

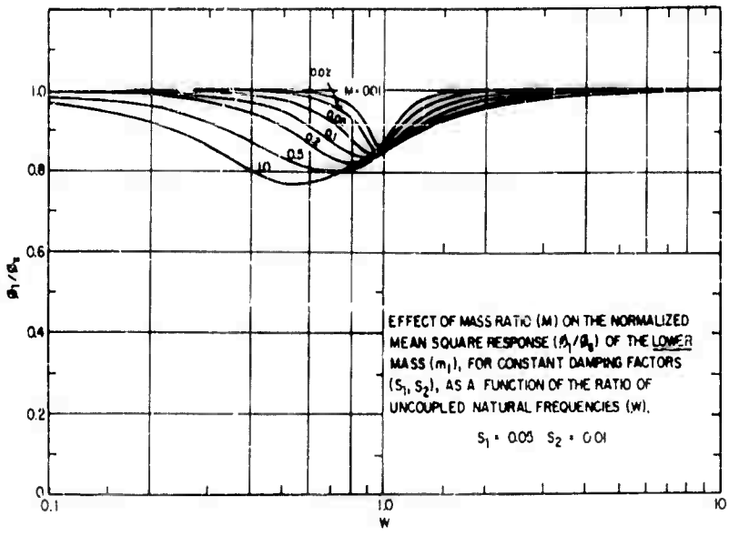

Fig. 9 - The response of a base-excited two-degree-of-freedom system to white-noise excitation

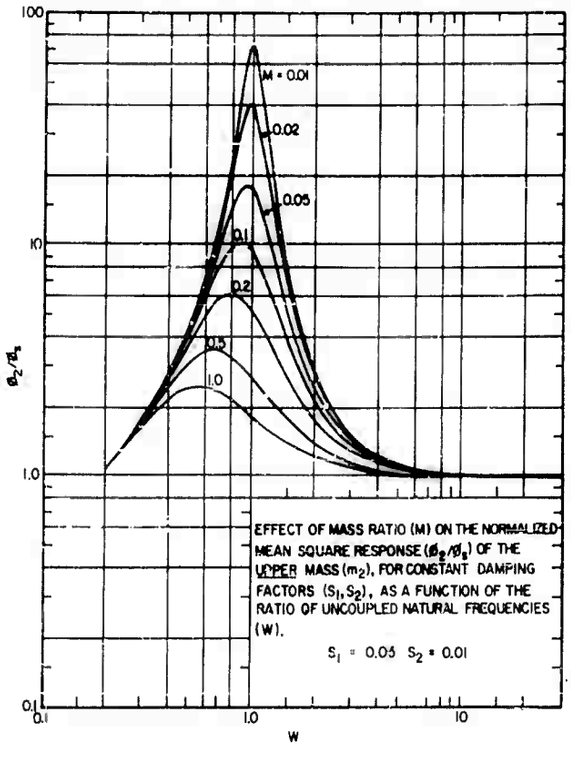

Fig. 10 - The response of a base-excited two-degree-of-freedom system to white-noise excitation

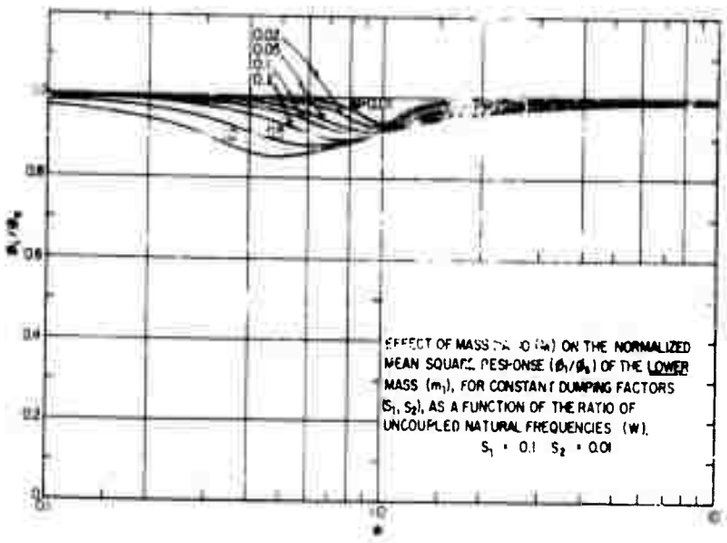

Fig. 11 - The response of a base-excited two-degree-of-freedom system to white-noise excitation

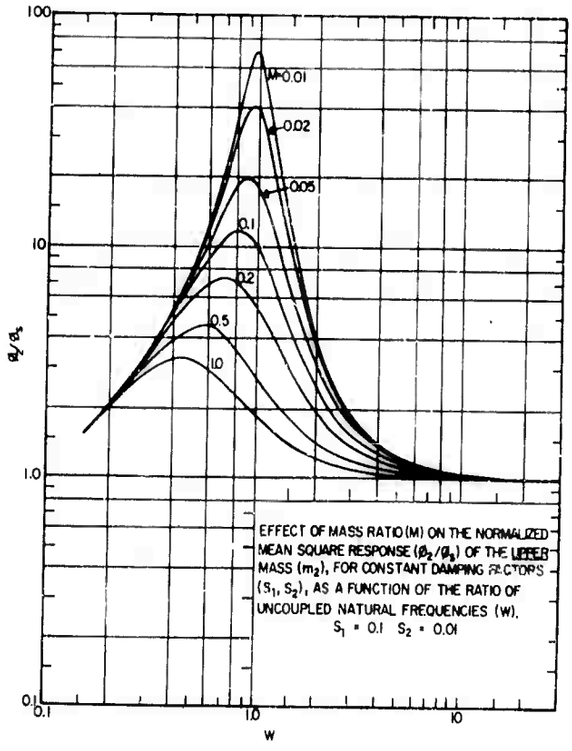

Fig. 12 - The response of a base-excited two-degree-of-freedom system to white-noise excitation

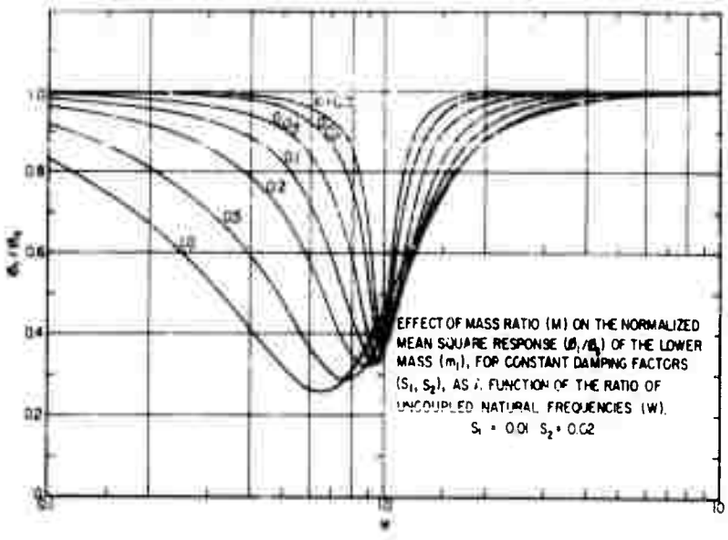

Fig. 13 - The response of a base-excited two-degree-of-freedom system to white-noise excitation

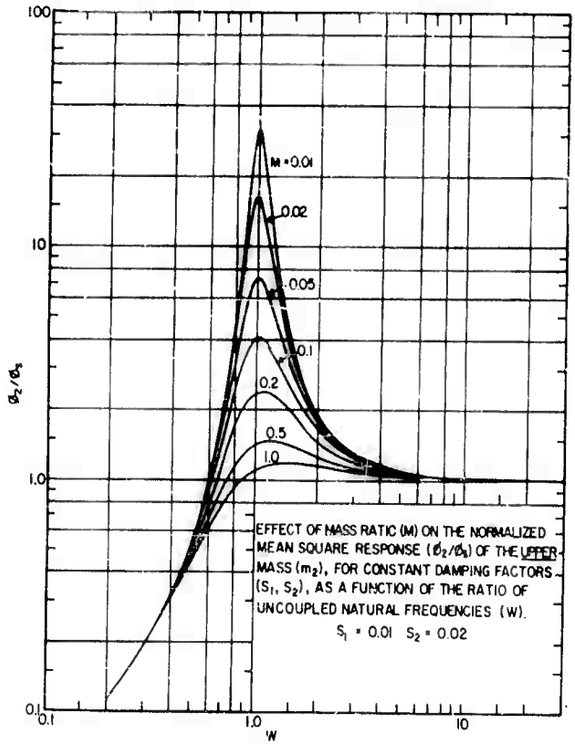

Fig. 14 - The response of a base-excited two-degree-of-freedom system to white-noise excitation

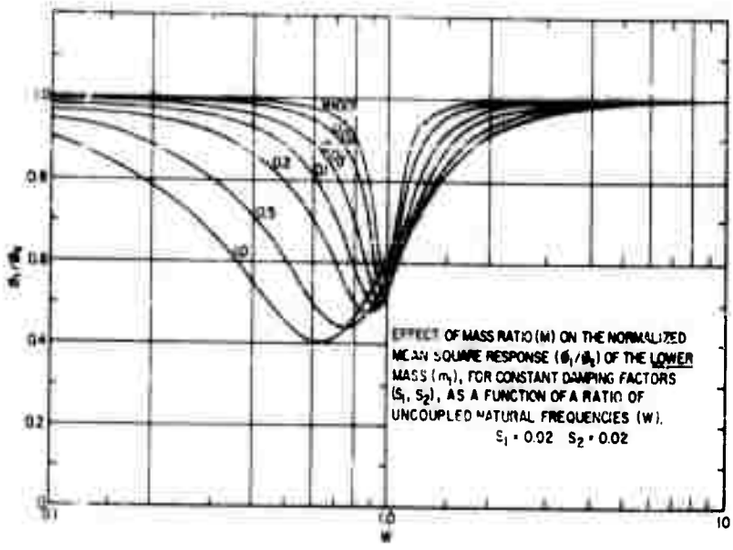

Fig. 15 - The response of a base-excited two-degree-of-freedom system to white-noise excitation

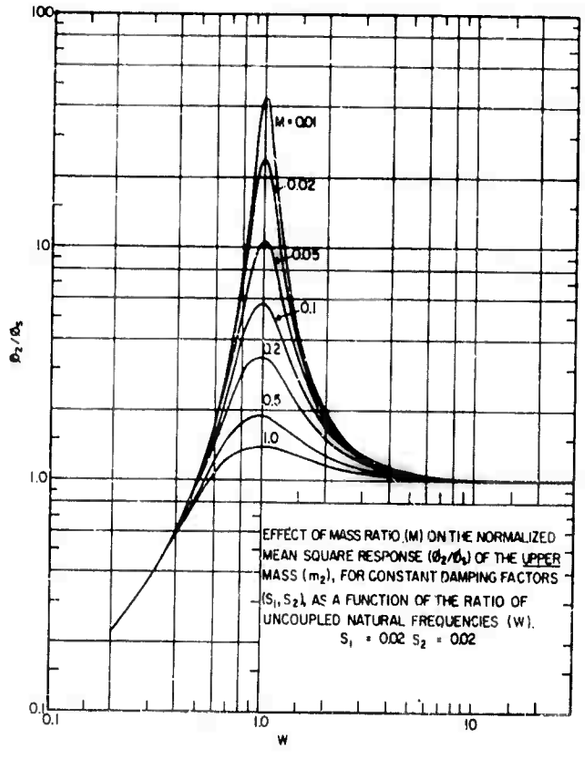

Fig. 16 - The response of a base-excited two-degree-of-freedom system to white-noise excitation

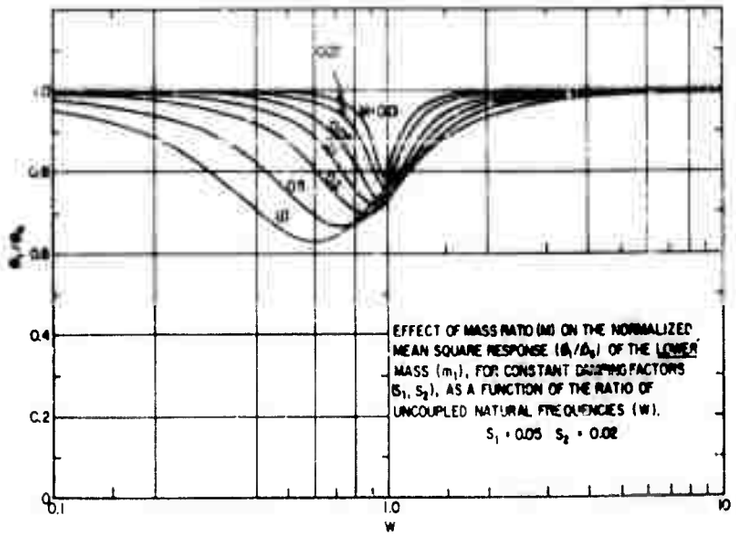

Fig. 17 - The response of a base-excited two-degree-of-freedom system to white-noise excitation

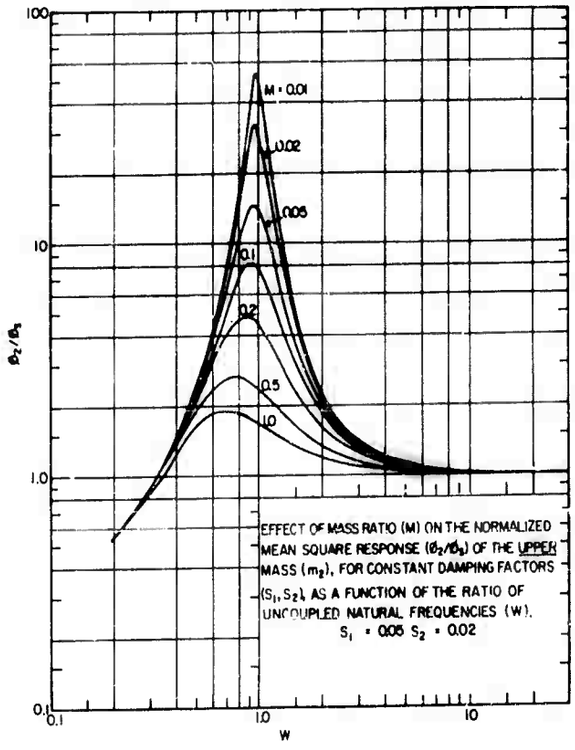

Fig. 18 - The response of a base-excited two-degree-of-freedom system to white-noise excitation

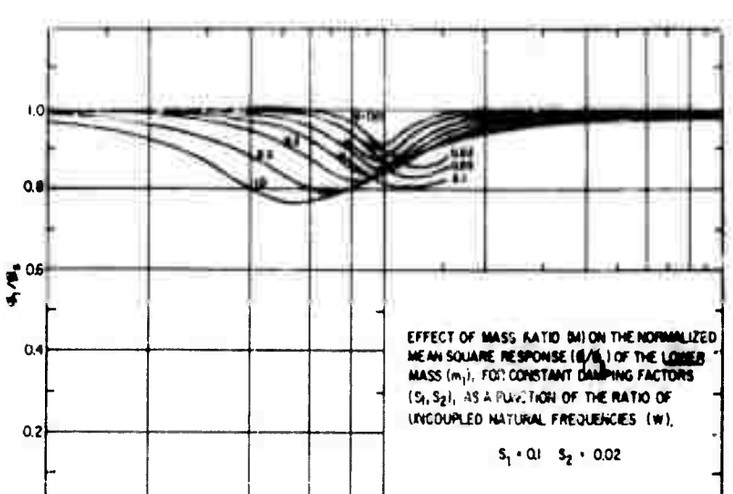

Fig. 19 - The response of a base-excited two-degree-of-freedom system to white-noise excitation

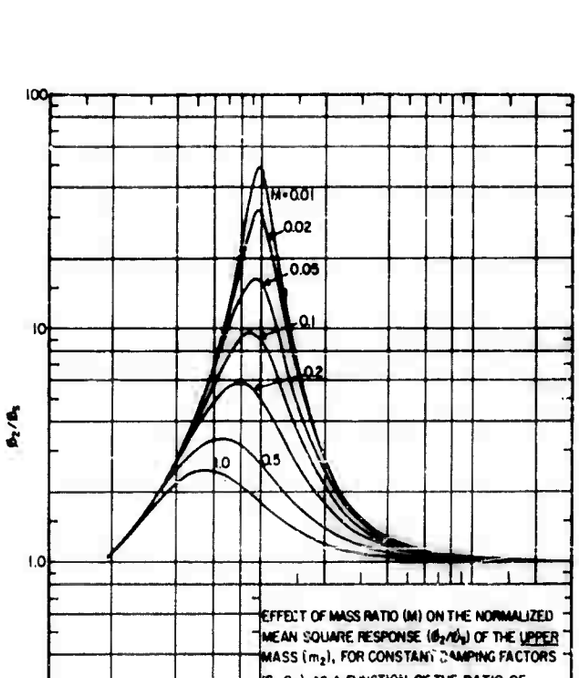

Fig. 20 - The response of a base-excited two-degree-of-freedom system to white-noise excitation.

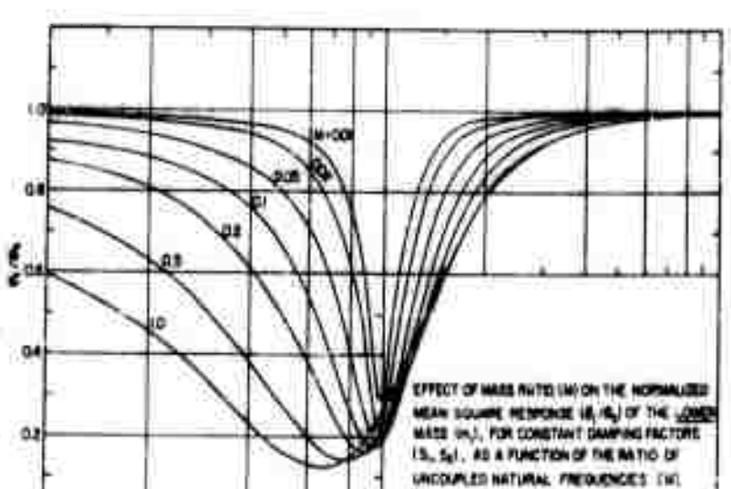

Fig. 21 - The response of a base-excited two-degree-of-freedom system to white-noise excitation

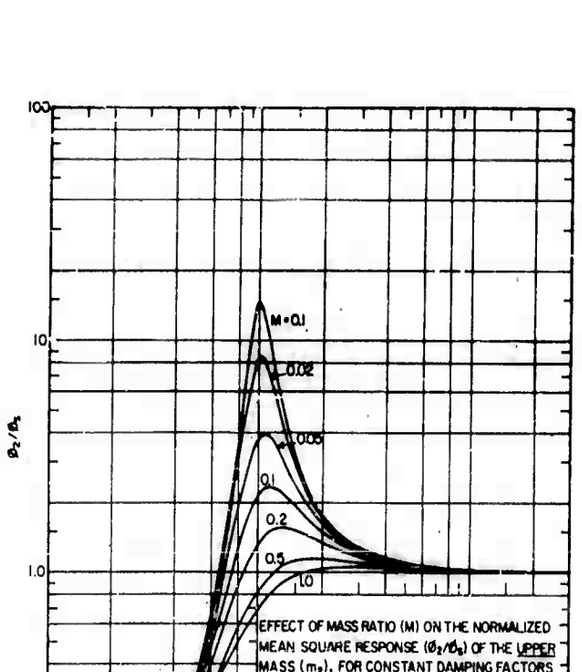

Fig. 22 - The response of a base-excited two-degree-of-freedom system to white-noise excitation

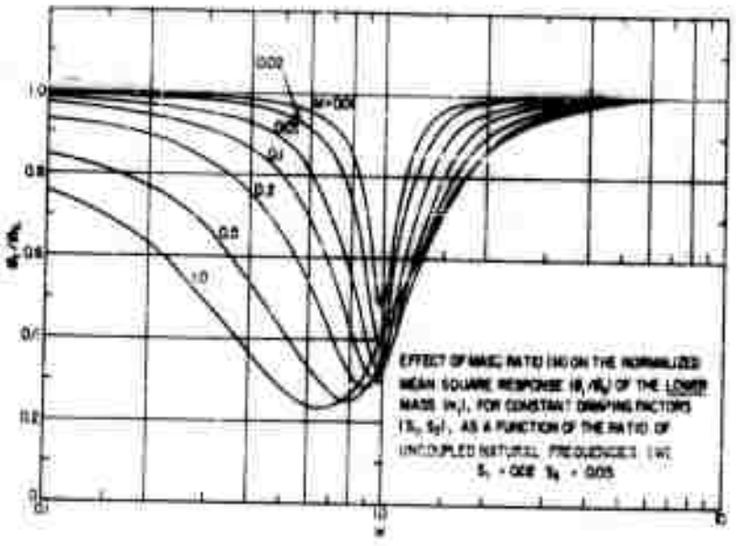

Fig. 23 - The response of a base-excited two-degree-of-freedom system to white-noise excitation

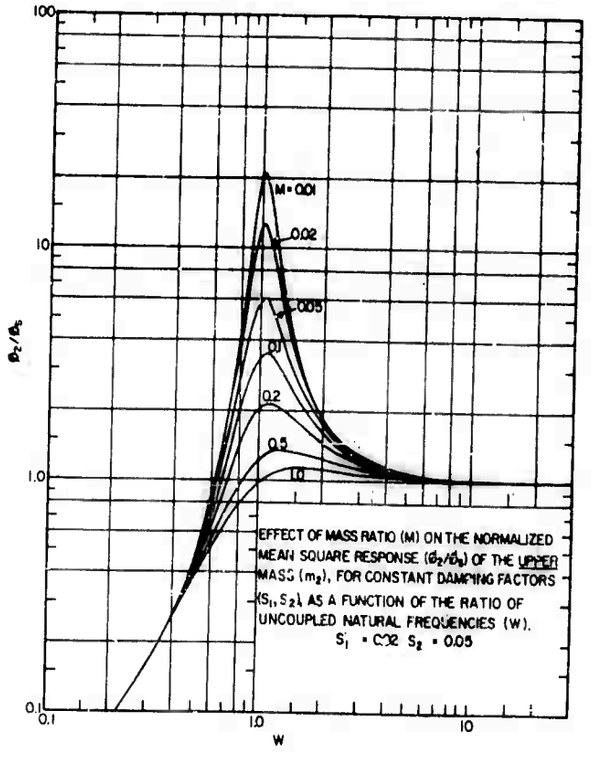

Fig. 24 - The response of a base-excited two-degree-of-freedom system to white-noise excitation

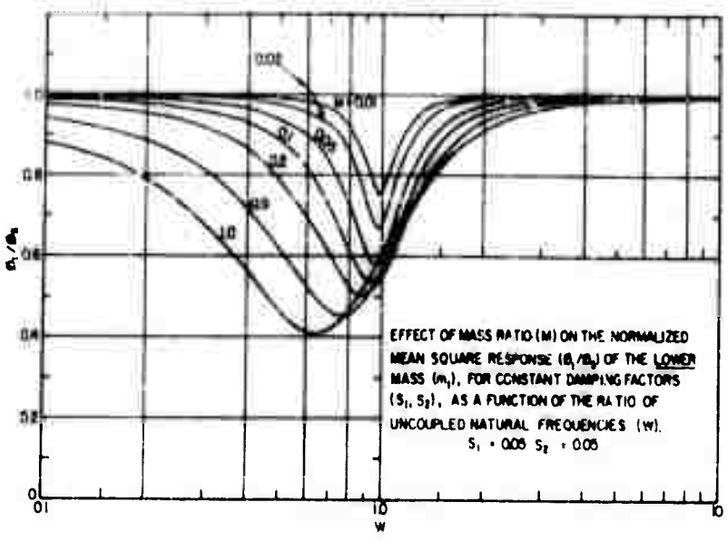

Fig. 25 - The response of a base-excited two-degree-of-freedom system to white-noise excitation

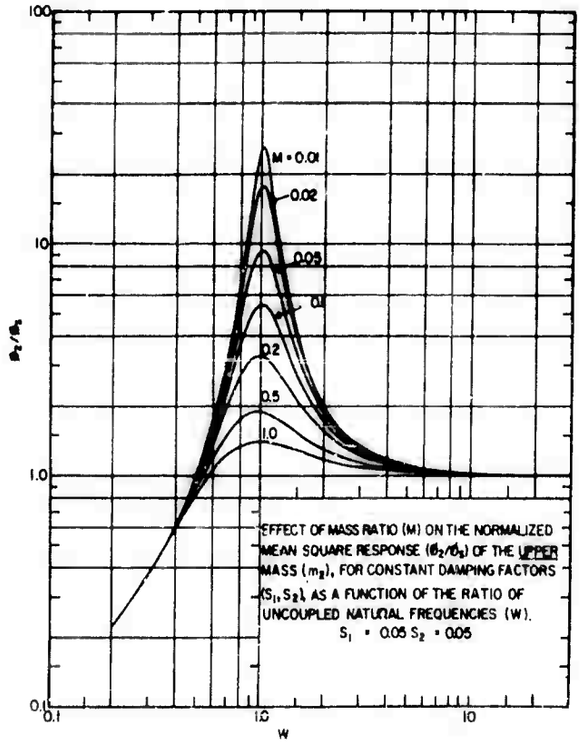

Fig. 26 - The response of a base-excited two-degree-of-freedom system to white-noise excitation

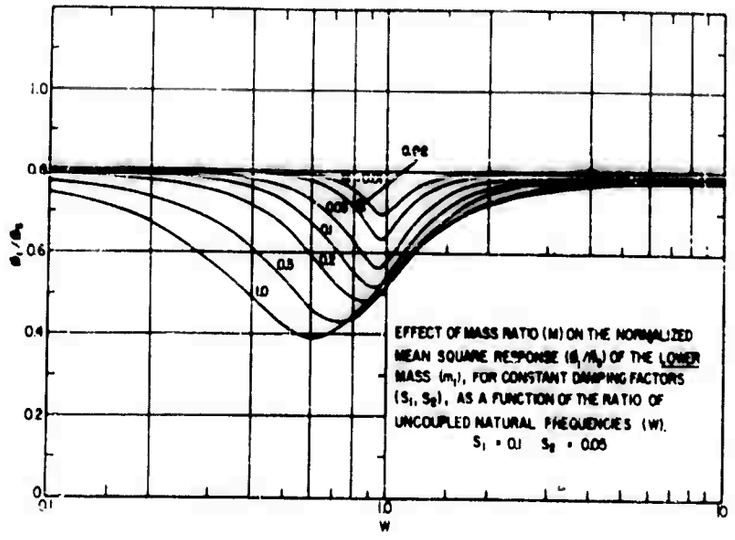

Fig. 27 - The response of a base-excited two-degree-of-freedom system to white-noise excitation

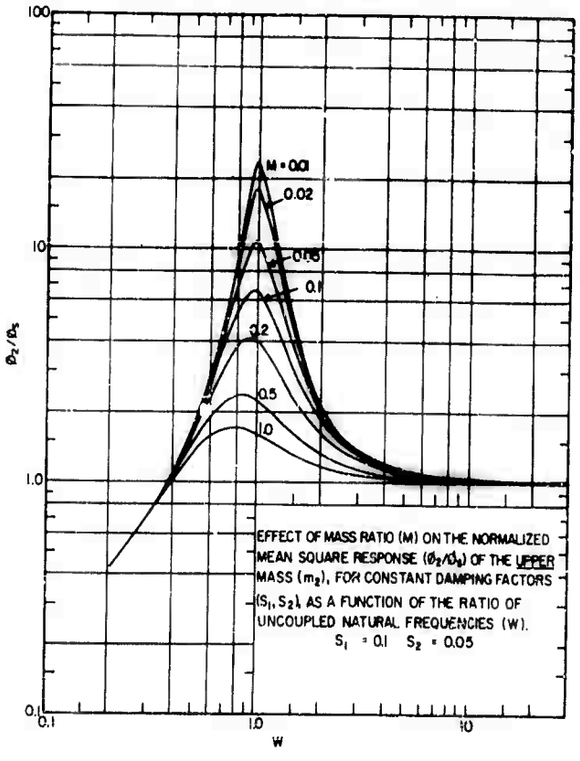

Fig. 28 - The response of a base-excited two-degree-of-freedom system to white-noise excitation

REFERENCES

1. S. H. Crandall, "Random Vibration," Technology Press of MIT, Cambridge, Mass., 1958.

2. C. T. Morrow and R. B. Muchmore, Journal of Applied Mechanics, 22:367 (1955).

3. W. T. Thomson and M. V. Barton, Journal of Applied Mechanics, 24:248 (1957).

4. J. W. Miles, J. Aero, Sc. Nov. 1954, p. 753.

5. L. A. Pipes, Applied Mathematics for Engineers and Physicists, McGraw-Hill, New York, 1946.

6. C. E. Crede and E. J. Lunney, "Establishment of Vibration and Shock Tests for Missile Electronics as Derived from the Measured Environment," WADC TR 56-503, ASTIA No. AD 118133, December 1956.

7. N. Granick and C. E. Thomas, "Aircraft Structural Vibration Induced by Jet Noise," WADC TN 56-514, ASTIA No. AD 110620, December 1956.

* * *

PANEL SESSION AND DISCUSSION

The Collection, Analysis, and Presentation of Shock and Vibration Data

PANEL SESSION AND DISCUSSION

The Collection, Analysis, and Presentation of Shock and Vibration Data

Panel Chairman: Dr. R. M. Mains, Knolls Atomic Power Lab.

Panel Members: Dr. T. P. Rona, M.I.T. and Boeing Airplane Co.
Mr. D. C. Kennard, Wright Air Dev. Div.
Dr. R. T. Othmer, Sandia Corporation
Mr. R. W. Blevins, Applied Physics Lab., JHU
Dr. A. J. Curtis, Hughes Aircraft Co.

Concluding Speaker: Dr. I. Vigness, U.S. Naval Research Lab.

FOREWORD

In the course of their visits to government laboratories and to contractors' plants, the staff of the Centralizing Activity (CA) became aware of some discontent among workers over the problems of data collection, analysis, and presentation. This discontent appeared to be primarily concerned with shock and vibration data. Because it is one of the aims of the CA to highlight problems as they arise so that solutions may be found, some means were sought to focus attention on the problem. A study group was organized and met at the U.S. Naval Research Laboratory in January 1960. The group discussed the evident discontent citing their own evidence, and determined some probable causes. They discussed possible improvements in current organization and methods and planned a panel presentation and discussion of the subject for the 28th Symposium.

That the subject was of considerable general interest was evident from the numbers who attended the seminar and who took part in the discussion. But whether any tangible results were achieved must be left to the reader to determine. The material that follows consists of the panel presentations, a narrative version of the main points brought out in the discussion and a summing up of the topics discussed at the panel session by an expert in the field.

Not all of the comments made during the panel session have been included in the narrative. Instead, an attempt has been made to consolidate comments on similar subject matter. Written comments on this topic or suggestions concerning this kind of session will be most welcome. Address all correspondence to Code 4021, U.S. Naval Research Laboratory, Washington 25, D. C.

CHAIRMAN'S PRESENTATION

Study Group Findings — Dr. Mains

Welcome to our panel session, ladies and gentlemen. This session was planned by a study group called together by the Centralizing Activity for Shock, Vibration, and Associated Environments. The group was chosen to represent a cross section of the interests and activities ordinarily represented at the Shock and Vibration Symposia, and it decided on the following procedure for this session. The Chairman will open with a survey of the situation as determined by the group and of possible action to improve

matters. The panel members will then be introduced by asking each a specific question, the answers to which are intended to bring forth each panelist's interest and background. The meeting will then be thrown open for questions from the floor. Finally, Dr. Vigness will summarize for us his impressions of what has been said this afternoon.

In the committee discussion of the present situation with regard to the collection, analysis, and presentation of shock and vibration data, there were about three points that stood out very strongly as being worthy of discussion this afternoon. During yesterday morning's session, yesterday afternoon's session, and this morning's session in particular, the participants played right into my hands. They gave me excellent material for the first point that there is a crying need for improvement of communication between the various disciplines involved in this business. For example, it would seem quite possible for a man to spend his days doing tests and have no notion of what it is he is testing, or why. How many times in the last two and a half days have you heard a question asked for which the answer was, "Well, I am sorry, that's not my department. I don't know the answer to that question." Well, this is a sad state of affairs. This is hiding behind a compartmentalization. This is saying that because I do testing I don't have to bother myself with analysis, or because I do analysis I don't have to ever go get my hands dirty. I am sorry. This won't work. We have reached a situation in which half of you can't talk to the other half. At the time the study group met we didn't know quite how far this had gone, but apparently it is a much more advanced disease than we had realized.

Now the second item is one that I think may be recognized also on the basis of what we have heard in these discussions during the last two and a half days. The point is that there is a severe need for standardization of nomenclature, techniques, and data presentation so that experience in one program can be carried over to another program. We must start talking the same language. When we say spectral density, or 10 g, it should mean the same thing to all of us, and 10 g must be accompanied by some qualifying words.

The third item that came forth in the study group was the fact that there is a need for devising an organizational structure which fosters rather than hampers cross-fertilization between these various special interest groups. I don't know how it happens that a chap can get into the business of doing shock and vibration work and, let's say, spend all of his days doing nothing but running a shake machine. This was incomprehensible to me until a few years ago when I got involved in industry. Around universities, you see, everybody had to be his own technician, his own calculator, and his own test setup man. He had to do the whole job because he never had anything but a shoestring to work on and a scrap pile for equipment. Apparently, in industrial work everybody gets compartmentalized into a little slot. Perhaps a man spends several years buying pumps. He knows all there is to know about pumps, but that is all he knows. This gets to be real unfortunate. We need then a means of organizing ourselves in our work so that cross talk between us is fostered rather than hindered.

The purpose of collecting, analyzing, and presenting shock and vibration data is really quite clear to me, and it seemed clear to our study group. We want these data to define the "loads" for the problem. Now I am using the term "loads" here in quotes in a generalized sense. Whether you think of shock, impact, vibration, transients or steady-state loads, I am not sure that it is worthwhile trying to distinguish between them. They are all just loads. They should all be defined statistically, just as the failure problem is a statistical problem that we should treat from a larger point of view than to make one test and try to draw general conclusions from that.

We want to use these data in specifying the design environment, then in designing the equipment, and then in testing the result. Data that are gathered are only useful when they contribute directly to these functions. We are, therefore, concerned with getting shock and vibration data into a form which enables us to predict the response of mechanical structures.

Now someone will immediately say, "But I am interested in vacuum tubes." Well, isn't a vacuum tube a mechanical structure? You get into difficulty in a vibration test with a vacuum tube not because it happens to have electricity in it, but because the grid element happens to bang into the plate element and cause a short, or because the grid wires go into resonance and cause malfunction. It is a mechanical structure problem, so we want to use the data for the purpose of determining the response of mechanical structures to shock and vibration.

The form for the data needs to be such that we can use it either with normal mode and frequency analyses or with test response information such as a measured response spectrum. We can then go on to predict the behavior of the structure when it is subjected to this environment. The process is really quite simple, especially since we have such things as digital machines to do computations for us. We can solve 12, 15, or 20 degree systems that we would never think of doing by hand and ask the machine to do a thousand computations on that system because it does so in a couple of minutes. This is a very handy tool.

The things we are concerned with in terms of response of this mechanical structure to the excitation are stress, acceleration, velocity, and displacement. I think everything else that we would like to derive from these data can be tied on to one of these four quantities, and probably we can leave the stress out because it depends upon either acceleration, velocity, or displacement.

Once we have predicted how the structure is going to respond to the excitation which we have determined by the data gathering process, what is the next thing? Well, the next thing is to predict damage, or its inverse, reliability. This is the part of the picture in which the state of the art is least well developed. It does us no good at all to argue about whether a spectral density picture looks like this because we have used a ten-cycle bandpass instead of a one-cycle bandpass. It does us no good to argue how that spectral density is going to affect a response unless we know what the response means when we get through. If you can't define the damage process then how are you going to predict damage? If you can't predict damage you'd better quit. The whole design process is aimed at getting something which survives with a given amount of reliability. Unless you know what the damage process is and how it progresses you can't do this.

Let's take a slightly different tack. Let's ask the question, why do we measure a shock and vibration environment? The reason for measuring a shock and vibration environment is to define the motional environment, because we suspect that it affects the reliability of equipment. We would like to anticipate this, to design for it, and to test for it. For example, if we measure the motional environment of a missile that we are interested in during the manufacturing processes, and the shipping processes, during storage, and the firing of the missile, we may well find quite different motional environments in those four cases so that different design requirements derive from them.

We might also ask the question of where to measure these environments. Well, you could debate this one for quite a while. I believe the place to measure is on the primary structure. On a ship, for example, you don't measure on a bracket; you measure on a floor, an inner bottom, or a bulkhead so that you can find the impedance of the primary structure and deduce what is going to change in the response when you put on a load in the form of the equipment you are concerned with. In making these measurements, it doesn't matter what instruments you use as long as they are rugged enough, have range enough, and have the necessary response. Each of us has his own pet instruments.

As to which recording system to use, well, the important thing is selecting one that has good fidelity. If you happen to like FM FM telemetering for missile work and the ground station happens to have a good Ampex recorder, this is fine, but I am sure there are other ways to do it that work well, too.

What kind of analysis should one do? Well, one should analyze for vibration in such a way that you get curves of rms acceleration spectral density versus frequency. In trying to do this you may find that you do not have random noise at all, but you still would like to have rms values and you still would like to know at what frequencies. In addition, you need histograms, probability plots or amplitude distributions at various frequencies. You need a time history of the variation in rms values, the area under the spectrum, or some other function which defines the change in environment with maneuver status as in the airplane, with the amount of fuel that has been used up in a missile, or a similar situation for other bits of equipment. For this you need either the excitation or the response at some point where the impedances are known. Just putting a gauge on a structure and hoping that when you get through it will mean something won't help you. You may get specific data that is useable for that particular place and that particular piece of equipment, but that is all you will get. If, on the other hand, you know what the impedance at that point is, both looking back into the structure and looking ahead into the package, then you can do something with it.

For shock, these analyses need to produce motion versus time for the rms or for the maximum shock intensity, or a shock spectrum of maximum motion versus frequency. If you like, a Fourier analysis of the rms, or the maximum, shock intensity may be used. The significance of a Fourier analysis of an rms shock would make an interesting question to debate. For shock also, it is necessary to measure either the excitation or the response at some point on the structure where you know the impedance looking both ways. Otherwise we can't carry it over into the next problem.

When the data has been worked over the specification writer needs to do an analysis, an operational analysis if you like, to determine how much to ask for in design and in test. The economics of the project are established right at this point because the specification establishes a ceiling and a floor between which the design must fit. If you ask for a shock capacity which turns out to be unreasonable, then you pay an unreasonable cost for the equipment when you don't really need to. Similarly, you may not get good enough equipment if you don't keep your requirements high enough. The specification writer has a real tough job.

Once the specification is written the design engineer uses the specification data to determine the structural characteristics that his equipment must have in order to stay within specified damage limits under the required excitation. As often as not he must also make some supplemental studies to determine what the damage process is and what the damage limits are for the subcomponents he intends to use in the equipment. This is a key part of the design process.

He also needs to live within functional requirements entirely irrespective of what the other specification had to say; shock or vibration or no, if the radar fails just when you want to shoot back, you are going to be unhappy.

Now the test engineer takes this specification and tries to apply the specified environment to the equipment and to measure the resulting damage. The test engineer needs to know something about the damage process also, because proper simulation of an environment consists of just one thing, and that is producing similar damage processes. You may want to produce these at an accelerated rate in order not to have to wait ten years for a failure, but unless the test depends upon an equivalent damage process you are making the wrong approach. If the failure is in structural fatigue, say a stress fatigue failure, and your test is geared to produce a static tensile fracture, you are testing the wrong way.

Another link in the chain is the production engineer who tries to produce in quantity items that were as good as the prototype that passed the test. This is sometimes quite a problem, because the one that passed the test may have been carefully hand selected and babied through the tests in order to get that contract. Then the production engineer is stuck with trying to produce items that will live up to that one test. The quality control engineer then sees to it that the production items continue to pass the test if he possibly can.

Each step in this chain is dependent upon the other, and it is necessary that they all be coordinated from the beginning. We need improved cross-talk between the various disciplines and an organization to foster it, so that we each understand the other fellow's work better and don't have to say, "Well, I'm sorry, that's not my department." When we get through with that we need to have some commonality of nomenclature, some common verbiage to use so that we can understand each other. We need standardized techniques so that when we talk about a shock test we are all talking about the same thing. And, we need uniform presentation of results so that power spectral density, and so on, means the same to each of us.

PANELISTS' PRESENTATIONS

Instrumentation — Dr. Rona

Dr. Maine: Our first panelist is Dr. T. P. Rona of MIT and Boeing Airplane Company. Dr. Rona, what kind of instruments do we need to determine the response to a 10-g excitation?

Dr. Rona: Well, this is a very interesting question. It's like trying to do a crossword puzzle when only one clue is available.

This question, how to determine what kind of instruments you would need to determine response to a 10-g excitation, contains a number of undertones and catches. My first reaction would be, if we don't know anything else about the problem then we had better

take the best instrument that exists, a pencil and paper, and try to figure it out theoretically. If we have any information on the structure concerned, probably one of the best methods is the analytical approach. Since this was not specified in the question, I assume that we are looking for something else. Is this 10 g a transient, a steady sinusoidal excitation, or a random excitation? When we talk about response, are we faced with a one-dimensional, multidimensional or possibly a nonanalytical structure where we cannot freely talk about degrees of freedom? One must not forget that we are more often than not faced with structures which fail at points which are precisely nonanalytical. Therefore, I will attempt to sneak out of the difficulty by simplifying the problem considerably.

First, I will assume that we do have test equipment on hand that will produce at the location we are interested in an arbitrary force or acceleration input. If you have anything to do with testing you realize this is a big assumption and, in general, this facility is not available. Second, I will assume that the system is linear. This in my judgment is the only condition for which we can speak freely of response, although many nonlinear systems are often used in such definitions. Third, I assume that we did select with proper care the point where measurement of response is significant from the viewpoint of impedance analysis. After the above is accomplished, which may represent several weeks or months of work, only then are we in a position to specify instrumentation intelligently.

Instrumentation for this purpose will consist essentially of a device which will sense the response under a specified force input. This we will call a transducer. Criteria on transducers are rather well known as of now. This is probably the strongest portion of our wealth of information. Transducers must be such that they will give information output without interfering with the essential phenomena. This means light weight, sufficient frequency response, sufficient dynamic range, accuracy, and environmental behavior. This means, for instance, that if this structure has to operate at high temperature the transducer will not be affected.

Usually the second portion of our instrumentation will consist of a line which could possibly include preamplifiers, amplifiers, premodulators, modulators, and so forth.

You will notice that each time electronics specialists touch instrumentation systems the discussion invariably centers around multiplexing bandwidth, FM-FM, and so forth, even though these are not really essential to the measurement process. Although we are basically interested at the present time in missiles, we should not forget that a great number of very important vibration problems do not involve telemetry at all. So for the sake of simplicity let us forget about telemetry and assume that the signal is obtained at the place where we can analyze it. There is some question whether we should record it first and analyze thereafter or whether we should analyze directly. My personal belief is that, if we are just looking for an indication, it is better to analyze immediately. However, it is often not possible to do this. Thus, recording is a necessity, not for theoretical reasons but because instruments with sufficiently fast time response are not available. Recording usually deteriorates the data and playback will give us the signal, or a distorted version thereof, which will ultimately be subjected to analysis.

Finally, analysis is performed. In analysis we mean either simply determination of the peak signal, peak acceleration, or displacement after suitable conversion, or the display frequency, power spectral distribution, amplitude probability distribution, or possibly even more sophisticated data.

Well, this is the kind of thing I would do to determine the response to a 10-g excitation. I hasten to add that the answer would probably be the same for just about any value of input excitation.

Data Analysis and Presentation — Mr. D. C. Kennard

Dr. Mains: Our second panelist is Clint Kennard from the Wright Air Development Division, Air Research and Development Command. I will ask him how he would analyze a 10-g signal and how he would present the findings.

Mr. Kennard: Well, inherent in this question, I think, is one gem that is very difficult to uncover in a group like this, and that is an area of mutual agreement. I think everybody would agree that we cannot specify vibration by g alone — g is a motion that has to be expressed in terms of a frequency. In

other words, a 10-g vibration at 10 cps is certainly an entirely different situation from 10-g at 10,000 cps. Or if we go to shock, a 10-g shock for 10 milliseconds is certainly different from a 10-g shock for one-tenth of a millisecond. So, in our method of presentation we must be sure that we are completely defining the phenomenon and our first concern is to match up some sort of a frequency or time function with the motional properties.

Now if the 10-g load is a steady state vibration, we simply analyze it for frequency content. We might present it in terms of a spectrum with an array of discrete frequencies, for example. If our load is a random vibration, we may present this data in terms of a spectrum which is a continuous spectral plot of motion versus frequency, such as many of the power spectral density plots. However, in so doing we must be very careful that we specify all the inherent characteristics of the data reduction process. For example, bandwidth, frequency range, etc., may be important to define the limitations of the analysis equipment so that we know within certain ranges that our analysis is done with a certain amount of accuracy. It is going to be very difficult to reach a point of standardizing analysis and presentation, but we can go a long way in that direction, I think, if we very carefully specify the characteristics of the equipment we are using and the limitations of it so that others will be aware of these limitations in reviewing and using the data. In other words, we should follow the scientific precept that we should endeavor, insofar as possible, to define the phenomenon of shock and vibration in basic terms that are independent of the methods of measurement, analysis, and presentation.

I think the data presenter has to consider a little bit what the people who are going to use the data are going to look for. The designer may not always be satisfied with a simple frequency spectrum or power spectral density plot. In the first place, he may not understand it. A lot of designers don't understand g^2/cps. In the second place, it represents a vibration at only one point, in only one direction and under only one set of conditions. It does not indicate the value of instantaneous peak loads, so the designer may want some further information. We tend to go to a histogram type of presentation to give him more of a statistical look at the phenomenon. The histogram will show quantitative data on load repetition characteristics, amplitude or acceleration levels at certain frequencies, and so forth. This can be done either in terms of rms response for maximum values, or a similar type presentation in terms of individual load counts which occur instantaneously. The histogram presentation has the advantage of being able to combine masses of data so that you can get a broad look at the conditions that you are faced with in service. In other words, you can group locations in various vehicles, directions, conditions of operation, and things of this type to obtain a wide statistical view of an operational profile.

Of course, one of the important problems in presentation is to consider the use that the data will be put to, for various types of presentation lend themselves to different uses. For example, you have a situation where, in an operational profile, the conditions that you encounter may be a series of stabilized conditions as far as vibration is concerned. You can conceivably treat each stabilized condition as a steady state, or something similar to a steady state, vibration. But then you have the other condition where the vibration is continually varying, according to a continually varying operational cycle. Dr. Mains pointed out the example of a missile going through its profile. You have a continual change from launch to reentry and landing. We may want to have a different form of presentation for that. I will leave it to your imagination what would be the best way to present a profile of that type. Perhaps we shall have some questions on that later.

The Designer's Viewpoint — Dr. R. T. Othmar

Dr. Mains: Our next panelist is Dr. Othmar of Sandia Corporation. I am sure he has often had someone come to him with this question, how do I design for 10 g's?

Dr. Othmar: From what the previous two panelists have said I will assume that we now have the 10 g's defined extremely well either in terms of sinusoidal vibration, random vibration, or shock. Of course, we have left out the man between the two previous panelists and myself, the specification writer. The designer is always interested in knowing what the actual conditions are that he has to design to since many times the specification writer will slip in a little amplification or factor of safety that the designer isn't always aware of. When faced with a particular specification the designer also is apt to

throw in an additional factor or margin of safety. He also has to have some idea as to what damage is going to be involved.

Not only the people that are concerned with shock and vibration, but the people that are concerned with the function are involved in the complete design. Many times the designer who first starts to work on a given problem is someone like an electrical engineer who is concerned primarily with the function. He has got to get out a component that will perform in operation. He is not well versed in shock and vibration analysis, so he concentrates on the functional aspects of design. The individual who has to deal with the control of that item to survive the various shock and vibration environments has the problem of taking what is already designed and trying to fit a box around it, or some sort of a mount, so that it will be well protected.

Here, I think, is another good place for an improvement in communications. The electrical and mechanical engineers should get together early in the program and discuss each others problems. Just as we need better communications between those concerned with instruments, data reduction and presentation, design and test, so we also need better communications within the design group itself. Once the mechanical engineer understands better the problems of the electrical engineer he can help influence how the design goes instead of having to work with an item that is already designed. This, obviously, will take a lot of diplomacy.

In the final analysis of the design, then, there are many different means available all the way from straight theoretical analysis to various models or complete tests.

I think that we are quite often like a certain gentleman quoted in the Readers Digest who was describing intelligence tests. He said that the way they used to weigh hogs in Texas was to find a plank and a crossbar; catch the hog and tie him on one end of the plank and then find a suitable rock or stone to balance the hog. After it was balanced they would guess the weight of the stone.

I think that in our designs we are often doing the same thing. That is, we have a lot of complex systems, which are not possible to treat as linear systems, or as single degree, two degree, or three degree of freedom systems. We have to guess at what we are to use for the parameters. When we guess we are somewhat like the individual who is weighing the hog; that is, we have a better idea of what the weight of a stone is than what we have for the weight of the live hog.

The Test Engineer's Viewpoint – Mr. R. W. Blevins

Dr. Mains: Our fourth panelist, Ralph Blevins from the Applied Physics Laboratory, Johns Hopkins University, represents the test engineer's point of view. The question I ask him is, how do you make a 10-g test?

Mr. Blevins: In discussing the test problem I want to emphasize four points, and in doing so I am going to duck the issue of what do we mean by 10 g. The other panelists have covered this, and we will assume that we have the equipment available and that we know what we mean by 10 g. This is a big assumption.

The first point that I would like to bring out is the question of where to measure the 10 g. Our moderator touched on this when he was discussing the problem of acquiring vibration data, but it is rather important for the test man to agree upon the point on the structure into which he wants to put a specified input. As an example, if we are testing a complete missile we want to apply the acceleration in the transverse plane, the structure will respond somewhat as a free-free beam, not ideally of course, but there will be some point on that structure where the excitation is zero or close to zero. There will be other points on the structure where the excitation will be quite high. When I test this at 10 g, can we agree that this is 10 g maximum or is it something else? Again when we consider the subassembly or the smaller component we face the same problem. Where do we measure the input? This is generally done by choosing rather arbitrarily a support point on this particular structure. I think the important thing to emphasize here is that at a very minimum, we must in some way simulate the support of the individual component to the basic airframe when we test it.

Now the second problem that I would like to mention is the fixture problem. If you will recall last year in El Paso there was a panel which spent considerable time discussing this. The specification generally

reads that we are required to apply 10 g along a particular axis. It says nothing about crosstalk. It seems to me there are two points of view here, and I am not going to stand on either one. But the first argument is that if we are able to apply the acceleration in one plane and one plane only without any crosstalk in the other planes, then we have a little better chance of performing some damage analysis, or we are closer to a theory that we understand. On the other hand, the argument goes that if you have a little bit of crosstalk you are much closer to an actual simulation of flight. I think the point I would like to emphasize here is that it is very important that we understand just what is the test excitation. In addition to the plane in which the 10-g excitation is to be applied, the motion in the other two planes should certainly be measured and understood.

A third point has also been mentioned by Dr. Mains, and that is a question of the definition of failure. If we are testing an item which fails by breakage or fails by yield, generally we have a pretty good chance of understanding this. However, in many equipments that we are asked to test, the criterion of failure is one of performance. It is a gyro, and failure is defined as a certain drift rate; or it is an amplifier and failure is defined as a certain signal-to-noise ratio. I think the important point here is that the test engineer must work very closely with the other disciplines involved to understand the implications of what he is defining as failure.

As an example, assume you have an amplifier which is a part of a guidance system. You realize that you will have a certain signal-to-noise ratio coming out of the amplifier under vibration. It is a rather complicated analysis to determine an acceptable amount of signal-to-noise ratio that will affect the guidance system and how the effect upon the guidance system will change the kill probability of the missile. The test engineer is here dependent on cooperation with the other disciplines involved. He must understand the problems and understand the implications of his test.

The last point I would like to mention concerns the type of data that we ought to get from our tests. I think we can all agree that the type of data we want is some kind of data that is useful in design. Here I am thinking primarily of data from the so-called type test, not a routine acceptance test. If we simply say a component did not work, did not pass the test, or exceeded some pre-set value under 10-g excitation, this gives the designer really very little information. It doesn't tell him whether that component would pass 5 g, 7 g or something else.

Therefore, in looking for information useful to the designer, I think we have to realize that in addition to passing an arbitrary specification we should be analyzing the equipment to obtain the method of failure and the points at which it failed.

Now we have found that the so-called "g-to-failure" test, which results in an inverse resonance curve as the test result, is a very useful type of investigation. Here we determine the force level at which the component fails as a function of frequency. This has the advantage of telling the designer where the critical points on that piece of equipment are.

Obviously these are not all of the problems the test engineer runs into, but I believe they are the major ones.

Organization – Dr. A. J. Curtis

Dr. Mains: Our final panelist is Dr. Curtis of Hughes Aircraft Company and he will tackle the question how do you organize so as to best integrate the whole shock and vibration business in a company of any given size?

Dr. Curtis: I think we must give this question a broader context than simply the integration of efforts on shock and vibration. Shock and vibration certainly is a very important part, but really it is only a part of an environmental program which, in turn, is one part of a reliability program for any project. Since it is such a part it must be integrated then with the whole reliability program of a given project.

How can we go about integrating all these various efforts, the ones that have been described by the previous panelists? I think we have to start applying the weapons system concept to these efforts. We need something like a system integration department. Most projects of any size have something which may be called a system analysis department or synonyms therefor. They say that this bird shall have a given probability of hit or it shall last so long. They define all the system parameters. What we need

then is some organization that decides the system parameters for environmental matters, reliability matters and, as part of that, shock and vibration requirements.

I am sure we are going to have to retain our usual organizations of flight test, instrumentation-data analysis, and design departments. We can't get away from it. But we need in addition to this a system activity.

What must this system activity be able to achieve and what kind of people can make up such an activity? Certainly they have to have a very broad area of technical competence. I am sure qualified people exist, but I am also sure they are going to be pretty hard to find, since they must fully appreciate the problems of the designer, the instrumentation man, the flight test man, etc. This appreciation must be in the sense of being able to conduct a technical evaluation, not merely to smile and nod knowingly. They must be pretty sharp cookies altogether.

Now to whom should this organization report? Well, certainly they come under the project manager for any project that they are working on. But sometimes project managers are a little biased in their outlook. They kind of feel that their project is the most important one that the company has in hand, and so I think it would be well that this organization report to top management directly and perhaps the project manager indirectly. In this way they can maintain a fairly impartial and objective view. For example, if the boss asks, "Well, how is this project coming? Is it going to be a reliable system? Are we going to be able to market this? — they can answer truthfully and objectively. Certainly these people must have some project loyalty, but this should not be overdone. Otherwise we will lose the ability of transferring the knowledge that we gained on project A to the next project B which comes along. We must hopefully learn by our past mistakes and make our giant steps forward instead of in the usual backwards direction.

Another thing they have to do is to make sure that the degree of effort which is put on the particular phases of this reliability program are kept in balance. Within the limitations of the three M's — standing for men, money, and months — a good overall balance should be maintained. For example, let's not spend every available data channel to measure the environment of one vacuum tube of a whole 15-foot missile. That's an extreme example, but I am sure you get the point. Also, we are always short of channels. So let's use each one to its optimum extent. A system type organization should be able to insure that, with appropriate choice of instrumentation and data analysis, this one channel can be made to serve the purposes of several of the panelists that you heard from before. Both the test engineer and the structural designer, for instance, can get the same information from the same data channel. At the present time in many projects they wind up competing for channels; let's get them together and sharing channels.

The things I have said are colored by the fact that I have worked on projects which have been largely in house where the control and flexibility required is quite feasible. When we have a project which is largely out of house or subcontracted with a systems management organization, I think you can see a similar organization to the one I have just proposed as part of a systems management effort. But when you have small subcontracts at the beginning of the program, how do you arrive at a reasonable set of requirements upon which a potential subcontractor is willing to bid, when you still do not know the environment? You have to tell him something, otherwise he won't give you a reasonable price or bid on the contract. If you are overly conservative it can be pretty costly and, if you are not conservative enough, this can be even worse. You usually find out right at the end that you are in trouble, and it is pretty expensive to correct your mistakes.

Well, how can we improve this art of estimating environments before we have even begun to design some vehicle. Here I think is the point where we really need this standardization of data analysis techniques. Perhaps it means we have to do it two ways. If you have a pet way of doing it, perhaps you do that, but also do it in a more standard way so that other people can understand it and your experience can be relayed to them. We should have some organization which could keep track of what kind of data and measurements have been made on various projects and types of vehicles. If this data or a description of what was measured where, when, and on what kind of a vehicle or structure could be collected together, we might do better in this preliminary estimating of environments.

NARRATIVE OF THE DISCUSSION

The Problem of Compartmentation

Mr. H. J. Parry, Lockheed, Burbank, commented that he agreed with Dr. Main's statements about the need for more communication between the various groups working on programs. However, it is probably unavoidable to have some people saying, "That part of it is not in my area and I don't care to get into it." Such a statement is quite natural since no one likes to talk for someone else. The only people who can cover the field are those who know all facets of the big programs.

Dr. C. Morrow of STL commented as follows: "I agree heartily that we have to have some way of getting around the present degree of compartmentation that has infected us in our industrial work on the shock and vibration problem. It is quite essential if we are to make progress, that we each learn a little bit of the other fellow's problem and a little more about what he does. But after we have exerted our best effort in this direction it is very likely that some compartmentation will still persist, though hopefully a little less than there is now. Some minimum level of compartmentation is quite characteristic of industry, so I would raise this question: Do we have a good solution to the shock and vibration problem unless it can be applied with a reasonable degree of compartmentation of effort? The work we do in solving the shock and vibration problems should not be based on any misconception of the organization problems involved."

Mr. H. W. Cordes, Lockheed, Sunnyvale commented as follows: "My question is simply, why should we change our present plan of operation? At an earlier session we heard that we should measure higher frequencies. From the floor came the questions: Why should we measure them, we haven't had any failures? Who has had any failures? No one responded and I don't think anyone has had any failures. Perhaps our present method is pretty good. We look at some previous data, use a crystal ball and come up with design criteria. Experience, at least from what has been said here, seems to have shown that no failures occur. Perhaps the way to get management behind us is to crystallize this problem of compartmentation. Actually the five representatives on this panel represent only a small portion of the people involved. Communications, data reduction, and other parts should also be linked. Maybe our present system is all right until we advertise our failures instead of our successes."

Dr. Curtis responded: "I don't think we are suggesting a change. The suggestion I made, hopefully, earlier this afternoon was just to make ourselves more efficient. A few years ago the customer was reasonably happy if you could design a weapon system which had an overall reliability of 60 or 70 percent. I don't think we can afford the luxury of that 30-percent unreliability anymore. We are now striving for reliabilities of 95 percent and our objectives for environments, which are more severe than they used to be, are several orders of magnitude more difficult to achieve. I don't believe we have the time, the men, or the money to be as inefficient as we are. These are the main reasons why we should modify and improve our approach."

Dr. Mains also responded to Mr. Cordes' remarks. ".... I remember calling attention to a particular piece of shipboard gear not long ago and commenting that it was poorly designed and not adequate for shock. I was told that these items were on several ships and had not failed yet. On asking whether any of them had received a shock, I was told, 'Oh, no; but none of them have failed yet.' If you are designing to withstand combat conditions and during noncombat conditions you have had no failures, this is no test. We have got to break down some of this complacency and satisfaction with the status quo. The way to ensure that our sons have a chance of returning from the next scrap is to build the stuff right — now. And this does not mean 'rule of thumb'."

To which Mr. Cordes replied: "May I add, for the record, that I am 100 percent behind the necessity of your approach. The point I am trying to bring out is that since we fly very few instruments in our space vehicles, how can we tell if we have had a vibration failure? It is extremely hard to prove that we have had a vibration failure at one point when we measured at another. Nor can we prove that we can save a lot of weight by reducing our design criteria. I am striving in practically the same direction as you are — to get the same sort of cooperation and coordination — because I think it is very essential."

Mr. R. M. Hurt of ABMA also commented on the points just raised. He pointed out that although it had been said there were no

failures, in fact this was not so. There had been failures and valuable lessons had been learned from them. A very serious effort must be made to obtain environmental data to ensure that specifications are realistic. At ABMA attempts are made to define environmental conditions early enough to do some good in the design stage. Often 'rule of thumb' applies but 'they try to apply what data they can when they can.'

Feedback of Information to the Designer

Mr. Treadwell, University of California Radiation Laboratory, brought out the point that power spectral density (psd) plots, although most useful for measuring input excitation, seem rather inadequate when discussing the response of an item with a design engineer. As an example, if a designer is shown the psd plots of the input and of the response at selected, possible, weak points on a piece of gear, tested to a requirement of say 0.1 g^2 per cps over a certain bandwidth, his reaction is often, "So what?" He does not know how to relate these plots to damage. If the equipment survived without damage he does not know how much he had overdesigned. Conversely if the piece failed he does not know how much stronger he should make it. How then should such information be presented to make it meaningful to the design engineer?

Mr. Blevins suggested testing at increasing levels of psd to the point of failure. This gives the designer, in general terms, the kind of safety factor he wants – how much above the specification level the item will take in terms of psd.

Mr. Treadwell complained about this answer since, in general, items are not available for testing to destruction. He suggested several possible ways for presenting the information. Psd plots, probability density of peak "g" or probability distribution of peak stresses. He wanted to know what other people used and how designers can apply such data to improving their design.

Mr. Gertel of Allied Research Associates commented that information related to fatigue could provide the designer with a good design technique. The problem of fatigue design for structures, using fatigue or endurance curves, has been with the aircraft designers for years. They have attempted to elaborate on the effects of random amplitudes in terms of cumulative fatigue damage. When a structural system, probably with a very high Q, is subjected to a random vibration, it will respond essentially sinusoidally at its resonant frequency. Neglecting other modes for simplicity, the missing link is how to relate the fatigue from random amplitudes to a single frequency sinusoid of constant amplitude that would produce the same damage. The data here is incomplete and inconclusive.

Dr. Mains pointed out again that the real problem here is that the damage process is not yet clearly defined so that the question cannot be answered.

Mr. Kerley, Kerley Engineering, felt that, from the standpoint of a designer, the passing on of data and other information is not directed to the proper places. There must be an integration of effort from the project manager right down the line. Although the designer is responsible for producing the design – it is his imagination which must create it – he is frequently well down the list for receipt of technical information. He does not have sufficient responsibility in the organization and until he does, the quality of design will continue to suffer. Also, those in management should retain close contact with laboratory tests and field tests so that they can appreciate the designer's problems.

Mr. Yaeger, Chrysler Corporation continued the discussion. He commented that the great bulk of the design of military hardware today was done by 'rule of thumb.' People do not calculate electronic chassis assembly frequencies. They design by taking a pencil and putting lines on pieces of paper. They are unimpressed by specifications in terms of 'g' values, frequencies, noise levels or any other description of vibration. The only way to impress them is to get them into the laboratory to work with the laboratory people. The answer then to Mr. Treadwell's question is to get them in the lab, test a gadget they have designed and when it fails, work out three acceptable fixes for it. This gives the designers a feel for what should go into a good design job and the only way to give it to them is in the lab.

Dr. Mains agreed that designers should be exposed to lab environmental tests.

Mr. Yaeger went on to suggest that what designers really need is a handbook of 'hints and kinks.' This is the level of information which they deal with. This they can understand. He illustrated his statement by an

example. He was asked to give a 16-session course to designers on the work of the vibration lab. About 15 minutes of this course was given over to a man from the structures branch who spoke on how thick panels should be and how you should avoid sharp corners. "Needless to say this 15 minutes was voted the most valuable item on the course."

Dr. Morrow, STL, went on to comment on the phrase 'knowing the mechanism of failure.' "In practice with equipment, we don't often know much about the 'mechanism of failure', whereas in structural problems of airframes we usually know a good deal. I don't think we are going to get quickly to the point where we understand all the mechanisms of failure in great detail on particular pieces of apparatus. This is probably one of the main reasons why we put so much emphasis on tests in the equipment problem. It is easy to define what is meant by failure in terms of the test results, the inspection of the item afterwards, related to the 'black box' specification for the item. It is much easier to do this than to explain in detail what corresponds to failure at every interior point." Dr. Morrow then posed this question, "Is not our interest in the capability of computing responses to vibration often more related to a desire to evaluate the significance of a particular test than to provide a method to be used by design engineers?"

Dr. Rona replied that it was his personal opinion that the tendency was definitely to attempt to correlate vibration test results with design criteria. However, as yet, there had not been much progress in this direction and he did not know of any case where significant results had been obtained. For the time being he would agree that the answer to Dr. Morrow's question was, yes.

Mr. Galef, Radioplane, discussed the problem of the designer. "If any of us here became designers and were given the task of designing to the mythical 10 g, perhaps we could design something, but I question whether it would be any different if we had been asked to design for 12 g. Now either the 10 g design is not good enough for 12 g or it is good enough for 12 g and therefore overdesigned for 10 g. There is, of course, the third way which in fact the designers are always giving us. This is the design which is good for neither 10 g nor 12 g, but which we test, find the weak points and then beef up locally for 10 g or 12 g. Maybe there is a lot to be said for this cut-and-try approach, unless any of you here think you can design something to take 10 g and not 12 g."

Nobody offered to do this but Dr. Mains argued that excitation times, required reliability and other information must be specified and that when they had been, this could make quite a difference in the design.

Mr. Forkois of the Naval Research Laboratory suggested that 95 percent of the environmental information made available at the symposia, etc. was never used in the initial concept and design of any sort of vehicle. He went on, "Actually a missile is a concept which involves a certain range, a certain payload, and other requirements. Based upon these requirements weight estimations are made which ultimately allow a certain weight for the structure. The design engineer is then told to design a structure to meet the general requirements but which must not exceed this weight. So regardless of any other requirements all he can do is to optimize the design for the weight conditions given. He does this by getting the minimum stress for the amount of material which is available. I don't mind how many figures you give him, this is the best that can be done." ".... The basic hull of a missile is very weak and I am awfully suspicious of a structure which cannot support its own weight. It's possible that a source of improvement in the reliability of missiles will have to be in more weight being appropriated for the structure itself. If this is done maybe we can get some different kinds of simulation which may not be as severe as the ones we are contending with at the present time."

Standardization of Data Presentation

Mr. Oleson of the Naval Research Laboratory raised the question of what we mean by standardization of data presentation and analysis techniques. He suggested we may be going beyond what we are technically capable of understanding. He posed the question, "What does the panel mean by standardization and how far do they propose to try and push it now?"

Mr. Kennard replied, "I agree that it is a pretty big order to standardize on data analysis and presentation. That is why I said earlier that I don't think we will ever achieve standardization in its true essence. I don't think we would want to because we do not want to restrict our thinking in an evolving

technology. But I think sometimes we lose sight of the precepts of good scientific methodology – we consider instrumentation infallible or we consider machines infallible. You have a machine to perform a frequency analysis and all you have to do is to feed the data into it and take the output. That is your answer. We must remember that the machine is only the process of our mental efforts and that, in considering the use and output of machines, we must establish limits and tolerances and be very conscious of these at all times. In doing this we aren't really standardising, but we are expressing our information in terms of fundamentals that can be used in a standardized manner."

Analysis of Random Vibration

Mr. R. W. Mustain or Northrop Corporation stated that he felt that there has been a lot of power spectral density work accomplished without anyone defining the rms-to-peak values and that possibly a lot of past data may be wrong. He asked Dr. Morrow to comment on this. He also asked Dr. Allen Curtis to comment on why he is backing probability density analyzers.

Dr. Curtis responded as follows: "I did not wish to appear to be backing one method of analysis or another. I think the point I was trying to make this morning was that often, when we analyze data, we pass the data through a filter whose bandwidth is known. We look at the output of the filter on a meter of some kind which gives some sort of an average value, but we really don't know what it is the average of. In other words, the usual methods of spectral analysis do not provide enough information to know whether you have a random function, a sinusoidal function, a phase-coherent function, a quasi sinusoid, or a mixture of all these things. If the test engineer is going to be able to use this data, the data analyst must, during the analysis process, do sufficient analysis to determine what kind of a process he is analyzing. There are many ways of doing this. My only point is that we don't do it often enough. I don't back any one system. I am just talking about principles. Let's really find out what kind of a signal we have."

Dr. Charles Morrow of STL commented as follows: "As Allen Curtis states his position now, I agree with him. Regarding the question from the floor, I think there probably is quite a bit of power spectral density data taken to date that could be improved. However, this is probably not connected with whether the probability distributions were measured or not. In many cases there has been insufficient care taken with the examination of raw data before the power spectral density analyses were done, as Dr. Curtis has been pointing out. In taking the data there has been insufficient care with the bandwidths used and the averaging times used. Now, as I think has been emphasized in the past, one of the virtues of the power spectral density plot properly used is that it tends to make the result independent of the apparatus used in getting the power spectrum. However, this is true only if the vibration is random, if the bandwidths are narrow enough to reveal the detailed interest in the power spectrum, and if the averaging time is long enough to correspond to the bandwidth that was selected."

Acoustic Noise Testing

Mr. D. E. Brown of Consolidated Electrodynamics Corporation asked for comments from anyone with experience in the field of acoustic noise testing. He had found no evidence of standardization in this field. He wanted to hear about the reasons for noise testing and something about the effect of the type of chamber and the type of excitation upon the final results of the test.

Comments on acoustic testing were made by Mr. R. W. Mustain of Northrop Corporation, Mr. W. D. Trotter of Boeing Airplane Company and Mr. G. S. November, General Electric, Lynn, Massachusetts.

Mr. Mustain said, "On the Snark missile the regular qualification program included the usual vibration tests such as resonance, flight cycle and a launch test which was fairly severe. In addition, after the sinusoidal vibration testing, we decided to investigate the acoustic effects on the equipment. We had previously qualified something like 200 components by vibration testing and we now selected 20 and tested them acoustically. For flight simulation testing we used a speaker system (130 db overall) and to simulate the launch phase we used pulse jets which gave 150 db. I think the type of facility must depend on what you are testing, electronic equipment, structures, or something else." As an example, Mr. Mustain said they had had panel failures on a trainer. To test the panels high-pressure air was supplied to a modulator consisting of an orifice plate with

numerous holes in it, driven by an MB C5 shaker. This gave random signals similar to those obtained on an airplane. This particular problem was cleared up satisfactorily but it was hard to specify a particular testing facility.

Mr. Trotter spoke of an interesting development, a small air bell which generates high acoustic levels. They are being considered for generating high acoustic levels in a jacket around a missile section. In this way it is felt that the actual launch excitation can be simulated as accurately as it has ever been done.

Mr. November said he had done acoustic evaluation of jet engines which might be of interest since the same things can happen on missiles. "In these examples you have organ pipes which are excellent sources of excitation. The problem is that the frequencies are always changing with load condition and with time. So if there is a mechanical resonance just changing due to a part becoming loose, or because of a temperature change, and there is also acoustic excitation, you may test one day and everything works well. Then the next day you have a great big fire. What has happened is that the resonance frequencies and the acoustic frequencies have come together."

Comments of General Interest

Dr. Charles Morrow of STL commented that there is a great tendency to bring up problems in connection with random vibration and infer that they are new, when they have been with us for some time. It impressed him a great deal the number of people who ask, "How can you compute a response to a random vibration?" when they have no intention of doing so and wouldn't do so for the periodic case either. Probably some of the interest in safety margins touches on a similar problem.

Mr. John Salter of the Armament Research and Development Establishment, Fort Halstead, England made the following comments: "Back home we have been bedeviled by two problems; the generalized specification and the committees which produce these specifications. I was quite shattered to hear earlier in this session that you proposed to follow us into that morass.

I do really ask you to look back on your previous experience. Let's start with the committee that writes the specification. Every establishment, as a matter of pride, has to have a representative on it. The result is that the size of the committee is already well into the fourth Parkinson area, where it is self propagating. In general there are two members of the committee who have pet ideas. One is all in favor of spectral densities and a few other technical terms and the other is in favor of simple sinusoids. The meeting starts, goes on for a hot two hours with arguments between these two, and at the end of the day the secretary goes away and writes the specification.

In general we have found that the specifications which emerge are based, roughly speaking, on the worst vital statistics which can be achieved. Most of the information we use, I'm sorry to say, originated in past years at this distinguished gathering. By the time that the curves have been enveloped, families of curves have been re-enveloped, and factors of safety have been added – usually a factor of two but some of the factors have a standard deviation of about 2-1/2 – we have found in England that we have ended up with power requirements to shake quite moderate articles of hardware which would need the whole resources of our nationalised industries. Unfortunately there is a real danger that once a committee, officially sponsored and set up, has put something on paper it then becomes a whip for the backs of everybody. If in doubt, play safe, call for your generalised specification. The result is that things which may be given quite a happy ride on a missile are treated as if they were going to be fastened on the tail of the jet itself. It really does lead to nonsenses."

The following comments were sent in after the session by Mr. K. Kuoppamaki, Lockheed, Sunnyvale: The reduced weight Mr. Forkois referred to is an interesting subject. (They tell us that an agent for a foreign power staring at Washington Monument shouted: "Impressive all right, but they'll never get it off the ground.") Reducing weight by performing an analysis of vibration characteristics has an increased importance in missile design, especially in the ballistic missiles, compared with the vibration analysis performed earlier on piloted aircraft. The volume of data collection is growing to new dimensions. In flight testing of one IRBM model alone the number of vibration channels is counted in hundreds and the analyzed events are counted in thousands.

In addition, the requirements for expediency in data presentation are increasing in the present-day high-priority projects. This adds a fourth one to the three Mr's Allen Curtis described: Money, Men, Months (for preparation) and Minutes (for presentation). The answers are required immediately after the test.

In order to obtain the answers in minutes in a tightly scheduled series of tests the preparation for obtaining the required information on shock and vibration has to be divided among a number of departments each one taking care of its own portion of the specific steps involved, such as: establishing the objectives, planning the measurements, designing the circuits, implementing the instrumentation and determining the performance characteristics of the measurement system, getting the calibration data for scaling and corrections, performing the test, reducing and presenting the data, running the analysis of the measurements, writing the reports for presentation of the conclusions drawn and recommendations made, using the information obtained for the benefit of the present design and to advance systems being developed.

Allen Curtis gave a clear-cut picture of the integrated effort necessary in managing the continuous flow of "the game" involved in making large-scale vibration measurements. In management of a high-priority project the ball cannot be carried successfully from individual to individual within one department and further from department to department without established rules of the game.

In preparing the rules for the game two categories of measurements are considered: first, determination of the overall system characteristics obtained by the integrated departmentalized effort listed above; second, the special projects which have to be steamrollered through or around the departmental systems as a one-shot deal. It is advisable to start preparing the rules for the first category of measurements as an integrated effort. One important step in standardized procedure has already been taken at Lockheed: the overall system characteristics have been determined by concentrating the measurements so as to indicate the response of the primary structure at indicated points and in indicated directions. A second step towards standardized procedure is being taken in the area of data reduction: (a) the response of the primary structure is being presented in the form of shock spectra, indicating the zero to peak amplitudes in the frequency ranges of interest with specific damping ratios; (b) the response to stationary inputs is being measured by the root-mean-square value of the vibration amplitude taken with a specific averaging time; (c) the frequency characteristics of a specific time interval of the rms value is being presented in form of a power spectral density plot.

In establishing the above starting points for the ground rules of the ball game the continuing task of the integrated departmental effort consists of assuring that the measured values have the same meaning in expressing the expected variability in the frequency levels and vibration amplitudes. Information of this variability is being determined among the various vehicles of the same model. Attempts are also being made to determine the variability between different models of the same weapon system as well as models from different weapons systems of the same general category.

Two papers, presented this morning, are of significant nation-wide importance from the standpoint of standardized data handling techniques. The paper of Atchison* shows possibilities of standardized techniques in the presentation of shock spectra. The paper of Brown† indicates that handling of vibration data is also approaching a new era of standardization. These papers emphasized the use of digital computer facilities. These facilities have high potentials for improving the resolution characteristics and rapidity of data presentation and for expanding the usefulness of the presented data in the analyzing effort.

Once the data is in digital form a wide variety of computations are within easy reach and fast access. The main portion of calibration data is available prior to flight. Intelligence for corrections in respect to mount resonances, transducer response characteristics and distortion of the transmitted signal can be processed before the flight to be ready for computer use. This reduces the time necessary in processing the intelligence for corrections for system noise and for effects of temperature and altitude on measurements made during the flight. Once the intelligence for corrective computations is in the computer then the

*Ref. to position in Bulletin.
†Ref. to position in Bulletin.

measured data in corrected form become available in only minutes of time.

Because of the expense of preparing computer programs, the use of digital computers makes it mandatory to standardize the techniques of measurements and methods of analysis. Programs for the use of Fourier integrals and autocorrelation function have already been adopted as standard routines. It can be predicted that the possibility of correlation of data for elimination of biased errors for increasing the statistical significance of the measurements made by using digital computer routines will lead towards uniform techniques employed by the various projects within one company as well as within the missile and space programs nation wide. It can be stated that contacts made at the DOD Shock and Vibration Symposia will have an important role in getting techniques formulated for uniform presentation of shock and vibration data.

SUMMARY OF PANEL SESSION AND DISCUSSION

Dr. Vigness

Dr. Mains: At this stage I would like to call on Dr. Vigness to summarize briefly for us his reactions to this afternoon's session.

Dr. Vigness: When one summarizes something it is difficult to keep from injecting ones own opinions, so I expect you will find some personal bias in what I am going to say.

I will not try to cover the individual panelists' presentations, but I will say a word about the 10-g specification. Of course it was a gag, but quite a sensible gag at that, because in almost all our specifications and our talking we say, rather glibly, "How many g is it?" This is only permissible provided something is implied about the waveform and the time function of that g. If this isn't understood by the person to whom you are talking then 10 g will make no sense to him and he will be unable to proceed with a design. If you have a sinusoid of 10 g amplitude at a certain frequency and you are going to design a system which might be resonant at that frequency, you have one problem. If the 10 g is an equivalent static acceleration you have another. If the 10 g is the maximum value of a pulse you have a third; and there are many others. I have eight or nine points I will try to cover. They are not necessarily in a logical order, but simply in the order I wrote them down.

My first point is compartmentalization. Presumably this is bad because, if you are in a compartment, you don't know what other people are doing, and if you don't know what the others are doing you may not be able to do your own job properly. However, some compartmentalization may be necessary and good. One person can learn only so much. If the person performing tests is required also to know all about the field shock conditions, the methods of shock analysis, and how the specifications are written, then he won't have any time to do his tests. He can be an expert of good competence in only one particular phase of the whole problem. I believe a degree of compartmentation is necessary so that a man can find time to become an expert in a particular area. However, a good smattering of knowledge in other areas is necessary so that his special knowledge can be dovetailed into the general problem.

In Mr. Forkois' group at our Laboratory we have a method of getting people out of their compartments and improving their education. Working for the Government under a rigid ceiling, in our particular activity, we don't have many people to help us do a job. So when someone asks us to do a shock or vibration test we say, "Certainly, but come down yourselves. We will provide the machines and tell you what to do, but you must come down and help." In this way we get the designers, the people who built the apparatus and the project engineers from the Bureaus who are responsible for the contracts. We see to it that the test is properly performed. We find out what goes wrong and we write up the test. The visitors see what happens when their equipment is tested. They are 'broken out of their compartment' and are shown an adjoining area, a knowledge of which is very necessary for the most effective performance in their own area. I suggest this can be done anywhere.

To get back to the summary. Another point is cross-fertilization of which the above is one example. Let the persons associated with a piece of equipment in one phase of a project experience what is going on with their equipment in other phases of the project, but don't require that these individuals learn and become expert in all phases. When you are a designer you are designing

primarily to a specification, and that specification is the law. It's what your equipment is going to have to withstand. It's not the field conditions that you should be worried about. Somebody, presumably very highly qualified, has written the specifications and most of them, even those which come in for most adverse comment here, have some good points in them. The designer, normally, might better spend his time improving his design so that it will pass specifications, rather than trying to find reasons for changing the specifications. Of course some exceptions to this rule may exist.

Specifications are usually written for very general conditions and you may find when you apply them to a particular test that they do not provide detailed information as to how to perform the test. The test engineer must then use a little judgment. If he is not permitted to exercise the required responsibility he must go to the project engineer responsible for the test and find out what he should do. As an example, let us take the question that was asked earlier. Where do you measure this 10 g? You have a specification calling for this level. You have your piece on the vibration table and you measure three different levels at three different points. Often it is impossible to have only one level. At one meeting a description was given of a plate, 8 feet long, that was pushed on a slippery table by a vibration machine at about 1000 cps. Measurements at each end of the plate gave a certain value of amplitude at 1000 cps. They did not say what they measured in-between, but with those dimensions and a speed of sound in the plate of around 16,000 fps, you will find the natural frequency of the plate in compression to be about 1000 cps. Probably the middle of the plate was standing still while approximately the same measurements were made at either end.

We have conditions like that to a lesser degree in a great many of our vibration tests. We may have the bottom of a certain piece of equipment going at a certain amplitude while the top bulkhead mounts, perhaps 6 feet away, are going at different amplitudes. Yet all the specification says is 60 mils double amplitude over a certain frequency range. Clearly something must be done about the interpretation of the specification. Something must be worked out between the persons doing the test and the persons who are responsible for the writing of the specifications for the particular piece of equipment. This must also be understood by all people involved so that attempts are not made to do the impossible. In the El Paso meeting* in the seminar on jigs and fixtures we heard about attempts to do this. The fixtures got bigger and bigger, yet they were still getting rocking modes and other modes of unwanted vibration.

My next point is standardization. Workers in research laboratories are very sensitive on this point. They don't like to have standards which tell them that they must do something a certain way or present their findings in a particular manner. This is quite natural. However, when things are standardized it is done for the convenience of everybody. If, for instance, we were to standardize the presentation of shock spectra at various values of damping -- we might standardize spectra at the equivalent of zero damping, at 2 percent critical and at 10 percent critical, etc. One would then have less trouble comparing the works of different groups. There are many aspects of our work which need this form of standardization. Standards in this area are not generally compulsory. They are primarily suggestions as to a common method of performance or presentation. If there are reasons to do things in another way, they can be done in another way. Standards are suggested ways of doing things so as to be in line with other people doing the same things. Common nomenclature, a similar manner for presentation of curves, the same general techniques, provide common means of comparison which makes understanding much easier.

The fourth point I have is this: before measurements are made something should be known about the purpose for which they are being made. Perhaps the main reason why most measurements which are made turn out not to be useful to those who look them up later is that the originator of the measurements made them for a specific purpose. Since that purpose is not the same as the purpose for which the new individuals want the data, it is then said that the data isn't any good since it does not give the information sought. But that does not mean that the measurements were not any good to begin with. It is often said that there are volumes of measurements in the literature that are of no use. It is quite probable that they were useful for the person who made them because he made them for a specific purpose, but to others they may be useless.

*27th Symposium

However, I believe we should have more guidance and a better idea as to why we make measurements and what we are going to do with them. If we are going to analyze things a certain way then we ought to make measurements of a certain kind. We should know where we are to make the measurements. If we make measurements on a piece of equipment, the information may be useful for a particular user of that equipment but it probably won't be useful to anyone else. However, if we make our measurements on main structural members of ships or missiles those measurements will generally be useful to a large number of individuals. That is provided the information covers a broad frequency range and the data can be trusted.

My fifth point was to have been the damage process, what it is and how to design for it in terms of environment, but it is late, so I must leave it out.

Lately we have been quite concerned with mechanical impedance. If measurements are made at a certain location, the measurement will have greater significance if the mechanical characteristics of the load and the structure are known at that point. If these characteristics are the mechanical impedance then it would be desirable to know the impedance at that point as we look into the structure, and the impedance of an equipment that might be mounted there, then any measurements we make at that point will be useable under any conditions. However, in my opinion, this approach is at the present time something to be worked toward. Currently we must rely on available statistics. Although I hope for sufficient scientific ability to get the impedance measurements and to use them, I think the problem is enormous and that it will be five or ten years hence before we are using impedance measurements together with field measurements on a statistical basis.

My final points concern the analyses of vibration and shock. If the source of an excitation is periodic then the vibration will be periodic. The common way of analyzing that is by Fourier or sine spectrum analysis. If, however, the vibration is more complicated the common way of doing it is by spectral density curves or power spectra. If there is a combination of random vibration and sinusoids it would probably be preferable to use spectral density curves for the whole thing. Sinusoids can readily be separated from narrow band random vibrations by looking at their amplitude probability density curves.

Shock specifications are frequently given in terms of shock spectra. When this is done it is desirable to give, in addition, some shock motions that are equivalent to the shock spectra. Then either the motion representation or the shock spectra may be used for design calculations or tests. It is generally quite simple for the specification writer to provide this extra information.

As a final point I might remark that although many think that shock spectra are used primarily by designers, actually they have been least used by designers. They have been used to a much greater extent by those who wish to make shock machines duplicate a given field condition of shock. The spectra have been used to compare the intensities of the machine shocks with either specified shock spectra values or with a shock spectrum which has been taken as an average value for some field condition. So shock spectra are used primarily to compare shock intensities.

* * *

INFORMATION EXCHANGE

The purpose of this section of the Bulletin is to act as an additional means of disseminating information. Within the limits of security and policy, the Centralizing Activity for Shock, Vibration, and Associated Environments will publish inquiries and answers, abstracts, bibliographies, and other relevant material. Items for inclusion should be addressed to:

The Centralizing Activity for Shock, Vibration,
and Associated Environments
Code 4021
U. S. Naval Research Laboratory
Washington 25, D. C.

INFORMATION EXCHANGE

BRITTLE-FRACTURE TRANSITION OF SOME CONCRETE REINFORCING STEELS

Allan L. Tarr
Office Chief of Research and Development
Army Research Office

INTRODUCTION

Catastrophic "brittle-fracture" service failures have occurred in structures made from steels which were considered to be ductile as judged by the results of tensile tests. Many of these failures occurred with extreme suddeness, without any noticeable deformation and under conditions where the nominal stress was at very low values, well below the yield strength values determined by tensile tests.

Another feature of these failures is that they occurred at temperatures which were in or below the range of temperatures where notch-bar impact tests show a marked decrease in energy-absorbing capacity and the nature of fracture changes from ductile, with a large proportion of shear failure and considerable deformation; to brittle, with fracture largely of the cleavage type accompanied by little or no noticeable deformation. Detailed studies have indicated that low-strength catastrophic failures appear to be the result of a small notch, crack or other defect, combined with the presence of unfavorable residual stress, a sufficiently low temperature, and a certain minimum level of load stress.

To avoid brittle fracture, or at least minimize probability of such, in ships and pressure vessels steps are now being taken to limiting the operating temperature relative to the transition temperature of the steel used, limiting residual stress, limiting load stress, or limiting defect size. However, there is little or no indication that such practices have been given any consideration for "blast resistant" protective structures or any other type of reinforced concrete structures. There is apparently no report on the evaluation of the resistance of such structures at low-atmospheric temperatures. This appears to be a serious oversight when it is realized that the transition range of steels used for reinforcing steel bars may be expected to lie in the range of ordinary atmospheric temperatures and that the deformations on the surface of reinforcing bars along with other irregularities may provide numerous locations for the initiation of cracks which could propagate into catastrophic failures.

The recent disastrous failure of the Malpasset Dam in France may possibly be attributed to brittle failure of the reinforcing steel. It may be anticipated now that the application of newer methods of structural design, referred to as "limit design," wherein the ultimate load can only be realized if the members can undergo plastic deformations, will be accompanied by an outbreak of catastrophic failures in structures unless special attention is paid to the selection of reinforcing steels. Steels of suitable low temperature notch toughness are not likely to be furnished under specifications which are normally used in the United States.

To emphasize the need for concern about such steels brittle fracture data on seven reinforcing steels is presented in this paper. Judging from the negative results of solicitation for such data, this brittle-fracture

transition data may be the first of its kind on concrete reinforcing steels.

STEELS STUDIED

Reinforcing bars are classified in the United States as structural, intermediate, or as hard grade. The separation of grades, in the commonly used ASTM specification A15, is made on the basis of strength requirements with yield strength limits set at 33,000, 40,000 and 50,000 psi, respectively. Two other ASTM specifications, A431-58T and A432-59T, have minimum yield strength requirements of 75,000 psi and 60,000 psi, respectively. In the United States, steels having up to about 0.30-percent carbon are found in the structural grade. The intermediate grades may run to about 0.50-percent carbon. The hard grades usually have more than 0.50-percent carbon. In Europe strength may result from cold working by stretching or twisting or by using much higher manganese content than is normally used in the United States. (The USSR specifies a low alloy open hearth steel for ribbed, i.e., deformed, concrete reinforcing bars with a yield point of 56,900 psi minimum. The specified composition is 0.20- to 0.29-percent carbon, 1.2- to 1.6-percent manganese, 0.6- to 0.9-percent silicon, with sulphur and phosphorous not above 0.05 percent.) In addition to the primary steel production sources of open hearth, acid bessemer, basic oxygen, and electric furnace, secondary sources such as rerolled rail steel and rerolled axle steel are permitted by some specifications in the United States. The most commonly used bars are in the intermediate grade.

The reinforcing bars used for obtaining the data for this paper represents the products of several steel producers. Both hot-rolled and cold-worked bars are included. The compositions and strength levels cover a wide range, and most of the bars tested were of the very commonly used No. 7 size. The bars are identified only as indicated in the table of results given herein.

RESULTS OF TESTS

The tabulation of results of tests presents chemical analyses of the seven steels, the results of tensile tests, and some of the results of Charpy V-notch bar impact tests.

DISCUSSION

Examination of the results of tests reveals that under the conditions of the Charpy V-notch bar impact test, some of the steels tested are very brittle at room temperature. The cold-worked and stress-relieved steels (C7 and W7, respectively) are very brittle at temperatures well above ordinary atmospheric ranges. Charpy V-notch tests are a means of checking relative embrittlement properties of materials but no claim is made here that there is any simple or direct relationship of the results of such tests and action of the material in specific structural situations. However, in view of the probability that there will be increased use of structural reinforced concrete in cold areas and in new designs for which there is limited experience, the alarming decrease in resistance of Charpy samples with decrease in temperature suggests that it will be prudent to give some careful attention to the evaluation of the performance of steels in reinforced concrete structures intended for use in low temperature service. The specification by the USSR of a low alloy steel which can have excellent low-temperature toughness suggests that the Soviets have already made such an evaluation.

CONCLUSION

The results of limited tests reveal that reinforcing steel likely to be furnished to specifications now used in the United States can be expected to have relatively high ductile to brittle transition temperatures as judged by Charpy V-notch bar tests. Use of such reinforcing steel in structures subject to exposure to cold or even mild atmospheric temperatures may result in catastrophic brittle failures under sudden dynamic loading or even with sudden unique changes of temperature. Consequently, it will be prudent for those who are responsible for the integrity of protective structures to take steps to evaluate materials and designs for low-temperature service quite thoroughly, particularly for new design methods. Moreover, new specifications for reinforcing steels are needed to provide for procurement of steels for low-temperature service.

BRITTLE-FRACTURE TRANSITION OF SOME CONCRETE REINFORCING STEELS

Identity of Steel Bars Tested		TEMPERATURE OF CHARPY BARS AT THE TIME OF FRACTURE															
	C	40	-	0	+	40	+	80	+	120	+	160	+	200	356	240	C
	F	-	4	32	68	+	140	+	212	+	252	+	356	+		+	F
		ENERGY TO FRACTURE (ft-lb) and PERCENT BRITTLE FRACTURE															
G7	E	4.4	.	7.3	20.5	.	32.2	.	44.4	51.8	.	57.2	.	50.9	.	.	E
	%	100	.	90	80	.	55	.	20	5	.	0	.	0	.	.	%
B9	E	4.2	.	10.9	27.6	33.7	43.6	47.8	54.5	.	.	.	.	50.5	.	.	E
	%	100	.	90	65	40	20	5	0	.	.	.	.	C	.	.	%
R7	E	1.8	3.0	(-10 C)	15.8	.	34.1	58.6	58.2	.	59.1	.	.	.	.	.	E
	%	100	95	.	80	.	50	10	10	.	0	.	.	.	.	.	%
B7	E	.	.	2.5	5.0	12.4	(50 C)	21.9	30.2	35.3	38.6	(150 C)	.	37.7	.	.	E
	%	.	.	100	95	75	.	50	20	10	0	.	.	0	.	.	%
Y7	E	.	.	.	10.3	10.9	(50 C)	19.1	28.3	32.6	36.1	(150 C)	39.	44.0			E
	%	.	.	.	95	80	.	60	35	20	5	.	0	0	.	.	%
O7	E	.	.	.	3.7	.	7.0	.	8.9	.	.	.	.	29.5	.	31.8	E
	%	.	.	.	100	.	95	.	85	.	.	.	.	0	.	0	%
W7	E	.	.	.	4.7	.	.	.	4.8	.	19.4	.	.	28.3	.	29.1	E
	%	.	.	.	100	.	.	.	90	.	40	.	.	0	.	0	%

Note: (a) Velocity of impact = 16.8 ft/sec

MECHANICAL PROPERTIES OF STEELS

Steel Bars	Tensile Strength (psi)	Yield Strength[b] (psi)	Elongation Percent in 8 inches	"Nil-Ductility"[c] Temperature	
				(C)	(F)
G7	107,100	69,000 (1)	16.0	-10	+ 14
B9	78,000	42,500 (1)	16.9	-20	- 4
R7	67,000	37,800 (1)	26.8	-20	- 4
B7	78,400	68,800 (2)	29.7	+20	+ 68
Y7	128,000	90,900 (2)	7.2	+20	+ 68
O7	126,500	104,500 (2)	8.5	+60	+140
W7	123,900	106,400 (2)	8.1	+60	+140

Note: (b) (1) Yield by drop of beam; (2) Yield by 0.2 percent offset.
Note: (c) "Nil-Ductility" is arbitrarily based on 95 percent brittle fracture.

CHEMICAL ANALYSIS OF STEELS (Percent)

Steel Bars	C	MN	Si	S	P	Ni	Cr	Mo	N
G7	0.42	1.65	0.24	0.028	0.024	nil	0.05	nil	0.007
B9	0.37	0.65	0.13	0.035	0.023	"	0.06	"	0.007
R7	0.33	0.49	0.07	0.021	0.016	"	0.003	"	0.005
B7	0.41	0.33	0.26	0.033	0.041	"	0.04	"	0.007
Y7	0.45	1.87	0.09	0.026	0.024	"	0.13	"	0.026
O7	0.60	0.92	0.23	0.026	0.043	"	0.05	"	0.008
W7	0.60	0.93	0.23	0.024	0.038	"	0.05	"	0.006

ACKNOWLEDGMENTS

Materials tested and their physical properties were furnished by Messrs. D. Watstein and R. G. Mathey, both of the Structural Engineering Section of the National Bureau of Standards, Washington, D. C. Chemical analyses and Charpy impact test data were obtained from Messrs. S. Vigo and D. Driscoll of the Watertown Arsenal Laboratories, Watertown Arsenal, Watertown, Massachusetts.

* * *

FREE-FIELD EFFECTS DUE TO AN EXPLOSION ON THE SURFACE OF A SEMI-INFINITE LINEAR-ELASTIC SOLID

Hans H. Bleich,
Consultant to Weidlinger and Salvadori,
New York City

The talk presented at the Symposium was an extract of results presented in a report entitled: "Survivability of Air Defense Systems, Progress Report on Ground Shock at High-Intensity Pressure Levels," October 1959 (Secret), submitted by Guy B. Panero, Engineers, to the MITRE Corporation (Attention of Mr. Walter Attridge), Bedford, Massachusetts. The report was prepared under subcontract by Paul Weidlinger, Consulting Engineer, New York City, in cooperation with a number of academic consultants.

In view of the fact that copies of the report are available, no formal paper for publication in the Proceedings of the Symposium is submitted.

For readers interested in the theoretical background a list of unclassified references utilized follows.

REFERENCES

D. Graffi, "Sui Teoremi di Reciprocita nei Fenomini Dipendendi dal Tempo, Annali di Matematica," Ser. 4, Vol. 18, 1939, pp. 178-200.

C. L. Pekeris and H. Lifson, "Motion of the Surface of a Uniform Elastic Half-Space Produced by a Buried Pulse," J. Acoust. Soc. America, 29:1233-1238.

C. Chao, "Dynamical Response of an Elastic Half Space to Tangential Surface Loading," ONR Proj. Nr 064-401, Report No. 11, Inst. of Flight Structures, Columbia University, March 1958.

J. D. Cole and J. H. Huth, "Impulsive Loading on an Elastic Half Plane," RAND Report P-437, December 1953.

J. D. Cole and J. H. Huth, "Elastic Stresses Produced in a Half-Plane by Steadily Moving Loads," RAND Report P-854, January 1956.

M. Salvadori, R. Skalak, and P. Weidlinger, "Stress Waves in Dissipative Media," Trans. New York Academy of Sciences, Ser II, Vol. 21, March 1959.

F. L. DiMaggio and H. H. Bleich," An Application of a Reciprocal Theorem," Jour. of Applied Mechanics, December 1959, p. 678.

M. Salvadori, R. Skalak, and P. Weidlinger, "Waves and Shocks in Locking and Dissipative Media," forthcoming in Proc. ASCE.

J. Sackman and H. H. Bleich, "Load Moving with Superseismic Speed Over a Layered Elastic Solid" (Submitted for publication as a RAND Report).

M. L. Baron, "Effect of Plane Shock Waves on a Cylindrical Cavity in an Elastic Solid" (to be submitted for publication as a RAND report).

* * *

THE DESIGN AND DEVELOPMENT OF A SHOCK RESPONSE ANALYZER

Abstract of a paper by
Ward P. Barnes
Boeing Airplane Company

INTRODUCTION

The objective of this paper is to describe the equipment employed by the Boeing Airplane Company to assure that the shock test requirements of certain recent research and development programs are satisfied. Previous test requirements have specified that a shock environment be a description of the shock pulse itself, in terms of intensity, duration and wave form. The requirements of these recent programs, however, depart from this concept by specifying the shock environment in terms of a response to the shock pulse. This response is described by a shock response spectrum.

The test requirements presently specify that the positive shock response spectrum envelope shall be between 90 and 150 g's at frequencies between 700 and 100 cps, reducing uniformly to no response at 0 cps. Facing the test engineer is the problem of assuring that the shock spectrum experienced by the test specimen is within these limits. To accomplish this, a method of presenting a spectrum of a shock is required.

THE SHOCK ANALYSIS SYSTEM

It was decided that a response spectrum would be best presented in the form of a bar-chart, each bar representing the acceleration response of a spring-mass system of a specified natural frequency. In view of the difficulty of devising a mechanical system to accomplish the desired results, an analogous electrical system has been employed.

A block diagram of the analysis system is shown in Fig. 1. The voltage output from the accelerometer can be traced through an amplifier to a tape recorder, where the signal is stored on a magnetic-tape loop. This signal is played back to each tuned circuit of a shock response analyzer, their response being displayed on an oscilloscope and recorded by means of a polaroid camera. The accelerometer, amplifier, tape recorder, oscilloscope and polaroid camera were all readily available. It remained for Boeing to develop the analyzer.

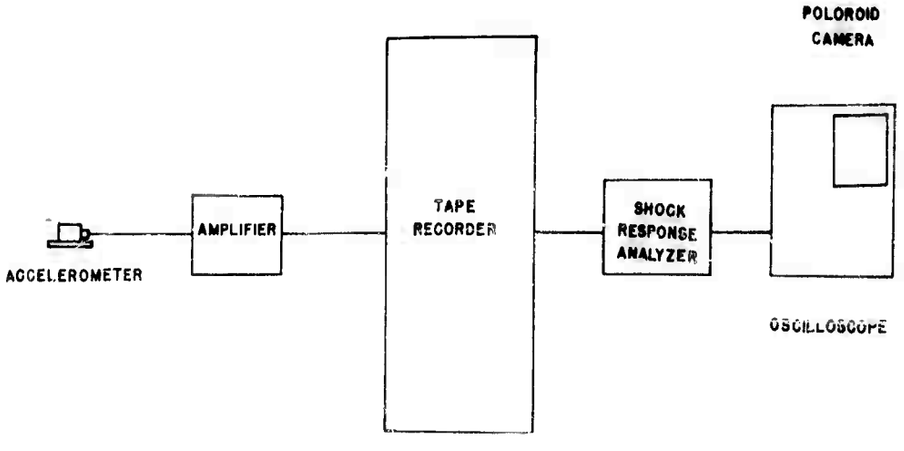

Fig. 1 - The shock analysis system

THE SHOCK RESPONSE ANALYZER

The analyzer is essentially a device that will respond to the electrical voltage signals from the tape recorder as a simple spring-mass system would respond to the original shock pulse; in other words, an electrical analogy of a Reed Gage.

Electro-Mechanical Analogy

The mechanical system to be duplicated electrically is similar to the system illustrated in Fig. 2a. A simple spring-mass system (k) and (M_1) represents a specimen component with natural frequency $\omega = \sqrt{k/M_1}$. This specimen is attached to a shock table (M_2) of such mass that the ratio M_1/M_2 is quite small. This small ratio minimizes the effect of the spring force (F_k) on the acceleration of the table under an applied force (F_a).

The following electromechanical analogy can be made:

Mechanical

Force (pound) F
Mass (lb sec^2/in.) M
Compliance (in./lb) 1/k

Electrical

Voltage (volt) e
Inductance (henry) L
Capacitance (farad) C

The analogous electrical circuit, therefore, is as shown in Fig. 2b. A small inductance (L_1) and a capacitance (C) represent a spring-mass system with natural frequency $\omega = \sqrt{1/L_1C}$. The large inductance L_2 represents the shock table, and as in the mechanical system, the ratio L_1/L_2 should be small to minimize the effect of the response voltage (e_c) on the current through L_2 due to the applied voltage (e).

In the mechanical system the acceleration of the shock table may be approximated by F_a/M_2 (neglecting the effect of M_1, which can be done provided M_1/M_2 is small), and the acceleration of the test specimen is equal to F_k/M_1. Similarly, it can be shown in the analogous electrical circuit that the acceleration of the shock table is approximately a function of e/L_1. If the voltage input (e) is proportional to the acceleration of the shock table, as it is with an accelerometer output, it follows that the acceleration of a specimen component of natural frequency ($\omega = \sqrt{1/L_1C}$) will be a function of e_c.

The Analyzer Circuit

Figure 3 represents the circuit diagram of the shock response analyzer. The complete circuit is essentially an extension of the analogous circuit previously illustrated, and is comprised of 20 tuned L-C circuits, each using the same inductances. It should be noted that L_2 is 90 times L_1. The resistance circuit, with its switch coupled to the L-C circuit switch, functions as a voltage divider for locating the position of the response signal on the horizontal axis of an oscilloscope.

Tape Speed Up

It is difficult to obtain a simple electrical circuit with a natural frequency less than 100 cps. This problem was effectively met by using circuits in the frequency range of from 100 to 5600 cps and playing the recording of the shock pulse back at 8 times the

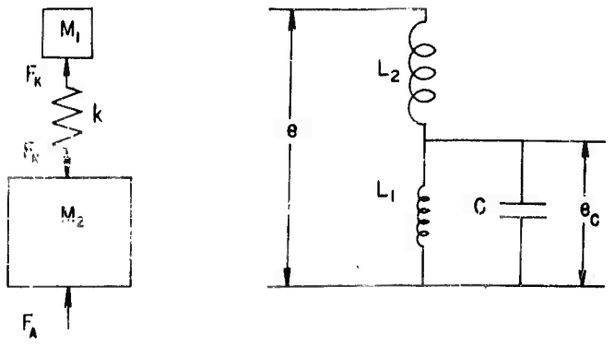

Fig. 2 - Analogous electrical and mechanical systems

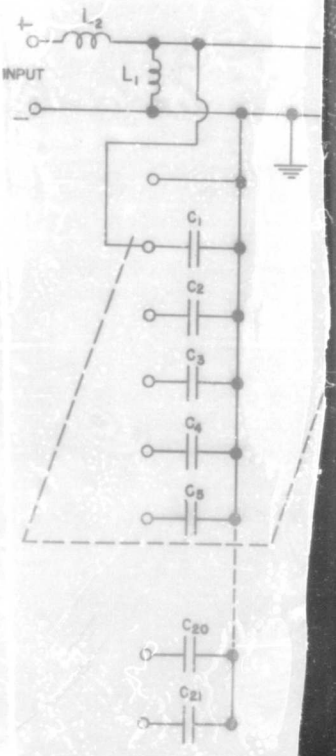

Fig. 3 - Circuit d
shock respon

recorded speed. The response of these circuits, therefore, is equivalent to the response of circuits with natural frequencies from 12.5 to 700 cps to the original shock pulse.

Damping

In the electrical circuit, as in any real mechanical spring-mass system, there is a certain amount of resistance or damping. The mechanical system called out in the test specification is theoretical, however, with no damping. It is therefore desirable to keep the resistance in the electrical circuit as low as possible. The problem faced in the use of an L-C circuit, is that the coils necessary to produce inductance will also create resistance. It can be shown that the damping in the circuit is a function of the term $e = (r_{L_1}t)/(2L_1)$. It is advantageous, therefore, to obtain an inductance with a value of $r_{L_1}/2L_1$ as low as possible. A value of 0.045 has proven to be satisfactory.

UNCLASSIFIED